Design and synthesis of small molecule chemical probes for bromodomain-containing proteins.

Duncan Alexander Hay

Corpus Christi College, Trinity 2014

A thesis submitted to the Faculty of Physical Sciences at the University of Oxford in partial fulfilment of the requirements of the degree of Doctor of Philosophy.

Bromodomains (BRDs) are protein modules which bind to acetylated lysines on histones and transcriptional regulating proteins. BRD-containing proteins are involved in a large variety of critical cellular processes and their misregulation, or mutation of the genes encoding for them, has been linked to pathogenesis in humans. The generation of chemical probes (potent, selective and cell permeable small molecules) in cellular experiments to investigate the biological role of the BRDs is thus desirable.

A chemical probe for the CREB (cyclic-AMP response element binding protein) binding-protein (CBP) and E1A binding protein (p300) BRDs was developed, starting from a low molecular weight, weak and non-selective dimethylisoxazole benzimidazole compound. Parallel synthesis was used to optimise the initial hit into a weak, but selective CBP inhibitor. Further modification of the two *N*-1 and *C*-2 moieties of the benzimidazole scaffold, led to highly potent and selective CBP inhibitors. Structure-guided design was then applied to optimise the selectivity of the series for CBP over the first domain of bromodomain-containing protein 4 BRD4(1). A strategy to reduce the flexibility of the *N*-1 and *C*-2 ethylene linker groups through the incorporation of conformational constraints led to inhibitors with increased selectivity. The optimal compound was highly potent for the CBP and p300 BRDs (K_d 21 nM and 32 nM, respectively) and selective over BRD4(1) (40-fold and 27-fold, respectively). On-target cellular activity was observed in a fluorescence recovery after photobleaching (FRAP) assay (0.1 μM), a p53 reporter gene assay (IC_{50} 1.5 μM) and a Förster resonance energy transfer (FRET) assay (5 μM).

A weak indolizine bromodomain-containing protein 9 (BRD9) inhibitor was used as the starting point for the development of a BRD9/BRD7 chemical probe. Analogues were synthesised via [3+2] cycloadditions. An optimised compound was found to be highly potent (68 nM) and selective over BRD4(1) (34-fold). On-target cellular activity was observed in a FRAP assay (5 μM). Efforts were made to improve the cellular activity through the introduction of an ionisable centre to aid solubility. A selection of piperazine analogues were shown to be potent and selective, and these compounds warrant further investigation of their selectivity and cellular activity.

Overall, the work has led to the first potent and selective inhibitors of the CBP/p300 and BRD9 BRDs. It also highlights the role of structural analysis in the development of inhibitors that modulate protein-protein interactions.

Dedicated to my two special ladies…

ACKNOWLEDGEMENTS

I would like to thank Chris Schofield and Paul Brennan for their supervision, guidance and support throughout my DPhil studies, and for giving me the chance to come to Oxford to work on various very interesting projects. Thanks to the Structural Genomics Consortium (SGC) and to Chas Bountra in particular, for contributing to college fees. Thanks also to the following colleagues at the SGC and Target Discovery Institute (TDI), who have contributed to the work presented herein: Oleg Fedorov, Sarah Martin, Octavia Monteiro and Anthony Tumber (primary binding assays), Sarah Picaud (protein purification, ITC, crystallography and providing training for protein purification and ITC), Panagis Filippakopoulos (X-ray crystallography data refinement and ITC advice), Cynthia Tallant Blanco (protein purification, ITC and crystallography), Clarence Yapp, Chris Wells, Martin Philpott and Dean Singleton (cellular assays), Stefan Knapp and Susanne Müller-Knapp (project direction, advice and instigation of collaborations), Brian Marsden and James Crowe (IT support), and to all other SGC/TDI colleagues who have offered advice and made me feel welcome.

Thanks also go to the following colleagues in the Schofield group: Louise Walport for help with biological techniques and proof reading, Adam Hardy for IT support, help with biological techniques and proof reading, Clarisse Lejeune for a warm welcome and helping me to get set up at the beginning, Cyrille Thinnes and Richard Hopkinson for proof reading, Mike McDonough for advice on electron density maps, and Wendy Sobey, Jenny Houlsby and Valerie De Newtown for keeping the Schofield group running smoothly behind the scenes. Thanks to all the colleagues in LG1 who I have borrowed reagents and starting materials from, who have offered advice, helpful discussion and support, and have generally worked hard to keep the lab tidy and running safe and efficiently; in particular, thanks to Katherine England, Clarisse Lejeune, Martin Muenzel, Sander Van Berkel, Cyrille Thinnes, Jacob Bush, Greg McSweeney, Marina Demetriades, Rob Lesniak and Anna Rydzik. Thanks also to all the

other Schofield group members, of whom there are too many to mention here, who have been welcoming and friendly and kept a smile on my face throughout my studies. Thanks also to Stuart Conway and his group members, in particular Timothy Rooney, David Hewings and Brian Wilson, who have worked collaboratively with me on projects with overlapping areas of interest, and have offered useful advice on target design. Thanks to Peter Clark in Darren Dixon's group for help with *er* determination.

I wish to thank Mark Bunnage and Pfizer for allowing me to begin my research at the Sandwich laboratories and for the use of the facilities there. Thanks to Katie Bainbridge and Steve Collins who conducted HPLC purification of the initial set of parallel synthesis target compounds.

Thanks to all the support staff in the CRL who have provided help with NMR and mass spectrometry determinations, stores facilitating and finance and administration. Thanks also to support staff at the SGC provide support in areas including ordering of consumables, wash-up service and autoclaving of media, and to those who have provided HR, finance and administration support.

Thanks to my parents, David and Isobel Hay, who have always been hugely supportive and encouraging throughout my life and education; thanks to my dad for catalysing my interest in chemistry and science in general. Finally, a special big thanks to my wife, Tanya Hay, who has been immensely supportive throughout my studies. She has provided encouragement, motivation and support, and has been extremely understanding of the extra time that I have needed to commit to the writing of my thesis. During this tough and stressful time, my wife also brought the most special thing in our lives into the world when our daughter, Fia, was born in August 2013. Thanks also go to Fia for sleeping so well during the night, and for providing Tanya and I with endless supplies of smiles and giggles that have helped to keep us smiling during times of stress.

LIST OF EXPERIMENTS INCLUDED IN THESIS DONE BY OTHERS

- HPLC purification of the initial set of parallel synthesis compounds in Chapter 1 was carried out by Katie Bainbridge and Steve Collins (Pfizer).
- All primary binding assays were carried out by Oleg Fedorov, Sarah Martin, Octovia P. Monteiro and Anthony Tumber (SGC/TDI).
- Crystallography and refinement of crystallographic data was carried out by Sarah Picaud, Panagis Filippakopoulos (SGC) and Cynthia Tallant Blanco (SGC/TDI), as indicated in the text. The crystallisation screen for the complex of compound **306** and BRD4(1) was carried out by the author under the guidance of Sarah Picaud.
- Isothermal titration calorimetry (ITC) was carried out by Sarah Picaud, Stefan Knapp and Cynthia Tallant Blanco (SGC/TDI) as stated in the text. Where not stated, the ITCs were carried out by the author.
- Protein expression and purification were carried out by various scientists at the SGC, with the exception of protein required for ITC experiments conducted by the author, which was prepared by the author under the guidance of Sarah Picaud.
- Fluorescence recovery after photobleaching (FRAP) assays were carried out by Dean Singleton and Martin Philpott (SGC/TDI).
- The p53 reporter-gene assay was carried out by Christopher Wells (SGC).
- The Förster resonance energy transfer (FRET) assay was carried out by Clarence Yapp (SGC/TDI).

CONTENTS

Abbreviations x

Chapter 1. Introduction 1

1.1 Chromatin and epigenetics 1

1.2 Definitions of epigenetics 3

1.3 DNA Methylation 4

1.4 Histone tail modifications 9

1.4.1 Lysine methylation 10

1.4.2 Lysine acetylation 15

1.5 Chemical probes for research into transcriptional regulating proteins 24

1.6 Project Aim 25

Chapter 2. CBP/p300 26

2.1 CBP/p300: transcriptional coactivators and lysine acetyl transferases 26

2.2 CBP/p300 in development and disease 30

2.2.1 CBP/p300 in development and RTS 30

2.2.2 CBP/p300 in memory and neurodegenartive disorders 31

2.2.3 CBP/p300 in cancer 32

2.2.4 CBP/p300 in inflammation 33

2.2.5 CBP/p300 in viral infection 34

2.2.6 CBP/p300 and p53 34

2.2.7 CBP/p300 in hypoxia 35

2.3 Inhibitors of CBP/p300 36

Chapter 3. CBP/p300 chemical probe: developing a non-selective fragment into a lead 39

3.1 Starting point 39

3.2 CBP vs BRD4(1) 40

3.3 Carboxylic acid-containing analogues 42

3.4 Neutral and basic analogues 44

3.5 Summary 49

Chapter 4. CBP/p300 chemical probe: improving potency and selectivity 52

4.1 Structure of compound **263** complexed to CBP 52

4.2 *C*-2 analogues 54

4.3 *N*-1 analogues 56

4.4 Further *C*-2 optimsation 60

4.5 Summary 66

Chapter 5. CBP/p300 chemical probe: structure-guided selectivity optimisation 68

5.1 Structure-guided design 68

5.2 Indole synthesis 71

5.2 Synthesis of ether-linked analogues 72

5.3 Screening results for benzimidazole core and *C*-2 linker analgoues 75

5.4 *N*-1 linker analogues 77

5.5 Screening results for *N*-1 linker analogues 79

5.6 Structure of compound **397** bound to CBP and BRD4(1) 83

5.7 Selectivity over other BRD subfamily members 85

5.8 Summary 86

Chapter 6. CBP/p300 chemical probe: characterisation of compound **397** 88

6.1 FRAP assays 88

6.2 p53-Reporter gene assay 89

6.3 FRET assay 90

6.4 Cytotoxicity of compound **397** 91

6.5 Wider profiling of compound **397** 92

6.6 Summary 93

Chapter 7. Towards a chemical probe for BRD9/BRD7 95

7.1 BRD9/BRD7 95

7.2 Starting point 96

7.3 *C*-1 analogues 98

7.4 Selectivity profiling of compound **425** 105

7.5 Structure of compound **425** bound to BRD9 106

7.6 Cellular characterisation of compound **425** 107

7.7 Improving solubility 109

7.8 *C*-3 Analogues 111

7.9 Summary 113

Chapter 8. Summary 115

8.1 CBP/p300 chemical probe 115

8.2 Towards a BRD9/BRD7 chemical probe 122

Experimental – Synthetic procedures 127

General experimental 127

General procedure A 129

General procedure B 130

General procedure C 130
General procedure D 163
General procedure E 170
General procedure F 195
General procedure G 207
General procedure H 207
General procedure I 208
Experimental – Protein expression and purification 344
Experimental – Isothermal titration calorimetry 347
Experimental – Crystallisation trials 348
References 349
Appendix 1. Carboxylic acid heteroaryl bromides for parallel Suzuki couplings 361
Appendix 2. Additional SAR for carboxylic acids from parallel Suzuki couplings 362
Appendix 3. Neutral and basic heteroaryl bromides for parallel Suzuki couplings 365
Appendix 4. Additional SAR from neutral and basic parallel Suzuki analogues 368
Appendix 5. Aldehydes for parallel benzimidazole-forming reactions 378
Appendix 6. Additional SAR from parallel benzimidazole forming reactions 379
Appendix 7. CEREP wide-ligand profiling for compound **397** 383

ABBREVIATIONS

α2A - adrenergic receptors A
α2C - adrenergic receptors C
2OG – α-Ketoglutarate
5caC – 5-Carboxycytosine
5mC – 5-Methylcytosine
5fC – 5-Formylcytosine
5hmC – 5-Hydroxymethylcytosine
Ac – Acetate
ADDP – Azodicarbonyldipiperidine
ADME – Absorption, distribution, metabolism, and excretion
AIL – Autoinhibitory loop
AlphaScreen – Amplified luminescent proximity homogeneous assay screen
AML – Acute myeloid leukaemia
AMP - Adenosine monophosphate
ApoA-I - apolipoprotein A-I
Aq. – Aqueous
Ar – Aryl
BAF – BRG1/BRM-associated factors
BAZ2A – Bromodomain adjacent to zinc finger domain A
BAZ2B – Bromodomain adjacent to zinc finger domain B
BER – Base excision repair
BET – Bromodomain and extra-terminal
Boc – *tert*-Butoxycarbonyl
BINAP – 2,2'-Bis(diphenylphosphino)-1,1'-binaphthyl
Bn – Benzyl
BRD – Bromodomain
BRD2-4 – Bromodomain-containing proteins 2-4
BRD7 – Bromodomain-containing protein 7
BRD9 – Bromodomain-containing protein 9
BRPF1 - Bromodomain and PHD finger containing protein 1
BTM – Basal transcriptional machinery
CAD – Carboxy-terminal activation domain
CBP – CREB binding protein
CC_{50} – 50% cytotoxicity concentration
CDI – 1,1'-Carbonyldiimidazole
CDKN2A – Cyclin-dependent kinase inhibitor 2A
CECR2 – Cat eye syndrome critical region protein 2
CFP – Cyan fluorescent protein
CH1-3 – Cysteine-histidine rich regions 1-3
clogP – Calculated partition coefficient
CoA – Co-enzyme A
CODDD – Carboxy-terminal oxygen-dependent degradation domain
COPD – Chronic obstructive pulmonary disease
COX-2 – Cyclooxygenase-2
CREB – Cyclic-AMP response element binding protein
CTC – Cutaneous T-cell lymphoma
CVs – Column volumes
DAD – Diode Array Detector
Dba – Dibenzylidineacetone

DDQ – 2,3-Dichloro-5,6-dicyano-1,4-benzoquinone
Dec – Decomposition (during melting point determination)
DMAP – 4-(Dimethylamino)pyridine
DME – 1,2-Dimethoxyethane
DMF – Dimethylformamide
DMSO – Dimethyl sulfoxide
DNMT – DNA methyltransferase
DRPLA – Dentatorubropallidoluysian atrophy
DSF – Differential scanning fluorimetry
E1A – Adenovirus early region 1A protein
EDCI – *N*-(3-Dimethylaminopropyl)-N′-ethylcarbodiimide hydrochloride
ELSD – Evaporative Light Scattering Detector
er – Enantiomeric ratio
ERK1/2 – Extracellular signal-regulated kinases 1/2
ERα – Oestrogen receptor α
ESI – Electrospray Ionisation
Et – Ethyl
EtOAc – Ethyl acetate
EtOH – Ethanol
EZH2 – Enhancer of zeste homolog 2
FAD – Flavin-adenine dinucleotide
FALZ – Foetal Alzheimer antigen
FASD – Foetal alcohol spectrum disorder
FIH – Factor inhibiting hypoxia
FRAP – Fluorescence recovery after photobleaching
FRET – Förster resonance energy transfer
GFP – Green fluorescent protein
GNAT – Gcn5-related *N*-acetyltransferase
GSTF – Gene-specific transcription factor
H1-4 – Histones 1-4
HBTU – *N,N,N′,N′*-Tetramethyl-*O*-(1*H*-benzotriazol-1-yl)uronium hexafluorophosphate
HDL – High density lipoprotein
HLM – Human liver microsome
HIF – Hypoxia-inducible factor
HIV – Human immunodeficiency virus
HPLC – High Performance Liquid Chromatography
HRMS – High Resolution Mass Spectrometry
IC_{50} – Half maximal inhibitory concentration
ITC – Isothermal titration calorimetry
JmjC – Jumonji C-terminal domain
Kac – Acetyl lysine
KAT – Lysine acetyl transferase
K_d – Dissociation constant
KDAC - Lysine deacetylase
KID – Kinase inducible domain
KIX – KID interacting domain
KDM – Lysine demethylase
KMT – Lysine methyl transferase
LE – Ligand efficiency
LiPE – Lipophilic ligand efficiency
LRMS – Low Resolution Mass Spectrometry
MeCN – Acetonitrile
MeCP – Methyl-CpG-binding protein
MBP – 5-methyl cytosine binding proteins

MBT – Malignant brain tumour domain
MDS – Myelodysplastic syndrome
MGE – Medial ganglionic eminence
MLH1 – MutL homolog 1, colon cancer, nonpolyposis type 2
MLL – Mixed lineage leukaemia
mp – Melting point
MOZ – Monocytic leukaemia zinc finger
mRNA – Messenger RNA
MS – Mass spectrometry
MW – Molecular weight
MYST – MOZ, Ybf2, Sas2, Tip60
NAD^+ – Nicotinamide adenine dinucleotide
NF-κB – Nuclear factor κB
NMP – 1-Methyl-2-pyrrolidinone
NODDD – Amino-terminal oxygen-dependent degradation domain
NOG – *N*-Oxalylglycine
NRC – Receptor coactivator interlocking domain
NSCLC – Non-small-cell lung cancer
NUT – Nuclear in the testis
Oxone – Potassium peroxymonosulfate
p53 – Tumour suppressor protein p53
p300 – E1A binding protein (p300)
PAD – Platelet-activating factor
PBS – Phosphate buffered saline
PBAF – Poly-bromo-associated BAF
PCAF – p300/CBP-associated factor
PDE5 – Phosphodiesterase-5
P-gp – P-glycoprotein
Ph – Phenyl
PHD – Plant homeodomain
PKA – Protein kinase A
PKCδ – Protein kinase Cδ
polyQ – Poly glutamine
PTCL – Peripheral T-cell lymphoma
PTM – Post-translational modification
pVHL – Von Hippel–Lindau tumour suppressor
R_f – Retardation factor
RING – Really interesting new gene
RISK – RNAi silencing complex
RNAi – RNA interference
RST – Rubinstein-Taybi Syndrome
SAM – *S*-Adenosyl methionine
SAH – *S*-Adenosyl homocysteine
SAHA – Suberoylanilide hydroxamic acid
SBMA – Spinobulbar muscular atrophy
SCX – Strong cation exchange
SEM – Standard error in the mean
SET – Suvar3-9, enhancer-of-zeste, trithorax
SCA – Spinocerebellar ataxia
SGC – Structural Genomics Consortium
shRNA – Short hairpin RNA
SIR2 – Silent information regulator 2
siRNA – Small interfering RNA
Succ – Succinate

SWI/SNF – SWItch/Sucrose Non-Fermentable
α-Syn - α-Synuclein
T3P – Propane phosphonic acid anhydride
Tat – Transactivator of transcription
TAZ – Transcription adaptor putative zinc finger-type
TDG – Thymidine-DNA glycolase
TDI – Target Discovery Institute
TEBAC - Benzyltriethylammonium chloride
TET – Ten-eleven translocation
THF – Tetrahydrofuran
TIPS – Triisopropylsilyl
TLC – Thin Layer Chromatography
ΔT_m – Change in denaturing temperature (in DSF assay)
t_r – Retention time
VPR – Viral protein R
YFP – Yellow fluorescent protein
ZF – Zinc finger

CHAPTER 1. INTRODUCTION

The elucidation of the processes which transcribe and translate the information contained in DNA into functional proteins is one of the defining scientific achievements of the 20th century.[1] However, the fact that the information to make every protein in an organism's proteome is contained in chromosomal DNA presents an interesting conundrum: if each individual cell contains the entire genome, where does the selectivity arise that leads to the multitude of cellular phenotypes in a given organism? The implication is that there exists an additional *epigenetic* layer of control which directs the translation or transcription of particular genes according to the cell type and/or environmental conditions. This realisation has prompted studies of the proteins that package DNA in the cell nucleus as a superstructure known as chromatin.[1-3] In recent years, molecules which interact with chromatin have been subject to intensive research interest, as the scientific community seeks to understand these fundamental biological processes and discover new targets for therapeutic intervention.

1.1 CHROMATIN AND EPIGENETICS

In linear form, human DNA molecules would be around 2 m long; however, in cells, DNA is efficiently packaged within chromatin into nuclei that are approximately 5-8 μm in diameter.[1-3] Chromatin is made up of DNA spooled around histone proteins in a 'beads-on-a-string' type structure (Figure 1A). The smallest unit of chromatin is the nucleosome, which consists of ~146 base pairs of DNA wrapped round a core octamer of histone proteins (Figure 1B-D). The octamer is made up of two of each of the histone proteins H2A, H2B, H3 and H4. Histones are rich in the positively-charged amino acid residues lysine and arginine, which impart an electrostatic attraction to the negatively-charged phosphate groups on DNA and helps to hold the DNA in place. Histone H1 sits on the outside of the nucleosome, apparently holding the DNA strands in place. Chromatin is further compacted into fibres by

the interaction of two H1 proteins, then further still by packing of these fibres onto scaffolding proteins.

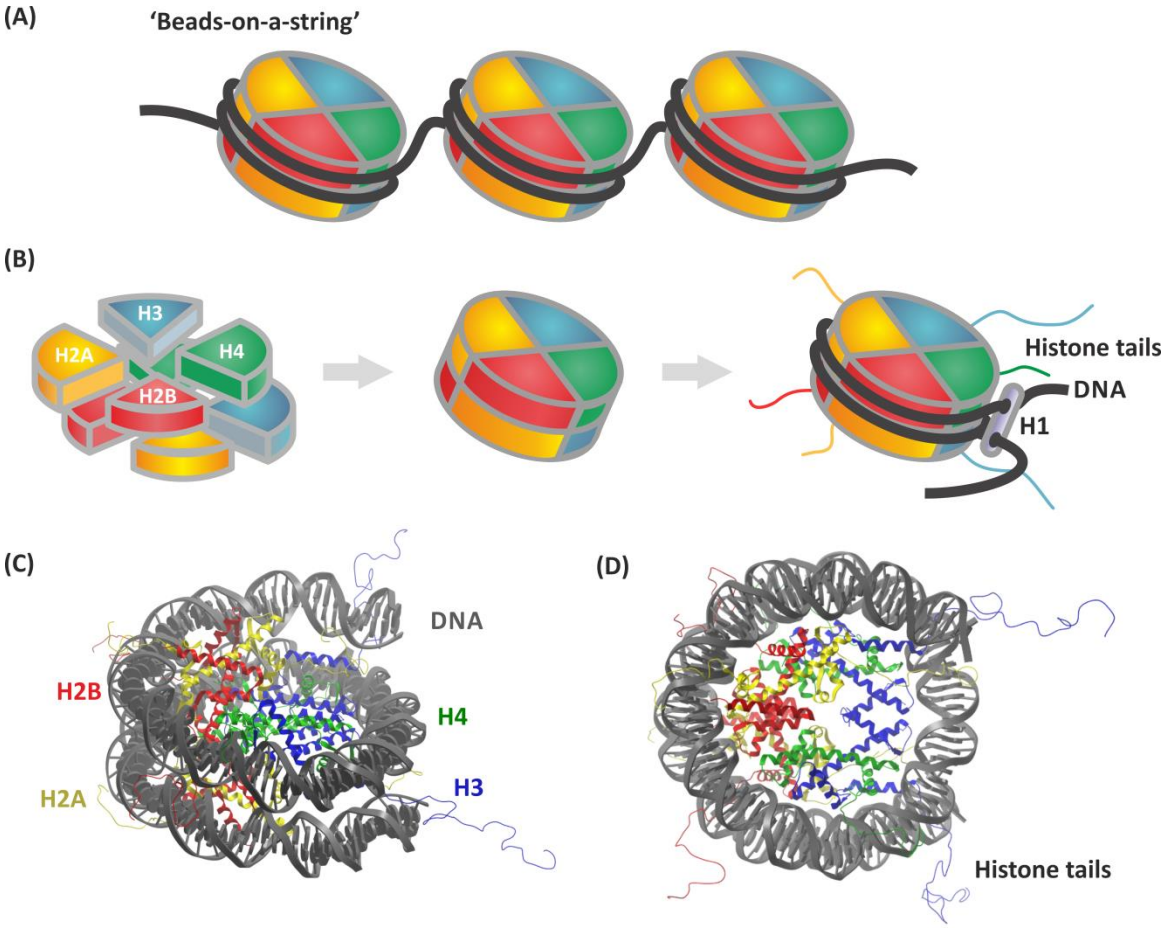

Figure 1. (A) Repeating nucleosomes and internucleosomal DNA as 'beads-on-a-string'. (B) Nucleosomes are composed of histone proteins (wedges). H3 pairs with H4 and H2A pairs with H2B. Two of each of these pairs combine to make the histone octamer, around which DNA (thick dark grey line) is spooled. (C) X-ray crystal structure of a nucleosome (PDB 1KX5). Coloured proteins represent histones and dark grey double helix is DNA. (D) 'Top-down' view of nucleosome with N-terminal histone tails protruding.

In addition to the canonical histones, there exist several histone variants with their own important functions. For example, the H2A variant H2A.Z is associated with the promoter regions of actively transcribed genes and H2A.X has roles in genomic stability and DNA repair.[4]

The degree of packing of DNA in chromatin is an important component of control of transcription.[2, 3] In an open state, accessible to the transcriptional machinery, chromatin is referred to as euchromatin and is associated with active gene transcription; heterochromatin is more densely packaged and consequently transcriptionally inactive.[5] Heterochromatin is further categorised into facultative chromatin, which is tissue specific

and varies with cell type, and constitutive chromatin, which is found in all cell types and performs a structural role.

Changes in chromatin structure and reversible covalent modification of the DNA and histones represent two of the main known mechanisms of *epigenetic* transcriptional control, with the others being through alternative RNA splicing and the function of non-coding RNA.[6-8] Post-translational modification (PTM) of chromatin will be discussed in subsequent sections. However, before going further, it is worth looking in more detail at how the term *epigenetics* is defined, as this has been a source of considerable debate.

1.2 DEFINITIONS OF EPIGENETICS

In 1942, Conrad Waddington devised the term *epigenetics*, with the Greek prefix *epi-* denoting 'over' or 'above' the genome.[9] Specifically, he defined this as *"the branch of biology which studies the causal interactions between genes and their products, which bring the phenotype into being"*. Today, definitions given have tended to fall into two categories, with the main difference being whether heritability is required. A commonly used definition states "*Epigenetics is the study of mitotically and/or meiotically heritable changes in gene function that cannot be explained by changes in DNA sequence.*".[10] However, it has also been defined without reference to heritability as "*the structural adaptation of chromosomal regions so as to register, signal or perpetuate altered activity states.*" and "*the study of changes in gene transcription that are based on chromatin and cannot be explained by changes in DNA sequence.*"[11, 12] In 2008, an attempt to put forward a consensus definition returned to the inclusion of heritability, stating "*An epigenetic trait is a stably heritable phenotype resulting from changes in a chromosome without alterations in the DNA sequence.*"[13] With the various definitions still being used interchangeably depending on the context, it is clear that a consensus on the definition has still to be agreed. The following sections will discuss how post-translational modifications of chromatin affect transcription. In order to avoid

confusion, the term *epigenetic* shall only be applied in the text that follows to phenomenon that fit the stricter definition which includes heritability as a requirement.

1.3 DNA METHYLATION

Post-translational methylation of the DNA itself is a well-studied epigenetic mechanism.[14] In eukaryotes, methylation of DNA occurs predominantly at the 5-position of cytosine on CpG dinucleotides. Due to base pairing, there is symmetry with a CpG on the complimentary DNA strand, allowing the mark to be maintained in cell divisions. DNA is methylated by *de novo* DNA methyltransferases (DNMTs), which in mammals are DNMT3a and DNMT3b.[15, 16] After cell-division, hemi-methylated DNA is methylated by DNMT1, which provides the mechanism for mitotic heritability of this epigenetic mark.[17, 18]

DNMTs function by transferring a methyl group from the cosubstrate *S*-adenosyl methionine (SAM) to the 5-position of cytosine, to give 5-methylcytosine (5mC) and *S*-adenosyl homocysteine (SAH) (Figure 2A).[16] In the mechanism, a thiolate side-chain of a cysteine residue adds to the 4-position of cytosine to generate an activated enamine intermediate.[19] This can react with the nearby SAM to install a methyl group in the 5-position. β-Elimination then yields the 5mC product. Figure 2B shows a view from the crystal structure of a bacterial DNMT1 with a modified cysteine base flipped into the active site.[20] Figure 2C is a close-up view of the active site showing the proximity of the base to SAH.

Demethylation of DNA can occur through passive demethylation, via down-regulation of DNMTs and failure to propagate the epigenetic mark upon cell division.[21, 22] However, 5mC demethylation can also occur without cell replication, perhaps pointing to the presence of an active process.[23] A complete picture has yet to emerge, but the ten-eleven translocation (TET) oxygenases have been implicated.[23-25] A proposed demethylation mechanism involves TET-mediated oxidation of 5mC to 5-hydroxycytosine (5hmC), then to 5-

hydroxymethylcytosine (5hmC), 5-formylcytosine (5fC) and 5-carboxycytosine (5caC) (Figure 3A). 5caC can be removed by thymidine-DNA glycolase (TDG) and replaced by cytosine via a base excision repair (BER) mechanism.[23-25] It has also been proposed that 5hmC is an epigenetic DNA modification in its own right, and not simply an intermediate in the demethylation pathway.[26] However, no specific 5hmC binding-proteins involved in epigenetic regulation have been described to date.

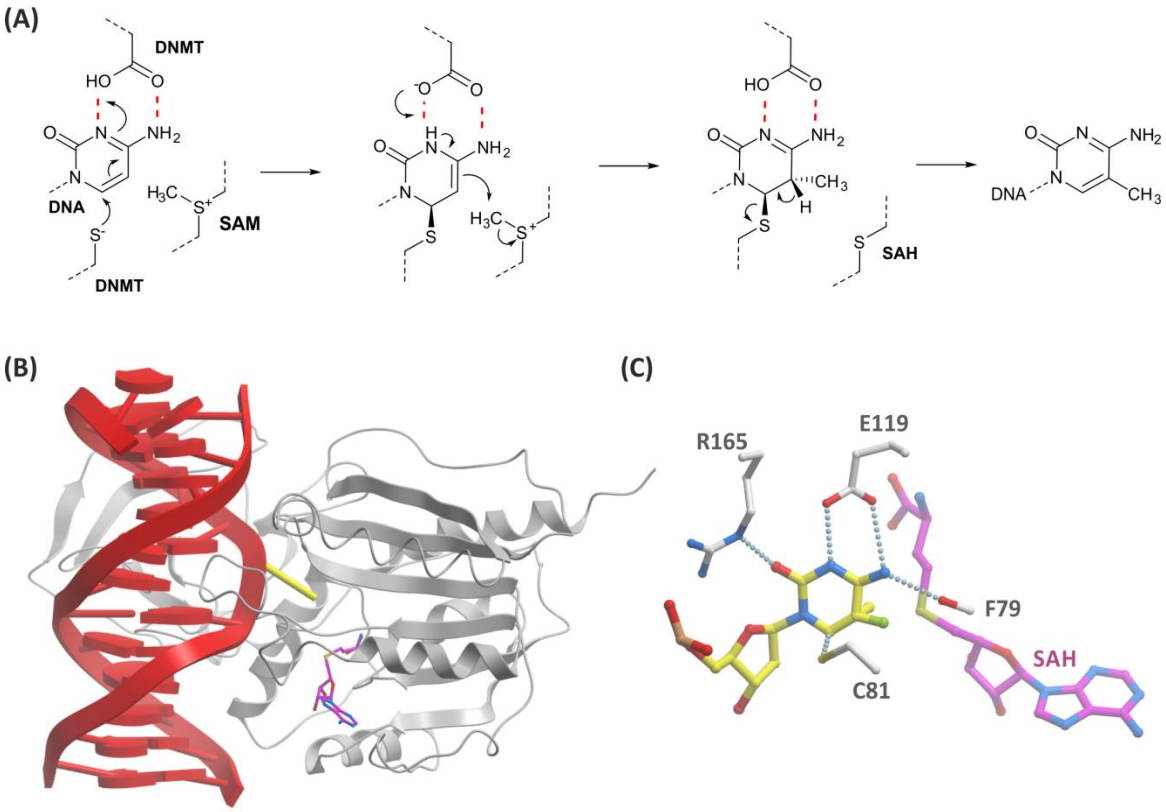

Figure 2. DNMTs. (A) Proposed mechanism of methylation of cytosine by DNMTs using SAM as cosubstrate.[19, 20] (B) View from an X-ray structure of bacterial (*haemophilus haemolyticus*) DNMT1 complexed to a 5-fluorocytosine-containing DNA strand (red) and SAH (carbon=magenta) (PDB 1MHT).* The 5-fluorocytosine base (yellow) is flipped out towards the active site.[20] (C) View from active site of (B) showing the cytosine binding residues and close proximity to SAH.

The TET enzymes are α-ketoglutarate- (2OG-) dependent dioxygenases which catalyse oxidation of the substrates with concurrent reduction of O_2 and 2OG to CO_2 and succinate (succ), respectively (Figure 3B). Figures 3C and D show views from a crystal structure of DNA complexed to TET2. The binding site (Figure 3C) shows 5mC bound in close proximity

*Images of X-ray crystal structures throughout were created using Molsoft ICM-Pro.

to the catalytic site, containing the metal ion, metal binding residues, and 2OG the mimic *N*-oxalylglycine (NOG).

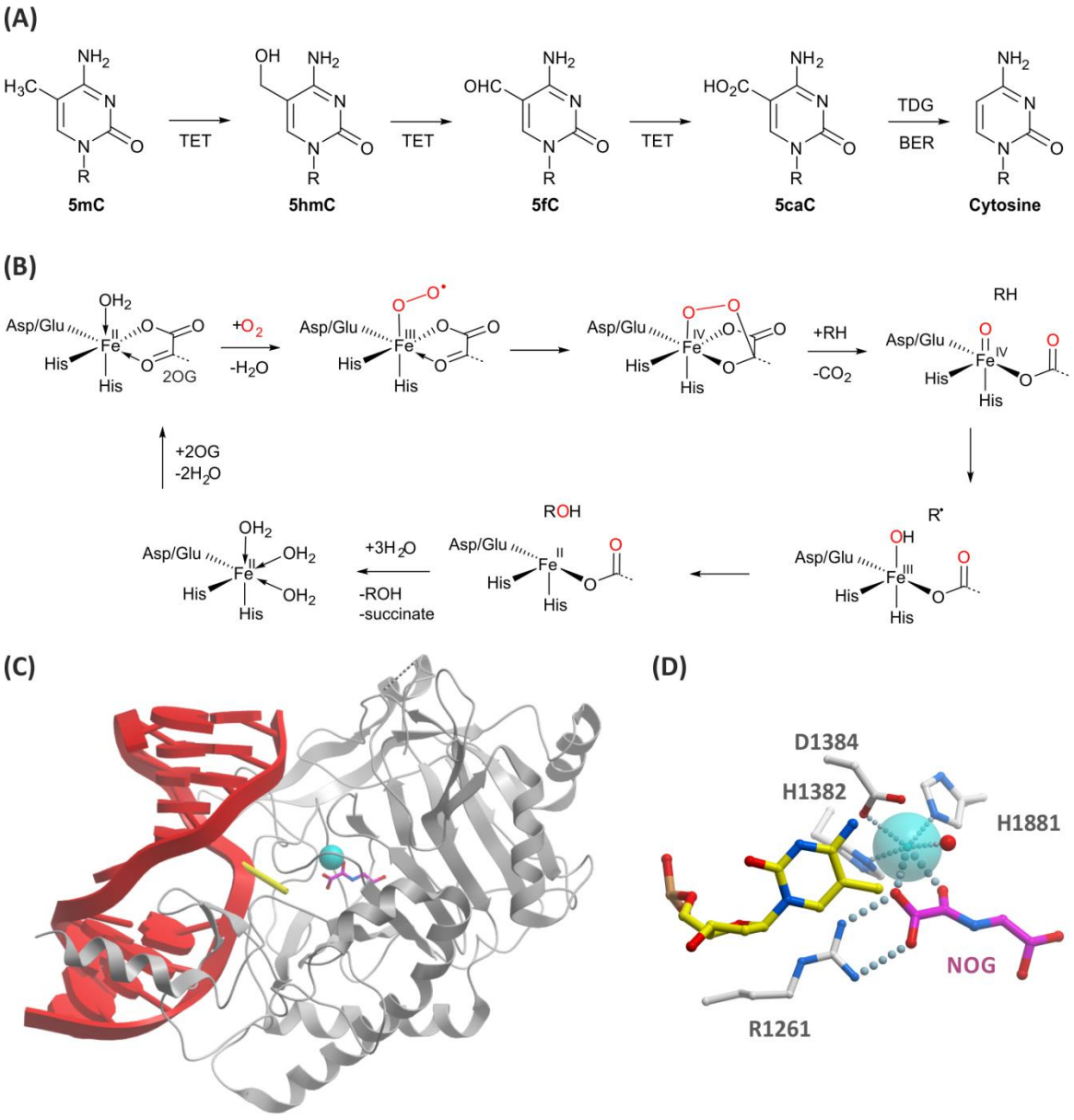

Figure 3. 5mC oxidation and possible DNA demethylation. (A) Proposed mechanism for demethylation of cytosine shown. The TET proteins oxidise 5mC to 5hmC, then to 5fC and 5caC. 5acC is removed by TDG and substituted by cytosine via BER.[25] (B) Consensus mechanism for oxidation of a substrate (RH) by Fe(II)-containing 2OG-dependent oxygenases, such as TETs.[27] (C) View from X-ray crystal structure of human TET2 (grey) complexed with methylated DNA (red) (PDB 4NM6).[28] 5mC (yellow) is flipped towards the catalytic site containing Fe(II) (blue sphere) and *N*-oxalylglycine (NOG, carbon=magenta), a catalytically inactive analogue of 2OG. (D) Catalytic site from (C) showing Fe binding residues and crystallographic water (red sphere). 5mC is positioned in close proximity to NOG and Fe.

CpG methylation is generally associated with gene silencing.[29] The inactivation occurs through binding of 5-methyl cytosine binding proteins (MBPs), such as methyl-CpG-binding

proteins 1 and 2 (MeCP1 and MeCP2).[30-32] These proteins may contain a DNA-binding domain and a transcriptional repression domain, or they can recruit a chromatin condensing factor in order to inactivate transcription.[31, 32] Alternatively, they can function by preventing the binding of transcription factors.[33] Figure 4 shows the binding of methylated DNA to the methyl-binding domain of MeCP2.[34] The methyl group sits in a relatively hydrophilic binding pocket and appears to make a series of non-bonding interactions to water molecules and polar side-chains.

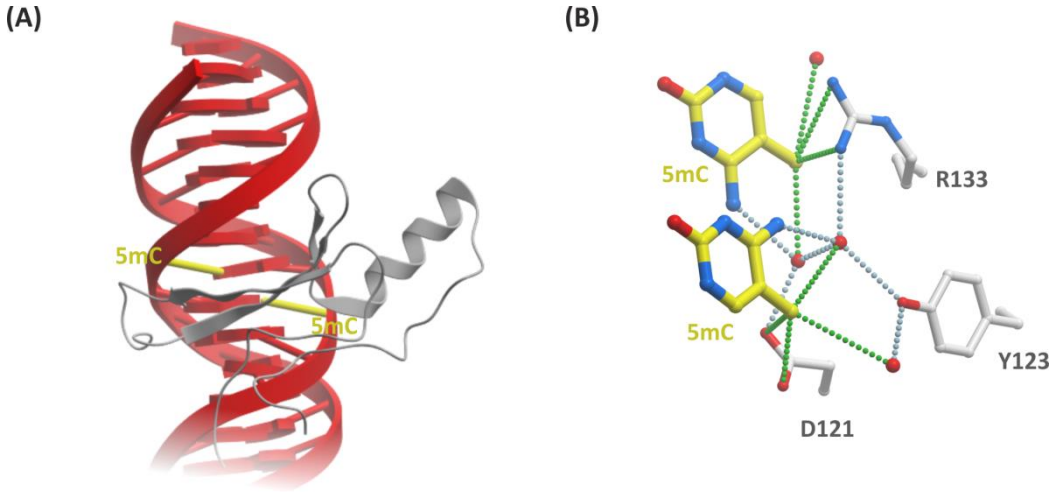

Figure 4. (A) View from an X-ray crystal structure of the methyl-binding domain of MeCP2 (grey) complexed with a DNA strand (red) (PDB 3C2I).[34] The 5mC bases are shown in yellow. (B) View from (A) showing 5mC binding site and key residues and crystallographic waters (red spheres). Hydrogen-bonds are shown as blue dotted lines and possible non-bonding interactions to the 5mC methyl groups are shown as green dotted lines.

CpGs are found clustered together in CpG islands which often occur at gene promoter regions.[35] CpG islands tend to be unmethylated so as to avoid inactivation during expression.[36] The unmethylated CpGs CpG islands represent a small fraction of the total CpGs (1-2%).[14] CpGs are also found in intergenic regions and repetitive elements, where they are usually methylated to avoid transcription.[37] The methylation of these regions is thought to promote genomic stability.[38]

DNA methylation plays a vital role in development.[14] It is essential for embryonic development in mammals, as evidenced by early lethality in *DNMT*-null mice models.[39] It has also been linked to chromosomal dosage compensation in females through inactivation of one X chromosome through hypermethylation of promoter CpGs.[40] With this vital

developmental role, it is not surprising that aberrant methylation signatures are ubiquitous in human cancers.[38, 41] CpG islands of tumour suppressor genes can become hypermethylated, resulting in their transcriptional silencing and subsequent tumourigenesis.[42] Genes with key roles in cancer biology, such as *CDKN2A (cyclin-dependent kinase inhibitor 2A), MLH1 (MutL homolog 1, colon cancer, nonpolyposis type 2)* and *BRCA1*, have been shown to be susceptible to methylation-associated silencing in cancer cells.[43] Conversely, intergenic regions can become hypomethylated, with evidence in mice models suggesting that this can lead to genomic instability and tumourigenesis.[44] Additionally, DNA methylation is linked to neurodegenerative diseases, such as Rett syndrome, Fragile X syndrome and Friedrich's ataxia.[45]

The proteins which regulate DNA methylation are therefore interesting targets for therapeutic intervention, and DNMTs have successfully been targeted by hypomethylating agents. 5-Azacytidine (compound **1**, Celgene) and decitabine (compound **2**, Eisai/Johnson & Johnson) are two compounds which have been approved for treatment of myelodysplastic syndromes and are undergoing clinical trials for other forms of cancer (Figure 5).[45-47] Both drugs are cytosine analogues where the base has been replaced by a triazine core. These can be incorporated into DNA and recognised by DNMTs. Without the ability to undergo the required β-elimination, they are left covalently bound to the DNMTs, and therefore DNMT action is blocked.[48] However, recent evidence suggests that their mechanism of action may not be limited to their hypomethylating action.[48, 49]

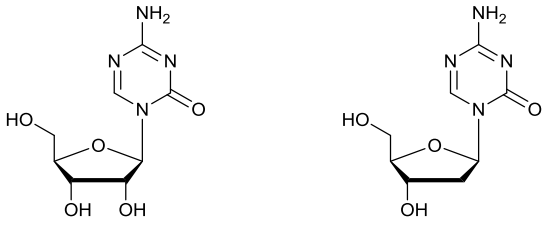

Figure 5. Vidaza and Dacogen: approved inhibitors of DNMTs for the treatment of myelodysplastic syndromes.

1.4 HISTONE TAIL MODIFICATIONS

In contrast to DNA, where identified covalent modifications are predominantly restricted to methylation and oxidation, histones are susceptible to a far wider variety of covalent modifications in animals, including acetylation, methylation, ubiquitination, biotinylation, phosphorylation, sumoylation, ADP-ribosylation and citrullination.[50-54] There are over 50 identified sites on histones which undergo PTMs, with most occurring on the *N*-terminal tails which protrude from the nucleosome core.[55] Most occur on H3 and H4, but they also occur on H2A and H2B. Certain positions can be modified by more than one type of mark, leading to a complex and flexible mechanism for transcriptional control (Figure 6).

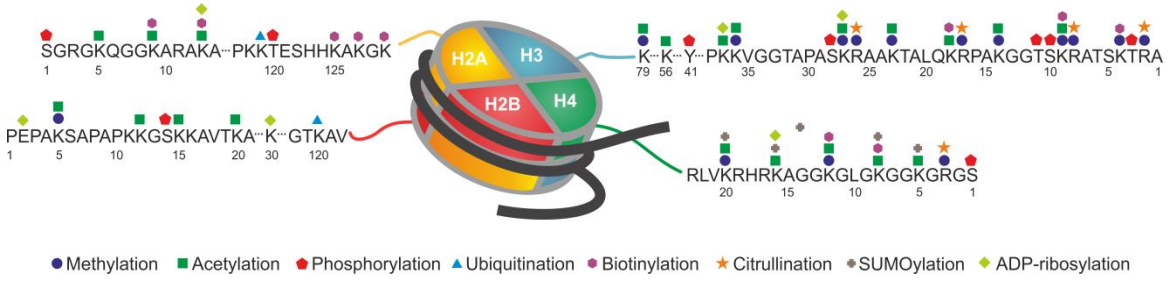

Figure 6. Known post-translational modifications of the core histones in humans.

Known human histone PTMs are listed in Table 1, along with the residues which are modified and their known functions.[50, 54] It has been suggested that PTMs may work in combination with neighbouring marks, perhaps pointing to the presence of a 'histone code' akin to the genetic code; however, much work is needed to understand how the relevance of cross-talk between PTMs.[56-58] Specific protein domains are responsible for the attachment ('writing'), removal ('erasing') and recognition ('reading') of histone PTMs.[59, 60] These domains often work in concert, as part of multidomain proteins and/or protein complexes. Among the best characterised histone PTMs are acetylation and methylation, which are discussed in more detail in the following sections.

Table 1.Histone modifications and functions.

Histone PTM	*Residue(s)*	*Chromatin reader domain*	*Function*
Acetylation	K	Bromodomain	Transcription, repair, replication, condensation.
Methylation (mono, di or tri)	K, R	Chromodomain, Tudor domain, MBT, PHD	Transcription, repair.
Ubiquitination	K	UIM, IUIM	Transcription.
Phosphorylation	S, T	BRCT	Transcription, repair, condensation.
Sumoylation	K	SIM	Transcription.
ADP-ribosylation	E, K	Macro domain, PDZ domain	Transcription.
Biotinylation	K		Transcription, condensation.
Citrullination	R		Transcription.

1.4.1 LYSINE METHYLATION

Histone lysine methylation (Kme) is a chromatin PTM which may be activating or deactivating depending on the context.[61-63] The potential for Kme marks to propagate through cell generations means Kme may be considered epigenetic.[61-63] Lysines may be mono-, di- or tri-methylated, in each case resulting in retention of the positive charge on the amino side-chain. For example, H3 lys-4 trimethylation (H3K4me3) is a promoter-specific mark which is associated with active transcription, whereas H3K9me3 is highly correlated with constitutive heterochromatin and H3K27me3 with facultative heterochromatin.[64-68] The Kme mark is written by lysine methyl transferases (KMTs) and erased by lysine demethylases (KDMs).[61-63, 69-71] A variety of protein modules exist that recognise the various Kme marks; these include plant homeodomains (PHDs), chromodomains, Tudor domains and malignant brain tumour domains (MBTs).[72-81]

In humans, all known KMTs contain a conserved SET (Suvar3-9, enhancer-of-zeste, trithorax) domain, apart from DOT1L.[82] The SET domains transfer a methyl group from the cosubstrate SAM to the lysine side-chain (Figure 7A).[83] Although DOT1L contains a different

catalytic domain, it still uses SAM as the cosubstrate.[84] Figure 7C shows a view of the active site of the SET domain of SET7/9.[83] The lysine side-chain is apparently held in the catalytically productive orientation next to the cosubstrate by a hydrogen-bond to a tyrosine side-chain and a water molecule.

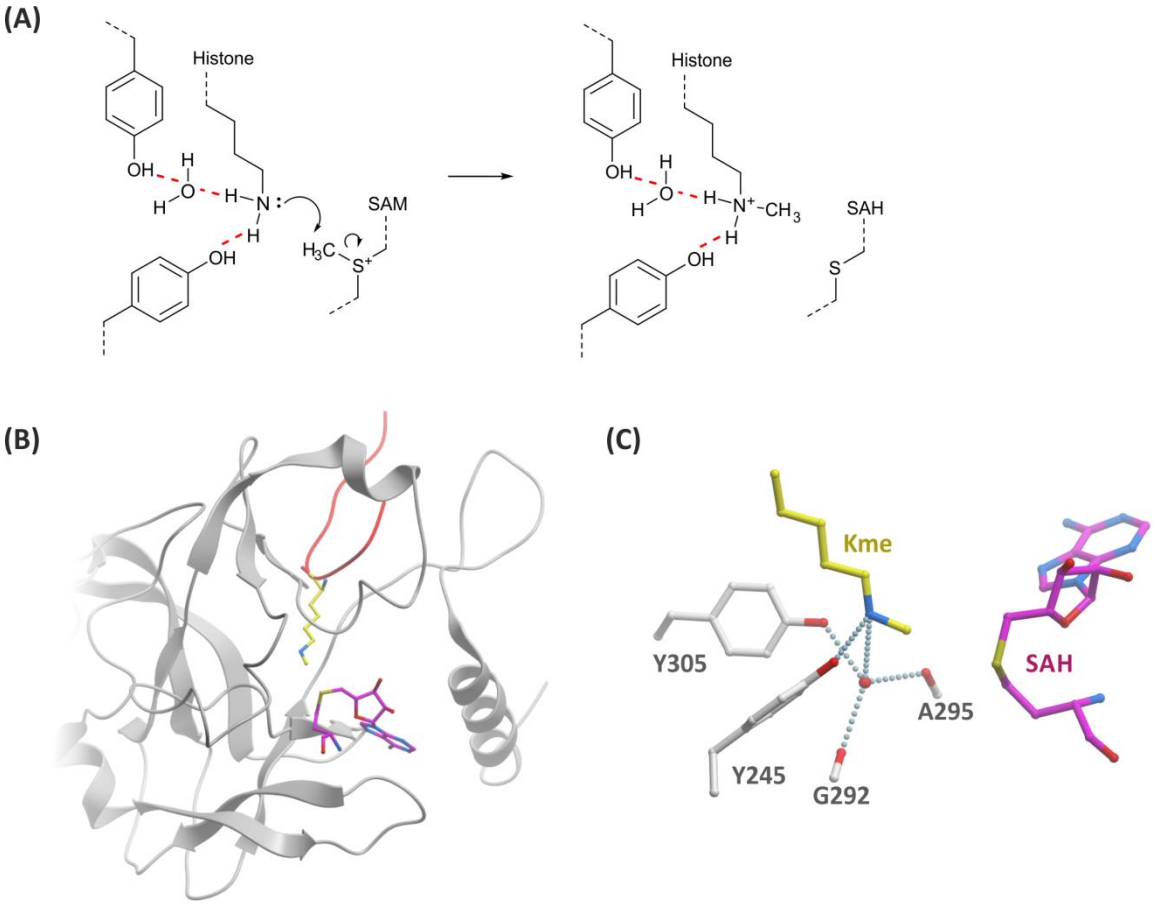

Figure 7. (A) Proposed mechanism of methylation of lysine side-chains by KMTs using SAM as the methyl source;[83] (B) A view from the X-ray crystal structure of the binding domain of SET7 (grey ribbon) complexed with a peptide with a methylated lysine side-chain (carbon=yellow) and SAH (carbon=magenta) (PDB 1O9S).[83] (C) Catalytic site of SET7/9. The lysine side-chain is oriented toward the sulfur atom of SAH by hydrogen-bonding to Y245 and a water molecule (red sphere).

Views from the X-ray structures of typical Kme reader domains are shown in Figure 8, along with their respective binding site residues. Aromatic side-chains are a common feature in Kme binding domains. These form 'aromatic-cages' which interact with the positively charged lysine side-chain through cation-π interactions. Figure 8D also shows a salt-bridge interaction between an aspartic acid and a dimethyl lysine side-chain.

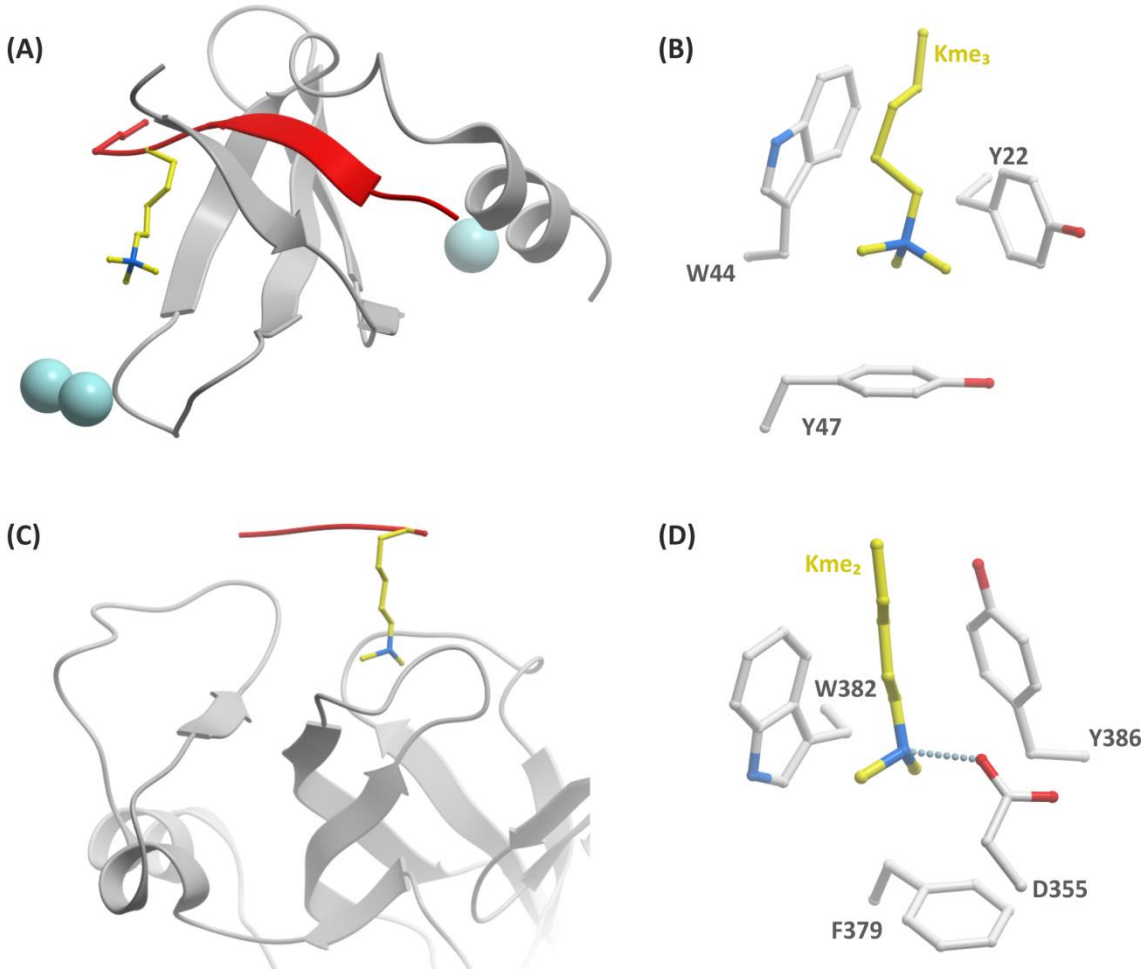

Figure 8. Views from X-ray crystal structures of typical Kme reader domains. The substrates are displayed as red ribbons with the methylated lysine side-chain in stick form (carbon=yellow). Metal ions are shown as blue spheres. (A) H3K9me3 peptide complexed to chromodomain protein 1 (Chp1) chromodomain (PDB 3G7L).[85] (B) Binding site of (A) with Kme_3 side-chain bound in an 'aromatic cage' binding pocket. (C) H1.5K27me2 complexed to lethal (3) malignant brain tumour-like protein 1 (L3MBTL1) MBT domain (PDB 2RHI).[86] (D) Binding site of (C) showing the hydrogen-bond between Kme2 and an Asp side-chains and the aromatic cage residues.

The KDMs are classed into two superfamilies.[71] The first class to be discovered was the flavin-adenine dinucleotide (FAD)-dependent amine oxidases, which consists of only 2 of the known KDMs.[70] These enzymes oxidise methyl lysines via a hydride-transfer mechanism to give an imine intermediate (Figure 9).[87] The imine is hydrolysed to yield the demethylated lysine product and formaldehyde. The reduced FADH2 is re-oxidised by oxygen to FAD. Due to the requirement for a lone pair to form the imine, this class of enzymes can oxidize mono- and di-methylated lysine but not quaternised trimethyl lysine side chains. Views from the X-ray structures of the catalytic site of a FAD-dependent KDM are shown in Figure 9B and C.

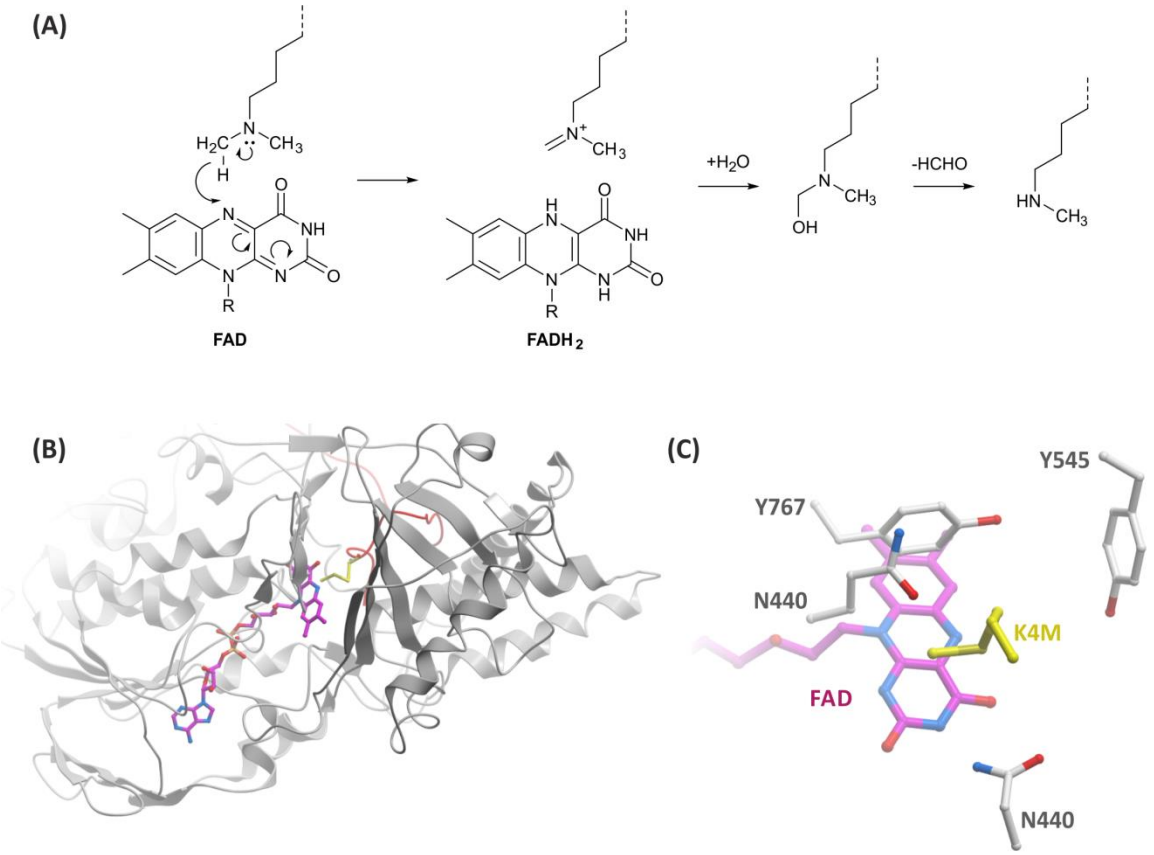

Figure 9. (A) Proposed mechanism of lysine demethylation by the FAD-dependent KDMs.[87] (B) View from X-ray crystal structure of methionine mutant substrate, H3K4M, complexed to lysine-specific demethylase 2 (LSD2). FAD is shown in stick representation (carbon=magenta) and the K4M side chain in yellow. (PDB 4GU0).[88] (C) Active site from (B) showing K4M bound in substrate site near the FAD cosubstrate.

The second class of KDMs to be discovered was the Jumonji C-terminal domain (JmjC)-containing enzymes.[69, 71] JmjC enzymes make up most of the known KDMs. The JmjC-containing KDMs belong to the same superfamily as the TET enzymes and employ Fe^{2+}, 2OG and oxygen as cofactors/cosubstrates. The methyl group is oxidised, converting 2OG to succinate and CO_2 in the process in a manner analogues to that shown in Figure 3. The intermediate hemiaminal loses formaldehyde to yield the demethylated lysine product (Figure 10). Because there is no requirement for a lone pair in this mechanism, the JmjC-containing KDMs can demethylate mono-, di- and tri-methyl lysine side-chains.

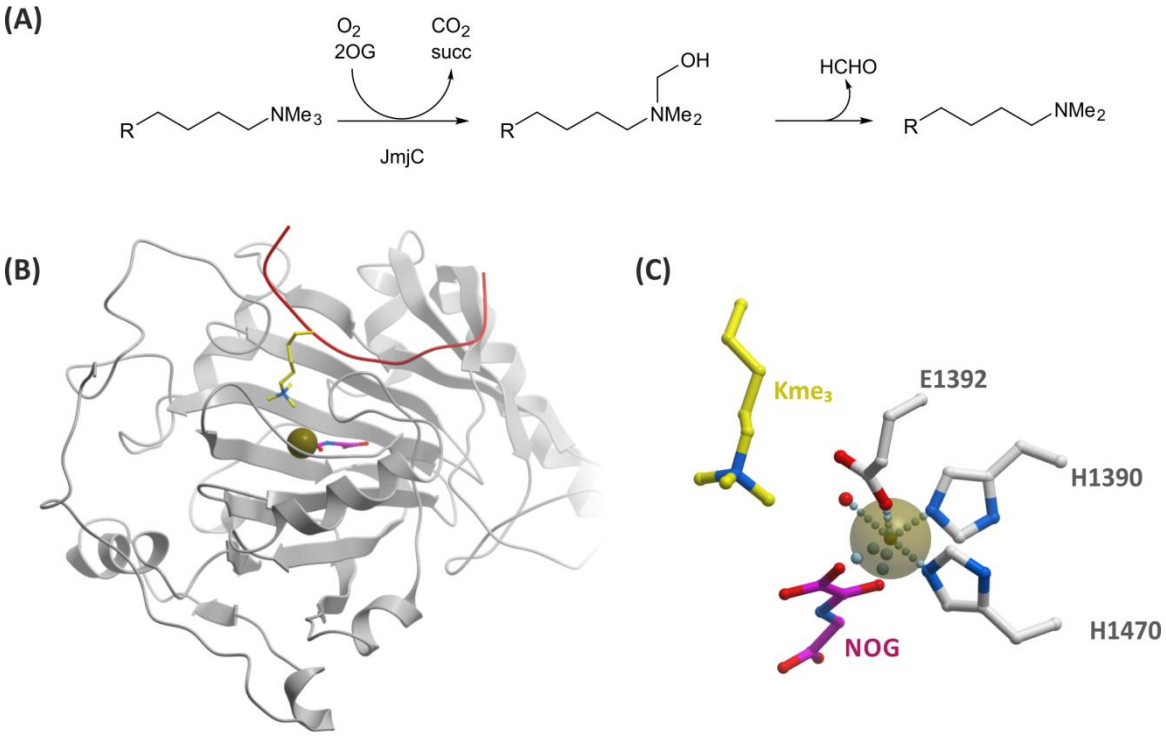

Figure 10. (A) Lysine demethylation of KMe3 by 2OG-dependent KDMs.[69] (B) View from X-ray crystal structure of H3K27me3 (red ribbon with Kme3 in yellow) complexed to lysine-specific demethylase 6B (KDM6B) (PDB 4EZH).[89] (C) Active site from (B) showing metal binding residues and proximity of substrate to metal.

Lysine methylation has been implicated in important developmental processes. For example, H3K27 methylation has been linked to homeotic gene silencing, X inactivation and genomic imprinting.[90] Aberrant lysine methylation is also linked to various human diseases and developmental disorders, including cancer and X-linked mental retardation.[91] There is robust *in vivo* data that suggests inhibition of the KMT EZH2 (enhancer of zeste homolog 2) reduces H3K27 methylation states and tumour proliferation. High EZH2 levels are also associated with poor prognosis in solid tumours.[45, 92]

Although no approved drugs are known to target histone lysine methylation, there are KMT inhibitors in late stages of development. EPZ-6438 (compound **3**, Epizyme/Eisai) is a small molecule inhibitor of EZH2 undergoing Phase I/II clinical trials for the treatment of non-Hodgkin's lymphoma.[93, 94] EPZ-5676 (compound **4**, Epizyme/Celgene) is a DOT1L inhibitor, in Phase 1 clinical trials for acute leukaemia (Figure 11).[95, 96] With the multitude of proteins which are involved in lysine methylation it should be expected that many more compounds will be developed to target this important epigenetic mark.

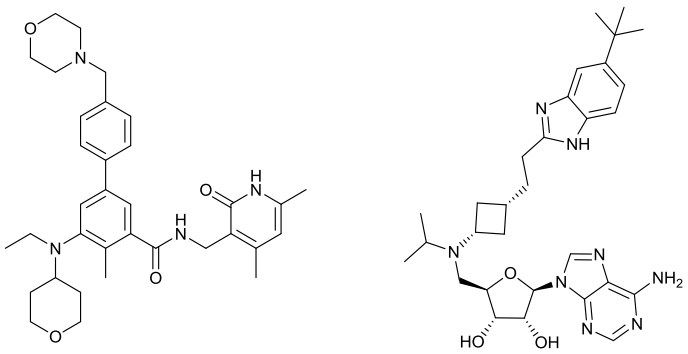

3
EPZ-6438

4
EPZ-5676

Figure 11. EPZ-6438 and EPZ-5676: compounds in clinical trials targeting histone lysine methylation.

1.4.2 LYSINE ACETYLATION

Lysine acetylation (Kac) is a very dynamic histone PTM, which is generally associated with transcriptional activation.[97-100] Unlike DNA and histone methylation, lysine acetylation is not considered to be epigenetic according to the stricter definition.[13] Regardless of the semantics, lysine acetylation plays a vital role in chromatin function, including nucleosome assembly, chromatin condensation, and transcription.[97-101] Additionally, acetylation plays an important role in non-nuclear cellular processes, including protein folding, cytoskeleton dynamics and cellular metabolism.[102]

Acetylation results in neutralisation of the positive charge on the lysine side-chain. It was originally proposed that this resulted in a decrease in the electrostatic interaction between positively charged lysine side-chains and the negatively charged phosphodiester backbone of DNA, making the DNA more accessible to the transcription machinery.[103] However, this is now generally accepted to be an oversimplification. It is now known that the Kac 'reading' event can also be important in transcriptional activation, where Kac is bound by bromodomain (BRD) containing proteins, which themselves act to activate transcription.[104-107] The BRD protein recruits other transcription factors, coactivators, etc., resulting in transcriptional activation. The domain responsible for writing the Kac mark is the lysine acetyl transferase (KAT) domain (also known as histone acetyl transferase, or HAT, domain)

whilst the eraser domain is the lysine deacetylase (KDAC) domain (also known as histone deacetylase, or HDAC, domain).[108-111] KATs transfer an acetyl group from acetyl co-enzyme A (acetyl-CoA), whilst the KDACs use water as the cosubstrate to remove the acetyl mark, giving acetate as a by-product.

KATs are clustered into three sub-families based on structural considerations (Figure 12).[112] The Gcn5-related *N*-acetyltransferase (GNAT) family are generally characterised by up to 4 conserved motifs found within the KAT domain. They generally possess a BRD and they acetylate residues on histones H2B, H3 and H4. The MYST (acronym for MOZ, Ybf2, Sas2, Tip60) family typically possess chromodomains and zinc fingers. They have been shown to acetylate histones H2A, H3 and H4. The remaining KATs can be grouped into an "orphan" family, which includes CREB (cyclic-AMP response element binding protein) binding-protein (CBP) and E1A binding protein (p300).

The mechanism for acetylation by KATs involves general base catalysis, via a water-mediated deprotonation of the histone lysine by a glutamate side-chain carboxylate. This frees the lysine side-chain for nucleophilic attack of the acetyl-CoA carbonyl (Figure 12B). Figures 12C and D show views from an X-ray crystal structure of a complex between the acetyl transferase domain of *Tetrahymena* GCN5, a histone H3 peptide and co-enzyme A (CoA).[113]

The KDAC proteins belong to two families: silent information regulator 2 (SIR2) family of NAD^+-dependent KDACs, and the 'classical' KDAC family.[114-116] The classical KDACs are divided into two phylogenetic classes: class I, which are related to the yeast transcriptional regulator RPD3, and class II, which are related to yeast HDA1.[114] The 'classic' KDACs are metalloenzymes which employ a metal in its +2 oxidation state. Typically, *in vitro* experiments use Zn^{2+}-containing enzymes, but there is evidence that the enzyme may use Fe^{2+}, Mn^{2+} *in vivo*.[117]

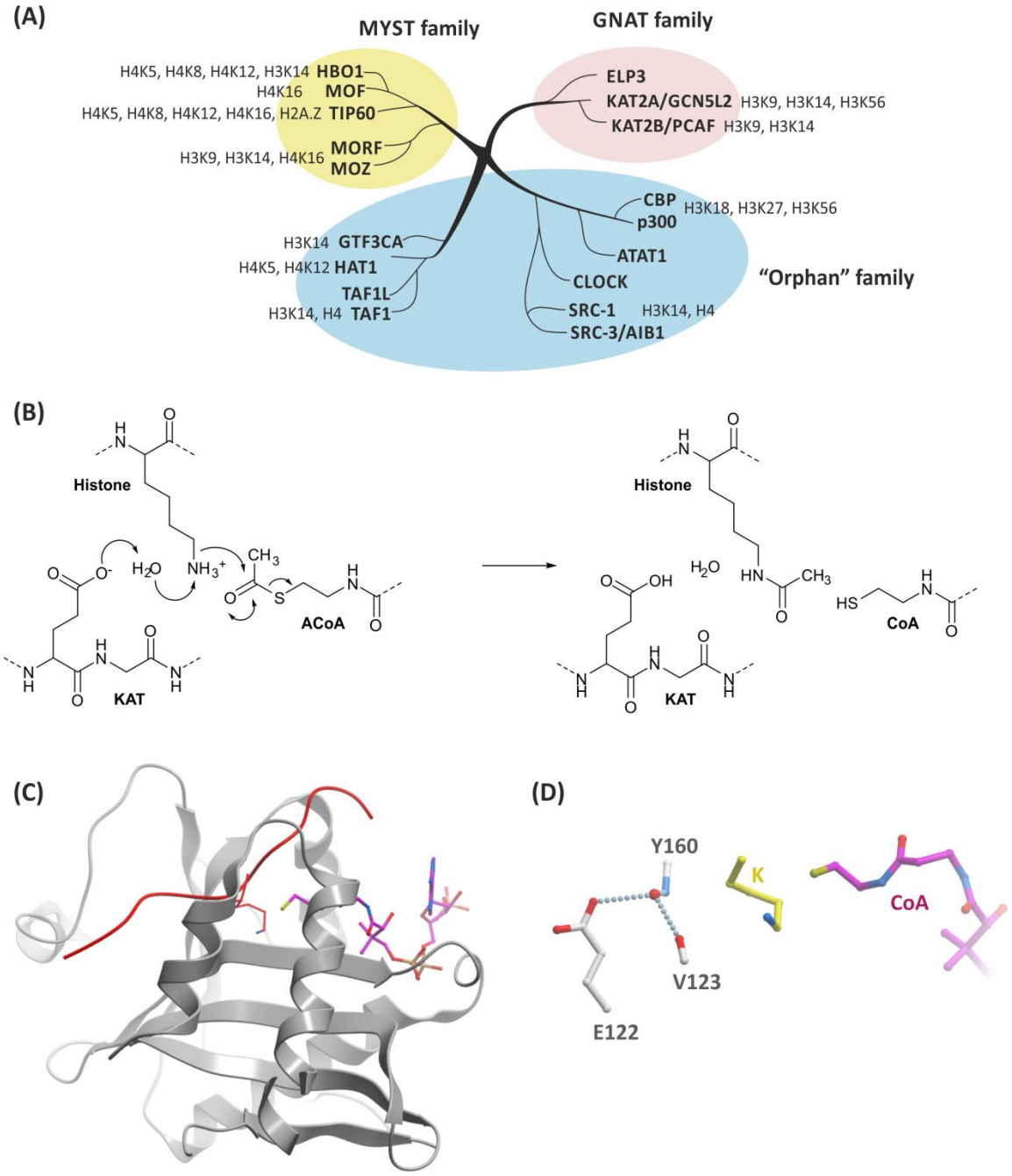

Figure 12. Lysine acetyl transferases. (A) Human KAT phylogenetic tree (adapted from De Cerbo, *et al*[112]). Reported major histone substrates are shown. (B) Proposed general base catalysed mechanism for acetylation of histones by KATs. Glutamate deprotonates a water molecule in the catalytic site, which in turn deprotonates the histone lysine side-chain. The deprotonation of the primary amine increases its nucleophilicity, allowing it to react with the electrophilic carbonyl group of acetyl-CoA. (C) View from a crystal structure of acetyl transferase domain of *Tetrahymena* GCN5 (grey ribbon) with bound acetyl-CoA (magenta) and H3 peptide (red ribbon and stick) (PDB 1QSN).[113] (D) Active site residues from (C) showing the key water hydrogen-bonded to a Glu side-chain and the GCN5 backbone. The lysine side-chain of the histone sits between this water molecule and the acetyl-CoA.[113] Hydrogen-bonds are shown as dotted lines.

A proposed deacetylation mechanism for KDACs is shown in Figure 13A. A histidine side-chain acts as a general base. This deprotonates a metal-bound water which is the nucleophile that attacks the carbonyl of the Kac side-chain. The Lewis acidity of the metal ion enhances the electrophilicity of the Kac carbonyl and/or acidifies the bound water.

Figure 13B and C show views from an X-ray crystal structure of a bacterial KDAC homologue and the key residues in the active site.[118]

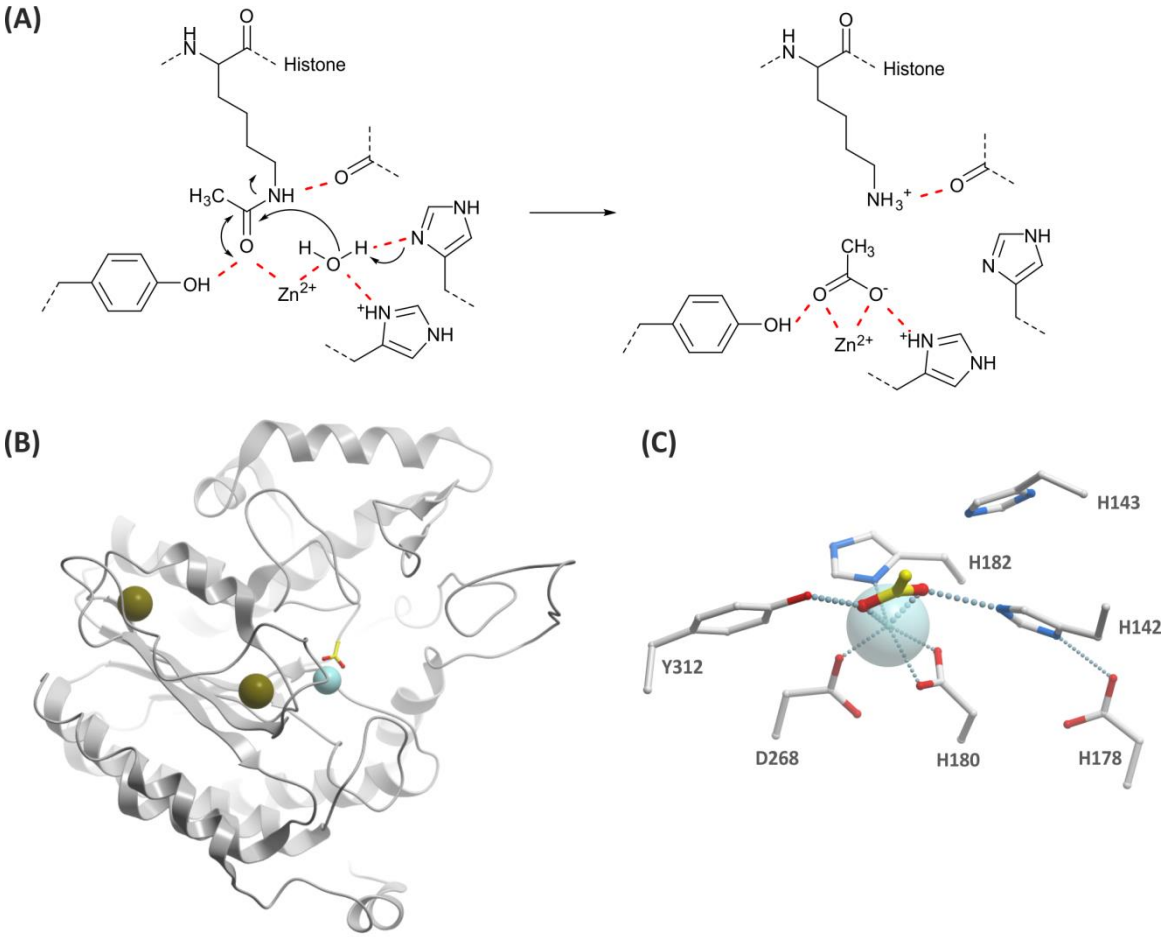

Figure 13. Lysine deacetylation by 'classical' KDACs. (A) Proposed metal-mediated general-base catalysed mechanism of deacetylation of Kac side-chains. A histidine side-chain deprotonates a metal-bound water, which adds to the Kac carbonyl. Acetate is released as the by-product of deacetylation. (B) View from a crystal structure of a KDAC homolog FB188 HDAH (histone deacetylase-like amidohydrolase) shown as grey ribbon. Potassium ions are shown as gold spheres, Zn^{2+} as a blue sphere and a metal-bound acetate as sticks (carbon = yellow). (PDB 1ZZ0). (C) Active site residues from (B) show zinc-binding residues and residues which hydrogen-bond to acetate.[118] Hydrogen-bonds and metal-ligand interactions are shown as dotted lines.

The SIR2 family of KDACs use nicotinamide adenine dinucleotide (NAD^+) as the cosubstrate.[116, 119] Unlike a typical NAD^+ dependent oxidase, the mechanism is thought to proceed via S_N2 substitution of the nicotinamide moiety of NAD^+ by the oxygen atom of the acetamide to give an imidate intermediate (Figure 14A). SIRT protein side-chains then activate the 2'-hydroxy, allowing it to displace the imidate. This leads to a bicyclic intermediate dioxolanamine which undergoes hydrolysis to the free lysine, giving acetylated ribose by-products.[120] The crystal structure of a complex between a yeast NAD-dependent

deacetylase, a Kac peptide and 2'-*O*-acetyl ADP ribose as an NAD surrogate is shown in Figure 14, along with the active site from the structure.

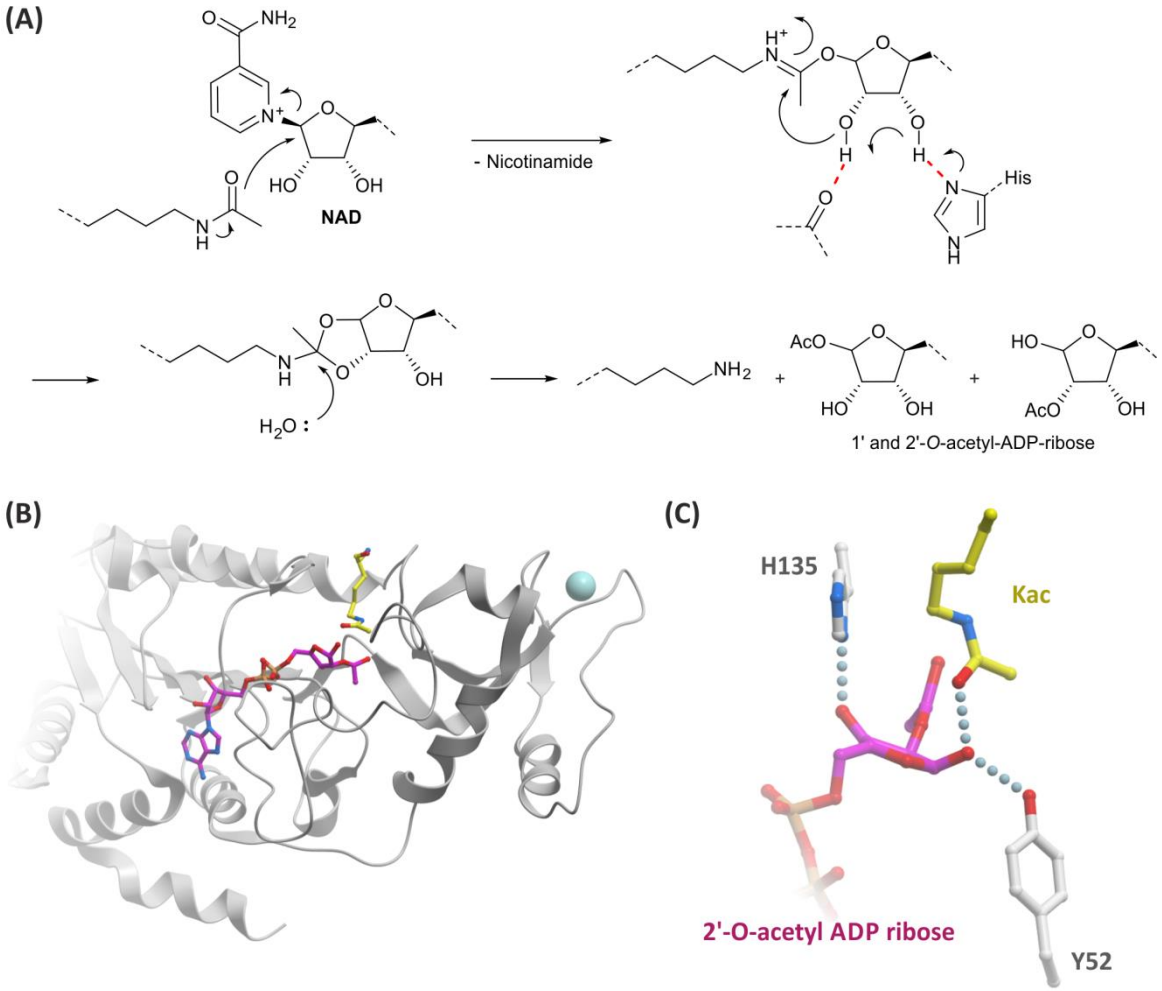

Figure 14. SIR2 KDACs. (A) Proposed deacetylation mechanism. The acetylated lysine undergoes a substitution reaction with NAD, displacing nicotinamide. The 2'-hydroxy, which is activated by neighbouring side-chains, attacks the intermediate, resulting in a bicylic intermediate. Hydrolysis of the cyclic intermediate yields the deacetylated lysine and acetylated ADP-ribose by-products.[120] (B) Structure of the yeast Hst2 protein deacetylase in complex with 2'-*O*-acetyl ADP ribose (carbon=magenta) and a Kac histone peptide (carbon=yellow).[121] (C) Active site from (B) showing proximity of a key histidine side-chain to ribose (carbon = magenta) and proximity of Kac side-chain (carbon = yellow) to the cosubstrate surrogate.

The Kac recognition modules, bromodomains, are named after the *Drosophila* gene *brahma* where they were originally identified. They are made up of approximately 110 amino acids residues arranged in a characteristic tertiary structure made up of 4 α-helices (αZ, αA, αB, αC) in what is termed the BRD-fold (Figure 15A). Two interhelical loop regions (ZA- and BC-loops) make up a largely hydrophobic Kac binding pocket. The base of the pocket is well-conserved and usually contains two key Kac binding residues, tyrosine (Y) and asparagine (N), and a hydrogen-bonded group of at least 4 crystallographically well-ordered water

molecules. One of these waters mediates a hydrogen-bond from the Kac carbonyl to the phenolic hydroxyl of tyrosine. A direct hydrogen-bond is also formed from the Kac carbonyl to the side-chain carboxamide-NH_2 of asparagine. This asparagine is highly conserved, being present in 48 of the 61 bromodomains in the human genome. In other examples, the asparagine is replaced by threonine (4 examples), tyrosine (8 examples) or aspartic acid (1 example) (Figure 15C–E).

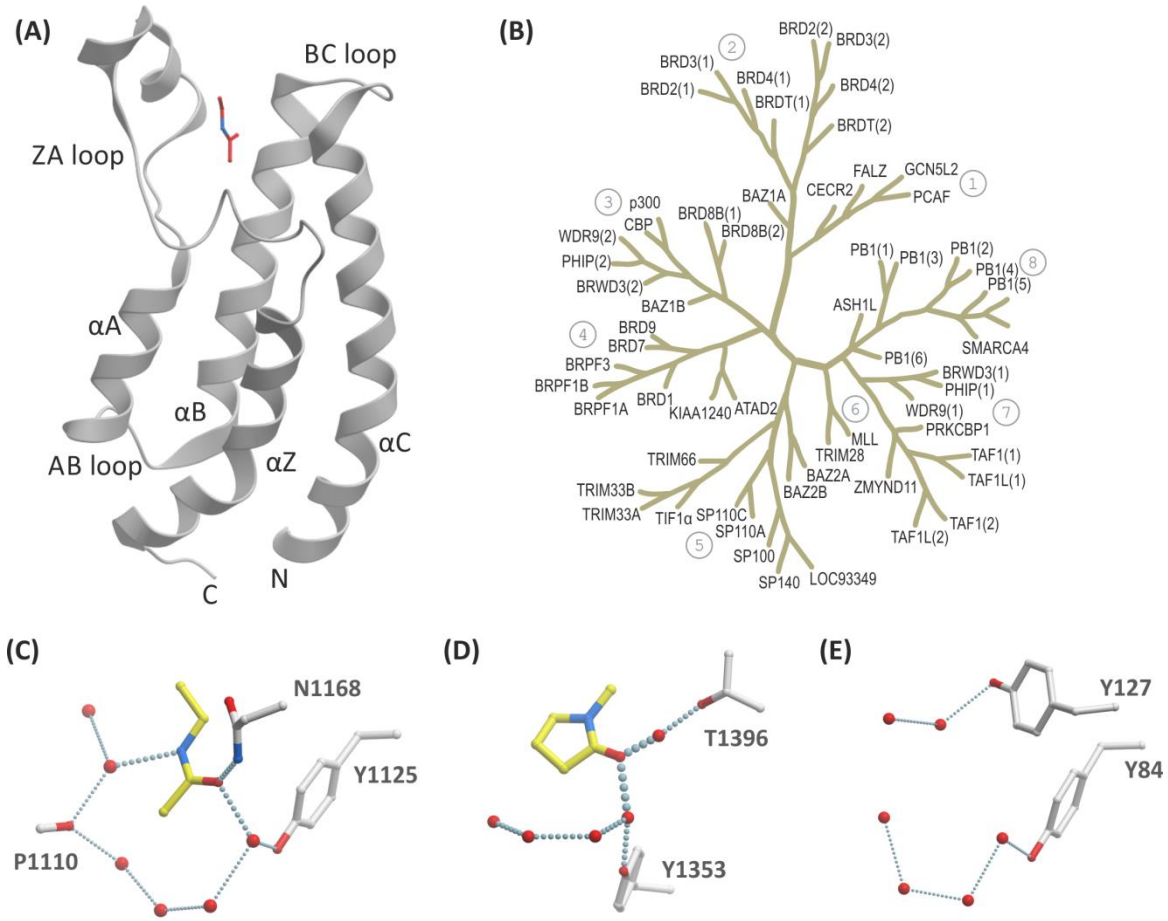

Figure 15. BRD reading of histone Kac PTM. (A) View from X-ray crystal structure of CBP BRD (grey) with an acetyl lysine side-chain bound (carbon=red) (PDB 3P1C).[122] Helical and loop regions are annotated. The ZA and BC loops form the Kac binding pocket. (B) BRD-containing protein phylogenetic tree.[123] (C) Binding site of (A) showing Kac binding-residues. Kac is bound by a hydrogen-bond from the Kac carbonyl to N1168, a water-mediated hydrogen-bond to Y1125 and a water-mediated hydrogen-bond from the Kac side-chain nitrogen to a backbone carbonyl of P1110. (D) Kac binding site of PHIP(2) BRD complexed with 1-methyl-2-pyrrolidinone (NMP) (carbon=yellow). The NMP carbonyl is bound to a Thr instead of Asn (PDB 3P1D).[122] (E) View from X-ray structure of apo of PB1(1) showing Y127 as Kac-binding residue.

The 61 known human BRDs are found in 46 different proteins, with some of these containing more than one BRD. These BRDs have been clustered according to sequence similarity into a phylogenetic tree containing 8 families (Figure 15B).[122] Few BRD protein ligands have been reported and mapped to specific sites. Additionally, reported affinities

suggest weak interactions. It has therefore been suggested that BRDs work in combination with other protein-interaction modules in order to generate selectivity and increased binding affinities.[122, 124]

Lysine acetylation is involved in diverse biological processes.[101] Aberrant lysine acetylation is associated with several age-related disorders, including cancer, diabetes and neurodegenerative disorders.[45, 125] Rubinstein-Taybi Syndrome (RTS) is a developmental condition, characterised by mental retardation and physical abnormalities, where patients have a predisposition to cancer.[126, 127] Research has implicated haploinsufficiency in the genes which transcribe the KDACs CBP and p300 as probable causes of RTS.[126-133]

Vorinostat (compound **5**, Merck, also known as SAHA) and romidepsin (compound **6**, Celgene) were the first approved drugs to target histone modifications (Figure 16A).[45, 134, 135] These compounds inhibit classical metal-containing KDACs, causing the accumulation of acetylated histones, and this is thought to reset normal levels of transcription of important regulatory proteins in cancerous cells.[136] Both are approved treatments of cutaneous T-cell lymphoma (CTCL); romidepsin is also indicated for peripheral T-cell lymphoma (PTCL). Additionally, vorinostat is undergoing Phase II trials for acute myeloid leukaemia (AML) and myelodysplastic syndrome (MDS).[137]

Figure 16B shows a view from the crystal structure of vorinostat bound to HDAC2, which shows how the hydroxamic acid functionality forms a bidendate interaction with the zinc ion. [138] Romidepsin is thought to act as a prodrug, whereby the disulfide bond is reduced *in vivo*, freeing up one of the thiols to coordinate to the zinc ion in the KDAC active site.[139, 140] A wave of second generation KDAC inhibitors is in development on the back of the success of these drugs.[45] These include CI-994 (compound **7**, Pfizer) and Panobinostat (compound **8**, Novartis) which are in Phase III trials for non-small-cell lung cancer (NSCLC) and lymphomas respectively (Figure 16C).

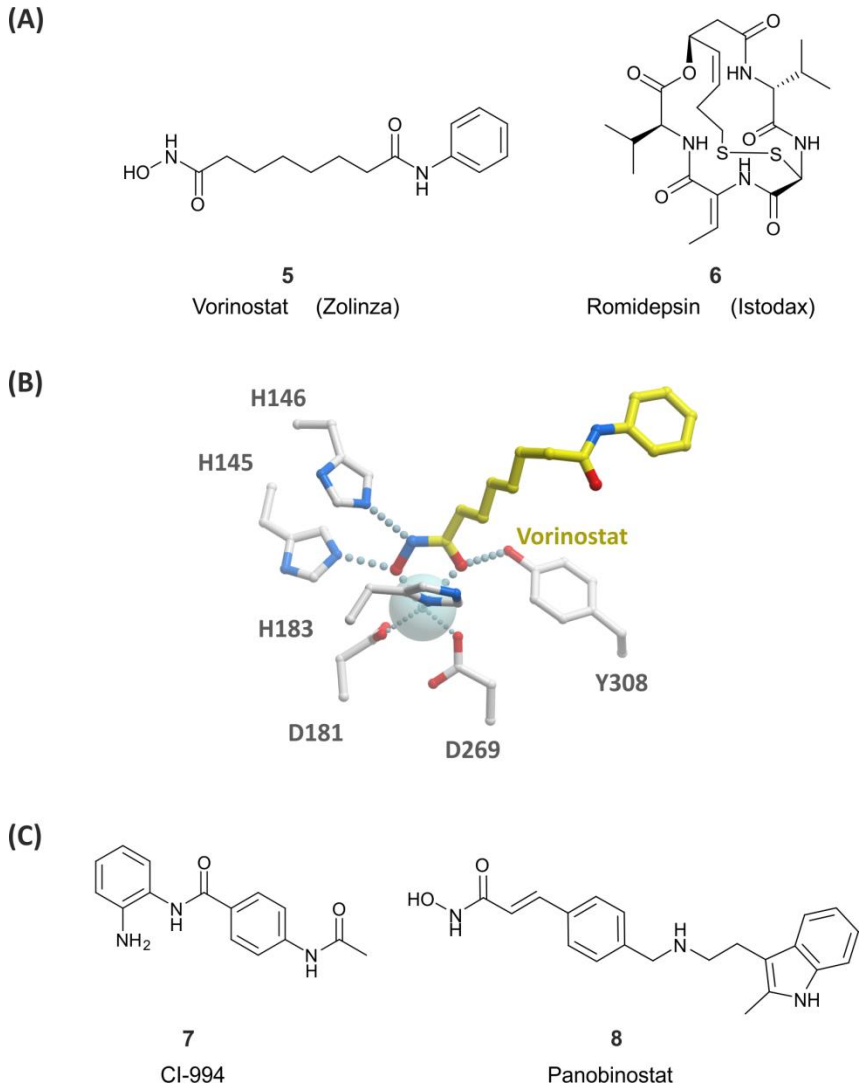

Figure 16. (A) Approved KDAC inhibiting drugs, Zolinza and Istodax. (B) View of active site from X-ray crystal structure of a complex of vorinostat (carbon-yellow) and a KDAC (PDB 4LXZ). (C) Developmental KDAC inhibitors CI-994 and panobinostat.

In addition to inhibitors of lysine deacetylation, compounds which target acetyl lysine recognition in the bromodomain and extra–terminal (BET) family of BRD-containing proteins are showing promise in clinical trials. The majority of patients with nuclear protein in the testis (NUT) midline carcinoma have a gene fusion between *NUT* and *BRD4* which codes for the BET family member BRD4.[141] iBET762 (compound **9**, GSK) is a pan-BET inhibitor in Phase I/II for the treatment of NUT-midline carcinoma and other cancers (Figure 17A).[142, 143] RVX-208 (compound **10,** Resverlogix Corporation) is also a pan-BET inhibitor, but it has been shown to be more selective for the second bromodomain of than

proteins over the first (Figure 17A).[144] RVX-208 was discovered to raise apolipoprotein A-I (apoA-I) levels, the main protein component of high density lipoprotein (HDL), in a phenotypic screening and this compound is now in Phase IIb for treatment of atherosclerosis.[144, 145] Figure 17B and C show crystallographically how these compounds mimic the acetyl lysine binding interactions in BRDs.

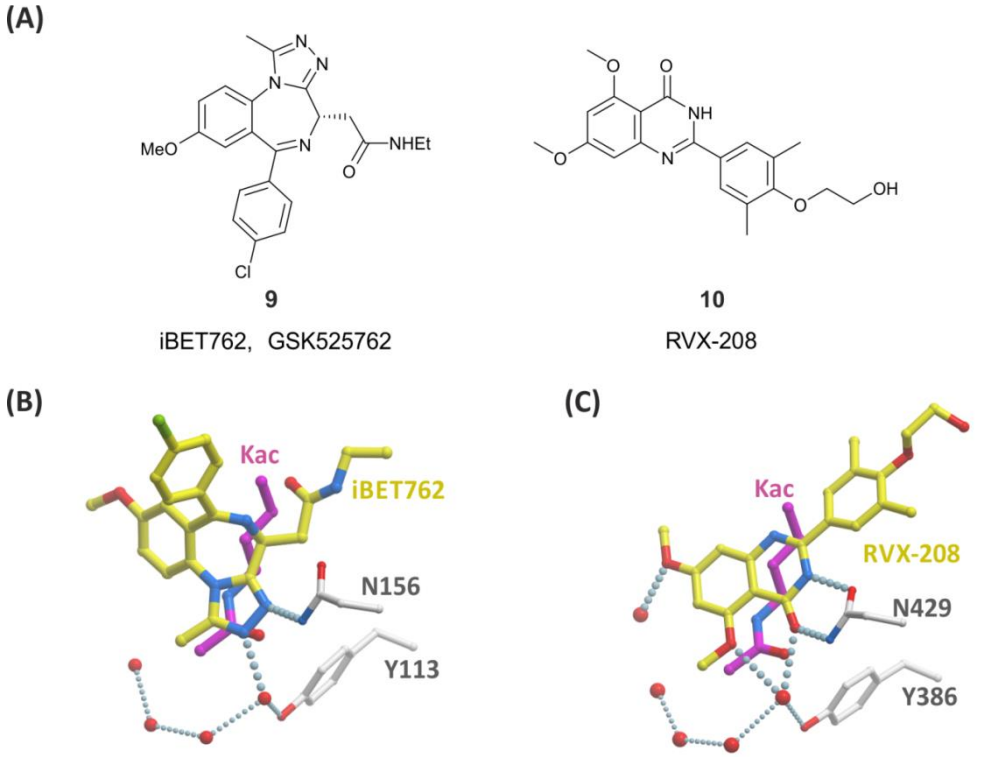

Figure 17. (A) iBET762 and RVX-208: Clinically used inhibitors of BET bromodomains. (B) iBET762 in complex with the first BRD of BRD-containing protein 4 (BRD4(1)) with key interactions with Asp and Tyr side-chains. Crystallographically well-conserved waters are shown (red spheres) (PDB 2YEK).[146] (C) RVX-208 in complex with BRD2(2) (PDB 4MR6).[144] (B) and (C) are overlaid with Kac (carbon = magenta) from an acetylated peptide complexed to BRD4(1) (PDB 3UVW).

Inhibition of the BET BRDs also leads to down-regulation of the oncogene *MYC*, meaning small molecule BET inhibitors may have broader application in oncology.[147, 148] Indeed, BET inhibitors are currently in clinical trials for a number of malignancies, including CPI-0610 (Constellation), in Phase I for treatment of lymphomas; TEN-010 (Tensha Therapeutics), in Phase I for solid tumours; and OTX015 (Oncoethix), in Phase I for haematological malignancies.[149-151]

1.5 CHEMICAL PROBES FOR RESEARCH INTO TRANSCRIPTIONAL REGULATING PROTEINS

Although much progress has been made in identifying the proteins that modify and interact with chromatin, little is known about the precise roles that these play in cellular processes, development and disease. When studying the function of proteins, it is often informative to inhibit the protein and measure the change in phenotype compared to a control. A number of genetic methods exist which are used to reduce target protein concentrations, such as RNA interference (RNAi).[152] RNAi makes use of small interfering RNA (siRNA) or short hairpin RNA (shRNA), which have complementary sequences to the messenger RNA (mRNA) of the target gene. The introduced RNA forms an RNAi silencing complex (RISC), which binds to and causes degradation of the target mRNA, thus inhibiting translation. Alternatively, a pharmacological approach involves the use of a small molecule chemical probe to inhibit the protein.[153-156] The probe should be designed to potently and selectively inhibit a domain of the target protein.

The generation of siRNA and shRNA constructs is rapid and economical. In contrast, the pharmacological approach requires laborious and expensive iterative cycles of design, synthesis and screening in order to optimise potency and selectivity characteristics.[152] Therefore RNAi is a popular technique in probing protein function. However, there are a number of advantages to the pharmacological approach that make the investment in compound optimisation worthwhile. For example, in RNAi the entire gene is targeted, resulting in 'knock down' of the target protein. Small molecule chemical probes, on the other hand, generally target one specific domain, potentially leaving some functions of the target protein unaffected. The selectivity of the pharmacological approach is particularly relevant when dealing with large, multidomain proteins, where it may be desirable to inhibit different domains in order to investigate their individual functions. Additionally, chemical

probes could be used as leads for drug discovery, where optimisation of the compound properties could deliver new clinical candidates for disease intervention.

Chemical probes which target transcription factors and chromatin associated proteins will help elucidate the cellular processes which govern transcriptional control, and could help to further demystify the field of epigenetics. It was recently argued that the discovery and dissemination of BET inhibitors accelerated research efforts and made a significant impact to the validation of these proteins as therapeutic targets.[157] Others have argued that more probes are needed to help the validation of more new targets from the field of chromatin and epigenetics.[59]

The BRD-containing proteins, CREB (cyclic-AMP response element binding protein) binding-protein (CBP) and E1A binding protein (p300) are large, multidomain transcriptional coactivators and KATs linked to a large variety of human diseases and developmental conditions, including leukaemia, pain and inflammation, and Rubinstein-Taybi syndrome (see Chapter 2). In contrast to CBP/p300, bromodomain containing proteins 9 and 7 (BRD9 and BRD7) are relatively sparsely studied. BRD9 and BRD7 are believed to play a role in chromatin remodelling and have been linked to a number of human cancers (see Chapter 7). Chemical probes are therefore important tools to understand the function of CBP/p300 and BRD9, and to investigate their potential as therapeutic targets.

1.6 PROJECT AIM

The aim of this project was the discovery of small molecule chemical probes for CBP/p300 and BRD9/BRD7. In order to generate probes which would produce meaningful and robust data in cellular experiments, the following criteria were targeted: *in vitro* potency ≤ 100 nM, ≥ 30-fold selectivity vs. other BRD subfamily members, and micromolar on-target cellular efficacy.[123]

CHAPTER 2. CBP/P300

2.1 CBP/P300: TRANSCRIPTIONAL COACTIVATORS AND LYSINE ACETYL TRANSFERASES

CBP and p300 are ubiquitous acetyl transferases that function as pleiotropic transcriptional coactivators.[158-162] Despite their substantially non-redundant roles, they are often referred to together as CBP/p300. CBP (also referred to as CREBBP or KAT3A) was first identified as a nuclear protein which binds to phosphorylated CREB (cyclic-AMP response element binding protein), whereas p300 (also known as EP300 or KAT3B) was originally recognised as a binding partner for the adenosine early region 1A protein (E1A).[163-165] CBP/p300 contain at least 9 functional domains which allow them to interact with transcription factors, the basal transcriptional machinery, and other coactivators (Figure 18).[158, 160, 166] Both proteins possess a BRD and KAT domain, meaning CBP and p300 are able to both read *and* write the Kac PTM. Although the sequences of CBP and p300 are only ~60% similar, there is higher conservation within the domains, including the BRD, which is 96% similar.

The other well conserved domains include a zinc finger, transcription adaptor putative zinc finger-type (ZF TAZ 1 and 2); a kinase inducible domain interacting domain (KIX); a zinc finger, ZZ-type (ZF ZZ); and a nuclear receptor coactivator interlocking domain (NRC). ZF TAZ I (also known as cysteine-histidine rich region 1, or CH1) is involved in the hypoxia-inducible factor (HIF) hypoxic response. ZF TAZ I binds to HIF-1α through the transcriptional activation domain, which prompts HIF target gene expression (see section 2.2.7).[167, 168] KIX binds to the kinase inducible domain (KID) of the transcription factor CREB in a phosphorylation-dependent manner.[169] Phosphorylation of CREB at Ser-133 by protein kinase A (PKA) induces complex formation between CREB and CBP, which stimulates CREB target gene expression. The third cysteine-histidine-rich region (CH3) of CBP/p300 consists

of two independently folding zinc finger domains, ZF ZZ and ZF TAZ II.[170] ZF TAZ II has been shown to bind p53 (tumour protein p53) and E1A. The function of the ZF ZZ is unclear, although it is structurally similar to the "cross-brace" family of ZF proteins which include really interesting new gene (RING), plant homeodomain (PHD) and FYVE.[170]

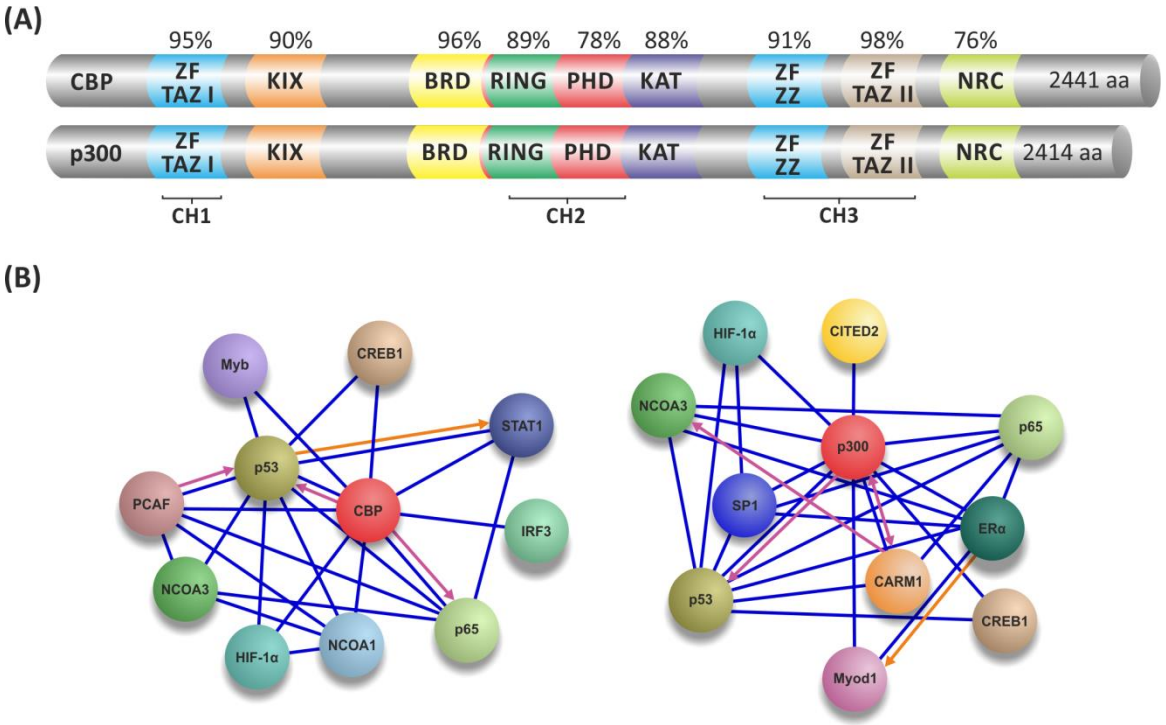

Figure 18. (A) Percent conservation and domain organization of human CBP (accession no. Q92793) and p300 (accession no. Q09472). (B) Partial protein-protein interaction maps for CBP and p300, based on maps generated by STRING 8.[171] Blue lines indicate binding between proteins, pink lines represent a PTM (arrows show directionality), and orange lines represent expression. Abbreviations: p53 (tumour protein p53); p65 (transcription factor p65); NCOA3 (nuclear receptor coactivator 3); IRF3 (interferon regulatory transcription factor 3; HIF-1α (hypoxia inducible factor, 1α); NCOA1 (nuclear receptor coactivator 1); STAT1 (signal transducer and activator of transcription 1); PCAF (p300/CBP-associated factor); Myb (v-myb myeloblastosis viral oncogene homolog (avian)); ERα (oestrogen receptor α); CITED2 (CBP/p300-interacting transactivator, with Glu/Asp-rich carboxy-terminal domain); SP1 (SP1 transcription factor); Myod1 (myogenic differentiation 1); CARM1 (coactivator-associated arginine methyltransferase 1.

With their variety of functional domains and modes of actions, CBP and p300 are among the most heavily connected nodes in the known mammalian protein-protein interactome with over 400 known interacting partners. Figure 18B depicts a selection of the known interactions for CBP and p300, which include CREB, HIF 1α and p53. The figure illustrates how the proteins have overlapping and independent interacting partners.

The importance of the BRD in the catalytic activity was demonstrated by the impairment of nucleosomal KAT activity in a mutated CBP construct lacking the BRD.[172] Additionally mutation or deletion of the p300 BRD impairs acetylation specificity and activity.[173, 174] A

structure of the 'catalytic core' of p300, which includes the BRD, CH2 and KAT domains, was recently solved (Figure 19A).[166] The CH2 domain was shown to consist of a discontinuous PHD interrupted by a RING finger, both in non-canonical forms. The authors propose a mechanism of autoregulation and substrate binding, based on observations from the crystal structure and from deletions/mutations of the various core domains (Figure 19B). In the proposed mechanism, the inactive state of the catalytic core is obstructed by the bound autoinhibitory loop (AIL) of the KAT domain and by the RING.[175] p300 is then recruited to an enhancer where it is autoacetylated in *trans* at the AIL. This process reveals the catalytic core of the KAT domain, allowing it to bind and acetylate substrates. Acetylated substrate binds to the BRD, resulting in positive feedback and maintenance of the p300 signal. KDACs such as SIRT2 deacetylate p300, returning it to the inactive state.[176]

Acetylation of lysines is one of the three mechanisms by which CBP and p300 exert transcriptional control.[177] The acetylation of histones alters the chromatin structure and lays down a mark for the recruitment of transcriptional coactivators or chromatin remodellers.[178, 179] CBP/p300 can acetylate all four core histones, with a preference for H3 and H4.[180, 181] Acetylation of non-histone proteins, such as transcription factors, can also contribute to transcriptional activation.[182, 183] In the second mechanism, CBP/p300 may act as a bridge between a gene-specific transcription factor (GSTF) and the basal transcriptional machinery (BTM).[177] Finally, CBP/p300 can act as a scaffold where binding to a GTFS is followed by binding of other transcriptional coactivators.

With the multitude of different roles that CBP and p300 play in cellular processes, they consequently play a pivotal role in development and their misregulation is implicated in a number of human diseases and developmental disorders.[158, 160]

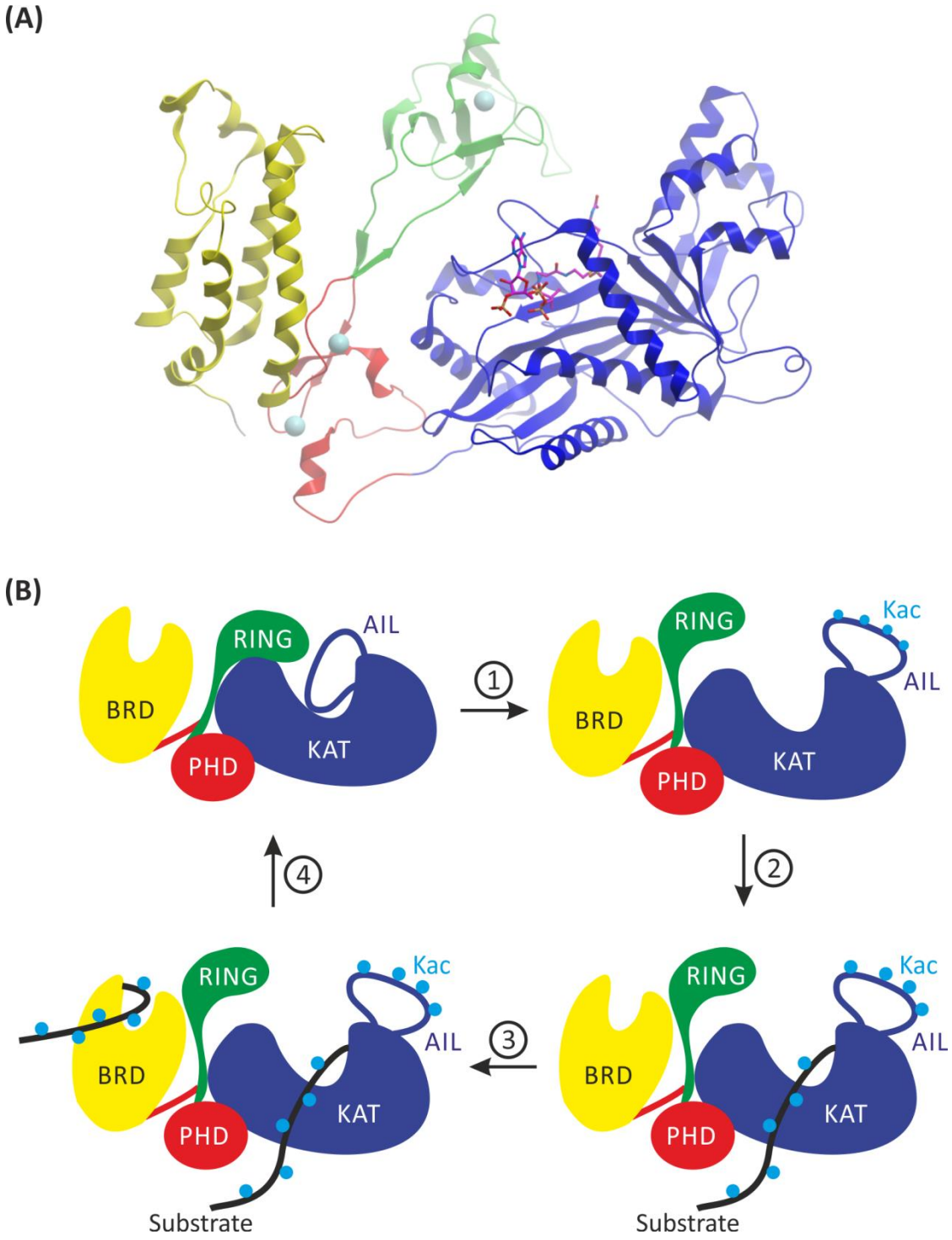

Figure 19. Catalytic core of p300.[166] (A) View from X-ray crystal structure of p300 catalytic core in complex with SAH (carbon=magenta) showing BRD (yellow), PHD (red), RING (green) and KAT (purple). Construct has a deletion of the AIL (Δ1520–1581) in the KAT domain (PDB 4BHW). (B) Proposed mechanism of autoregulation and substrate acetylation. In the inactive state (top-left), the AIL and RING block the substrate binding site of the KAT. In the first step, recruitment to an enhancer results in *trans* autoacetylation of the AIL with concurrent exposure of the KAT binding site (top-right). Binding and acetylation of the substrate is then possible (bottom-right). Binding of acetylated substrate to the BRD results in positive feedback and maintenance of p300 signal (bottom-left). Deacetylation of p300 is regulated by KDAC, such as SIRT2, resulting in inactivation.[166, 176]

2.2 CBP/P300 IN DEVELOPMENT AND DISEASE

2.2.1 CBP/P300 IN DEVELOPMENT AND RTS

The importance of CBP in development can be seen in Rubinstein-Taybi Syndrome (RTS), a congenital disorder characterised by stunted growth, facial abnormalities, broad toes and thumbs, epilepsy, and mental retardation.[126] RTS patients are also more susceptible to a variety of tumours. It was demonstrated by Petrij *et al.* that a cohort of RTS patients had heterozygous mutations in *CBP,* which indicated that RTS could be caused by a haploinsufficiency of CBP.[184] This was also supported by a screen of 92 RTS patients, which found that 36 had mutations in *CBP* and 3 had mutations in *p300*.[128]

The proliferation and differentiation of different cell lineages, including those within the nervous system, is controlled by CBP/p300 and they are required for neural tube closure in mammalian embryos.[185] Pioneering knockout studies published in the 1990s gave further insight into the importance of CBP/p300 in development. Homozygous null mutations in CBP and p300 led to early embryonic death in mice models. The $CBP^{-/-}$ mutant embryos show severe defects in neural tube closure, haematopoiesis and vascular angiogenesis, whilst $p300^{-/-}$ mutants also display neural tube defects, defective cell proliferation and abnormal heart development.[186-188] Heterozygotes also exhibit severe developmental abnormalities; $CBP^{+/-}$ mutant mice showed growth retardation, craniofacial abnormalities akin to RTS, skeletal abnormalities, splenomegaly, defects in hematopoietic differentiation, and were susceptible to leukaemia and sarcomas.[133, 188] Mutations of the CBP KIX, PHD and KAT domain have also been found in patients with RTS.[189] $p300^{+/-}$ mutants were prone to embryonic lethality, again displaying developmental retardation. Compound heterozygotes were also lethal to embryos.[187] Taken in combination these data suggest that full complements of CBP and p300 are required for normal development. Additionally, a

haplodeficiency in one gene cannot be compensated for by a full complement of its paralogue.

Abnormal *CBP* expression has also been postulated to explain epilepsy in individuals with RTS.[190] *CBP* is expressed in neural precursors in the embryonic medial ganglionic eminence (MGE), where most cortical interneurons are generated, and knockdown of *CBP* negatively effects differentiation of neural precursors into interneurons and oligodendrocytes.

In a further demonstration of the importance of CBP/p300 in development, studies in rat which modelled foetal alcohol spectrum disorder (FASD) demonstrated reduced CBP expression and H3/H4 acetylation levels.[191]

2.2.2 CBP/P300 IN MEMORY AND NEURODEGENARTIVE DISORDERS

Experiments in transgenic mice which express CBP with no KAT activity demonstrated that transformation of short-term into long-term memory was impaired.[192] In addition, conditional knock-out experiments in mice indicate that CBP is required for both short- and long-term memory formation.[193-195]

Mutations in presenilins, a family of transmembrane proteins that function as part of the γ-secretase complex, are found in the majority of cases of familial Alzheimer's disease. Loss of presenilins causes a reduction in the expression of CBP and CREB target gene in the cerebral cortex.[196, 197] Similar effects have also been reported for p300.[198]

CBP/p300 have been linked to neurological conditions, including poly-glutamine (polyQ) diseases.[190, 199-201] PolyQ diseases are a class of trinucleotide repeat disorders where abnormal expansion of CAG repeats in a gene result in extended polyQ expression.[202] Human polyQ disorders include Huntington's disease, dentatorubropallidoluysian atrophy (DRPLA), spinobulbar muscular atrophy (SBMA, aka Kennedy disease) and several forms of spinocerebellar ataxia (SCA). It has been proposed that aberrantly regulated polyQ chains

interact with a glutamine rich region of CBP (C-terminus, residues 1760–2440) and lure it from its normal nuclear location. [190, 199-201, 203] Additionally, brain autopsies from people who had Huntington's disease indicate dramatically reduced levels of CBP expression.[200]

In Parkinson's disease, it has been suggested that native α-synuclein (α-syn) offers neuroprotection against neurotoxins through the down-regulation of p300.[204] This causes a further down-regulation of protein kinase Cδ (PKCδ) expression, which causes dopaminergic neuronal death. However, misfolded α-syn, associated with pathogenesis of Parkinson's disease, cannot regulate p300 effectively, resulting in p300 transactivation of PKCδ and dopaminergic cell death.

2.2.3 CBP/P300 IN CANCER

CBP/p300 appear to have various context specific roles in tumours, with evidence suggesting they can act as tumour suppressors or promoters.[205] This may be due to the delicate balance of acetylation required for normal cell function.[112] Hypoacetylation from reduced CBP/p300 expression or mutation to the catalytic core can reduce the expression of tumour suppressor proteins. Conversely, hyperacetylation from overexpression of CBP/p300 can increase the expression of oncogenes, oncofusion proteins and viral oncoproteins.

Mixed lineage leukaemia (*MLL*) and monocytic leukaemia zinc finger (*MOZ*) have been found to undergo chromosomal translocations with *CBP*/*p300* in cases of myeloid and lymphoid acute leukaemia and therapy-related myelodysplasia following treatment with DNA topoisomerase II targeting drugs.[206-208] Additionally, CBP/p300 are recruited as transcriptional coactivators during leukaemogenesis by the translocation generated fusion proteins NUP98-HOXA9 and MOZ-TIF2.[209, 210]

The role of CBP and p300 in cancer is not limited to haematological malignancies. Mutations which inactivate CBP/p300 are common in the major forms of B-cell non-Hodgkin's

lymphoma; *CBP* and *p300* are highly expressed in advanced prostate cancer; and mutations to *CBP* have been detected in ovarian and bladder cancers whilst mutations to *p300* have been observed in colorectal, bladder, breast, ovarian and gastric tumours. [129, 211-214]

Examples of mutations in cancer cell lines have emerged which demonstrate the importance of the BRD in regulating normal cell function. A mutation which results in loss of the p300 BRD and which prevent p300-mediated p21 activation was observed in SiHa cervical carcinoma cell lines, suggesting a critical role for the BRD in p300 tumour suppressor function.[215] Additionally, a 21-base pair deletion within the *p300* BRD have been observed in a T-lymphoblastic leukaemia cell line (CEM).[216] Mutation experiments, in which the BRD and KAT domains in a tumorigenic MLL-CBP fusion construct were substituted, showed that both domains were important in the MLL disease phenotype.[217]

2.2.4 CBP/P300 IN INFLAMMATION

Inflammatory lung diseases, such as asthma, chronic obstructive pulmonary disease (COPD) and cystic fibrosis, are characterised by overexpression of inflammatory genes. The pro-inflammatory protein complex NF-κB (nuclear factor κB) regulates the transcription of several genes involved in airway inflammation. The transcriptional activity and target gene affinity of the p65 subunit of NF-κB are regulated by CBP/p300 acetylation.[218] Increased acetylation of histones H3/H4 and NF-κB by CBP/p300 has been linked to cigarette smoke-mediated pro-inflammatory cytokine release in COPD.[219]

Additionally, p300 has been implicated as the predominant coactivator of cyclooxygenase-2 (COX-2) transcriptional activation. COX-2 is involved in the conversion of arachidonic acid to pro-inflammatory prostaglandins.[220] Inhibition of the p300 KAT domain was also shown to reduce COX-2 expression and neuropathic pain in an *in vivo* model.[221]

2.2.5 CBP/P300 IN VIRAL INFECTION

The human immunodeficiency virus (HIV) requires the viral protein, transactivator of transcription (Tat), for replication.[222] Tat recruits CBP/p300 to enhance HIV transcription.[223] Additionally, the activity of HIV integrase, which enables the viral genome to be integrated into this host DNA, is regulated by p300 acetylation.[224] Also, nuclear import of the HIV pre-integration complex is regulated by the HIV viral protein R (Vpr), which has been shown to interact with CBP/p300.[225]

2.2.6 CBP/P300 AND P53

Mutations of the *p53* gene are common, with around 50% of human cancers encoding such mutations.[226-228] In response to cellular stress, p53 undergoes post translational modifications (PTMs) of the *C*- and *N*-terminal regions, including acetylation at the *C*-terminal region by p300 and p300/CBP-associated factor (PCAF), which results in changes in the p53-dependent activation of target genes leading to cell cycle arrest, senescence or apoptosis.[228-230] Lysine acetylation at lysine 382 (K382) of p53 is responsible for recruitment of CBP to p53 via its bromodomain, as shown by NMR titration of the CBP bromodomain with acetylated p53 peptides, and transfection of $p53^{-/-}$ cells with mutated *p53*.[231] Additionally, in a p21 luciferase assay, the CBP-p53 Kac interaction was shown to be crucial for p53-induced p21-mediated G_1 cell cycle arrest. Also, chemo- and radio-therapy can cause p53-mediated tissue damage of non-cancerous tissue, implying p53 inhibition could be used to protect healthy tissue during these therapies.[232] In addition to its important tumour suppressor role, hyperactive p53 is implicated in Alzheimer's disease, Parkinson's disease, spinal cord diseases, multiple sclerosis, ischemic brain injury, infectious and autoimmune diseases, and myocardial ischemia.[233-238]

2.2.7 CBP/P300 IN HYPOXIA

In humans, the cellular response to hypoxia is mediated by hypoxia-inducible factors (HIFs). HIFs are transcription factors which mediate processes such as angiogenesis and erythropoiesis. The HIF pathway is vital to human development, but also important in the growth of solid tumours.[239] HIFs are made up of two subunits, α and β. The β sub-unit is constitutively expressed, whereas the α subunit is controlled by various oxygen sensing mechanisms. In HIF-1α and HIF-2α, there are two main mechanisms that control HIF target gene expression (Figure 20). In the first mechanism, Pro-402 and -564 on HIF (HIF-1α numbering) are hydroxylated by a proline hydroxylase domain.[240, 241] Hydroxylation leads to polyubiquitination, mediated by Von Hippel–Lindau tumour suppressor (pVHL), and subsequent proteasomal degradation. Secondly, HIF Asn-803 is hydroxylated by factor-inhibiting HIF (FIH).[168, 242] The hydroxylation prevents HIF binding to its coactivators, CBP/p300. Under hypoxic conditions, the Pro and Asn residues are less hydroxylated, as their activity is limited by oxygen availability in physiologically relevant ranges. The non-hydroxylated HIF-1α is then able to translocate to the nucleus, where it dimerises with HIF-1β and binds to p300, leading to transcription of HIF target genes. Thus CBP/p300 play an important role in the HIF pathway, and inhibitors of CBP/p300-mediated HIF-target gene transcription are potentially relevant in oncology.

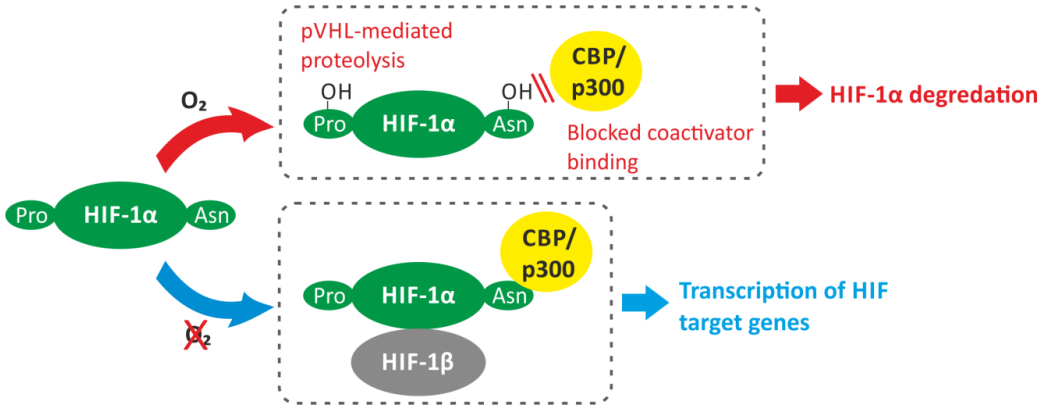

Figure 20. HIF-1α mediated hypoxic response. In normoxia, PHDs and FIH downregulate and inactivate HIF-1α. PHDs hydroxylate prolyl residues in the amino- and carboxy-terminal oxygen-dependent degradation domains (NODDD and CODDD), which promotes pVHL-dependent proteolysis of HIF-1α. FIH hydroxylates an asparagine residue in the carboxy-terminal activation domain (CAD), which blocks CBP/p300 co-activator recruitment. Under hypoxic conditions, HIF hydroxylases are inactive and these processes are suppressed, which allows the formation of a transcriptionally active complex and consequently transcription of HIF target genes.

2.3 INHIBITORS OF CBP/P300

With the pleiotropic roles that CBP and p300 play in development and disease, inhibitors of their various domains have the potential to be valuable tools in studying their biology and validating new therapeutic strategies for disease intervention. To date, the majority of inhibitors of CBP/p300 described target the KAT domain, whilst inhibitors of the KIX and BRD have also been reported.

Figure 21 shows reported CBP/p300 KAT inhibitors, together with their reported activities. Anardic acid (compound **11**), a natural product from cashew nut shell liquid, has been reported to inhibit the KAT activity of p300, with an IC_{50} of 8.5 μM.[243] This compound is non-specific and also inhibited the KAT activity of PCAF (IC_{50} 5 μM). Interestingly, CTPB, an amide analogue of anardic acid, activates p300 KAT activity, but not that of PCAF. Subsequently, garcinol (compound **12**), found in the rinds of the mangosteen fruit, was shown to have similar inhibitory capability to anardic acid against p300 and PCAF, and was shown to induce apoptosis in HeLa cells.[244] Garcinol has also been shown to inhibit p300-mediated acetylation of p53 and inhibit the multiplication of HIV.[245] An analogue of garcinol, LTK-14 (compound **13**), has been reported to be selective for the CBP/p300 KAT over PCAF, and also inhibits HIV multiplication.[246] Other reported CBP/p300-specific KAT inhibitors include the turmeric component, curcumin (compound **14**); plumbagin (compound **15**), an extract from *Plumbago rosea* root; an isothiazolopyridinone (compound **16**); a quinone, L002 (compound **17**); and dihydropyrazolones, C107 (compound **18**) and C646 (compound **19**).[247-255]

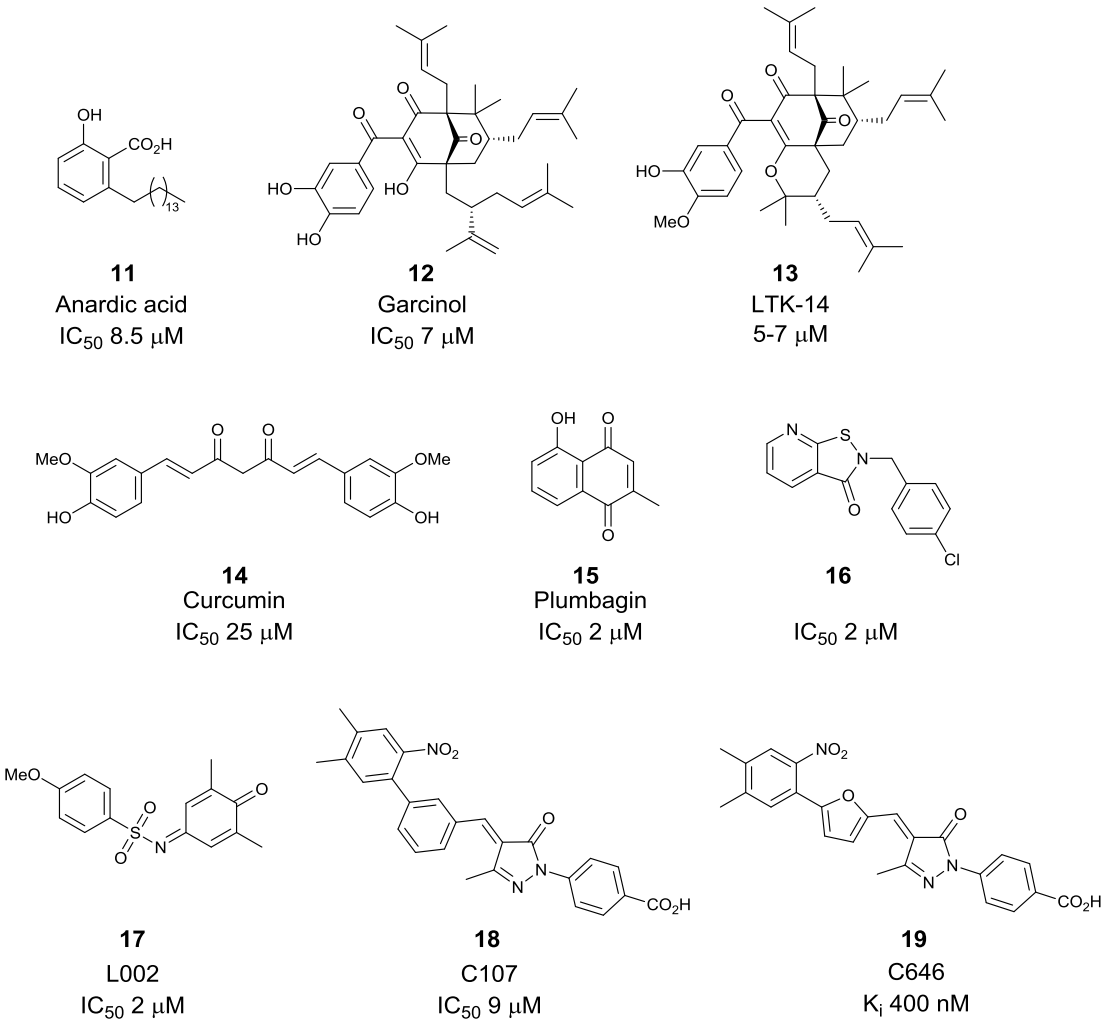

Figure 21. Reported small molecule and natural product inhibitors of CBP/p300 KAT domain.

Figure 22 shows reported inhibitors of the CBP/p300 KIX domain. Naphthol AS-E (compound **20**) is a cell-permeable inhibitor which inhibits CREB-dependent gene transcription in cells.[256] The depside compound, sekikaic acid (compound **21**) and the depsidone, lobaric acid (compound **22**) are allosteric inhibitors of the KIX domain of CBP/p300 which down-regulate *CCND1* expression.[257]

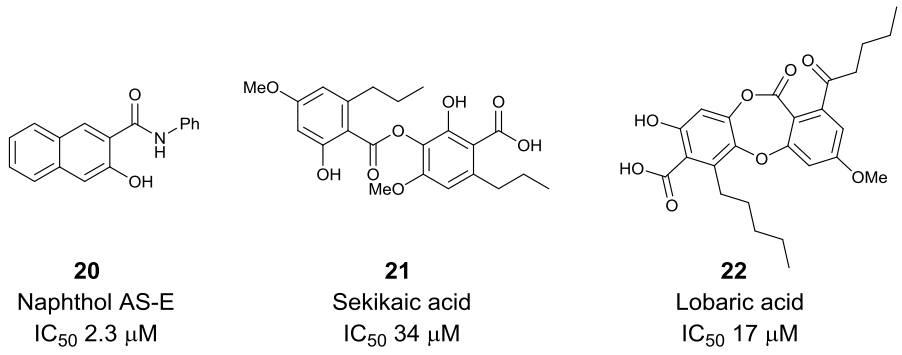

Figure 22. Reported small molecule and natural product inhibitors of the CBP/p300 KIX domain.

Pioneering work on the inhibition of the CBP BRD was carried out by the Zhou group which reported several compounds with micromolar affinities (Figure 23).[258-260] The *N*-acetyl indole MS7972 (compound **23**, K_d 19.6 μM) was shown to block the p53-CBP interaction at 50 μM in a competition assay.[258] Ischemin (compound **24**, *in vitro* affinity: K_d 19 μM) inhibited p53-induced p21 activation in a luciferase reporter-gene assay (IC_{50} 5 μM) and down-regulated p53 target gene expression under oxidative stress conditions.[259] The cyclic peptide **25** shown in Figure 23 has also been shown to bind CBP (IC_{50} 13.1 μM) and to inhibit p53 activity in a reporter gene assay.[260]

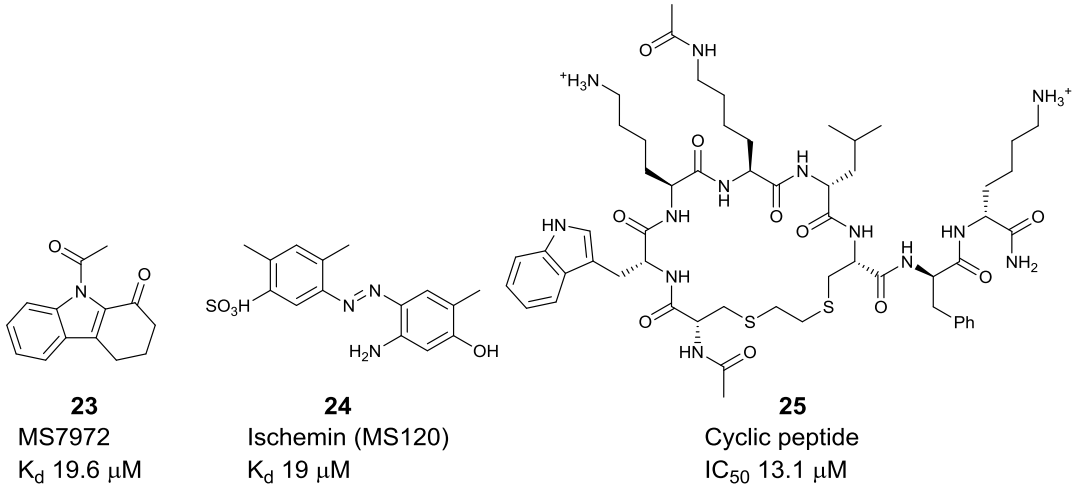

Figure 23. Known CBP bromodomain ligands.

CBP and p300 are ubiquitous and pervasively implicated in human cellular processes; consequently, their misfunction through mutations or abnormal expression patterns is implicated in a multitude of diseases and developmental disorders. Although the CBP/p300 inhibitors described previously could serve as useful tool compounds, they lack the potency and full characterisation in terms of selectivity and cellular activity that allow robust conclusions to be made from their use. Limited genetic evidence has pointed to the role of the BRD and KAT domains in CBP/p300 pathogenesis. As such, potent, selective and cell-permeable chemical probes for the CBP/p300 BRD and KAT domains are still needed to aid in the interrogation of their function and potential application as therapeutic targets.

CHAPTER 3. CBP/P300 CHEMICAL PROBE: DEVELOPING A NON-SELECTIVE FRAGMENT INTO A LEAD

3.1 STARTING POINT

The starting point for developing selective CBP/p300 inhibitors was the reported weak and non-selective dimethylisoxazole hit compound **26** (Figure 24).[261] Compound **26** was considered to be an attractive fragment to develop CBP-selective inhibitors because it has a low molecular weight (213 Da), reasonable lipophilic efficiency (LiPE)[262] (3.5) and ligand efficiency (LE)[263, 264] (0.46) for CBP and has various points useful for diversification of the core scaffold.

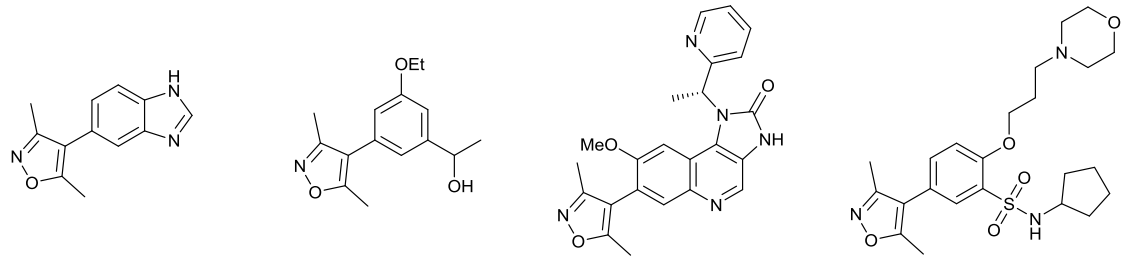

26
CBP IC_{50} 5.4 μM
BRD4(1) IC_{50} 5.2 μM

27
CBP IC_{50} 28 μM
BRD4(1) IC_{50} 1.6 μM

28
(I-BET151)
BRD4(1) K_d 0.1 μM

29
BRD4(1) IC_{50} 2.6 μM

Figure 24. Dimethylisoxazole inhibitors of bromodomains.

One potential obstacle for developing dimethylisoxazole compounds into CBP chemical probes is the potency for such compounds against BRD4; compound **26** is equipotent against the first domain of BRD4 (BRD4(1)). Additionally, there have been several reports of dimethylisoxazole inhibitors that are selective for BRD4(1), such as compounds **27**, **28** and **29** (Figure 24). Therefore, it was decided to screen all compounds against both CBP and BRD4(1) in order to optimise the selectivity of the inhibitors for CBP.[261, 265-267]

3.2 CBP VS BRD4(1)

The Kac binding sites of the BRDs of CBP and BRD4(1) are very similar. However, comparison of X-ray crystal structures of CBP and BRD4(1) suggests differences which may aid the design of CBP selective compounds. Figure 25 shows a comparison of the binding sites of CBP and BRD4(1). The key residues involved in Kac binding are identical, i.e. Y1125 (CBP), Y97 (BRD4(1)) and N1168 (CBP), N140 (BRD4(1)). The hydrophobic residues which line the binding pocket are very similar, with subtle differences in I1122 (CBP) vs L94 (BRD4(1)) and V1174 (CBP) vs. I146 (BRD4(1)). However, the most significant difference are in a 'shelf' region just outside the base of the binding pocket, which is termed the WPF (Trp, Pro, Phe) shelf in BRD4(1) (Figure 25B and D). The main feature of the BRD4(1) WPF shelf is the indole side-chain of W81 which protrudes from the surface. In CBP, the equivalent amino acid is L1109, which leads to a flatter surface in this area. The main feature of the CBP shelf region is the guanidine side-chain of R1173. The D145 side-chain in the equivalent position in BRD4(1) is oriented away from the shelf region. Thus building into a vector which can access this shelf region is a potential strategy for the design of CBP-selective inhibitors. For example, acidic moieties could form salt-bridge interactions with R1173 in CBP, but no equivalent interaction could occur in BRD4(1). Also, since W81 forms a more enclosed surface on BRD4(1) compared to the same area in CBP, bulky moieties which form unfavourable steric interactions with W81 could increase selectivity of inhibitors for CBP.

It was considered that the benzimidazole scaffold would lend itself well to the strategy of targeting the shelf region of the CBP and BRD4(1) BRDs. The *N*-1 and *C*-2 positions (Figure 26) can be varied readily, and substituents that build from these regions could target the shelf region. For example, Figure 26 shows a benzimidazole analogue (compound **30**) which has been docked into the CBP BRD. This supported the strategy of targeting the shelf region through *N*-1 and/or *C*-2 substitution of the benzimidazole core. The salt-bridge interaction

shown in Figure 26 between the carboxylic acid of compound **30** and R1173 could be exploited to increase potency for CBP, whilst acidic moieties cannot form the same interactions in BRD4(1), meaning selectivity may also be increased.

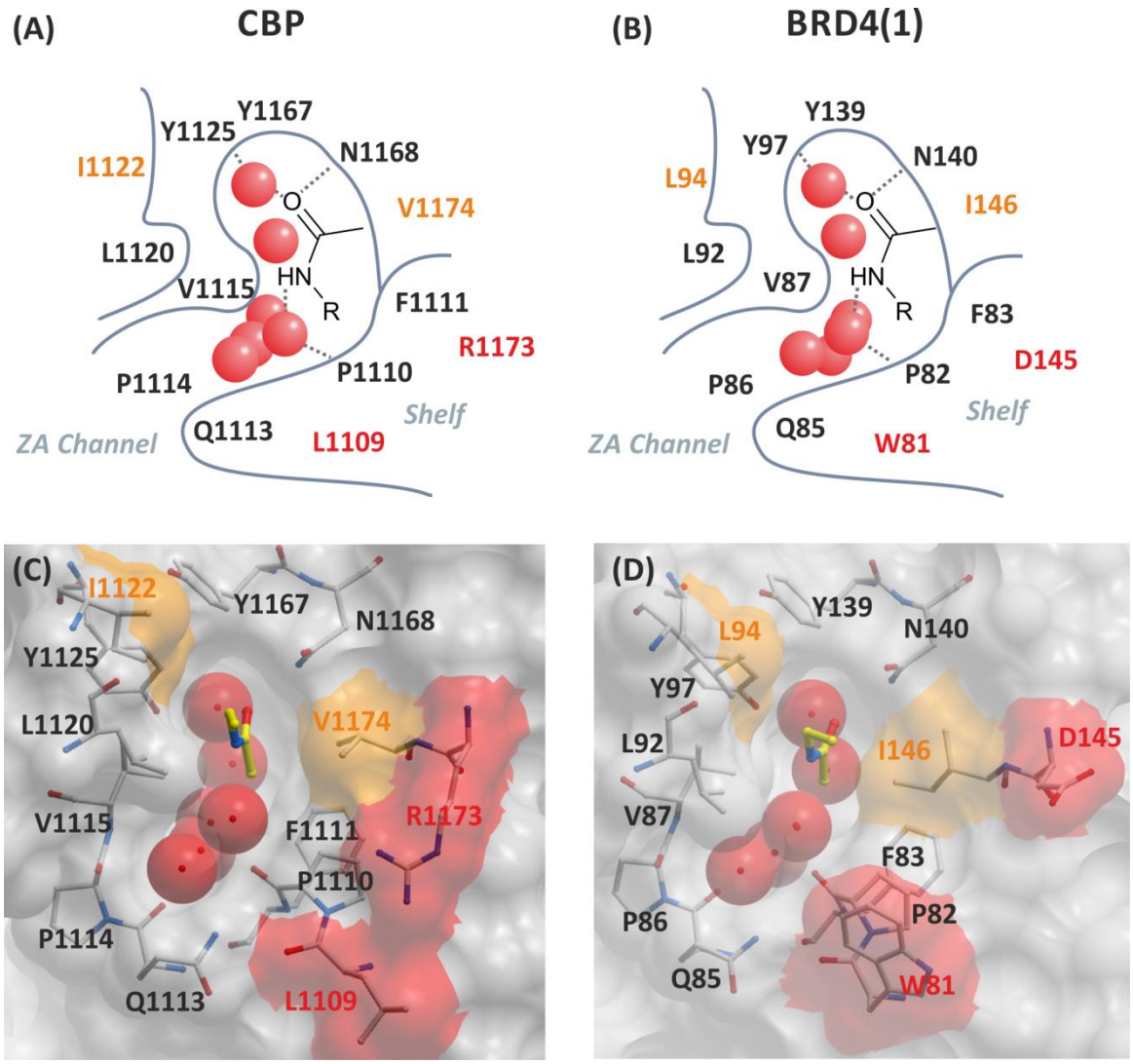

Figure 25. Comparison of binding pockets of CBP and BRD4(1). (A) and (B): CBP and BRD4(1) Kac binding pockets. Residues which are equivalent in CBP and BRD4(1) are shown in grey font. Those with minor differences are coloured orange. Significantly different amino acid residues are shown in red font. Crystallographically well conserved waters are shown as red spheres. (C) and (D): Views from binding pocket of CBP (PDB 3P1C) and BRD4(1) (PDB 3UVW). Differences in the surfaces are colour-coded as per (A) and (B).

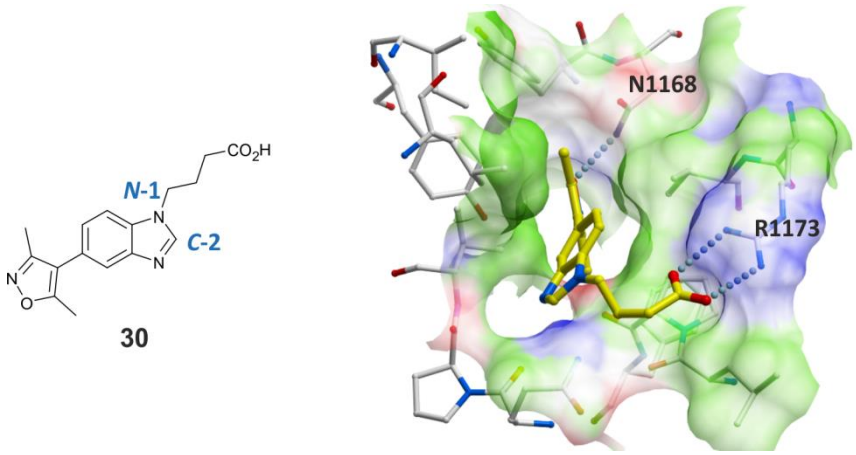

Figure 26. Docking of compound **30** into CBP (PDB 3P1C).* This demonstrates the potential to simultaneously form an H-bond from the dimethylisoxazole to N1168 and a salt bridge between a carboxylic acid and R1173.

3.3 CARBOXYLIC ACID-CONTAINING ANALOGUES

The initial strategy involved retaining the dimethylisoxazole moiety as the Kac mimic, whilst varying substitution on the 5-membered ring of the core (Figure 27). Although the lead possessed a benzimidazole, it was envisaged that other 5,6-heterocycles would also be suitable analogues. A retrosynthesis of the targeted compounds involved disconnecting across the C-C bond between the dimethylisoxazole and the heterocyclic core to give metal-catalysed cross-coupling partners. One permutation of this disconnection is a metallic dimethylisoxazole, coupled with heterocyclic halides (Figure 27). Heteroaryl bromides were chosen, as these had a reasonable overlap of availability and reactivity. Since various boron-containing dimethylisoxazoles, such as compound **31**, were commercially available, these were chosen as the other coupling partner, meaning the forward reaction would be a Suzuki reaction. As the project was at an early stage, elaborating on a fragment hit, it was desirable to test a significant number of compounds with structural diversity. Therefore, this one-step approach to test compounds was beneficial to building a structure-activity relationship (SAR).

*Docking of analogues was carried out using Molsoft ICM-Pro using the default settings.

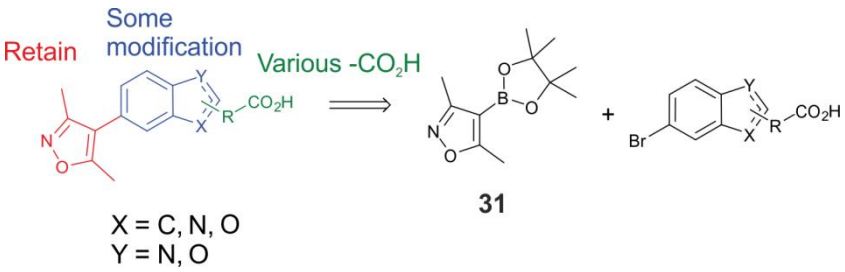

Figure 27. Strategy for acid-containing analogues. The dimethylisoxazole moiety was retained whilst the core and core side-chains were varied. In order to build out to the shelf region, modifications on the 5-membered ring of the heterocyclic core were prioritised. Disconnection of the desired targets across the dimethylisoxazole-heterocyclic core C-C bond gives precursors for a metal-catalysed cross-coupling.

The cross-coupling reactions were carried out at Pfizer's Sandwich laboratories, which were equipped with facilities for parallel chemistry and automated purification, and also possessed in-house sets of monomers. A set of 23 carboxylic acid-containing 5,6-heteroaryl bromides (compounds **32-55**, Appendix 1) were chosen from the Pfizer monomers. The heteroaryl bromides included indoles, benzofurans and benzimidazoles with a variety of functionality and substitution patterns. The reactions were carried out in parallel, then the crude reaction mixtures were purified either by flash column chromatography, or worked up in parallel prior to automated HPLC purification. This procedure resulted in the isolation of 17 products (compounds **56-73**) out of the set of 23, in sufficient quantity and purity for biological screening.

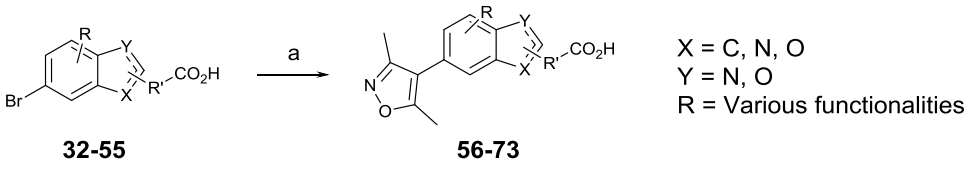

Scheme 1. Coupling of acid-containing 5,6-heteroaryl bromides. Reagents and conditions: (a) **31**, $Pd(dppf)Cl_2$, $NaHCO_3$, DME/H_2O, 100 °C (10-55%, mean yield 28%).

The compounds obtained were screened by AlphaScreen (amplified luminescent proximity homogeneous assay screen).* [268] The potency of compounds **56-73** against CBP ranged from 1.8-64 μM (Appendix 2). Disappointingly, most compounds displayed poor selectivity for CBP, or a slight preference for BRD4(1). However, notable exceptions included compound

*All primary binding assays were carried out by Oleg Fedorov, Sarah Martin, Octovia P. Monteiro and Anthony Tumber (SGC/TDI).

56 which was around 3 times more potent for CBP than BRD4(1) and compound **57** which was over 30-fold selective for CBP (Table 2). Even with this selectivity, the potency of these compounds (IC_{50} 8.9 μM and 14 μM respectively), was still well below the targeted criteria. The most potent CBP inhibitor from this set was compound **58** (IC_{50} 1.9 μM). However, compound **58** displayed little selectivity over BRD4(1) (IC_{50} 2.1 μM) and was approximately equipotent with the initial lead **26**. Whilst this series suggested that selectivity for CBP was attainable, it did not lead to improved potency. It was therefore decided to widen the scope of the target compounds beyond carboxylic acid-containing heterocycles.

Table 2. SAR for CBP and BRD4(1) binding as determined by AlphaScreen for selected carboxylic acid-containing analogues.

		*AlphaScreen IC_{50} (μM)**		
Cmpd	*Structural formula*	*CBP*	*BRD4(1)*	*CBP selectivity (-fold)*
56	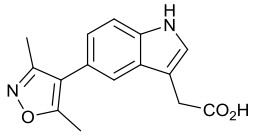	8.9	28	3.1
57	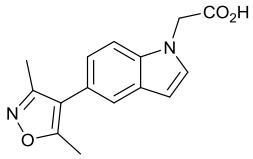	14	450	32
58	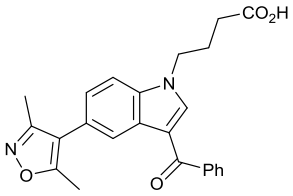	1.9	2.1	1.1

3.4 NEUTRAL AND BASIC ANALOGUES

A set of heteroaryl bromides was chosen from the Pfizer compound collection. The monomers were selected so that products obtained would have Lipinski compliant properties (e.g. clog P <5 and MW <500) and the majority of the compounds were targeted at around clog P 2-4 and MW 300-400. The set chosen consisted of 78 heteroaryl bromides

(compounds **74**-**151**, Appendix 3), which had a variety of substituents on the heterocyclic core. The starting materials featured polar, non-polar, aromatic, heteroaromatic, basic and neutral substituents and the heterocycles included benzimidazole, indoles, benzofurans and benzothiophenes. It was envisaged that the diverse nature of the heteroaryl bromides would maximise the chances of interacting with the shelf regions of CBP and BRD4(1). The set of starting monomers was coupled with compound **31** in the same way as for the acid-containing compounds (Scheme 2).

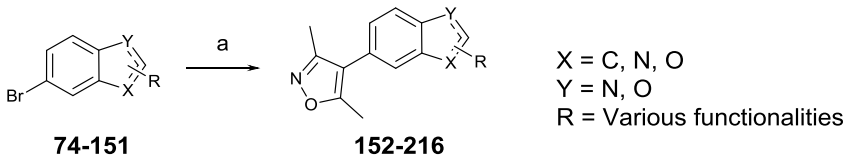

Scheme 2. Synthesis of neutral and basic analogues. Suzuki coupling of various heteroaryl bromides with **31**. Reagents and conditions: (a) **31**, $Pd(dppf)Cl_2$, $NaHCO_3$, DME/H_2O, 100 °C (5-93%, mean yield 42%)

A set of 65 target compounds (compounds **152**-**216**) were obtained from the 78 heteroaryl bromides. Gratifyingly, certain products displayed selectivity for CBP over BRD4(1) (Appendix 4 and Table 3). Table 3 shows selected examples of non-selective, CBP-selective and BRD4(1)-selective hits from the library. Compound **152**Error! Reference source not found. was reasonably potent against both CBP (IC_{50} 1.2 μM) and BRD4(1) (IC_{50} 1.1 μM). The CBP-selective examples **153**-**156** all possessed a substituent on the *C*-2 position of the 5-6-heterocycle, implying this was important for CBP-selectivity over BRD4(1). This could be due to a steric clash of the *C*-2 moieties with W81 of BRD4(1). In contrast, the alkyl chain on the *N*-1 position of the benzimidazole of **157** resulted in selective binding for BRD4(1) over CBP (IC_{50} 0.44 μM and 4.8 μM, respectively). However, compound **156**, which possessed an *N*-1 dimethylamino ethyl group and bulky *C*-2 neopentyl group was around 9-fold selective for CBP over BRD4(1) (IC_{50} 1.6 μM and 15 μM, selectively). The basic *N*-1 moiety of compound **156** was in contrast to the original strategy of incorporating a negatively charged carboxylate in compounds **56**-**73**. The balance of potency and selectivity meant compound **156** was seen as an attractive scaffold for further investigation.

Table 3. Selected AlphaScreen results for basic and neutral analogues.

Cmpd	*Structural formula*	*AlphaScreen IC_{50} (μM)*		*Selectivity*
		CBP	*BRD4(1)*	
152	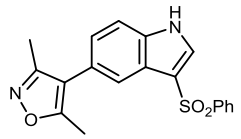	1.2	1.1	Non-selective
153	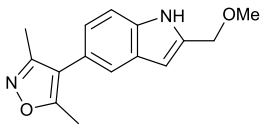	4.1	15	CBP, 3.7-fold
154	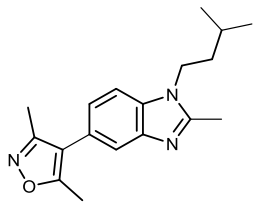	2.0	8.2	CBP, 4.1-fold
155	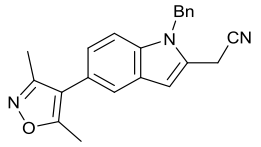	2.2	11	CBP, 5.0-fold
156	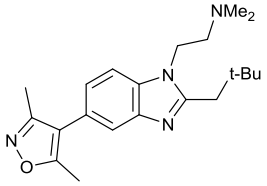	1.6	15	CBP, 9.4-fold
157	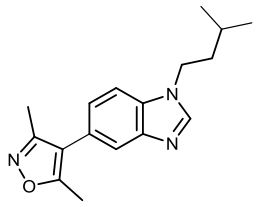	4.8	0.44	BRD4(1) 11-fold

Initially, it was decided to retain the benzimidazole and *N*-1 moiety of compound **156** whilst varying the *C*-2 substituent (Figure 28). Such targets could be accessed by a benzimidazole-forming reaction between nitroaniline **217** and an aldehyde. A set of 32 aldehydes (**218-249**) was selected from the Pfizer compound collection. A variety of aldehydes were chosen

to include alkyl, polar, aromatic and heteroaromatic moieties (Appendix 5). In order to keep the molecular weight (MW) of the products relatively low, the aldehydes chosen had MW <140.

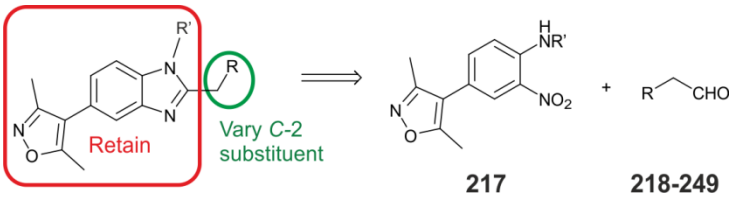

Figure 28. C-2 variation. The benzimidazole ring can be disconnected to a nitroaniline and aldehyde precursors.

The required nitroaniline precursor was synthesised according to Scheme 3. Commercial 4-bromo-1-fluoro-2-nitrobenzene **217** was coupled with compound **31** to yield compound **251**, which underwent S_NAr with *N,N*-dimethylenediamine to yield compound **217**. Compound **217** was then reacted with a set of aldehydes (**218-249**) in the presence of sodium dithionite to yield the target compounds (**252-270**), which were purified by automated HPLC. The desired products were isolated from 19 out of 32 reactions.

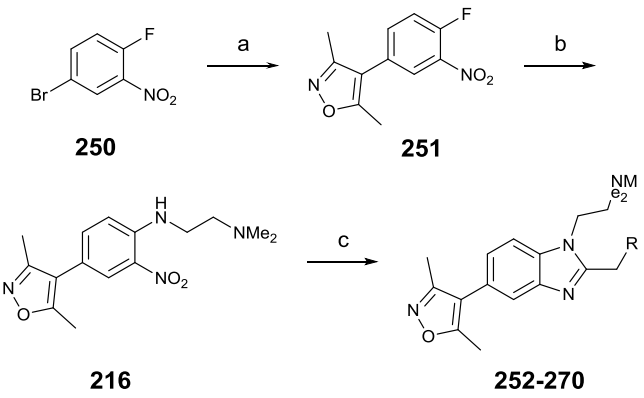

Scheme 3. Reagents and conditions: (a) **31**, $Pd(dppf)Cl_2$, $NaHCO_3$, DME/H_2O, 73%; (b) *N,N*-Dimethylenediamine, DIPEA, THF, 86%; (c) RCH_2CHO, $Na_2S_2O_4$, H_2O, EtOH, DMSO, 80 °C (8-54%, mean yield 28%).

In this instance, the compounds were screened for binding to CBP and BRD4(1) using a differential scanning fluorimetry (DSF) assay, which had been found to be a reliable and high-throughput surrogate for the more complicated and lower throughput AlphaScreen assay (Appendix 6).[269] DSF measures changes in the denaturing temperature (ΔT_m) of proteins upon ligand binding and a high ΔT_m value should correlate with potent affinity.

Table 4 summarises a selection of SAR data obtained for the *C*-2 analogues. Encouragingly, the selectivity for CBP over BRD4(1) was maintained with most compounds showing minimal effect on BRD4(1) (ΔT_m <1 °C). This result supported the hypothesis that the *C*-2 substitution pattern is detrimental for BRD4(1) binding. Alkyl substituents (compounds **252**-**257**) gave a ΔT_m value in the range of 1.4-3.8 °C for CBP, and bulky groups tended to give higher ΔT_m values than small groups. Polar functionality, such as amide **258** and amine **259** seemed to be poorly tolerated by CBP (ΔT_m <1 °C). Aryl groups were well tolerated (compounds **260**-**265**), with ΔT_m in the range of 2.2-6.3 °C. The highest affinity for CBP was for compound **263** (ΔT_m 6.3 °C) which possessed phenethyl substitution at *C*-2 of the benzimidazole. AlphaScreen was used to determine that this ΔT_m corresponded to an IC_{50} of 0.49 μM, which represented a 10-fold improvement in potency for CBP compared to the starting compound **26**. It had therefore been demonstrated that 1,2-disubstituted benzimidazoles, could give potent compounds with selectivity for CBP over BRD4(1). Future close-in analogues were therefore planned based on the series exemplified by compound **263**.

Table 4. SAR for CBP and BRD4(1) binding as determined by DSF assay for selected *C*-2 substituted benzimidazole products.

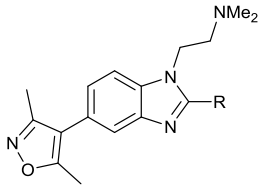

		DSF ΔT_m (°C)[*]	
Cmpd	*R*	*CBP*	*BRD4(1)*
252	-Et	1.4 ± 0.12 (2)	0.35 (1)
253	-*n*-Pr	3.0 (1)	0.20 (1)
254	-*n*-Bu	2.0 ± 0.075 (2)	0.71 (1)

Cmpd	R	DSF ΔT_m (°C)*	
		CBP	BRD4(1)
255		1.9 ± 0.32 (2)	0.42 (1)
256		3.2 ± 0.060 (2)	0.55 (1)
257	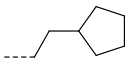	3.8 ± 0.41 (2)	0.78 (1)
258	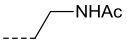	0.84 ± 0.080 (2)	0.17 (1)
259	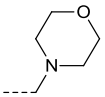	0.78 ± 0.16 (2)	0.14 (1)
260	-Bn	3.1 ± 0.43 (2)	0.25 (1)
261	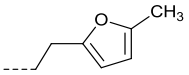	3.0 ± 0.24 (2)	0.75 (1)
262	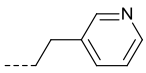	2.2 ± 0.040 (2)	0.53 (1)
263	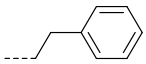	6.3 ± 0.27 (3)	2.9 ± 0.20 (3)
264	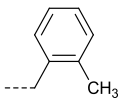	2.7 ± 0.44 (2)	0.27 (1)
265	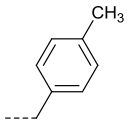	4.0 ± 0.075 (2)	0.38 (1)

*Mean ΔT_m ± SEM (number of measurements).

3.5 SUMMARY

Figure 29 shows a summary of the compounds developed in this chapter. A weak binding and non-selective dimethylisoxazole fragment **26** was chosen as the starting point for the

development of a CBP-selective chemical probe. A strategy of introducing carboxylic acids to interact with R1173 was initially pursued. 17 target compounds were synthesised by parallel Suzuki coupling reactions (Scheme 1). The resulting compounds showed poor potency and selectivity for CBP (Table 2). A set of 65 diverse neutral and basic analogues were synthesised (Scheme 2). These demonstrated that *C*-2 substitution on the heteroaryl core could impart selectivity over BRD4(1) (Table 3), as exemplified by the *C*-2 neopentyl compound **156**. Compound **156** potentially exploits unfavourable steric interactions with the BRD4(1) binding pocket (e.g. W81 on the WPF shelf). The series was further optimised using a set of benzimidazole-forming reactions (Scheme 3). This yielded a set of 19 compounds which displayed selectivity for CBP over BRD4(1) (Table 4). The SAR again implied that bulky groups at *C*-2, and in particular the phenethyl group in compound **263**, were beneficial for CBP binding. The potency of the series was improved 10-fold from the starting point of compound **26**. Additionally, DSF results imply that the selectivity of the series for CBP over BRD4(1) improved. The LE and LiPE have suffered relative to the starting compound **26**. This has been driven by the increase in clogP (calculated partition coefficient), caused by the introduction of substitution on *N*-1 and *C*-2. However, this was necessary in order to get selectivity for CBP over BRD4(1). Compound **263** exemplifies the lead series which was selected for further optimisation.

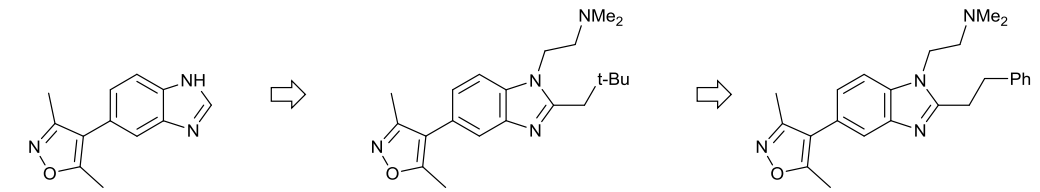

26 **156** **263**

	CBP ΔT_m 4.5 °C BRD4(1) ΔT_m 3.2 °C	CBP ΔT_m 6.3 °C BRD4(1) ΔT_m 2.9 °C
CBP IC_{50} 5.4 μM BRD4(1) IC_{50} 5.2 μM	CBP IC_{50} 1.6 μM BRD4(1) IC_{50} 15 μM	CBP IC_{50} 0.48 μM
clogP 1.9 CBP LiPE 3.4 CBP LE 0.46	clogP 4.4 CBP LiPE 1.3 CBP LE 0.31	clog P 4.9 CBP LiPE 1.4 CBP LE 0.31

Figure 29. Summary of development of fragment into lead compounds using parallel chemistry.

CHAPTER 4. CBP/P300 CHEMICAL PROBE: IMPROVING POTENCY AND SELECTIVITY

4.1 STRUCTURE OF COMPOUND **263** COMPLEXED TO CBP

In order to guide the optimisation of compound **263**, an X-ray crystal structure of the ligand bound to the CBP BRD (residues 1081-1197) was obtained (Figure 30). The structure revealed that the dimethylisoxazole ring forms the expected hydrogen-bonds to N1168 and to Y1125 via a water molecule. In addition, the benzimidazole *N*-3 nitrogen, which possesses a free lone pair, is hydrogen-bonded to another well-conserved water molecule. However, the crystal structure did not show any significant interactions of the *N*-1 and *C*-2 substituents. The phenyl ring of **263** is situated near the side-chains of L1120 and L1121, but the dimethylamino group of **263** only appears to be interacting with bulk water, which does not explain the increase in potency and selectivity for CBP achieved through incorporation of this group.

The orientation of these side-chains may be influenced by packing artefacts, whereby the ligand interacts with atoms from a neighbouring asymmetric unit.[270, 271] Therefore, compound **263** was also docked into the CBP structure to suggest alternative binding modes which may help explain the potency and selectivity of the ligand. Figure 30C depicts an overlay of a docked conformation of compound **263** with the experimentally determined co-crystal structure. In the docked structure, the benzimidazole of **263** is bound in a flipped conformation, and the *N*-1 and *C*-2 substituents occupy opposite areas of the protein compared to the crystal structure. If this binding mode is indeed important, it was postulated that a cation-π interaction could be formed between the aryl ring on the *C*-2 substituent of **263** and R1173. The *N*-1 substituent of **263** may also be able to interact with R1173, if it is oriented as in the crystal structure in Figure 30B. Alternatively, if the docked

structure is more representative of the solution-phase binding, then it is possible that moieties on *N*-1 could interact with the conserved water molecules in the channel region. Therefore, analogues of compound **263** which varied at positions *C*-2 and *N*-1 were designed in order to find functional groups with optimal interactions with the CBP BRD.

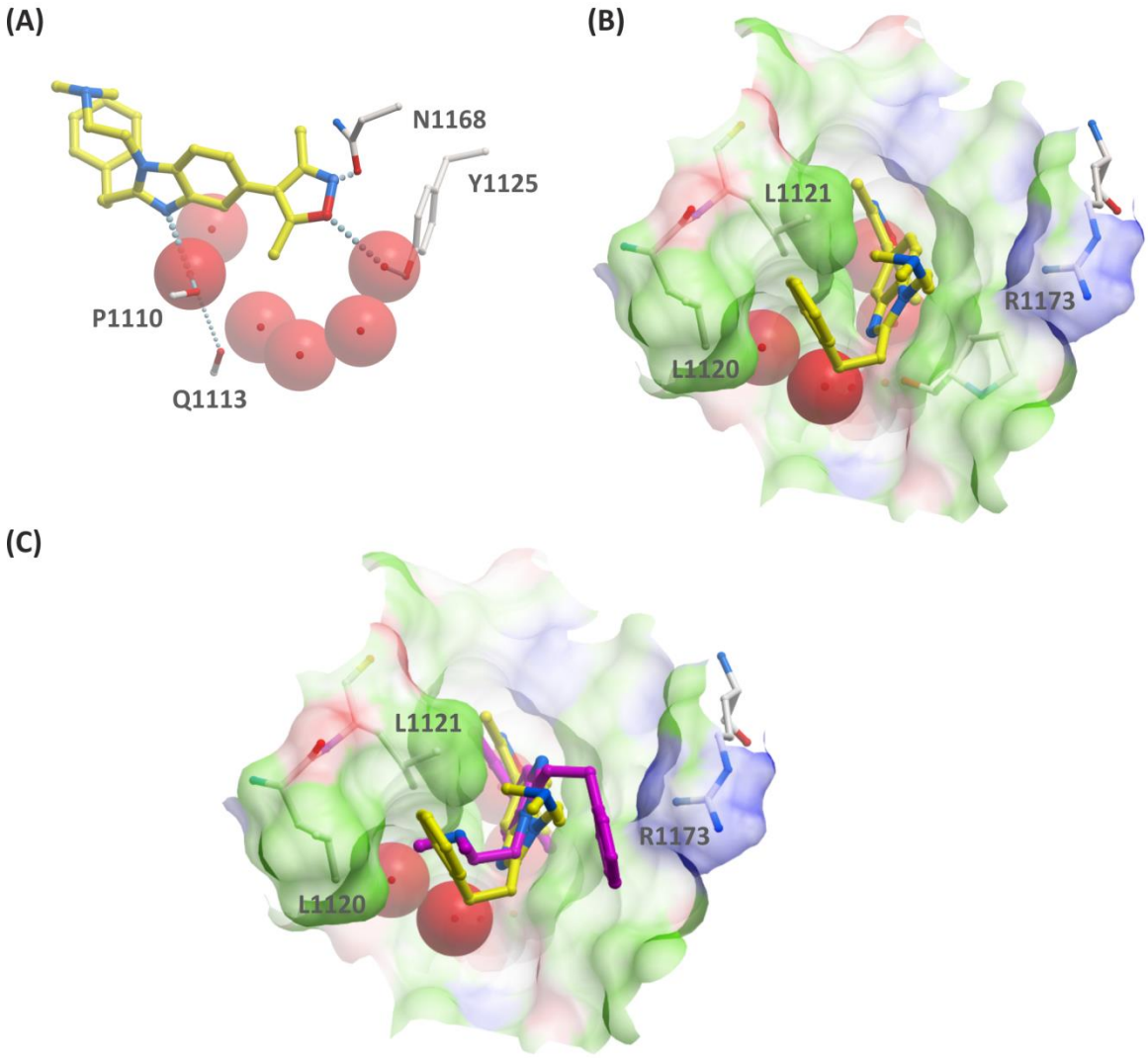

Figure 30. (A) View from X-ray crystal structure of **263** (carbon=yellow) bound to CBP BRD, showing hydrogen-bond between isoxazole oxygen atom and N1168 side-chain (3.35 Å) and a water-mediated hydrogen-bond from isoxazole nitrogen to Y1125 (3.02 Å from isoxazole oxygen to water).* There are also two water-mediated hydrogen-bonds between the *N*-3 of the benzimidazole P1110 and Q1113 (3.08 Å from benzimidazole nitrogen to water). (B) View from the same structure as (A) showing pocket surface and selected residues on the edge of the pocket near the benzimidazole *N*-1 and *C*-2 moieties. (C) As in (B) with overlay of **263** docked structure (carbon= magenta). In the docked structure the ligand is bound in a flipped binding mode compared to the co-crystal structure with the *N*-1 and *C*-2 moieties occupying the opposite regions. In the docked structure, the phenyl ring is oriented towards the R1173 side-chain.

*Crystallography and refinement of crystallographic data was carried out by Sarah Picaud and Panagis Filippakopoulos (SGC).

4.2 *C*-2 ANALOGUES

A series of analogues of compound **263** was designed where the *C*-2 aryl ring was varied to introduce electron-donating and electron-withdrawing substituents. Although the methodology used thus far allowed for late-stage variation of the *C*-2 substituent, there were insufficient aldehydes available with the desired functionality. Therefore other synthetic approaches were pursued (Scheme 4). Nitroaniline **217** was reduced to phenylenediamine **271** using sodium dithionite, then **271** was reacted with triethyl orthoacetate to furnish 2-methyl substituted benzimidazole **272**. Compound **272** underwent a Knoevenagel condensation with an aryl aldehyde at high temperature to yield an unsaturated intermediate **273**, which was hydrogenated to give the target compound **274**.[272] Alternatively, lateral lithiation of compound **272** with *n*-BuLi, followed by quenching with benzylic halides yielded target compounds (**275**-**280**).[273] Phenylenediamine **271** was also coupled with carboxylic acids under peptide coupling conditions, then cyclised by heating in acetic acid to yield products **281**-**283**.

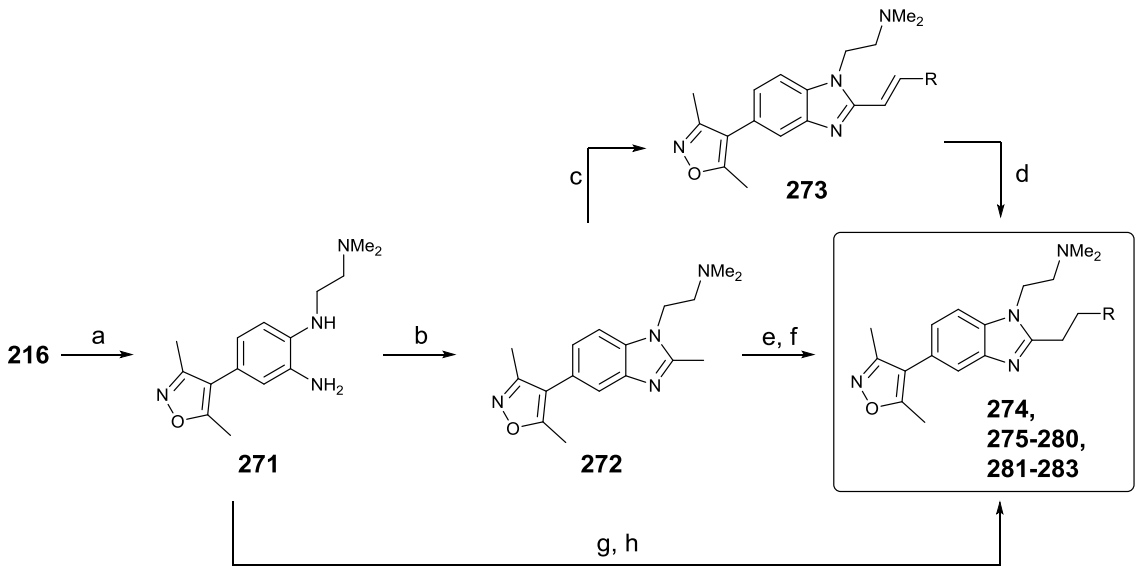

Scheme 4. Synthesis of *C*-2 aryl variants. Reagents and conditions: (a) $Na_2S_2O_4$, H_2O, EtOH, 80 °C (67%); (b) $CH_3(OEt)_3$, EtOH, 60 °C, (80%); (c) ArCHO, Ac_2O, chlorobenzene, MW, 250 °C (28%); (d) H_2 (1 atm), 10% Pd/C, AcOH (20%); (e) *n*-BuLi, THF, -78 °C; (f) RCH_2Br, -78 °C RT (16-50%); (g) $ArCH_2CH_2CO_2H$, HBTU, DIPEA, DMF; (h) AcOH, MW 180 °C (49-69% over two steps).

The screening results for the aryl analogues are shown in Table 5. The results indicated that, in general, compounds with electron-donating substituents (**274**, **281**-**283**) and halogens

(**275**-**277**) were more potent than those containing electron-withdrawing nitrile substituents (**278**-**280**). The AlphaScreen data indicated that the 3-methoxy analogue **281** was the most potent of this set (IC_{50} 0.23 μM), whilst the 4-chloro analogue **277** was also potent in AlphaScreen (IC_{50} 0.36 μM) and DSF (ΔT_m 6.7 °C). All analogues showed weak potency against BRD4(1), confirming that *C*-2 arylethyl substituents imparted selectivity for CBP over BRD4(1). Attention now turned to the *N*-1 position of the benzimidazole core, with a view to combining the best *N*-1 and *C*-2 moieties.

Table 5. SAR for CBP and BRD4(1) binding as determined by AlphaScreen and DSF for *C*-2 arylethyl analogues.

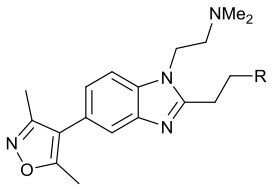

		AlphaScreen IC_{50} (μM)[*]		*CBP Selectivity*	*DSF ΔT_m (°C)*[*]	
Cmpd	*R*	*CBP*	*BRD4(1)*	*(-fold)*	*CBP*	*BRD4(1)*
274	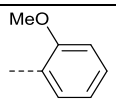	1.3 (1)	6.6 (1)	5.1	2.7 ± 0.72 (2)	1.5 (1)
281	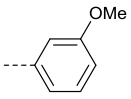	0.23 (1)	3.1 (1)	13	4.0 (1)	1.9 (1)
282	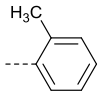	0.38 (1)				
283	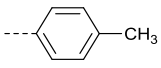	0.30 (1)				
275	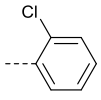	0.64 (1)			5.3 ± 0.039 (4)	2.5 ± 0.075 (2)
276	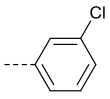	0.82 (1)	23 (1)	28	5.4 ± 0.030 (4)	1.6 ± 0.14 (2)

Cmpd	R	AlphaScreen IC_{50} (μM)* CBP	AlphaScreen IC_{50} (μM)* BRD4(1)	CBP Selectivity (-fold)	DSF ΔT_m (°C)* CBP	DSF ΔT_m (°C)* BRD4(1)
277	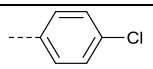	0.36 (1)			6.7 ± 0.14 (4)	1.9 ± 0.040 (2)
278	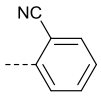	0.88 (1)	19 (1)	22	3.3 ± 0.23 (3)	1.4 ± 0.0050 (2)
279	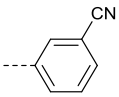	1.4 (1)	8.5 (1)	6.1	4.3 ± 0.060 (2)	2.2 (1)
280	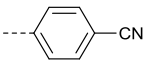	1.4 (1)	15 (1)	11	4.3 ± 0.37 (2)	2.0 (1)

*Mean value ± SEM (number of measurements).

4.3 *N*-1 ANALOGUES

In order to maximise the chances of making new interactions with the CBP BRD, a set of analogues was designed to include lipophilic, aryl, heteroaryl, polar and basic functionality on the *N*-1 position of the benzimidazole scaffold. Additionally, to further test the original hypothesis of gaining selectivity through acidic moieties binding to R1173 (see 3.2) acidic analogues were also included.

The synthesis of the non-basic *N*-1 analogues in Scheme 5 was similar to routes used for previously described target compounds. The original approach was to carry out the S_NAr reaction on **217** as the first step to yield bromo-nitro intermediates **284**-**286**. These were then coupled with compound **31** to give precursors (**287**-**289**), which were reduced and cyclised to give target compounds **290**-**292**. Although successful, this approach introduced the variation at an early stage, meaning synthesis of analogues was laborious. Therefore, a second route was also used where the S_NAr was carried out on **251** instead. Additionally, it was found that the benzimidazole-forming reaction could be combined with the S_NAr in a two-step, one-pot procedure. This gave a simple, rapid late-stage synthetic route to the *N*-1

analogues **293**-**298**. The esters of target compounds **296**-**298** were saponified to give carboxylic acid targets **299**-**301**.

The screening results from the compounds thus obtained are shown in Table 6. DSF results generally correlated well with those from AlphaScreen; due to the more rapid throughput of the DSF assay, DSF was now used as the primary binding assay. According to the DSF data, *N*-1 alkyl, ether and aryl/heteroaryl analogues **290**-**295** suffered in terms of CBP potency or selectivity for CBP over BRD4(1). Although the DSF results implied that ester-containing analogues (**296**-**298**) and acid-containing analogous (**299**-**301**) were mostly potent against CBP (with the exception of the less potent compound **299**, CBP ΔT_m 2.4 °C), the potency of these compounds was not as good as for the amine compound **263**. This suggested that it was not possible to achieve selectivity for CBP by interacting with R1173 through a salt-bridge interaction with *N*-1 substituents.

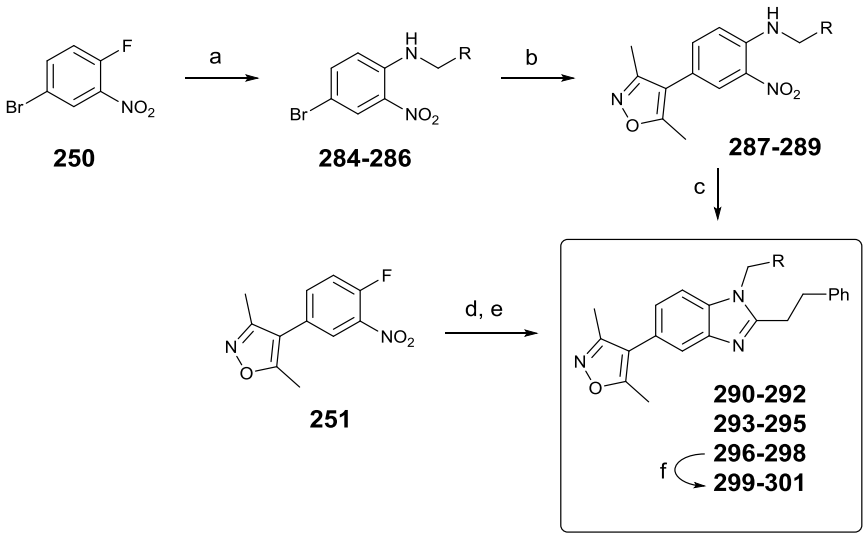

Scheme 5. Synthesis of N-1 variants. Reagents and conditions: (a) RCH_2NH_2, DIPEA, THF (29-75%); (b) **31** $Pd(dppf)Cl_2$, $NaHCO_3$, H_2O, DME, 80 °C (65-84%); (c) $PhCH_2CH_2CHO$, $Na_2S_2O_4$, H_2O, EtOH, DMSO, 80 °C (25-75%); (d) RCH_2NH_2, DMSO, 80 °C; (e) $PhCH_2CH_2CHO$, $Na_2S_2O_4$, H_2O, EtOH, DMSO, 80 °C (22-64%, over two steps); (f) LiOH, H_2O, MeOH (62-71%).

Table 6. SAR for CBP and BRD4(1) binding as determined by DSF and AlphaScreen assays for *N*-1 analogues.

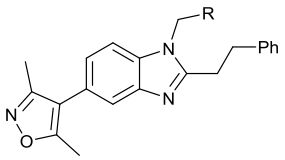

		DSF ΔT_m (°C)[*]		*AlphaScreen IC_{50} (μM)*[*]
Cmpd	*R*	*CBP*	*BRD4(1)*	*CBP*
290	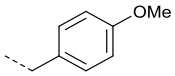	3.9 ± 0.14 (2)		1.4 ± 0.050 (2)
291	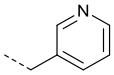	4.4 ± 0.16 (2)		2.0 ± 0.19 (2)
292	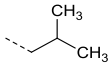	4.5 ± 0.20 (2)		3.5 ± 0.11 (2)
293		5.3 ± 0.21 (2)		3.9 ± 0.070 (2)
294		4.1 ± 0.36 (2)	1.9 (1)	2.5 ± 0.13 (2)
295	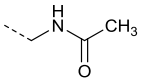	4.0 (1)	2.0 (1)	1.9 (1)
296		5.7 ± 0.23 (2)	0.61 (1)	2.7 (1)
297	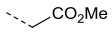	5.9 ± 0.44 (2)	1.4 (1)	3.6 (1)
298	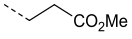	5.6 ± 0.12 (2)	1.2 (1)	3.3 (1)
299		2.4 (1)		1.1 (1)
300	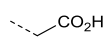	4.2 (1)		2.9 (1)
301	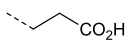	5.0 ± 0.24 (2)	1.3 (1)	3.3 (1)

[*]Mean value ± SEM (number of measurements).

Attention therefore turned to synthesising *N*-1 amine analogues, which would be closer to the structure of compound **263**. Attempted nucleophilic substitution of the chloro-

intermediate **302** with piperidine at high temperature failed to yield appreciable amounts of the amine product, instead giving mainly unreacted starting material (Scheme 6). It was therefore envisaged that these analogues could instead be accessed via a final-stage reductive amination. The dimethylacetal compound **303** was synthesised according to routes described for previous analogues, then deprotected by acid-promoted hydrolysis to yield the aldehyde precursor **304**. Reductive aminations furnished the targeted compounds **305-313**.

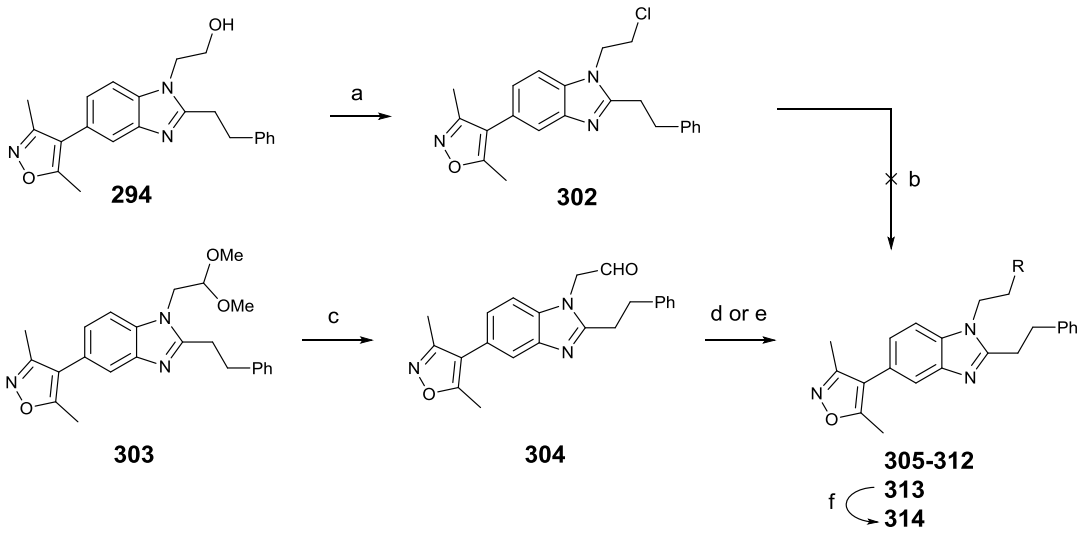

Scheme 6. *N*-1 Amine variation. Reagents and conditions: (a) $SOCl_2$, CH_2Cl_2 (95%); (b) Piperidine, KI, NMP, 140 °C; (c) CF_3CO_2H, H_2O, CH_2Cl_2, MW 150 °C (99%); (d) Amine (RH), $NaBH(OAc)_3$, AcOH, THF (35-86%); (e) Amine (RH), $NaCNBH_3$, AcOH, MeOH (42%); (f) F_3CCO_2H, (67%).

Gratifyingly, screening of the products thus obtained demonstrated that certain amino-analogues gave an improvement in potency when compared to dimethylamino compound **263** (Table 7). The azetidine analogue **305** lost potency for CBP (ΔT_m 0.27 °C), while pyrrolidine and piperidine analogues **306** and **307** were reasonably potent against CBP in DSF (ΔT_m 4.4 °C and 5.4 °C, respectively) and AlphaScreen (IC_{50} 0.57 μM and 0.84 μM, respectively). The morpholine-containing analogue **308** was particularly potent against CBP (ΔT_m 6.5 °C, IC_{50} 0.18 μM) and was 13-fold selective over BRD4(1). The remaining amine analogues, **309** - **314** were either less potent against CBP than compound **308**, or less selective for CBP over BRD4(1). Thus the morpholine moiety of compound **308** was regarded as the optimal amino substituent for future analogues.

Table 7. SAR for CBP and BRD4(1) binding as determined by DSF and AlphaScreen for *N*-1 amino analogues.

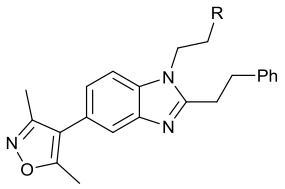

		DSF ΔT_m (°C)		*AlphaScreen IC_{50} (μM)*		*CBP selectivity*
Cmpd	*R*	*CBP*	*BRD4(1)*	*CBP*	*BRD4(1)*	*(-fold)*
305		0.27 ± 0.13 (3)	0.60 ± 0.076 (3)	460 (1)		
306		4.4 ± 0.15 (3)	2.6 ± 0.35 (3)	0.57 (1)		
307	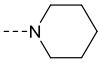	5.4 ± 0.45 (3)	2.7 ± 0.22 (3)	0.84 ± 0.57 (2)	9.1 (1)	11
308	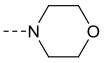	6.5 ± 0.18 (2)	2.7 ± 0.64 (3)	0.18 ± 0.041 (6)	2.4 ± 1.0 (7)	13
309	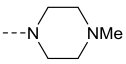	3.9 ± 0.17 (2)	2.1 ± 0.14 (3)	1.6 (1)		
310	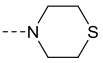	6.5 ± 0.12 (3)	4.0 ± 0.23 (3)	0.75 (1)		
311	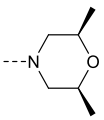	6.6 ± 0.20 (3)	3.9 ± 0.31 (3)	0.44 (1)		
312	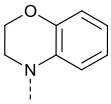	1.5 ± 0.083 (4)	0.20 ± 0.062 (3)			
313	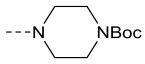	5.5 ± 0.010 (2)	2.2 (1)	1.2 (1)		
314	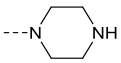	2.0 ± 0.24 (3)	1.2 ± 0.23 (3)	3.9 (1)		

*Mean value ± SEM (number of measurements).

4.4 FURTHER *C*-2 OPTIMSATION

With the preferred *N*-1 moiety selected, further *C*-2 analogues were prepared by dehydrative benzimidazole formation from suitable carboxylic acids and phenylenediamine **316** (Scheme 7). It was found that the coupling and dehydration steps could be performed

in one simple operation with the use of the dehydrating reagent, propylphosphonic anhydride (T3P), or under acidic conditions to yield targets **317**-**346**. In order to confirm if the SAR still followed the same trends as for the dimethylamino compound **263**, the targets were designed to include a variety of electron-donating and electron-withdrawing substituents. Additionally, disubstituted aryl groups and heterocycles were included in the targets.

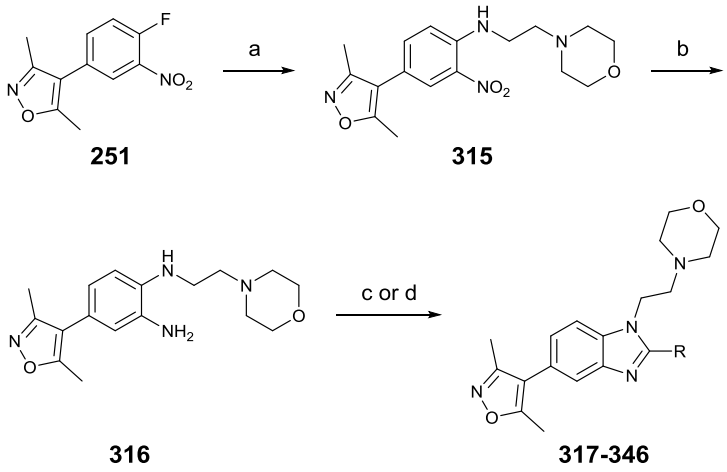

Scheme 7. *C*-2 Variation. Reagents and conditions: (a) 4-(2-Aminoethyl)morpholine, DIPEA, THF (94%); (b) $Na_2S_2O_4$, H_2O, EtOH, 80 °C (87%); (c) RCO_2H, T3P, EtOAc, reflux (31-62%); (d) RCO_2H, 6 M aq. HCl, MW 210 °C (16-55%).

The SAR shown in Table 8 correlated well with previously observed trends for *C*-2 analogues; electron-donating groups (e.g. compounds **317**-**321**) and halogens (e.g. compounds **323**-**325**) on the aryl ring were favourable for CBP potency, whereas electron-withdrawing groups were detrimental (e.g. compounds **328**-**330**). The 4-methoxy aryl compound **321** gave particularly encouraging CBP potency (ΔT_m 8.1 °C, IC_{50} 0.13 μM) and 20-fold selectivity over BRD4(1) according to AlphaScreen. For halogen substitution, the DSF results suggested that the 3-position of compound **324** was favoured for CBP potency (ΔT_m 7.1 °C). Disubstituted analogues which combined the 4-methoxy and 3-halogen moieties, compounds **335** and **337**, showed particularly high potency for CBP in DSF (ΔT_m 9.0 °C and 9.6 °C respectively) and AlphaScreen (IC_{50} 0.069 μM and 0.23 μM respectively). Additionally, compounds **335** and **337** showed good selectivity for CBP over BRD4(1). Out

of the heterocycles tested, the electron-rich indole compound **341** was best, with high potency against CBP (ΔT_m 8.9 °C, IC_{50} 0.052 μM) and selectivity for CBP over BRD4(1). Additionally, another disubstituted analogue **336** (CBP ΔT_m 8.1 °C, IC_{50} 0.083 μM) and the benzodioxole compound **338** (CBP ΔT_m 6.7 °C, IC_{50} 0.069 μM) also had a reasonable balance of potency and selectivity and were worthy of further investigation.

Table 8. SAR for CBP and BRD4(1) binding as determined by DSF and AlphaScreen for *C*-2 arylethyl analogues.

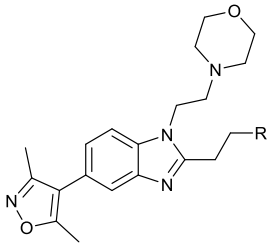

		DSF ΔT_m (°C)[*]		*AlphaScreen IC_{50} (μM)*[*]		*CBP selectivity*
Cmpd	*R*	*CBP*	*BRD4(1)*	*CBP*	*BRD4(1)*	*(-fold)*
317	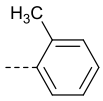	6.4 ± 0.30 (3)	3.8 ± 0.45 (3)	0.27 ± 0.033 (4)	1.7 ± 0.21 (2)	6.3
318	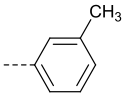	6.3 ± 0.23 (3)	2.7 ± 0.085 (2)	0.48 ± 0.088 (3)	2.3 ± 0.26 (2)	4.8
319	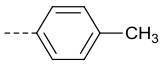	7.4 ± 0.21 (3)	3.8 ± 0.24 (3)	0.22 ± 0.033 (5)	1.8 ± 0.55 (3)	8.2
320	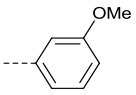	6.2 ± 0.22 (4)	2.4 (1)	0.39 ± 0.053 (4)	2.1 ± 0.26 (2)	5.4
321	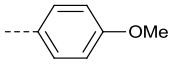	8.1 ± 0.27 (4)	2.4 ± 0.57 (4)	0.13 ± 0.037 (4)	2.6 ± 0.48 (4)	20
322	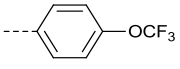	7.0 ± 0.17 (4)	2.3 ± 0.63 (3)	0.26 (1)	12 (1)	46
323	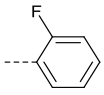	6.2 ± 0.31 (4)	2.6 ± 0.069 (3)	0.22 (1)	1.48 (1)	6.7
324	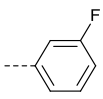	7.1 ± 0.39 (4)	2.8 ± 0.27 (3)			

		DSF ΔT_m (°C)*		AlphaScreen IC_{50} (μM)*		CBP selectivity
Cmpd	R	CBP	BRD4(1)	CBP	BRD4(1)	(-fold)
325	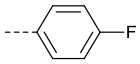	6.4 ± 0.092 (4)	3.1 ± 0.27 (3)	0.11 (1)	1.6 (1)	15
326	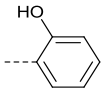	6.0 ± 0.70 (4)	2.1 ± 0.39 (5)	0.12 ± 0.058 (2)	1.4 ± 0.81 (4)	12
327	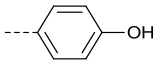	6.5 ± 0.32 (3)	2.8 ± 0.010 (2)	0.12 (1)	2.90 (1)	24
328	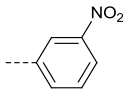	5.4 (1)	2.3 (1)	0.44 (1)		
329	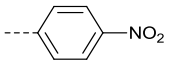	5.2 (1)	2.5 (1)	0.49 (1)		
330	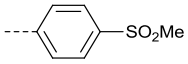	4.9 (1)	1.9 (1)	0.28 ± 0.11 (2)	3.6 (1)	13
331	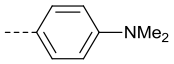	6.3 (1)	3.4 ± 0.10 (2)	0.18 ± 0.022 (2)	8.7 ± 4.6 (2)	48
332	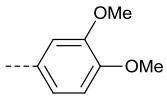	4.5 ± 0.54 (2)	1.9 ± 0.32 (2)	0.89 (1)		
333	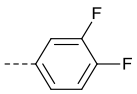	7.7 ± 0.13 (4)	3.2 ± 0.10 (3)			
334	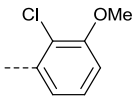	7.0 ± 0.15 (4)	2.6 ± 0.39 (3)			
335	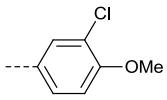	9.0 ± 0.27 (4)	1.9 ± 0.10 (3)	0.069 ± 0.0013 (2)	4.7 (1)	68
336	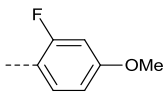	8.1 (1)	2.4 ± 0.1 (2)	0.083 ± 0.015 (2)	14 ± 6.2 (2)	170
337	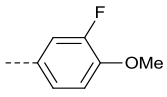	9.6 ± 0.17 (3)	3.2 ± 0.10 (2)	0.23 ± 0.21 (2)	31 (1)	130
338	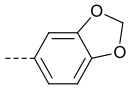	6.7 (1)	2.5 (1)	0.069 ± 0.017 (2)		
339	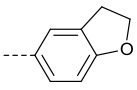	6.8 (1)	2.8 (1)	0.17 ± 0.031 (2)	3.3 (1)	19

		DSF ΔT_m (°C)[*]		*AlphaScreen IC_{50} (μM)*[*]		*CBP selectivity*
Cmpd	*R*	*CBP*	*BRD4(1)*	*CBP*	*BRD4(1)*	*(-fold)*
340		6.0 ± 0.47 (2)	3.4 ± 0.30 (2)	0.48 (1)		
341	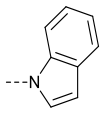	8.9 ± 0.17 (3)	2.8 ± 0.10 (2)	0.052 ± 0.021 (2)	2.7 (1)	52
342	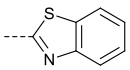	6.2 ± 0.52 (2)	3.1 ± 0.80 (2)	0.48 (1)		
343	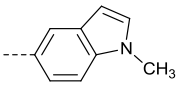	7.0 (1)	2.7 ± 0.045 (2)	0.18 ± 0.10 (2)	14 (1)	78
344	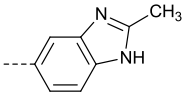	4.0 ± 0.31 (6)	2.5 ± 0.14 (4)	0.14 ± 0.14 (4)	6.7 ± 4.4 (4)	48
345	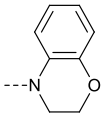	6.3 (1)	2.0 ± 0.015 (2)	0.13 (1)	1.1 (1)	8.5
346	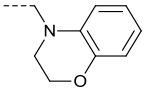	5.8 (1)	2.6 ± 0.040 (2)	0.30 ± 0.078 (2)	9.7 ± 4.0 (2)	32

[*]Mean value ± SEM (number of measurements).

In order to ascertain if any of these compounds met the targeted probe criteria for potency and selectivity, isothermal titration calorimetry (ITC) was used to obtain the dissociation constant (K_d) for the most promising analogues against CBP and BRD4(1) (Table 9). The unsubstituted phenyl analogue **308** was reasonably potent against CBP (K_d 0.32 μM), and was only 2.9-fold selective over BRD4(1). The 4-methoxyphenyl compound **321** was more potent against CBP (K_d 0.050 μM), and was 11-fold selective over BRD4(1). Thus, compound **321** was the first to meet the targeted chemical probe criteria in terms of *in vitro* affinity. However, the selectivity of compound **321** for CBP over BRD4(1) needed to be improved in order to meet the targeted probe criteria. The benzodioxole compound **338** was also potent (K_d 0.098 μM) but only 4.7-fold selective over BRD4(1). The disubstituted and indole compounds **335**, **337** and **341** were even more potent against

CBP, (K_d 0.022-0.030 μM) and were significantly more selective over BRD4(1) (17-22 fold). Although the selectivity of analogues **335**, **337** and **341** was a significant improvement over compound **338**, the selectivity was still insufficient to meet the targeted criteria.

The energy terms from the ITC indicated that the binding of this series was mostly enthalpically driven, as all compounds measured a large negative enthalpic contribution (ΔH). The entropic contribution (-TΔS) to CBP binding seemed to only be significant for the less selective compound **308**. This suggested that the binding to CBP was due to strong intermolecular interactions and not down to entropically driven non-specific binding.[274]

Table 9. Determination of CBP and BRD4(1) binding constants by ITC for selected analogues.

	CBP			*BRD4(1)*			*CBP selectivity (-fold)*
Cmpd	K_d *(μM)*	*ΔH (kcal/mol)*	*-TΔS (kcal/mol)*	K_d *(μM)*	*ΔH (kcal/mol)*	*-TΔS (kcal/mol)*	
308*	0.32	-5.76	-2.90	0.94	-5.86	-2.51	2.9
321*	0.050	-9.70	0.0674	0.55	-8.74	-0.501	11
335	0.028	-9.63	-0.346	0.48	-8.02	-0.331	17
337	0.022	-10.8	0.760	0.44	-9.99	1.67	20
338	0.098	-9.01	-0.242	0.46	-9.34	-1.02	4.7
341	0.030	-9.30	-0.638	0.66	-9.34	1.24	22

In order to confirm that this series of compounds also inhibited p300, compound **308** was tested against p300 by ITC. The results summarised in Table 10 show that the K_d and energy terms were similar to those for CBP inhibition, which was expected from their high sequence similarity (see section 2.1).

*Carried out by Sarah Picaud (SGC).

Table 10. Determination of p300 binding constant by ITC for compound **308**.*

Cmpd	*p300 K_d (μM)*	*p300 ΔH (kcal/mol)*	*p300 -TΔS (kcal/mol)*
308	0.35	-6.09	-2.51

4.5 SUMMARY

In this section, optimisation of the *C*-2 and *N*-1 substituents of the benzimidazole core has been described, which led to improvements in potency and selectivity. Figure 31 summarises the progress made. Initially, *C*-2 aryl analogues were synthesised via lateral lithiation, Knoevenagel condensation/hydrogenation, or dehydrative benzimidazole formation (Scheme 4). The SAR suggested that electron-donating and halogen-containing analogues were preferred on the aryl ring (Table 5). *N*-1 Analogues were synthesised, including a set of amine variants which were accessed via late-stage reductive aminations (Schemes 5 and 6). Screening of these compounds implied that the morpholine of compound **308** was the optimal amine group in terms of potency and selectivity (Tables 6 and 7). Whilst retaining this morpholine feature, *C*-2 analogues were again prepared by dehydrative benzimidazole formation (Scheme 7); the SAR implied that electron-rich and halogenated aryl rings were favoured (Table 8). The particular substitution pattern of the aryl ring which proved optimal was the 3-halo-4-methoxy pattern of compounds **335** and **337**, which were particularly potent and selective. The indole of compound **341** was also a potent electron-rich aromatic group. Compounds with ΔT_m >9 °C were obtained with <50 nM binding by AlphaScreen, which also measured high selectivity over BRD4(1). However, ITC screening revealed that the best compounds were only around 20-fold selective, which is short of the targeted 30-fold probe selection criterion (Table 9). Overall, the potency and LiPE of the series, exemplified by analogues such as **341**, was significantly improved from the lead

* Carried out by Sarah Picaud (SGC).

compound **263** (Figure 31). However, further optimisation of the selectivity was still required to meet the targeted probe criteria.

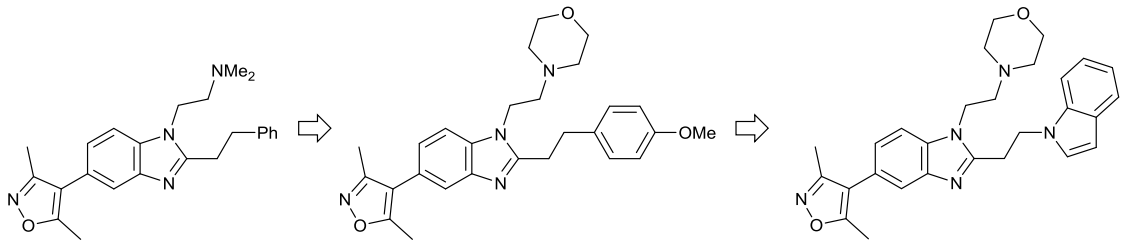

263	**321**	**341**
CBP ΔT_m 5.2 °C	CBP ΔT_m 8.1 °C	CBP ΔT_m 8.9 °C
BRD4(1) ΔT_m 0.58 °C	BRD4(1) ΔT_m 2.4 °C	BRD4(1) ΔT_m 2.8 °C
CBP IC_{50} 0.48 μM	CBP K_d 0.050 μM	CBP K_d 0.030 μM
	BRD4(1) K_d 0.55 μM	BRD4(1) K_d 0.66 μM
CBP LE 0.31	CBP LE 0.30	CBP LE 0.30
CBP LIPE 1.4	CBP LIPE 2.9	CBP LIPE 2.7

Figure 31. Summary of the optimisation of lead compound **263** to potent and selective CBP inhibitors such as compound **341**.

CHAPTER 5. CBP/P300 CHEMICAL PROBE: STRUCTURE-GUIDED SELECTIVITY OPTIMISATION

5.1 STRUCTURE-GUIDED DESIGN

In order to investigate features which could be exploited to improve the selectivity of the series, compound **308** was crystallised in complex with both the CBP and BRD4(1) BRDs (Figure 32). In the CBP X-ray structure, compound **308** is bound in a flipped binding-mode in comparison to the structure of **263** obtained (Chapter 4, Figure 30). The binding mode is much more similar to the docking of compound **263** (Chapter 4, Figure 30C). The polar morpholine ring of compound **308** is positioned in a relatively hydrophilic channel region, lined by residues L1109, P1110, Q1113 and a crystallographically conserved water molecule. The aryl ring of compound **308** is oriented close to the side-chain of L1120. With no strong interactions formed, the positioning of the aryl substituent did not help explain the potency of these analogues. Nor did the lipophilic interaction with L1120 explain the SAR obtained for this moiety, which indicated that electron-donating substituents were preferred. As for the structure of compound **263** complexed to CBP, it was again questioned if crystallographic artefacts could have led to a structure which is not representative of the binding of the ligand in solution. Additionally, the positioning of the flexible *N*-1 and *C*-2 aryl groups of **308** was poorly defined (Figure 32A). Nevertheless, the structure of compound **308** complexed with CBP was compared to the equivalent structure of **308** complexed with BRD4(1) in order to suggest areas which could be exploited to improve selectivity.

A structure of compound **308** complexed with BRD4(1) revealed that the ligand binds in a flipped binding mode where the benzimidazole *N*-3 nitrogen is hydrogen-bonded via a water molecule to the carbonyl of P82 and to the amide side-chain of Q85. If this binding-mode is important for BRD4(1) potency then it suggests that replacement of the

benzimidazole core with a heterocycle which does not possess a hydrogen-bond donor in this position could improve selectivity for CBP.

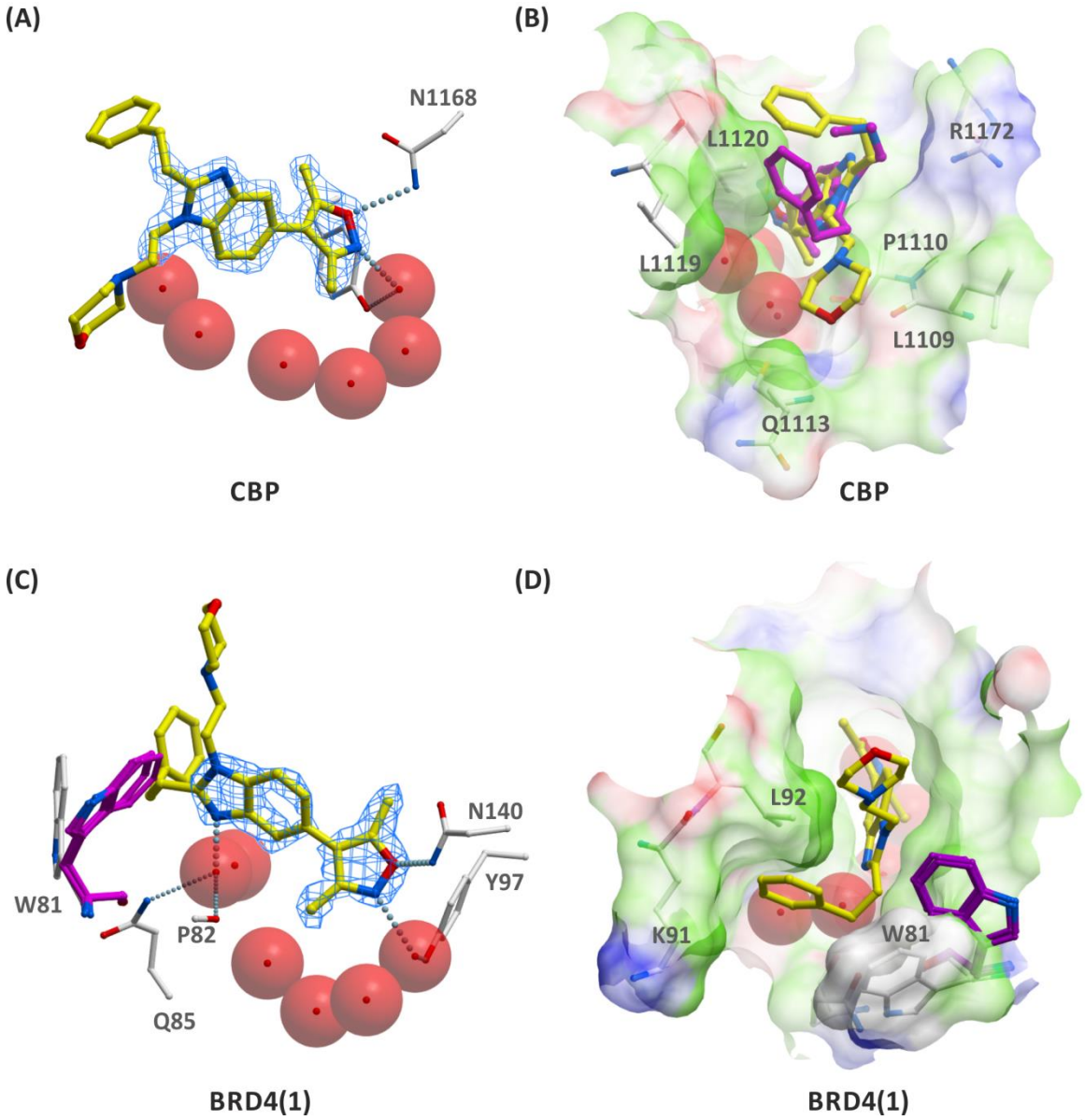

Figure 32. Views from X-ray crystal structure **308** complexed to CBP (PDB 4NR5) and BRD4(1) (PDB 4NR8).* (A) View from compound **308** complexed to CBP showing hydrogen-bonding between isoxazole oxygen atom and N1168 (3.02 Å), and isoxazole nitrogen and a water molecule (2.75 Å). The 2Fo-Fc ligand map (σ 2.0) is shown as a blue mesh. (B) View from compound **308** complexed to CBP showing surface of binding pocket and selected residues in close proximity to the benzimidazole *N*-1 and *C-2* substituents. Compound **263** is overlaid for comparison (carbon = magenta). (C) View from compound **308** complexed to BRD4(1) showing hydrogen-bonding between isoxazole oxygen atom and N140 (3.05 Å), and isoxazole nitrogen and a water molecule (2.72 Å). Water mediated hydrogen-bonds from the benzimidazole of **308** *N*-3 to Q85 and the carbonyl of P82 are also shown (3.54 Å from **308** benzimidazole *N*-3 to water molecule). W81 is shown overlaid with the same side-chain from published ligand-bound X-ray structures of BRD4(1) (carbon = magenta) (PDB 3MXF, 4E96, 4C67);[269, 275, 276] The 2Fo-Fc ligand map (σ 2.0) is shown as a blue mesh. (D) View from compound **308** complexed to BRD4(1) showing surface of binding pocket and selected residues in close proximity to the benzimidazole *N*-1 and *C-2* substituents. W81 is again shown from other structures for comparison (carbon = magenta).

*Crystallography carried out by Sarah Picaud (SGC). Refinement of crystallographic data was carried out by Panagis Filippakopoulos (SGC). The crystallisation screen for the BRD4(1) complex was carried out by the author.

It was also envisaged that the binding mode of compound **308** in CBP could be favoured through the introduction of a hydrogen-bonding motif on the benzimidazole. For example, a hydroxyl group could form a hydrogen bond to one of the well conserved waters in the CBP ZA channel (Figure 33). Stabilising the CBP binding mode could increase the CBP selectivity over BRD4(1) through an increase in CBP potency.

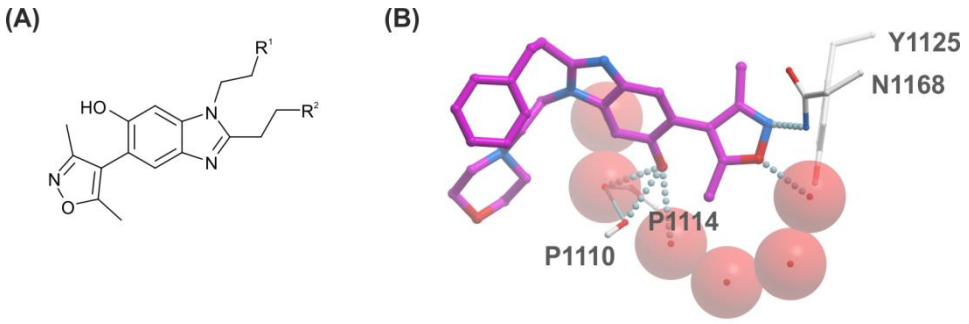

Figure 33. Postulated 6-hydroxybenzimidazole targets. (B) Docking of a 6-hydroxybenzimidazole target into CBP BRD. Possible hydrogen-bonds between the phenolic OH and waters, and between the phenol and the backbone carbonyl oxygen of P1110, are shown.

Additionally, in BRD4(1) the *C*-2 phenethyl group of compound **308** is positioned in a hydrophobic region of the ZA loop and partly occupies the shelf region. The structure also revealed a shift in the position of W81 relative to the usual position observed in reported ligand-bound structures, presumably to accommodate the *C*-2 phenethyl group of **308** (Figure 32C, D).[265, 271, 272] This difference could be exploited to design more selective compounds. For example, if one of the two methylenes which link the benzimidazole from the *C*-2 position to the aryl group were replaced with an ether linkage, the resultant increase in polarity could disfavour binding to the hydrophobic region of BRD4(1). Compounds with reduced conformational flexibility in the *C*-2 linker moiety may also hinder binding to BRD4(1), due to the reduced ability of such compounds to avoid steric clashes with side-chains of residues such as W81. Figure 34 summarises the structure-guided strategies adopted in order to improve selectivity, based on comparison of the CBP and BRD4(1) ligand-bound structures.

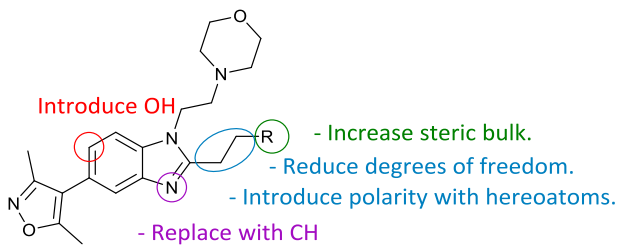

Figure 34. Summary of structure-guided design strategies for improving selectivity for CBP over BRD4(1).

5.2 INDOLE SYNTHESIS

The synthesis of an indole analogue was based on a reported base-promoted cyclisation of phosphorus ylides with amides (Scheme 8).[277] 3-Bromobenzylbromide **347** was nitrated to give nitro compound **348**.[278] The bromide in compound **348** was then substituted with PPh_3 to yield phosphonyl bromide **349**. Reduction with Zn/AcOH furnished aniline **350** which was acylated to give the precursor to the indole, **351**. The indole forming reaction was achieved by heating compound **351** with KO*t*-Bu under microwave irradiation to yield compound **352**. Compound **352** was alkylated under forcing conditions to give the precursor **353** which was cross-coupled to yield the desired indole analogue **354**.

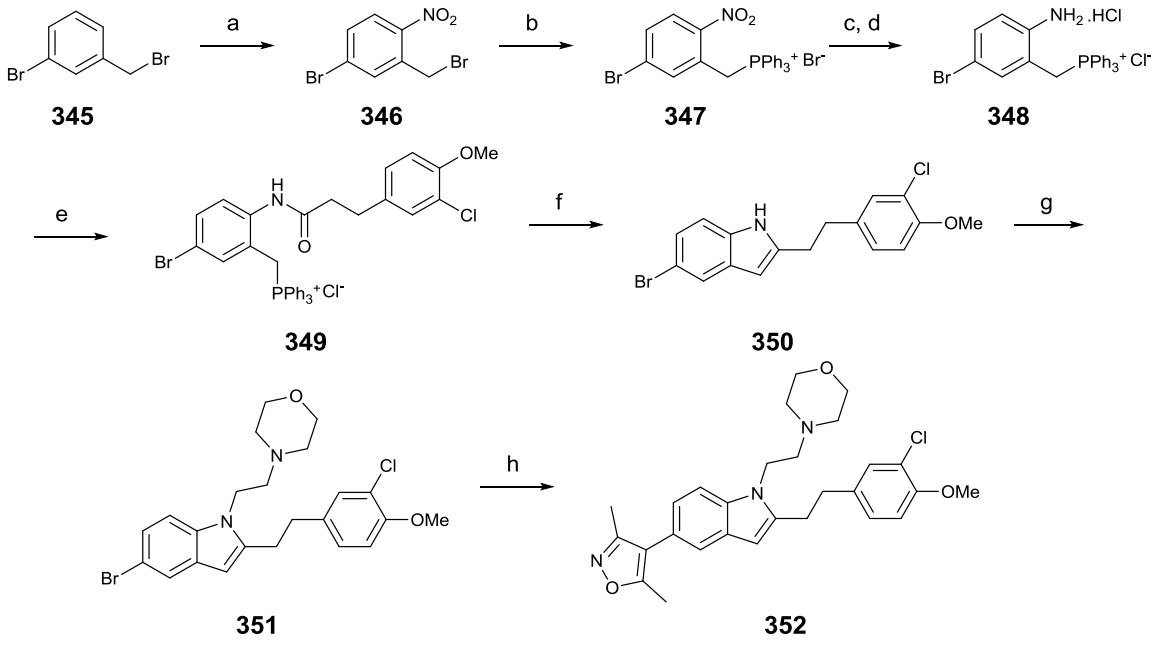

Scheme 8. Synthesis of indole analogue. Reagents and conditions: (a) *conc.* HNO_3, *conc.* H_2SO_4, 0 °C, 39%; (b) PPh_3, $CHCl_3$, quant.; (c) Zn/AcOH; (d) HCl, quant. over 2 steps; (e) 3-(3-chloro-4-methoxyphenyl)propanoyl chloride, DMF, pyridine, 56%; (f) KO*t*-Bu, toluene, MW, 130 °C, 56%; (g) 4-(2-chloroethyl)morpholine hydrochloride, NaH, KI, DMF, 80 °C, 24%, (h) 3,5-Dimethylisoxazole-4-boronic acid pinacol ester, $Pd(dppf)Cl_2$, $NaHCO_3$, DME/H_2O, 43%.

5.2 SYNTHESIS OF ETHER-LINKED ANALOGUES

Scheme 9 shows attempts at synthesising ether-linked targets via a chlorinated precursor. Treatment of alcohol **355** with $SOCl_2$ did not give the desired product, so this was instead synthesised directly by condensation of phenylenediamine **316** with chloroacetic acid (Scheme 9). However, reaction of the chloro-compound **356** with nucleophiles failed to give the expected products, instead yielding alkene **357** as the major product.

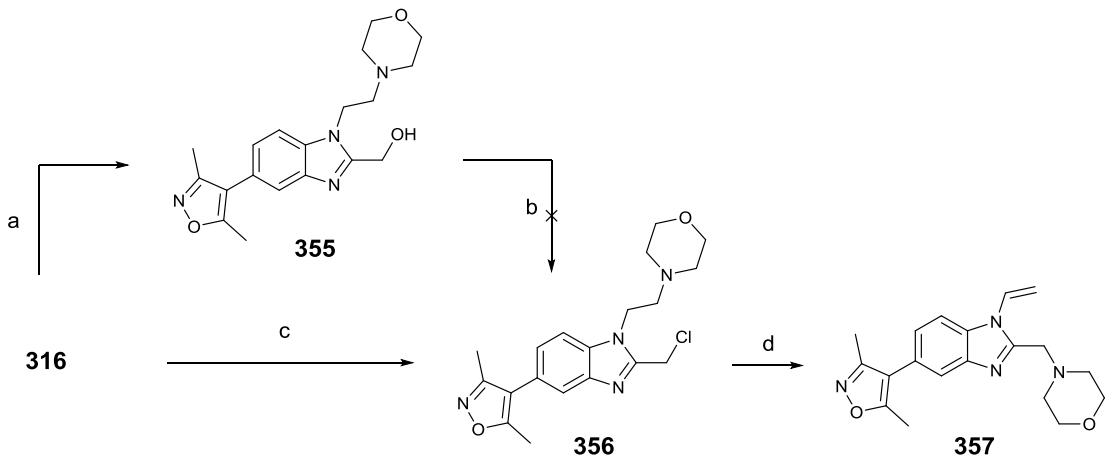

Scheme 9. Attempted synthesis of heteroatom linked targets. Reagents and conditions: (a) 2-Hydroxyacetic acid, 6 M aq. HCl, MW, 180 °C (62%); (b) $SOCl_2$, CH_2Cl_2; (c) Chloroacetic acid, 6 M aq. HCl, 100 °C (14%); (d) 3-Chloro-4-methoxyaniline, K_2CO_3, DMF (41%).

A similar problem arose with the use of a 2-chlorobenzimidzole intermediate (Scheme 10). Reaction of **316** with CDI afforded compound **358**, which was chlorinated with $POCl_3$ to give compound **359**. Compound **359** did not react as initially expected with nucleophiles, but instead gave the alkene **360** (Scheme 10). A possible mechanism for the formation of the alkene by-products is shown in Scheme 11. In each case, an intramolecular substitution reaction by the morpholine nitrogen gives quaternised intermediates. Base-promoted E2 elimination then gives the observed by-products. Both of these reactions represent novel routes to these aminobenzimidazoles, and the by-products were considered worthy of primary screening as inhibitors. However, this meant that alternative routes to the desired targets needed to be investigated.

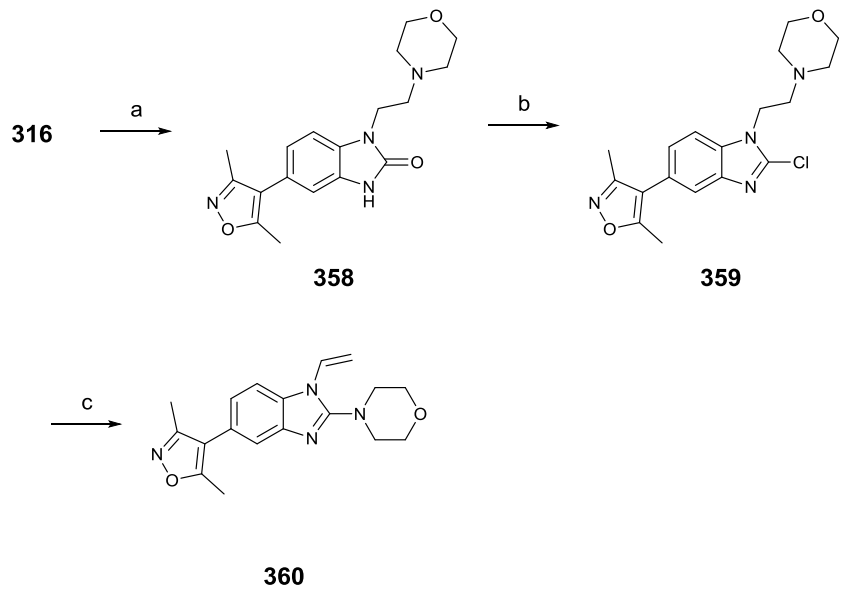

Scheme 10. Attempted synthesis of heteroatom linked targets. Reagents and conditions: (a) CDI, THF, 78%; (b) $POCl_3$, MeCN, reflux (55%); (c) 4-Methoxybenzyl alcohol, KOH, DMSO, 70 °C (38%).

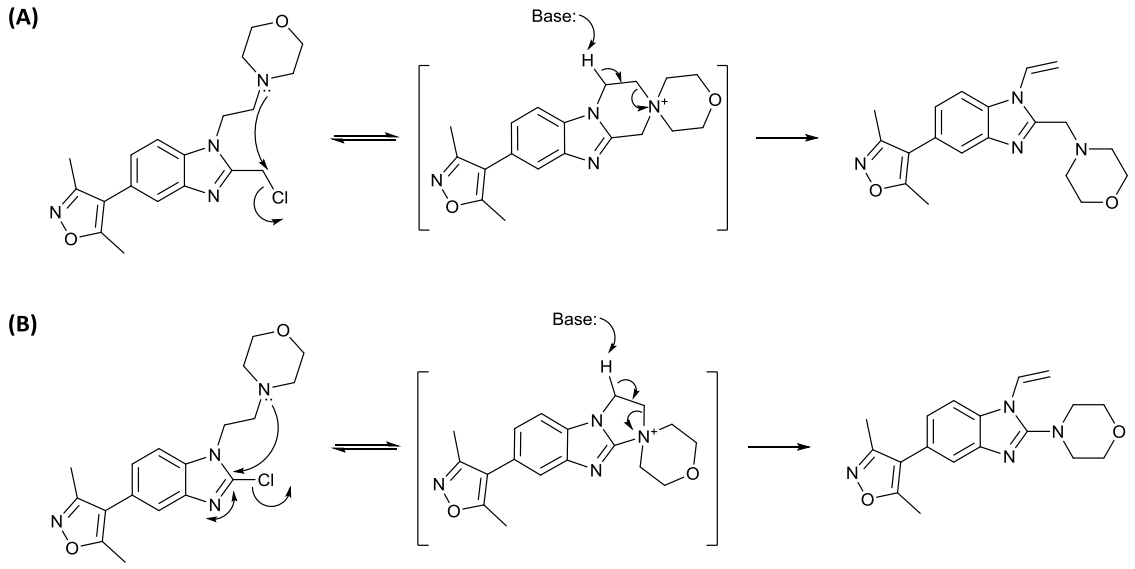

Scheme 11. Postulated mechanism for by-product formation from chlorinated precursors.

The successful synthesis of *O*-linked targets is shown in Scheme 12. Modified Mitsunobu conditions were used to form ether **361** from the alcohol precursor **355**.[279] Alkylation of the cyclic urea **358** tended to be highly selective for the undesired *N*-alkylated isomer. However, the use of Ag_2CO_3 as base helped to shift the ratio of isomers towards the desired *O*-alkyalted product **362**, which could then be separated from the *N*-alkylated isomer.[280-283]

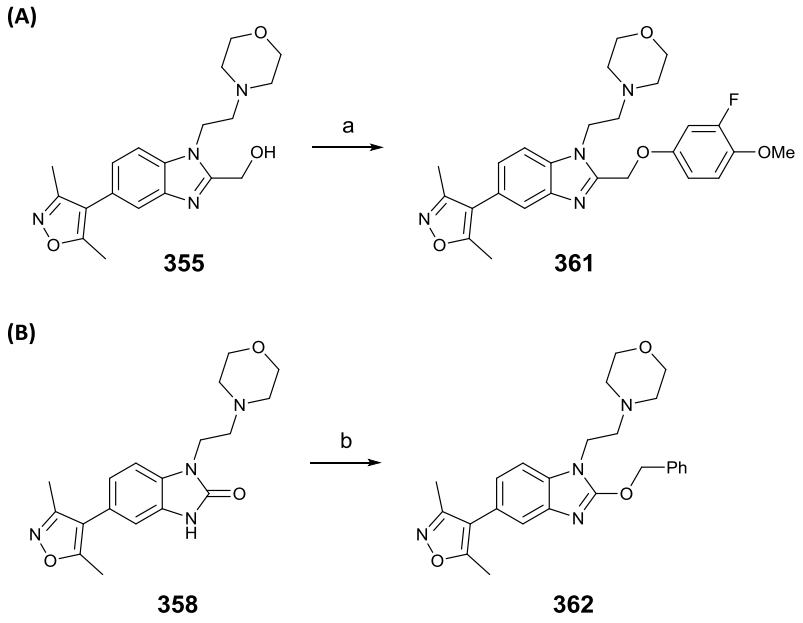

Scheme 12. Synthesis of *O*-linked targets. Reagents and conditions: (a) 3-Fluoro-4-methoxyphenol, azodicarbonyldipiperidine (ADDP), P(*n*-Bu)$_3$, CH_2Cl_2, 67%; (b) BnBr, Ag_2CO_3, toluene, 80 °C (18%).

The 6-hydroxybenzimidazole **367** was synthesised according to Scheme 13. The synthesis started from the difluoro aryl compound **363**, which underwent S_NAr to give compound **364**, and Suzuki cross-coupling to give compound **365**. Compound **365** was reduced and cyclised to the fluoro-precursor **366**, which underwent S_NAr hydrolysis to yield hyroxybenzimidazole target compound **367**.

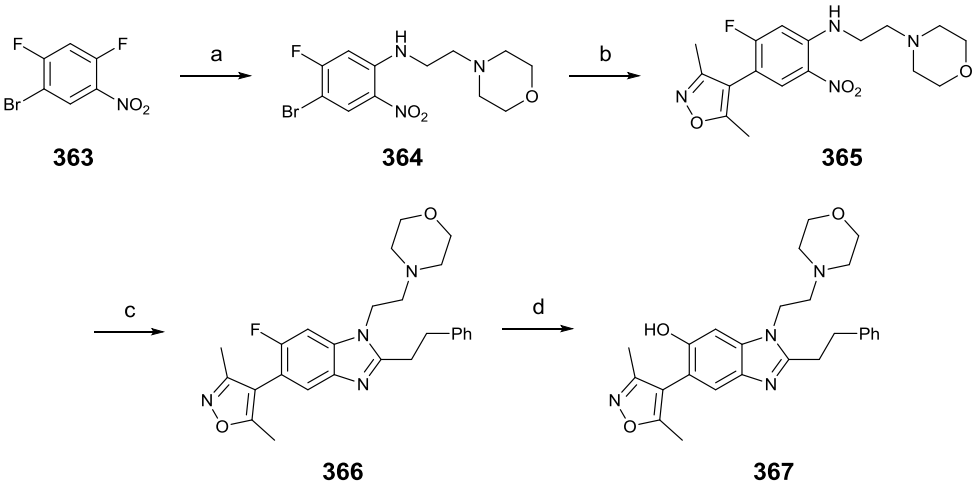

Scheme 13. Synthesis of 6-substituted analogues. Reagents and conditions: (a) 4-(2-Aminoethyl)morpholine, DIPEA, THF, 0°C-RT (66%); (b) 3,5-Dimethylisoxazole-4-boronic acid pinacol ester, Pd(dppf)Cl_2, $NaHCO_3$, DME/H_2O (16%); $PhCH_2CH_2CHO$, $Na_2S_2O_4$, H_2O, EtOH, DMSO, 80 °C (quant.); (d) KOH, H_2O, DMSO, 80 °C (71%).

Analogues with conformationally constrained groups on the *C*-2 position, compounds **368-377**, were prepared by dehydrative cyclisation of the phenylenediamine intermediate **316** according to the methods previously described (Chapter 4, Scheme 7).

5.3 SCREENING RESULTS FOR BENZIMIDAZOLE CORE AND *C*-2 LINKER ANALGOUES

As hoped, indole **354** was completely inactive against BRD4(1) (ΔT_m < 1 °C) (Table 11). Unfortunately compound **354** was also not very potent against CBP (ΔT_m 2.0 °C). This implies that although the crystal structure of **308** complexed to CBP shows no hydrogen-bond to the protein backbone, interaction of the electron-poor benzimidazole of compound **308** with the CBP protein is favoured over the electron-rich indole of compound **354**. Although, the 6-hydroxy group of compound **367** was tolerated (ΔT_m 5.4 °C, 0.35 μM) there was no improvement in potency compared to the unsubstituted analogue **308** (ΔT_m 6.5 °C, 0.18 μM). Of the ether-linked analogues, compound **361** was encouraging, as it appeared to be potent (ΔT_m 6.8 °C, IC_{50} 0.13 μM) and >150-fold selective over BRD4(1) by AlphaScreen. However, the CBP K_d for compound **361** was measured at only 0.41 μM by ITC (Table 12. Additionally, compound **361** was only 4-fold selective over BRD4(1).

Disappointingly, most conformationally constrained analogues **368-377** showed no improvement in terms of potency and selectivity; indeed, the selectivity was invariably worse for these compounds. The most encouraging compound of this set was the racemic compound **370** (ΔT_m 8.9 °C, IC_{50} 0.049 μM), which may warrant further testing of the single enantiomers. In the absence of a route to reasonable quantities of the enantiomers of compound **370**, attention shifted to analogues of the *N*-1 linker, where in a similar approach to *C*-2 substitution, conformational constraints were designed to improve selectivity for CBP for BRD4(1).

Table 11. SAR for CBP and BRD4(1) binding as determined by DSF and AlphaScreen assays for indole analogue, constrained/polar *C*-2 linker analogues and 6-substituted analogues.

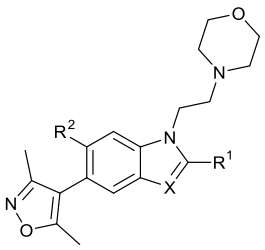

				*DSF ΔT_m (°C)**		*AlphaScreen IC_{50} (μM)**		
Cmpd	*R^1*	*R^2*	*X*	*CBP*	*BRD4(1)*	*CBP*	*BRD4(1)*	*CBP selectivity (-fold)*
354	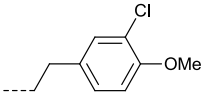	H	C	2.0 ± 0.055 (3)	0.42 ± 0.24 (3)			
361	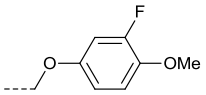	H	N	6.8 ± 0.21 (1)	2.9 ± 0.13 (3)	0.13 ± 0.0026 (2)	21 ± 11 (2)	160
362	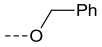	H	N	4.9 ± 0.16 (3)	3.2 ± 0.19 (3)	0.71 ± 0.28 (2)	10 ± 6.0 (2)	14
366	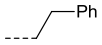	F	N	4.6 ± 0.44 (3)	2.2 ± 0.050 (2)	0.24 (1)	1.6 (1)	6.7
367	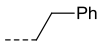	OH	N	5.4 ± 0.43 (3)	2.1 ± 0.10 (2)	0.35 (1)	1.1 (1)	3.1
368	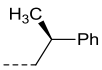	H	N	7.2 ± 0.59 (2)	3.6 ± 0.34 (2)	0.21 (1)	1.4 ± 0.17 (3)	6.7
369	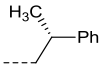	H	N	5.2 ± 0.32 (3)	3.2 ± 0.66 (3)			
370	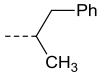	H	N	8.9 ± 0.26 (3)	2.9 ± 0.73 (3)	0.049 (1)		
371	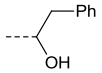	H	N	3.6 ± 0.38 (4)	1.5 ± 0.39 (5)	0.47 ± 0.15 (2)	1.9 ± 0.86 (4)	4.0
372	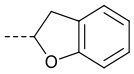	H	N	3.9 ± 0.15 (4)	3.3 ± 0.28 (3)	0.73 (1)	1.3 (1)	1.8
373	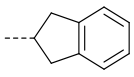	H	N	4.9 ± 0.15 (4)	3.7 ± 0.66 (3)	0.29 (1)	0.65 (1)	2.2
374	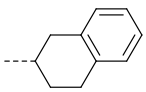	H	N	5.8 ± 0.24 (4)	2.8 ± 0.13 (3)	0.24 (1)	0.94 (1)	3.9
375	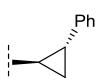	H	N	4.2 ± 0.26 (4)	2.8 ± 0.11 (3)	7.1 (1)	12 (1)	1.7

Cmpd	R^1	R^2	X	DSF ΔT_m (°C)*		AlphaScreen IC_{50} (μM)*		CBP selectivity (-fold)
				CBP	BRD4(1)	CBP	BRD4(1)	
376	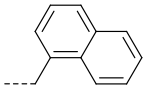	H	N	5.8 ± 0.062 (3)	2.6 ± 0.35 (3)			
377	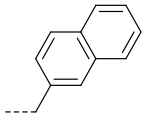	H	N	8.4 (1)	4.0 (1)			

*Mean value ± SEM (number of measurements).

Table 12. Determination of CBP and BRD4(1) binding constants by ITC for compound **361**.*

Cmpd	CBP			BRD4(1)			CBP selectivity
	K_d (μM)	ΔH (kcal/mol)	-TΔS (kcal/mol)	K_d (μM)	ΔH (kcal/mol)	-TΔS (kcal/mol)	
361	0.41	-8.19	-0.239	1.64	-8.72	-1.08	4.0-fold

5.4 *N*-1 LINKER ANALOGUES

The *N*-1 ethylene group which links the morpholine and the benzimidazole was seen as another region which could be modified to increase potency. The X-ray structure of compound **308** bound to BRD4(1) (Figure 32) suggests that the *N*-1 ethyl group linking the benzimidazole to the morpholine ring has steric demands placed on it by the BRD4(1) residues L92 and W81. In contrast, the structure of compound **308** bound to CBP shows that this group is positioned in a more open channel region. Therefore, analogous with the *C*-2 linker strategy, it was again envisaged that the introduction of conformational constraints to the *N*-1 ethyl linker could help to increase the selectivity of the series for CBP over BRD4(1). Also, it was hypothesised that moving the aryl substituent onto the *N*-1 linker may greatly reduce the size and flexibility of the scaffold, resulting in improved potency and selectivity. These strategies are summarised in Figure 35.

* Carried out by Stefan Knapp (SGC/TDI)

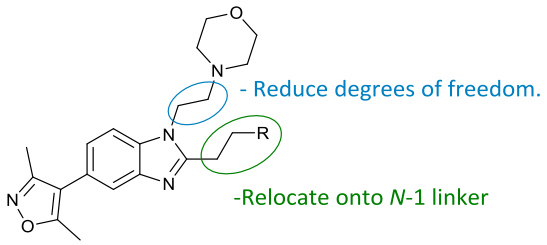

Figure 35. Strategy for *N*-1 ethylene linker: introduce linker substitution to reduce degrees of freedom; relocate aryl ring onto *N*-1 to reduce degrees of freedom.

The synthetic route to the compounds where the aryl group was relocated to the *N*-1 linker is shown in Scheme 14. S_NAr reaction of the appropriate amines with the fluoro-nitro compound **251** yielded nitro compounds **378-379**. The nitro-group of compounds **378-379** was reduced and the resultant phenylenediamines were condensed with orthoesters to yield target compounds **380-383**, which were isolated and tested as racemates in the first instance. The route to compounds with methyl-substituted *N*-1 linkers is shown in Scheme 15, which follows previously described methodology. Racemic compounds **386-389** were isolated and submitted for screening.

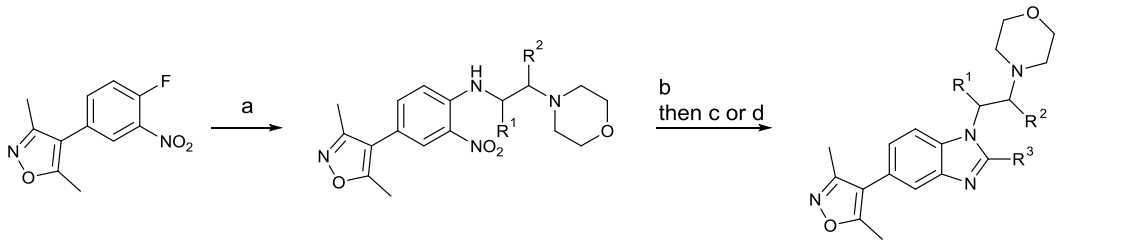

251

378 R^1 = Ph, R^2 = H
379 R^1 = H, R^2 = Ph

380 R^1 = Ph, R^2 = H, R^3 = H
381 R^1 = Ph, R^2 = H, R^3 = CH_3
382 R^1 = H, R^2 = Ph, R^3 = H
383 R^1 = H, R^2 = Ph, R^3 = CH_3

Scheme 14. Relocation of aryl onto *N*-1 linker. Reagents and conditions: (a) Amine, DIPEA, THF, sealed vial, 80 °C (59-68%); (b) $Na_2S_2O_4$, EtOH, H_2O, 80 °C; (c) $CHOEt_3$, EtOH, reflux (25-81% over 2 steps); (d) $CH_3(OEt)_3$, EtOH, reflux (17-45% over 2 steps).

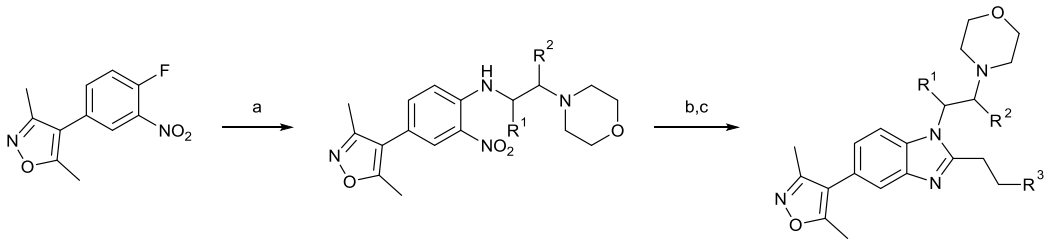

Scheme 15. Synthesis of methylated *N*-1 linker targets. Reagents and conditions: (a) Amine, DIPEA, THF, sealed vial, 80 °C (68-81%); (b) $Na_2S_2O_4$, EtOH, H_2O, 80 °C; (c) $R^3CH_2CH_2CO_2H$, T3P, DIPEA, EtOAc, reflux (23-39%).

5.5 SCREENING RESULTS FOR *N*-1 LINKER ANALOGUES

The screening results for the compounds where the aryl is substituted on the *N*-1 linker are summarised in Table 13. Compounds **380-383** were only moderately potent against CBP (ΔT_m 2.3-3.8 °C), implying the aryl ring was no longer able to make the same interactions as the *C*-2 substituted aryl group in previous compounds.

Table 13. SAR for CBP and BRD4(1) binding as determined by DSF for *N*-1 aryl analogues.

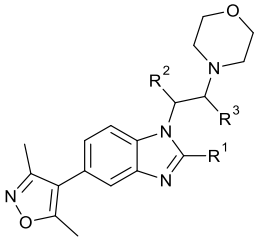

Cmpd	*R^1*	*R^2*	*R^3*	*DSF ΔT_m (°C)**	
				CBP	*BRD4(1)*
380	H	H	Ph	2.3 ± 0.28 (5)	1.9 ± 0.27 (3)
381	CH_3	H	Ph	2.4 ± 0.35 (5)	1.8 ± 0.56 (3)
382	H	Ph	H	3.3 ± 0.18 (5)	2.1 ± 0.045 (3)
383	CH_3	Ph	H	3.8 ± 0.25 (5)	2.6 ± 0.19 (3)

*Mean ΔTm ± SEM (number of measurements).

Table 14 shows the SAR for the compounds with methyl-substituted *N*-1 linkers. Substitution was not well tolerated proximal to the benzimidazole ring (compounds **386**

and **387**, CBP ΔT_m 5.8 °C, 5.6 °C, respectively). However, when the methyl group was substituted on the carbon adjacent to the morpholine ring (compounds **388** and **389**) the compounds were highly potent against CBP in DSF (ΔT_m of 9.4 °C and 9.4 °C, respectively). AlphaScreen results confirmed the high potency of compounds **388** and **389** against CBP (IC_{50} 0.022 μM and 0.10 μM, respectively). Results also suggested that compounds **388** and **389** were selective over BRD4(1) (ΔT_m of 2.0 °C and 2.4 °C, respectively; IC_{50} 17 μM and 16 μM, respectively). Therefore, it was decided to synthesise the single enantiomers of compounds containing methyl substitution on the carbon adjacent to the morpholine ring, in order to determine if the CBP and BRD4(1) potency resided predominantly with one enantiomer.

Table 14. SAR for CBP and BRD4(1) binding as determined by DSF and AlphaScreen for conformationally constrained *N*-1 linkers. Compounds are racemic except where indicated.

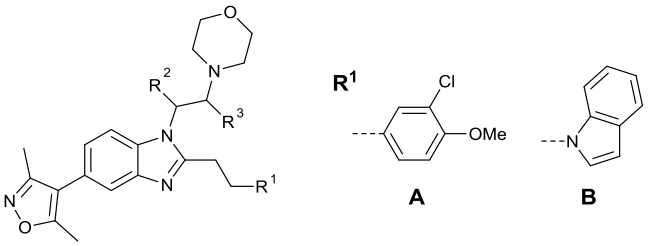

				*DSF ΔT_m (°C)**		*AlphaScreen IC_{50} (μM)**		*CBP Selectivity*
Cmpd	*R^1*	*R^2*	*R^3*	*CBP*	*BRD4(1)*	*CBP*	*BRD4(1)*	*(-fold)*
386	A	CH_3	H	5.8 ± 0.092 (3)	1.9 ± 0.27 (2)			
387	B	CH_3	H	5.6 ± 0.29 (3)	1.2 ± 0.070 (2)			
388	A	H	CH_3	9.4 ± 0.58 (5)	2.0 ± 0.33 (3)	0.022 (1)	17 ± 10 (2)	770
389	B	H	CH_3	9.1 ± 0.44 (5)	2.4 ± 0.25 (3)	0.10 ± 0.034 (2)	16 ± 7.5 (2)	160

*Mean value ± SEM (number of measurements).

The synthesis of the single enantiomers proceeded according to the route shown in Scheme 16. Commercially acquired (*R*)- and (*S*)-1,2-diaminopropane were reacted with compound **251**, predominantly at the less sterically hindered amine distal to the methyl group. This

gave an inseparable 4:1 mixture of isomers in favour of the desired compounds (**390** and **391**). The morpholine ring was formed by alkylation with 2-bromoethyl ether to give compounds **392** and **393**. At this stage, the isomeric by-products from the S_NAr step could be separated from the desired isomers. Nitro reduction followed by benzimidazole formation yielded the target compounds **394**-**399** in ≥99:1 enantiomeric ratio (*er*).

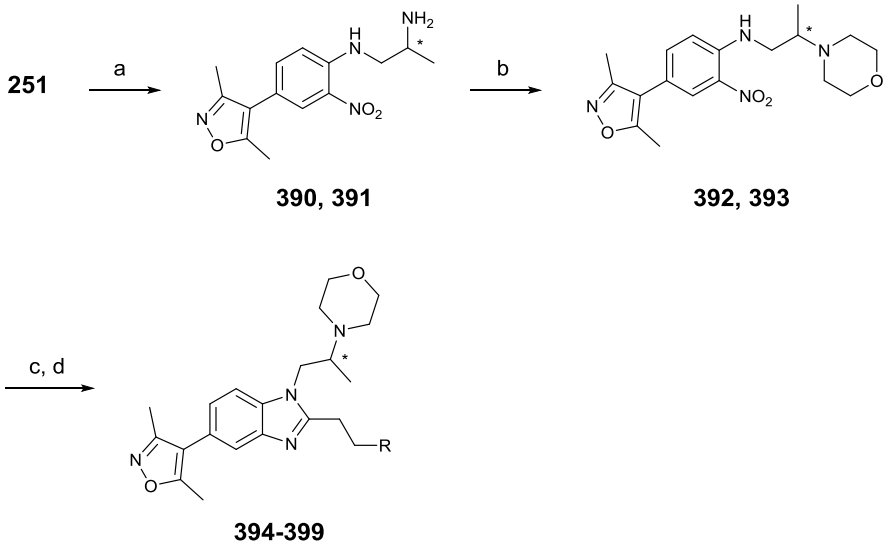

Scheme 16. Route to single enantiomers (asterisks denote stereogenic centres). Reagents and conditions: (a) (*R*)- or (*S*)-1,2-diaminoropane dihydrochloride, K_2CO_3, DMF, 80 °C (38-41%); (b) 2-bromoethylether, K_2CO_3, DMF, 70 °C (27-37%); (c) $Na_2S_2O_4$, H_2O, EtOH, 80 °C; (d) $RCH_2CH_2CO_2H$, T3P, EtOAc, reflux (38-52% over two steps).

Gratifyingly, the (*R*)- and (*S*)-enantiomers displayed different affinities for CBP (Table 15). The (*R*)-enantiomers (compounds **394**-**396**) were moderately potent against CBP (ΔT_m 7.2-7.5 °C, IC_{50} 0.18-0.45 μM). However, the (*S*)-enantiomers (compounds **397**-**399**) were significantly more potent against CBP (ΔT_m 9.7-11 °C, IC_{50} 0.045-0.069 μM). Therefore it was decided to determine the K_d of a representative set of the most potent *N*-1 methyl-substituted analogues by ITC.

Table 15. SAR for CBP and BRD4(1) binding as determined by DSF and AlphaScreen assays for conformationally constrained *N*-1 linkers.

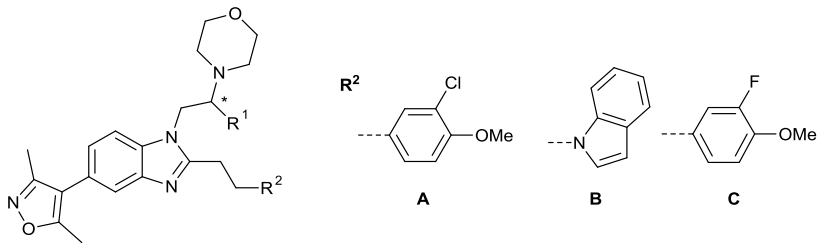

Cmpd	R^1	R^2	*DSF* ΔT_m *(°C)**		*AlphaScreen* IC_{50} *(μM)**
			CBP	*BRD4(1)*	*CBP*
394	(*R*)-CH_3	A	7.5 ± 0.10 (3)	2.0 ± 0.040 (2)	0.45 (1)
395	(*R*)-CH_3	B	7.2 ± 0.21 (3)	2.3 ± 0.25 (2)	0.42 (1)
396	(*R*)-CH_3	C	7.3 ± 0.058 (3)	3.4 ± 0.54 (2)	0.18 (1)
397	(*S*)-CH_3	A	9.7 ± 0.31 (4)	1.8 ± 0.71 (4)	0.069 (1)
398	(*S*)-CH_3	B	11 ± 0.17 (3)	3.3 ± 0.57 (2)	0.045 (1)
399	(*S*)-CH_3	C	10 ± 0.11 (3)	2.3 ± 0.25 (2)	0.059 (1)

*Mean value ± SEM (number of measurements).

Table 16 summarises the ITC results obtained for the set of *N*-1 substituted analogues. As expected from DSF and AlphaScreen, the (*R*)-methyl compounds **394** and **396** were less potent against CBP (K_d 0.37 μM and 0.24 μM, respectively) than the (*S*)-methyl compounds **397- 399** (K_d 0.021-0.039 μM). Compounds **394** and **396** were only around 3-fold selective for CBP over BRD4(1). Gratifyingly the (*S*)-methyl analogues **397- 399** were significantly more selective. Compound **397**, was 40-fold selective for CBP over BRD4(1), meaning the selectivity had surpassed the targeted chemical probe criteria. The introduction of a chiral methyl onto the morpholino-ethylene moiety thus has the desired effect of improving selectivity over BRD4(1) whilst maintaining CBP potency and validates the design strategy of introducing conformational restraints into the ethylene linker of the target compounds. In order to confirm that compound **397** was also an inhibitor of p300, it was tested against p300 by ITC. The ITC results showed that the p300 K_d (0.032 μM) and thermodynamic parameters were similar to those for CBP inhibition (Table 17).

Table 16. Determination of CBP and BRD4(1) binding constants by ITC for selected compounds.*

	CBP			*BRD4(1)*			*CBP selectivity*
Cmpd	K_d *(μM)*	*ΔH (kcal/mol)*	*-TΔS (kcal/mol)*	K_d *(μM)*	*ΔH (kcal/mol)*	*-TΔS (kcal/mol)*	*(-fold)*
394	0.37	-14.0	-1.71	1.2	-8.50	0.725	3.2
396	0.24	-12.5	-1.17	0.68	-9.21	1.12	2.8
397	0.021	-10.9	0.817	0.85	-8.47	0.817	40
398	0.026	-9.59	-0.420	0.53	-7.46	-0.844	20
399	0.039	-11.1	1.37	0.63	-9.15	-0.292	16

Table 17. Determination of p300 binding constant by ITC for compound **397**.†

Compound	*p300* K_d *(μM)*	*p300 ΔH (kcal/mol)*	*p300 -TΔS (kcal/mol)*
397	0.032	-10.5	0.638

5.6 STRUCTURE OF COMPOUND **397** BOUND TO CBP AND BRD4(1)

In order to better understand differences in binding modes which give rise to the selectivity of compound **397**, it was crystallised in complex with the CBP and BRD4(1) BRDs (Figure 36). In the CBP complex, in addition to the previously described Kac-mimicking interactions of the isoxazole, a notable feature of the structure obtained is a cation-π interaction between the aryl ring of compound **397** and R1173. The interaction is formed in an induced pocket, where R1173 has moved relative to the position observed in previous structures (Figure 36B). The cation-π interaction may explain why electron-donating substituents were favoured on the aryl ring. The chiral methyl group on the *N*-1 linker of compound **397** is positioned on the other side of the aryl ring and may help stabilise this conformation. The methoxy and chlorine substituents on the aryl ring of compound **397** sit in a hydrophobic region of the induced pocket. The reduced flexibility of the *N*-1 and *C*-2 moieties is apparent from their generally well defined electron density (Figure 36A).

*Carried out by Stefan Knapp (SGC/TDI), with the exception of compounds **394** and **396** with CBP, which were carried out by the author.

† Carried out by Sarah Picaud (SGC).

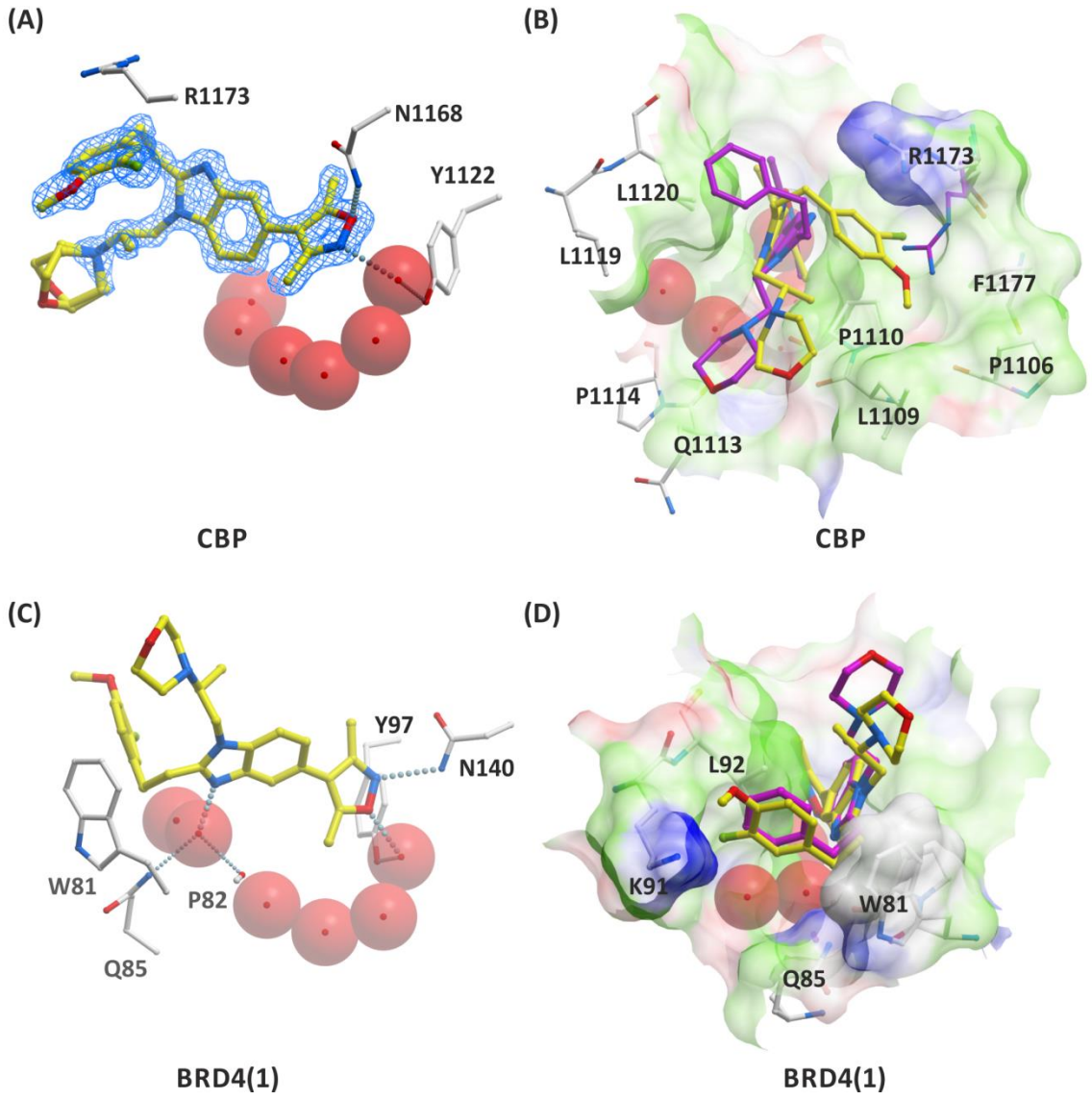

Figure 36. Views from X-ray structure of compound **397** (carbon = yellow) complexed to CBP (PDB 4NR7) and BRD4(1);* (A) Hydrogen-bonding interactions between isoxazole oxygen and N1168 of CBP (3.08 Å) and isoxazole nitrogen and a conserved water molecule (2.83 Å) are shown. The 2Fo-Fc ligand map (σ 3.0) is shown as a blue mesh. (B) View showing surface of binding pocket of CBP and selected residues on the outside of the binding pocket which are in close proximity with the ligand *N*-1 and *C*-2 substituents. A cation-π interaction is formed between the aryl ring of compound **397** and R1173 (3.54 Å between nearest atoms of compound **397** and R1173). The cation-π interaction occurs in an induced pocket, where R1173 moves relative to the position observed in the structure of CBP in complex with compound **308**, which is overlaid for comparison (carbon = magenta). (C) Hydrogen-bonding interactions between isoxazole oxygen and N140 of BRD4(1) (3.04 Å) and isoxazole nitrogen and a conserved water molecule (2.97 Å) are shown. (D) View showing surface of BRD4(1) binding pocket and selected residues on the outside of the binding pocket which are in close proximity with the ligand *N*-1 and *C*-2 substituents. The complex of compound **308** and BRD4(1) is overlaid for comparison (carbon = magenta).

The structure of compound **397** complexed to BRD4(1) is very similar to that of compound **308** complexed to BRD4(1) (see overlay in Figure 36D). The main difference in the two structures is the positioning of the *N*-1 moiety. The chiral methyl group on compound **397**

*Crystallography and refinement of crystallographic data was carried out by Sarah Picaud and Panagis Filippakopoulos (SGC).

appears to make it more difficult for the *N*-1 moiety to avoid unfavourable steric interactions with L92 and W81 on BRD4(1).

5.7 SELECTIVITY OVER OTHER BRD SUBFAMILY MEMBERS

Although efforts thus far had focussed on obtaining selectivity for CBP over structurally similar BRD4(1), it was important to profile the series more broadly to see if the scaffold was selective over other BRD sub-family members. Figure 37 summarises the DSF results from screening of compounds **308** and **397** against different BRDs from various sub-family members. Compound **308** is only around 3-fold selective for CBP over BRD4(1) (see Chapter 4). However, the DSF selectivity panel demonstrated that compound **308** had little affinity for any of the other BRDs tested, with the main affinity for CBP and p300 (ΔT_m 6.7 °C and 7.9 °C, respectively), and off-target against the first domain of the BET sub-family members, BRD2-BRD4 (ΔT_m 2.4-2.6 °C). Weak affinity (ΔT_m 1-2 °C) was detected for compound **308** binding to BAZ1A, BRDT(1), CECR2, PHIP(1), LOC93349, TIF-1α and BRD9, and all other targets showed negligible affinity (ΔT_m < 1.0 °C). Compound **397** appeared to be significantly more selective than compound **308**. As expected, the main affinity for compound **397** was for binding to CBP and p300 (ΔT_m 9.7 °C for both targets). Weak affinity (ΔT_m 1-2 °C) was observed for the first domain of the BET sub-family members, BRD2-BRD4 and BRPF1B, and all other targets tested showed negligible affinity for compound **397** (ΔT_m < 1.0 °C). Thus, the data implies that compounds **308** and **397** are selective for CBP/p300, with compound **397** showing very high selectivity over other targets tested. The selectivity data supports the use of compound **397** as a chemical probe, as interference from other BRD-containing proteins should be minimal.

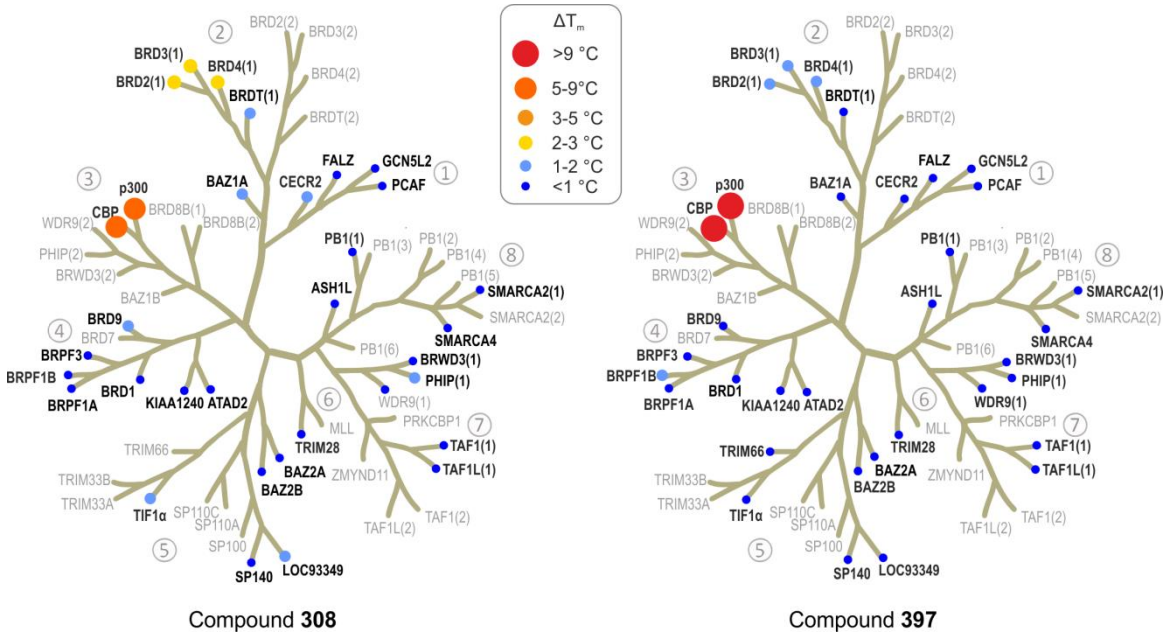

Figure 37. DSF selectivity profiling of compounds **308** and **397** against various BRD subfamily members.

5.8 SUMMARY

In this section, several structure-guided approaches aimed at improving the selectivity of the series for CBP over BRD4(1) were described. The synthesis of an indole analogue, compound **354**, which was designed to disfavour the BRD4(1) binding mode observed in a crystal structure, was achieved via an intramolecular cyclisation of an amide with a phosphorus ylide (Scheme 8). Disappointingly, indole **354** lost potency against both CBP and BRD4(1) (Table 11). Attempts to favour a binding mode seen in CBP but not in BRD4(1) through the introduction of a 6-hydroxybenzimidazole **367** also gave no signs of selectivity improvement (Table 11). Ether analogues, **361** and **362** were made via Ag_2CO_3 mediated *O*-alkylation of a urea precursor, and by a Mitsunobu reaction between a phenol and an alcohol precursor (Scheme 12). Compounds **361** and **362** were designed to disfavour binding in a hydrophobic region of BRD4(1), but they gave no signs of improvements in the selectivity for CBP over BRD4(1) (Table 11). Several attempts were made to introduce conformational constraints through the introduction of substituents on the *C*-2 linker of target compounds in order to disfavour binding of this moiety to a relatively narrow pocket

of BRD4(1), but no improvement in selectivity was observed (Table 11). In a similar approach, attempts were made to modify the *N*-1 linker of the target compounds in order to reduce the flexibility and disfavour BRD4(1) binding. The introduction of a methyl group on the methylene next to the morpholine ring gave encouraging potency and selectivity in primary screening (Table 14). The single enantiomers were therefore synthesised, making use of a chiral diamine starting material and a morpholine ring forming reaction (Scheme 16). The (*S*)-form was found to be more potent against CBP and compound **397** showed high selectivity (40-fold) for CBP over BRD4(1), as determined by ITC (Table 16). DSF screening with a selection of BRD targets demonstrated that compounds **308** and **397** are selective for CBP/p300 (Figure 37). In particular, compound **397** was highly selective, with very little affinity observed for any of the other BRD targets tested.

The use of X-ray structures of ligand-protein complexes gave valuable insights and was used to design targets which could be selective for CBP over BRD4(1). Most of the ideas tried were unsuccessful in this aim, likely reflecting the difficulty in interpreting static structures which may not be indicative of the solution-phase environment and do not take into account the dynamic and flexible nature of proteins. However, the structure-guided approach was eventually fruitful and the compounds obtained through modification of the *N*-1 linker meet the targeted potency and selectivity criteria for a CBP chemical probe. The next chapter looks at a characterisation of compound **397** in cells to test if on-target cellular activity is observed.

CHAPTER 6. CBP/P300 CHEMICAL PROBE: CHARACTERISATION OF COMPOUND **397**

6.1 FRAP ASSAYS

On-target cellular efficacy for the CBP BRD was investigated using a fluorescence recovery after photo-bleaching (FRAP) assay (Figure 38).[284] HeLa cells transfected with a construct encoding a green fluorescent protein (GFP) tagged multimerised (3×) CBP BRD showed a rapid recovery time ($t_{½}$ 0.59 s) upon photobleaching of a small area of the nucleus. The broad-spectrum KDAC inhibitor, SAHA (suberoylanilide hydroxamic acid), was used to increase the extent of global lysine acetylation, increasing recovery time ($t_{½}$ 0.79 s) and expanding the assay window. An equivalent increase in the recovery time was not observed in cells transfected with a CBP BRD construct carrying the N1168F mutation, consistent with the critical role of N1168 in Kac binding, and supporting the proposal that the increase in assay window due to SAHA addition is due to BRD binding.

SAHA-treated cells were treated with 3 dimethylisoxazole inhibitors with different selectivity profiles for comparison. Compound **400** is a reported BRD4(1)-selective inhibitor,[261] and compounds **308** and **400** are CBP-selective (2.9-fold and 40-fold, respectively). Treatment of SAHA-treated cells with compound **397** at 0.1 μM was sufficient to reduce FRAP recovery times back to unstimulated levels ($t_{½}$ 0.60 s), equivalent to the N1168F mutant. The effect is indicative of displacement of the CPB BRD from acetylated chromatin. The weaker and less selective CBP inhibitor, compound **308** and the BRD4(1)-selective inhibitor **400** were unable to significantly alter the FRAP at this concentration ($t_{½}$ 0.66 and 0.74 s, respectively). Conversely, in an equivalent assay using GFP-tagged BRD4, only the BRD4-selective inhibitor **400** significantly affected FRAP recovery times, with CBP inhibitors **308** and **397** showing no significant effect at 0.1 μM (Figure 38B). The results

therefore demonstrate the specificity of the compounds for their respective targets in a cellular context.

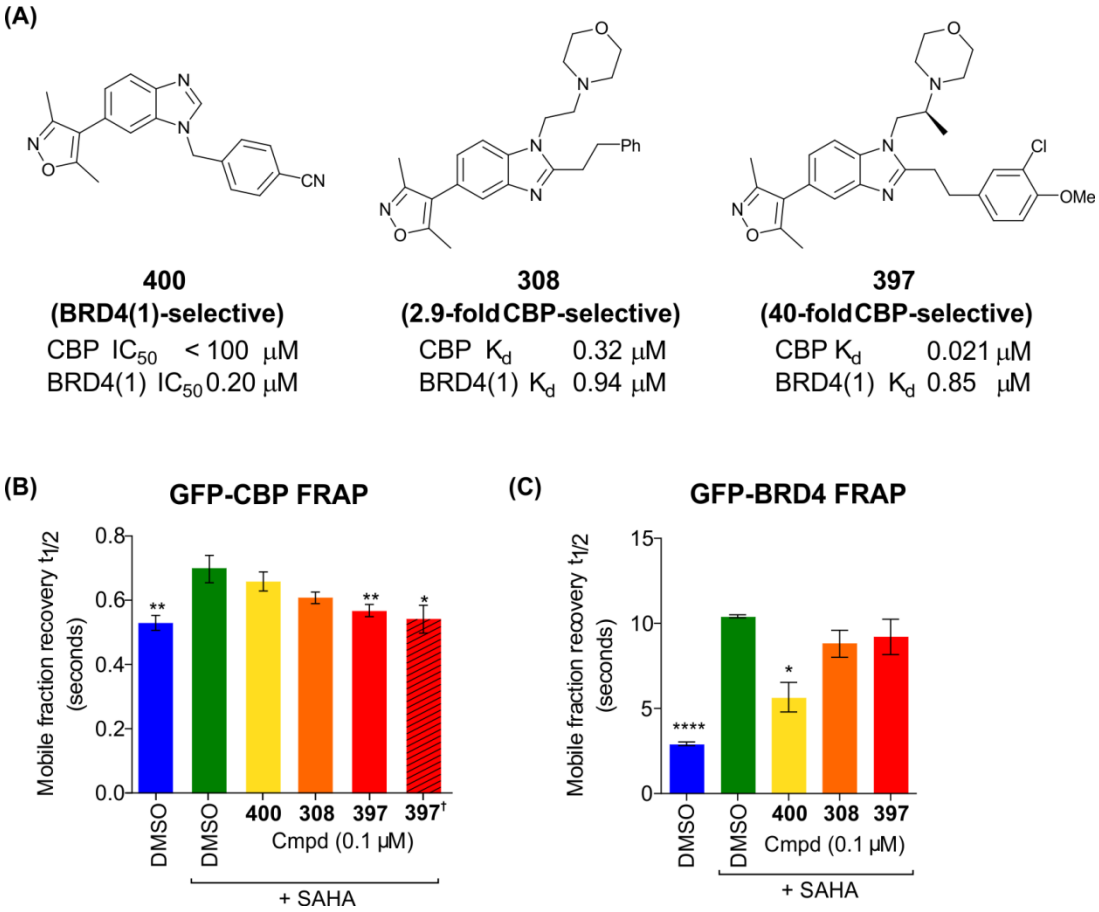

Figure 38. (A) Compounds used in FRAP assay.* (B) Time dependence of fluorescent recovery in the bleached area in FRAP assays with GFP-tagged 3×CBP BRD construct (B) and full length BRD4 (C). Half times of fluorescence recovery ($t_{½}$) are shown as bars, which are coloured according to DMSO control (blue), DMSO + SAHA (green), 0.1 μM BRD4(1)-selective inhibitor **400** (yellow), 0.1 μM compound **308** (orange), 0.1 μM compound **397** (red). †N1168F mutant (red hashed). Bars represent the mean ± SEM $t_{½}$ calculated from 2-3 independent experiments. Significance of groups compared with the control was determined by *t*-tests *p<0.05, **p<0.01, ****p<0.0001.

6.2 P53-REPORTER GENE ASSAY

To investigate the effect of compound **397** on the CBP-p53 association in a functional cellular context, a luciferase reporter assay for p53 induction was used.[285] Doxorubicin induced p53 activity was effectively inhibited by compound **397** in a dose-dependent manner (IC_{50} 1.5 μM) (Figure 39). These results suggest that the CBP BRD inhibitor **397** inhibits the CBP coactivation of p53 target genes in cells and demonstrate the utility of **397**

* The FRAP assays were carried out by Dean Singleton (TDI).

in a cellular context. The effect on p53 regulation by compound **397** is most likely due to its CBP inhibition, not its weaker BRD4 inhibition, as the much more potent BRD4 inhibitor, JQ1 shows p53 mediated effects at similar concentrations.[286, 287] However, it was not possible to analyse the effects of less selective CBP inhibitors in the p53 reporter gene assay due to their BRD4(1) activity and the confounding effects of BRD4 inhibition on p53.[286]

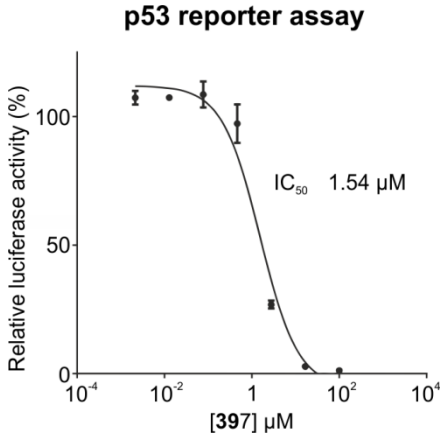

Figure 39. Inhibition of p53-driven luciferase activity by compound **397**.* RKO cells were transfected with p53 reporter plasmid. Cells were treated with compound **397** at the indicated concentrations for 24 h and subsequently with doxorubicin at 0.3 µM for 16 h. Each value is the mean ± SEM.

6.3 FRET ASSAY

In order to provide further evidence for inhibition of the CBP BRD interaction with acetylated p53 in cells, a Förster resonance energy transfer (FRET) assay was used.[288] HeLa cells were transfected with cyan fluorescent protein (CFP) tagged p53 and yellow fluorescent protein (YFP) tagged CBP constructs (Figure 40). Upon laser excitation of CFP and YFP, a FRET signal was observed, implying close proximity of the tagged CBP and p53 constructs (Figure 40C). Treatment of cells with 5 µM of compound **397** diminished the FRET signal. The inhibition of the FRET signal by **397** implied that the tagged constructs were not in close proximity and were therefore not interacting.

* The p53 reporter-gene assay was carried out by Christopher Wells (SGC).

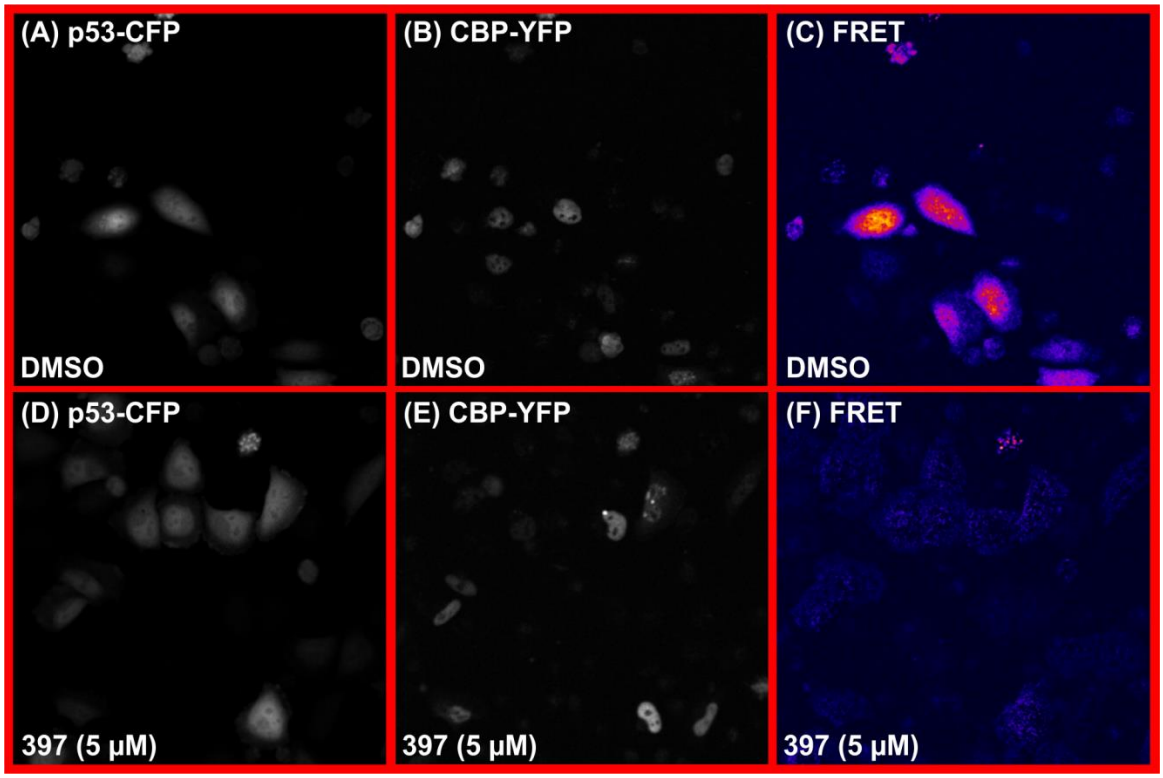

Figure 40. FRET assay using p53-CFP and CBP-YFP constructs.* (A)-(C) are DMSO control experiments. (D)-(F) are in the presence of 5 μM compound **397**. (A) and (D) – Cells expressing p53-CFP in the cyan channel. (B) and (E) – Cells expressing CBP-YFP in the YFP channel. (C) and (F) – Intensity of FRET signal.

6.4 CYTOTOXICITY OF COMPOUND **397**

To test if CBP/p300 BRD inhibition by compound **397** is cytotoxic at the concentrations where on-target efficacy was observed, U2OS osteosarcoma cells were treated with compound **397** for 24 h and cell viability was determined using a standard MTT (3-(4,5-dimethylthiazol-2-yl)-2,5-diphenyltetrasolium bromide) turnover assay (Figure 41).[289] This showed that compound **397** had modest cytotoxicity (CC_{50} 80 μM), well above the levels where on-target efficacy was observed in the FRAP and p53 reporter gene assays. After 72 h of treatment with compound **397**, cytotoxicity in U2OS cells increased (CC_{50} 8.1 μM). Compound **397** is ~10-fold less cytotoxic in U2OS cells treated for 72 h than the BET-selective inhibitor JQ1 (CC_{50} 8.1 and 0.73 μM, respectively).[290] The lower cytotoxicity of

* The FRET assay was carried out by Clarence Yapp (SGC).

compound **397** compared to JQ1 gives further evidence for the lack of BRD4 inhibition by compound **397** in a cellular context.

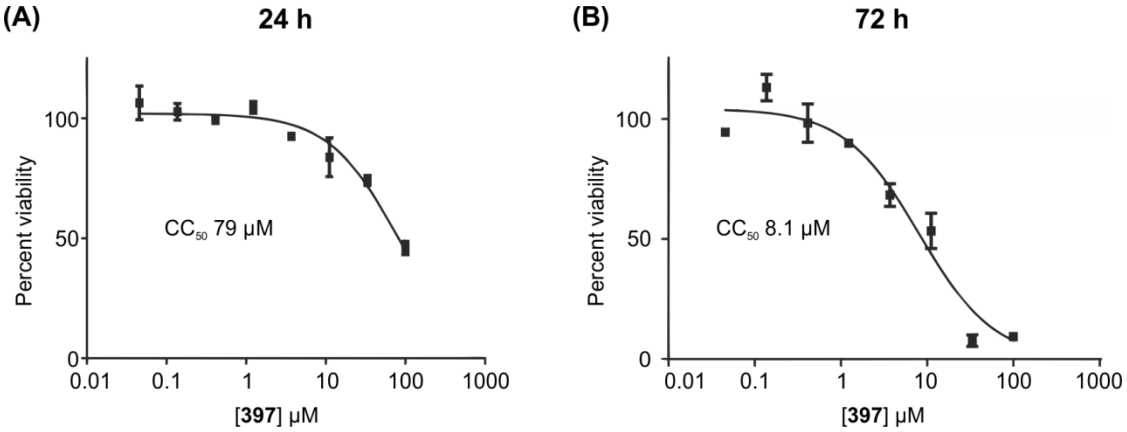

Figure 41. (A) Compound **397** in U2OS MTT cytotoxicity assays, 24 h treatment. (B) Compound **397** in U2OS MTT cytotoxicity assays, 72 h treatment.

6.5 WIDER PROFILING OF COMPOUND **397**

In order to investigate if compound **397** could also serve as a probe in animals, it was tested in *in vitro* ADME (absorption, distribution, metabolism, and excretion) physiochemical assays (Table 18). The moderate solubility of compound **397** (38 μM, pH 7.4), combined with high permeability (CACO-2, A-B 37×10^{-6} cm/s) imply that absorption would be sufficient for oral dosing at doses ≤ 1 mg/kg.[291] Drug-drug interactions with P-glycoprotein (P-gp) substrates are not anticipated, due to the low P-gp inhibition of compound **397** (21% @ 10 μM).[292] In a human liver microsome (HLM) stability assay, no compound was detected after 60 min, implying the metabolism of compound **397** may be too rapid for it to be useful as an oral *in vivo* probe.[293] ADME properties would therefore have to be optimised if utilising compound **397** as the starting point for the development of an oral *in vivo* probe or for drug discovery efforts.

Table 18. ADME properties for compound **397**

log D (PBS, pH 7.4)	3.9
Solubility (PBS, pH 7.4)	38 μM
CACO-2 (A-B)	37×10^{-6} cm/s
P-gp inhibition	21% @ 10 μM
HLM (remaining after 60 min)	0%

The selectivity of compound **397** against other target classes was assessed using wide ligand profiling (Appendix 7). When tested against 136 GPCR, ion channel, enzyme and kinase targets, compound **397** showed IC_{50}'s of < 1 μM only for the adrenergic receptors α2C (0.11 μM) and α2A (0.57 μM), phosphodiesterase-5 (PDE5) (0.15 μM) and platelet-activating factor (PAF) (0.54 μM). The low promiscuity of compound **397** implies interference from off-target inhibition is expected to be minimal. For the majority of cell assays, the targets which were inhibited by compound **397** at < 1 μM are unlikely to interfere with results. However, if compound **397** is used as a starting point for drug discovery, affinity for α2C, α2A, PDE5 and PAF should be monitored in order to avoid off-target toxicity.

6.6 SUMMARY

On-target cellular activity of the CBP/p300 inhibitors was investigated using a FRAP assay with GFP-tagged CBP multimerised BRD (Figure 38). The results showed that at 0.1 μM, compound **397** inhibited SAHA-enhanced FRAP recovery times back to unstimulated levels. Compound **397** inhibited doxorubicin-induced p53 activation in a reporter-gene assay (IC_{50} 1.5 μM) (Figure 39). Additionally, compound **397** inhibited the FRET between a CYP-tagged p53 and YFP-tagged CBP (Figure 40). The p53 reported-gene and FRET assays are

consistent with on-target inhibition of the CBP BRD interaction with p53 in a cellular context. On-target cellular activity has therefore been demonstrated, albeit in an artificial system, at levels consistent with the targeted criteria. Compound **397** was moderately cytotoxic, at concentration much less than those where on-target cellular activity was observed (Figure 41). ADME profiling showed that compound **397** possessed reasonable solubility and cell-permeability, and did not inhibit P-gp. However, HLM clearance was high and would have to be further optimised for oral dosing in *in vivo* studies or for drug discovery efforts. Wide-ligand profiling demonstrated relatively few hits for off-target inhibition, implying that interference in cell studies from other proteins should be minimal. The data demonstrates the utility of compound **397** as a cellular probe which should prove useful in elucidating the biological function of CBP and could also be applied to target-validation in the pharmaceutical industry.

CHAPTER 7. TOWARDS A CHEMICAL PROBE FOR BRD9/BRD7

7.1 BRD9/BRD7

Unlike CBP/p300 and the BET family of BRD-containing proteins, very little is known about the function of bromodomain-containing protein 9 (BRD9). BRD9 contains 598 amino acids and the BRD is the only functional domain that has been assigned to date.[122] Proteomic analysis suggested that BRD9 is associated with human BAF-type (BRG1/BRM-associated factors) SWI/SNF (SWItch/Sucrose Non-Fermentable) chromatin remodelling complexes.[294] Recently, it has been shown that BRD9 is a dedicated and non-exchangeable sub-unit of SWI/SNF.[295] The BRD9 paralog, bromodomain-containing protein 7 (BRD7), is a subunit of PBAF (poly-bromo-associated BAF) SWI/SNF complexes.[294, 296, 297] It has been suggested that BRD7 regulates transcription through the binding of its BRD to H3K14ac.[298] Overall, BRD7 and BRD9 are only 36% similar at the amino acid level, but the similarity of the BRD is high (72%).

Evidence is emerging that indicates that BRD9 and BRD7 may have important roles in oncology. *BRD9* has been identified as part of a group of genes with copy number variations in non-small cell lung cancer (NSCLC) tumour samples, implying that a chromosomal imbalance in *BRD9* could be involved in tumourigenesis.[299] Similar analysis of cervical cancer tumour samples also found copy number increases in *BRD9.*[300]

It has been suggested that *BRD7* is a tumour-suppressor gene, which inhibits G1-S progression by blocking the translocation of β-catenin from the cytoplasm to the cell nucleus and negatively regulating the extracellular signal-regulated kinases 1/2 (ERK1/2) pathway.[301, 302] Additionally, BRD7 has been shown to be a critical regulator of tumour suppressor p53.[303-305] It also regulates oestrogen receptor α (ERα) expression through BRCA1 recruitment.[306] Analysis of tumour biopsies shows that *BRD7* is down-regulated in

nasopharyngeal carcinoma, colorectal cancer and epithelial ovarian cancers.[301, 307, 308] In colorectal cancer, BRD7 expression is negatively collated with survival time.[307] The *BRD7* locus is frequently deleted in breast cancer tumours.[304] However, it was found that *BRD7* mutation represent a rare polymorphism in breast cancer, with no pathogenic effect.[309] MicroRNA-200c, which is up-regulated in endometrial carcinoma, inhibits BRD7 expression.[310]

With little known about the function of BRD7, and even less in the case of BRD9, chemical probes would be valuable tools; these could help further the understanding of transcriptional control by BRD9 and BRD7 and help elucidate their roles in oncology and other human diseases. However, to date no small molecule inhibitors of BRD9 and BRD7 have been described. This chapter describes efforts toward a BRD9/BRD7 chemical probe.

7.2 STARTING POINT

The indolizine ketone, GSK2801 (compound **401**), is a GSK/SGC derived chemical probe for the BAZ2A/BAZ2B (bromodomain adjacent to zinc finger domain A and B) BRDs (Table 19).[311] During the development of this probe, BRD9 affinity was observed for a *C*-1 pyridine analogue of GSK2801, compound **402** (BRD9 IC_{50} 1.2 μM). Another *C*-1 pyridine analogue, compound **403**, was even more potent against BRD9 (IC_{50} 0.45 μM) and was over 5-fold selective for BRD9 over BAZ2B. However, compound **403** was also potent against BRD4(1), as measured by DSF (ΔT_m 4.4 °C). Nevertheless, the BRD9 potency of compounds **402** and **403** made them attractive starting points for the development of potent and selective BRD9 inhibitors.

An X-ray crystal structure of a complex between compound **401** and BAZ2B is shown in Figure 42, which demonstrates how the ketone group mimics the Kac interaction with N1944 and Y1901. There is also an additional hydrogen-bond from the sulfone of compound **401** to the protein backbone (N1894). Figure 42B and C show how the outside of the Kac

pocket is relatively open, especially when compared to an overlaid structure of BRD9 (Figure 42D). The residues L1197 and L1950 in BAZ2B correspond to I53 and Y106 in BRD9, which results in a flatter and narrower pocket in BRD9 and may explain the differences in BRD9 potency of compounds **401** and **403**. In compound **401**, the aryl group sits close to perpendicular with the indolizine core. However, the presence of the pyridine nitrogen atom in compound **403** allows it to adopt a flatter conformation, consistent with a reduction in biaryl torsional strain.[312] It may be that the reduction in bi-aryl strain is important in allowing compounds *C*-1 pyridine analogue to bind into the narrower BRD9 pocket.

Table 19. Comparison of lead compounds **402** and **403** with BAZ2B probe, GSK2801.

	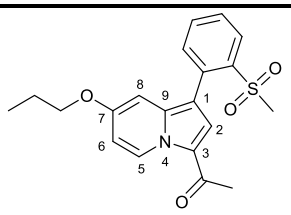	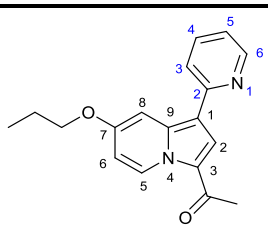	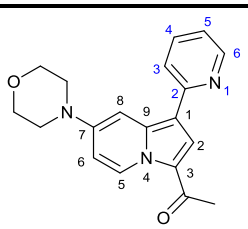
Cmpd	**401** (GSK2801)	**402**	**403**
AlphaScreen IC_{50}			
BAZ2B	0.66 μM (K_d 0.14 μM, ITC)	2.5 μM	2.6 μM
BRD9	15 μM	1.2 μM	0.45 μM
ΔT_m			
BAZ2A	3.7 °C	1.9 °C	3.7 °C
BRD9	1.3 °C	4.4 °C	8.7 °C
BRD4(1)	0.32 °C	1.7 °C	4.4 °C

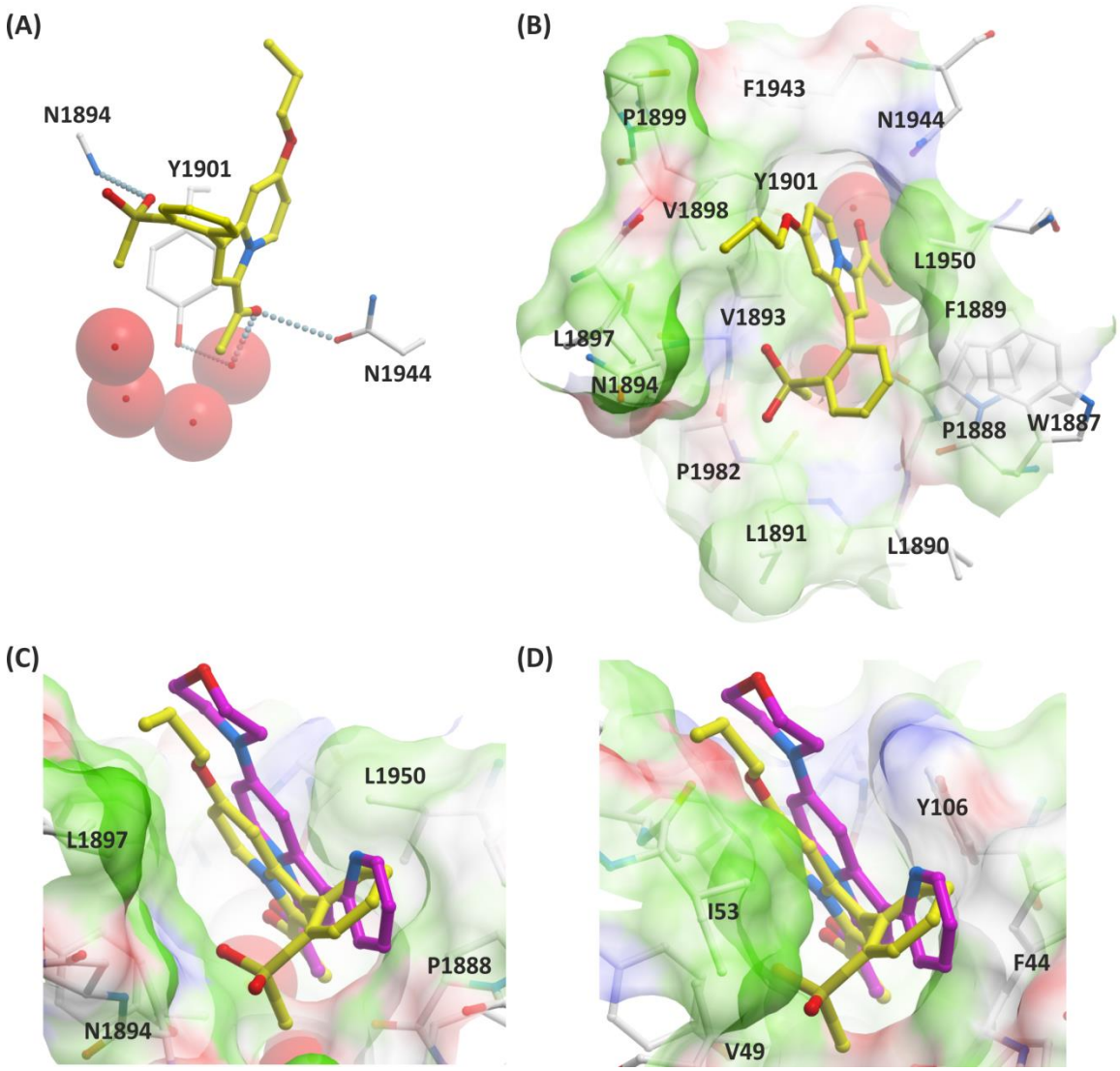

Figure 42. (A) View from X-ray crystal structure of BAZ2B complexed with GSK2801 showing hydrogen-bonding interactions between indolizine and protein. There is a hydrogen-bond from the ketone to N1944 and a water-mediated hydrogen-bond to Y1901. There is also a hydrogen-bond from the sulfone to the protein back-bone (N1894). (B) As in (A) showing a view with the pocket surface. (C) As in (B) with an aligned X-ray crystal structure of compound **403**-BAZ2B complex overlaid for comparison. A significant difference in the torsional angle of the aryl/pyridyl group relative to the indolizine can be seen. (D) As in (C) with an aligned BRD9 X-ray structure overlaid for comparison, showing a narrow binding pocket lined by residues I53 and Y106.

7.3 *C*-1 ANALOGUES

Initial targets for BRD9 inhibition were designed to test the effects of varying the *C*-1 heteroaryl group, through synthesis of substituted pyridines and replacing it with different heterocyclic analogues. In order to confirm the importance of the *C*-7 morpholine moiety, some *C*-7 *n*-propoxy analogues were also synthesised. The targeted compounds were synthesised by base-promoted [3+2] cycloaddition with commercially acquired

alkynes.[313, 314] Additional alkynes that were not readily available commercially were synthesised according to Scheme 17 and Scheme 18. Sonogashira coupling of a silyl protected alkyne with 2-bromopyridine, **404**, followed by TBAF deprotection yielded 2-ethynylpyridine **406**.[315, 316] Bestmann-Ohira homologation of aldehyde **407**, yielded 2-ethynyl-1-methylimidazole **408**. However, no product was isolated from the indolizine forming reaction for the alkyne **408**.[317]

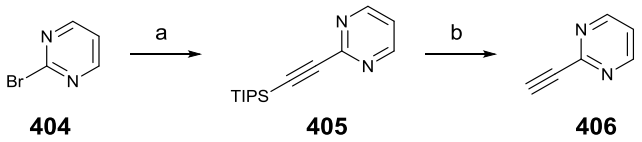

Scheme 17. Synthesis of 2-ethynylpyrimidine. Reagents and conditions: (a) TIPS-acetylene, $Pd(PPh_3)_2Cl_2$, CuI, Et_3N, DMF, 45%; (b) TBAF on silica, THF, 45%.

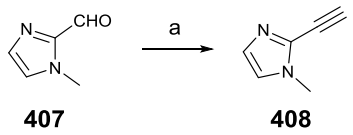

Scheme 18. Synthesis of 2-ethynyl-1-methylimidazole. Reagents and conditions: (a) Bestmann-Ohira reagent, MeOH, K_2CO_3, 86%.

The *C*-1 *n*-propoxy analogues were synthesised through S_NAr reaction of 4-chloropyridine **409** with *n*-PrONa, to yield compound **410**. Compound **410** was then alkylated with chloroacetone to yield the pyridinium **411** (Scheme 19).[318] Compound **411** underwent base-promoted [3+2] cycloaddition with alkynes to yield the target compounds (**412** and **413**).[313, 314] *C*-1 morpholine analogues were made in an analogous fashion, starting from commercially acquired 4-morpholinopyridine, **414**, which yielded targeted compounds **416**-**427** (Scheme 20).

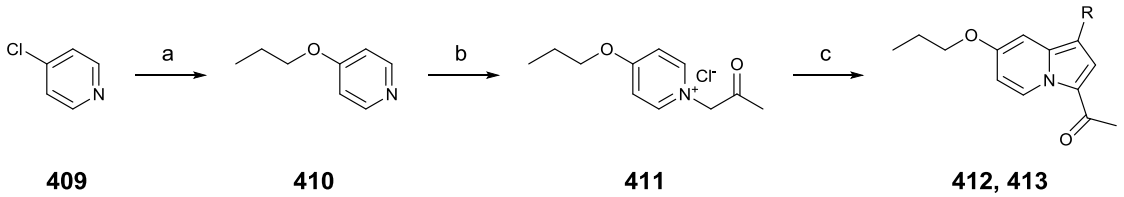

Scheme 19. Synthesis of *C*-1 analogues of an *n*-propxy indolizine. Reagents and conditions: (a) *n*-PrONa, *n*-PrOH, reflux (93%); (b) chloroacetone, THF, 75%; (c) alkyne (RH), K_2CO_3, DMF, 90 °C, 19-39%.

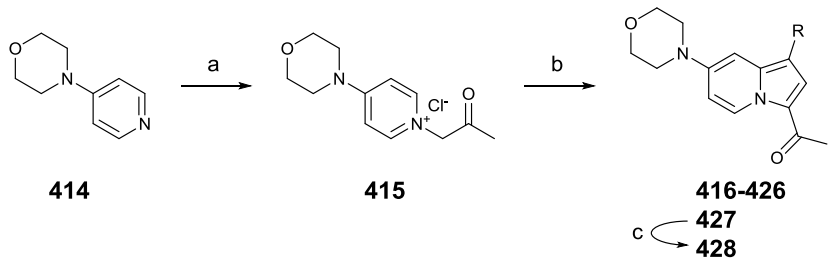

Scheme 20. Synthesis of *C*-1 analogues of a morpholino indolizine. Reagents and conditions: (a) Chloroacetone, THF, 91%; (b) Alkyne (RH), K_2CO_3, DMF, 90 °C, 4-40%.; (c) LiOH, H_2O, THF, MeOH (78%).

The yields for the [3+2] cycloaddition reactions were moderate to poor (4-40%). The low yield of the desired products was partly explained by the formation of several by-products. It was decided to isolate the main by-product from one of the reactions in order to help improve the synthesis. The main by-product isolated was the dihydroindolizinone **429** (Scheme 21).

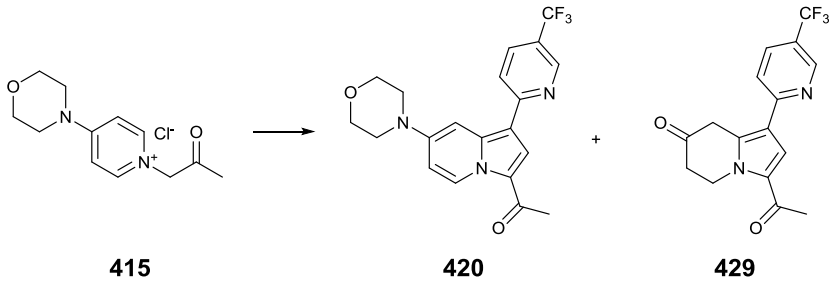

Scheme 21. Isolation of a ketone by-product **429** from a [3+2] cycloaddition reaction.

It was postulated that the ketone by-product **429** was formed prior to aromatisation of the indolizine ring; a proposed mechanism is shown in Scheme 22. The [3+2] cycloaddition yields intermediate **430**. Instead of aromatising to the desired indolizine, compound **430** undergoes a [1,5] prototropic shift to compound **431**. Compound **431** then undergoes a [1,7] prototropic shift to give enamine intermediate **432**, which can be protonated to give iminium **433**, then hydrolysed to the ketone by-product **429**.

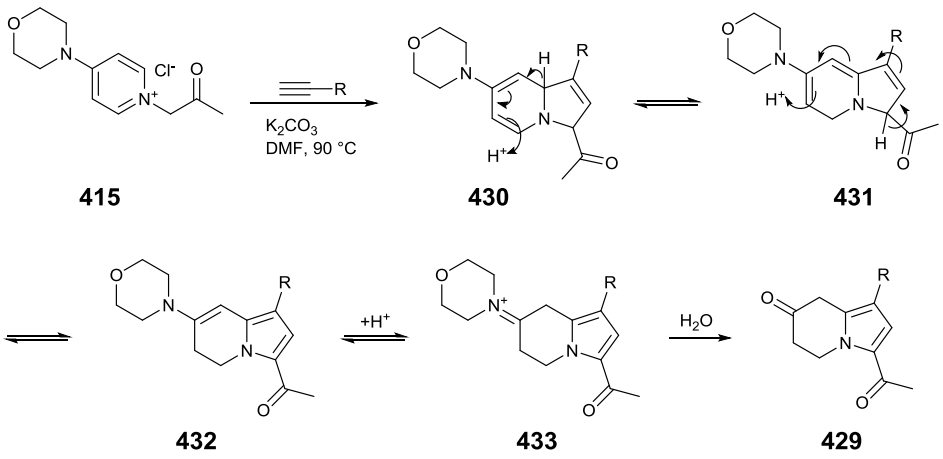

Scheme 22. A proposed mechanism for the formation of ketone by-product **429**.

Screening of alternative reaction conditions failed to change the reaction profile favourably. The addition of an oxidation reagent, such as 2,3-dichloro-5,6-dicyano-1,4-benzoquinone (DDQ), was considered to improve the yield of the desired product; however, it was found to be more practicable to separate the by-product and accept the low yields in order to rapidly generate targeted compounds.

The *C*-1 analogues were screened against BRD9 by DSF (Table 20). Additionally, the selectivity of the series was monitored by screening them against BAZ2A and BRD4(1). Generally, the selectivity of the series of compounds was good, with almost all analogues showing a higher ΔT_m for BRD9 compared with BAZ2A or BRD4(1). *C*-7 propoxy analogues **412** and **413** (BRD9 ΔT_m 0.48 °C and 0.50 °C, respectively) were significantly less potent against BRD9 than the corresponding morpholino analogues **416** and **427** (BRD9 ΔT_m 3.0 °C and 3.2 °C, respectively). The difference in ΔT_m confirms that the *C*-7 morpholine moiety is important for BRD9 potency. The introduction of substitution onto the 3-, 4-, 5- and 6-positions of the pyridine ring (compounds **416**-**422**, **427**, **428**) generally led to a drop in BRD9 potency compared to the original lead compound, **403** (ΔT_m 8.7 °C). In particular, substitution on the 3-position of the pyridine ring (compounds **419**, **420** and **422**) was poorly tolerated (ΔT_m ≤1.1 °C). The most potent substituted pyridine analogues were compounds **417** (BRD9 ΔT_m 8.5 °C) and **421** (BRD9 ΔT_m 5.0 °C). Analogues which replaced

the pyridine ring with an alternative heterocycle (**423**-**425**) had low to moderate affinity for BRD9 (ΔT_m 2.0-5.0 °C). The most potent of the *C*-1 heterocyclic analogues was the *C*-1 imidazopyridine compound **425** (BRD9 ΔT_m 5.0 °C).

Table 20. SAR for BRD9, BAZ2A and BRD4(1) binding as determined by DSF assay for indolizine analogues.

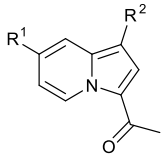

			DSF ΔT_m (°C)[*]		
Cmpd	*R^1*	*R^2*	*BRD9*	*BAZ2A*	*BRD4(1)*
412	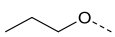	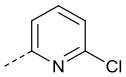	0.48 ± 0.10 (2)	-0.34 (1)	-0.55 (1)
413		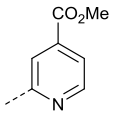	0.50 ± 0.36 (2)	-0.1 (1)	0.15 (1)
416		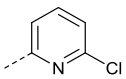	3.0 (1)	0.53 (1)	2.1 (1)
417		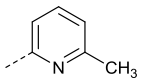	8.5 ± 0.15 (3)		3.0 (1)
418		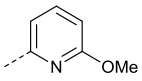	3.6 ± 0.66 (3)		3.1 (1)
419		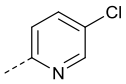	0.91 ± 0.055 (2)	0.060 (1)	0.097 ± 0.15 (3)
420		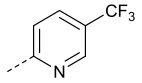	1.0 ± 0.27 (2)	0.34 (1)	-0.24 ± 0.058 (3)
421			5.0 ± 0.081 (3)		0.50 (1)

			DSF ΔT_m (°C)*		
Cmpd	*R^1*	*R^2*	*BRD9*	*BAZ2A*	*BRD4(1)*
422		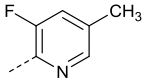	1.1 ± 0.11 (3)		0.40 (1)
423			3.4 ± 1.1 (2)	3.2 (1)	3.8 ± 1.1 (3)
424		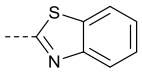	2.0 ± 0.23 (3)		1.9 (1)
425		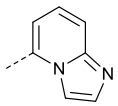	5.0 ± 0.37 (5)	0.92 ± 0.093	1.7 ± 0.18 (9)
426		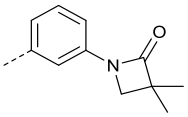	Ambiguous		6.1 (1)
427		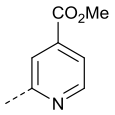	3.2 (1)	1.2 (1)	2.8 (1)
428		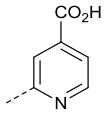	2.3 (1)	1.0 (1)	2.8 (1)

*Mean ΔT_m ± SEM (number of measurements).

The IC_{50} values against BRD9 and BZ2B were determined by AlphaScreen for the most potent of the *C*-1 analogues (compounds **417**, **421** and **425**) (Table 21). Compound **417** was potent against BRD9 (IC_{50} 0.46 μM). The potency of compound **417** was similar to the unsubstituted compound **403**, (IC_{50} 0.45 μM). However, compound **417** was ~30-fold selective over BAZ2B (IC_{50} 14 μM), which was a significant improvement on compound **403** (5.8-fold selective). This demonstrated that modification of the *C*-1 substituent could improve selectivity for BRD9 over BAZ2B. However, the potency of the series still needed to be improved to meet the targeted probe criteria.

Compound **421** was not very potent against BRD9 (IC_{50} 7.8 μM). However, compound **425** was highly potent (IC_{50} 0.10 μM) and was almost completely inactive against BAZ2B (34% inhibition at 100 μM compound concentration). The potency and selectivity of compound **425** warranted the determination of thermodynamic binding parameters by ITC (Table 22). The ITC results indicate that compound **425** is highly potent (K_d 0.068 μM), and the binding of compound **425** is driven by a large enthalpic contribution (ΔH -10.7 kcal/mol).

Since the DSF results had indicated that there may be some potency against BRD4(1) the K_d was also determined for compound **425** against BRD4(1). Pleasingly, the results show there is 34-fold selectivity for BRD9 over BRD4(1) with K_d 2.3 μM. Therefore compound **425** meets the targeted chemical probe criteria for *in vitro* potency and selectivity. Further characterisation of the selectivity and cellular activity of **425** was therefore carried out.

Table 21. SAR for BRD9 and BAZ2B binding as determined by AlphaScreen assay for selected *C*-1 indolizine analogues.

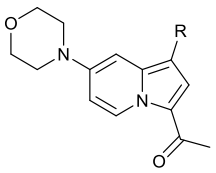

Cmpd	*R^2*	*AlphaScreen IC_{50} (μM)*		*BRD9 selectivity (-fold)*
		BRD9	*BAZ2B*	
417	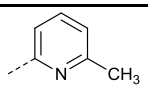	0.46	14	30
421		7.8	14% @ 100 μM	>13
425	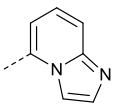	0.10	34% @ 100 μM	>1000

Table 22. Determination of BRD9 binding constant by ITC for compound **425**.

	BRD9			*BRD4(1)*			
Cmpd	*K_d (μM)*	*ΔH (kcal/mol)*	*-TΔS (kcal/mol)*	*K_d (μM)*	*ΔH (kcal/mol)*	*-TΔS (kcal/mol)*	*BRD9 selectivity (-fold)*
425*	0.068	-10.7	1.32	2.3	-4.51	-3.04	34

7.4 SELECTIVITY PROFILING OF COMPOUND **425**

The selectivity of compound **425** was assessed by DSF for a representative set of BRD proteins and the results were compared to those for the lead compound **403** (Figure 43). Compound **403** was found to be fairly non-selective; in addition to BRD9, compound **403** showed moderate affinity for BRD4(1), BAZ2A, CECR2 (cat eye syndrome critical region protein 2), BAZ2A, BRPF1B (BRD and PHD finger containing protein 1, isoform B) and CBP. The broad-spectrum affinity mean that compound **403** could find potential utility as a pan-BRD inhibitor.[319] As expected, compound **425** was potent against the BRD9 paralog, BRD7 (ΔT_m 5.6 °C). Encouragingly, compound **425** is very selective for BRD9/BRD7, with little affinity (T<1°C) across families 5-8, including BAZ2A and BAZ2B. Compound **425** has minor affinity for CBP, p300 and FALZ (Foetal Alzheimer antigen) (ΔT_m 1.8, 2.0 and 1.1 °C respectively). The high selectivity of compound **425** for BRD9/BRD7 imply that this compound could be used to investigate the biology of BRD9 and BRD7 without interference from other BRD proteins, and thus supports its use as a chemical probe.

*Carried out by Cynthia Tallant Blanco (TDI).

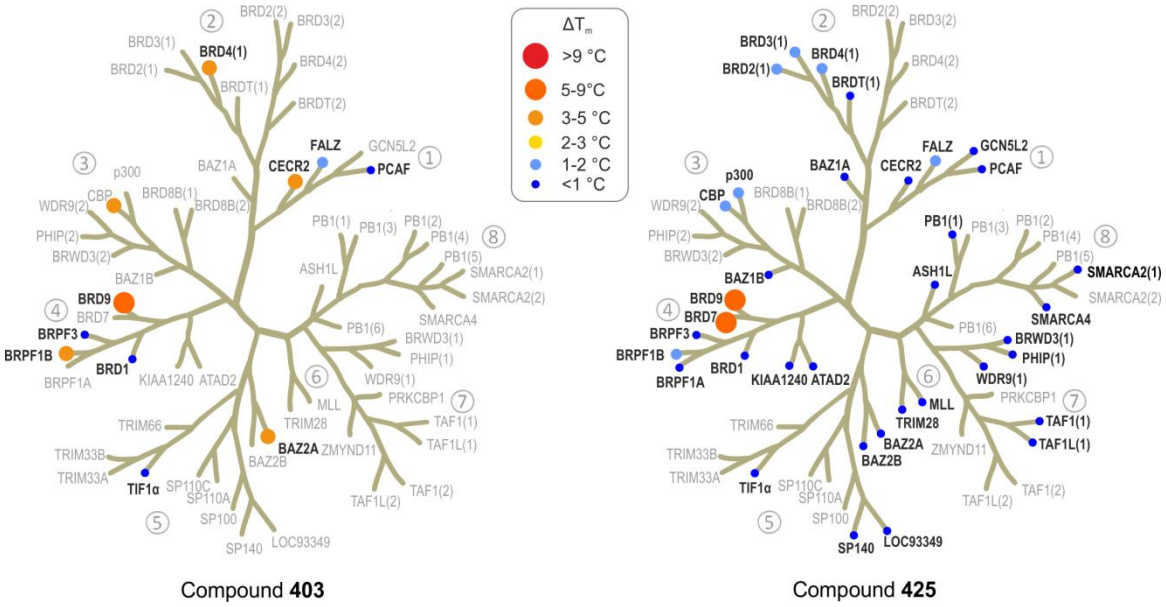

Figure 43. DSF screening of compounds **403** and **425** against various BRD subfamily member. Compound **403** is a broad-spectrum BRD inhibitor. Compound **425** is selective for BRD9 and BRD7.

7.5 STRUCTURE OF COMPOUND **425** BOUND TO BRD9

In order to understand the binding of compound **425** to BRD9, an X-ray crystal structure was determined (Figure 44). The ketone carbonyl of compound **425** forms the expected Kac mimicking interactions between N216 and Y163. Additionally, the indolizine ring of compound **425** forms a π-π interaction with Y222. The *C*-7 morpholino moiety of compound **425** is in a hydrophilic region between I169 and Y173, whereas the *C*-1 imidazopyridine moiety is situated in a lipophilic region, sandwiched between the I169 and F160 side-chains. Interestingly, the *C*-1 heterocycle of compound **425** has apparently displaced a water molecule which is usually well conserved in complexes of BRD9 (e.g. Figure 44C).

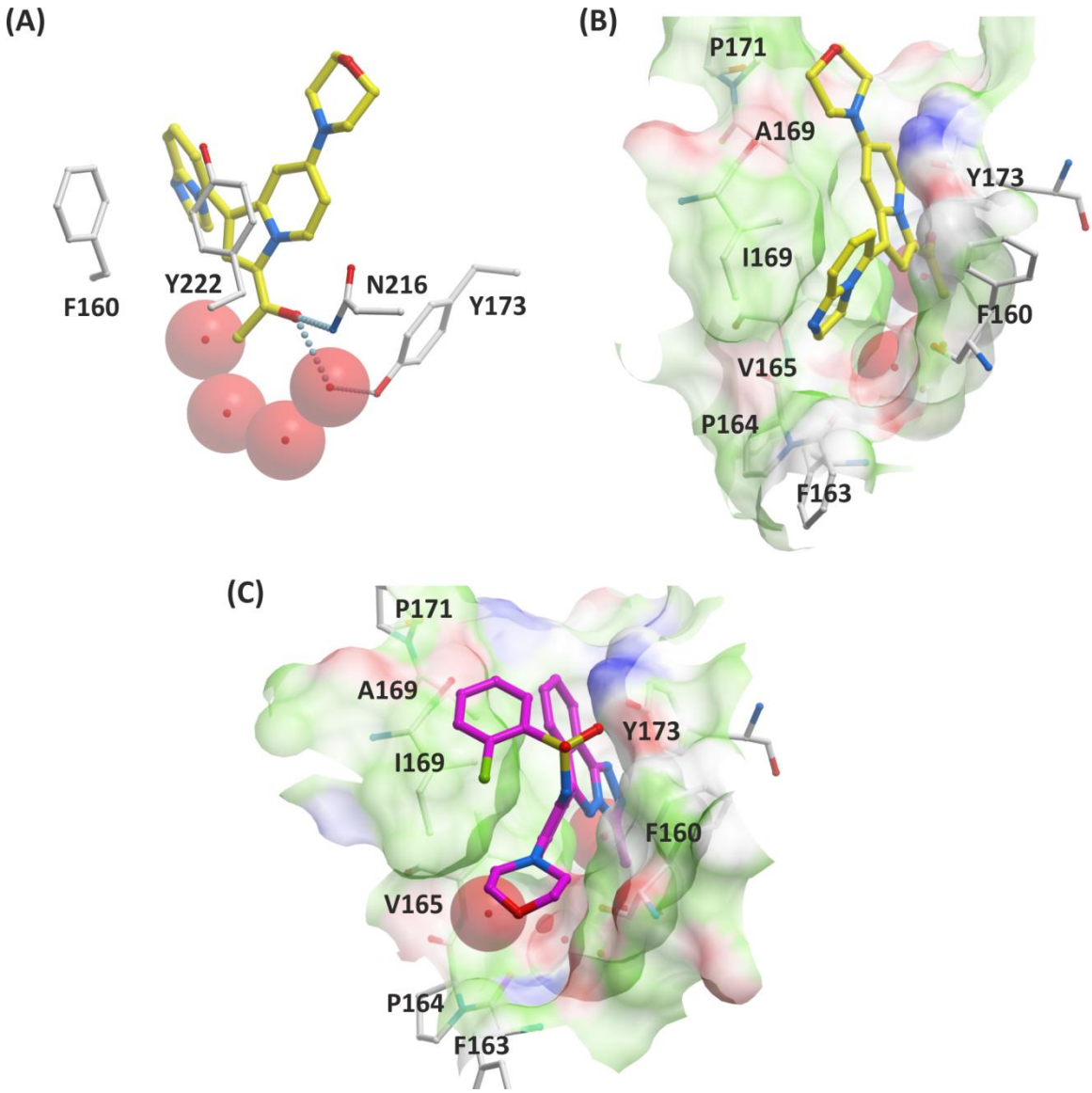

Figure 44. (A) View from X-ray crystal structure of compound **425** complexed to BRD9 showing hydrogen-bond from ketone to N216 (3.06 Å) and a water molecule (2.92 Å). An apparent π-π interaction is also observed between the indolizine ring of **425** and Y222;* (B) As in (A) showing the surface of the binding pocket and selected residues which are in close proximity to **425**. (C) View from X-ray crystal structure of a ligand bound to BRD9 showing a water molecule in the ZA channel next to F163 and P164 which has been displaced in the complex with **425** as seen in (B) (PDB 4NQM).

7.6 CELLULAR CHARACTERISATION OF COMPOUND **425**

The on-target cellular efficacy of compound **425** was investigated using a FRAP-based assay (Figure 45). U2OS cells transfected with a construct encoding GFP-tagged murine BRD9† showed a quick recovery time (t½ 1.8 s) upon photobleaching of a small area of the nucleus.

*Crystallography and refinement of crystallographic data was carried out by Cynthia Tallant Blanco (TDI).
†Murine BRD9 is 94.8% similar to human BRD9 and the BRD is 99% similar.

Stimulation with the broad-spectrum KDAC inhibitor, SAHA, to increase global lysine acetylation and expand the assay window increased recovery time (t½ 2.7 s). Treatment of cells with compound **425** at 1 μM reduced the FRAP recovery time (t½ 2.2 s). Cells needed to be treated with 5 μM of **425** in order to reduce the FRAP recovery time back to unstimulated levels (t½ 1.6 s).

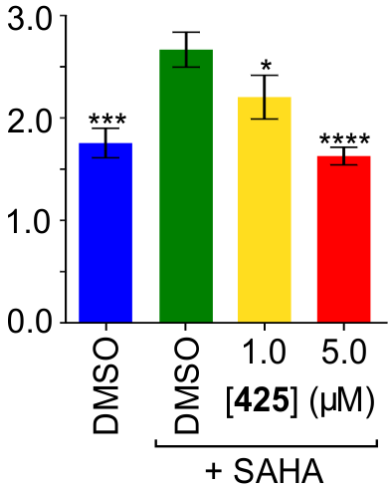

Figure 45. FRAP assay with **425**.† Half times of fluorescence recovery ($t_{½}$). Bars represent the mean $t_{½}$ calculated from individual recovery curves of at least 10 cells per group. First column (blue) GFP-tagged murine BRD9 construct; second column (green): construct treated with 2.5 μM SAHA; third column (yellow): construct treated with 2.5 μM SAHA and 1 μM compound **425**; fourth column (red): construct treated with 2.5 μM SAHA and 5 μM compound **425**. The significance of groups compared with the control was determined by *t*-tests *p<0.05, ***p<0.001, ****p<0.0001;

The relatively low cellular potency of **425** in the FRAP assay was surprising, given its high *in vitro* potency. In some assays using **425**, precipitation had been observed, so it was postulated that low solubility of **425** may limit the cellular potency. Therefore, it was desirable to synthesise more soluble analogues in order to potentially increase cellular potency.

† FRAP assay was carried out by Martin Philpott (SGC/TDI).

7.7 IMPROVING SOLUBILITY

The calculated pKa_H of the imidazopyridine moiety in compound **425** is 6.5 (Table 23).[320] Thus compound **425** is predominantly uncharged at physiological pH (~7.4). Replacement of the morpholino moiety with a piperazine ring would introduce a new basic centre into the scaffold which could improve aqueous solubility. Table 23 shows the calculated pKa_H values and solubilities of compound **425** and a selection of possible piperazine targets. The calculated pKa_H for the piperazine compounds **434** and **435** is 7.1 and 8.5, respectively for the first protonation. Additionally, the piperazine targets give a 4-5 fold increase in calculated solubility in comparison to compound **425**. The improvement in calculated solubility values supports the synthesis of *C*-7 piperazine analogues.

Table 23. Calculated pKa_H and solubility (ACD iLAB) for compound **425** and potential piperazine targets.[320]

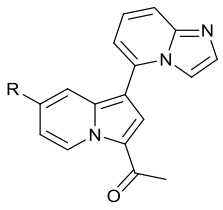

Cmpd	*R*	*cpKa$_H$ (1)*	*cpKa$_H$ (2)*	*cSolubility (mg/mL)*
425	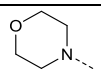	6.5	-	0.2
434	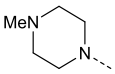	7.1	6.5	0.8
435	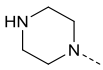	8.5	6.5	1.0

C-7 piperazine analogues were synthesised according to Scheme 23. The commercially acquired pyridinyl piperazine, **436**, was methylated or Boc-protected, then quaternised and cyclised with alkynes as described for previous analogues.

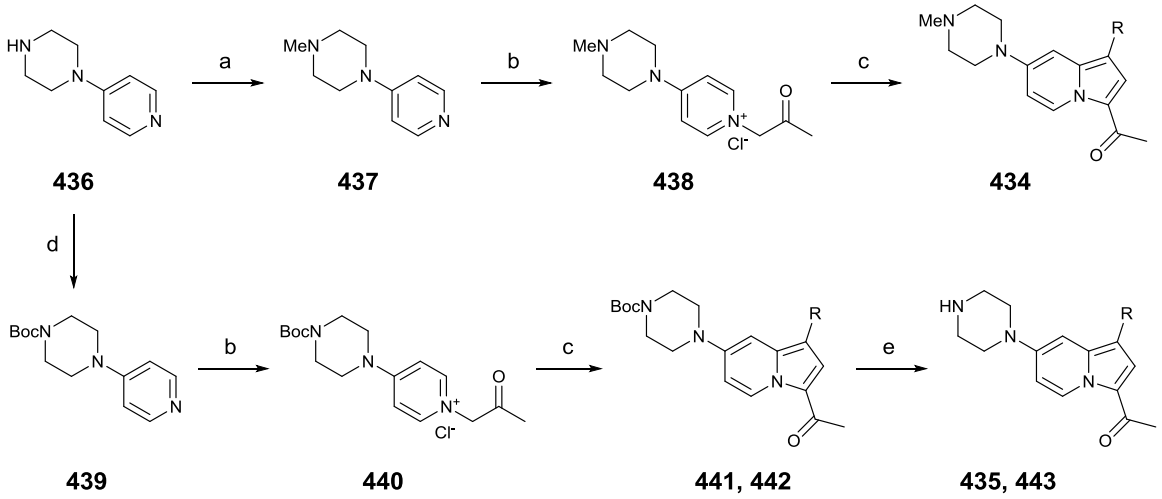

Scheme 23. Synthesis of *C*-1 analogues of an *n*-propxy indolizine. Reagents and conditions: (a) MeI, K_2CO_3 DMF, 56%; (b) Chloroacetone, THF, 34-65%; (c) Alkyne (RH), K_2CO_3, DMF, 90 °C, 3-21%; (d) di-*tert*-butyl dicarbonate, THF, 89%; (e) HCl, dioxane (quant).

The DSF results indicated that the *C*-7 piperazine analogues, **434**, **435** and **443**, were highly potent against BRD9 (ΔT_m 7.2-8.3 °C) (Table 24). However, the piperazine analogues were also potent against BRD4(1) (2.9-3.8 °C) and CBP (3.1-5.7 °C). Therefore, further modification of the series was required in order to improve selectivity for BRD9 over BRD4(1) and CBP, whilst maintaining the postulated solubility enhancement afforded by the basic *C*-7 piperazine moiety. As was previously shown, the *C*-1 imidazopyridine ring is important for potency and selectivity for BRD9 over BAZ2B. Therefore, it was decided to modify the *C*-3 ketone group to investigate if BRD9 selectivity could be improved.

Table 24. SAR for BRD9, BRD4(1) and CBP binding as determined by DSF assay for *C*-7 piperazine analogues.

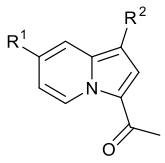

			DSF ΔT_m (°C)*		
Cmpd	R^1	R^2	*BRD9*	*BRD4(1)*	*CBP*
434	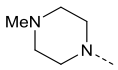	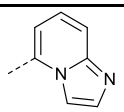	7.2 ± 1.0 (2)	2.9 ± 1.4 (2)	5.7 (1)
435	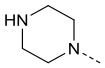	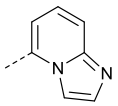	8.3 (1)		
443	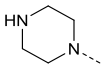		7.3 ± 0.43 (3)	3.8 (1)	3.1 (1)

*Mean ΔT_m ± SEM (number of measurements).

7.8 *C*-3 ANALOGUES

Alternative *C*-3 substituents were incorporated into targets as shown in Scheme 24. Commercially acquired α-halo ketones were reacted with pyridines, **414** and **437**, to yield the pyridinium precursors, **444**-**450**, for the indolizine forming cycloaddition. An α-halo ketone that was not available commercially was prepared by chlorination of β-keto ester **458** to yield compound **459**, followed by decarboxylation to yield compound **460** (Scheme 25).

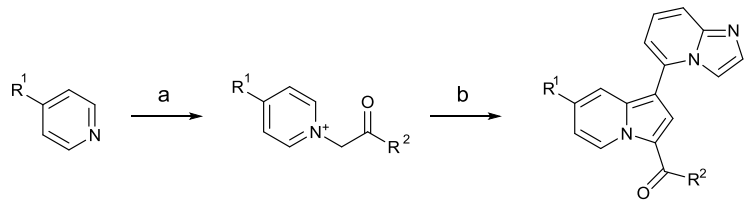

Scheme 24. Reagents and conditions: (a) R^2COCH_2X (X = Cl, Br), THF or acetone (15-89%); (b) 5-ethynylimidazo[1,2-*a*]pyridine,, K_2CO_3 90 °C (2.3-20%).

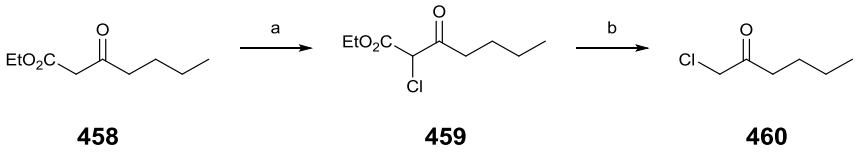

Scheme 25. Reagents and conditions: (a) $SOCl_2$, CH_2Cl_2, 98%; (b) *conc.* H_2SO_4, H_2O, reflux, 64%.

The DSF results for the *C*-3 ketone analogues **451-457** indicated that they were less potent against BRD9 (ΔT_m 0.070-4.1 °C) than their *C*-3 methyl ketone equivalents, compounds **425** and **434** (BRD9 ΔT_m 5.0 °C and 7.2 °C, respectively). The data therefore suggested that the BRD9 Kac binding site may be able to accommodate substituents larger than methyl ketones, although the affinity seems less than for the methyl ketone equivalents (Table 25). In particular, the *C*-3 cyclopropyl ketone analogue, **455**, was inactive against BRD9 (ΔT_m 0.070 °C). The low affinity of the cyclopropyl analogue could be due to the greater degree of sp^2 character in the cyclopropane ring, which changes the electronics, the flexibility, and the orientation of the carbon atoms in comparison to acyclic analogues.[321] BRD4(1) affinity was observed for analogues **451-454** (ΔT_m 1.5-3.2 °C), which was similar to the affinity of the *C*-3 methyl ketone analogues **425** and **434** (BRD4(1) ΔT_m 0.92 °C and 2.9 °C, respectively). However, the *C*-3 trifluoromethyl analogue, **457**, was encouraging as it was moderately potent against BRD9 (ΔT_m 4.0 °C) and inactive against BRD4(1) and CBP (ΔT_m < 1 °C). Compound **457** therefore warrants further testing to determine its IC_{50} and selectivity profile. Further, the *n*-butyl analogue **456** had some potency against BRD9 (ΔT_m 3.3 °C) and was selective over BRD4(1) (ΔT_m 0.83 °C), so this analogue may warrant further testing. Overall, the results suggest that the BRD9 Kac binding site may be able to accommodate

substituents larger than methyl ketones, although the affinity appears to be less than for the methyl ketone equivalents.

Table 25. SAR for BRD9, BRD4(1) and CBP binding as determined by DSF assay for *C*-3 ketone analogues.

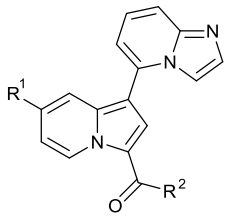

			DSF ΔT_m (°C)*		
Cmpd	R^1	R^2	*BRD9*	*BRD4(1)*	*CBP*
451	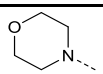	-Et	4.1 (1)	1.7 (1)	0.68 ± 0.070 (2)
452		-CF_3	3.4 (1)	1.5 (1)	0.38 ± 0.15 (2)
453	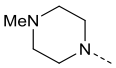	-Et	3.9 (1)	3.2 (1)	1.9 ± 0.0050 (2)
454	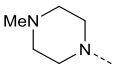	-*i*-Pr	2.0 ± 0.11 (3)	1.8 (1)	
455	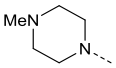	*c*-Pr	0.070 ± 0.13 (3)	0.53 (1)	
456	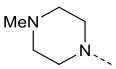	-*n*-Bu	3.3 ± 0.23 (3)	0.83 (1)	
457	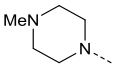	-CF_3	4.0 ± 0.97 (4)	0.62 ± 0.21 (3)	0.040 (1)

*Mean ΔT_m ± SEM (number of measurements).

7.9 SUMMARY

Potent and selective small molecule inhibitors of the BRD9/BRD7 BRD were developed. *C*-1 analogues of the indolizine lead series were prepared via a [3+2] cycloaddition reaction

(Scheme 20). Low yields were found to be partly due to the formation of a cyclic ketone by-product (Scheme 21). A mechanism was postulated for the formation of the by-product whereby an enamine, which is formed prior to indolizine aromatisation, is hydrolysed to the ketone (Scheme 22). *C*-1 analogues gave potent compounds (Tables 20 and 21Table 20); the optimal compound, **425**, was highly potent *in vitro* (K_d 68 nM) and selective (~30-fold) over the BET subfamily member, BRD4(1) (Table 22). DSF implied that compound **425** was selective over the other BRD sub-families, with only modest affinity against the BET family, CBP/p300 and FALZ (Figure 43). On target cellular efficacy of compound **425** was demonstrated in a FRAP assay, although relatively high concentrations of inhibitor (5 μM) were required to show an effect (Figure 45). It was thought that low solubility of the indolizine compounds may give rise to lower than anticipated cellular activity. Therefore, *C*-7 piperazine analogues were prepared in order to increase the solubility of target compounds (Scheme 23). The *C*-7 piperazine analogues were highly potent against BRD9 (ΔT_m > 7 °C); however, these analogues were also potent against BRD4(1) and CBP (Table 24). Attempts to improve the selectivity through the synthesis of *C*-3 ketone analogues (Schemes 24 and 25) gave reduced BRD9 potency (Table 25). The trifluoromethyl analogue **457** was the most potent and selective of the *C*-3 analogues and warrants further investigation to determine potency and selectivity.

CHAPTER 8. SUMMARY

8.1 CBP/P300 CHEMICAL PROBE

CBP and p300 are ubiquitous pleiotropic transcriptional coactivators and lysine acetyl transferases (Chapter 2). CBP/p300 play vital roles in development and disease. Mice knockout studies show that CBP/p300 are vital for embryonic development, and a haploinsufficiency in CBP/p300 is linked to the developmental disorder Rubinstein-Taybi Syndrome. CBP/p300 are important for normal cell function; aberrant expression and mutations have been linked to a variety of cancers. In particular, haematological malignancies such as myeloid and lymphoid acute leukaemia and therapy-related myelodysplasia have been linked to CBP/p300. In addition to their roles in oncology, CBP/p300 are thought to be important in several neurodegenerative disorders, pain and inflammation and viral infection.

CBP/p300 exert their multitude of functions through 9 conserved domains which interact with transcription factors and coactivators, and basal transcriptional machinery (Figure 46A). The lysine-acetyl transferase (KAT) domain of CBP/p300 is responsible for adding an acetyl group to the ε-amino group of lysine side-chains on histones and various non-histone proteins. Acetylation neutralises the positive charge on the lysine side-chain, which can affect the interaction with neighbouring residues, such as the negatively charged phosphodiester backbone of DNA (Chapter 1). When acetylated, the electrostatic interaction between histone lysines and DNA is reduced, making the DNA more accessible to transcriptional machinery. Additionally, acetylated lysines can act as a 'mark' for binding to proteins which contain a bromodomain (BRD).

The BRD binds to acetylated lysines, which allows for the recruitment of BRD-containing proteins and for the assembly of multicomponent transcriptional complexes. CBP and p300

contain a BRD which is thought to work in concert with the KAT domain, helping to maintain and amplify the catalytic activity (Figure 46B-D).

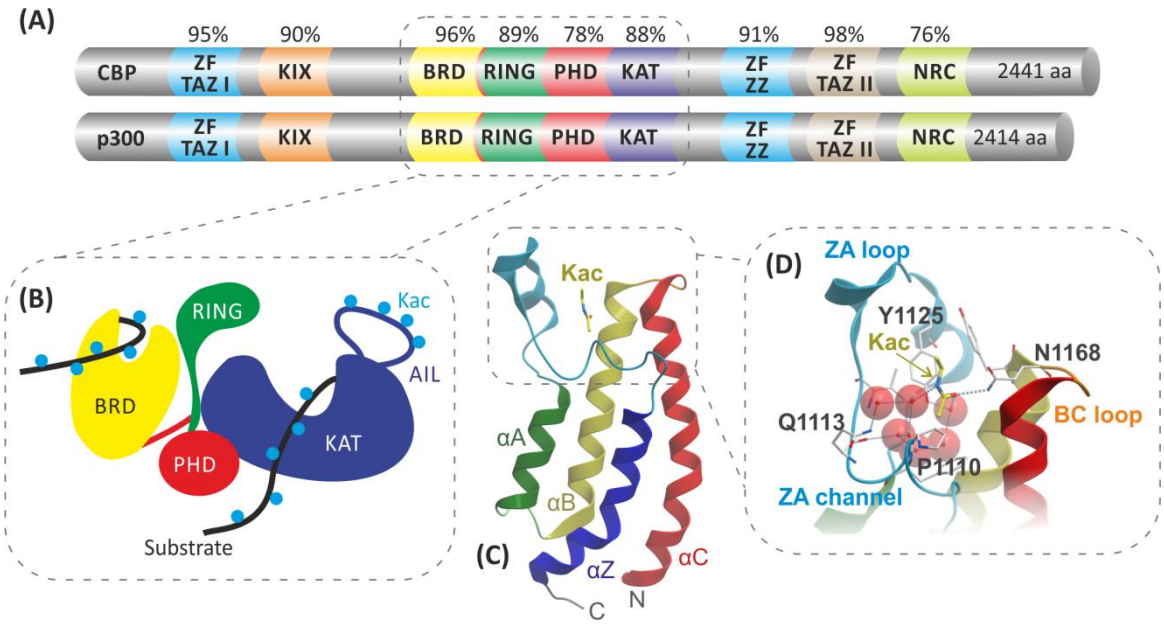

Figure 46. (A) Percent conservation and domain organization of human CBP (accession no. Q92793) and p300 (accession no. Q09472). (B) 'Catalytic' core of p300. Following activation via acetylation of the autoinhibitory loop (AIL) and subsequent substrate acetylation, binding of acetylated substrate to the BRD results in positive feedback and maintenance of p300 catalytic signal. (C) CBP 'BRD-fold' depicting the four α-helices (αZ, αA, αB, αC) and the ZA and BC loops that form the Kac binding pocket (derived from PDB 3P1C). (D) Structure of an acetyl lysine (yellow – only partial structure shown) and CBP BRD complex. Key interactions are shown, including H-bond (dotted lines) from the Kac carbonyl to N1168 and a water-mediated H-bond from the Kac carbonyl to Y1125 (PDB 3P1C).

The study of the various domains of CBP/p300 will help to further our understanding of their biological function, and may give mechanistic insight into how they contribute to the multitude of CBP/p300 disease phenotypes. The use of chemical probes to study protein domains complements genetic approaches. Therefore, potent and selective inhibitors can contribute to the study of the CBP/p300 domains and could help to validate new targets for the pharmaceutical industry. The aim of this project was to design and synthesise a potent and selective inhibitor of the CBP/p300 BRD which could be used as a cellular tool compound. In order to provide useful and unambiguous readouts from cell assays, the criteria set for a chemical probe were that it should be potent *in vitro* (≤100 nM), selective over other BRD subfamilies (≥30-fold) and active in cells (≤1 μM).

The project began with a dimethylisoxazole benzimidazole compound **26** (Figure 47), which is a weak and non-selective inhibitor of CBP and BRD4(1) (Chapter 3). Compound **26** was

viewed as an attractive starting point, due to its fragment-like high ligand efficiency (LE 0.46) and suitability for rapid synthresis of analogues. However, it was recognised that obtaining selectivity for CBP/p300 over BRD4(1), represented a significant challenge. It was initially envisaged that substitution on the *N*-1 and *C*-2 positions of the benzimidazole core would access areas of where the BRDs of CBP and BRD4(1) differ, thus giving rise to selective compounds. In particular, the 'shelf' regions of CBP and BRD4(1) contain prominent features that differ in each protein. The CBP shelf contains an arginine (R1173), which could interact with suitable compound substituents, and the BRD4(1) shelf contains a tryptophan side-chain (W81) which could be exploited through, for example, the introduction of unfavourable steric interactions with compound substituents.

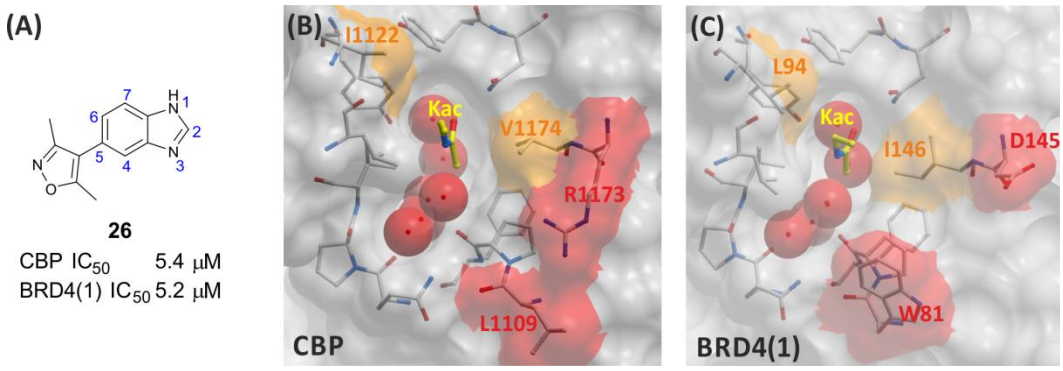

Figure 47. (A) Compound **26**, a non-selective dimethylisoxazole benzimidazole inhibitors of CBP and BRD4(1). (B) and (C): CBP and BRD4(1) BRD, Kac binding pockets. Residues which differ, but retain similar side-chain characteristics are coloured orange. Significantly different amino acid residues are shown in red.

Initially, diversity was introduced into the scaffold through parallel Suzuki cross-couplings and benzimidazole forming reactions. Compounds were screened using DSF (differential scanning fluorimetry) and AlphaScreen (amplified luminescent proximity homogeneous assay screen). The structure-activity relationship (SAR) observed for the products obtained indicated that 1,2-disubstituted benzimidazole compounds could give rise to compounds which were selective for CBP over BRD4(1). The optimal hit compound from this initial set was compound **263** (Figure 48A), which was potent against CBP by AlphaScreen (IC_{50} 0.48 μM) and selective for CBP over BRD4(1) by DSF (ΔT_m 6.3 °C and 2.9 °C, respectively).

Compound **263** was therefore selected as the basis for further optimisation of potency and selectivity.

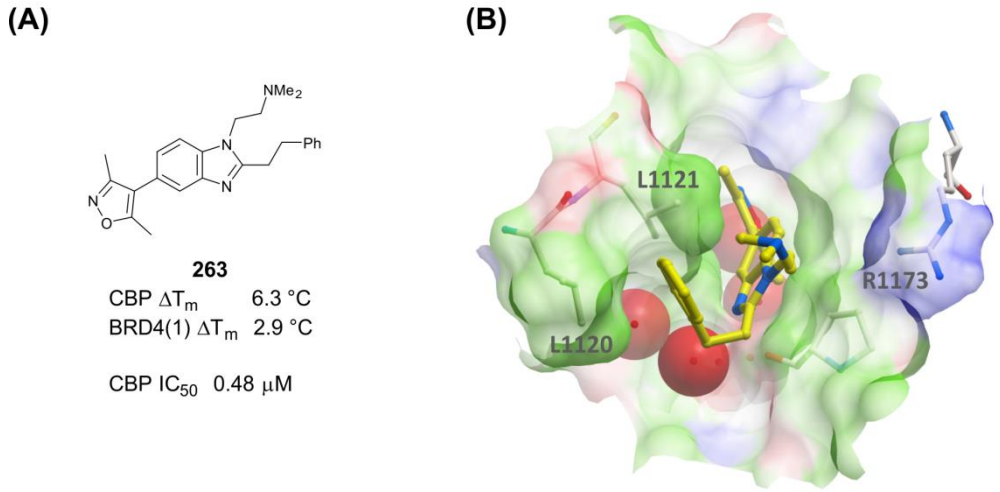

Figure 48. (A) Compound **263**, a selective CBP hit compound. (B) View from X-ray crystal structure of **263** (carbon=yellow) bound to CBP BRD, showing pocket surface and selected residues on the edge of the pocket in close proximity to the benzimidazole *N*-1 and *C*-2 moieties.

In order to guide the design of potent and selective analogues, compound **263** was crystallised bound to the CBP BRD (Chapter 4). The structure obtained was ambiguous due to the potential influence of crystallographic artefacts, but did imply that varying the *N*-1 and *C*-2 substituents could bring about favourable interactions with R1173 (Figure 48B). *C*-2 analogues were synthesised through various synthetic approaches, including lateral lithiation, Knoevenagel condensation and dehydrative benzimidazole formation reactions. *N*-1 analogues were prepared by benzimidazole forming reactions, or via reductive aminations. The SAR showed that the dimethylamino moiety of compound **263** could be replaced by cyclic amines; in particular, morpholine analogues such as compound **308** were potent against CBP (Figure 49A). Isothermal titration calorimetry confirmed that compound **308** was potent against CBP (K_d 0.32 μM). However, ITC also revealed that compound **308** was only 2.7-fold selective over BRD4(1). Optimisation of the *C*-2 linked aryl ring indicated that electron-rich and halogen-containing aryl or heteroaryl rings were preferred over equivalent electron poor aryl groups. Optimal compounds were highly potent and selective, for example compound **321** (CBP K_d 0.050 μM, 11-fold selective over BRD4(1)) and compound **341** (CBP K_d 0.030 μM, 22-fold selective over BRD4(1)).

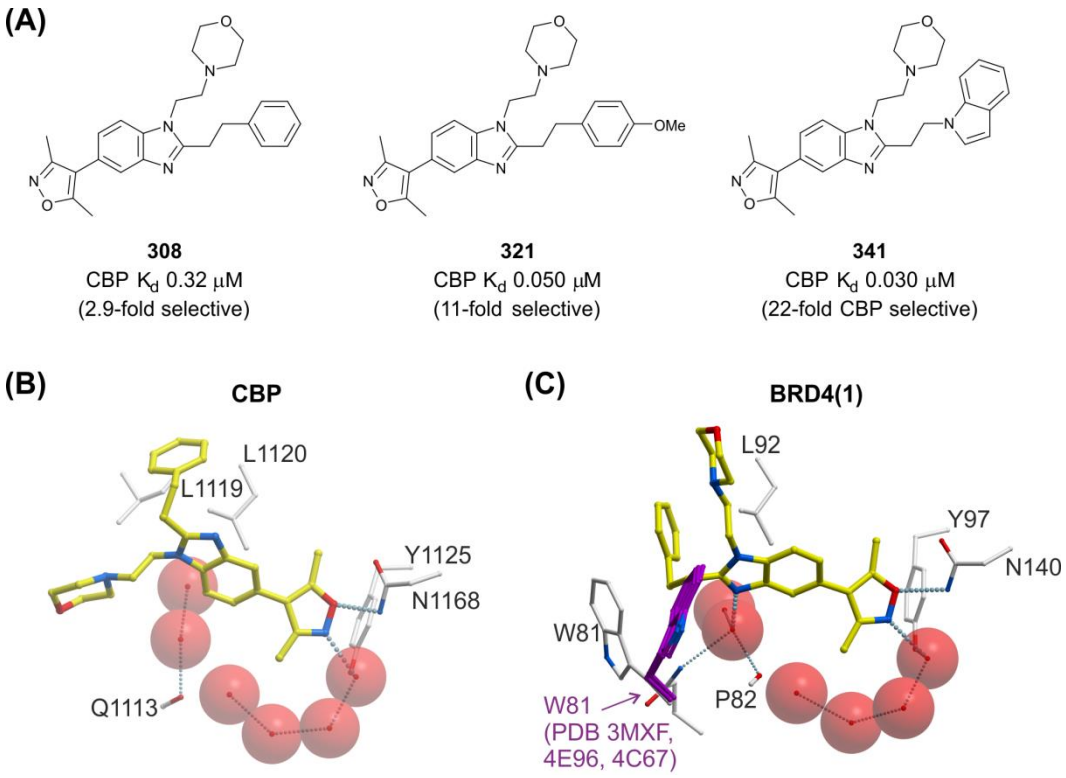

Figure 49. (A) Optimisation of the *N*-1 ethylamino and *C*-2 ethylaryl moieties led to potent and selective CBP inhibitors (the selectivity values quoted in parenthesis are for CBP over BRD4(1)). (B) View from X-ray crystal structure **308** complexed to CBP showing hydrogen-bonding between isoxazole oxygen atom and N1168 (3.02 Å), and isoxazole nitrogen and a water molecule (2.75 Å). (B) View from compound **308** complexed to BRD4(1) showing hydrogen-bonding between isoxazole oxygen atom and N140 (3.05 Å), and isoxazole nitrogen and a water molecule (2.72 Å). Water mediated hydrogen-bonds from the benzimidazole of **308** *N*-3 to Q85 and the carbonyl of P82 are also shown (3.54 Å from **308** benzimidazole *N*-3 to water molecule). W81 is shown overlaid with the same side-chain from other published ligand-bound X-ray structures of BRD4(1) (carbon = magenta).

With highly potent compounds in hand, attention turned to the optimisation of selectivity for CBP over BRD4(1) through the use of structure-guided design (Chapter 5). Compound **308** was crystallised bound to the CBP and BRD4(1) BRDs (Figure 49B and C). In the BRD4(1) complex, W81 had moved considerably from the usual orientation found in ligand-bound structures, in order to accommodate the *C*-2 phenethyl group. Therefore, it was envisaged that substitution of the *N*-1 and *C*-2 ethylene linkers with polar or conformationally constrained groups could further disfavour BRD4(1) binding through the introduction of unfavourable electrostatic, or steric interactions with W81. Additionally, a different binding mode was observed between the ligand bound to CBP and BRD4(1). The benzimidazole moiety of compound **308** is bound in a 'flipped' conformation in BRD4(1) compared to CBP (Figure 49B and C). In the BRD4(1) structure, the binding mode is stabilised through a water mediated hydrogen-bond from the *N*-3 nitrogen of **308** to the backbone of P82 and the amide

side-chain of Q82. An equivalent interaction is not present in the complex of compound **308** and CBP. Therefore, compounds were designed to disfavour the BRD4(1) binding mode, through replacement of the benzimidazole core with an indole which could not make the same water-mediated hydrogen-bonds to the protein. Additionally, it was envisaged that 6-substitued analogues could favour the CBP binding mode through the potential formation of hydrogen-bonds to well-conserved water molecules in the CBP binding pocket. Figure 50 summarises the various structure-guided design strategies for the optimisation of CBP selective compounds.

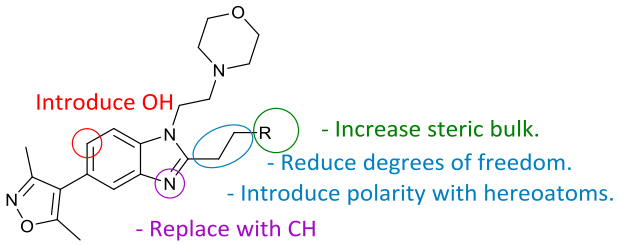

Figure 50. Summary of structure-guided designs, targeted at improving selectivity for CBP over BRD4(1).

Disappointingly, an indole core and 6-hydroxy analogues gave no improvements in potency or selectivity. Additionally, analogues which replaced the *C*-2 ethylene linker with polar or conformationally restrained groups were less potent or selective than their equivalent ethylene linked analogues. Attention then turned to substitution of the *N*-1 ethylene linker. Compounds with a chiral branching methyl group on the *N*-1 ethylene linker gave encouraging results, with the (*S*)-forms being highly potent by ITC ($K_d \leq 69$ nM). The optimal analogue, compound **397**, is 40-fold selective for CBP over BRD4(1) (Figure 51A).

Compound **397** was crystallised bound to CBP and was shown to possess a key cation-π interaction between the aryl ring of **397** and the guanidinium side-chain of R1173, which was not present in the equivalent structure of compound **308** (Figure 51B and C). The chiral methyl group is positioned below the aryl ring and appears to 'lock' this in place. In order to investigate the selectivity over other BRD sub-families, compound **397** was screened against a selection of BRDs and was found to be highly selective for CBP/p300 (Figure 51D).

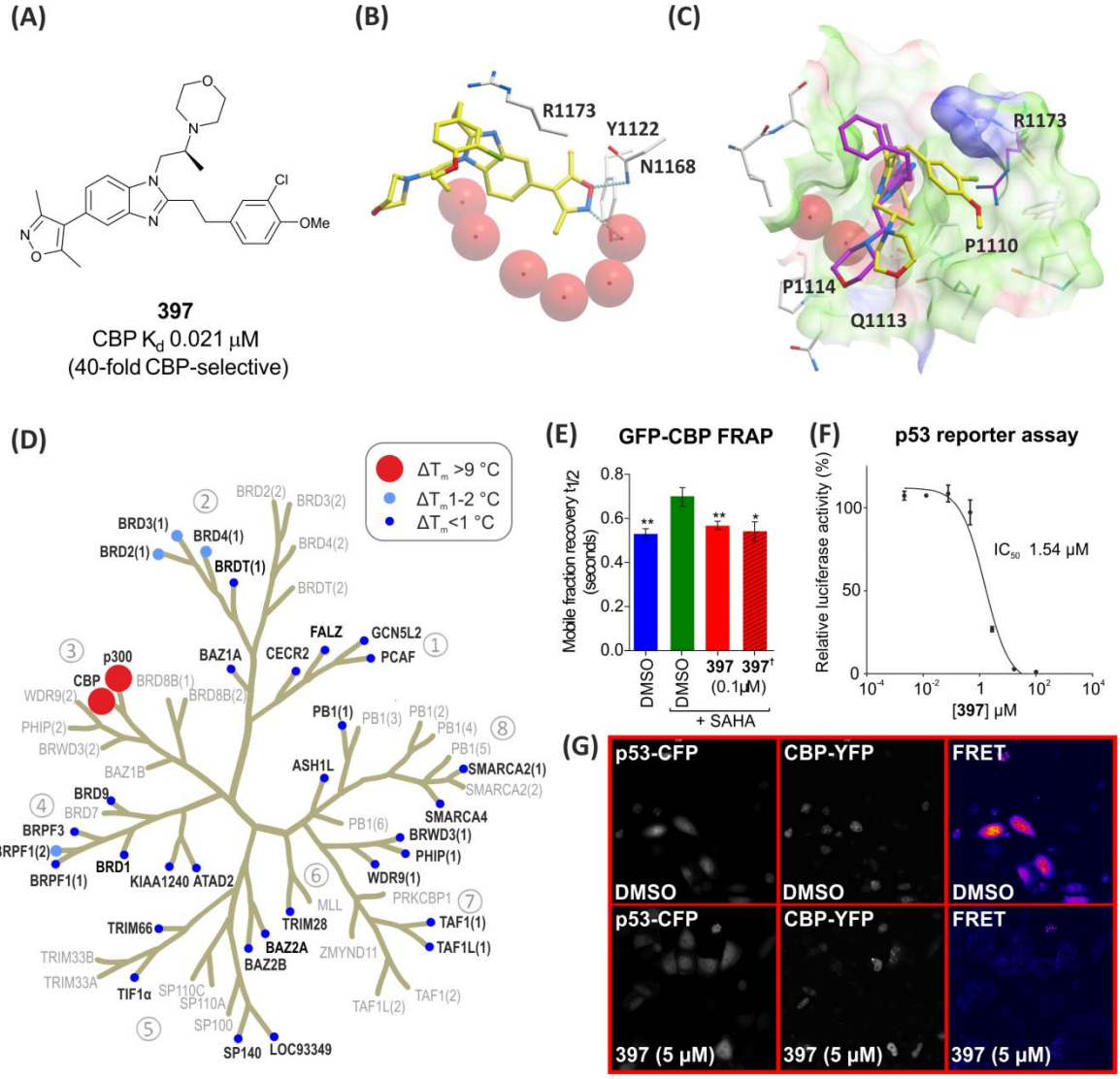

Figure 51. (A) Compound **397** (the selectivity value quoted in parenthesis is for CBP over BRD4(1)). (B) and (C): Views from X-ray structure of compound **397** (carbon = yellow) complexed to CBP BRD. Hydrogen-bonding interactions between isoxazole oxygen and N1168 (3.08 Å) and isoxazole nitrogen and a conserved water molecule (2.83 Å) are shown in (B). In (C), a cation-π interaction is observed between the aryl ring of compound **397** and R1173 (3.54 Å between nearest atoms of compound **397** and R1173). The cation- π interaction is made possible by R1173 flipping out from the position observed in other structures such as for compound **308**, which is overlaid for comparison (carbon = magenta). An induced-pocket is formed through the movement of R1173. (D) DSF selectivity profiling of compound **397** against various BRD subfamily members, indicating high selectivity for CBP/p300. (E) Time dependence of fluorescent recovery in the bleached area in FRAP assays with GFP-tagged 3×CBP BRD construct. Half times of fluorescence recovery ($t_{½}$) are shown as bars, which are coloured according to DMSO control (blue), DMSO + SAHA (green), 0.1 μM compound **397** (red). †N1168F mutant (red hashed). Significance of groups compared with the control was determined by *t*-tests *p<0.05, **p<0.01, ****p<0.0001. (F) Inhibition of p53-driven luciferase activity by compound **397**. (G) FRET assay using p53-CFP and CBP-YFP constructs. The top row is DMSO control experiments and the bottom row is in the presence of 5 μM compound **397.** Images on the left are cells expressing p53-CFP in the cyan channel. Images in the centre are cells expressing CBP-YFP in the YFP channel. Images on the right show the intensity of FRET signal.

On-target cellular activity of compound **397** was investigated (Chapter 6). In a FRAP (fluorescence recovery after photobleaching) assay in cells which had been transfected with a GFP-tagged CBP construct (Figure 51E). Histone acetylation was stimulated with the broad-spectrum lysine deacetylase inhibitor, SAHA, which resulted in an increase in FRAP recovery times. Compound **397** effectively inhibited FRAP recovery times back to unstimulated levels.

In a p53-reporter gene assay, compound **397** inhibited doxorubicin-induced p53 activity in a dose-dependent manner (IC_{50} 1.5 μM, Figure 51F). Additionally, compound **397** inhibited FRET (Förster resonance energy transfer) between a CYP-tagged p53 construct and a YFP-tagged CBP construct (Figure 51G). On-target cellular activity of compound **397** had therefore been demonstrated using a variety of techniques.

CBP inhibitors were developed from a weak and non-selective starting point (compound **26**) into a series of highly potent and selective compounds. Selectivity for CBP over BRD4(1) was optimised through structure-guided design. Compound **397 is** a highly potent and selective chemical probe with on-target cellular activity. Compound **397** is expected to be a useful chemical probe for furthering the understanding of the biological roles of CBP/p300, and could be used to validate the CBP/p300 BRD as a new therapeutic target for disease intervention. Work with collaborators using compound **395** has already begun to show the unique role of CBP BRD inhibition in inflammatory and proliferative disorders, demonstrating the application to the investigation of disease mechanisms and the validation of new pharmaceutical strategies.

8.2 TOWARDS A BRD9/BRD7 CHEMICAL PROBE

In comparison to CBP/p300, very little is known about BRD9 and its paralog, BRD7 (Chapter 7). They are BRD-containing proteins thought to be play a role in SWI/SNF (SWItch/Sucrose Non-Fermentable) chromatin remodelling complexes. Evidence indicates that BRD9 and BRD7 may have important roles in oncology. *BRD9* has been linked to non-small cell lung cancer (NSCLC) and cervical cancer, whilst *BRD7* is a postulated tumour-suppressor gene. Additionally, BRD7 has been shown to regulate tumour suppressor p53, and to regulate oestrogen receptor α (ERα) expression through BRCA1 recruitment. *BRD7* has been further linked to nasopharyngeal, colorectal, breast, endometrial and epithelial ovarian cancers. With little known about their function, chemical probes would be valuable tools to further the

understanding of transcriptional control by BRD9 and BRD7 and to elucidate their roles in oncology and other human diseases. The aim of this project was to design and synthesise potent and selective inhibitors of the BRD of BRD9 and BRD7 for use as chemical probes.

The starting point for the project was an indolizine ketone compound, **403**, initially synthesised as a BAZ2B inhibitor (Figure 52A). Compound **403** was found to inhibit BRD9 (ΔT_m 8.7 °C, IC_{50} 0.45 μM). However, compound **403** was also potent against BRD4(1) (ΔT_m 4.4 °C) and various other BRD subfamily members (Figure 52B). Therefore, efforts were made to improve the BRD9 potency and selectivity of the indolizine series.

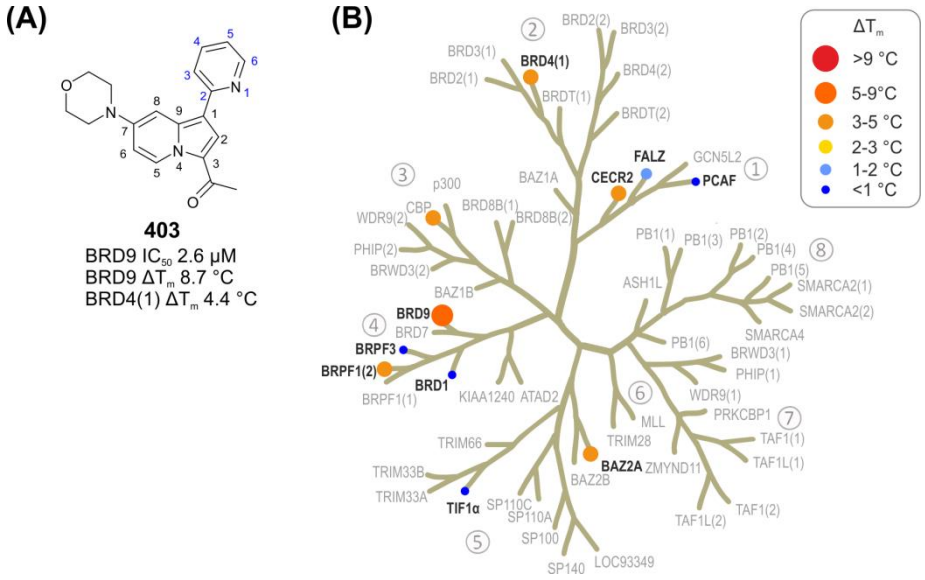

Figure 52. (A) Indolizine compound **403**. Indolizine and pyridine ring numbering are shown in black and blue respectively. (B) DSF selectivity profiling of compound **403** indicating promiscuous affinity across BRD subfamily members.

Target compounds which varied the *C*-1 heteroaryl group were prepared via a base-promoted [3+2] cycloaddition of pyridinium compounds with alkynes. Substitution on the *C*-1 pyridine ring generally led to a drop in BRD9 potency compared to unsubstituted analogues. Alternative *C*-1 heterocycles were generally also poorly tolerated. The most encouraging *C*-1 analogue was the imidazopyridine compound **425** (Figure 53A), which is potent against BRD9 (ΔT_m 5.0 °C, IC_{50} 0.10 μM). The binding constant was determined by ITC for BRD9, which confirmed that compound **425** is highly potent (K_d 68 nM). Additionally, ITC results indicated that compound **425** is 34-fold selectivity for BRD9 over BRD4(1). Wider

profiling against a representative set of BRD proteins indicated that of compound **425** is selective for BRD9 and BRD7 (Figure 53B). Compound **425** was crystallised complexed to BRD9 (Figure 53C and D). The structure obtained shows the ketone carbonyl of compound **425** forming the expected Kac mimicking interactions between N216 and Y163, and a π-π interaction between the indolizine ring of compound **425** with Y222.

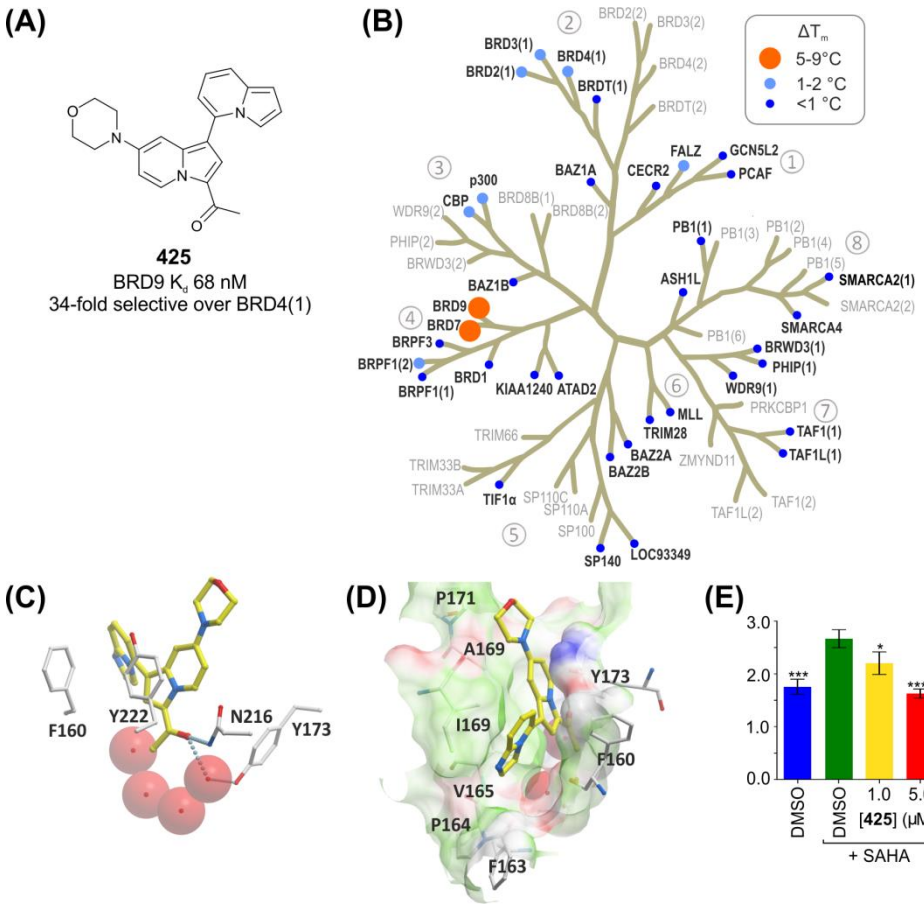

Figure 53. (A) Compound **425**. (B) DSF profiling of compound **425**. (C) and (D): Views from X-ray structure of compound **425** complexed to BRD9. (C) Shows hydrogen-bond from ketone of **425** to N216 (3.06 Å) and to a water molecule (2.92 Å). A π-π interaction is observed between the indolizine ring of **425** and Y222. (E) FRAP assay with compound **425**. Half times of fluorescence recovery ($t_{½}$). Bars represent the mean $t_{½}$ calculated from individual recovery curves. First column (blue): GFP-tagged BRD9 construct; second column (green): construct treated with 2.5 μM SAHA; third column (yellow): construct treated with 2.5 μM SAHA and 1 μM compound **425**; fourth column (red): construct treated with 2.5 μM SAHA and 5 μM compound **425**. Significance of groups compared with the control was determined by *t*-tests *p<0.05, ***p<0.001, ****p<0.0001

On-target cellular activity was demonstrated in a FRAP-based assay, where treatment of SAHA stimulated cells with compound **425** at 5 μM reduced the FRAP recovery time equivalent to unstimulated levels (Figure 53E). Although active in cells, the relatively high concentration of compound **425** required in the FRAP assay, combined with observations of

potential precipitation in buffered aqueous solutions, led to concerns that solubility of compound **425** may be limiting the cellular activity.

It was envisaged that *C*-7 piperazine analogues of compound **425** could improve the solubility of the series through the introduction of a new ionisable centre. The SAR obtained indicated that the *C*-7 piperazine analogues were highly potent against BRD9 (ΔT_m 7.2-8.3 °C), but were also potent against BRD4(1) (2.9-3.8 °C) and CBP (3.1-5.7 °C). Therefore, it was decided to modify the *C*-3 ketone group to investigate if the BRD9 selectivity of the piperazine series could be improved.

The SAR indicated that BRD9 could accommodate substituents larger than methyl ketones, although the affinity was less than for the methyl ketone equivalents. However, the *n*-butyl analogue **456** was moderately potent against BRD9 (ΔT_m 3.3 °C) and selective over BRD4(1) (ΔT_m 0.83 °C) (Figure 54). Also, the *C*-3 trifluoromethyl analogue, **457**, was encouraging as it was moderately potent against BRD9 (ΔT_m 4.0 °C) and inactive against BRD4(1) and CBP (ΔT_m < 1 °C). Compounds **457** and **456** therefore warrant further testing to fully profile their potency and selectivity.

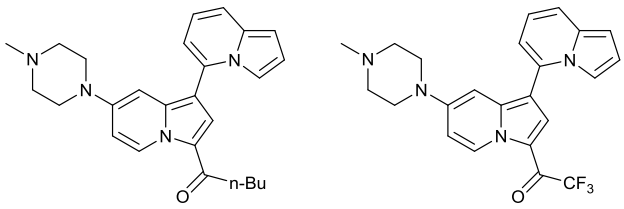

456
BRD9 ΔT_m 3.3 °C
BRD4(1) ΔT_m 0.83 °C

457
BRD9 ΔT_m 4.0 °C
BRD4(1) ΔT_m 0.62 °C

Figure 54. Compounds **456** and **457**; potential selective BRD9 inhibitors.

Although more work is required to understand the potency and selectivity of the indolizine series, it is anticipated that compounds such as **425**, **457**, and **456** could be useful tool compounds to study the biological function and pathogenesis of BRD9 and BRD7.

Overall, this work represents the discovery of the first potent and selective inhibitors for the BRDs of CBP/p300 and BRD9/BRD7. The approach highlights the role of iterative design, synthesis and screening cycles to optimise the potency and selectivity of inhibitors. Additionally, the work underline the role of X-ray crystal structural analysis to guide the design of inhibitors which modulate protein-protein interactions.

EXPERIMENTAL – SYNTHETIC PROCEDURES

GENERAL EXPERIMENTAL

All reactions involving moisture-sensitive reagents were carried out under a nitrogen atmosphere using standard vacuum line techniques and glassware that was oven dried and cooled under nitrogen before use. Commercial anhydrous solvents used in reactions and HPLC grade solvents were employed for work-up and chromatography. Water was purified using an Elix UV-10 system. All other reagents were used as supplied (analytical or HPLC grade) without prior purification. Parallel synthesis was carried out using a Radleys GreenHouse reactor. Parallel work-ups were carried out using a Radleys stacker and Isolute phase separation cartridges. Parallel evaporation was carried out using a Radleys BlowDown Evaporator. Microwave experiments were carried out using a Biotage Initiator 8. Flash column chromatography was performed either on a Presearch Isco Combiflash Companion using Presearch columns or a Biotage SP4 automated flash column chromatography platform using Biotage SNAP columns. Thin layer chromatography was performed on aluminium plates coated with 60 F_{254} silica. Plates were visualised using UV light (254 nm) or 1% aq. $KMnO_4$. R_f values are quoted to the nearest 0.05. Melting points were recorded on a Gallenkamp Hot Stage apparatus or a Stuart Automatic Melting Point SMP40. Optical rotations were recorded on a Perkin-Elmer 241 polarimeter with a water-jacketed 10 cm cell. Specific rotations are reported in 10^{-1} deg cm^2 g^{-1} and concentrations in g/100 mL. IR spectra were recorded on a Bruker Tensor 27 FT-IR spectrometer; selected characteristic peaks are reported in cm^{-1}. NMR spectra were recorded on a Varian Mercury or a Bruker Avance using the solvent as internal deuterium lock. Spectra were recorded at room temperature unless otherwise stated. The field was locked by external referencing to the relevant deuteron resonance. Coupling constants (J) are quoted in Hz and are recorded to the nearest 0.5 Hz. Identical proton coupling constants are averaged in each spectrum

and reported to the nearest 0.5 Hz. When peak multiplicities are reported, the following abbreviations are used: s = singlet, d = doublet, t = triplet, q = quartet, quin = quintet, sxt = sextet, m = multiplet, br = broadened, dd = doublet of doublets, dt = doublet of triplets, td = triplet of doublets. LRMS were recorded on a Waters LCT Premier, equipped with electrospray ionisation source and TOF analyser, acquiring in positive and negative ionisation modes or on and Agilent 6100 mass spectrometer operated with an electrospray ionisation source via flow injection analysis with an Agilent 1200 isocratic pump; data acquisition and processing was performed using Waters Masslynx 4.1 software or Agilent chemstation software. HRMS were run on either a Bruker MicroTOF internally calibrated with polyalanine or sodium formate, or on a Micromass GCT instrument fitted with a Scientific Glass Instruments BPX5 column (15 m × 0.25 mm) using amyl acetate as a lock mass. *m/z* values are reported in Daltons. Elemental analyses were recorded by the elemental analysis service of the London Metropolitan University. HPLC were performed on the following systems: System A: stationary phase: Agilent SB C18 50×3 mm with 3 micron particle size, 50 °C; detection: UV: 210 nm–450 nm DAD– ELSD–MS; mobile phase: A: H_2O + 0.1% formic acid, B: MeCN + 0.1% formic acid; gradient: 95% A 1 min hold, 95-0% A over 8 min, 2.5 min hold, 0.50 min re-equilibration; flow rate: 1.2 mL/min; System B: stationary phase: Agilent SB C18 50×3 mm with 1.8 micron particle size, 50 °C; detection: UV: 200 nm–290 nm DAD–MS; mobile phase: A: H_2O + 0.05% F_3CCOOH, B: MeCN + 0.05% F_3CCOOH; gradient: 95% A 1 min hold, 95-0% A over 8 min, 2.5 min hold, 0.50 min re-equilibration; flow rate: 1.2 mL/min; System C: stationary phase: Gemini-NX 3um C18 110A, ambient temperature; detection: UV 225 nm–ELSD–MS; system/data file: CTC–MUX1; injection volume: 5 µL; flow rate: 1.5 mL/min, mobile phase (acidic conditions): A: H_2O + 0.1% formic acid, B: MeCN + 0.1% formic acid; Gradient (Time/min, %B) – (0,5), (3,95), (4,95), (4.1,5), (5,5); (basic conditions): mobile phase: A: H_2O + 0.1% ammonia, B: MeCN + 0.1% ammonia; gradient (Time/min, %B) (0,5), (3,95), (4,95), (4.1,5), (5,5). Preparative HPLC purification was carried out using: stationary phase: Gemini NX 5um C18 100x21.2, ambient

temperature; detection: ELSD–MS; injection volume: 1000 µL; flow rate: 18 mL/min. The mobile phase used was: acidic conditions: A: H_2O + 0.1% formic acid, B: MeCN + 0.1% formic acid; gradient (time/min %B) (0-1, 5),(1-7, 5-98),(7-9, 98),(9-9.1, 98-5),(9.1-10, 5); basic conditions: A: H_2O + 0.1% diethylamine, B: MeCN + 0.1% diethylamine; gradient (Time/min,%B) - (0-1, 5),(1-7, 5-98),(7-9, 98),(9-9.1, 98-5),(9.1-10, 5). Products from HPLC purification were assessed to be ≥80% peak area by UV at 225 nm, ≥90% peak area by ELSD, and ≥50% spectral purity in ES^+ or ES^-. LRMS were recorded on a Waters LCT Premier, equipped with electrospray ionisation source and TOF analyser, acquiring in positive and negative ionisation modes; System D: WATERS sunfire C18 column (150 mm × 4.6 mm, 5 µm) using a linear gradient of solvent A (water + 0.01% CF_3CO_2H) and solvent B (acetonitrile + 0.01% CF_3CO_2H), eluting at a flow rate of 1 mL/min and monitoring at 254 nm: 0% B over 2 min, 0% B to 100% B over 16 min and 100% B over 2 min; System E: Merk Millipore Chromolith Performance RP-18e column (100 mm × 2 mm, 1.6 µm) using a linear gradient of solvent A (water + 0.01% CF_3CO_2H) and solvent B (acetonitrile + 0.01% CF_3CO_2H), eluting at a flow rate of 1 mL/min and monitoring at 254 nm: 2% B over 2 min, 2% B to 100% B over 8 min and 100% B over 1 min. HPLC t_r are quoted to the nearest 0.1 min.

GENERAL PROCEDURE A

3,5-Dimethylisoxazole-4-boronic acid pinacol ester was dissolved in DME to make a 0.3 M stock solution. Aliquots (1.0 mL, 0.3 mmol) of the stock solution were added to GreenHouse reaction tubes containing the aryl bromide compounds (0.20 mmol) and $Pd(dppf)Cl_2$ (7 mg, 0.01 mmol). The mixtures were stirred then 1.0 M aq. $NaHCO_3$ solution (0.6 mL, 0.6 mmol) was added to each tube. The tubes were placed in a Radley's GreenHouse reactor then degassed by evacuating the apparatus then refilling with nitrogen several times. The mixtures were heated under reflux (block temperature set to 100 °C) for 24 h. Another portion of catalyst (7 mg, 0.01 mmol) was added to each tube then the mixtures were

refluxed for a further 24 h. The reaction mixtures were each worked up as follows 0.5 M aq. HCl (1 mL) and EtOAc (1 mL) were added. The aqueous phase was added onto an Isolute HM-N phase-separation cartridge using a pipette then left to equilibrate on the cartridge for 5 min. The organic phase was then added onto the cartridge followed by elution with more EtOAc to extract the organics. The eluted organic phases were evaporated by blow-down under a nitrogen stream. The crude material thus obtained was purified by preparative HPLC purification.

GENERAL PROCEDURE B

3,5-Dimethylisoxazole-4-boronic acid pinacol ester was dissolved in DME to make a 0.3 M stock solution. Aliquots (1.0 mL, 0.3 mmol) of the stock solution were added to GreenHouse reaction tubes containing the aryl bromide compounds (0.20 mmol) and Pd(dppf)Cl_2 (7 mg, 0.01 mmol). The mixtures were stirred then 1.0 M aq. $NaHCO_3$ solution (0.6 mL, 0.6 mmol) was added to each tube. The tubes were placed in a Radley's GreenHouse reactor then degassed by evacuating the apparatus then refilling with nitrogen several times. The mixtures were heated under reflux (block temperature set to 100 °C) for 24 h. The reaction mixtures were partitioned between water (3 mL) and CH_2Cl_2 (3 mL). The organic phases were separated from the aqueous by passing them through a hydrophobic frit then evaporated by blow-down using a stream of nitrogen. The crude residues were dissolved in DMSO (1 mL) then purified by preparative HPLC.

GENERAL PROCEDURE C

Compound **215** was dissolved in DMSO to make a 0.1 M stock solution. Aliquots of this stock (1.0 mL, 0.10 mmol) were dispensed into the reaction vials. The aldehydes were dissolved in ethanol to make 0.67 M stock solutions. Portions of the aldehyde stocks (0.30 mL, 0.20 mmol) were then dispensed to the appropriate vials. 1.0 M aq. $Na_2S_2O_4$ solution (0.3 mL, 0.3

mmol) was added to each vial then the reactions were heated in a GreenHouse reactor at 80 °C for 18 h. The reaction mixtures were allowed to cool then analysed by LCMS. The reactions were concentrated by half under blow-down then partitioned between CH_2Cl_2 (2 mL) and 2 M aq. ammonia (2 mL). The organic phases were collected by passing through a hydrophobic frit then evaporated by blow-down. The residues were dissolved in DMSO (1 mL) then purified by preparative HPLC.

Cmpd	*General synthesis procedure*	*Structure*	*Mass obtained (mg)*	*Yield (%)*	*LCMS* t_r *(min)*	*LCMS m/z*	*LCMS UV purity (%)*	*LCMS ELSD purity (%)*	*^{1}H NMR (400 MHz) δ ppm*
56	A	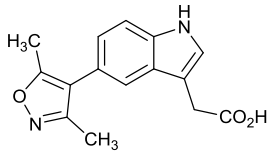	5	10	2.8[c]	(ESI$^+$) 271 [MH$^+$], (ESI$^-$) 269 [(M-H)$^-$]	>99	>99	ND
57	A	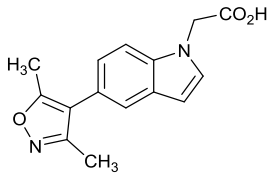	25	46	1.9[d]	(ESI$^+$) 271 [MH$^+$], (ESI$^-$) 269 [(M-H)$^-$]	>99	>99	ND
58	A	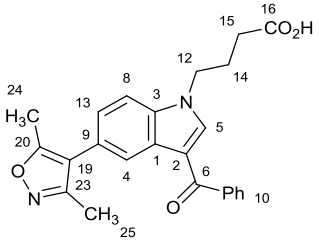	44	55	5.0[a]	(ESI$^+$) 403 [MH$^+$], (ESI$^-$) 401 [(M-H)$^-$]	>99	>99	(DMSO-d_6) 1.99 - 2.08 (m, 2 H, C(14)H_2), 2.22 (s, 3 H, C(25)H_3), 2.25 (t, J=7.0 Hz, 2 H, C(15)H_2), 2.40 (s, 3 H, C(24)H_3), 4.33 (t, J=7.0 Hz, 2 H, C(12)H_2), 7.30 (dd, J=8.5, 2.0 Hz, 1 H, C(13)H), 7.50 - 7.57 (m, 2 H, 2×PhH), 7.58 - 7.64 (m, 1 H, PhH), 7.74 (dd, J=8.5, 1.0 Hz, 1 H, C(8)H), 7.77 - 7.82 (m, 2 H, 2×PhH), 8.07 (s, 1 H, C(5)H), 8.18 (dd, J=2.0, 1.0 Hz, 1 H, C(8)H) 12.16 (br. s, 1 H, OH)
59	A	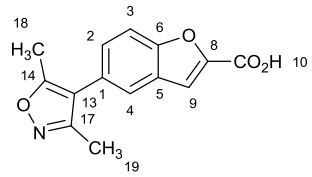	28	54	4.1[a]	(ESI$^+$) 258 [MH$^+$], (ESI$^-$) 256 [(M-H)$^-$]	>99	>99	(DMSO-d_6), 2.23 (s, 3 H, C(19)H_3), 2.41 (s, 3 H, C(18)H_3), 7.49 (dd, J=8.5, 2.0 Hz, 1 H, C(2)H), 7.67 (d, J=1.0 Hz, 1 H, C(9)H), 7.76 - 7.81 (m, 2 H, C(3)H+C(4)H) 13.66 (s, 1 H, OH)

Cmpd	*General synthesis procedure*	*Structure*	*Mass obtained (mg)*	*Yield (%)*	*LCMS* t_r *(min)*	*LCMS m/z*	*LCMS UV purity (%)*	*LCMS ELSD purity (%)*	*^{1}H NMR (400 MHz) δ ppm*
60	A	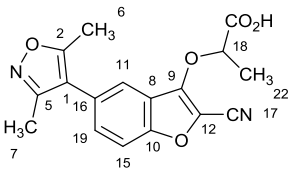	11	17	4.9[a]	(ESI$^+$) 327 [MH$^+$], (ESI$^-$) 325 [(M-H)$^-$]	>99	>99	(DMSO-d_6) 1.65 (d, J=6.5 Hz, 3 H, C(22)H_3), 2.22 (s, 3 H, C(7)H_3), 2.40 (s, 3 H, C(6)H_3), 5.36 (q, J=6.5 Hz, 1 H, C(18)H), 7.62 (dd, J=9.0, 2.0 Hz, 1 H, C(19)H), 7.74 - 7.78 (m, 2 H, C(11)H+C(15)H)
61	A	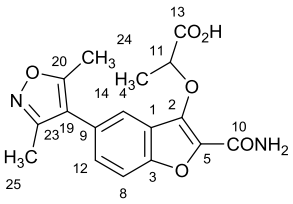	13	19	3.8[a]	(ESI$^+$) 345 [MH$^+$], (ESI$^-$) 343 [(M-H)$^-$]	>99	>99	(DMSO- d_6) 1.59 (d, J=7.0 Hz, 3 H, C(14)H_3), 2.22 (s, 3 H, C(25)H_3), 2.40 (s, 3 H, C(20)H_3), 5.41 (q, J=7.0 Hz, 1 H, C(11)H), 7.46 (dd, J=8.5, 2.0 Hz, 1 H, C(12)H), 7.66 (dd, J=8.5, 0.5 Hz, 1 H, C(8)H), 7.71 (br. s, 2 H, NH_2), 7.74 (dd, J=2.0, 0.5 Hz, 1 H, C(4)H), 10.88 (br. s, 1 H, OH)
62	A	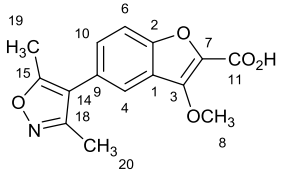	12	21	4.1[d]	(ESI$^+$) 288 [MH$^+$], (ESI$^-$) 286 [(M-H)$^-$]	>99	>99	(DMSO-d_6), 2.24 (s, 3 H, C(20)H_3), 2.42 (s, 3 H, C(19)H_3), 4.19 (s, 3 H, OCH_3), 7.51 (dd, J=8.5, 2.0 Hz, 1 H, C(10)H), 7.71 (dd, J=8.5, 0.5 Hz, 1 H, C(6)H), 7.85 (dd, J=2.0, 0.5 Hz, 1 H, C(4)H) 13.23 (br. s, 1 H, OH)
63	A	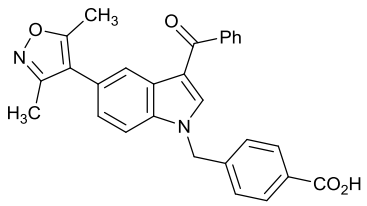	18	20	2.3[d]	(ESI$^+$) 451 [MH$^+$], (ESI$^-$) 449 [(M-H)$^-$]	>99	>99	ND

Cmpd	*General synthesis procedure*	*Structure*	*Mass obtained (mg)*	*Yield (%)*	*LCMS* t_r *(min)*	*LCMS m/z*	*LCMS UV purity (%)*	*LCMS ELSD purity (%)*	*^{1}H NMR (400 MHz) δ ppm*
64	A	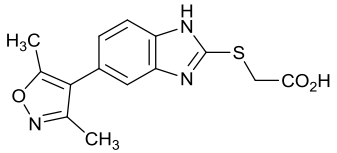	21	35	3.0[a]	(ESI+) 304 [MH+], (ESI-) 302 [(M-H)-]	>99	>99	ND
65	A	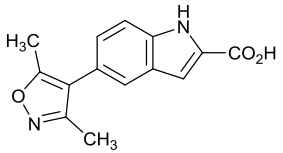	12	24	2.8[c]	257 [MH+], (ESI-) 255 [(M-H)-]	>99	>99	ND
66	A	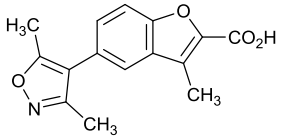	9	16	3.0[c]	(ESI+) 272 [MH+], (ESI-) 270 [(M-H)-]	96	89	ND
67	A	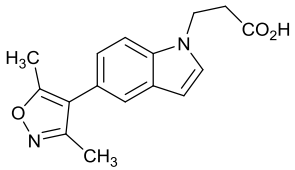	16	28	2.1[d]	(ESI+) 285 [MH+], (ESI-) 283 [(M-H)-]	>99	99	ND
68	A	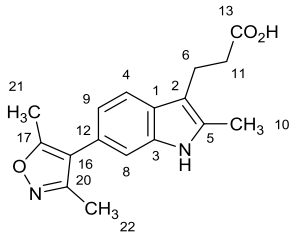	6	10	4.8[a]	(ESI+) 299 [MH+]	>99%	ND	($CDCl_3$), 2.28 (s, 3 H, C(22)H_3), 2.41 (s, 3 H, C(21)H_3), 2.43 (s, 3 H, C(10)H_3), 2.70 (t, J=7.5 Hz, 2 H, C(11)H_2), 3.07 (t, J=7.5 Hz, 2 H, C(6)H_2), 6.96 (dd, J=8.0, 1.0 Hz, 1 H, C(9)H), 7.14 (d, J=1.0 Hz, 1 H, C(8)H), 7.55 (d, J=8.0 Hz, 1 H, C(4)H), 7.90 (s, 1 H, NH)

Cmpd	*General synthesis procedure*	*Structure*	*Mass obtained (mg)*	*Yield (%)*	*LCMS* t_r *(min)*	*LCMS m/z*	*LCMS UV purity (%)*	*LCMS ELSD purity (%)*	*^{1}H NMR (400 MHz) δ ppm*
69	A	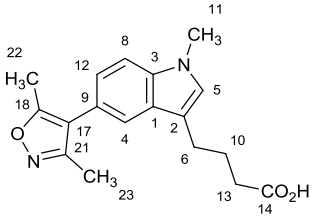	8	13	5.4[a]	(ESI+) 313 [MH+]	81	ND	($CDCl_3$), 2.01 - 2.11 (m, 2 H, C(10)H_2), 2.31 (s, 3 H, C(23)H_3), 2.42 - 2.49 (m, 5 H, C(22)H_3+C(13)H_2), 2.81 - 2.88 (m, 2 H, C(6)H_2), 3.80 (s, 3 H, C(11)H_3), 6.94 (s, 1 H, C(5)H), 7.11 (dd, J=8.5, 1.5 Hz, 1 H, C(12)H), 7.36 (dd, J=8.5, 0.5 Hz, 1 H, C(8)H), 7.47 (dd, J=1.5, 0.5 Hz, 1 H, C(4)H)
70	A	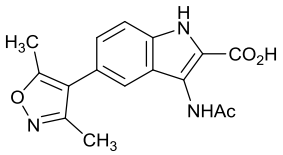	9	15	2.6[c]	(ESI+) 314 [MH+]	95	>99	ND
71	A	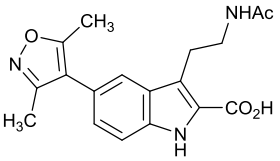	31	45	2.6[c]	(ESI+) 342 [MH+], (ESI-) 340 [(M-H)-]	>99	>99	ND
72	A	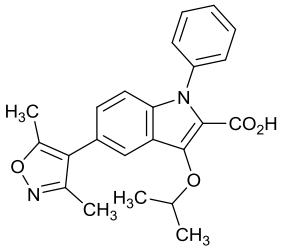	24	31	2.3[d]	(ESI+) 391 [MH+], (ESI-) 389 [(M-H)-]	97	98	ND

Cmpd	*General synthesis procedure*	*Structure*	*Mass obtained (mg)*	*Yield (%)*	*LCMS*				*^{1}H NMR (400 MHz) δ ppm*
					t_r (min)	*m/z*	*UV purity (%)*	*ELSD purity (%)*	
73	A	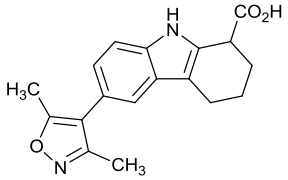	25	41	2.3[d]	(ESI$^+$) 311 [MH$^+$], (ESI$^-$) 309 [(M-H)$^-$]	95	>99	ND
152	B	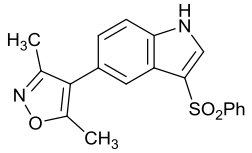	27	38	3.1[d]	(ESI$^+$) 353 [MH$^+$], (ESI$^-$) 351 [(M-H)$^-$]	>99	>99	ND
153	B	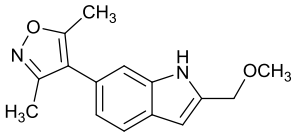	9	17	3.2[c]	(ESI$^+$) 257 [MH$^+$], (ESI$^-$) 255 [(M-H)$^-$]	>99	>99	ND
154	B	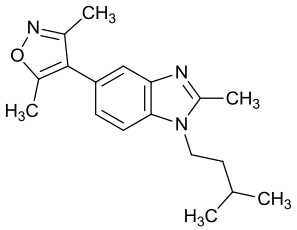	31	52	3.4[d]	(ESI$^+$) 298 [MH$^+$]	>99	>99	ND

Cmpd	*General synthesis procedure*	*Structure*	*Mass obtained (mg)*	*Yield (%)*	*LCMS*				*^{1}H NMR (400 MHz) δ ppm*
					t_r (min)	*m/z*	*UV purity (%)*	*ELSD purity (%)*	
155	B	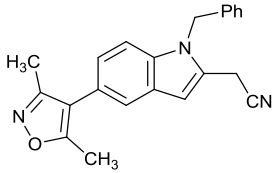	9	13	3.6[d]	(ESI$^+$) 342 [MH$^+$], (ESI$^-$) 340 [(M-H)$^-$]	>99	>99	ND
156	B	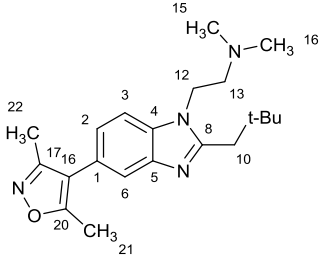	37	52	2.1[c]	353 [MH$^+$], (ESI$^-$) 351 [(M-H)$^-$]	98	>99	($CDCl_3$) δ ppm 1.11 (s, 9 H, 9×*t*-Bu-*H*), 2.30 (s, 3 H, C(22)H_3), 2.35 (s, 6 H, C(15)H_3+C(16)H_3), 2.42 (s, 3 H, C(21)H_3), 2.53 - 2.68 (m, 2 H, C(13)H_2), 2.83 (s, 2 H, C(10)H_2), 4.26 - 4.34 (m, 2 H, C(12)H_2), 7.11 (dd, *J*=8.5, 1.5 Hz, 1 H, C(2)*H*), 7.38 (d, *J*=8.5 Hz, 1 H, C(3)*H*), 7.62 (d, *J*=1.5 Hz, 1 H, C(6)*H*)
157	B	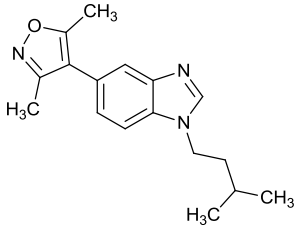	13	23	1.9[d]	(ESI$^+$) 284 [MH$^+$], (ESI$^-$) 283 [(M-H)$^-$]	>99	>99	ND
158	B	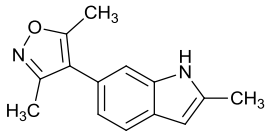	26	58	3.4[d]	(ESI$^+$) 227 [MH$^+$], (ESI$^-$) 225 [(M-H)$^-$]	97	>99	ND

Cmpd	*General synthesis procedure*	*Structure*	*Mass obtained (mg)*	*Yield (%)*	*LCMS*				*^{1}H NMR (400 MHz) δ ppm*
					t_r (min)	*m/z*	*UV purity (%)*	*ELSD purity (%)*	
159	B	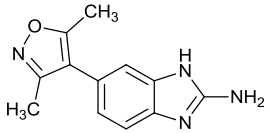	22	48	2.3[d]	(ESI$^+$) 229 [MH$^+$], (ESI$^-$) 227 [(M-H)$^-$]	>99	92	ND
160	B	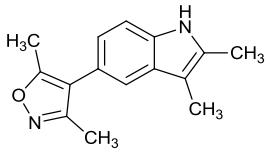	24	50	3.4[d]	(ESI$^+$) 241 [MH$^+$], (ESI$^-$) 239 [(M-H)$^-$]	96	>99	ND
161	B	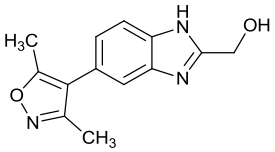	31	63	1.1[c]	(ESI$^+$) 244 [MH$^+$], (ESI$^-$) 242 [(M-H)$^-$]	71	54	ND
162	B	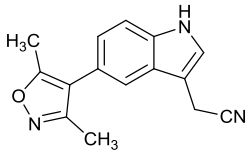	31	61	3.0[d]	(ESI$^+$) 252 [MH$^+$], (ESI$^-$) 250 [(M-H)$^-$]	91	98	ND
163	B	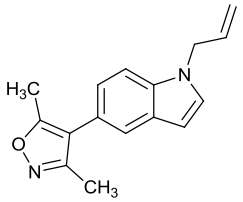	24	48	3.5[c]	(ESI$^+$) 253 [MH$^+$], (ESI$^-$) 251 [(M-H)$^-$]	>99	>99	ND

Cmpd	*General synthesis procedure*	*Structure*	*Mass obtained (mg)*	*Yield (%)*	*LCMS* t_r *(min)*	*LCMS m/z*	*LCMS UV purity (%)*	*LCMS ELSD purity (%)*	*^{1}H NMR (400 MHz) δ ppm*
164	B	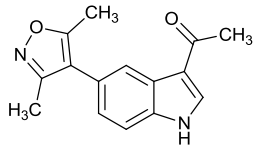	23	45	2.7[d]	(ESI+) 255 [MH+], (ESI-) 253 [(M-H)-]	97	97	ND
165	B	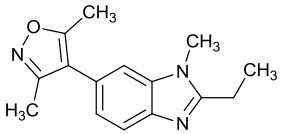	38	74	2.9[d]	(ESI+) 256 [MH+], (ESI-) 254 [(M-H)-]	95	>99	ND
166	B	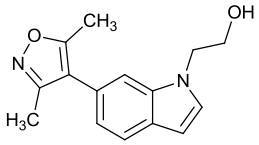	12	23	2.8[d]	(ESI+) 257 [MH+], (ESI-) 255 [(M-H)-]	>99	94	ND
167	B	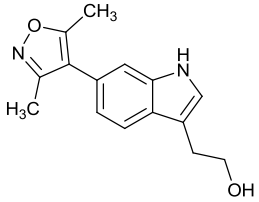	34	66	2.8[c]	(ESI+) 257 [MH+], (ESI-) 255 [(M-H)-]	>99	>99	ND
168	B	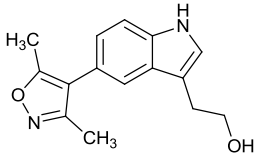	18	36	2.6[d]	(ESI+) 257 [MH+], (ESI-) 255 [(M-H)-]	>99	95	ND

Cmpd	*General synthesis procedure*	*Structure*	*Mass obtained (mg)*	*Yield (%)*	*LCMS*				*^{1}H NMR (400 MHz) δ ppm*
					t_r (min)	*m/z*	*UV purity (%)*	*ELSD purity (%)*	
169	B	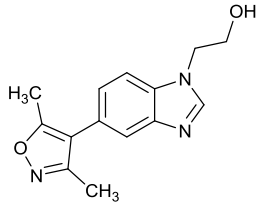	36	70	1.9[c]	(ESI$^+$) 258 [MH$^+$], (ESI$^-$) 256 [(M-H)$^-$]	98	95	ND
170	B	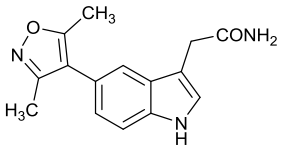	24	44	2.6[c]	(ESI$^+$) 270 [MH$^+$], (ESI$^-$) 268 [(M-H)$^-$]	81	93	ND
171	B	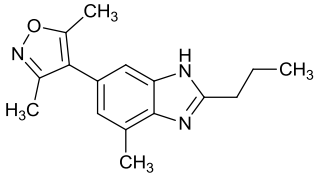	32	59	2.9[c]	(ESI$^+$) 270 [MH$^+$], (ESI$^-$) 268 [(M-H)$^-$]	>99	95	ND
172	B	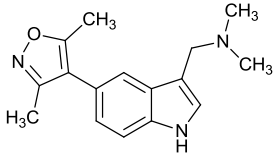	5	9	3.1[d]	(ESI$^+$) 270 [MH$^+$], (ESI$^-$) 268 [(M-H)$^-$]	97	91	ND
173	B	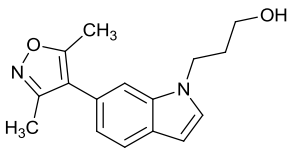	21	39	3.1[c]	271 [MH$^+$], (ESI$^-$) 269 [(M-H)$^-$]	93	>99	ND

Cmpd	*General synthesis procedure*	*Structure*	*Mass obtained (mg)*	*Yield (%)*	*LCMS* t_r *(min)*	*LCMS m/z*	*LCMS UV purity (%)*	*LCMS ELSD purity (%)*	*^{1}H NMR (400 MHz) δ ppm*
174	B	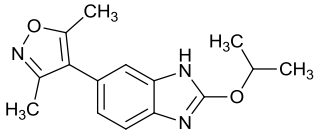	18	33	2.6[c]	(ESI+) 272 [MH+], (ESI-) 270 [(M-H)-]	87	>99	ND
175	B	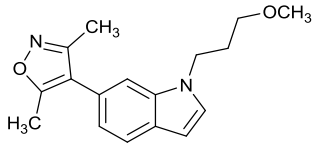	40	70	3.5[d]	(ESI+) 285 [MH+]	>99	>99	ND
176	B	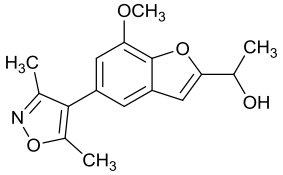	53	93	3.1[d]	(ESI+) 288 [MH+], (ESI-) 286 [(M-H)-]	>99	>99	ND
177	B	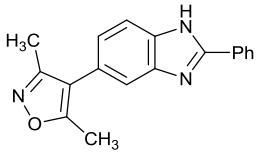	13	23	2.5[c]	(ESI+) 290 [MH+], (ESI-) 288 [(M-H)-]	94	>99	ND
178	B	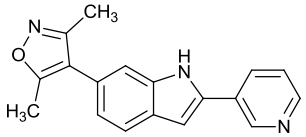	25	44	3.2[d]	(ESI+) 290 [MH+], (ESI-) 288 [(M-H)-]	>99	>99	ND

Cmpd	*General synthesis procedure*	*Structure*	*Mass obtained (mg)*	*Yield (%)*	*LCMS* t_r *(min)*	*LCMS m/z*	*LCMS UV purity (%)*	*LCMS ELSD purity (%)*	*^{1}H NMR (400 MHz) δ ppm*
179	B	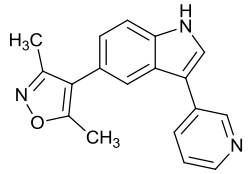	36	62	3.0[d]	290 [MH$^+$], (ESI$^-$) 288 [(M-H)$^-$]	>99	>99	ND
180	B	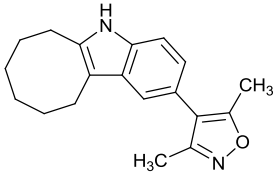	37	62	3.8[c]	295 [MH$^+$], (ESI$^-$) 293 [(M-H)$^-$]	>99	>99	ND
181	B	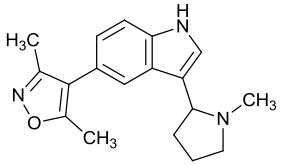	48	81	3.3[d]	296 [MH$^+$], (ESI$^-$) 294 [(M-H)$^-$]	>99	>99	ND
182	B	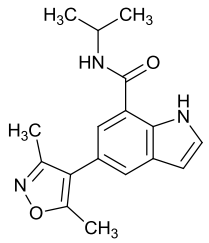	41	70	3.3[d]	(ESI$^+$) 298 [MH$^+$], (ESI$^-$) 296 [(M-H)$^-$]	95	>99	ND

Cmpd	*General synthesis procedure*	*Structure*	*Mass obtained (mg)*	*Yield (%)*	*LCMS* t_r *(min)*	*LCMS m/z*	*LCMS UV purity (%)*	*LCMS ELSD purity (%)*	*^{1}H NMR (400 MHz) δ ppm*
183	B	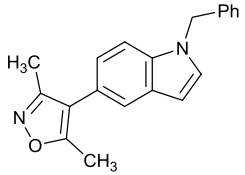	35	58	3.7[c]	(ESI+) 303 [MH+]	>99	97	ND
184	B	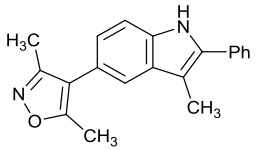	24	40	3.7[d]	(ESI+) 303 [MH+], (ESI-) 301 [(M-H)-]	96	97	ND
185	B	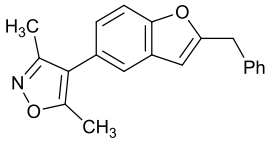	28	46	3.9[d]	(ESI+) 304 [MH+], (ESI-) 302 [(M-H)-]	>99	>99	ND
186	B	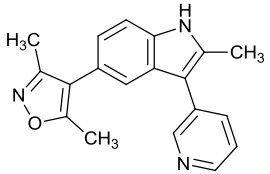	16	26	3.1[d]	(ESI+) 304 [MH+], (ESI-) 302 [(M-H)-]	>99	>99	ND
187	B	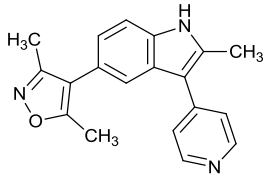	7	11	3.0[d]	(ESI+) 304 [MH+], (ESI-) 302 [(M-H)-]	96	97	ND

Cmpd	*General synthesis procedure*	*Structure*	*Mass obtained (mg)*	*Yield (%)*	*LCMS* t_r *(min)*	*LCMS m/z*	*LCMS UV purity (%)*	*LCMS ELSD purity (%)*	*^{1}H NMR (400 MHz) δ ppm*
188	B	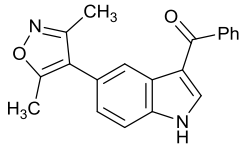	3	5	3.3[d]	(ESI+) 317 [MH+], (ESI-) 315 [(M-H)-]	>99	>99	ND
189	B	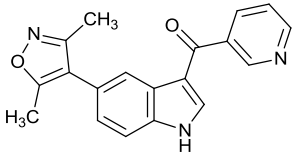	22	35	2.9[d]	(ESI+) 318 [MH+]	>99	>99	ND
190	B	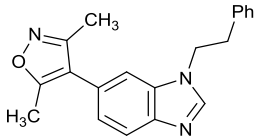	15	23	3.2[d]	(ESI+) 318 [MH+], (ESI-), 316 [(M-H)-]	>99	>99	ND
191	B	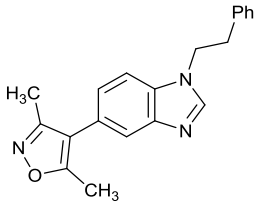	13	21	3.3[d]	(ESI+) 318 [MH+], (ESI-) 316 [(M-H)-]	>99	>99	ND
192	B	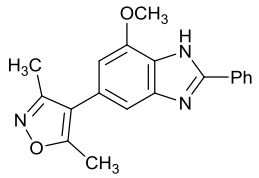	17	27	3.1[d]	(ESI+) 320 [MH+], (ESI-) 318 [(M-H)-]	>99	>99	ND

Cmpd	*General synthesis procedure*	*Structure*	*Mass obtained (mg)*	*Yield (%)*	*LCMS*				*^{1}H NMR (400 MHz) δ ppm*
					t_r (min)	*m/z*	*UV purity (%)*	*ELSD purity (%)*	
193	B	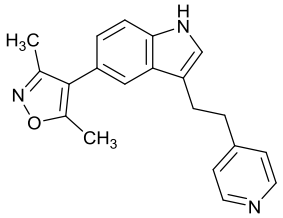	36	56	3.1[d]	(ESI$^+$) 318 [MH$^+$], (ESI$^-$) 316 [(M-H)$^-$]	>99	>99	ND
194	B	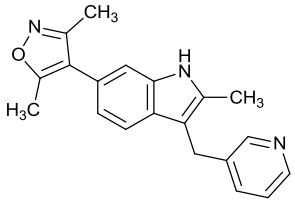	22	34	3.2[d]	(ESI$^+$) 318 [MH$^+$], (ESI$^-$) 316 [(M-H)$^-$]	>99	>99	ND
195	B	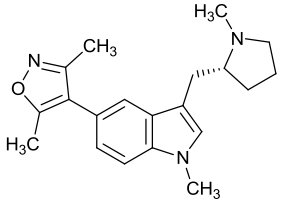	20	31	3.7[d]	(ESI$^+$) 324 [MH$^+$]	>99	>99	ND
196	B	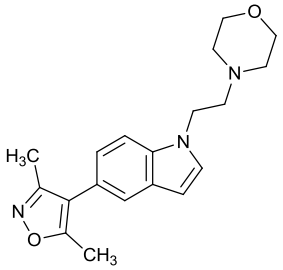	51	79	3.2[d]	(ESI$^-$) 324 [(M-H)$^-$]	>99	>99	ND

Cmpd	*General synthesis procedure*	*Structure*	*Mass obtained (mg)*	*Yield (%)*	*LCMS*				*^{1}H NMR (400 MHz) δ ppm*
					t_r (min)	*m/z*	*UV purity (%)*	*ELSD purity (%)*	
197	B	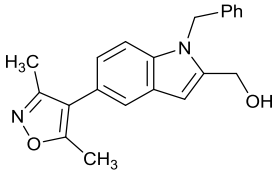	26	39	3.3[d]	333 [MH$^+$], (ESI$^-$) 331 [(M-H)$^-$]	>99	>99	ND
198	B	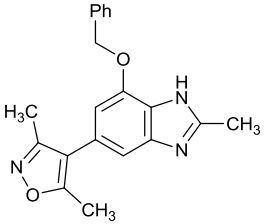	26	39	3.3[d]	333 [MH$^+$], (ESI$^-$) 331 [(M-H)$^-$]	>99	>99	ND
199	B	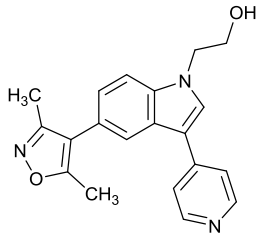	17	25	2.2[c]	(ESI$^+$) 334 [MH$^+$], (ESI$^-$) 332 [(M-H)$^-$]	>99	>99	ND
200	B	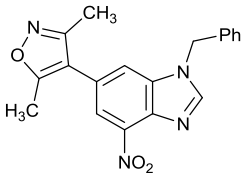	13	19	3.1[d]	(ESI$^+$) 349 [MH$^+$], (ESI$^-$) 347 [(M-H)$^-$]	>99	>99	ND

Cmpd	*General synthesis procedure*	*Structure*	*Mass obtained (mg)*	*Yield (%)*	*LCMS*				*^{1}H NMR (400 MHz) δ ppm*
					t_r (min)	*m/z*	*UV purity (%)*	*ELSD purity (%)*	
201	B	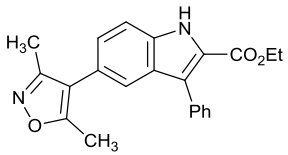	8	11	3.6[c]	(ESI$^+$) 361 [MH$^+$], (ESI$^-$) 359 [(M-H)$^-$]	>99	>99	ND
202	B	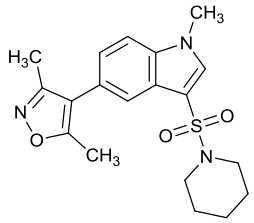	13	18	3.4[d]	(ESI$^+$) 374 [MH$^+$], (ESI$^-$) 372 [(M-H)$^-$]	>99	>99	ND
203	B	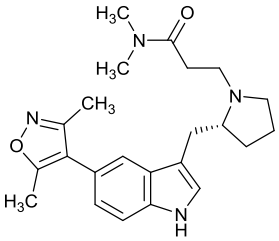	21	27	3.0[d]	(ESI$^+$) 395 [MH$^+$], (ESI$^-$) 393 [(M-H)$^-$]	96	98	ND
204	B	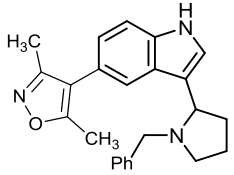	27	37	2.4[d]	(ESI$^+$) 372 [MH$^+$], (ESI$^-$) 370 [(M-H)$^-$]	>99	>99	ND

Cmpd	*General synthesis procedure*	*Structure*	*Mass obtained (mg)*	*Yield (%)*	*LCMS*				*^{1}H NMR (400 MHz) δ ppm*
					t_r (min)	*m/z*	*UV purity (%)*	*ELSD purity (%)*	
205	B	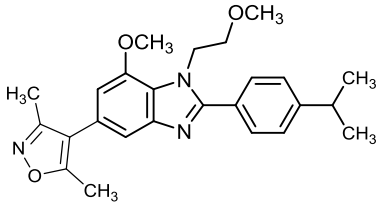	27	32	3.0[c]	(ESI$^+$) 420 [MH$^+$], (ESI$^-$) 418 [(M-H)$^-$]	>99	>99	ND
206	B	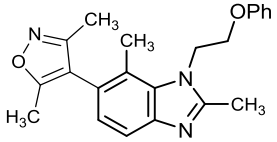	15	21	2.5[c]	(ESI$^+$) 362 [MH$^+$], (ESI$^-$) 360 [(M-H)$^-$]	88	97	ND
207	B	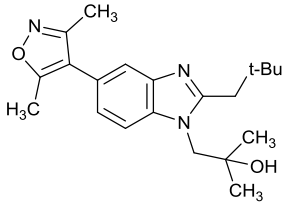	11	15	2.4[c]	(ESI$^+$) 356 [MH$^+$], (ESI$^-$) 354 [(M-H)$^-$]	95	98	ND
208	B	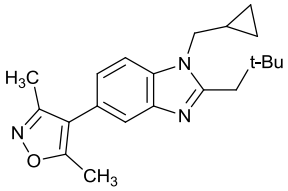	38	57	2.5[c]	(ESI$^+$) 338 [MH$^+$], (ESI$^-$) 336 [(M-H)$^-$]	>99	>99	ND

Cmpd	*General synthesis procedure*	*Structure*	*Mass obtained (mg)*	*Yield (%)*	*LCMS* t_r *(min)*	*LCMS m/z*	*LCMS UV purity (%)*	*LCMS ELSD purity (%)*	*^{1}H NMR (400 MHz) δ ppm*
209	B	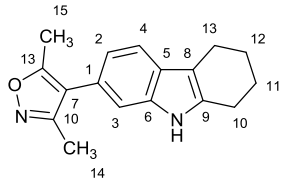	29	54	3.7[d]	(ESI+) 267 [MH+], (ESI-) 265 [(M-H)-]	84	88	($CDCl_3$) δ ppm 1.85 - 2.00 (m, 4 H, C(11)H_2+C(12)H_2), 2.28 (s, 3 H, C(14)H_3), 2.41 (s, 3 H, C(15)H_3), 2.71 - 2.81 (m, 4 H, C(10)H_2+C(13)H_2), 6.96 (dd, *J*=8.0, 1.0 Hz, 1 H, C(2)*H*), 7.15 (d, *J*=1.0 Hz, 1 H, C(3)*H*), 7.52 (d, *J*=8.0 Hz, 1 H, C(4)*H*), 7.80 (br. s., 1 H, N*H*)
210	B	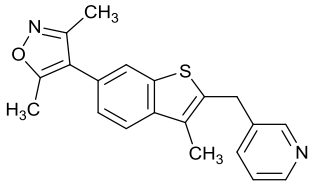	33	50	3.6[d]	(ESI+) 335 [MH+]	99	>99	ND
211	B	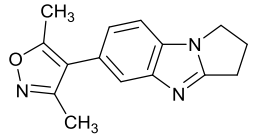	15	30	2.0[c]	(ESI+) 254 [MH+], (ESI-) 252 [(M-H)-]	>99	>99	ND
212	B	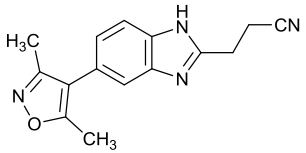	5	10	2.6[d]	(ESI+) 267 [MH+], (ESI-) 265 [(M-H)-]	>99	>99	ND
213	B	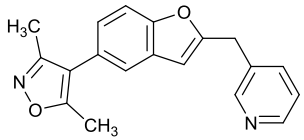	26	42	2.6[d]	(ESI+) 305 [MH+], (ESI-) 303 [(M-H)-]	95	>99	ND

Cmpd	*General synthesis procedure*	*Structure*	*Mass obtained (mg)*	*Yield (%)*	*LCMS* t_r *(min)*	*LCMS m/z*	*LCMS UV purity (%)*	*LCMS ELSD purity (%)*	*^{1}H NMR (400 MHz) δ ppm*
214	B	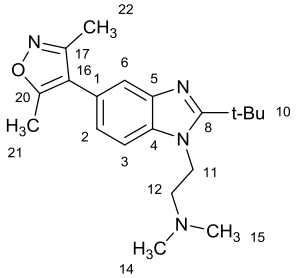	9	13	1.2[c]	(ESI+) 341 [MH+]	>99	>99	($CDCl_3$) δ ppm 1.59 (s, 9 H, *t*-Bu), 2.28 (s, 3 H, C(22)H_3), 2.41 (s, 9 H, C(14)H_3+C(15)H_3+C(21)H_3), 2.72 - 2.81 (m, 2 H, C(12)H_2), 4.43 - 4.53 (m, 2 H, C(11)H_2), 7.13 (dd, *J*=8.0, 1.5 Hz, 1 H, C(2)H), 7.39 (d, *J*=8.0 Hz, 1 H, C(3)H), 7.64 (d, *J*=1.5 Hz, 1 H, C(6)H)
215	B	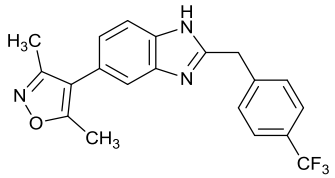	61	82	3.4[d]	(ESI+) 372 [MH+], (ESI-) 370 [(M-H)-]	97	95	ND
216	B	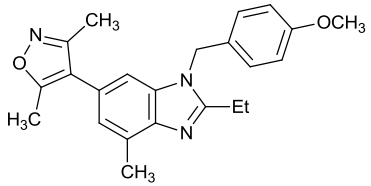	49	68	2.5[c]	(ESI+) 376 [MH+], (ESI-) 374 [(M-H)-]	>99	>99	ND
252	C	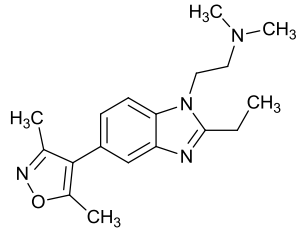	10	31	2.9[d]	(ESI+) 313 [MH+], (ESI-) 311 [(M-H)-]	98	>99	ND

Cmpd	*General synthesis procedure*	*Structure*	*Mass obtained (mg)*	*Yield (%)*	*LCMS* t_r *(min)*	*LCMS m/z*	*LCMS UV purity (%)*	*LCMS ELSD purity (%)*	*^{1}H NMR (400 MHz) δ ppm*
253	C	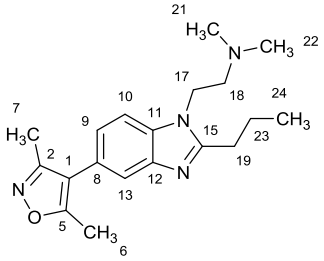	10	30	1.0[c]	(ESI+) 327 [MH+]	>99	>99	ND
254	C	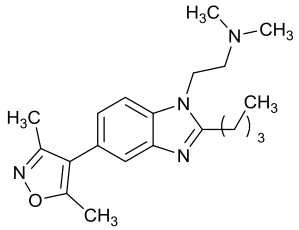	6	17	1.9[c]	(ESI+) 341 [MH+], (ESI-) 339 [(M-H)-]	98	>99	ND
255	C	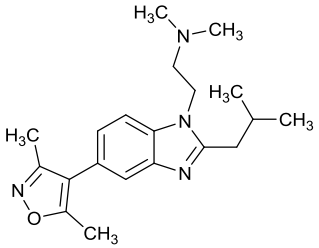	17	49	3.2[d]	(ESI+) 341 [MH+], (ESI-), 339 [(M-H)-]	99	>99	ND

Cmpd	*General synthesis procedure*	*Structure*	*Mass obtained (mg)*	*Yield (%)*	*LCMS*				*^{1}H NMR (400 MHz) δ ppm*
					t_r (min)	*m/z*	*UV purity (%)*	*ELSD purity (%)*	
256	C	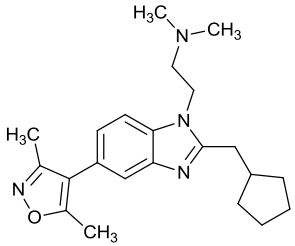	18	50	3.5[d]	(ESI$^+$) 367 [MH$^+$], (ESI$^-$) 365 [(M-H)$^-$]	>99	98	ND
257	C	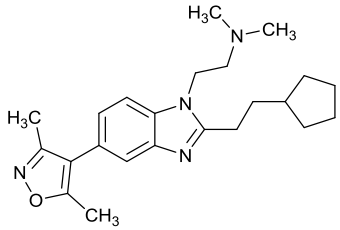	3	9	3.6[d]	(ESI$^+$) 381 [MH$^+$], (ESI$^-$) 379 [(M-H)$^-$]	99	>99	ND
258	C	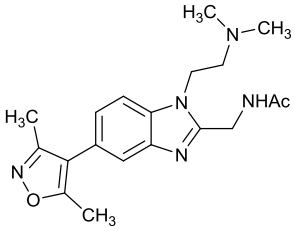	19	54	2.6[d]	(ESI$^+$) 370 [MH$^+$], (ESI$^-$) 368 [(M-H)$^-$]	>99	>99	ND
259	C	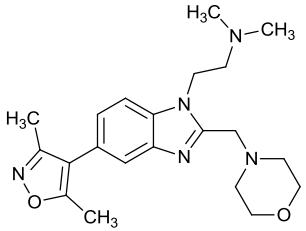	5	13	2.9[d]	(ESI$^+$) 384 [MH$^+$]	90	>99	ND

Cmpd	*General synthesis procedure*	*Structure*	*Mass obtained (mg)*	*Yield (%)*	*LCMS* t_r *(min)*	*LCMS m/z*	*LCMS UV purity (%)*	*LCMS ELSD purity (%)*	*^{1}H NMR (400 MHz) δ ppm*
260	C	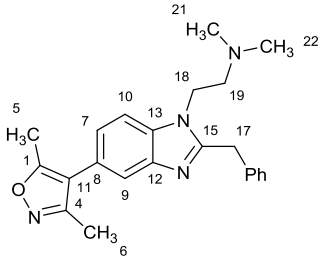	9	24	3.2[b]	(ESI+) 375 [MH+]	90	ND	($CDCl_3$) δ ppm 2.23 (s, 6 H, C(21)H_3+C(22)H_3), 2.32 (s, 3 H, C(6)H_3), 2.38 (t, J=7.52 Hz, 2 H, C(19)H_2), 2.45 (s, 3 H, C(5)H_3), 4.14 (t, J=7.5 Hz, 2 H, C(18)H_2), 4.40 (s, 2 H, CH_2Ph), 7.15 (dd, J=8.0, 1.5 Hz, 1 H, C(7)H), 7.27 - 7.38 (m, 6 H, C(10)H+5×PhH), 7.66 (d, J=1.5 Hz, 1 H, C(9)H)
261	C	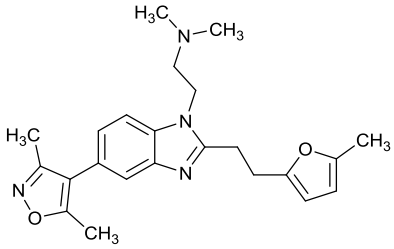	5	12	3.3[d]	(ESI+) 393 [MH+], (ESI-) 391 [(M-H)-]	>99	>99	ND
262	C	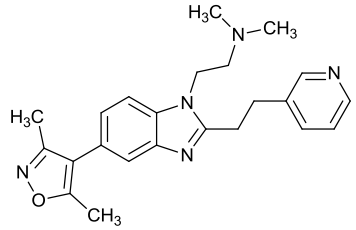	13	34	2.8[c]	(ESI+) 390 [MH+], (ESI-) 388 [(M-H)-]	>99	>99	ND

Cmpd	*General synthesis procedure*	*Structure*	*Mass obtained (mg)*	*Yield (%)*	*LCMS*				*^{1}H NMR (400 MHz) δ ppm*
					t_r (min)	*m/z*	*UV purity (%)*	*ELSD purity (%)*	
263	C	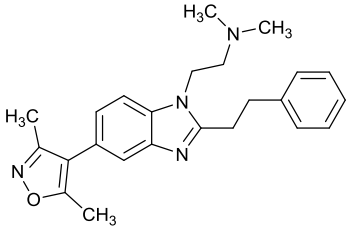	26	34	3.4[d]	(ESI$^+$) 389 [MH$^+$], (ESI$^-$) 387 [(M-H)$^-$]	>99	>99	ND
264	C	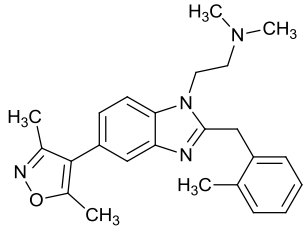	3	8	3.4[c]	389 [MH$^+$]	95	98	ND
265	C	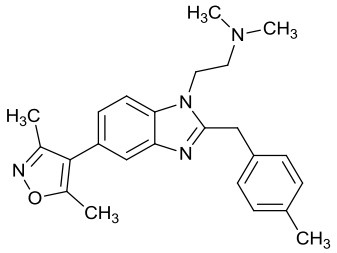	13	34	3.4[d]	(ESI$^+$) 389 [MH$^+$], (ESI$^-$) 387 [(M-H)$^-$]	95	99	ND
266	C	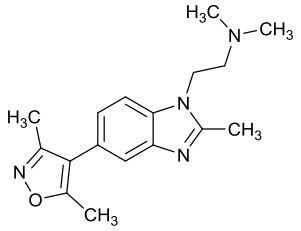	16	54	2.8[d]	(ESI$^+$) 299 [MH$^+$], (ESI$^-$) 297 [(M-H)$^-$]	92	>99	ND

Cmpd	*General synthesis procedure*	*Structure*	*Mass obtained (mg)*	*Yield (%)*	*LCMS* t_r *(min)*	*LCMS m/z*	*LCMS UV purity (%)*	*LCMS ELSD purity (%)*	*^{1}H NMR (400 MHz) δ ppm*
267	C	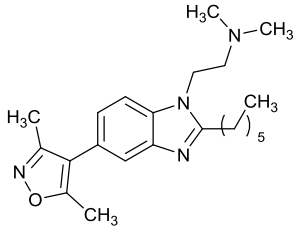	13	36	2.1[c]	(ESI+) 369 [MH+], (ESI-) 367 [(M-H)-]	>99	>99	ND
268	C	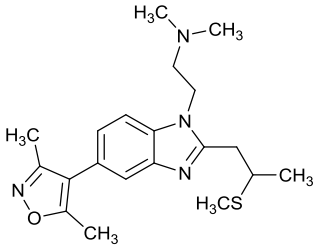	4	10	3.1[c]	(ESI+) 373 [MH+], (ESI-), 371 [(M-H)-]	98	>99	ND
269	C	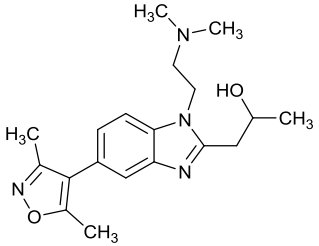	5	16	2.8[c]	(ESI+) 343 [MH+], (ESI-) 341 [(M-H)-]	92	>99	ND

Cmpd	*General synthesis procedure*	*Structure*	*Mass obtained (mg)*	*Yield (%)*	*LCMS*				*^{1}H NMR (400 MHz) δ ppm*
					t_r (min)	*m/z*	*UV purity (%)*	*ELSD purity (%)*	
270	C	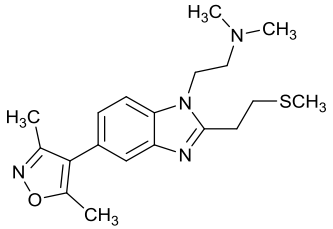	4	12	2.0[c]	(ESI$^+$) 359 [MH$^+$], (ESI$^-$) 357 [(M-H)$^-$]	96	>99	ND

[a] LCMS system A
[b] LCMS system B
[c] LCMS system C (acidic conditions)
[d] LCMS system C (basic conditions)

4-(4-Fluoro-3-nitrophenyl)-3,5-dimethyl-1,2-oxazole (251)

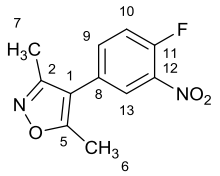

$Pd(dppf)Cl_2$ (1.81 g, 2.47 mmol) was added to a solution of 4-bromo-1-fluoro-2-nitrobenzene (10.87 g, 49.4 mmol) and 3,5-dimethylisoxazole-4-boronic acid pinacol ester (12.68 g, 56.8 mmol) in DME (100 mL). The mixture was stirred then saturated aq. $NaHCO_3$ solution (100 mL) was added. The mixture was degassed by evacuating and refilling with nitrogen (×3) then heated at 80 °C for 3 h. The reaction was allowed to cool then partitioned between EtOAc (100 mL) and water (100 mL). The phases were separated then $MgSO_4$ and activated charcoal was added. The solid was filtered then the filtrate was evaporated. The resultant residue was re-dissolved in the minimum of methylene chloride then purified by flash column chromatography on a silica column (330 g). The column was eluted with a gradient of EtOAc:*c*-hexane, which was increased linearly from 10:90 to 30:70 over 10 CVs (some product crystallised on the column but re-dissolved as the percentage of EtOAc increased). The desired fractions were combined and evaporated. Et_2O (30 mL) was added, resulting in crystallisation of the product. The supernatant was decanted off with a pipette then the process was repeated. The solid was dried under vacuum to yield the product as a beige solid (8.57 g, 73%); R_f 0.25 (EtOAc:*n*-hexane, 30:70); mp 128-131 °C; ν_{max} (neat) 3063 (C-H), 2933 (C-H), 1538 (N-O), 1354 (N-O); ^{1}H NMR (400 MHz, $CDCl_3$) δ ppm 2.29 (s, 3 H, C(7)H_3), 2.44 (s, 3 H, C(6)H_3), 7.41 (dd, *J*=10.5, 8.5 Hz, 1 H, C(10)*H*), 7.54 (ddd, *J*=8.5, 4.0, 2.5 Hz, 1 H, C(9)*H*), 7.96 (dd, *J*=7.0, 2.5 Hz, 1 H, C(13)*H*); ^{13}C NMR (101 MHz, $CDCl_3$) δ ppm 10.8 (s, 1 C, *C*(7)), 11.8 (s, 1 C, *C*(6)), 114.2 (s, 1 C, *C*(1)), 119.3 (d, *J*=21.5 Hz, 1 C, *C*(10)), 126.5 (d, *J*=2.5 Hz, 1 C, *C*(13)), 127.9 (d, *J*=5.0 Hz, 1 C, *C*(8)), 136.1 (d, *J*=8.0 Hz, 1 C, *C*(9)), 137.8 (d, *J*=6.5 Hz, 1 C, *C*(12)), 154.9 (d, *J*=266.0 Hz, 1 C, *C*(11)), 158.2 (s, 1 C, *C*(2)), 166.4 (s, 1 C, *C*(5)); ^{19}F NMR (377 MHz, $CDCl_3$) δ ppm -118.5 (s, 1 F); LRMS *m/z* (ESI^+) 237 [MH^+]; HRMS

(ESI$^+$) found 259.0492, calculated for $C_{11}H_9FN_2NaO_3^+$ 259.0489; HPLC (System D): t_r 15.1 min (99%).

_N'_-[4-(3,5-Dimethyl-1,2-oxazol-4-yl)-2-nitrophenyl]-_N,N_-dimethylethane-1,2-diamine (217)

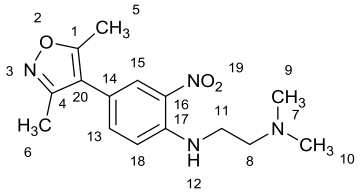

N,N-Dimethylenediamine (0.694 mL, 6.35 mmol) was added drop-wise to a solution of compound **251** (1.00 g, 4.23 mmol) and EtN(*i*-Pr)$_2$ (1.1 mL, 6.4 mmol) in THF (10 mL). The mixture was left to stir at room temperature for 16 h then partitioned between EtOAc (20 mL) and water (20 mL). The phases were separated then the organic phase was washed with water (20 mL) and brine (20 mL) then dried over $MgSO_4$ and evaporated to an orange solid. Ether (10 mL) was added then the resultant suspension was agitated then allowed to settle. The supernatant was decanted off with a pipette then more ether (10 mL) was added. This was again agitated, allowed to settle then decanted as before. The resultant solid was dried under vacuum to yield the product as an orange solid (1.10 g, 86%); R_f 0.15 (EtOAc:MeOH:NEt$_3$, 90:10:1); mp 118-119 °C; ν_{max} (neat) 3355 (N-H), 2951 (C-H), 2876 (C-H), 2795 (C-H), 1554 (N-O), 1354 (N-O); ^{1}H NMR (400 MHz, $CDCl_3$) δ ppm 2.27 (s, 3 H, C(6)H_3), 2.33 (s, 6 H, C(9)H_3+C(10)H_3), 2.41 (s, 3 H, C(5)H_3), 2.67 (t, *J*=6.0 Hz, 2 H, C(8)H_2), 3.40 (q, *J*=6.0 Hz, 2 H, C(11)H_2), 6.93 (d, *J*=9.0 Hz, 1 H, C(18)*H*), 7.34 (dd, *J*=9.0, 2.0 Hz, 1 H, C(13)*H*), 8.08 (d, *J*=2.0 Hz, 1 H, C(15)*H*), 8.40 (br. s., 1 H, N*H*); ^{13}C NMR (101 MHz, $CDCl_3$) δ ppm 10.7 (s, 1 C, *C*(6)), 11.5 (s, 1 C, *C*(5)), 40.8 (s, 1 C, *C*(11)), 45.2 (s, 2 C, *C*(9)+*C*(10)), 57.3 (s, 1 C, *C*(8)), 114.6 (s, 1 C, *C*(18)), 114.9 (s, 1 C, *C*(20)), 117.2 (s, 1 C, *C*(14)), 127.0 (s, 1 C, *C*(15)), 131.9 (s, 1 C, *C*(16)), 136.7 (s, 1 C, *C*(13)), 144.5 (s, 1 C, *C*(17)), 158.6 (s, 1 C, *C*(4)), 165.3 (s, 1 C, *C*(1)); HPLC (System D) t_r 3.6 min, *m/z* 305 [MH$^+$]; LRMS (ESI$^+$) *m/z* 631

[(2M+Na)$^+$], 609 [(2M+H)$^+$], 327 [(M+Na)$^+$], 305 [MH$^+$]; (ESI$^-$) 303 [(M-H)$^-$]; HRMS (ESI$^+$) found 305.1614, calculated for $C_{15}H_{21}N_4O_3^+$ 305.1608; HPLC (System D) t_r 10.3 min (99%).

N^1-[2-(Dimethylamino)ethyl]-4-(3,5-dimethyl-1,2-oxazol-4-yl)benzene-1,2-diamine (271)

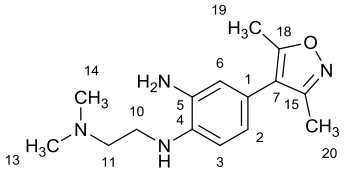

1 M aq. $Na_2S_2O_4$ (17.3 mL, 17.3 mmol) was added to a suspension of compound **217** (1.32 g, 4.34 mmol) in EtOH (20 mL). The mixture was heated at 80°C for 3 h then allowed to cool. The resultant mixture was concentrated *in vacuo* to remove some of the ethanol then partitioned between 10% aq. NH_3 (25 mL) and EtOAc (25 mL). The phases were separated then the aqueous phase further extracted with EtOAc (2×25 mL). The combined organic phases were dried over $MgSO_4$ and evaporated to yield the product as a brown gum (800 mg, 67%); R_f 0.10 (CH_2Cl_2:MeOH:NH_4OH, 90:10:1); ^{1}H NMR (400 MHz, $CDCl_3$) δ ppm 2.26 (s, 3 H, C(20)H_3), 2.27 (s, 6 H, C(13)H_3+C(14)H_3), 2.38 (s, 3 H, C(19)H_3), 2.62 (t, J=6.0 Hz, 2 H, C(11)H_2), 3.18 (t, J=6.0 Hz, 2 H, C(10)H_2), 3.50 (br. s., 2 H, NH_2), 4.05 (br. s., 1 H, NH), 6.59 (t, J=1.0 Hz, 1 H, C(2)H), 6.69 (d, J=1.0 Hz, 2 H, C(3)H+C(6)H); ^{13}C NMR (101 MHz, $CDCl_3$) δ ppm 10.8 (s, 1 C, C(20)), 11.5 (s, 1 C, C(19)), 41.4 (s, 1 C, C(10)), 45.3 (s, 2 C, C(13)+C(14)), 58.1 (s, 1 C, C(11)), 111.6 (s, 1 C, C(3/6)), 116.5 (s, 1 C, C(2)), 116.8 (s, 1 C, C(7)), 120.0 (s, 1 C, C(1)), 121.2 (s, 1 C, C(3/6)), 134.5 (s, 1 C, C(5)), 137.2 (s, 1 C, C(4)), 159.0 (s, 1 C, C(15)), 164.4 (s, 1 C, C(18)); LRMS *m/z* (ESI$^+$) 275 [MH$^+$], (ESI$^-$) 273 [(M-H)$^-$]; HRMS (ESI$^+$) found 275.1868, calculated 275.1866; HPLC (System D) t_r 8.3 min (93%).

2-[5-(3,5-Dimethyl-1,2-oxazol-4-yl)-2-methyl-1*H*-benzimidazol-1-yl]-*N,N*-dimethylethanamine (272)

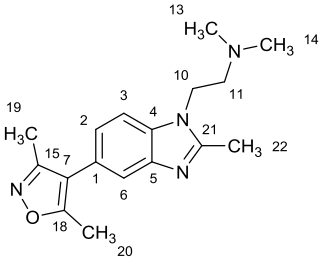

A mixture of compound **271** (0.74 g, 2.70 mmol), triethyl orthoacetate (10 mL) and ethanol (10 mL) was heated at 60 °C for 2 h then allowed to cool. The mixture was concentrated *in vacuo* then purified by flash column chromatography on silica (25 g). The column was eluted with a gradient of CH_2Cl_2:MeOH:NH_4OH, which was increased linearly from 95:5:0.5 to 90:10:1 over 10 CVs. The desired fractions were combined and evaporated to yield the product as a brown gum (0.64 g, 80%); R_f 0.35 (CH_2Cl_2:MeOH:NH_4OH, 90:10:1); ν_{max} 2983 (C-H), 2923 (C-H), 2857 (C-H), 2773 (C-H); ^{1}H NMR (400 MHz, $CDCl_3$) δ ppm 2.28 (s, 3 H, C(19)H_3), 2.33 (s, 6 H, C(13)H_3+C(14)H_3), 2.41 (s, 3 H, C(20)H_3), 2.61 - 2.70 (m, 5 H, C(11)H_2+C(22)H_3), 4.22 (t, *J*=7.0 Hz, 2 H, C(10)H_2), 7.11 (dd, *J*=8.0, 1.5 Hz, 1 H, C(2)*H*), 7.35 (d, *J*=8.0 Hz, 1 H, C(3)*H*), 7.55 (d, *J*=1.5 Hz, 1 H, C(6)*H*); ^{13}C NMR (101 MHz, $CDCl_3$) δ ppm 10.8 (s, 1 C, *C*(19)), 11.5 (s, 1 C, *C*(20)), 13.9 (s, 1 C, *C*(17)), 42.46 (s, 1 C, *C*(10)), 45.9 (s, 2 C, *C*(13)+*C*(14)), 58.4 (s, 1 C, *C*(11)), 109.2 (s, 1 C, *C*(3)), 117.1 (s, 1 C, *C*(7)), 119.7 (s, 1 C, *C*(6)), 123.3 (s, 1 C, *C*(2)), 124.0 (s, 1 C, *C*(1)), 134.5 (s, 1 C, *C*(4)), 143.0 (s, 1 C, *C*(5)), 152.6 (s, 1 C, *C*(21)), 159.0 (s, 1 C, *C*(15)), 165.0 (s, 1 C, *C*(18)); LRMS *m/z* (ESI^+) 619 [$(2M+Na)^+$], 321 $(M+Na)^+$], 299 [MH^+]; HRMS (ESI^+) found 299.1867, calculated for $C_{17}H_{23}N_4O^+$ 299.1866; HPLC (System D) t_r 8.0 min (99%).

2-{5-(3,5-Dimethyl-1,2-oxazol-4-yl)-2-[(*E*)-2-(2-methoxyphenyl)ethenyl]-1*H*-benzimidazol-1-yl}-*N*,*N*-dimethylethanamine (273)

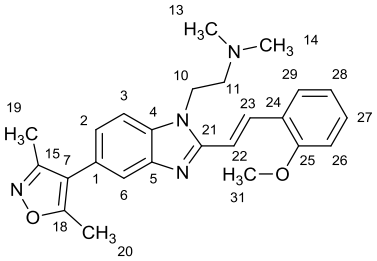

Acetic anhydride (23 µL, 0.24 mmol) was added to a solution of compound **272** (60 mg, 0.20 mmol) in chlorobenzene (1 mL). The solution was heated under microwave irradiation for 10 min at 180 °C. More acetic anhydride (0.10 mL, 1.06 mmol) was added then the solution was heated under microwave irradiation for 10 min at 220 °C then for 15 min at 250 °C. The reaction mixture was loaded directly onto a pre-equilibrated silica column (10 g) then eluted with a gradient of CH_2Cl_2:MeOH:NH_4OH, which was increased linearly from 99:1:0.1 to 90:10:1 over 10 CVs. The desired fractions were combined and evaporated to a brown gum. This material was columned again on a silica column (4 g). The column was eluted with a gradient of EtOAc:MeOH:NEt_3, which was increased linearly from 94:6:0.6 to 90:10:1 over 20 CVs. The desired fractions were combined and evaporated to yield the product as a yellow/brown gum (23 mg, 28%); R_f 0.50 (CH_2Cl_2:MeOH:NH_4OH, 90:10:1); ^{1}H NMR (400 MHz, $CDCl_3$) δ ppm 2.31 (s, 3 H, C(19)H_3), 2.39 (s, 6 H, C(13)H_3+C(14)H_3), 2.44 (s, 3 H, C(20)H_3), 2.74 (t, *J*=7.5 Hz, 2 H, C(11)H_2), 3.94 (s, 3 H, OCH_3), 4.38 (t, *J*=7.5 Hz, 2 H, C(10)H_2), 6.96 (d, *J*=8.5 Hz, 1H, C(26)*H*), 7.01 (t, *J*=7.5 Hz, 1H, C(28)*H*), 7.13 (dd, *J*=8.5, 1.5 Hz, 1 H, C(2)*H*), 7.29 - 7.36 (m, 2 H, C(22)*H*+C(27)*H*), 7.40 (d, *J*=8.5 Hz, 1 H, C(3)*H*), 7.60 (d, *J*=7.5Hz, 1H, C(29)*H*), 7.65 (d, *J*=1.5 Hz, 1H, C(6)*H*), 8.23 (d, *J*=16.0 Hz, 1 H, C(23)*H*); ^{13}C NMR (101 MHz, $CDCl_3$) δ ppm 10.9 (s, 1 C, *C*(19)), 11.55 (s, 1 C, *C*(20)), 42.0 (s, 1 C, *C*(10)), 45.8 (s, 2 C, *C*(13)+*C*(14)), 55.4 (s, 1 C, *C*(31)), 58.7 (s, 1 C, *C*(11)), 109.3 (s, 1 C, *C*(3)), 111.1 (s, 1 C, *C*(26)), 113.9 (s, 1 C, *C*(22)), 117.1 (s, 1 C, *C*(7)), 119.9 (s, 1 C, *C*(6)), 120.8 (s, 1 C, *C*(28)), 123.6 (s, 1 C, *C*(2)), 124.6 (s, 1 C, *C*(1/24)), 124.8 (s, 1 C, *C*(1/24)), 128.9 (s, 1 C, *C*(29)), 130.2

(s, 1 C, *C*(27)), 133.8 (s, 1 C, *C*(23)), 134.8 (s, 1 C, *C*(4)), 143.6 (s, 1 C, *C*(5)), 152.4 (s, 1 C, *C*(21)), 158.1 (s, 1 C, *C*(25)), 159.0 (s, 1 C, *C*(15)), 165.0 (s, 1 C, *C*(18)); LRMS *m/z* (ESI^+) 833 [$(2M+H)^+$], 417 [MH^+]; HRMS (ESI^+) found 417.2289, calculated for $C_{25}H_{29}N_4O_2^+$ 417.2285.

2-{5-(3,5-Dimethyl-1,2-oxazol-4-yl)-2-[2-(2-methoxyphenyl)ethyl]-1*H*-benzimidazol-1-yl}-*N*,*N*-dimethylethanamine (274)

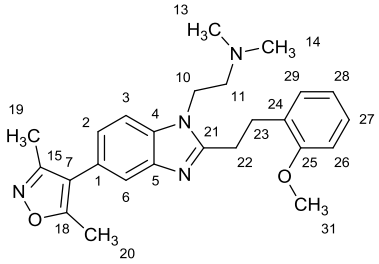

A mixture of compound **273** (20 mg, 0.05 mmol) and 10% Pd/C (5 mg) in acetic acid was stirred under a hydrogen atmosphere for 4 h. The mixture was filtered through a Celite pad then the filtrate was evaporated. The residue was partitioned between saturated aq. $NaHCO_3$ (5 mL) and EtOAc (5 mL). The phases were separated then the organic phase was washed with water (5 mL) and brine (5 mL) then dried over $MgSO_4$ and evaporated. The crude material was purified by flash column chromatography on a silica column (4 g). The column was eluted with a gradient of CH_2Cl_2:MeOH:NH_4OH, which was increased linearly from 98:2:0.2 to 90:10:1 over 20 CVs. The desired fractions were combined and evaporated to a pale yellow gum (13 mg). This material was re-dissolved in MeOH (1 mL) then purified using semi-preparative reverse-phase HPLC, performed on a WATERS Sunfire C18 column (150 mm x 10 mm, 5 μm). Separation was achieved using a linear gradient of solvent A (water + 0.1% F_3CCOOH) and solvent B (acetonitrile + 0.1% F_3CCOOH), eluting at a flow rate of 5 mL/min and monitoring at 254 nm: 0% B over 2 min and 0% B to 50% B over 30 min. The material obtained was loaded onto an SCX cartridge (1 g), which was eluted with MeOH then 7 M ammonia in MeOH. The ammonia eluent was evaporated to yield the product as a colourless gum (4 mg, 20%); R_f 0.40 (CH_2Cl_2:MeOH:NH_4OH, 90:10:1); ^1H NMR (500 MHz, $CDCl_3$) δ ppm 2.30 (s, 3 H, C(19)H_3), 2.32 (s, 6 H, C(13)H_3+C(14)H_3), 2.43 (s, 3 H, C(20)H_3),

2.61 (t, *J*=7.5 Hz, 2 H, C(11)H_2), 3.14 - 3.26 (m, 4 H, C(22)H_2+C(23)H_2), 3.86 (s, 3 H, C(31)H_3), 4.19 (t, *J*=7.5 Hz, 2 H, C(10)H_2), 6.87 - 6.93 (m, 2 H, C(26)*H*+C(28)*H*), 7.12 (dd, *J*=8.0, 1.5 Hz, 1 H, C(2)*H*), 7.19 (dd, *J*=8.0, 1.5 Hz, 1 H, C(29)*H*), 7.25 (td, *J*=8.0, 1.5 Hz, 1 H, C(27)*H*), 7.37 (d, *J*=8.0 Hz, 1 H, C(3)*H*), 7.63 (d, *J*=1.5 Hz, 1 H, C(6)*H*); ^{13}C NMR (126 MHz, $CDCl_3$) δ ppm 10.9 (1 C, s, *C*(19)), 11.5 (1 C, s, *C*(20)), 27.9 (1 C, s, *C*(23)), 29.6 (1 C, s, *C*(22)), 42.0 (1 C, s, *C*(10)), 45.8 (2 C, s, *C*(13)+*C*(14)), 55.2 (1 C, s, *C*(31)), 58.3 (1 C, s, *C*(11)), 109.4 (1 C, s, *C*(3)), 110.3 (1 C, s, *C*(26)), 117.2 (1 C, s, *C*(7)), 119.9 (1 C, s, *C*(6)), 120.7 (1 C, s, *C*(28)), 123.3 (1 C, s, *C*(2)), 124.0 (1 C, s, *C*(1)), 127.9 (1 C, s, *C*(27)), 129.0 (1 C, s, *C*(24)), 130.2 (1 C, s, *C*(29)), 134.4 (1 C, s, *C*(4)), 143.1 (1 C, s, *C*(5)), 155.9 (1 C, s, *C*(21)), 157.5 (1 C, s, *C*(25)), 159.0 (1 C, s, *C*(15)), 165.0 (1 C, s, *C*(18)); LRMS *m/z* (ESI^+) 859 [$(2M+Na)^+$], 837 [$(2M+H)^+$], 441 [$(M+Na)^+$], 419 [MH^+]; HRMS (ESI^+) found 419.2446, calculated for $C_{25}H_{31}N_4O_2^+$ 419.2442.

GENERAL PROCEDURE D

An oven-dried and nitrogen flushed sealable vial with septum was charged with a solution of compound **272** (45 mg, 0.15 mmol) in THF (2 mL). The vial was placed in an aluminium block which was cooled in a dry-ice acetone bath. *n*-BuLi (1.6 M in THF, 110 μL, 0.2 mmol) was added then the reaction was stirred for 30 min. A the appropriate benzylic halide (0.18 mmol) in THF (0.5 mL) was added then the resultant solution was stirred in the cooling bath for 30 min. The reaction mixture was then allowed to warm to room temperature then kept stirring for a further 4 h. The crude reaction was loaded directly onto a pre-equilibrated silica column (10 g) then eluted with a gradient of CH_2Cl_2:MeOH:NH_4OH, which was increased linearly from 96:4:0.4 to 91:9:0.9 over 10 CVs. The desired fractions were combined and evaporated to yield the products.

2-{2-[2-(2-Chlorophenyl)ethyl]-5-(3,5-dimethyl-1,2-oxazol-4-yl)-1*H*-benzimidazol-1-yl}-*N*,*N*-dimethylethanamine (275)

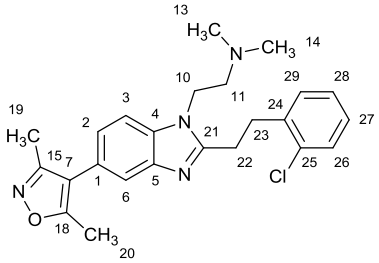

Compound **272** (45 mg, 0.15 mmol) was reacted with 1-(bromomethyl)-2-chlorobenzene (37 mg, 0.18 mmol) according to general procedure D to yield the product as a pale yellow gum (20 mg, 32%); TLC (CH_2Cl_2:MeOH:NH_4OH, 90:10:1) R_f 0.50; ν_{max} (neat) 2974 (C-H), 2945 (C-H), 2854 (C-H), 2821 (C-H), 2773 (C-H); ^{1}H NMR (400 MHz, $CDCl_3$) δ ppm 2.30 (s, 9 H, C(13)H_3+C(14)H_3+C(19)H_3), 2.43 (s, 3 H, C(20)H_3), 2.58 (t, *J*=7.5 Hz, 2 H, C(11)H_2), 3.17 - 3.26 (m, 2 H, C(22)H_2), 3.33 - 3.45 (m, 2 H, C(23)H_2), 4.16 (t, *J*=7.5 Hz, 2 H, C(10)H_2), 7.13 (dd, *J*=8.5, 1.5 Hz, 1 H, C(2)*H*), 7.16 - 7.23 (m, 2 H, C(27)*H*+C(28)*H*), 7.25 - 7.29 (m, 1 H, C(26)*H*), 7.37 (d, *J*=8.5 Hz, 1 H, C(3)*H*), 7.39 - 7.42 (m, 1 H, C(29)*H*), 7.63 (s, 1 H, C(6)*H*); ^{13}C NMR (101 MHz, $CDCl_3$) δ ppm 10.9 (s, 1 C, *C*(19)), 11.5 (s, 1 C, *C*(20)), 27.6 (s, 1 C, *C*(22)), 32.3 (s, 1 C, *C*(23)), 42.2 (s, 1 C, *C*(10)), 45.8 (s, 2 C, *C*(13)+*C*(14)), 58.3 (s, 1 C, *C*(11)), 109.5 (s, 1 C, *C*(3)), 117.1 (s, 1 C, *C*(7)), 119.9 (s, 1 C, *C*(6)), 123.4 (s, 1 C, *C*(2)), 124.1 (s, 1 C, *C*(1)), 127.2 (s, 1 C, *C*(27)), 128.1 (s, 1 C, *C*(28)), 129.6 (s, 1 C, *C*(29)), 130.8 (s, 1 C, *C*(26)), 133.8 (s, 1 C, *C*(25)), 134.3 (s, 1 C, *C*(4)), 138.28 (s, 1 C, *C*(24)), 143.1 (s, 1 C, *C*(4)), 155.0 (s, 1 C, *C*(21)), 159.0 (s, 1 C, *C*(15)), 165.0 (s, 1 C, *C*(18)); LRMS *m/z* (ESI$^+$) 847 [(2M(^{37}Cl)+Na)$^+$], 845 [(2M(^{35}Cl)+Na)$^+$], 447 [(M(^{37}Cl)+Na)$^+$], 445 [(M(^{35}Cl)+Na)$^+$], 425 [M(^{37}Cl)H$^+$], 423 [M(^{35}Cl)H$^+$]; HRMS (ESI$^+$) found 423.1939, calculated for $C_{24}H_{28}{}^{35}ClN_4O^+$ 423.1946; HPLC (System D) t_r 9.9 min (>99%).

2-{2-[2-(3-Chlorophenyl)ethyl]-5-(3,5-dimethyl-1,2-oxazol-4-yl)-1*H*-benzimidazol-1-yl}-*N*,*N*-dimethylethanamine (276)

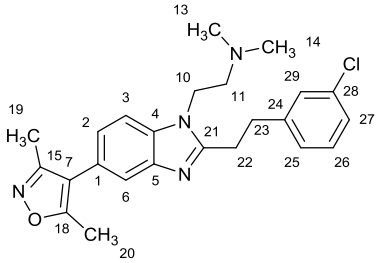

Compound **272** (45 mg, 0.15 mmol) was reacted with 1-(bromomethyl)-3-chlorobenzene (37 mg, 0.18 mmol) according to general procedure D to yield the product as a pale yellow gum (32 mg, 50%); R_f 0.50 (CH_2Cl_2:MeOH:NH_4OH, 90:10:1); ν_{max} (neat) 2976 (C-H), 2950 (C-H), 2924 (C-H), 2857 (C-H), 2826 (C-H), 2799 (C-H), 2777 (C-H); ^{1}H NMR (400 MHz, $CDCl_3$) δ ppm 2.30 (s, 9 H, C(13)H_3+C(14)H_3+C(19)H_3), 2.43 (s, 3 H, C(20)H_3), 2.57 (t, *J*=7.0 Hz, 2 H, C(11)H_2), 3.14 - 3.21 (m, 2 H, C(22)H_2), 3.26 - 3.32 (m, 2 H, C(23)H_2), 4.14 (t, *J*=7.0 Hz, 2 H, C(10)H_2), 7.10 - 7.16 (m, 2 H, C(2)*H*+Ar*H*), 7.19 - 7.28 (m, 3 H, 3×Ar*H*), 7.36 (d, *J*=8.5 Hz, 1 H, C(3)*H*), 7.63 (d, *J*=1.5 Hz, 1 H, C(6)*H*); ^{13}C NMR (101 MHz, $CDCl_3$) δ ppm 10.9 (s, 1 C, *C*(19)), 11.5 (s, 1 C, *C*(20)), 29.1 (s, 1 C, *C*(22)), 33.3 (s, 1 C, *C*(23)), 42.2 (s, 1 C, *C*(10)), 45.9 (s, 2 C, *C*(13)+ *C*(14)), 58.4 (s, 1 C, *C*(11)), 109.4 (s, 1 C, *C*(3)), 117.1 (s, 1 C, *C*(7)), 119.9 (s, 1 C, *C*(6)), 123.5 (s, 1 C, *C*(2)), 124.2 (s, 1 C, *C*(1)), 126.6 (s, 1 C, *C*(25/27)), 126.6 (s, 1 C, *C*(25/27)), 128.5 (s, 1 C, *C*(29)), 129.9 (s, 1 C, *C*(26)), 134.3 (s, 1 C, *C*(4/28)), 134.3 (s, 1 C, *C*(4/28)), 142.9 (s, 1 C, *C*(5/24)), 143.0 (s, 1 C, *C*(5/24)), 154.8 (s, 1 C, *C*(21)), 159.0 (s, 1 C, *C*(15)), 165.0 (s, 1 C, *C*(18)); LRMS *m/z* (ESI$^+$) 869 [(2M(^{37}Cl)+Na)$^+$], 867 [(2M(^{35}Cl)+Na)$^+$], 847 [(2M(^{37}Cl)+H)$^+$], 845 [(2M(^{35}Cl)+H)$^+$], 447 [(M(^{37}Cl)+Na)$^+$], 445 [(M(^{35}Cl)+Na)$^+$], 425 [M(^{37}Cl)H$^+$], 423 [M(^{35}Cl)H$^+$]; HRMS (ESI$^+$) found 423.1940, calculated for $C_{24}H_{28}{}^{35}ClN_4O^+$ 423.1946; HPLC (System D) t_r 10.2 min (96%).

2-{2-[2-(4-Chlorophenyl)ethyl]-5-(3,5-dimethyl-1,2-oxazol-4-yl)-1*H*-benzimidazol-1-yl}-*N*,*N*-dimethylethanamine (277)

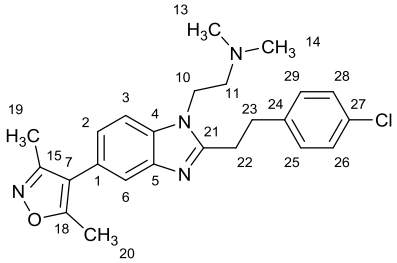

Compound **272** (45 mg, 0.15 mmol) was reacted with 1-(bromomethyl)-4-chlorobenzene (37 mg, 0.18 mmol) according to general procedure D to yield the product as a pale yellow gum (27 mg, 43%); R_f 0.50 (CH_2Cl_2:MeOH:NH_4OH, 90:10:1); ν_{max} (neat) 2932 (C-H), 2855 (C-H), 2823 (C-H), 2773 (C-H); ^{1}H NMR (400 MHz, $CDCl_3$) δ ppm 2.29 (s, 6 H, C(13)H_3+C(14)H_3), 2.30 (s, 3 H, C(19)H_3), 2.43 (s, 3 H, C(20)H_3), 2.53 (t, *J*=7.0 Hz, 2 H, C(11)H_2), 3.11 - 3.20 (m, 2 H, C(23)H_2), 3.23 - 3.31 (m, 2 H, C(22)H_2), 4.11 (t, *J*=7.0 Hz, 2 H, C(10)H_2), 7.13 (dd, *J*=8.0, 1.5 Hz, 1 H, C(2)*H*), 7.15 - 7.21 (m, 2 H, C(25)*H*+C(29)*H*), 7.24 - 7.29 (m, 2 H, C(26)*H*+C(28)*H*), 7.36 (d, *J*=8.5 Hz, 1 H, C(3)*H*), 7.62 (d, *J*=1.5 Hz, 1 H, C(6)*H*); ^{13}C NMR (101 MHz, $CDCl_3$) δ ppm 10.9 (s, 1 C, *C*(19)), 11.5 (s, 1 C, *C*(20)), 29.3 (s, 1 C, *C*(22)), 33.2 (s, 1 C, *C*(23)), 42.2 (s, 1 C, *C*(10)), 45.9 (s, 2 C, *C*(13)+*C*(14)), 58.3 (s, 1 C, *C*(11)), 109.4 (s, 1 C, *C*(3)), 117.1 (s, 1 C, *C*(7)), 119.9 (s, 1 C, *C*(6)), 123.5 (s, 1 C, *C*(2)), 124.2 (s, 1 C, *C*(1)), 128.7 (s, 2 C, *C*(26)+*C*(28)), 129.8 (s, 2 C, *C*(25)+*C*(29)), 132.2 (s, 1 C, *C*(27)), 134.3 (s, 1 C, *C*(4)), 139.3 (s, 1 C, *C*(24)), 143.0 (s, 1 C, *C*(5)), 154.9 (s, 1 C, *C*(21)), 159.0 (s, 1 C, *C*(15)), 165.0 (s, 1 C, *C*(18)); LRMS *m/z* (ESI$^+$) 847 [(2M(^{37}Cl)+H)$^+$], 845 [(2M(^{35}Cl)+H)$^+$], 447 [(M(^{37}Cl)+Na)$^+$], 445 [(M(^{35}Cl)+Na)$^+$], 425 [M(^{37}Cl)H$^+$], 423 [M(^{35}Cl)H$^+$]; HRMS (ESI$^+$) found 423.1948, calculated for $C_{24}H_{28}{}^{35}ClN_4O^+$ 423.1946; HPLC (System D) t_r 10.2 min (95%).

2-(2-{1-[2-(Dimethylamino)ethyl]-5-(3,5-dimethyl-1,2-oxazol-4-yl)-1*H*-benzimidazol-2-yl}ethyl)benzonitrile (278)

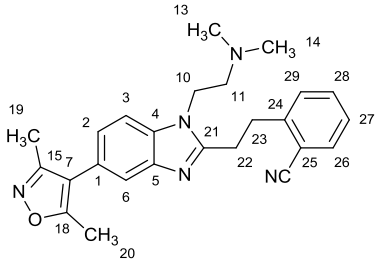

Compound **272** (45 mg, 0.15 mmol) was reacted with 2-(bromomethyl)benzonitrile (35 mg, 0.18 mmol) according to general procedure D to yield the product as a pale brown solid (27 mg, 43%); mp 48-52 °C; R_f 0.50 (CH_2Cl_2:MeOH:NH_4OH, 90:10:1); ν_{max} (neat) 2968 (C-H), 2945 (C-H), 2863 (C-H), 2828 (C-H), 2770, (C-H), 2219 (C≡N); ^{1}H NMR (400 MHz, $CDCl_3$) δ ppm 2.30 (s, 9 H, C(13)H_3+C(14)H_3+C(19)H_3), 2.43 (s, 3 H, C(20)H_3), 2.62 (t, *J*=7.0 Hz, 2 H, C(11)H_2), 3.24 - 3.31 (m, 2 H, C(22)H_2), 3.46 - 3.53 (m, 2 H, C(23)H_2), 4.23 (t, *J*=7.0 Hz, 2 H, C(10)H_2), 7.14 (dd, *J*=8.0, 1.5 Hz, 1 H, C(2)*H*), 7.33 - 7.41 (m, 2 H, C(3)*H*+C(27)H_3), 7.45 (d, *J*=7.5 Hz, 1 H, C(29)*H*), 7.50 - 7.57 (m, 1 H, C(28)*H*), 7.62 (s, 1 H, C(6)*H*), 7.68 (d, *J*=8.0 Hz, 1 H, C(26)*H*); ^{13}C NMR (101 MHz, $CDCl_3$) δ ppm 10.8 (s, 1 C, *C*(19)), 11.5 (s, 1 C, *C*(20)), 28.6 (s, 1 C, *C*(22)), 32.8 (s, 1 C, *C*(23)), 42.4 (s, 1 C, *C*(10)), 45.9 (s, 2 C, *C*(13)+*C*(14)), 58.4 (s, 1 C, *C*(11)), 109.6 (s, 1 C, *C*(3)), 112.3 (s, 1 C, *C*(25)), 117.1 (s, 1 C, *C*(7)), 118.0 (s, 1 C, *C*N) 119.9 (s, 1 C, *C*(6)), 123.6 (s, 1 C, *C*(2)), 124.2 (s, 1 C, *C*(1)), 127.2 (s, 1 C, *C*(27)), 130.1 (s, 1 C, *C*(29)), 132.9 (s, 1 C, *C*(26/28)), 133.2 (s, 1 C, *C*(26/28)), 134.4 (s, 1 C, *C*(4)), 143.0 (s, 1 C, *C*(5)), 144.7 (s, 1 C, *C*(24)), 154.2 (s, 1 C, *C*(21)), 159.0 (s, 1 C, *C*(15)), 165.0 (s, 1 C, *C*(18)); LRMS *m/z* (ESI$^+$) 849 [(2M+Na)$^+$], 827 [(2M+H)$^+$], 436 [(M+Na)$^+$], 414 [MH$^+$]; HRMS (ESI$^+$) found 414.2287, calculated for $C_{25}H_{28}N_5O^+$ 414.2288; HPLC (System E) t_r 3.4 min (94%).

3-(2-{1-[2-(Dimethylamino)ethyl]-5-(3,5-dimethyl-1,2-oxazol-4-yl)-1*H*-benzimidazol-2-yl}ethyl)benzonitrile (279)

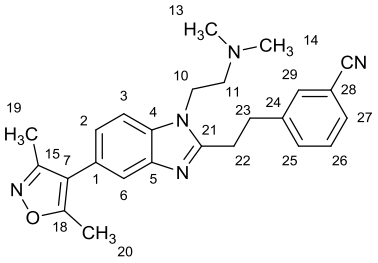

Compound **272** (45 mg, 0.15 mmol) was reacted with 3-(bromomethyl)benzonitrile (35 mg, 0.18 mmol) according to general procedure D to yield the product as a pale yellow gum (10 mg, 16%); R_f 0.40 (CH_2Cl_2:MeOH:NH_4OH, 90:10:1); ν_{max} (neat) 2858 (C-H), 2826 (C-H), 2800 (C-H), 2772 (C-H), 2229 (C≡N); ^{1}H NMR (500 MHz, $CDCl_3$) δ ppm 2.27 - 2.32 (m, 9 H, C(19)H_3+C(13)H_3+C(14)H_3), 2.44 (s, 3 H, C(20)H_3), 2.60 (t, *J*=7.0 Hz, 2 H, C(11)H_2), 3.19 - 3.24 (m, 2 H, C(22)H_2), 3.35 - 3.41 (m, 2 H, C(23)H_2), 4.17 (t, *J*=7.0 Hz, 2 H, C(10)H_2), 7.15 (dd, *J*=8.0, 1.5 Hz, 1 H, C(2)*H*), 7.37 (d, *J*=8.0 Hz, 1 H, C(3)*H*), 7.42 (t, *J*=7.5 Hz, 1 H, C(26)*H*), 7.51 - 7.56 (m, 2 H, C(25)*H*+C(27)*H*), 7.58 (s, 1 H, C(29)*H*), 7.63 (d, *J*=1.5 Hz, 1 H, C(6)*H*); ^{13}C NMR (126 MHz, $CDCl_3$) δ ppm 10.9 (s, 1 C, *C*(19)), 11.6 (s, 1 C, *C*(20)), 28.8 (s, 1 C, *C*(22)), 32.9 (s, 1 C, *C*(23)), 42.3 (s, 1 C, *C*(10)), 45.9 (s, 2 C, *C*(13)+*C*(14)), 58.5 (s, 1 C, *C*(11)), 109.4 (s, 1 C, *C*(3)), 112.7 (s, 1 C, *C*(28)), 117.0 (s, 1 C, *C*(7)), 118.8 (s, 1 C, *C*N)), 120.0 (s, 1 C, *C*(6)), 123.6 (s, 1 C, *C*(2)), 124.3 (s, 1 C, *C*(1)), 129.4 (s, 1 C, *C*(26)), 130.2 (s, 1 C, *C*(27)), 131.9 (s, 1 C, *C*(29)), 133.1 (s, 1 C, *C*(25)), 134.3 (s, 1 C, *C*(4)), 142.3 (s, 1 C, *C*(24)), 142.9 (s, 1 C, *C*(5)), 154.3 (s, 1 C, *C*(21)), 159.0 (s, 1 C, *C*(15)), 165.0 (s, 1 C, *C*(18)); LRMS *m/z* (ESI^+) 827 [$(2M+H)^+$], 436 [$(M+Na)^+$], 414 [MH^+]; HRMS (ESI^+) found 414.2296, calculated for $C_{25}H_{28}N_5O^+$ 414.2288; HPLC (System D) t_r 9.7 min (94%).

4-(2-{1-[2-(Dimethylamino)ethyl]-5-(3,5-dimethyl-1,2-oxazol-4-yl)-1*H*-benzimidazol-2-yl}ethyl)benzonitrile (280)

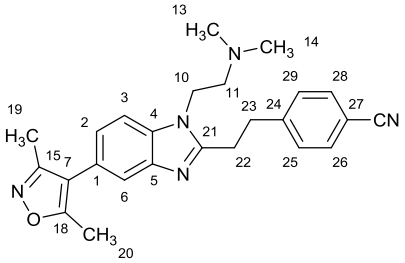

Compound **272** (45 mg, 0.15 mmol) was reacted with 4-(bromomethyl)benzonitrile (35 mg, 0.18 mmol) according to general procedure D to yield the product as a pale brown solid (17 mg, 27%); R_f 0.35 (CH_2Cl_2:MeOH:NH_4OH, 90:10:1); mp 189-195 °C; ν_{max} (neat) 2924 (C-H), 2854 (C-H), 2832 (C-H), 2775 (C-H), 2225 (C≡N); ^{1}H NMR (500 MHz, $CDCl_3$) δ ppm 2.27 - 2.31 (m, 9 H, C(19)H_3+C(13)H_3+C(14)H_3), 2.43 (s, 3 H, C(20)H_3), 2.58 (t, *J*=7.0 Hz, 2 H, C(11)H_2), 3.16 - 3.24 (m, 2 H, C(22)H_2), 3.35 - 3.42 (m, 2 H, C(23)H_2), 4.15 (t, *J*=7.0 Hz, 2 H, C(10)H_2), 7.14 (dd, *J*=8.0, 1.5 Hz, 1 H, C(2)*H*), 7.31 - 7.44 (m, 3 H, C(14)*H*+C(25)*H*+C(29)*H*), 7.55 - 7.69 (m, 3 H, C(6)*H*+C(26)*H*+C(28)*H*); ^{13}C NMR (126 MHz, $CDCl_3$) δ ppm 10.9 (s, 1 C, *C*(19)), 11.6 (s, 1 C, *C*(20)), 28.6 (s, 1 C, *C*(22)), 33.5 (s, 1 C, *C*(23)), 42.2 (s, 1 C, *C*(10)), 45.9 (s, 2 C, *C*(13)+*C*(14)), 58.4 (s, 1 C, *C*(11)), 109.4 (s, 1 C, *C*(3)), 110.4 (s, 1 C, *C*(22)), 117.0 (s, 1 C, *C*(7)), 118.8 (s, 1 C, *C*N) 119.9 (s, 1 C, *C*(6)), 123.6 (s, 1 C, *C*(2)), 124.3 (s, 1 C, *C*(1)), 129.2 (s, 2 C, *C*(25)+*C*(29)), 132.4 (s, 2 C, *C*(26)+*C*(28)), 134.3 (s, 1 C, *C*(4)), 142.9 (s, 1 C, *C*(5)), 146.5 (s, 1 C, *C*(24)), 154.3 (s, 1 C, *C*(21)), 159.0 (s, 1 C, *C*(15)), 165.0 (s, 1 C, *C*(18)); LRMS *m/z* (ESI$^+$) 849 [(2M+Na)$^+$], 827 [(2M+H)$^+$], 436 [(M+Na)$^+$], 414 [MH$^+$]; HRMS (ESI$^+$) found 414.2295, calculated for $C_{25}H_{28}N_5O^+$ 414.2288; HPLC (System D) t_r 9.7 min (97%).

GENERAL PROCEDURE E

HBTU (102 mg, 0.27 mmol) and EtN(*i*-Pr)$_2$ (63 μL, 0.36 mmol) were added to a stirred solution of the appropriate carboxylic acid (0.19 mmol) in DMF (1 mL). The mixture was stirred at room temperature for 5 min then compound **271** (50 mg, 0.18 mmol) was added. The solution was stirred at room temperature for 18 h then partitioned between EtOAc (2 mL) and saturated aq. K_2CO_3 solution (2 mL). The phases were separated then the organic phase was washed with water (2 mL) and brine (2 mL) then passed through a hydrophobic frit then concentrated *in vacuo*. The residue was re-dissolved in AcOH (1 mL) then the resultant solution was heated under microwave irradiation for 10 min at 180 °C. The solution was neutralized by addition of 1 M aq. NaOH solution then extracted with CH_2Cl_2 (2×2 mL). The combined organic phases were passed through a hydrophobic frit then evaporated by nitrogen blow-down. The crude material was purified by flash column chromatography on silica (10 g). The column was eluted with a gradient of CH_2Cl_2:MeOH:NH_4OH, which was increased linearly from 99:1:0.1 to 92:8:0.8 over 10 CVs. The desired fractions were combined and evaporated to yield the product.

2-{5-(3,5-Dimethyl-1,2-oxazol-4-yl)-2-[2-(3-methoxyphenyl)ethyl]-1*H*-benzimidazol-1-yl}-*N*,*N*-dimethylethanamine (281)

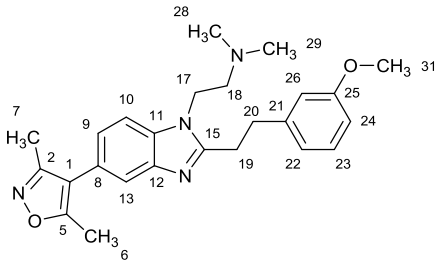

3-(3-Methoxyphenyl)propionic acid (34 mg, 0.19 mmol) was reacted with compound **271** (50 mg, 0.18 mmol) according to general procedure E to yield the product as a pale yellow gum (37 mg, 49%); R_f 0.50 (CH_2Cl_2:MeOH:NH_4OH, 90:10:1); ν_{max} 2941 (C-H), 2825 (C-H), 2743 (C-H); ^{1}H NMR (400 MHz, $CDCl_3$) δ ppm 2.23 - 2.33 (m, 9 H, C(7)*H*$_3$+C(28)*H*$_3$+C(29)*H*$_3$),

2.42 (s, 3 H, C(6)H_3), 2.54 (t, J=7.5 Hz, 2 H, C(18)H_2), 3.15 - 3.22 (m, 2 H, C(19)H_2), 3.22 - 3.31 (m, 2 H, C(20)H_2), 3.73 (s, 3 H, OCH_3), 4.10 (t, J=7.5 Hz, 2 H, C(17)H_2), 6.74 - 6.80 (m, 2 H, C(24)H+C(26)H), 6.84 (d, J=7.5 Hz, 1 H, C(22)H), 7.12 (dd, J=8.5, 1.5 Hz, 1 H, C(9)H), 7.19 - 7.25 (m, 1 H, C(23)H), 7.36 (d, J=8.5 Hz, 1 H, C(10)H), 7.62 (d, J=1.5 Hz, 1 H, C(13)H); ^{13}C NMR (101 MHz, $CDCl_3$) δ ppm 10.8 (s, 1 C, C(7)), 11.5 (s, 1 C, C(6)), 29.4 (s, 1 C, C(19)), 34.0 (s, 1 C, C(20)), 42.1 (s, 1 C, C(17)), 45.8 (s, 2 C, C(28)+C(29)), 55.0 (s, 1 C, C(31)), 58.3 (s, 1 C, C(18)), 109.4 (s, 1 C, C(10)), 111.8 (s, 1 C, C(24)), 114.1 (s, 1 C, C(26)), 117.1 (s, 1 C, C(1)), 119.8 (s, 1 C, C(13)), 120.7 (s, 1 C, C(22)), 123.4 (s, 1 C, C(9)), 124.1 (s, 1 C, C(8)), 129.6 (s, 1 C, C(23)), 134.3 (s, 1 C, C(11)), 142.4 (s, 1 C, C(21)), 143.0 (s, 1 C, C(12)), 155.2 (s, 1 C, C(15)), 159.0 (s, 1 C, C(2)), 159.7 (s, 1 C, C(25)), 165.0 (s, 1 C, C(5)); LRMS m/z (ESI$^+$) 859 [(2M+Na)$^+$], 837 [(2M+H)$^+$], 441 [(M+Na)$^+$], 419 [MH$^+$]; HRMS (ESI$^+$) found 419.2447, calculated for $C_{25}H_{31}N_4O_2^+$ 419.2442; HPLC (System D) t_r 9.7 min (94%).

2-{5-(3,5-Dimethyl-1,2-oxazol-4-yl)-2-[2-(2-methylphenyl)ethyl]-1*H*-benzimidazol-1-yl}-*N*,*N*-dimethylethanamine (282)

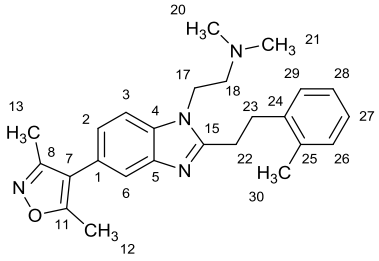

2-Methylhydrocinnamic acid (34 mg, 0.19 mmol) was reacted with compound **271** (50 mg, 0.18 mmol) according to general procedure E to yield the product as a colourless gum (37 mg, 51%); R_f 0.45 (CH_2Cl_2:MeOH:NH_4OH, 90:10:1); ν_{max} (neat) 2949 (C-H), 2886 (C-H), 2696 (C-H), 2633 (C-H), 2539 (C-H); ^{1}H NMR (400 MHz, $CDCl_3$) δ ppm 2.28 (s, 6 H, C(20)H_3+C(21)H_3), 2.30 (s, 3 H, C(13)H_3), 2.38 (s, 3 H, C(30)H_3), 2.43 (s, 3 H, C(12)H_3), 2.56 (t, J=7.5 Hz, 2 H, C(18)H_2), 3.11 - 3.20 (m, 2 H, C(22)H_2), 3.25 - 3.33 (m, 2 H, C(23)H_2), 4.09 (t, J=7.5 Hz, 2 H, C(17)H_2), 7.08 - 7.23 (m, 5 H, 5×ArH), 7.36 (d, J=8.5 Hz, 1 H, C(3)H), 7.64 (d,

J=1.0 Hz, 1 H, C(6)*H*); ^{13}C NMR (101 MHz, $CDCl_3$) δ ppm 10.8 (1 C, s, *C*(13)), 11.5 (1 C, s, *C*(12)), 19.3 (1 C, s, *C*(30)), 28.2 (1 C, s, *C*(22)), 31.3 (1 C, s, *C*(23)), 42.1 (1 C, s, *C*(17)), 45.8 (2 C, s, *C*(20)+*C*(21)), 58.3 (1 C, s, *C*(18)), 109.4 (1 C, s, *C*(3)), 117.1 (1 C, s, *C*(7)), 119.9 (1 C, s, *C*(6)), 123.4 (1 C, s, *C*(2)), 124.1 (1 C, s, *C*(1)), 126.3 (1 C, s, *C*(27/28)), 126.6 (1 C, s, *C*(27/28)), 128.8 (1 C, s, *C*(29)), 130.4 (1 C, s, *C*(26)), 134.3 (1 C, s, *C*(4)), 135.9 (1 C, s, *C*(25)), 139.0 (1 C, s, *C*(24)), 143.0 (1 C, s, *C*(5)), 155.4 (1 C, s, *C*(15)), 159.0 (1 C, s, *C*(8)), 164.9 (1 C, s, *C*(11)); LRMS *m/z* (ESI$^+$) 827 [(2M+Na)$^+$], 805 [(2M+H)$^+$], 425 [(M+Na)$^+$], 403 [MH$^+$]; HRMS (ESI$^+$) found 403.2493, calculated for $C_{25}H_{31}N_4O^+$ 403.2492; HPLC (System D) t_r 9.8 min (>99%).

2-{5-(3,5-Dimethyl-1,2-oxazol-4-yl)-2-[2-(4-methylphenyl)ethyl]-1*H*-benzimidazol-1-yl}-*N,N*-dimethylethanamine (283)

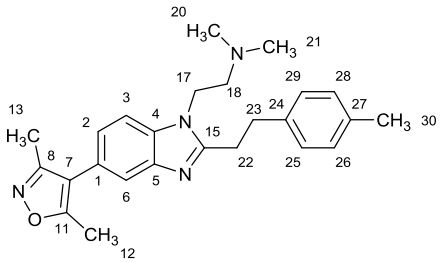

3-(*p*-Tolyl)-propionic acid (34 mg, 0.19 mmol) was reacted with compound **271** (50 mg, 0.18 mmol) according to general procedure E to yield the product as a cream solid (50 mg, 69%); R_f 0.45 (CH_2Cl_2:MeOH:NH_4OH, 90:10:1); mp 122-126 °C; ν_{max} (neat) 2951 (C-H), 2860 (C-H), 2828 (C-H), 2790 (C-H); ^{1}H NMR (400 MHz, $CDCl_3$) δ ppm 2.28 (s, 6 H, C(20)H_3+C(21)H_3), 2.30 (s, 3 H, C(13)H_3), 2.33 (s, 3 H, C(30)H_3), 2.42 (s, 3 H, C(12)H_3), 2.53 (t, *J*=7.5 Hz, 2 H, C(18)H_2), 3.13 - 3.20 (m, 2 H, C(22)H_2), 3.22 - 3.28 (m, 2 H, C(24)H_2), 4.10 (t, *J*=7.5 Hz, 2 H, C(17)H_2), 7.10 - 7.16 (m, 5 H, 5×Ar*H*), 7.36 (d, *J*=8.5 Hz, 1 H, C(3)*H*), 7.63 (d, *J*=1.0 Hz, 1 H, C(6)*H*); ^{13}C NMR (101 MHz, $CDCl_3$) δ ppm 11.3 (1 C, s, *C*(13)), 12.0 (1 C, s, *C*(12)), 21.4 (1 C, s, *C*(30)), 30.1 (1 C, s, *C*(22)), 34.0 (1 C, s, *C*(23)), 42.5 (1 C, s, *C*(17)), 46.2 (2 C, s, *C*(20)+*C*(21)), 58.7 (1 C, s, *C*(18)), 109.8 (1 C, s, *C*(3)), 117.5 (1 C, s, *C*(7)), 120.3 (1 C,

s, *C*(6)), 123.8 (1 C, s, *C*(2)), 124.5 (1 C, s, *C*(1)), 128.7 (2 C, s, *C*(24/27)+*C*(25/26)), 129.7 (2 C, s, *C*(24/27)+*C*(25/26)), 134.7 (1 C, s, *C*(4)), 136.4 (1 C, s, *C*(27)), 138.2 (1 C, s, *C*(24)), 143.5 (1 C, s, *C*(5)), 155.8 (1 C, s, *C*(15)), 159.4 (1 C, s, *C*(8)), 165.4 (1 C, s, *C*(11)); LRMS *m/z* (ESI$^+$) 827 [(2M+Na)$^+$], 805 [(2M+H)$^+$], 425 [(M+Na)$^+$], 403 [MH$^+$]; HRMS (ESI$^+$) found 403.2495, calculated for $C_{25}H_{31}N_4O^+$ 403.2492; HPLC (System D) t_r 10.0 min (>99%).

4-Bromo-*N*-(4-methoxybenzyl)-2-nitroaniline (284)

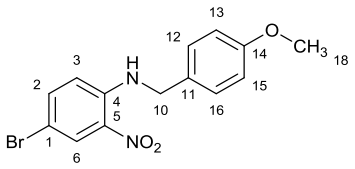

4-Methoxybenzylamine (0.745 g, 5.5 mmol) was added to a cooled (0 °C) solution of 4-bromo-1-fluoro-2-nitrobenzene (1.10 g, 5.0 mmol) and EtN(*i*-Pr)$_2$ (1.31 mL, 7.5 mmol) in THF (20 mL). The solution was allowed to warm gradually to room temperature over 1 hour then stirred at this temperature for 3 h. The reaction mixture was partitioned between EtOAc (25 mL) and water (25 mL). The phases were separated then the organic phase was washed with water (25 mL) and brine (25 mL) then dried over $MgSO_4$ and evaporated to an orange solid. MeOH (3 mL) was added resulting in a suspension. The supernatant was decanted off using a pipette. This process was repeated twice then the resultant solid was dried under vacuum to yield the product as a bright orange solid (1.18 g, 70%); R_f 0.25 (EtOAc:*c*-hexane, 10:90); mp 118-124 °C; ν_{max} (neat) 3398 (N-H), 2839 (C-H), 1562 (N-O), 1347 (N-O); ^{1}H NMR (400 MHz, $CDCl_3$) δ ppm 3.82 (s, 3 H, C*H*$_3$), 4.47 (d, *J*=5.6 Hz, 2 H, C*H*$_2$), 6.75 (d, *J*=9.2 Hz, 1 H, C(3)*H*), 6.90 (d, *J* = 8.9 Hz, 2 H, C(13)*H*+C(15)*H*), 7.24 (d, *J* = 8.9 Hz, 2 H, C(12)*H*+C(16)*H*), 7.45 (dd, *J*=9.2, 2.4 Hz, 1 H, C(2)*H*), 8.29 - 8.40 (m, 2 H, C(6)*H*+N*H*); ^{13}C NMR (101 MHz, $CDCl_3$) δ ppm 46.7 (s, 1 C, *C*H$_2$) 55.3 (s, 1 C, O*C*H$_3$) 106.8 (s, 1 C, *C*(1)), 114.4 (s, 2 C, *C*(13)+*C*(15)), 116.0 (s, 1 C, *C*(6)), 128.4 (s, 2 C, *C*(12)+*C*(16)), 128.7 (s, 1 C, *C*(11)), 128.9 (s, 1 C, *C*(6)), 132.5 (s, 1 C, *C*(5)), 138.9 (s, 1 C, *C*(2)), 144.1 (s, 1 C, *C*(5)), 159.3 (s, 1 C,

C(4)); LRMS *m/z* (ESI$^+$) 359, 361 [(M+Na)$^+$]. HRMS (ESI$^+$) found 359.0005, calculated for $C_{14}H_{13}BrN_2NaO_3^+$ 359.0002; HPLC (System D) t_r 18.6 min (99%).

4-Bromo-2-nitro-*N*-(pyridin-3-ylmethyl)aniline (285)

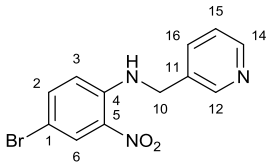

3-Picolylamine (0.28 mL, 2.8 mmol) was added to a cooled (0 °C) solution of 4-bromo-1-fluoro-2-nitrobenzene (550 mg, 2.5 mmol) and EtN(*i*-Pr)$_2$ (0.65 mL, 3.8 mmol) in THF (10 mL). The solution was stirred at 0 °C for 2 h, allowed to warm to room temperature then left to stir at room temperature for 18 h. The reaction mixture was partitioned between EtOAc (10 mL) and water (10 mL). The phases were separated then the organic phase was washed with water (10 mL) and brine (10 mL) then dried over $MgSO_4$ and evaporated. Ethanol (5 mL) was added resulting in crystallisation of a solid. The supernatant was decanted off using a pipette. This process was repeated twice then the resultant solid was dried under vacuum to yield the product as a bright orange solid (376 mg). NMR indicated unreacted starting aryl fluoride so the solid was taken up in 1 M aq. HCl (15 mL). The mixture was extracted with CH_2Cl_2 (2×15 mL) then these organic extracts were discarded. The aqueous phase was made basic by addition of 1 M aq. NaOH solution then extracted with CH_2Cl_2 (2×15 mL). The combined organic phases were dried over $MgSO_4$ and evaporated to yield the product as a pale orange solid (222 mg, 29%); R_f 0.10 (EtOAc:*n*-hexane, 50:50); mp 109-111 °C; ν_{max} (neat) 3342 (N-H), 2929 (C-H), 1553 (N-O), 1348 (N-O); ^{1}H NMR (400 MHz, $CDCl_3$) δ ppm 4.58 (d, *J*=6.0 Hz, 2 H, CH_2), 6.70 (d, *J*=9.0 Hz, 1 H, C(3)*H*), 7.32 (dd, *J*=8.0, 5.0 Hz, 1 H, C(15)*H*), 7.47 (dd, *J*=9.0, 2.5 Hz, 1 H, C(2)*H*), 7.60 - 7.71 (m, 1 H, C(16)*H*), 8.35 (d, *J*=2.5 Hz, 1 H, C(6)*H*), 8.36 - 8.43 (m, 1 H, N*H*), 8.59 (dd, *J*=5.0, 1.5 Hz, 1 H, C(14)*H*), 8.64 (d, *J*=1.5 Hz, 1 H, C(12)*H*); ^{13}C NMR (101 MHz, $CDCl_3$) δ ppm 44.7 (s, 1 C, CH_2) 107.5 (s, 1 C, *C*(1)), 115.6 (s, 1 C, *C*(3)), 123.8 (s, 1 C, *C*(15)), 129.1 (s, 1 C, *C*(6)), 132.4 (s, 1 C, *C*(5/11)), 132.9 (s, 1 C,

C(5/11)), 134.6 (s, 1 C *C*(16)), 139.0 (s, 1 C, *C*(2)), 143.6 (s, 1 C, *C*(4)), 148.8 (s, 1 C, *C*(14)), 149.5 (s, 1 C, *C*(12)); LRMS *m/z* (ESI^+) 330, 332 [$(M+Na)^+$], 308, 310 [MH^+], (ESI^-) 306, 308 [$(M-H)^-$]; HRMS (ESI^+) found 308.0026, calculated for $C_{12}H_{11}BrN_3O_2^+$ 308.0029; HPLC (System D) t_r 10.8 min (>99%).

4-Bromo-*N*-isopentyl-2-nitroaniline (286)

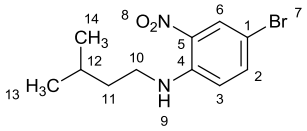

Isopentylamine (320 µL, 2.8 mmol) was added to a cooled (0 °C) solution of 4-bromo-1-fluoro-2-nitrobenzene (550 mg, 2.5 mmol) and EtN(*i*-Pr)$_2$ (650 µL, 3.8 mmol) in THF (10 mL). The solution was stirred at 0 °C for 2 h, allowed to warm to room temperature then left to stir at room temperature for 18 h. The reaction mixture was partitioned between EtOAc (10 mL) and water (10 mL). The phases were separated then the organic phase was washed with water (10 mL) and brine (10 mL) then dried over $MgSO_4$ and evaporated. The crude material was purified by flash column chromatography on a silica column (25 g). The column was eluted with a gradient of EtOAc:40-60 petroleum spirit, which was increased linearly from 5:95 to 20:80 over 10 CVs. The desired fractions were combined and evaporated to yield the product as an orange oil (540 mg, 75%); R_f 0.40 (EtOAc:*n*-hexane, 20:80); ν_{max} (neat) 3376 (N-H), 3099 (C-H), 2956 (C-H), 2927 (C-H), 2867 (C-H), 1537 (N-O), 1348 (N-O); ^{1}H NMR (400 MHz, $CDCl_3$) δ ppm 0.99 (d, *J*=6.5 Hz, 6 H, C(13)H_3+C(14)H_3), 1.63 (q, *J*=7.0 Hz, 2 H, C(11)H_2), 1.70 - 1.84 (m, 1 H, C(12)*H*), 3.30 (td, *J*=7.5, 5.0 Hz, 2 H, C(10)H_2), 6.77 (d, *J*=9.0 Hz, 1 H, C(3)*H*), 7.49 (dd, *J*=9.0, 2.5 Hz, 1 H, C(2)*H*), 8.00 (br. s., 1 H, N*H*), 8.31 (d, *J*=2.5 Hz, 1 H, C(6)*H*); ^{13}C NMR (101 MHz, $CDCl_3$) δ ppm 22.4 (s, 2 C, *C*(13)+*C*(14)), 25.9 (s, 1 C, *C*(12)), 37.7 (s, 1 C, *C*(11)), 41.4 (s, 1 C, *C*(10)), 106.1 (s, 1 C, *C*(1)), 115.5 (s, 1 C, *C*(3)), 128.9 (s, 1 C, *C*(6)), 132.0 (s, 1 C, *C*(5)), 138.9 (s, 1 C, *C*(2)), 144.5 (s, 1 C, *C*(4)); LRMS *m/z*

(ESI$^+$) 309, 311 [(M+Na)$^+$], 287, 289 [MH$^+$], 285, (ESI$^-$) 287 [(M-H)$^-$]; HRMS (ESI$^+$) found 309.0202, calculated for $C_{11}H_{15}N_2NaO_2^+$ 309.0209; HPLC (System D) t_r 20.2 min (96%).

4-(3,5-Dimethyl-1,2-oxazol-4-yl)-*N*-(4-methoxybenzyl)-2-nitroaniline (287)

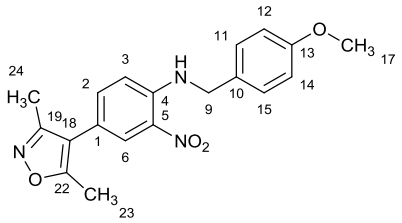

Pd(dppf)Cl_2 (22 mg, 0.030 mmol) was added to a solution of compound **284** (500 mg, 1.5 mmol) and 3,5-dimethylisoxazole-4-boronic acid pinacol ester (500 mg, 1.5 mmol) in 1,4-dioxane (5 mL). The mixture was stirred then 1.0 M aq. $NaHCO_3$ solution (4.4 mL, 4.4 mmol) was added. The mixture was heated under reflux for 3 h then more catalyst (22 mg, 0.030 mmol) was added. The mixture was reflux for a further 18 h then more catalyst (22 mg, 0.030 mmol) and boronic ester (200 mg, 0.90 mmol) were added. The reaction was heated under reflux for 5 h then allowed to cool. The mixture was partitioned between EtOAc (15 mL) and water (15 mL). The phases were separated then the organic phase was washed with water (15 mL) and brine (15 mL) then dried over $MgSO_4$ and evaporated. The crude material was purified by flash column chromatography on a silica column (25 g). The column was eluted with a gradient of EtOAc:40-60 petroleum spirit, which was increased linearly from 5:95 to 20:80 over 10 CVs then 20:80 to 30:70 over 5 CVs. Unreacted starting aryl bromide was recovered as an orange solid (327 mg, 65%) and the product was obtained as an orange residue (98 mg, 19%); R_f 0.15 (EtOAc:*n*-hexane, 20:80); ν_{max} (neat) 3376 (N-H), 2916 (C-H), 2841 (C-H), 1514 (N-O), 1351 (N-O); ^{1}H NMR (400 MHz, $CDCl_3$) δ ppm 2.26 (s, 3 H, C(24)H_3), 2.40 (s, 3 H, C(23)H_3), 3.82 (s, 3 H, OCH_3), 4.52 (d, *J*=5.6 Hz, 2 H, CH_2), 6.87 - 6.97 (m, 3 H, C(3)*H*+C(12)*H*+C(14)*H*), 7.30 (m, 3 H, C(2)*H*+C(11)*H*+C(15)*H*), 8.10 (d, *J*=2.0 Hz, 1 H, C(6)*H*), 8.42 (t, *J*=5.2 Hz, 1 H, N*H*); ^{13}C NMR (101 MHz, $CDCl_3$) δ ppm 10.7 (s, 1 C, *C*(24)), 11.5 (s, 1 C, *C*(23)), 46.7 (s, 1 C, *C*H_2) 55.3 (s, 1 C, O*C*H_3) 114.4 (s, 2 C,

C(12)+*C*(14)), 114.8 (s, 1 C, *C*(18)), 114.8 (s, 1 C, *C*(3)), 117.8 (s, 1 C, *C*(1)), 126.9 (s, 1 C, *C*(6)), 128.4 (s, 2 C, *C*(11) +*C*(15)), 128.9 (s, 1 C, *C*(10)), 132.1 (s, 1 C, *C*(5)), 136.7 (s, 1 C, *C*(2)), 144.4 (s, 1 C, *C*(4)), 158.5 (s, 1 C, *C*(19)), 159.2 (s, 1 C, *C*(13)), 165.3 (s, 1 C, *C*(22)); LRMS *m/z* (ESI$^+$) 729 [(M+Na)$^+$] 354 [MH$^+$], (ESI$^-$) 352 [(M-H)$^-$]; HRMS (ESI$^+$) found 376.1267, calculated for $C_{19}H_{19}N_3NaO_4^+$ 376.1268; HPLC (System D) t_r 17.3 min (97%).

4-(3,5-Dimethyl-1,2-oxazol-4-yl)-2-nitro-*N*-(pyridin-3-ylmethyl)aniline (288)

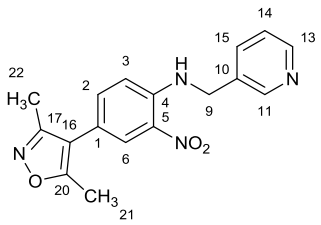

$Pd(dppf)Cl_2$ (42 mg, 0.057 mmol) was added to a solution of compound **285** (177 mg, 0.57 mmol) and 3,5-dimethylisoxazole-4-boronic acid pinacol ester (191 mg, 0.89 mmol) in DME (2 mL). The mixture was stirred then 1.0 M aq. $NaHCO_3$ solution (1.7 mL, 1.7 mmol) was added. The mixture was degassed by evacuating and refilling with nitrogen (×3) then heated under reflux for 2 h. The reaction was allowed to cool then partitioned between EtOAc (10 mL) and water (10 mL). The phases were separated then the organic phase was washed with water (10 mL) and brine (10 mL) then dried over $MgSO_4$. The crude material was purified by flash column chromatography on a silica column (10 g). The column was eluted with a gradient of EtOAc. The desired fractions were combined and evaporated to yield the product as a yellow solid (148 mg, 80%); R_f 0.25 (EtOAc); mp 170-174 °C ; ν_{max} (neat) 3341 (N-H), 2929 (C-H), 1553 (N-O), 1348 (N-O); ^{1}H NMR (400 MHz, $CDCl_3$) δ ppm 2.26 (s, 3 H, C(22)*H*$_3$), 2.40 (s, 3 H, C(21)*H*$_3$), 4.64 (d, *J*=5.5 Hz, 2 H, C*H*$_2$), 6.88 (d, *J*=8.5 Hz, 1 H, C(3)*H*), 7.29 - 7.37 (m, 2 H, C(2)*H*+C(14)*H*), 7.68 - 7.76 (m, 1 H, C(13)*H*), 8.12 (d, *J*=2.0 Hz, 1 H, C(6)*H*), 8.48 (t, *J*=5.5 Hz, 1 H, N*H*), 8.60 (dd, *J*=5.0, 1.5 Hz, 1 H, C(13)*H*), 8.67 (d, *J*=2.5 Hz, 1 H, C(15)*H*); ^{13}C NMR (101 MHz, $CDCl_3$) δ ppm 10.7 (s, 1 C, *C*(22)), 11.6 (s, 1 C, *C*(21)), 44.7 (s, 1 C, *C*H$_2$) 114.6 (s, 1 C, *C*(3)), 114.7 (s, 1 C, *C*(16)), 118.6 (s, 1 C, *C*(1)), 123.9 (s, 1 C, *C*(14)),

127.0 (s, 1 C, *C*(6)), 132.5 (s, 1 C, *C*(5/10)), 132.7 (s, 1 C, *C*(5/10)), 134.7 (s, 1 C, *C*(15)), 136.9 (s, 1 C, *C*(2)), 143.9 (s, 1 C, *C*(4)), 148.8 (s, 1 C, *C*(13)), 149.4 (s, 1 C, *C*(11)), 158.5 (s, 1 C, *C*(17)), 165.5 (s, 1 C, *C*(20)); LRMS *m/z* (ESI^+) 671 [$(2M+Na)^+$], 649 [$(2M+H)^+$], 347 [$(M+Na)^+$], 325 [MH^+], (ESI^-) 323 [$(M-H)^-$]; HRMS (ESI^+) found 325.1296, calculated for $C_{17}H_{17}N_4O_3^+$ 325.1295; HPLC (System D) t_r 10.5 min (98%).

4-(3,5-Dimethyl-1,2-oxazol-4-yl)-*N*-(3-methylbutyl)-2-nitroaniline (289)

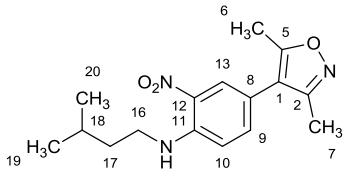

$Pd(dppf)Cl_2$ (127 mg, 0.17 mmol) was added to a solution of compound **286** (500 mg, 1.74 mmol) and 3,5-dimethylisoxazole-4-boronic acid pinacol ester (873 mg, 3.92 mmol) in DME (6 mL). The mixture was stirred then 1.0 M aq. $NaHCO_3$ solution (5.2 mL, 5.2 mmol) was added. The mixture was degassed by evacuating and refilling with nitrogen (×3) then heated under reflux for 2 h. The reaction was allowed to cool then partitioned between EtOAc (10 mL) and water (10 mL). The phases were separated then the organic phase was washed with water (10 mL) and brine (10 mL) then dried over $MgSO_4$. The crude material was pre-adsorbed onto silica then purified by flash column chromatography on silica. The column was eluted with a gradient of EtOAc:*n*-hexane (15:85). The desired fractions were combined and evaporated to yield the product as a dark orange solid (445 mg, 84%); R_f 0.35 (EtOAc:*n*-hexane, 20:80); mp 70-73 °C; ν_{max} (neat) 3377 (N-H), 2973 (C-H), 2954 (C-H), 2923 (C-H), 2871 (C-H), 1525 (N-O), 1356 (N-O); ^{1}H NMR (400 MHz, $CDCl_3$) δ ppm 1.01 (d, *J*=6.6 Hz, 6 H, C(19,20)H_3), 1.67 (q, *J*=6.9 Hz, 2 H, C(17)H_2), 1.72 - 1.86 (m, 1 H, C(18)*H*), 2.27 (s, 3 H, C(7)H_3), 2.41 (s, 3 H, C(6)H_3), 3.37 (m, 2 H, C(16)H_2), 6.95 (d, *J*=8.8 Hz, 1 H, C(10)*H*), 7.34 (dd, *J*=8.8, 2.0 Hz, 1 H, C(9)*H*), 7.97 - 8.16 (m, 2 H, C(13)*H*,N*H*); ^{13}C NMR (101 MHz, $CDCl_3$) δ ppm 10.7 (s, 1 C, *C*(7)), 11.6 (s, 1 C, *C*(6)), 22.4 (s, 2 C, *C*(19)+*C*(20)), 26.0 (s, 1 C, *C*(18)), 37.8 (s, 1 C, *C*(17)), 41.3 (s, 1 C, *C*(16)), 114.4 (s, 1 C, *C*(10)), 114.9 (s, 1 C, *C*(1)), 117.2 (s, 1 C,

C(8)), 127.0 (s, 1 C, *C*(13)), 131.6 (s, 1 C, *C*(12)), 136.8 (s, 1 C, *C*(9)), 144.8 (s, 1 C, *C*(11)), 158.6 (s, 1 C, *C*(2)), 165.3 (s, 1 C, *C*(5)); LRMS *m/z* (ESI^+) 629 [$(2M+Na)^+$], 304 [MH^+], (ESI^-) 302 [$(M-H)^-$]; HRMS (ESI^+) found 359.1474, calculated for $C_{16}H_{21}N_3NaO_3^+$ 326.1475; HPLC (System D) t_r 18.9 min (99%).

5-(3,5-Dimethyl-1,2-oxazol-4-yl)-1-(4-methoxybenzyl)-2-(2-phenylethyl)-1*H*-benzimidazole (290)

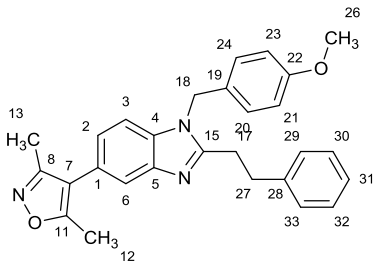

1.0 M aq. $Na_2S_2O_4$ (0.51 mL, 0.51 mmol) was added to a solution of compound **287** (60 mg, 0.17 mmol) and 2-phenylpropanal (24 mg, 0.18 mmol) in EtOH:DMSO (1:1, 1 mL). The mixture was heated at 80 °C for 16 h. The mixture was allowed to cool then 1% aq. ammonia solution (5 mL) was added. The mixture was extracted with EtOAc (5 mL) then the organic phase was washed with water (5 mL) and brine (5 mL) then dried over $MgSO_4$. The solvent was evaporated then the crude material was purified by flash column chromatography on a silica column (10 g). The column was eluted with a gradient of EtOAc:40-60 petroleum spirit, which was increased linearly from 50:50 to 100:0 over 10 CVs. The desired fractions were combined and evaporated to yield the product as a cream solid (56 mg, 75%); R_f 0.15 (EtOAc:*n*-hexane, 60:40); mp 112-117 °C; ν_{max} (neat) 3028 (C-H), 2935 (C-H), 2835 (C-H); ^{1}H NMR (400 MHz, $CDCl_3$) δ ppm 2.31 (s, 3 H, C(13)H_3), 2.43 (s, 3 H, C(12)H_3), 3.09 - 3.29 (m, 4 H, C(27)H_2+C(28)H_2), 3.78 (s, 3 H, OCH_3), 5.17 (s, 2 H, C(18)H_2), 6.84 (d, *J*=8.6 Hz, 2 H, C(21)*H*+C(23)H_2), 6.98 (d, *J*=8.6 Hz, 2 H, C(20)*H*+C(24)H_2), 7.09 (dd, *J*=8.2, 1.5 Hz, 1 H, C(2)*H*), 7.17 - 7.35 (m, 6 H, *Ph* C(3)*H*), 7.67 (d, *J*=1.5 Hz, 1 H, C(6)*H*); ^{13}C NMR (101 MHz, $CDCl_3$) δ ppm 10.9 (s, 1 C, *C*(13)), 11.6 (s, 1 C, *C*(12)), 29.7 (s, 1 C, *C*(17)), 33.9 (s, 1 C, *C*(27)), 46.5 (s, 1 C, *C*(18)), 55.3 (s, 1 C, O*C*H_3) 109.8 (s, 1 C, *C*(2)), 114.4 (s, 2 C, *C*(21)+*C*(23)), 117.1

(s, 1 C, *C*(7)), 119.9 (s, 1 C, *C*(6)), 123.6 (s, 1 C, *C*(2)), 124.2 (s, 1 C, *C*(1)), 126.4 (s, 1 C, *C*(31)), 127.5 (s, 2 C, *C*(20)+*C*(24)), 127.6 (s, 1 C, *C*(19)), 128.4 (s, 2 C, *Ph*) 128.6 (s, 2 C, *Ph*) 134.7 (s, 1 C, *C*(4)), 140.7 (s, 1 C, *C*(28)), 143.0 (s, 1 C, *C*(5)), 155.4 (s, 1 C, *C*(15)), 159.0 (s, 1 C, *C*(8/22)), 159.3 (s, 1 C, *C*(8/22) 165.0 (s, 1 C, *C*(11)); LRMS *m/z* (ESI^+) 438 [MH^+]; HRMS (ESI^+) found 438.2172, calculated for $C_{28}H_{28}N_3O_2^+$ 438.2176; HPLC (System D) t_r 12.6 min (97%).

5-(3,5-Dimethyl-1,2-oxazol-4-yl)-2-(2-phenylethyl)-1-(pyridin-3-ylmethyl)-1*H*-benzimidazole (291)

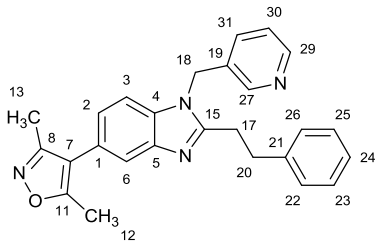

A freshly prepared aq. solution of $Na_2S_2O_4$ (1.0 M, 1.0 mL, 1.0 mmol) was added to a solution of compound **288** (114 mg, 0.35 mmol) and 2-phenylpropanal (50 mg, 0.37 mmol) in EtOH:DMSO (1:1, 2 mL). The mixture was heated at 80 °C for 18 h. More 2-phenylpropanal (24 mg, 0.18 mmol) and 1 M $Na_2S_2O_4$ (0.18 mL, 0.18 mmol) were added then the mixture was heated at 80 °C for a further 4 h. The mixture was allowed to cool then 10% aq. ammonia solution (5 mL) was added. The mixture was extracted with CH_2Cl_2 (5 mL) then the organic phase was washed with water (5 mL) and brine (5 mL) then dried over $MgSO_4$. The solvent was evaporated then the crude material was purified by flash column chromatography on a silica column (10 g). Eluted with CH_2Cl_2:MeOH:NH_4OH, which was increased linearly from 98:2:0.2 to 94:6:0.6 over 10 CVs. The desired fractions were combined and evaporated to yield the product as an amorphous solid (36 mg, 25%); R_f 0.30 (CH_2Cl_2:MeOH:NH_4OH, 95:5:0.5); ν_{max} (neat) 3505 (C-H), 2931 (C-H); ^1H NMR (400 MHz, $CDCl_3$) δ ppm 2.30 (s, 3 H, C(13)H_3), 2.43 (s, 3 H, C(12)H_3), 3.11 - 3.19 (m, 2 H, C(17)H_2), 3.20 - 3.30 (m, 2 H, C(20)H_2), 5.21 (s, 2 H, C(18)H_2), 7.10 (dd, *J*=8.5, 1.5 Hz, 1 H, C(2)*H*), 7.16 - 7.32

(m, 8 H, 5×Ph*H*+C(3)*H*+C(30)*H*+C(31)*H*), 7.68 (d, *J*=1.0 Hz, 1 H, C(6)*H*), 8.46 (s, 1 H, C(27)*H*), 8.56 (t, *J*=3.0 Hz, 1 H, C(29)*H*); ^{13}C NMR (101 MHz, $CDCl_3$) δ ppm 10.85 (s, 1 C, *C*(13)), 11.5 (s, 1 C, *C*(12)), 29.8 (s, 1 C, *C*(17)), 33.9 (s, 1 C, *C*(20)), 44.5 (s, 1 *C*(18)), 109.5 (s, 1 C, *C*(3)), 116.9 (s, 1 C, *C*(7)), 120.1 (s, 1 C, *C*(6)), 123.9 (s, 1 C, *C*(2/30)), 123.9 (s, 1 C, *C*(2/30)), 124.7 (s, 1 C, *C*(1)), 126.6 (s, 1 C, *C*(24)), 128.3 (s, 2 C, *C*(22/23)+*C*(25/26)), 128.7 (s, 2 C, *C*(22/23)+*C*(25/26)), 131.4 (s, 1 C, *C*(19)), 133.8 (s, 1 C, *C*(26)), 134.4 (s, 1 C, *C*(4)), 140.4 (s, 1 C, *C*(21)), 143.1 (s, 1 C, *C*(5)), 147.9 (s, 1 C, *C*(27)), 149.6 (s, 1 C, *C*(29)), 155.1 (s, 1 C, *C*(15)), 158.9 (s, 1, *C*(8)), 165.1 (s, 1 C, *C*(11)); LRMS *m/z* (ESI$^+$) 839 [(2M+Na)$^+$], 431 (M+Na)$^+$], 409 [MH$^+$]; HRMS found 409.2022, calculated for $C_{26}H_{25}N_4O^+$ 409.2023; HPLC (System D) t_r 9.8 min (97%).

5-(3,5-Dimethyl-1,2-oxazol-4-yl)-1-(3-methylbutyl)-2-(2-phenylethyl)-1H-benzimidazole (292)

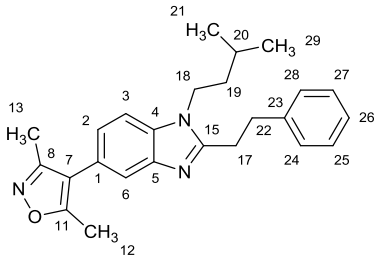

A freshly prepared aq. solution of $Na_2S_2O_4$ (1.0 M, 0.60 mL, 0.60 mmol) was added to a solution of compound **289** (61 mg, 0.20 mmol) and 2-phenylpropanal (29 mg, 0.21 mmol) in EtOH:DMSO (1:1, 1 mL). The mixture was heated at 80 °C for 16 h. The mixture was allowed to cool then 10% aq. ammonia solution (5 mL) was added. The mixture was extracted with CH_2Cl_2 (5 mL) then the organic phase was washed with water (5 mL) and brine (5 mL) then dried over $MgSO_4$. The solvent was evaporated then the crude material was purified by flash column chromatography on a silica column (10 g). The column was eluted with a gradient of EtOAc:*n*-hexane, which was increased linearly from 50:50 to 70:30 over 10 CVs. The desired fractions were combined and evaporated to yield the product as a colourless oil (48 mg, 62%); R_f 0.45 (EtOAc:*c*-hexane, 40:60); ^{1}H NMR (400 MHz, $CDCl_3$) δ ppm 1.00 (d, *J*=6.5 Hz, 6

H, C(21)H_3+C(29)H_3), 1.53 - 1.74 (m, 3 H, C(19)H_2+C(20)*H*), 2.31 (s, 3 H, C(13)H_3), 2.43 (s, 3 H, C(12)H_3), 3.13 - 3.20 (m, 2 H, C(17)H_2), 3.26 - 3.33 (m, 2 H, C(23)H_2), 3.93 - 4.05 (m, 2 H, C(18)H_2), 7.12 (dd, *J*=8.5, 1.5 Hz, 1 H, C(2)*H*), 7.20 - 7.36 (m, 6 H, C(3)*H*+5×Ph*H*), 7.64 (d, *J*=1.5 Hz, 1 H, C(6)*H*); ^{13}C NMR (101 MHz, $CDCl_3$) δ ppm 10.9 (s, 1C, *C*(13)H_3) 11.5 (s, 1 C, *C*(12)H_3) 22.4 (s, 2 C, *C*(21)+*C*(29)), 26.1 (s, 1 C, *C*(20)), 29.7 (s, 1 C, *C*(17)), 34.0 (s, 1 C, *C*(23)), 38.6 (s, 1 C, *C*(19)), 42.1 (s, 1 C, *C*(18)), 109.5 (s, 1 C, *C*(3)), 117.2 (s, 1 C, *C*(7)), 119.83 (s, 1 C, *C*(6)), 123.3 (s, 1 C, *C*(2)), 124.0 (s, 1 C, *C*(1)), 126.5 (s, 1 C, *C*(26)), 128.4 (s, 2 C, *C*(24/25)+*C*(28/27)), 128.7 (s, 2 C, *C*(24/25)+*C*(27/28)), 134.3 (s, 1 C, *C*(4)), 140.8 (s, 1 C, *C*(23)), 143.0 (s, 1 C, *C*(5)), 154.9 (s, 1 C, *C*(15)), 159.0 (s, 1 C, *C*(8)), 165.0 (s, 1 C, *C*(11)); LRMS *m/z* 797 [$(2M+Na)^+$], 775 [$(2M+H)^+$], 388 [MH^+], 386 [$(M-H)^-$]; HRMS (ESI^+) found 388.2376, calculated for $C_{25}H_{30}N_3O^+$ 388.2383; HPLC (System D) t_r 12.9 min (99%).

5-(3,5-Dimethyl-1,2-oxazol-4-yl)-1-(2-methoxyethyl)-2-(2-phenylethyl)-1*H*-benzimidazole (293)

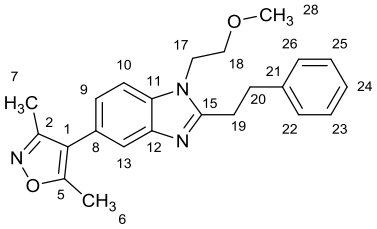

A solution of compound **251** (47 mg, 0.20 mmol) and 2-methoxymethylamine (17 µL, 0.20 mmol) in DMSO (0.2 mL) was heated at 80 °C for 1 hour. The solution was removed from the heat then a solution of 3-phenylpropanal (26 µL, 0.20 mmol) in ethanol (0.8 mL) was added, followed by $Na_2S_2O_4$ (104 mg, 0.60 mmol). The mixture was heated at 80 °C for 4 h then allowed to cool. The reaction mixture was partitioned between EtOAc (5 mL) and 10% aq. ammonia solution (5 mL). The phases were separated then the organic phase was washed with water (5 mL) and brine (5 mL) then dried over $MgSO_4$ and evaporated. The crude material was purified by flash column chromatography on a silica column (10 g). The column was eluted with a gradient of EtOAc:petroleum ether, which was increased linearly

from 60:40 to 80:20 over 10 CVs. The desired fractions were combined and evaporated to yield the product as a colourless gum (26 mg, 35%). R_f 0.35 (EtOAc:*n*-hexane, 80:20); ν_{max} (neat) 3026 (C-H), 2930 (C-H), 2893(C-H); ^{1}H NMR (400 MHz, $CDCl_3$) δ ppm 2.30 (s, 3 H, C(7)H_3), 2.43 (s, 3 H, C(6)H_3), 3.18 - 3.33 (m, 7 H, C(19)H_2+C(20)H_2+OCH_3), 3.63 (t, *J*=5.5 Hz, 2 H, C(18)H_2), 4.21 (t, *J*=5.5 Hz, 2 H, C(17)H_2), 7.12 (dd, *J*=8.5, 1.5 Hz, 1 H, C(9)*H*), 7.19 - 7.34 (m, 5 H, 5×Ph*H*), 7.37 (d, *J*=8.5 Hz, 1 H, C(10)*H*), 7.64 (d, *J*=1.5 Hz, 1 H, C(13)*H*); ^{13}C NMR (101 MHz, $CDCl_3$) δ ppm 10.8 (s, 1 C, *C*(7)), 11.5 (s, 1 C, *C*(6)), 29.5 (s, 1 C, *C*(19)), 33.9 (s, 1 C, *C*(20)), 43.7 (s, 1 C, *C*(17)), 59.1 (s, 1 C, O*C*H$_3$) 70.7 (s, 1 C, *C*(18)), 109.5 (s, 1 C, *C*(10)), 117.1 (s, 1 C, *C*(1)), 119.8 (s, 1 C, *C*(13)), 123.3 (s, 1 C, *C*(9)), 124.1 (s, 1 C, *C*(8)), 126.3 (s, 1 C, *C*(24)), 128.4 (s, 2 C, *C*(22/23)+*C*(26/25)), 128.6 (s, 2 C, *C*(22/23)+*C*(26/25)), 134.4 (s, 1 C, *C*(11)), 141.0 (s, 1 C, *C*(21)), 143.0 (s, 1 C, *C*(12)), 155.9 (s, 1 C, *C*(15)), 159.0 (s, 1 C, *C*(2)), 165.0 (s, 1 C, *C*(5)); LRMS *m/z* (ESI$^+$) 773 [(2M+Na)$^+$], 751 [(2M+H)$^+$], 398 [(M+Na)$^+$], 376 [MH$^+$]; HRMS (ESI$^+$) found 376.2017, calculated for $C_{23}H_{26}N_3O_2^+$ 376.2020; HPLC (System D) t_r 11.9 min (98%).

2-[5-(3,5-Dimethyl-1,2-oxazol-4-yl)-2-(2-phenylethyl)-1*H*-benzimidazol-1-yl]ethanol (294)

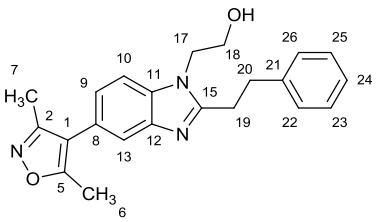

A solution of compound **251** (472 mg, 2.0 mmol) and ethanolamine (120 µL, 2.0 mmol) in DMSO (2 mL) was heated at 80 °C for 2 h. The solution was removed from the heat then a solution of 3-phenylpropanal (260 µL, 2.0 mmol) in ethanol (8 mL) was added, followed by a 1 M aq. solution of $Na_2S_2O_4$ (6 mL, 6 mmol). The mixture was heated at 80 °C for 3 h then allowed to cool. The reaction mixture was partitioned between EtOAc (15 mL) and 10% aq. ammonia solution (15 mL). The phases were separated then the organic phase was washed

with water (15 mL) then evaporated. Et_2O (10 mL) was added then the supernatant was decanted off with a pipette. This process was repeated with more Et_2O (2×10 mL) then the solid was dried under vacuum to yield the product as a white solid (465 mg, 64%); R_f 0.25 (EtOAc) mp 199-204 °C; ν_{max} (neat) 3189 (O-H), 2930 (C-H), 2869 (C-H); ^{1}H NMR (400 MHz, $CDCl_3$) δ ppm 2.23 (s, 3 H, C(7)H_3), 2.38 (s, 3 H, C(6)H_3), 2.98 - 3.08 (m, 2 H, C(19)H_2), 3.10 - 3.18 (m, 2 H, C(20)H_2), 3.26 (br. s., 1 H, O*H*), 3.95 (t, *J*=5.0 Hz, 2 H, C(18)H_2), 4.15 (t, *J*=5.0 Hz, 2 H, C(17)H_2), 7.10 (dd, *J*=8.5, 1.0 Hz, 1 H, C(9)*H*), 7.13 - 7.30 (m, 5 H, 5×Ph*H*), 7.38 (d, *J*=8.5 Hz, 1 H, C(10)*H*), 7.58 (d, *J*=1.0 Hz, 1 H, C(13)*H*); ^{13}C NMR (101 MHz, $CDCl_3$) δ ppm 10.8 (s, 1 C, *C*(7)), 11.5 (s, 1 C, *C*(6)), 29.5 (s, 1 C, *C*(19)), 33.9 (s, 1 C, *C*(20)), 45.9 (s, 1 C, *C*(17)), 60.8 (s, 1 C, *C*(18)), 109.8 (s, 1 C, *C*(10)), 117.0 (s, 1 C, *C*(1)), 120.0 (s, 1 C, *C*(13)), 123.5 (s, 1 C, *C*(9)), 124.2 (s, 1 C, *C*(8)), 126.4 (s, 1 C, *C*(24)), 128.3 (s, 2 C, *C*(22/23)+C(26/25)), 128.6 (s, 2 C, *C*(22/23)+C(26/25)), 134.5 (s, 1 C, *C*(11)), 140.7 (s, 1 C, *C*(21) 142.8 (s, 1 C, *C*(12)), 155.8 (s, 1 C, *C*(15)), 158.9 (s, 1 C, *C*(2)), 165.0 (s, 1 C, *C*(5)); LRMS *m/z* (ESI$^+$) 745 [(2M+Na)$^+$], 723 [(2M+H)$^+$], 362 [(M+Na)$^+$], (ESI$^-$) 360 [(M-H)$^-$]; HRMS (ESI$^+$) found 362.1854, calculated for $C_{22}H_{24}N_3O_2^+$ 362.1863; HPLC (System D) t_r 10.9 min (98%).

_N_-{2-[5-(3,5-dimethyl-1,2-oxazol-4-yl)-2-(2-phenylethyl)-1*H*-benzimidazol-1-yl]ethyl}acetamide (295)

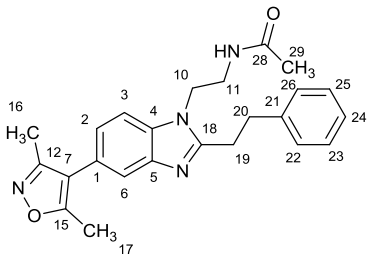

A solution of compound **251** (47 mg, 0.20 mmol) and *N*-(2-aminoethyl)acetamide (20 mg, 0.20 mmol) in DMSO (0.2 mL) was heated at 80 °C for 1 hour. The solution was removed from the heat then a solution of 3-phenylpropanal (26 µL, 0.20 mmol) in ethanol (0.8 mL) was added, followed by 1 M aq. $Na_2S_2O_4$ (0.60 mL, 0.60 mmol). The mixture was heated at 80 °C for 16 h then allowed to cool. The mixture was partitioned between EtOAc (5 mL) and

10% aq. NH_3 (5 mL). The organic phase was passed through a hydrophobic frit then evaporated. The crude material was purified by flash column chromatography on silica (10 g). The column was eluted with a gradient of CH_2Cl_2:MeOH:NH_4OH, which was increased linearly from 95:5:0.5 to 90:10:1 over 10 CVs. The desired fractions were combined and evaporated to yield the product as a pale-yellow foam (35 mg, 43%); R_f 0.30 (CH_2Cl_2:MeOH:NH_4OH, 90:10:1); ν_{max} (neat) 3252 (N-H), 2927 (C-H), 2854 (C-H), 1668 (C=O); ^{1}H NMR (400 MHz, $CDCl_3$) δ ppm 1.90 (s, 3 H, C(29)H_3), 2.25 (s, 3 H, C(16)H_3), 2.41 (s, 3 H, C(17)H_3), 3.07 - 3.17 (m, 2 H, C(19)H_2), 3.20 - 3.30 (m, 2 H, C(20)H_2), 3.46 (q, *J*=6.0 Hz, 2 H, C(11)H_2), 4.19 (t, *J*=6.0 Hz, 2 H, C(10)H_2), 5.79 (t, *J*=6.0 Hz, 1 H, N*H*), 7.12 (dd, *J*=8.5, 1.5 Hz, 1 H, C(2)*H*), 7.18 - 7.25 (m, 3 H, 3×Ph*H*), 7.25 - 7.33 (m, 2 H, 2×Ph*H*), 7.39 (d, *J*=8.5 Hz, 1 H, C(3)*H*), 7.62 (d, *J*=1.5 Hz, 1 H, C(6)*H*); ^{13}C NMR (101 MHz, $CDCl_3$) δ ppm 10.8 (s, 1 C, *C*(16)), 11.5 (s, 1 C, *C*(17)), 23.0 (s, 1 C, *C*(29)), 29.4 (s, 1 C, *C*(19)), 34.0 (s, 1 C, *C*(20)), 39.3 (s, 1 C, *C*(11)), 42.3 (s, 1 C, *C*(10)), 109.5 (s, 1 C, *C*(3)), 117.0 (s, 1 C, *C*(7)), 119.8 (s, 1 C, *C*(6)), 123.6 (s, 1 C, *C*(2)), 124.3 (s, 1 C, *C*(1)), 126.5 (s, 1 C, *C*(24)), 128.4 (s, 2 C, *C*(22/23)+*C*(26/25)), 128.6 (s, 2 C, *C*(22/23)+*C*(26/25)), 134.4 (s, 1 C, *C*(4)), 140.6 (s, 1 C, *C*(21)), 142.9 (s, 1 C, *C*(5)), 155.2 (s, 1 C, *C*(18)), 158.9 (s, 1 C, *C*(12)), 165.0 (s, 1 C, *C*(15)), 170.8 (s, 1 C, *C*(28)); LRMS *m/z* (ESI$^+$) 827 [(2M+Na)$^+$], 805 [(2M+H)$^+$], 425 [(M+Na)$^+$], 403, [MH$^+$], (ESI$^-$) 401 [(M-H)$^-$]; HRMS (ESI$^+$) found 403.2127, calculated for $C_{24}H_{27}N_4O_2^+$ 403.2129; HPLC (System D) t_r 11.5 min (>99%).

Methyl [5-(3,5-dimethyl-1,2-oxazol-4-yl)-2-(2-phenylethyl)-1*H*-benzimidazol-1-yl]acetate (296)

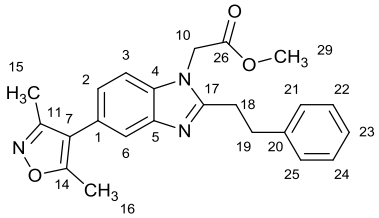

A solution of compound **251** (236 mg, 1.00 mmol), glycine methyl ester hydrochloride (126 mg, 1.00 mmol) and triethylamine (152 μL, 1.10 mmol) in DMSO (1 mL) was heated at 80 °C for 1 hour. The solution was removed from the heat then a solution of 3-phenylpropanal (132 μL, 1.00 mmol) in MeOH (4 mL) was added, followed by 1 M aq. $Na_2S_2O_4$ (3 mL, 3 mmol). The mixture was heated at 80 °C for 16 h then allowed to cool. The mixture was partitioned between EtOAc (5 mL) and 10% aq. NH_3 (5 mL). The organic phase was passed through a hydrophobic frit then evaporated. The crude material was purified by flash column chromatography on silica (10 g). The column was eluted with a gradient of EtOAc:*c*-hexane, which was increased linearly from 60:40 to 100:0 over 10 CVs. The desired fractions were combined and evaporated to yield the product as a cream solid (85 mg, 22%); R_f 0.50 (EtOAc); mp 135-138 °C; ν_{max} (neat) 2924 (C-H), 2853 (C-H), 1753 (C=O); ^{1}H NMR (400 MHz, $CDCl_3$) δ ppm 2.30 (s, 3 H, C(15)H_3), 2.42 (s, 3 H, C(16)H_3), 3.10 - 3.17 (m, 2 H, C(18)H_2), 3.25 - 3.32 (m, 2 H, C(19)H_2), 3.78 (s, 3 H, C(29)H_3), 4.71 (s, 2 H, C(10)H_2), 7.14 (dd, *J*=8.5, 1.5 Hz, 1 H, C(2)*H*), 7.22 - 7.29 (m, 4 H, C(3)*H*+3×Ph*H*), 7.29 - 7.35 (m, 2 H, 2×Ph*H*), 7.66 (d, *J*=1.5 Hz, 1 H, C(6)*H*); ^{13}C NMR (101 MHz, $CDCl_3$) δ ppm 10.8 (s, 1 C, *C*(15)), 11.5 (s, 1 C, *C*(16)), 29.5 (s, 1 C, *C*(18)), 33.6 (s, 1 C, *C*(19)), 44.5 (s, 1 C, *C*(10)), 52.9 (s, 1 C, *C*(29)), 109.0 (s, 1 C, *C*(3)), 117.0 (s, 1 C, *C*(7)), 120.1 (s, 1 C, *C*(6)), 123.9 (s, 1 C, *C*(2)), 124.6 (s, 1 C, *C*(1)), 126.5 (s, 1 C, *C*(23)), 128.3 (s, 2 C, *C*(21/22)+*C*(25/24)), 128.7 (s, 2 C, *C*(21/22)+*C*(25/24)), 134.5 (s, 1 C, *C*(4)), 140.6 (s, 1 C, *C*(20)), 142.9 (s, 1 C, *C*(5)), 155.3 (s, 1 C, *C*(17)), 159.0 (s, 1 C, *C*(11)), 165.0 (s, 1 C, *C*(14)), 167.6 (s, 1 C, *C*(26)); LRMS *m/z* (ESI^+) 801 [$(2M+Na)^+$], 779 [$(2M+H)^+$], 412 [$(M+Na)^+$], 390, [MH^+], (ESI^-) 388 [$(M-H)^-$]; HRMS (ESI^+) found 390.1812, calculated for $C_{23}H_{24}N_3O_3^+$ 390.1812; HPLC (System D) t_r 11.4 min (97%).

Methyl 3-[5-(3,5-dimethyl-1,2-oxazol-4-yl)-2-(2-phenylethyl)-1*H*-benzimidazol-1-yl]propanoate (297)

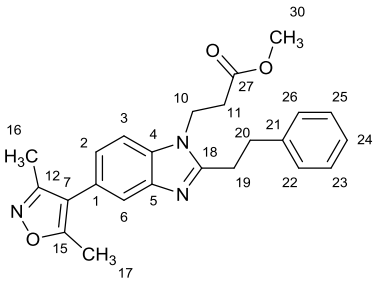

A solution of compound **251** (236 mg, 1.00 mmol), beta-alanine methyl ester hydrochloride (140 mg, 1.00 mmol) and triethylamine (152 µL, 1.10 mmol) in DMSO (1 mL) was heated at 80 °C for 1 hour. The solution was removed from the heat then a solution of 3-phenylpropanal (132 µL, 1.00 mmol) in MeOH (4 mL) was added, followed by 1 M aq. $Na_2S_2O_4$ (3 mL, 3 mmol). The mixture was heated at 80 °C for 16 h then allowed to cool. The mixture was partitioned between EtOAc (5 mL) and 10% aq. NH_3 (5 mL). The organic phase was passed through a hydrophobic frit then evaporated. The crude material was purified by flash column chromatography on silica (10 g). The column was eluted with a gradient of EtOAc:*c*-hexane, which was increased linearly from 60:40 to 100:0 over 10 CVs. The desired fractions were combined and evaporated to yield the product as a cream solid (259 mg, 64%); R_f 0.50 (EtOAc); mp 79-84 °C; ν_{max} (neat) 2927 (C-H), 2855 (C-H), 1730 (C=O); ^{1}H NMR (400 MHz, $CDCl_3$) δ ppm 2.30 (s, 3 H, C(16)H_3), 2.43 (s, 3 H, C(17)H_3), 2.72 (t, *J*=7.0 Hz, 2 H, C(11)H_2), 3.19 - 3.26 (m, 2 H, C(19)H_2), 3.26 - 3.32 (m, 2 H, C(20)H_2), 3.68 (s, 3 H, C(30)H_3), 4.34 (t, *J*=7.0 Hz, 2 H, C(10)H_2), 7.14 (dd, *J*=8.5, 1.5 Hz, 1 H, C(2)*H*), 7.22 - 7.29 (m, 3 H, 3×Ph*H*), 7.29 - 7.34 (m, 2 H, 2×Ph*H*), 7.37 (d, *J*=8.5 Hz, 1 H, C(3)*H*), 7.64 (d, *J*=1.5 Hz, 1 H, C(6)*H*); ^{13}C NMR (101 MHz, $CDCl_3$) δ ppm 10.8 (s, 1 C, *C*(16)), 11.5 (s, 1 C, *C*(17)), 29.5 (s, 1 C, *C*(19)), 33.8 (s, 1 C, *C*(11/20)), 34.0 (s, 1 C, *C*(11/20)), 39.0 (s, 1 C, *C*(10)), 52.1 (s, 1 C, *C*(30)), 109.4 (s, 1 C, *C*(3)), 117.0 (s, 1 C, *C*(7)), 120.0 (s, 1 C, *C*(6)), 123.6 (s, 1 C, *C*(2)), 124.4 (s, 1 C, *C*(1)), 126.5 (s, 1 C, *C*(24)C) 128.4 (s, 2 C, *C*(22/23)+*C*(26/25)), 128.7 (s, 2 C, *C*(22/23)+*C*(26/25)), 133.9 (s, 1 C, *C*(4)), 140.7 (s, 1 C, *C*(21)), 143.1 (s, 1 C, *C*(5)), 155.1 (s, 1

C, *C*(18)), 159.0 (s, 1 C, *C*(12)), 165.0 (s, 1 C, *C*(15)), 170.8 (s, 1 C, *C*(27)); LRMS *m/z* (ESI^+) 829 [$(2M+Na)^+$], 807 [$(2M+H)^+$], 426 [$(M+Na)^+$], 404 [MH^+]; HRMS (ESI^+) found 404.1970, calculated for $C_{24}H_{26}N_3O_3^+$ 404.1969; HPLC (System E) t_r 4.0 min (>99%).

Methyl 4-[5-(3,5-dimethyl-1,2-oxazol-4-yl)-2-(2-phenylethyl)-1*H*-benzimidazol-1-yl]butanoate (298)

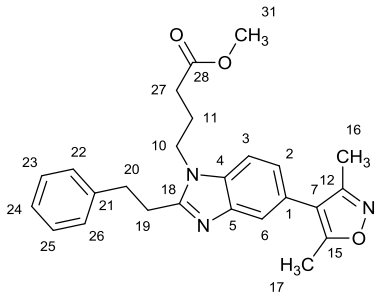

Triethylamine (152 µL, 1.10 mmol) was added to a stirred mixture of compound **251** (236 mg, 1.00 mmol) and methyl 4-aminobutanoate hydrochloride (154 mg, 1.00 mmol) in DMSO (1 mL). The mixture was heated at 80 °C for 1 hour then removed from the heat source. A solution of 3-phenylpropanal (132 µL, 1.00 mmol) in MeOH (4 mL) was added, followed by 1 M aq. $Na_2S_2O_4$ (3.0 mL, 3.0 mmol). The mixture was heated at 80 °C for a further 2 h then allowed to cool. The mixture was partitioned between EtOAc (5 mL) and 10% aq. NH_3 (5 mL) then dried over $MgSO_4$ and evaporated. The crude material was purified by flash column chromatography on a silica column (10 g). The column was eluted with a gradient of EtOAc:*c*-hexane, which was increased linearly from 50:50 to 100:0 over 10 CVs. The desired fractions were combined and evaporated to yield the product as a pale yellow solid (173 mg, 41%); R_f 0.25 (EtOAc:*c*-hexane, 60:40); ν_{max} (neat) 2953 (C-H), 2921 (C-H), 2857 (C-H), 2840 (C-H), 2798 (C-H); ^{1}H NMR (400 MHz, $CDCl_3$) δ ppm 2.04 (quin, *J*=7.0 Hz, 2 H, C(11)H_2), 2.30 (s, 3 H, C(16)H_3), 2.35 (t, *J*=7.0 Hz, 2 H, C(27)H_2), 2.43 (s, 3 H, C(17)H_3), 3.14 - 3.20 (m, 2 H, C(19)H_2), 3.26 - 3.33 (m, 2 H, C(20)H_2), 3.68 (s, 3 H, C(31)H_3), 4.10 (d, 2 H, *J*=7.0 Hz, C(10)H_2), 7.13 (dd, *J*=8.5, 1.5 Hz, 1 H, C(2)*H*), 7.20 - 7.34 (m, 5 H, 5×Ph*H*), 7.40 (d, *J*=8.5 Hz, 1 H, C(3)*H*), 7.64 (d, *J*=1.5 Hz, 1 H, C(6)*H*); ^{13}C NMR (101 MHz, $CDCl_3$) δ ppm 10.9 (s, 1 C,

C(16)), 11.5 (s, 1 C, *C*(17)), 24.7 (s, 1 C, *C*(26)), 29.5 (s, 1 C, *C*(19)), 30.4 (s, 1 C, *C*(27)), 33.9 (s, 1 C, *C*(20)), 42.5 (s, 1 C, *C*(10)), 51.8 (s, 1 C, *C*(31)), 109.6 (s, 1 C, *C*(3)), 117.1 (s, 1 C, *C*(7)), 119.9 (s, 1 C, *C*(6)), 123.5 (s, 1 C, *C*(2)), 124.2 (s, 1 C, *C*(1)), 126.4 (s, 1 C, *C*(24)), 128.4 (s, 2 C, *C*(22/23)+*C*(26/25)), 128.6 (s, 2 C, *C*(22/23)+*C*(26/25)), 134.3 (s, 1 C, *C*(4)), 140.8 (s, 1 C, *C*(21)), 143.0 (s, 1 C, *C*(5)), 155.0 (s, 1 C, *C*(18)), 159.0 (s, 1 C, *C*(12)), 165.0 (s, 1 C, *C*(15)), 172.8 (s, 1 C, *C*(28)); LRMS *m/z* (ESI$^+$) 857 [(2M+Na)$^+$], 835 [(2M+H)$^+$], 440 [(M+Na)$^+$], 418 [MH$^+$]; HRMS (ESI$^+$) found 418.2126, calculated for $C_{25}H_{28}N_3O_3^+$ 414.2125; HPLC (System E) t_r 4.2 min (>99%).

[5-(3,5-Dimethyl-1,2-oxazol-4-yl)-2-(2-phenylethyl)-1H-benzimidazol-1-yl]acetic acid (299)

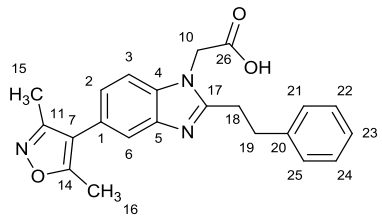

1.00 M aq. LiOH solution (0.80 mL, 0.80 mmol) was added to a stirred solution of compound **296** (64 mg, 0.16 mmol) in MeOH (4 mL). The resultant solution was heated at 50 °C for 3 h then allowed to cool. The solvent was evaporated then the residue was taken up in water (2 mL). Dilute aq. HCl was added until no more solid crashed out (pH~5) then the suspension was centrifuged. The supernatant was decanted off with a pipette. More water was added and the process was repeated. The resultant solid was dried under vacuum to yield the product as an off-white solid (37 mg, 62%); R_f 0.05 (streaky) (EtOAc:MeOH, 80:20); mp 268-274 °C (dec); ν_{max} 3373 (O-H), 2927 (C-H), 1725 (C=O); ^{1}H NMR (400 MHz, DMSO-d_6) δ ppm 2.23 (s, 3 H, C(15)H_3), 2.40 (s, 3 H, C(16)H_3), 3.05 - 3.19 (m, 4 H, C(18)H_2+C(19)H_2), 5.10 (s, 2 H, C(10)H_2), 7.14 - 7.25 (m, 2 H, C(2)*H*+C(23)*H*), 7.26 - 7.35 (m, 4 H, 4×Ph*H*), 7.54 - 7.60 (m, 2 H, C(3)*H*+C(6)*H*) 13.38 (br. s., 1 H, O*H*); ^{13}C NMR (101 MHz, DMSO-d_6) δ ppm 10.5 (s, 1 C, *C*(15)), 11.3 (s, 1 C, *C*(14)), 28.2 (s, 1 C, *C*(18)), 32.4 (s, 1 C, *C*(19)), 44.4 (s, 1 C, *C*(10)), 110.2

(s, 1 C, *C*(3)), 116.7 (s, 1 C, *C*(7)), 118.9 (s, 1 C, *C*(6)), 122.9 (s, 1 C, *C*(1/2)), 123.0 (s, 1 C, *C*(1/2)), 126.1 (s, 1 C, *C*(23)), 128.3 (s, 2 C, *C*(21/22)+*C*(25/24)), 128.4 (s, 2 C, *C*(21/22)+*C*(25/24)), 135.0 (s, 1 C, *C*(4)), 141.0 (s, 1 C, *C*(20)), 142.4 (s, 1 C, *C*(5)), 155.6 (s, 1 C, *C*(17)), 158.4 (s, 1 C, *C*(11)), 164.6 (s, 1 C, *C*(14)), 169.7 (s, 1 C, *C*(26)); LRMS *m/z* (ESI$^-$) 749 [(2M-H)$^-$], 374 [(M-H)$^-$]; HRMS (ESI$^+$) found 398.1475, calculated for $C_{22}H_{21}N_3NaO_3^+$ 398.1474; HPLC (System E) t_r 3.8 min (97%).

3-(5-(3,5-Dimethylisoxazol-4-yl)-2-phenethyl-1*H*-benzo[*d*]imidazol-1-yl)propanoic acid (300)

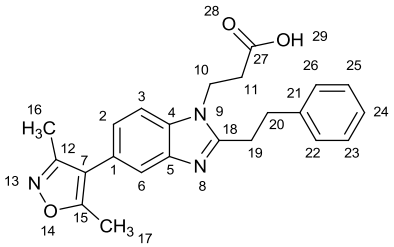

1.00 M aq. LiOH solution (2.8 mL, 2.8 mmol) was added to a stirred solution of compound **297** (226 mg, 0.56 mmol) in MeOH (14 mL). The resultant solution was heated at 50 °C for 3 h then allowed to cool. The solvent was evaporated then the residue was taken up in water (6 mL). Dilute aq. HCl was added until no more solid crashed out (pH~5) then the suspension was filtered. The solid was washed with a little water and MeCN then dried under vacuum to yield the product as an off-white solid (148 mg, 68%); R_f 0.40 (streaky) (EtOAc:MeOH, 80:20); mp 236-369 °C; ν_{max} 1715 (C=O); ^{1}H NMR (400 MHz, DMSO-d_6) δ ppm 2.23 (s, 3 H, C(16)H_3), 2.40 (s, 3 H, C(17)H_3), 2.73 (t, *J*=7.0 Hz, 2 H, C(11)H_2), 3.11 - 3.19 (m, 2 H, C(19)H_2), 3.20 - 3.27 (m, 2 H, C(20)H_2), 4.41 (t, *J*=7.0 Hz, 2 H, C(10)H_2), 7.15 - 7.24 (m, 2 H, C(2)*H*+C(24)H_3), 7.26 - 7.36 (m, 4 H, 4×Ph*H*), 7.57 (d, *J*=1.0 Hz, 1 H, C(6)*H*), 7.62 (d, *J*=8.0 Hz, 1 H, C(3)*H*) 12.49 (br. s., 1 H, O*H*); ^{13}C NMR (101 MHz, DMSO-d_6) δ ppm 10.5 (s, 1 C, *C*(16)), 11.3 (s, 1 C, *C*(17)), 28.2 (s, 1 C, *C*(19)), 32.7 (s, 1 C, *C*(20)), 33.8 (s, 1 C, *C*(11)), 38.9 (s, 1 C, *C*(10)), 110.4 (s, 1 C, *C*(3)), 116.7 (s, 1 C, *C*(7)), 118.9 (s, 1 C, *C*(3)), 122.8 (s, 1 C, *C*(1/2)), 122.9 (s, 1 C, *C*(1/2)), 126.1 (s, 1 C, *C*(24)), 128.3 (s, 2 C, *C*(22/23)+*C*(26/25)), 128.4 (s, 2 C,

C(22/23)+*C*(26/25)), 134.1 (s, 1 C, *C*(4)), 141.2 (s, 1 C, *C*(21)), 142.7 (s, 1 C, *C*(5)), 155.3 (s, 1 C, *C*(18)), 158.4 (s, 1 C, *C*(12)), 164.6 (s, 1 C, *C*(15)), 172.3 (s, 1 C, *C*(27)); LRMS *m/z* (ESI^-) 777 [$(2M-H)^-$], 388 [$(M-H)^-$]; HRMS (ESI^+) found 412.1621, calculated for $C_{23}H_{23}N_3NaO_3^+$ 412.1632; HPLC (System E) t_r 3.9 min (>99%).

4-(5-(3,5-Dimethylisoxazol-4-yl)-2-phenethyl-1*H*-benzo[*d*]imidazol-1-yl)butanoic acid (301)

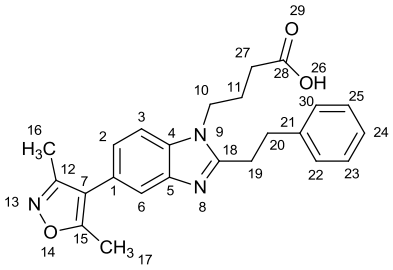

Aq. solution LiOH solution (1.00 M, 0.22 mL, 0.22 mmol) was added to a stirred solution of compound **298** (90 mg, 0.22 mmol) in MeOH (1 mL). The solution was left to stir at room temperature for 16 h then more 1.00 M aq. LiOH solution (1.0 mL, 1.0 mmol) was added. The resultant solution was heated at 60 °C for 1 hour then allowed to cool. The solvent was evaporated then the residue was taken up in water (2 mL). Dilute aq. HCl was added until no more solid crashed out (pH~5) then the suspension was diluted with water. The supernatant was decanted off with a pipette. More water was added and then decanted off then this was repeated once more. The resultant solid was dried under vacuum to yield the product as an off-white solid (63 mg, 71%); R_f 0.15 (streaky); mp 194-197 °C; (EtOAc); ν_{max} (neat) 3374 (O-H) 2929 (C-H), 1704 (C=O); ^{1}H NMR (400 MHz, DMSO-d_6) δ ppm 1.83 (quin, *J*=7.0 Hz, 2 H, C(11)H_2), 1.95 (t, *J*=7.0 Hz, 2 H, C(27)H_2), 2.22 (s, 3 H, C(16)H_3), 2.39 (s, 3 H, C(17)H_3), 3.07 - 3.21 (m, 4 H, C(19)H_2+C(20)H_2), 4.17 (t, *J*=7.0 Hz, 2 H, C(10)H_2), 7.12 (dd, *J*=8.5, 1.5 Hz, 1 H, C(2)*H*), 7.15 - 7.21 (m, 1 H, C(24)*H*), 7.24 - 7.35 (m, 4 H, 4×Ph*H*), 7.54 (d, *J*=1.5 Hz, 1 H, C(6)*H*), 7.66 (d, *J*=8.5 Hz, 1 H, C(3)*H*); ^{13}C NMR (101 MHz, DMSO-d_6) δ ppm 10.5 (s, 1 C, *C*(16)), 11.3 (s, 1 C, *C*(17)), 26.7 (s, 1 C, *C*(11)), 28.2 (s, 1 C, *C*(19)), 32.9 (s, 1 C,

C(20)), 34.6 (s, 1 C, *C*(27)), 43.0 (s, 1 C, *C*(10)), 110.6 (s, 1 C, *C*(3)), 116.8 (s, 1 C, *C*(7)), 118.8 (s, 1 C, *C*(6)), 122.5 (s, 1 C, *C*(1/2)), 122.6 (s, 1 C, *C*(1/2)), 126.0 (s, 1 C, *C*(24)), 128.3 (s, 2 C, *C*(22/23)+*C*(30/25)), 128.4 (s, 2 C, *C*(22/23)+*C*(30/25)), 134.6 (s, 1 C, *C*(4)), 141.1 (s, 1 C, *C*(21)), 142.6 (s, 1 C, *C*(5)), 155.1 (s, 1 C, *C*(18)), 158.4 (s, 1 C, *C*(12)), 164.5 (s, 1 C, *C*(15)), 175.8 (s, 1 C, *C*(28)); LRMS *m/z* (ESI^+) 426 [$(M+Na)^+$], 404, [MH^+], (ESI^-) 402 [$(M-H)^-$]; HRMS (ESI^+) found 404.1960, calculated for $C_{24}H_{26}N_3O_3^+$ 404.1969; HPLC (System D) t_r 10.8 min (>99%).

1-(2-Chloroethyl)-5-(3,5-dimethyl-1,2-oxazol-4-yl)-2-(2-phenylethyl)-1*H*-benzimidazole (302)

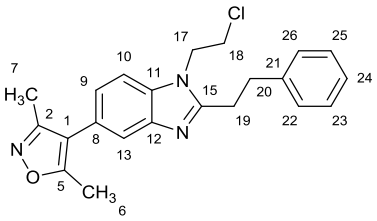

Thionyl chloride (400 μL, 5.5 mmol) was added to a suspension of compound **294** (200 mg, 0.55 mmol) in CH_2Cl_2 (3 mL). The resultant solution was stirred at room temperature for 18 h then evaporated. The residue was partitioned between EtOAc (15 mL) and saturated $NaHCO_3$ (15 mL). The phases were separated then the organic phase dried over $MgSO_4$ and evaporated to yield the product as a beige solid (198 mg, 95%); R_f 0.55 (EtOAc); mp 149-152 °C; ν_{max} (neat) 2889, (C-H); ^{1}H NMR (400 MHz, $CDCl_3$) δ ppm 2.30 (s, 3 H, C(7)*H*$_3$), 2.44 (s, 3 H, C(6)*H*$_3$), 3.24 - 3.30 (m, 2 H, C(19)*H*$_2$), 3.30 - 3.36 (m, 2 H, C(20)*H*$_2$), 3.70 (t, *J*=6.5 Hz, 2 H, C(18)*H*$_2$), 4.32 (t, *J*=6.5 Hz, 2 H, C(17)*H*$_2$), 7.17 (dd, *J*=8.5, 1.5 Hz, 1 H, C(9)*H*), 7.22 - 7.27 (m, 3 H, 3×Ph*H*), 7.28 - 7.34 (m, 2 H, 2×Ph*H*), 7.37 (d, *J*=8.5 Hz, 1 H, C(10)*H*), 7.69 (d, *J*=1.5 Hz, 1 H, C(13)*H*); ^{13}C NMR (101 MHz, $CDCl_3$) δ ppm 10.8 (s, 1 C, *C*(6)), 11.6 (s, 1 C, *C*(7)), 29.5 (s, 1 C, *C*(19)), 34.0 (s, 1 C, *C*(20)), 41.3 (s, 1 C, *C*(18)), 45.0 (s, 1 C, *C*(17)), 109.4 (s, 1 C, *C*(10)), 116.8 (s, 1 C, *C*(1)), 119.8 (s, 1 C, *C*(13)), 124.1 (s, 1 C, *C*(9)), 125.1 (s, 1 C, *C*(8)), 126.6 (s, 1 C, *C*(24)), 128.4 (s, 2 C, *C*(22/23)+C(26/25)), 128.7 (s, 2 C, *C*(22/23)+C(26/25)),

133.5 (s, 1 C, *C*(12)), 140.4 (s, 1 C, *C*(21)), 142.0 (s, 1C, *C*(12)), 155.2 (s, 1 C, *C*(15)), 158.9 (s, 1 C, *C*(2)), 165.2 (s, 1 C, *C*(5)); LRMS *m/z* (ESI$^+$) 783 [(2[(M(^{37}Cl)+Na)$^+$], 781 [(2[(M(^{35}Cl)+Na)$^+$], 761 [(2M(^{37}Cl)+H)$^+$], 759 [(2M(^{35}Cl)+H)$^+$], 404 [(M(^{37}Cl)+Na)$^+$], 402 [(M(^{35}Cl)+Na)$^+$], 383 [M(^{37}Cl)H$^+$], 381 [M(^{35}Cl)H$^+$]; HRMS (ESI$^+$) found 380.1515, calculated for $C_{22}H_{22}{}^{35}ClN_3O^+$ 380.1524; HPLC (System D) t_r 11.9 min (98%).

1-(2,2-Dimethoxyethyl)-5-(3,5-dimethyl-1,2-oxazol-4-yl)-2-(2-phenylethyl)-1*H*-benzimidazole (303)

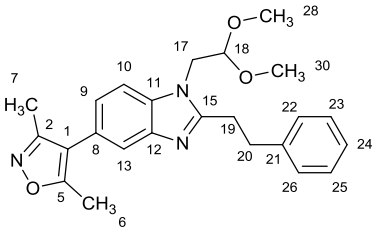

Aminoacetaldehyde dimethyl acetal (218 µL, 2.00 mmol) was added to a solution of compound **251** (472 mg, 2.00 mmol) in DMSO (1 mL). The solution was heated a t 80 °C for 2 h. The solution was removed from the heat then a solution of 3-phenylpropanal (263 µL, 2.00 mmol) in MeOH (4 mL) was added, followed by 1 M aq. $Na_2S_2O_4$ (3.0 mL, 3.0 mmol). The mixture was heated at 80 °C for 4 h then allowed to cool. The mixture was partitioned between EtOAc (15 mL) and 10% aq. ammonia solution (15 mL). The phases were separated then the organic phase was washed with water (15 mL) and brine (15 mL) then dried over $MgSO_4$ and evaporated. The crude material was purified by flash column chromatography on a silica column. The column was eluted with a gradient of EtOAc:*c*-hexane, which was increased linearly from 50:50 to 70:30 over 10 CVs. The desired fractions were combined and evaporated to yield the product as a white solid (525 mg, 65%); R_f 0.50 (EtOAc); mp 105-107 °C; ν_{max} (neat) 2396 (C-H), 2825 (C-H); ^{1}H NMR (400 MHz, $CDCl_3$) δ ppm 2.31 (s, 3 H, C(7)H_3), 2.44 (s, 3 H, C(6)H_3), 3.20 - 3.32 (m, 4 H, C(19)H_2+C(20)H_3), 3.36 (s, 6 H, C(28)H_3+C(30)H_3), 4.12 (d, *J*=5.0 Hz, 2 H, C(17)H_2), 4.50 (t, *J*=5.0 Hz, 1 H, C(18)*H*), 7.13 (dd, *J*=8.5, 1.5 Hz, 1 H, C(9)*H*), 7.23 - 7.35 (m, 5 H, 5×Ph*H*), 7.40

(d, *J*=8.5 Hz, 1 H, C(10)*H*), 7.64 (d, *J*=1.5 Hz, 1 H, C(13)*H*); ^{13}C NMR (101 MHz, $CDCl_3$) δ ppm 10.9 (s, 1 C, *C*(7)), 11.6 (s, 1 C, *C*(6)), 29.5 (s, 1 C, *C*(19)), 33.9 (s, 1 C, *C*(20)), 46.5 (s, 1 C, *C*(17)), 55.5 (s, 2 C, *C*(28)+*C*(30)), 103.1 (s, 1 C, *C*(18)), 109.6 (s, 1 C, *C*(10)), 117.1 (s, 1 C, *C*(1)), 119.8 (s, 1 C, *C*(13)), 123.5 (s, 1 C, *C*(9)), 124.3 (s, 1 C, *C*(8)), 126.4 (s, 1 C, *C*(24)), 128.4 (s, 2 C, *C*(22/23)+C(26/25)), 128.6 (s, 2 C, *C*(22/23)+C(26/25)), 134.6 (s, 1 C, *C*(11)), 141.0 (s, 1 C, *C*(21)), 142.9 (s, 1 C, *C*(12)), 156.0 (s, 1 C, *C*(15)), 159.0 (s, 1 C, *C*(2)), 165.0 (s, 1 C, *C*(5)); LRMS *m/z* (ESI$^+$) 833 [(2M+Na)$^+$], 811 [(2M+H)$^+$], 428 [(M+Na)$^+$], 406 [MH$^+$], (ESI$^-$) 404 [(M-H)$^-$]; HRMS (ESI$^+$) found 406.2118, calculated for $C_{24}H_{28}N_3O_3^+$ 406.2125; HPLC (System D) t_r 11.8 min (99%).

[5-(3,5-Dimethyl-1,2-oxazol-4-yl)-2-(2-phenylethyl)-1*H*-benzimidazol-1-yl]acetaldehyde (304)

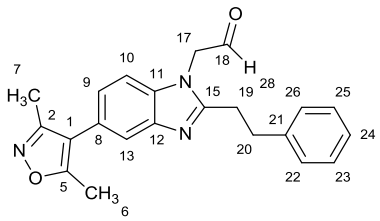

A mixture of compound **303** (1.15 g, 2.84 mmol), water (2.5 mL) CF_3CO_2H (2.5 mL) and CH_2Cl_2 (5 mL) was crimp-sealed in a microwave vial then heated under microwave irradiation for 20 min at 150 °C then for a further 30 min at 150 °C. The reaction mixture was added carefully to a conical flask containing saturated aq. $NaHCO_3$ solution (50 mL) then transferred to a separating funnel. The phases were separated then the organic phase was washed with 1:1 water:brine (50 mL) then brine (50 mL) then dried over $MgSO_4$ and evaporated to yield the product as a cream-coloured solid (1.01 g, 99%); 75-80 °C; R_f 0.30 (EtOAc); ν_{max} (neat) 2928 (C-H), 1733 (C=O); ^{1}H NMR (400 MHz, $CDCl_3$) δ ppm 2.29 (s, 3 H, C(7)H_3), 2.43 (s, 3 H, C(6)H_3), 3.05 - 3.15 (m, 2 H, C(19)H_2), 3.21 - 3.30 (m, 2 H, C(20)H_2), 4.69 (s, 2 H, C(17)H_2), 7.07 - 7.35 (m, 7 H, 7×Ar*H*), 7.67 (d, *J*=1.0 Hz, 1 H, C(13)*H*), 9.48 (s, 1 H, C*H*O); ^{13}C NMR (101 MHz, $CDCl_3$) δ ppm 10.8 (s, 1 C, *C*(7)), 11.5 (s, 1 C, *C*(6)), 29.6 (s, 1 C,

C(19)), 34.0 (s, 1 C, *C*(20)), 52.6 (s, 1 C, *C*(17)), 108.9 (s, 1 C, *C*(10)), 116.9 (s, 1 C, *C*(1)), 120.2 (s, 1 C, *C*(13)), 124.0 (s, 1 C, *C*(9)), 124.9 (s, 1 C, *C*(8)), 126.7 (s, 1 C, *C*(24)), 128.4 (s, 2 C, *C*(22/23)+C(26/25)), 128.8 (s, 2 C, *C*(22/23)+C(26/25)), 134.3 (s, 1 C, *C*(11)), 140.3 (s, 1 C, *C*(21)), 143.0 (s, 1 C, *C*(12)), 155.2 (s, 1 C, *C*(15)), 158.9 (s, 1 C, *C*(2)), 165.1 (s, 1 C, *C*(5)), 194.5 (s, 1 C, *C*HO); LRMS *m/z* (ESI$^-$) 358 [(M-H)$^-$]; HRMS (ESI$^-$) found 358.1563, calculated for $C_{22}H_{20}N_3O_2^-$ 358.1561; HPLC (System D) t_r 10.6 min (38%, aldehyde/hydrate), 11.3 min (62%, MeOH hemiacetal).

GENERAL PROCEDURE F

$NaBH(OAc)_3$ (42 mg, 0.20 mmol) was added to a stirred solution of compound **304** (50 mg, 0.14 mmol), the appropriate amine (0.20 mmol) and acetic acid (10 µL) in THF (1 mL). The mixture was left to stir at room temperature for 2 h then partitioned between CH_2Cl_2 (2 mL) and 1 M NaOH (2 mL). The phases were separated using a hydrophobic frit separation cartridge then the organic phase was evaporated by nitrogen blow-down. The crude material was purified by flash column chromatography on a silica column (10 g). The desired fractions were combined and evaporated to yield the product.

1-[2-(Azetidin-1-yl)ethyl]-5-(3,5-dimethyl-1,2-oxazol-4-yl)-2-(2-phenylethyl)-1*H*-benzimidazole (305)

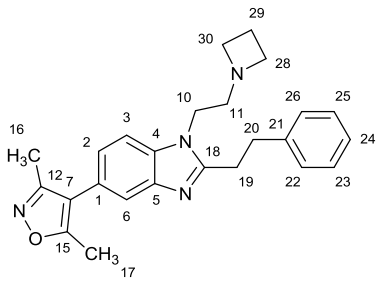

Azetidine (14 µL, 0.20 mmol) was reacted with compound **304** (50 mg, 0.14 mmol) according to general procedure F. Chromatography was carried out with a gradient of CH_2Cl_2:MeOH:NH_4OH, which was increased linearly from 98:2:0.2 to 90:10:1 over 10 CVs.

The product was obtained as a cream solid (48 mg, 86%); mp 163-165 °C; R_f 0.40 (CH_2Cl_2:MeOH:NH_4OH, 90:10:1); ν_{max} 2953 (C-H), 2921 (C-H), 2857 (C-H), 2840 (C-H), 2798 (C-H); ^{1}H NMR (400 MHz, $CDCl_3$) δ ppm 2.07 (quin, *J*=7.0 Hz, 2 H, C(29)H_2), 2.30 (s, 3 H, C(16)H_3), 2.43 (s, 3 H, C(17)H_3), 2.68 (t, *J*=7.0 Hz, 2 H, C(11)H_2), 3.16 (t, *J*=7.0 Hz, 4 H, C(28)H_2+C(30)H_2), 3.19 - 3.24 (m, 2 H, C(29)H_2, C(19)H_2), 3.25 - 3.32 (m, 2 H, C(20)H_2), 3.98 (t, *J*=7.0 Hz, 2 H, C(10)H_2), 7.12 (dd, *J*=8.5, 1.5 Hz, 1 H, C(2)*H*), 7.20 - 7.34 (m, 5 H, 5×Ph*H*), 7.36 (d, *J*=8.5 Hz, 1 H, C(3)*H*), 7.63 (d, *J*=1.5 Hz, 1 H, C(6)*H*); ^{13}C NMR (101 MHz, $CDCl_3$) δ ppm 10.8 (s, 1 C, *C*(16)), 11.5 (s, 1 C, *C*(17)), 17.9 (s, 1 C, *C*(29)), 29.5 (s, 1 C, *C*(19)), 33.9 (s, 1 C, *C*(20)), 42.1 (s, 1 C, *C*(10)), 55.7 (s, 2 C, *C*(28)+*C*(30)), 58.2 (s, 1 C, *C*(11)), 109.4 (s, 1 C, *C*(3)), 117.1 (s, 1 C, *C*(7)), 119.8 (s, 1 C, *C*(6)), 123.3 (s, 1 C, *C*(2)), 124.1 (s, 1 C, *C*(1)), 126.4 (s, 1 C, *C*(24)), 128.4 (s, 2 C, *C*(22/23)+*C*(26/25)), 128.6 (s, 2 C, *C*(22/23)+*C*(26/25)), 134.3 (s, 1 C, *C*(4)), 140.8 (s, 1 C, *C*(21)), 143.0 (s, 1 C, *C*(5)), 155.3 (s, 1 C, *C*(18)), 159.0 (s, 1 C, *C*(12)), 165.0 (s, 1 C, *C*(15)); LRMS *m/z* 823 [(2M+Na)$^+$], 801 [(2M+H)$^+$], 423 [(M+Na)$^+$], 401 [MH$^+$]; HRMS found 401.2334, calculated for $C_{25}H_{29}N_4O^+$ 401.2336); HPLC (System D) t_r 9.7 min (98%).

5-(3,5-Dimethyl-1,2-oxazol-4-yl)-2-(2-phenylethyl)-1-[2-(pyrrolidin-1-yl)ethyl]-1*H*-benzimidazole (306)

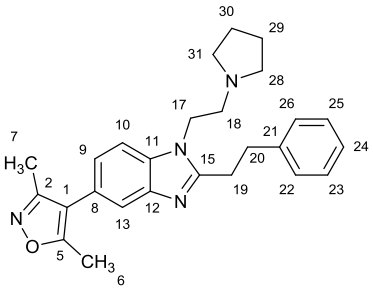

Pyrrolidine (16 μL, 0.20 mmol) was reacted with compound **304** (50 mg, 0.14 mmol) according to general procedure F. Chromatography was carried out with a gradient of EtOAc:MeOH:NEt_3, which was increased linearly from 92:8:0.8 to 90:10:1 over 10 CVs. The product was obtained as a colourless gum (39 mg, 67%); R_f 0.15 (EtOAc:MeOH:NEt_3,

90:10:1); ν_{max} 2960 (C-H), 2921 (C-H), 2794 (C-H); ^{1}H NMR (400 MHz, $CDCl_3$) δ ppm 1.76 - 1.84 (m, 4 H, C(29)H_2+C(30)H_2), 2.30 (s, 3 H, C(7)H_3), 2.43 (s, 3 H, C(6)H_3), 2.53 - 2.61 (m, 4 H, C(28)H_2+C(31)H_2), 2.69 - 2.77 (m, 2 H, C(18)H_2), 3.16 - 3.23 (m, 2 H, C(19)H_2), 3.25 - 3.34 (m, 2 H, C(20)H_2), 4.11 - 4.21 (m, 2 H, C(17)H_2), 7.12 (dd, *J*=8.5, 1.5 Hz, 1 H, C(9)*H*), 7.20 - 7.27 (m, 3 H, 3×Ph*H*), 7.28 - 7.33 (m, 2 H, 2×Ph*H*), 7.37 (d, *J*=8.5 Hz, 1 H, C(10)*H*), 7.63 (d, *J*=1.5 Hz, 1 H, C(13)*H*); ^{13}C NMR (101 MHz, $CDCl_3$) δ ppm 10.8 (s, 1 C, *C*(7)), 11.5 (s, 1 C, *C*(6)), 23.5 (s, 2 C, *C*(29)+*C*(30)), 29.5 (s, 1 C, *C*(19)), 33.9 (s, 1 C, *C*(20)), 43.0 (s, 1 C, *C*(17)), 54.5 (s, 2 C, *C*(28)), 55.0 (s, 1 C, *C*(31)), 109.4 (s, 1 C, *C*(10)), 117.1 (s, 1 C, *C*(1)), 119.8 (s, 1 C, *C*(13)), 123.4 (s, 1 C, *C*(9)), 124.1 (s, 1 C, *C*(8)), 126.4 (s, 1 C, *C*(24)), 128.3 (s, 2 C, *C*(22/23)+C(26/25)), 128.6 (s, 2 C, *C*(22/23)+C(26/25)), 134.3 (s, 1 C, *C*(11)), 140.8 (s, 1 C, *C*(21)), 143.0 (s, 1 C, *C*(11)), 155.2 (s, 1 C, *C*(15)), 159.0 (s, 1 C, *C*(2)), 165.0 (s, 1 C, *C*(5)); LRMS *m/z* (ESI$^+$) 851 [(2M+Na)$^+$], 829 [(2M+H)$^+$], 437 [(M+Na)$^+$], 415 [MH$^+$]; HRMS (ESI$^+$) found 415.2491, calculated for $C_{26}H_{31}N_4O^+$ 415.2492; HPLC (System D) t_r 9.7 min (99%).

5-(3,5-Dimethyl-1,2-oxazol-4-yl)-2-(2-phenylethyl)-1-[2-(piperidin-1-yl)ethyl]-1*H*-benzimidazole (307)

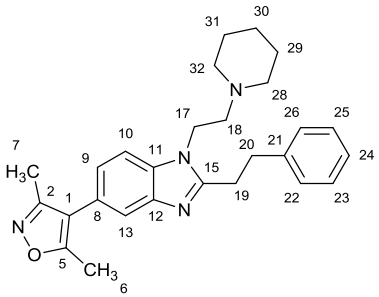

Piperidine (15 µL, 0.20 mmol) was reacted with compound **304** (50 mg, 0.14 mmol) according to general procedure F. Chromatography was carried out with a gradient of EtOAc:MeOH:NEt_3, which was increased linearly from 98:2:0.2 to 92:8:0.8 over 10 CVs. The product was obtained as a colourless gum (21 mg, 49%); R_f 0.15 (EtOAc); ν_{max} 2933 (C-H), 2857 (C-H), 2842, (C-H); ^{1}H NMR (400 MHz, $CDCl_3$) δ ppm 1.40 - 1.48 (m, 2 H, C(30)H_2), 1.53-1.62 (m, *J*=5.5 Hz, 4 H, C(29)H_2+C(31)H_2), 2.30 (s, 3 H, C(7)H_3), 2.42-2.45 (m, 7 H,

C(6)H_3+C(28)H_2+C(32)H_2), 2.57 (t, *J*=7.0 Hz, 2 H, C(18)H_2), 3.17 - 3.26 (m, 2 H, C(19)H_2), 3.26 - 3.34 (m, 2 H, C(20)H_2), 4.14 (t, *J*=7.0 Hz, 2 H, C(17)H_2), 7.12 (dd, *J*=8.5, 1.0 Hz, 1 H, C(9)*H*), 7.21 - 7.35 (m, 5 H, 5×Ph*H*), 7.37 (d, *J*=8.5 Hz, 1 H, C(10)*H*), 7.64 (d, 1 H, 1.0 Hz, C(13)*H*); ^{13}C NMR (101 MHz, $CDCl_3$) δ ppm 10.9 (s, 1 C, *C*(7)), 11.5 (s, 1 C, *C*(6)), 24.1 (s, 1 C, *C*(7)), 25.9 (s, 2 C, *C*(29)+*C*(31)), 29.5 (s, 1 C, *C*(19)), 33.8 (s, 1 C, *C*(20)), 41.7 (s, 1 C, *C*(17)), 55.1 (s, 2 C, *C*(28)+*C*(32)), 57.9 (s, 1 C, *C*(18)), 109.5 (s, 1 C, *C*(10)), 117.1 (s, 1 C, *C*(1)), 119.8 (s, 1 C, *C*(13)), 123.3 (s, 1 C, *C*(9)), 124.0 (s, 1 C, *C*(8)), 126.4 (s, 1 C, *C*(24)), 128.4 (s, 2 C, *C*(22/23)+C(26/25)), 128.6 (s, 2 C, *C*(22/23)+C(26/25)), 134.3 (s, 1 C, *C*(11)), 140.9 (s, 1 C, *C*(21)), 143.0 (s, 1 C, *C*(12)), 155.4 (s, 1 C, *C*(15)), 159.0 (s, 1 C, *C*(2)), 165.0 (s, 1 C, *C*(5)); LRMS *m/z* (ESI$^+$) 879 [(2M+Na)$^+$], 857 [(2M+H)$^+$], 451 [(M+Na)$^+$], 429 [MH$^+$]; HRMS (ESI$^+$) found 429.2643, calculated for $C_{27}H_{33}N_4O^+$ 429.2649; HPLC (System D) t_r 9.9 min (99%).

5-(3,5-Dimethyl-1,2-oxazol-4-yl)-1-[2-(morpholin-4-yl)ethyl]-2-(2-phenylethyl)-1*H*-benzimidazole (308)

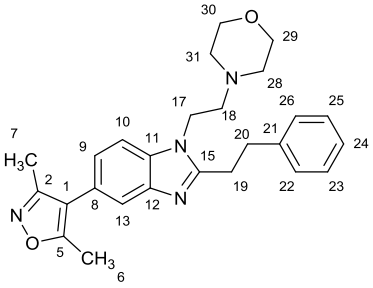

Morpholine (18 µL, 0.20 mmol) was reacted with compound **304** (50 mg, 0.14 mmol) according to general procedure F. Chromatography was carried out with a gradient of EtOAc:MeOH:NEt_3, which was increased linearly from 99:1:0.1 to 90:10:1 over 10 CVs. The product was obtained as a colourless gum (21 mg, 35%); R_f 0.40 (EtOAc:MeOH:NEt_3, 90:10:1); ν_{max} (neat) 2930 (C-H), 29 (C-H), 2855 (C-H), 2814 (C-H); ^{1}H NMR (400 MHz, $CDCl_3$) δ ppm 2.30 (s, 3 H, C(7)H_3), 2.43 (s, 3 H, C(6)H_3), 2.44 - 2.48 (m, 4 H, C(28)H_2+C(31)H_2), 2.61 (t, *J*=7.0 Hz, 2 H, C(18)H_2), 3.18 - 3.25 (m, 2 H, C(19)H_2), 3.27 - 3.34 (m, 2 H, C(20)H_2), 3.64 - 3.71 (m, 4 H, C(29)H_2+C(30)H_2), 4.12 (t, *J*=7.0 Hz, 2 H, C(17)H_2),

7.13 (dd, *J*=8.0, 1.5 Hz, 1 H, C(9)*H*), 7.22 - 7.28 (m, 3 H, 3×Ph*H*), 7.30 - 7.34 (m, 2 H, 2×Ph*H*), 7.36 (d, *J*=8.5 Hz, 1 H, C(10)*H*), 7.64 (d, *J*=1.0 Hz, 1 H, C(13)*H*); ^{13}C NMR (101 MHz, $CDCl_3$) δ ppm 10.9 (s, 1 C, *C*(7)), 11.6 (s, 1 C, *C*(6)), 29.6 (s, 1 C, *C*(19)), 33.8 (s, 1 C, *C*(20)), 41.4 (s, 1 C, *C*(17)), 54.0 (s, 2 C, *C*(28)+*C*(31)), 57.6 (s, 1 C, *C*(18)), 66.8 (s, 2 C, *C*(29)+*C*(30)), 109.4 (s, 1 C, *C*(10)), 117.1 (s, 1 C, *C*(1)), 119.9 (s, 1 C, *C*(13)), 123.4 (s, 1 C, *C*(9)), 124.2 (s, 1 C, *C*(8)), 126.5 (s, 1 C, *C*(24)), 128.4 (s, 2 C, *C*(22/23)+C(26/25)), 128.7 (s, 2 C, *C*(22/23)+C(26/25)), 134.3 (s, 1 C, *C*(11)), 140.9 (s, 1 C, *C*(21)), 143.0 (s, 1 C, *C*(11)), 155.3 (s, 1 C, *C*(15)), 159.0 (s, 1 C, *C*(2)), 165.0 (s, 1 C, *C*(5)); LRMS *m/z* (ESI$^+$) 883 [(2M+Na)$^+$], 861 [(2M+H)$^+$], 453 [(M+Na)$^+$], 431 [MH$^+$]; HRMS (ESI$^+$) found 431.2434, calculated for $C_{26}H_{31}N_4O_2^+$ 431.2442; HPLC (System E) t_r 3.4 min (93%).

5-(3,5-Dimethyl-1,2-oxazol-4-yl)-1-[2-(4-methylpiperazin-1-yl)ethyl]-2-(2-phenylethyl)-1*H*-benzimidazole (309)

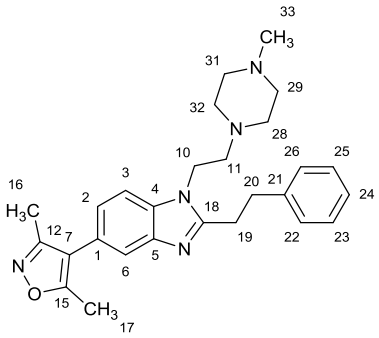

1-Methylpiperazine (14 μL, 0.20 mmol) was reacted with compound **304** (50 mg, 0.14 mmol) according to general procedure F. Chromatography was carried out with a gradient of CH_2Cl_2:MeOH:NH_4OH, which was increased linearly from 95:5:0.5 to 90:10:1 over 10 CVs. The product was obtained as a colourless gum (29 mg, 47%); R_f 0.30 (CH_2Cl_2:MeOH:NH_4OH, 90:10:1); ν_{max} (neat) 2863 (C-H), 2720 (C-H), 2625 (C-H); ^{1}H NMR (400 MHz, $CDCl_3$) δ ppm 2.28 (s, 3 H, C(33)H_3), 2.30 (s, 3 H, C(16)H_3), 2.36 - 2.56 (m, 11 H, C(17)H_3+C(28)H_2+C(29)H_2+C(31)H_2+C(32)H_2), 2.61 (t, *J*=7.0 Hz, 2 H, C(11)H_2), 3.17 - 3.25 (m, 2 H, C(19)H_2), 3.26 - 3.33 (m, 2 H, C(20)H_2), 4.11 (t, *J*=7.0 Hz, 2 H, C(10)H_2), 7.12 (dd,

J=8.0, 1.0 Hz, 1 H, C(2)*H*), 7.21 - 7.34 (m, 5 H, 5×Ph*H*), 7.35 (d, *J*=8.0 Hz, 1 H, C(3)*H*), 7.63 (d, *J*=1.0 Hz, 1 H, C(6)*H*); ^{13}C NMR (101 MHz, $CDCl_3$) δ ppm 10.8 (s, 1 C, *C*(16)), 11.5 (s, 1 C, *C*(15)), 29.6 (s, 1 C, *C*(19)), 33.8 (s, 1 C, *C*(20)), 41.6 (s, 1 C, *C*(10)), 45.9 (s, 1 C, *C*(33)), 53.5 (s, 2 C, *C*(29)+*C*(31)), 54.9 (s, 2 C, *C*(28)+*C*(32)), 57.1 (s, 1 C, *C*(11)), 109.4 (s, 1 C, *C*(3)), 117.1 (s, 1 C, *C*(7)), 119.8 (s, 1 C, *C*(6)), 123.4 (s, 1 C, *C*(2)), 124.1 (s, 1 C, *C*(1)), 126.4 (s, 1 C, *C*(24)), 128.4 (s, 2 C, *C*(22/23)+*C*(26/25)), 128.6 (s, 2 C, *C*(22/23)+*C*(26/25)), 134.3 (s, 1 C, *C*(4)), 140.9 (s, 1 C, *C*(21)), 143.0 (s, 1 C, *C*(5)), 155.4 (s, 1 C, *C*(18)), 159.0 (s, 1 C, *C*(12)), 165.0 (s, 1 C, *C*(15)); LRMS *m/z* (ESI$^+$) 909 [(2M+Na)$^+$], 887 [(2M+H)$^+$], 466 [(M+Na)$^+$], 444 [MH$^+$]; HRMS (ESI$^+$) found 444.2743, calculated for $C_{27}H_{34}N_5O^+$ 444.2758; HPLC (System D) t_r 9.8 min (>99%).

5-(3,5-Dimethyl-1,2-oxazol-4-yl)-2-(2-phenylethyl)-1-[2-(thiomorpholin-4-yl)ethyl]-1*H*-benzimidazole (310)

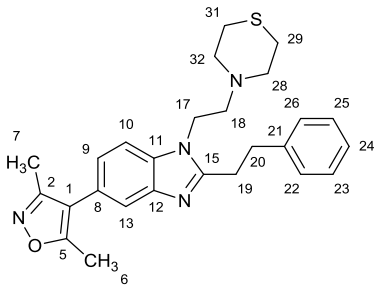

Thiomorpholine (20 μL, 0.20 mmol) was reacted with compound **304** (50 mg, 0.14 mmol) according to general procedure F. Chromatography was carried out with a gradient of CH_2Cl_2:MeOH:NH_4OH, which was increased linearly from 99:1:0.1 to 92:8:0.8 over 30 CVs. The desired fractions were combined and evaporated to yield the product as a colourless gum (37 mg, 59%); R_f 0.45 (CH_2Cl_2:MeOH:NH_4OH, 90:10:1); ν_{max} (neat) 2926 (C-H), 2813 (C-H); ^{1}H NMR (400 MHz, $CDCl_3$) δ ppm 2.30 (s, 3 H, C(7)H_3), 2.43 (s, 3 H, C(6)H_3), 2.64 (s, 6 H, C(7)H_3+C(29)H_2+C(31)H_2), 2.69 - 2.75 (m, 4 H, C(28)H_2+C(32)H_2), 3.17 - 3.24 (m, 2 H, C(19)H_2), 3.26 - 3.33 (m, 2 H, C(20)H_2), 4.09 (t, *J*=7.0 Hz, 2 H, C(17)H_2), 7.12 (dd, *J*=8.0, 1.5 Hz, 1 H, C(9)*H*), 7.23 - 7.28 (m, 3 H, 3×Ph*H*), 7.28 - 7.37 (m, 3 H, C(10)*H*+2×Ph*H*), 7.64 (d,

J=1.5 Hz, 1 H, C(13)*H*); ^{13}C NMR (101 MHz, $CDCl_3$) δ ppm 10.8 (s, 1 C, *C*(7)), 11.5 (s, 1 C, *C*(6)), 27.8 (s, 2 C, *C*(29)+*C*(31)), 29.7 (s, 1 C, *C*(19)), 33.8 (s, 1 C, *C*(20)), 41.6 (s, 1 C, *C*(17)), 55.4 (s, 2 C, *C*(28)+*C*(32)), 57.8 (s, 1 C, *C*(18)), 109.4 (s, 1 C, *C*(10)), 117.0 (s, 1 C, *C*(1)), 119.9 (s, 1 C, *C*(10)), 123.3 (s, 1 C, *C*(9)), 124.1 (s, 1 C, *C*(8)), 126.5 (s, 1 C, *C*(24)), 128.3 (s, 2 C, *C*(22/23)+*C*(26/25)), 128.7 (s, 2 C, *C*(22/23)+*C*(26/25)), 134.2 (s, 1 C, *C*(11)), 140.8 (s, 1 C, *C*(21)), 143.0 (s, 1 C, *C*(12)), 155.3 (s, 1 C, *C*(15)), 159.0 (s, 1 C, *C*(2)), 165.0 (s, 1 C, *C*(5)); LRMS *m/z* (ESI$^+$) 915 [(2M+Na)$^+$], 893 [(2M+H)$^+$], 447 [MH$^+$]; HRMS found 447.2204, calculated for $C_{26}H_{31}N_4OS^+$ 447.2213; HPLC (System E) t_r 3.6 min (86%).

1-{2-[(*cis*-2,6-Dimethylmorpholin-4-yl]ethyl}-5-(3,5-dimethyl-1,2-oxazol-4-yl)-2-(2-phenylethyl)-1*H*-benzimidazoledimethylmorpholine (311)

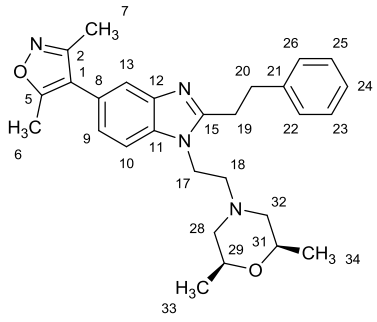

cis-2,6-Dimethylmorpholine (25 μL, 0.20 mmol) was reacted with compound **304** (50 mg, 0.14 mmol) according to general procedure F. Chromatography was carried out with a gradient of CH_2Cl_2:MeOH:NH_4OH, which was increased linearly from 99:1:0.1 to 92:8:0.8 over 30 CVs. The desired fractions were combined and evaporated to yield the product as a colourless gum (29 mg, 45%); R_f 0.45 (CH_2Cl_2:MeOH:NH_4OH, 90:10:1); ν_{max} (neat) 2973 (C-H), 2934 (C-H), 2870 (C-H); ^{1}H NMR (400 MHz, $CDCl_3$) δ ppm 1.13 (d, *J*=6.5 Hz, 6 H, C(33)*H*$_3$+C(34)*H*$_3$), 1.83 (t, *J*=10.5 Hz, 2 H, C(28)*H*+C(32)*H*), 2.30 (s, 3 H, C(7)*H*$_3$), 2.43 (s, 3 H, C(6)*H*$_3$), 2.58 (t, *J*=7.0 Hz, 2 H, C(18)*H*$_2$), 2.65 (d, *J*=10.5 Hz, 2 H, C(28)*H*+C(32)*H*), 3.16 - 3.24 (m, 2 H, C(19)*H*$_2$), 3.26 - 3.33 (m, 2 H, C(20)*H*$_2$), 3.56 - 3.67 (m, 2 H, C(29)*H*+C(31)*H*), 4.12 (t, *J*=7.0 Hz, 2 H, C(17)*H*$_2$), 7.13 (dd, *J*=8.5, 1.5 Hz, 1 H, C(9)*H*), 7.22 - 7.27 (m, 3 H, 3×Ph*H*), 7.29 - 7.38 (m, 3 H, C(9)*H*+2×Ph*H*), 7.64 (d, *J*=1.5 Hz, 1 H, C(13)*H*); ^{13}C NMR (101 MHz, $CDCl_3$) δ

ppm 10.9 (s, 1 C, *C*(7)), 11.5 (s, 1 C, *C*(6)), 19.0 (s, 2 C, *C*(33)+ *C*(34)), 29.7 (s, 1 C, *C*(19)), 33.7 (s, 1 C, *C*(20)), 41.3 (s, 1 C, *C*(17)), 57.2 (s, 1 C, *C*(18)), 59.7 (s, 2 C, *C*(28)+*C*(32)), 71.5 (s, 2 C, *C*(29)+*C*(31)), 109.4 (s, 1 C, *C*(10)), 117.1 (s, 1 C, *C*(1)), 119.9 (s, 1 C, *C*(13)), 123.4 (s, 1 C, *C*(9)), 124.1 (s, 1 C, *C*(8)), 126.5 (s, 1 C, *C*(24)), 128.3 (s, 2 C, *C*(22/23)+*C*(26/25)), 128.7 (s, 2 C, *C*(22/23)+*C*(26/25)), 134.3 (s, 1 C, *C*(11)), 140.9 (s, 1 C, *C*(21)), 143.0 (s, 1 C, *C*(12)), 155.3 (s, 1 C, *C*(15)), 159.0 (s, 1 C, *C*(2)), 165.0 (s, 1 C, *C*(5)); LRMS *m/z* (ESI^+) 939 [$(2M+Na)^+$], 917 [$(2M+H)^+$], 459 [MH^+]; HRMS (ESI^+) found 459.2756, calculated for $C_{28}H_{35}N_4O_2^+$ 459.2755; HPLC (System E) t_r 3.7 min (81%).

4-{2-[5-(3,5-Dimethyl-1,2-oxazol-4-yl)-2-(2-phenylethyl)-1*H*-benzimidazol-1-yl]ethyl}-3,4-dihydro-2*H*-1,4-benzoxazine (312)

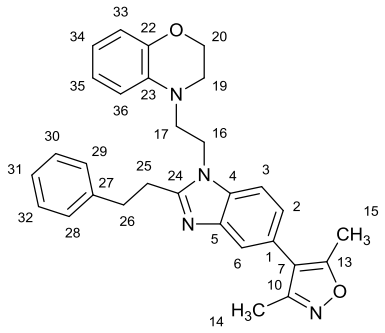

$NaCNBH_3$ (63 mg, 1.00 mmol) was added to a solution of 2-(5-(3,5-dimethylisoxazol-4-yl)-2-phenethyl-1*H*-benzo[*d*]imidazol-1-yl)acetaldehyde (61 mg, 0.45 mmol) in MeOH (2 mL). AcOH (0.1 mL) was added then the mixture was left to stir for 16 h at room temperature. The resultant mixture was partitioned between EtOAc (5 mL) and 1 M aq. NaOH (5 mL). The phases were separated then the organic phase was washed with water (5 mL) and brine (5 mL) then dried over $MgSO_4$ and evaporated. The crude material was purified by flash column chromatography on silica (4 g). The column was eluted with a gradient of EtOAc:*c*-hexane, which was increased linearly from 20:80 to 80:20 over 30 CVs. The desired fractions were combined and evaporated to yield the product as a brown/orange gum (22 mg, 42%); R_f 0.20 (EtOAc:*c*-hexane, 60:40); ν_{max} (neat) 2925 (C-H), 2855 (C-H); ^{1}H NMR (400 MHz, $CDCl_3$) δ ppm 2.31 (s, 3 H, C(14)H_3), 2.44 (s, 3 H, C(15)H_3), 2.87 - 2.94 (m, 2 H,

C(19)H_2), 3.10 (t, *J*=7.5 Hz, 2 H, C(25)H_2), 3.22 (t, *J*=7.5 Hz, 2 H, C(26)H_2), 3.59 (t, *J*=6.0 Hz, 2 H, C(17)H_2), 3.91 - 3.97 (m, 2 H, C(20)H_2), 4.22 (t, *J*=6.0 Hz, 2 H, C(16)H_2), 6.59 (d, *J*=8.0 Hz, 1 H, C(33)*H*), 6.71 (t, *J*=8.0 Hz, 1 H, C(35)*H*), 6.83 (d, *J*=8.0 Hz, 1 H, C(36)*H*), 6.88 (t, *J*=8.0 Hz, 1 H, C(34)*H*), 7.08 (d, *J*=7.0 Hz, 2 H, 2×Ph*H*), 7.14 (d, *J*=8.5 Hz, 1 H, C(3)*H*), 7.18 - 7.29 (m, 3 H, 3×Ph*H*), 7.32 (d, *J*=8.5 Hz, 1 H, C(3)*H*), 7.68 (s, 1 H, C(6)*H*); ^{13}C NMR (101 MHz, $CDCl_3$) δ ppm 10.9 (s, 1 C, *C*(14)), 11.6 (s, 1 C, *C*(15)), 29.4 (s, 1 C, *C*(25)), 33.8 (s, 1 C, *C*(26)), 41.0 (s, 1 C, *C*(16)), 48.5 (s, 1 C, *C*(19)), 50.5 (s, 1 C, *C*(17)), 64.0 (s, 1 C, *C*(20)), 109.5 (s, 1 C, *C*(3)), 110.9 (s, 1 C, *C*(33)), 116.9 (s, 1 C, *C*(7)), 117.1 (s, 1 C, *C*(36)), 118.4 (s, 1 C, *C*(35)), 119.8 (s, 1 C, *C*(6)), 121.9 (s, 1 C, *C*(34)), 123.8 (s, 1 C, *C*(2)), 124.7 (s, 1 C, *C*(1)), 126.5 (s, 1 C, *C*(31)), 128.3 (s, 2 C, *C*(28/32)+*C*(29/30)), 128.6 (s, 2 C, *C*(28/32)+*C*(29/30)), 133.8 (s, 2 C, *C*(4)+*C*(23)), 140.4 (s, 1 C, *C*(27)), 142.4 (s, 1 C, *C*(22)), 144.0 (s, 1 C, *C*(5)), 155.3 (s, 1 C, *C*(24)), 158.9 (s, 1 C, *C*(10)), 165.1 (s, 1 C, *C*(13)); LRMS (ESI$^+$) *m/z* 501 [(M+Na)$^+$], 479 [MH$^+$]; HRMS (ESI$^+$) found 479.2441, calculated for $C_{30}H_{31}N_4O_2^+$ 479.2442; HPLC (System E) t_r 5.0 min (74%).

tert-Butyl 4-{2-[5-(3,5-dimethyl-1,2-oxazol-4-yl)-2-(2-phenylethyl)-1*H*-benzimidazol-1-yl]ethyl}piperazine-1-carboxylate (313)

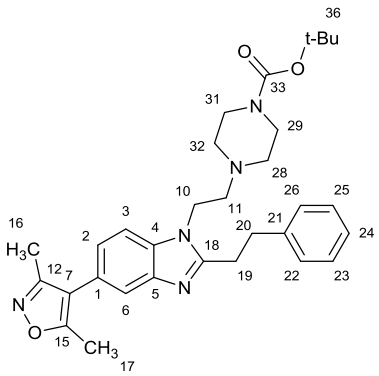

1-Boc-piperazine (37 mg, 0.20 mmol) was reacted with compound **304** (50 mg, 0.14 mmol) according to general procedure F. Chromatography was carried out with an isocratic gradient of EtOAc. The product was obtained as a colourless gum (52 mg, 70%); R_f 0.15 (CH_2Cl_2:MeOH:NH_4OH, 90:10:1); ν_{max} (neat) 2975 (C-H), 2930 (C-H), 2917 (C-H), 1688

(C=O); ^{1}H NMR (400 MHz, $CDCl_3$) δ ppm 1.45 (s, 9 H, C(CH_3)$_3$), 2.30 (s, 3 H, C(16)H_3), 2.35 - 2.45 (m, 7 H, C(17)H_3+C(28)H_2+C(32)H_2), 2.61 (t, *J*=7.0 Hz, 2 H, C(11)H_2), 3.15 - 3.24 (m, 2 H, C(19)H_2), 3.26 - 3.34 (m, 2 H, C(20)H_2), 3.35 - 3.44 (m, 4 H, C(29)H_2+C(31)H_2), 4.11 (t, *J*=7.0 Hz, 2 H, C(10)H_2), 7.12 (dd, *J*=8.5, 1.5 Hz, 1 H, C(2)*H*), 7.21 - 7.33 (m, 5 H, 5×Ph*H*), 7.35 (d, *J*=8.5 Hz, 1 H, C(3)*H*), 7.64 (d, *J*=1.5 Hz, 1 H, C(6)*H*); ^{13}C NMR (101 MHz, $CDCl_3$) δ ppm 10.9 (s, 1 C, *C*(16)), 11.6 (s, 1 C, *C*(17)), 28.4 (s, 3 C, C(*C*H_3)$_3$) 29.7 (s, 1 C, *C*(19)), 33.8 (s, 1 C, *C*(20)), 41.6 (s, 1 C, *C*(10)), 43.2 (s, 2 C, *C*(29)+*C*(31)), 53.4 (s, 2 C, *C*(28)+*C*(32)), 57.2 (s, 1 C, *C*(11)), 79.8 (s, 1 C *C*(CH_3)$_3$) 109.4 (s, 1 C, *C*(3)), 117.1 (s, 1 C, *C*(7)), 119.9 (s, 1 C, *C*(6)), 123.4 (s, 1 C, *C*(2)), 124.2 (s, 1 C, *C*(1)), 126.5 (s, 1 C, *C*(24)), 128.3 (s, 2 C, *C*(22/23)+*C*(26/25)), 128.7 (s, 2 C, *C*(22/23)+*C*(26/25)), 134.2 (s, 1 C, *C*(4)), 140.8 (s, 1 C, *C*(21)), 143.0 (s, 1 C, *C*(5)), 154.6 (s, 1 C, *C*(33)), 155.3 (s, 1 C, *C*(18)), 159.0 (s, 1 C, *C*(12)), 165.0 (s, 1 C, *C*(15)); LRMS *m/z* (ESI$^+$) 552 [(M+Na)$^+$], 530 [MH$^+$]; HRMS (ESI$^+$) found 530.3122, calculated for $C_{31}H_{40}N_5O_3^+$ 530.3126; HPLC (System E) t_r 4.2 min (89%).

5-(3,5-Dimethyl-1,2-oxazol-4-yl)-2-(2-phenylethyl)-1-[2-(piperazin-1-yl)ethyl]-1*H*-benzimidazole (314)

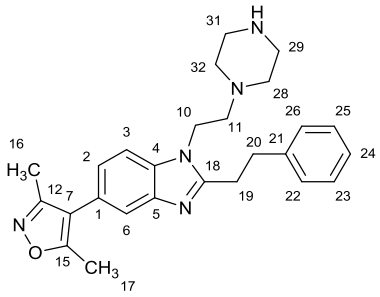

Compound **313** (50 mg, 0.094 mmol) was dissolved in F_3CCO_2H (2 mL) then stirred for 1 h. The excess F_3CCO_2H was evaporated then the residue purified by flash column chromatography on a silica column (4 g). Eluted with CH_2Cl_2:MeOH:NH_4OH, which was increased linearly from 95:5:0.5 to 90:10:1 over 5 CVs. The desired fractions were combined and evaporated to a golden-yellow gum. This material was dissolved in MeOH then loaded onto a pre-wetted SCX cartridge (1 g). The cartridge was eluted with MeOH then with 10%

NEt_3 in MeOH. The basic eluent was evaporated then dried under high vacuum to yield the product as a colourless gum (27 mg, 67%); R_f 0.20, (CH_2Cl_2:MeOH:NH_4OH, 90:10:1); ν_{max} (neat) 3373 (N-H), 2937 (C-H), 2811 (C-H); ^{1}H NMR (400 MHz, $CDCl_3$) δ ppm 2.29 - 2.31 (m, 3 H, C(16)H_3), 2.41 - 2.49 (m, 7 H, C(17)H_3+C(28)H_2+C(32)H_2), 2.59 (t, *J*=7.0 Hz, 2 H, C(11)H_2), 2.83 - 2.91 (m, 4 H, C(29)H_2+C(31)H_3), 3.17 - 3.25 (m, 2 H, C(19)H_2), 3.25 - 3.33 (m, 2 H, C(20)H_2), 4.11 (t, *J*=7.0 Hz, 2 H, C(10)H_2), 7.12 (dd, *J*=8.0, 1.0 Hz, 1 H, C(2)*H*), 7.19 - 7.34 (m, 5 H, 5×Ph*H*), 7.35 (d, *J*=8.5 Hz, 1 H, C(3)*H*), 7.63 (d, *J*=1.0 Hz, 1 H, C(6)*H*); ^{13}C NMR (101 MHz, $CDCl_3$) δ ppm 10.8 (s, 1 C, *C*(16)), 11.5 (s, 1 C, *C*(17)), 29.6 (s, 1 C, *C*(19)), 33.8 (s, 1 C, *C*(20)), 41.5 (s, 1 C, *C*(10)), 45.7 (s, 2 C, *C*(29)+*C*(31)), 54.5 (s, 2 C, *C*(28)+*C*(32)), 57.7 (s, 1 C, *C*(11)), 109.4 (s, 1 C, *C*(3)), 117.1 (s, 1 C, *C*(7)), 119.8 (s, 1 C, *C*(6)), 123.4 (s, 1 C, *C*(2)), 124.1 (s, 1 C, *C*(1)), 126.4 (s, 1 C, *C*(24)), 128.3 (s, 2 C, *C*(22/23)+*C*(26/25)), 128.6 (s, 2 C, *C*(22/23)+*C*(26/25)), 134.3 (s, 1 C, *C*(4)), 140.8 (s, 1 C, *C*(21)), 143.0 (s, 1 C, *C*(5)), 155.3 (s, 1 C, *C*(18)), 159.0 (s, 1 C, *C*(12)), 165.0 (s, 1 C, *C*(15)); LRMS *m/z* (ESI$^+$) 859 [(2M+H)$^+$], 430 [MH$^+$]; HRMS (ESI$^+$) found 430.2592, calculated for $C_{26}H_{32}N_5O^+$ 430.2601; HPLC (System E) t_r 3.4 min (92%).

4-(3,5-Dimethyl-1,2-oxazol-4-yl)-*N*-[2-(morpholin-4-yl)ethyl]-2-nitroaniline (315)

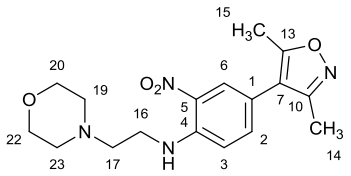

4-(2-Aminoethyl)morpholine (0.787 mL, 6.00 mmol) was added to a solution of compound **249** (1.18 g, 5.00 mmol) and EtN(*i*-Pr)$_2$ (1.05 mL, 6.00 mmol) in THF (25 mL). The mixture was left to stir for 16 h at room temperature then more 4-(2-aminoethyl)morpholine (0.262 mL, 2.00 mmol) was added and the reaction was left to stir for a further 5 h. The mixture was partitioned between EtOAc (20 mL) and water (20 mL). The phases were separated then the organic phase was washed with water (20 mL) and brine (20 mL) then dried over $MgSO_4$ and evaporated to yield the product as an orange solid (1.63 g, 94%); R_f 0.15

(EtOAc); mp 131-133 °C; ν_{max} (neat) 3343 (N-H), 2967 (C-H), 2941 (C-H), 2856 (C-H), 2811 (C-H), 1526 (N-O), 1352 (N-O); ^{1}H NMR (400 MHz, $CDCl_3$) δ ppm 2.26 (s, 3 H, C(14)H_3), 2.40 (s, 3 H, C(15)H_3), 2.50 - 2.60 (m, 4 H, C(19)H_2+C(23)H_2), 2.76 (t, *J*=6.0 Hz, 2 H, C(17)H_2), 3.35 - 3.45 (m, 2 H, C(16)H_2), 3.73 - 3.81 (m, 4 H, C(20)H_2+C(22)H_2), 6.92 (d, *J*=9.0 Hz, 1 H, C(3)*H*), 7.34 (dd, *J*=9.0, 2.0 Hz, 1 H, C(2)*H*), 8.09 (d, *J*=2.0 Hz, 1 H, C(6)*H*), 8.55-8.64 (m, 1 H, N*H*); ^{13}C NMR (101 MHz, $CDCl_3$) δ ppm 10.7 (s, 1 C, *C*(14)), 11.5 (s, 1 C, *C*(15)), 39.4 (s, 1 C, *C*(16)), 53.1 (s, 2 C, *C*(19)+*C*(23)), 55.9 (s, 1 C, *C*(17)), 67.0 (s, 2 C, *C*(20)+*C*(22)), 114.7 (s, 1 C, *C*(3)), 114.9 (s, 1 C, *C*(7)), 117.2 (s, 1 C, *C*(1)), 127.0 (s, 1 C, *C*(6)), 131.9 (s, 1 C, *C*(5)), 136.7 (s, 1 C, *C*(2)), 144.4 (s, 1 C, *C*(4)), 158.6 (s, 1 C, *C*(10)), 165.3 (s, 1 C, *C*(13)); LRMS *m/z* (ESI^+) 715 [$(2M+Na)^+$], 693 [$(2M+H)^+$], 369 [$(M+Na)^+$], 347 [MH^+]; HRMS (ESI^+) found 347.1714, calculated for $C_{17}H_{23}N_4O_4^+$ 347.1714; HPLC (System D) t_r 10.0 min (99%).

4-(3,5-Dimethyl-1,2-oxazol-4-yl)-*N*^{1}-[2-(morpholin-4-yl)ethyl]benzene-1,2-diamine (316)

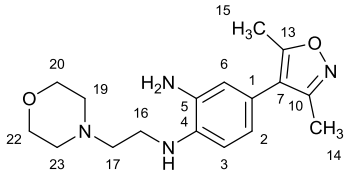

1.0 M aq. $Na_2S_2O_4$ (50 mL, 50 mmol) was added to a suspension of 4-(3,5-dimethylisoxazol-4-yl)-*N*-(2-morpholinoethyl)-2-nitroaniline (3.43 g, 3.43 mmol) in EtOH (50 mL). The reaction was heated under reflux for 1 hour then allowed to cool. The mixture was partitioned between 10% aq. NH_3 (50 mL) and EtOAc (50 mL). The phases were separated then the aqueous phase was extracted with more EtOAc (50 mL). The combined organic phases were washed with brine (50 mL) then dried over $MgSO_4$ and evaporated to yield the product as a pale yellow gum (2.737 g, 87%); R_f 0.40 (CH_2Cl_2:MeOH:NH_4OH, 90:10:1); ν_{max} (neat) 3339 (N-H), 2957 (C-H), 2854 (C-H), 2816 (C-H); ^{1}H NMR (400 MHz, $CDCl_3$) δ ppm 2.26 (s, 3 H, C(10)H_3), 2.39 (s, 3 H, C(13)H_3), 2.47 - 2.55 (m, 4 H, C(19)H_2+C(23)H_2), 2.72 (t, *J*=6.0 Hz, 2 H, C(17)H_2), 3.21 (t, *J*=6.0 Hz, 2 H, C(16)H_2), 3.48 (br. s., 2 H, NH_2), 3.70 - 3.78 (m,

4 H, C(20)H_2+C(22)H_2), 4.08 (br. s., 1 H, N*H*), 6.60 (s, 1 H, C(2)*H*), 6.69 (s, 2 H, C(3)*H*+C(6)*H*); ^{13}C NMR (101 MHz, $CDCl_3$) δ ppm 10.8 (s, 1 C, *C*(14)), 11.5 (s, 1 C, *C*(15)), 40.2 (s, 1 C, *C*(17)), 53.4 (s, 2 C, *C*(19)+*C*(23)), 57.2 (s, 2 C, *C*(20)+*C*(22)), 67.0 (s, 1 C, *C*(16)), 111.7 (s, 1 C, *C*(3)), 116.6 (s, 1 C, *C*(6)), 116.7 (s, 1 C, *C*(7)), 120.3 (s, 1 C, *C*(1)), 121.3 (s, 1 C, *C*(2)), 134.5 (s, 1 C, *C*(5)), 137.0 (s, 1 C, *C*(4)), 159.0 (s, 1 C, *C*(10)), 164.5 (s, 1 C, *C*(13)); LRMS *m/z* (ESI$^+$) 655 [(2M+Na)$^+$], 339 [(M+Na)$^+$], 317 [MH$^+$]; HRMS (ESI$^+$) found 317.1971, calculated for $C_{17}H_{25}NaO_3^+$ 317.1972; HPLC (System E) t_r 2.6 min (97%).

GENERAL PROCEDURE G

A solution of compound **316** (50 mg, 0.16 mmol), T3P (50 wt.% in EtOAc, 0.50 mL, 0.79 mmol), EtN(*i*-Pr)$_2$ (31 µL, 0.18 mmol) and the appropriate carboxylic acid (0.18 mmol) in EtOAc (0.5 mL) was crimp-sealed in a microwave vial then heated under microwave irradiation for 10 min at 150 °C. The reaction mixture was basified by addition of 1 M aq. NaOH solution then extracted with EtOAc (3 mL). The organic phase was washed with water (3 mL) and brine (3 mL) then the organic phase was passed through a hydrophobic frit then evaporated by nitrogen blow-down. The crude material was purified by flash column chromatography on silica (10 g). The desired fractions were combined and evaporated to yield the product.

GENERAL PROCEDURE H

A solution of compound **316** in EtOAc (0.25 M, 0.50 mL, 0.13 mmol) was added to a Radley's GreenHouse tube containing the appropriate carboxylic acid (0.14 mmol). EtN(*i*-Pr)$_2$ (25 µL, 0.14 mmol) was added, followed by T3P (50 wt.% in EtOAc, 0.39 mL, 0.65 mmol). The reaction tube was placed in a Radley's GreenHouse reactor with a reflux head and under a nitrogen atmosphere. The reaction was heated under reflux for 16 h then allowed to cool. The reaction mixture was partitioned between 1 M aq. NaOH (2 mL) and CH_2Cl_2 (2 mL). The

phases were separated by passing the organic phase through a hydrophobic frit with a small amount of $MgSO_4$ on the frit. The collected organic phase was evaporated by nitrogen blow-down then the crude material was purified by flash column chromatography on silica (4 g). The column was eluted with a gradient of EtOAc:MeOH:NEt_3, which was increased linearly from 99:1:0.1 to 95:5:0.5 over 20 CVs. The desired fractions were combined and evaporated to yield the product.

GENERAL PROCEDURE I

A mixture of compound **316** (40 mg, 0.13 mmol) and the appropriate carboxylic acid (0.26 mmol) in 6 M aq. HCl (0.5 mL) was crimp-sealed in a microwave vial then heated under microwave irradiation for 15 min at 210 °C. The mixture was neutralised by careful addition of saturated aq. $NaHCO_3$ solution then extracted with EtOAc (5 mL). The organic phase was dried by passing through a hydrophobic frit with a small amount of $MgSO_4$ on top. The crude material was purified by flash column chromatography on silica (4 g). The desired fractions were combined and evaporated to yield the product.

5-(3,5-Dimethyl-1,2-oxazol-4-yl)-2-[2-(2-methylphenyl)ethyl]-1-[2-(morpholin-4-yl)ethyl]-1*H*-benzimidazole (317)

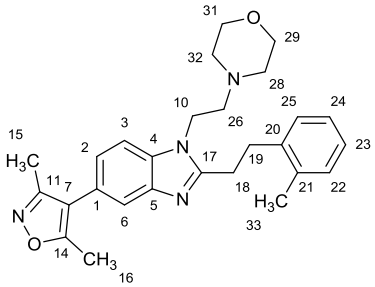

2-Methylhydrocinnamic acid (30 mg, 0.18 mmol) was reacted with compound **316** (50 mg, 0.16 mmol) according to general procedure G. Chromatography was carried out with a gradient of CH_2Cl_2:MeOH:NH_4OH, which was increased linearly from 99:1:0.1 to 90:10:1 over 10 CVs. The product was obtained as a beige solid (44 mg, 62%); mp 121-123 °C; ν_{max}

(neat) 2956 (C-H), 2930 (C-H), 2867 (C-H), 2826 (C-H); R_f 0.40 (CH_2Cl_2:MeOH:NH_4OH, 90:10:1); ν_{max} (neat) 2956 (C-H), 2931 (C-H), 2857 (C-H), 2826 (C-H); ^{1}H NMR (400 MHz, $CDCl_3$) δ ppm 2.30 (s, 3 H, C(15)H_3), 2.38 (s, 3 H, C(33)H_3), 2.43 (s, 3 H, C(16)H_3), 2.44 - 2.48 (m, 4 H, C(28)H_2+C(32)H_2), 2.62 (t, J=7.0 Hz, 2 H, C(26)H_2), 3.09 - 3.20 (m, 2 H, C(18)H_2), 3.25 - 3.34 (m, 2 H, C(19)H_2), 3.58 - 3.70 (m, 4 H, C(29)H_2+C(31)H_2), 4.11 (t, J=7.0 Hz, 2 H, C(10)H_2), 7.00 - 7.23 (m, 5 H, C(2)H+4×ArH), 7.36 (d, J=8.5 Hz, 1 H, C(3)H), 7.65 (s, 1 H, C(6)H); ^{13}C NMR (101 MHz, $CDCl_3$) δ ppm 10.8 (s, 1 C, C(15)), 11.5 (s, 1 C, C(16)), 19.3 (s, 1 C, C(33)), 28.3 (s, 1 C, C(18)), 31.1 (s, 1 C, C(19)), 41.4 (s, 1 C, C(10)), 54.0 (s, 2 C, C(28)+C(32)), 57.5 (s, 1 C, C(26)), 66.7 (s, 2 C, C(29)+C(31)), 109.4 (s, 1 C, C(3)), 117.0 (s, 1 C, C(7)), 119.9 (s, 1 C, C(6)), 123.4 (s, 1 C, C(2)), 124.1 (s, 1 C, C(1)), 126.3 (s, 1 C, C(23/24)), 126.6 (s, 1 C, C(23/24)), 128.8 (s, 1 C, C(25)), 130.4 (s, 1 C, C(22)), 134.2 (s, 1 C, C(4)), 135.9 (s, 1 C, C(21)), 139.0 (s, 1 C, C(20)), 143.0 (s, 1 C, C(5)), 155.4 (s, 1 C, C(17)), 158.9 (s, 1 C, C(11)), 164.9 (s, 1 C, C(14)); LRMS *m/z* (ESI$^+$) 911 [(2M+Na)$^+$], 889 [(2M+H)$^+$], 467 [(M+Na)$^+$], 445 [MH$^+$], (ESI$^-$) 443 [(M-H)$^-$]; HRMS (ESI$^+$) found 445.2595, calculated for $C_{27}H_{33}N_4O_2^+$ 445.2598; HPLC (System E) t_r 3.7 min (96%).

5-(3,5-Dimethyl-1,2-oxazol-4-yl)-2-[2-(3-methylphenyl)ethyl]-1-[2-(morpholin-4-yl)ethyl]-1*H*-benzimidazole (318)

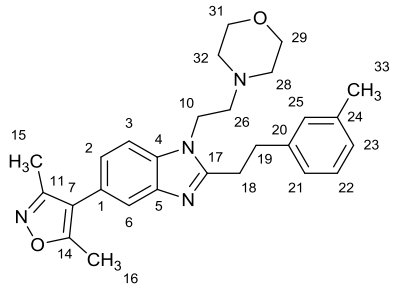

3-(3-Methylphenyl)propionic acid (30 mg, 0.18 mmol) was reacted with compound **316** (50 mg, 0.16 mmol) according to general procedure G. Chromatography was carried out with a gradient of CH_2Cl_2:MeOH:NH_4OH, which was increased linearly from 99:1:0.1 to 92:8:0.8 over 10 CVs. The product was obtained as a pale brown solid (22 mg, 31%); R_f 0.40

(CH_2Cl_2:MeOH:NH_4OH, 90:10:1); mp 68-70 °C; ν_{max} (neat) 2925 (C-H), 2815 (C-H), 2816 (C-H); ^{1}H NMR (400 MHz, $CDCl_3$) δ ppm 2.30 (s, 3 H, C(15)H_3), 2.34 (s, 3 H, C(33)H_3), 2.43 (s, 3 H, C(16)H_3), 2.45 - 2.51 (m, 4 H, C(28)H_2+C(32)H_2), 2.62 (t, *J*=7.0 Hz, 2 H, C(26)H_2), 3.16 - 3.24 (m, 2 H, C(18)H_2), 3.24 - 3.31 (m, 2 H, C(19)H_2), 3.63 - 3.73 (m, 4 H, C(29)H_2+C(31)H_2), 4.14 (t, *J*=7.0 Hz, 2 H, C(10)H_2), 7.00 - 7.10 (m, 3 H, C(21)*H*+C(23)*H*+C(25)*H*), 7.13 (dd, *J*=8.5, 1.5 Hz, 1 H, C(2)*H*), 7.18 - 7.24 (m, 1 H, C(22)*H*), 7.36 (d, *J*=8.5 Hz, 1 H, C(3)*H*), 7.64 (d, *J*=1.5 Hz, 1 H, C(6)*H*); ^{13}C NMR (101 MHz, $CDCl_3$) δ ppm 10.9 (s, 1 C, *C*(15)), 11.5 (s, 1 C, *C*(16)), 21.4 (s, 1 C, *C*(33)), 29.7 (s, 1 C, *C*(18)), 33.7 (s, 1 C, *C*(19)), 41.4 (s, 1 C, *C*(10)), 54.0 (s, 2 C, *C*(28)+*C*(32)), 57.6 (s, 1 C, *C*(26)), 66.8 (s, 2 C, *C*(29)+*C*(31)), 109.3 (s, 1 C, *C*(3)), 117.1 (s, 1 C, *C*(7)), 119.9 (s, 1 C, *C*(6)), 123.4 (s, 1 C, *C*(2)), 124.2 (s, 1 C, *C*(1)), 125.3 (s, 1 C, *C*(21)), 127.2 (s, 1 C, *C*(23)), 128.6 (s, 1 C, *C*(22)), 129.2 (s, 1 C, *C*(25)), 134.3 (s, 1 C, *C*(4)), 138.3 (s, 1 C, *C*(20)), 140.8 (s, 1 C, *C*(24)), 143.0 (s, 1 C, *C*(5)), 155.4 (s, 1 C, *C*(17)), 159.0 (s, 1 C, *C*(11)), 165.0 (s, 1 C, *C*(14)); LRMS *m/z* (ESI$^+$) 911 [(2M+Na)$^+$], 889 [(2M+H)$^+$], 467 [(M+Na)$^+$], 445 [MH$^+$]; HRMS (ESI$^+$) found 445.2587, calculated for $C_{27}H_{33}N_4O_2^+$ 445.2598; HPLC (System E) t_r 3.7 min (99%).

5-(3,5-Dimethyl-1,2-oxazol-4-yl)-2-[2-(4-methylphenyl)ethyl]-1-[2-(morpholin-4-yl)ethyl]-1*H*-benzimidazole (319)

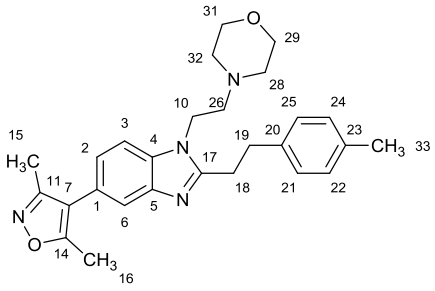

3-(*p*-Tolyl)propionic acid (30 mg, 0.18 mmol) was reacted with compound **316** (50 mg, 0.16 mmol) according to general procedure G. Chromatography was carried out with a gradient of CH_2Cl_2:MeOH:NH_4OH, which was increased linearly from 99:1:0.1 to 90:10:1 over 10 CVs. The product was obtained as a white solid (25 mg, 35%); R_f 0.40; (CH_2Cl_2:MeOH:NH_4OH,

90:10:1); mp 131-133 °C; ν_{max} (neat) 2962 (C-H), 2922 (C-H), 2860 (C-H), 2824 (C-H); ^{1}H NMR (400 MHz, $CDCl_3$) δ ppm 2.30 (s, 3 H, C(15)H_3), 2.34 (s, 3 H, C(33)H_3), 2.43 (s, 3 H, C(16)H_3), 2.44 - 2.49 (m, 4 H, C(28)H_2+C(32)H_2), 2.60 (t, J=7.0 Hz, 2 H, C(26)H_2), 3.14 - 3.22 (m, 2 H, C(18)H_2), 3.23 - 3.31 (m, 2 H, C(19)H_2), 3.65 - 3.71 (m, 4 H, C(29)H_2+C(31)H_2), 4.13 (t, J=7.0 Hz, 2 H, C(10)H_2), 7.10 - 7.17 (m, 5 H, C(2)H+4×ArH), 7.36 (d, J=8.5 Hz, 1 H, C(3)H), 7.64 (d, J=1.0 Hz, 1 H, C(6)H); ^{13}C NMR (101 MHz, $CDCl_3$) δ ppm 10.9 (s, 1 C, C(15)), 11.5 (s, 1 C, C(16)), 21.0 (s, 1 C, C(33)), 29.8 (s, 1 C, C(18)), 33.4 (s, 1 C, C(19)), 41.4 (s, 1 C, C(10)), 54.0 (s, 2 C, C(28)+C(32)), 57.5 (s, 1 C, C(26)), 66.8 (s, 2 C, C(29)+C(31)), 109.4 (s, 1 C, C(3)), 117.1 (s, 1 C, C(7)), 119.9 (s, 1 C, C(6)), 123.3 (s, 1 C, C(2)), 124.1 (s, 1 C, C(1)), 128.2 (s, 2 C, C(21/22)+C(25/24)), 129.3 (s, 2 C, C(21/22)+C(25/24)), 134.2 (s, 1 C, C(4)), 136.0 (s, 1 C, C(23)), 137.8 (s, 1 C, C(20)), 143.0 (s, 1 C, C(5)), 155.4 (s, 1 C, C(17)), 159.0 (s, 1 C, C(11)), 165.0 (s, 1 C, C(14)); LRMS m/z (ESI$^+$) 911 [(2M+Na)$^+$], 889 [(2M+H)$^+$], 467 [(M+Na)$^+$], 445 [MH$^+$], 443 [(M-H)$^-$]; HRMS (ESI$^+$) found 445.2590, calculated for $C_{27}H_{33}N_4O_2^+$ 445.2598; HPLC (System E) t_r 3.7 min (99%).

5-(3,5-Dimethyl-1,2-oxazol-4-yl)-2-[2-(3-methoxyphenyl)ethyl]-1-[2-(morpholin-4-yl)ethyl]-1*H*-benzimidazole (320)

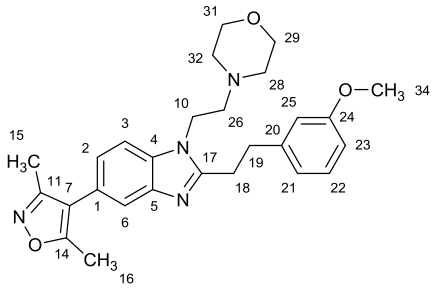

3-(Methoxyphenyl)propionic acid (32 mg, 0.18 mmol) was reacted with compound **316** (50 mg, 0.16 mmol) according to general procedure G. Chromatography was carried out with a gradient of CH_2Cl_2:MeOH:NH_4OH, which was increased linearly from 99:1:0.1 to 90:10:1 over 10 CVs. The product was obtained as a pale yellow gum (38 mg, 52%); R_f 0.40 (CH_2Cl_2:MeOH:NH_4OH, 90:10:1); ν_{max} (neat) 2957 (C-H), 2931 (C-H), 2854 (C-H); ^{1}H NMR

(400 MHz, $CDCl_3$) δ ppm 2.30 (s, 3 H, C(15)H_3), 2.43 (s, 3 H, C(16)H_3), 2.44 - 2.49 (m, 4 H, C(28)H_2+C(32)H_2), 2.60 (t, *J*=7.0 Hz, 2 H, C(26)H_2), 3.17 - 3.24 (m, 2 H, C(18)H_2), 3.25 - 3.33 (m, 2 H, C(19)H_2), 3.64 - 3.70 (m, 4 H, C(29)H_2+C(31)H_2), 3.74 (s, 3 H, C(34)H_3), 4.12 (t, *J*=7.0 Hz, 2 H, C(10)H_2), 6.75 - 6.81 (m, 2 H, C(23)*H*+C(25)*H*), 6.85 (d, *J*=7.5 Hz, 1 H, C(21)*H*), 7.13 (dd, *J*=8.5, 1.5 Hz, 1 H, C(2)*H*), 7.20 - 7.26 (m, 1 H, C(22)*H*), 7.35 (d, *J*=8.5 Hz, 1 H, C(3)*H*), 7.63 (d, *J*=1.5 Hz, 1 H, C(2)*H*); ^{13}C NMR (101 MHz, $CDCl_3$) δ ppm 10.8 (s, 1 C, *C*(15)), 11.5 (s, 1 C, *C*(16)), 29.5 (s, 1 C, *C*(18)), 33.9 (s, 1 C, *C*(19)), 41.4 (s, 1 C, *C*(10)), 54.0 (s, 2 C, *C*(28)+*C*(32)), 55.1 (s, 1 C, *C*(34)), 57.5 (s, 1 C, *C*(26)), 66.8 (s, 2 C, *C*(29)+*C*(31)), 109.4 (s, 1 C, *C*(3)), 111.7 (s, 1 C, *C*(23)), 114.2 (s, 1 C, *C*(25)), 117.1 (s, 1 C, *C*(7)), 119.9 (s, 1 C, *C*(6)), 120.6 (s, 1 C, *C*(21)), 123.4 (s, 1 C, *C*(2)), 124.2 (s, 1 C, *C*(1)), 129.7 (s, 1 C, *C*(22)), 134.3 (s, 1 C, *C*(4)), 142.4 (s, 1 C, *C*(20)), 143.0 (s, 1 C, *C*(5)), 155.3 (s, 1 C, *C*(17)), 159.0 (s, 1 C, *C*(11)), 159.8 (s, 1 C, *C*(34)), 165.0 (s, 1 C, *C*(14)); LRMS *m/z* (ESI$^+$) 943 [(2M+Na)$^+$], 921 [(2M+H)$^+$], 483 [(M+Na)$^+$], 461 [MH$^+$]; HRMS (ESI$^+$) found 461.2550, calculated for $C_{27}H_{33}N_4O_3^+$ 461.2547; HPLC (System E) t_r 3.5 min (99%).

5-(3,5-Dimethyl-1,2-oxazol-4-yl)-2-[2-(4-methoxyphenyl)ethyl]-1-[2-(morpholin-4-yl)ethyl]-1*H*-benzimidazole (321)

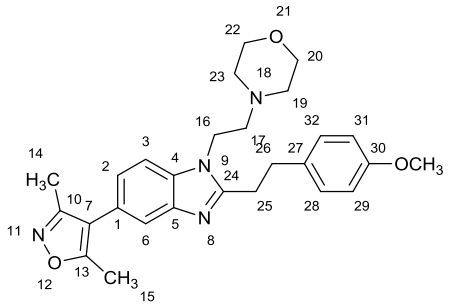

3-(4-Methoxyphenyl)propionic acid (32 mg, 0.18 mmol) was reacted with compound **316** (50 mg, 0.16 mmol) according to general procedure G. Chromatography was carried out with a gradient of CH_2Cl_2:MeOH:NH_4OH, which was increased linearly from 99:1:0.1 to 92:8:0.8 over 10 CVs. The product was obtained as a pale yellow gum (27 mg, 37%); R_f 0.50 (CH_2Cl_2:MeOH:NH_4OH, 90:10:1); ν_{max} (neat) 2956 (C-H), 2926 (C-H), 2854 (C-H); ^{1}H NMR

(400 MHz, $CDCl_3$) δ ppm 2.30 (s, 3 H, C(15)H_3), 2.43 (s, 3 H, C(16)H_3), 2.44 - 2.49 (m, 4 H, C(19)H_2+C(23)H_2), 2.60 (t, *J*=7.0 Hz, 2 H, C(17)H_2), 3.13 - 3.21 (m, 2 H, C(25)H_2), 3.21 - 3.28 (m, 2 H, C(26)H_2), 3.65 - 3.70 (m, 4 H, C(20)H_2+C(22)H_2), 3.79 (s, 3 H, OCH_3), 4.12 (t, *J*=7.0 Hz, 2 H, C(16)H_2), 6.81 - 6.88 (m, 2 H, C(29)*H*+C(31)*H*), 7.12 (dd, *J*=8.5, 1.5 Hz, 1 H, C(2)*H*), 7.14 - 7.18 (m, 2 H, C(28)*H*+C(32)*H*), 7.35 (d, *J*=8.5 Hz, 1 H, C(3)*H*), 7.63 (d, *J*=1.5 Hz, 1 H, C(6)*H*); ^{13}C NMR (101 MHz, $CDCl_3$) δ ppm 10.9 (s, 1 C, *C*(14)), 11.5 (s, 1 C, *C*(15)), 29.9 (s, 1 C, *C*(25)), 33.0 (s, 1 C, *C*(26)), 41.4 (s, 1 C, *C*(16)), 54.0 (s, 2 C, *C*(19)+*C*(23)), 55.2 (s, 1 C, O*C*H_3) 57.5 (s, 1 C, *C*(17)), 66.8 (s, 2 C, *C*(20)+*C*(22)), 109.4 (s, 1 C, *C*(3)), 114.0 (s, 2 C, *C*(29)+*C*(31)), 117.1 (s, 1 C, *C*(7)), 119.9 (s, 1 C, *C*(6)), 123.3 (s, 1 C, *C*(2)), 124.1 (s, 1 C, *C*(1)), 129.3 (s, 2 C, *C*(28)+*C*(32)), 132.9 (s, 1 C, *C*(27)), 134.2 (s, 1 C, *C*(4)), 143.0 (s, 1 C, *C*(5)), 155.4 (s, 1 C, *C*(24)), 158.2 (s, 1 C, *C*(30)), 159.0 (s, 1 C, *C*(10)), 165.0 (s, 1 C, *C*(13)); LRMS *m/z* (ESI$^+$) 943 [(2M+Na)$^+$], 921 [(2M+H)$^+$], 483 [(M+Na)$^+$], 461 [MH$^+$]; HRMS (ESI$^+$) found 461.2543, calculated for $C_{27}H_{33}N_4O_3^+$ 461.2547; HPLC (System E) t_r 3.5 min (91%).

5-(3,5-Dimethyl-1,2-oxazol-4-yl)-1-[2-(morpholin-4-yl)ethyl]-2-{2-[4-(trifluoromethoxy)phenyl]ethyl}-1*H*-benzimidazole (322)

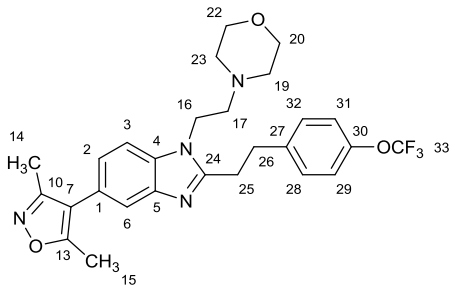

3-[4-(Trifluoromethoxy)phenyl]propanoic acid (33 mg, 0.14 mmol) was reacted with compound **316** (0.13 mmol) according to general procedure H. The product was obtained as a pale orange resin (32 mg, 51%); R_f 0.15 (EtOAc:MeOH:NEt_3, 95:5:0.5); ν_{max} (neat) 2926 (C-H), 2854 (C-H), 2815 (C-H); ^{1}H NMR (400 MHz, $CDCl_3$) δ ppm 2.30 (s, 3 H, C(14)H_3), 2.43 (s, 3 H, C(15)H_3), 2.44 - 2.49 (m, 4 H, C(19)H_2+C(23)H_3), 2.62 (t, *J*=7.0 Hz, 2 H, C(25)H_2), 3.17 - 3.24 (m, 2 H, C(26)H_2), 3.29 - 3.37 (m, 2 H, C(17)H_2), 3.63 - 3.70 (m, 4 H, C(20)H_2+C(22)H_2),

4.13 (t, *J*=7.0 Hz, 2 H, C(16)H_2), 7.10 - 7.19 (m, 3 H, C(3)*H*+C(29)*H*+C(31)*H*), 7.24 - 7.31 (m, 2 H, C(28)*H*+C(32)*H*), 7.36 (d, *J*=8.0 Hz, 1 H, C(2)*H*), 7.63 (s, 1 H, C(6)*H*); ^{13}C NMR (101 MHz, $CDCl_3$) δ ppm 10.8 (s, 1 C, *C*(14)), 11.5 (s, 1 C, *C*(15)), 29.4 (s, 1 C, *C*(25)), 32.9 (s, 1 C, *C*(26)), 41.5 (s, 1 C, *C*(16)), 54.0 (s, 2 C, *C*(19)+*C*(23)), 57.6 (s, 1 C, *C*(17)), 66.8 (s, 2 C, *C*(20)+*C*(22)), 109.4 (s, 1 C, *C*(3)), 117.0 (s, 1 C, *C*(7)), 119.9 (s, 1 C, *C*(6)), 120.4 (q, *J*=257.0 Hz, 1 C, *C*F_3) 121.2 (s, 2 C, *C*(29)+*C*(31)), 123.5 (s, 1 C, *C*(2)), 124.3 (s, 1 C, *C*(1)), 129.7 (s, 2 C, *C*(28)+*C*(32)), 134.2 (s, 1 C, *C*(4)), 139.6 (s, 1 C, *C*(27)), 142.9 (s, 1 C, *C*(5)), 147.8 (d, *J*=1.5 Hz, 1 C, *C*(30)), 154.8 (s, 1 C, *C*(24)), 158.9 (s, 1 C, *C*(10)), 165.0 (s, 1 C, *C*(13)); ^{19}F NMR (377 MHz, $CDCl_3$) δ ppm -57.9 (s, 3 F); LRMS (ESI^+) *m/z* 515 [MH^+]; HRMS (ESI^+) found 515.2251, calculated for $C_{27}H_{30}F_3N_4O_3^+$ 515.2265; HPLC (System D) t_r 10.7 min (94%).

5-(3,5-Dimethyl-1,2-oxazol-4-yl)-2-[2-(2-fluorophenyl)ethyl]-1-[2-(morpholin-4-yl)ethyl]-1*H*-benzimidazole (323)

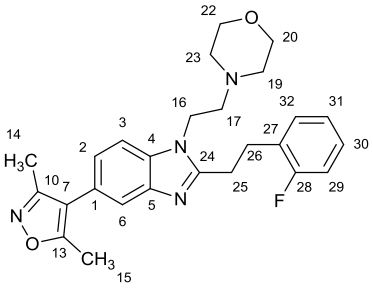

3-(2-Fluorophenyl)propanoic acid (23 mg, 0.14 mmol) was reacted with compound **316** (0.13 mmol) according to general procedure H. The product was obtained as a pale yellow gum (11 mg, 19%); R_f 0.35 (EtOAc:MeOH:NEt_3, 95:5:0.5); ν_{max} (neat) 2933 (C-H), 2856 (C-H), 2819 (C-H); ^{1}H NMR (500 MHz, $CDCl_3$) δ ppm 2.30 (s, 3 H, C(14)H_3), 2.43 (s, 3 H, C(15)H_3), 2.47 - 2.53 (m, 4 H, C(19)H_2+C(23)H_2), 2.68 (t, *J*=7.0 Hz, 2 H, C(17)H_2), 3.19 - 3.26 (m, 2 H, C(26)H_2), 3.27 - 3.34 (m, 2 H, C(25)H_2), 3.65 - 3.71 (m, 4 H, C(20)H_2+C(23)H_2), 4.21 (t, *J*=7.0 Hz, 2 H, C(16)H_2), 7.02 - 7.11 (m, 2 H, C(29)*H*+C(31)*H*), 7.14 (dd, *J*=8.0, 1.5 Hz, 1 H, C(2)*H*), 7.20 - 7.31 (m, 2 H, C(30)*H*+C(32)*H*), 7.38 (d, *J*=8.0 Hz, 1 H, C(3)*H*), 7.64 (d, *J*=1.5 Hz, 1 H C(6)*H*); ^{13}C NMR (126 MHz, $CDCl_3$) δ ppm 10.9 (s, 1 C, *C*(14)), 11.6 (s, 1 C, *C*(15)), 27.9 (d,

J=1.9 Hz, 1 C, *C*(26)), 28.1 (s, 1 C, *C*(25)), 41.5 (s, 1 C, *C*(16)), 54.0 (s, 2 C, *C*(19)+*C*(22)), 57.6 (s, 1 C, *C*(17)), 66.7 (s, 2 C, *C*(20)+*C*(22)), 109.5 (s, 1 C, *C*(3)), 115.4 (d, *J*=21.0 Hz, 1 C, *C*(29)), 117.0 (s, 1 C, *C*(7)), 119.9 (s, 1 C, *C*(6)), 123.5 (s, 1 C, *C*(2)), 124.3 (s, 1 C, *C*(1)), 124.4 (d, *J*=4.0 Hz, 1 C, *C*(31)), 127.5 (d, *J*=15.5 Hz, 1 C, *C*(27)), 128.4 (d, *J*=8.6 Hz, 1 C, *C*(30)), 130.9 (d, *J*=5.0 Hz, 1 C, *C*(32)), 134.2 (s, 1 C, *C*(4)), 142.8 (s, 1 C, *C*(5)), 155.1 (s, 1 C, *C*(24)), 159.0 (s, 1 C, *C*(10)), 161.2 (d, *J*=244.0 Hz, 1 C, *C*(28)), 165.0 (s, 1 C, *C*(13)); ^{19}F NMR (377 MHz, $CDCl_3$) δ ppm -118.8 (s, 1 F); LRMS *m/z* (ESI^+) 449 [MH^+]; HRMS (ESI^+) found 449.2337, calculated for $C_{26}H_{30}FN_4O_2^+$ 449.2347; HPLC (System D) t_r 9.4 min (92%).

5-(3,5-Dimethyl-1,2-oxazol-4-yl)-2-[2-(3-fluorophenyl)ethyl]-1-[2-(morpholin-4-yl)ethyl]-1*H*-benzimidazole (324)

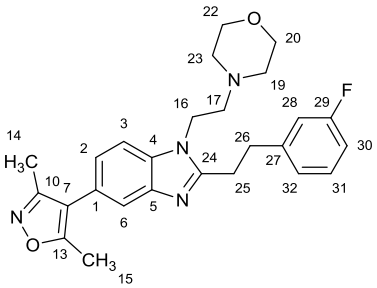

3-(3-Fluorophenyl)propanoic acid (23 mg, 0.14 mmol) was reacted with compound **316** (0.13 mmol) according to general procedure H. The product was obtained as a pale yellow gum (21 mg, 37%); R_f 0.25 (EtOAc:MeOH:NEt_3, 95:5:0.5); ν_{max} (neat) 2962 (C-H), 2929 (C-H), 2854 (C-H), 2825 (C-H); ^{1}H NMR (400 MHz, $CDCl_3$) δ ppm 2.30 (s, 3 H, C(14)H_3), 2.43 (s, 3 H, C(15)H_3), 2.44 - 2.52 (m, 4 H, C(19)H_2+C(23)H_2), 2.63 (t, *J*=7.0 Hz, 2 H, C(17)H_2), 3.18 - 3.24 (m, 2 H, C(25)H_2), 3.29 - 3.37 (m, 2 H, C(26)H_2), 3.61 - 3.72 (m, 4 H, C(20)H_2+C(22)H_2), 4.15 (t, *J*=7.0 Hz, 2 H, C(16)H_2), 6.90 - 6.95 (m, 1 H, C(30)*H*), 6.95 - 7.00 (m, 1 H, C(28)*H*), 7.04 (d, *J*=7.5 Hz, 1 H, C(32)*H*), 7.13 (dd, *J*=8.5, 1.5 Hz, 1 H, C(2)*H*), 7.24 - 7.31 (m, 1 H, C(23)*H*), 7.36 (d, *J*=8.5 Hz, 1 H, C(3)*H*), 7.63 (s, 1 H, C(6)*H*); ^{13}C NMR (101 MHz, $CDCl_3$) δ ppm 10.9 (s, 1 C, *C*(14)), 11.5 (s, 1 C, *C*(15)), 29.2 (s, 1 C, *C*(25)), 33.3 (s, 1 C, *C*(26)), 41.5 (s, 1 C, *C*(16)), 54.0 (s, 2 C, *C*(19)+*C*(23)), 57.6 (s, 1 C, *C*(17)), 66.8 (s, 2 C, *C*(20)+*C*(22)), 109.4 (s, 1 C, *C*(3)),

113.4 (d, *J*=21.5 Hz, 1 C, *C*(30)), 115.2 (d, *J*=21.0 Hz, 1 C, *C*(28)), 117.0 (s, 1 C, *C*(7)), 119.9 (s, 1 C, *C*(6)), 123.5 (s, 1 C, *C*(2)), 124.0 (d, *J*=3.0 Hz, 1 C, *C*(32)), 124.3 (s, 1 C, *C*(1)), 130.1 (d, *J*=8.0 Hz, 1 C, *C*(31)), 134.2 (s, 1 C, *C*(4)), 142.9 (s, 1 C, *C*(5)), 143.4 (d, *J*=7.0 Hz, 1 C, *C*(27)), 154.8 (s, 1 C, *C*(24)), 159.0 (s, 1 C, *C*(10)), 162.9 (d, *J*=246.0 Hz, 1 C, *C*(29)), 165.0 (s, 1 C, *C*(13)); ^{19}F NMR (377 MHz, $CDCl_3$) δ ppm -113.0 (s, 1 F); LRMS *m/z* (ESI^+) 449 [MH^+]; HRMS (ESI^+) found 449.2335, calculated for $C_{26}H_{30}FN_4O_2^+$ 449.2347; HPLC (System D) t_r 9.6 min (94%).

5-(3,5-Dimethyl-1,2-oxazol-4-yl)-2-[2-(4-fluorophenyl)ethyl]-1-[2-(morpholin-4-yl)ethyl]-1*H*-benzimidazole (325)

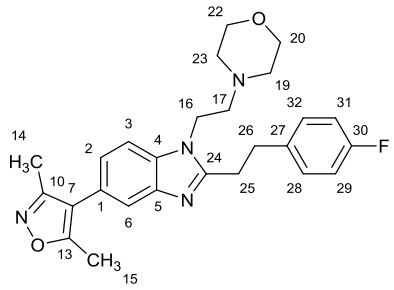

3-(4-Fluorophenyl)propanoic acid (23 mg, 0.14 mmol) was reacted with compound **316** (0.13 mmol) according to general procedure H. The product was obtained as an orange gum (22 mg, 39%); R_f 0.20 (EtOAc:MeOH:NEt_3, 95:5:0.5); ν_{max} (neat) 2926 (C-H), 2854 (C-H), 2815 (C-H); ^{1}H NMR (400 MHz, $CDCl_3$) δ ppm 2.30 (s, 3 H, C(14)H_3), 2.43 (s, 3 H, C(15)H_3), 2.44 - 2.49 (m, 4 H, C(19)H_2+C(23)H_2), 2.61 (t, *J*=7.0 Hz, 2 H, C(17)H_2), 3.15 - 3.22 (m, 2 H, C(25)H_2), 3.25 - 3.33 (m, 2 H, C(26)H_2), 3.60 - 3.71 (m, 4 H, C(20)H_2+C(22)H_2), 4.13 (t, *J*=7.0 Hz, 2 H, C(16)H_2), 6.99 (t, *J*=8.5 Hz, 2 H, C(29)*H*+C(31)*H*), 7.13 (dd, *J*=8.0, 1.5 Hz, 1 H, C(2)*H*), 7.20 (dd, *J*=8.5, 5.5 Hz, 2 H, C(28)*H*+C(32)*H*), 7.36 (d, *J*=8.0 Hz, 1 H, C(3)*H*), 7.63 (s, 1 H, C(6)*H*); ^{13}C NMR (101 MHz, $CDCl_3$) δ ppm 10.8 (s, 1, *C*(14)), 11.5 (s, 1 C, *C*(15)), 29.7 (s, 1 C, *C*(25)), 32.9 (s, 1 C, *C*(26)), 41.4 (s, 1 C, *C*(16)), 54.0 (s, 2 C, *C*(19)+*C*(23)), 57.6 (s, 1 C, *C*(17)), 66.8 (s, 2 C, *C*(20)+*C*(22)), 109.4 (s, 1 C, *C*(3)), 115.4 (d, *J*=21.5 Hz, 2 C, *C*(29)+*C*(31)), 117.0 (s, 1 C, *C*(7)), 119.9 (s, 1 C, *C*(6)), 123.4 (s, 1 C, *C*(2)), 124.2 (s, 1 C, *C*(1)), 129.8 (d, *J*=8.0 Hz, 2

C, *C*(28)+*C*(32)), 134.2 (s, 1 C, *C*(4)), 136.5 (s, 1 C, *C*(27)), 143.0 (s, 1 C, *C*(5)), 155.0 (s, 1 C, *C*(24)), 158.9 (s, 1 C, *C*(10)), 161.5 (d, *J*=253.0 Hz, 1 C, *C*(30)), 165.0 (s, 1 C, *C*(13)); ^{19}F NMR (377 MHz, $CDCl_3$) δ ppm -116.5 (s, 1 F); LRMS *m/z* (ESI^+) 449 [MH^+]; HRMS (ESI^+) found 449.2334, calculated for $C_{26}H_{30}FN_4O_2^+$ 449.2347; HPLC (System D) t_r 9.5 min (91%).

2-(2-{5-(3,5-Dimethyl-1,2-oxazol-4-yl)-1-[2-(morpholin-4-yl)ethyl]-1*H*-benzimidazol-2-yl}ethyl)phenol (326)

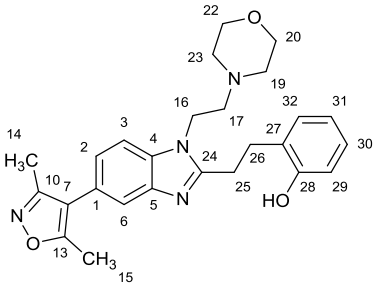

3-(2-Hydroxyphenyl)propionic acid (44 mg, 0.26 mmol) was reacted with compound **316** (40 mg, 0.13 mmol) according to general procedure I. Chromatography was carried out with a gradient of EtOAc:MeOH:NEt_3, which was increased linearly from 99:1:0.1 to 90:10:1 over 20 CVs. The product was obtained as a pale orange solid (32 mg, 55%); R_f 0.45 (EtOAc:MeOH:NEt_3, 90:10:1); mp 172-174 °C; ν_{max} (neat) 3198 (O-H), 2954 (C-H), 2859 (C-H); ^{1}H NMR (400 MHz, $CDCl_3$) δ ppm 2.28 (s, 3 H, C(14)H_3), 2.41 (s, 3 H, C(15)H_3), 2.44 - 2.51 (m, 4 H, C(19)H_2+C(23)H_2), 2.69 (t, *J*=6.5 Hz, 2 H, C(17)H_2), 3.34 (s, 4 H, C(25)H_2+C(26)H_2), 3.59 - 3.69 (m, 4 H, C(20)H_2+C(22)H_2), 4.20 (t, *J*=6.5 Hz, 2 H, C(16)H_2), 6.86 (td, *J*=7.5, 1.0 Hz, 1 H, C(31)*H*), 6.94 (dd, *J*=8.0, 1.0 Hz, 1 H, C(29)*H*), 7.07 - 7.16 (m, 2 H, C(2)*H*+C(30)*H*), 7.20 (dd, *J*=7.5, 1.5 Hz, 1 H, C(32)*H*), 7.35 (d, *J*=8.5 Hz, 1 H, C(3)*H*), 7.64 (d, *J*=1.0 Hz, 1 H, C(6)*H*) 11.59 (br. s., 1 H, O*H*); ^{13}C NMR (101 MHz, $CDCl_3$) δ ppm 10.8 (s, 1 C, *C*(14)), 11.5 (s, 1 C, *C*(15)), 25.5 (s, 1 C, *C*(26)), 29.9 (s, 1 C, *C*(25)), 41.6 (s, 1 C, *C*(16)), 54.0 (s, 2 C, *C*(19)+*C*(23)), 57.3 (s, 1 C, *C*(17)), 66.7 (s, 2 C, *C*(20)+*C*(22)), 109.4 (s, 1 C, *C*(3)), 116.8 (s, 1 C, *C*(7)), 119.1 (s, 1 C, *C*(29)), 119.5 (s, 1 C, *C*(6)), 120.2 (s, 1 C, *C*(31)), 124.1 (s, 1 C, *C*(2)), 124.8 (s, 1 C, *C*(1)), 128.0 (s, 1 C, *C*(30)), 128.7 (s, 1 C, *C*(27)), 130.5 (s, 1 C, *C*(32)), 134.3 (s, 1 C, *C*(4)),

140.9 (s, 1 C, *C*(5)), 155.4 (s, 1 C, *C*(24/28)), 155.7 (s, 1 C, *C*(24/28)), 158.8 (s, 1 C, *C*(10)), 165.1 (s, 1 C, *C*(13)); LRMS *m/z* (ESI$^+$) 447 [MH$^+$], 445 [(M-H)$^-$]; HRMS (ESI$^+$) found 447.2387, calculated for $C_{26}H_{31}N_4O_3^+$ 447.2391; HPLC (System E) t_r 3.3 min (96%).

4-(2-{5-(3,5-Dimethyl-1,2-oxazol-4-yl)-1-[2-(morpholin-4-yl)ethyl]-1H-benzimidazol-2-yl}ethyl)phenol (327)

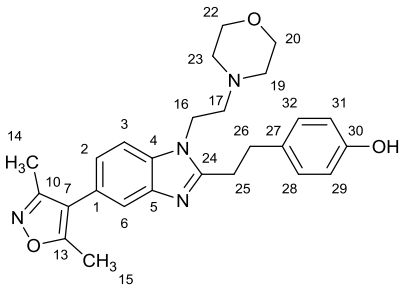

3-(2-Hydroxyphenyl)propionic acid (44 mg, 0.26 mmol) was reacted with compound **316** (40 mg, 0.13 mmol) according to general procedure I. Chromatography was carried out with a gradient of EtOAc:MeOH:NEt_3, which was increased linearly from 99:1:0.1 to 90:10:1 over 30 CVs. The product was obtained as a brown gum (26 mg, 45%); R_f 0.35 (EtOAc:MeOH:NEt_3, 90:10:1); ν_{max} (neat) 3438 (O-H), 2952 (C-H), 2929 (C-H), 2850 (C-H); ^{1}H NMR (400 MHz, DMSO-d_6) δ ppm 2.23 (s, 3 H, C(14)H_3), 2.40 (s, 7 H, C(15)H_3+C(19)H_2+C(23)H_2), 2.53 (t, *J*=6.5 Hz, 2 H, C(17)H_2), 3.00 - 3.09 (m, 2 H, C(26)H_2), 3.10 - 3.18 (m, 2 H, C(25)H_2), 3.47 - 3.57 (m, 4 H, C(20)H_2+C(22)H_2), 4.25 (t, *J*=6.5 Hz, 2 H, C(16)H_2), 6.68 (d, *J*=8.5 Hz, 2 H, C(29)*H*+C(31)*H*), 7.08 (d, *J*=8.5 Hz, 2 H, C(28)*H*+C(32)*H*), 7.16 (dd, *J*=8.0, 1.5 Hz, 1 H, C(2)*H*), 7.51 - 7.61 (m, 2 H, C(3)*H*+C(6)*H*), 9.23 (s, 1 H, O*H*); ^{13}C NMR (101 MHz, DMSO-d_6) δ ppm 10.6 (s, 1 C, *C*(14)), 11.4 (s, 1 C, *C*(15)), 28.8 (s, 1 C, *C*(25)), 32.0 (s, 1 C, *C*(26)), 40.5 (s, 1 C, *C*(16)), 53.6 (s, 2 C, *C*(19)+*C*(23)), 57.5 (s, 1 C, *C*(17)), 66.2 (s, 2 C, *C*(20)+*C*(22)), 110.4 (s, 1 C, *C*(3)), 115.2 (s, 2 C, *C*(29)+*C*(31)), 116.8 (s, 1 C, *C*(7)), 118.9 (s, 1 C, *C*(6)), 122.7 (s, 1 C, *C*(1/2)), 122.8 (s, 1 C, *C*(1/2)), 129.3 (s, 2 C, *C*(28)+*C*(32)), 131.3 (s, 1 C, *C*(27)), 134.5 (s, 1 C, *C*(4)), 142.6 (s, 1 C, *C*(5)), 155.7 (s, 1 C, *C*(24/30)), 155.7 (s, 1 C, *C*(24/30)), 158.5 (s, 1 C, *C*(10)), 164.6 (s, 1 C, *C*(13)); LRMS *m/z* (ESI$^+$) 445 [(M-H)$^-$]; HRMS

(ESI$^+$) found 447.2397, calculated for $C_{26}H_{31}N_4O_3^+$ 447.2391; HPLC (System D) t_r 8.5 min (96%).

5-(3,5-Dimethyl-1,2-oxazol-4-yl)-1-[2-(morpholin-4-yl)ethyl]-2-[2-(3-nitrophenyl)ethyl]-1*H*-benzimidazole (328)

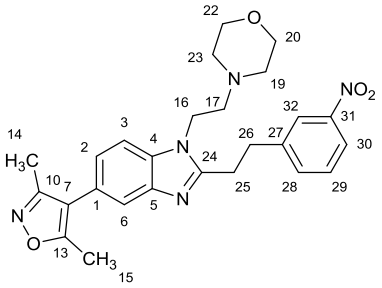

3-(3-Nitrophenyl)propanoic acid (27 mg, 0.14 mmol) was reacted with compound **316** (0.13 mmol) according to general procedure H. The product was obtained as a brown gum (23 mg, 37%); R_f 0.20 (EtOAc:MeOH:NEt_3, 95:5:0.5); ν_{max} (neat) 2960 (C-H), 2931 (C-H), 2855 (C-H), 2816 (C-H), 1582 (N-O), 1350 (N-O); ^{1}H NMR (400 MHz, $CDCl_3$) δ ppm 2.30 (s, 3 H, C(14)H_3), 2.43 (s, 3 H, C(15)H_3), 2.45 - 2.52 (m, 4 H, C(19)H_2+C(23)H_2), 2.68 (t, *J*=6.5 Hz, 2 H, C(17)H_2), 3.28 (t, *J*=8.5 Hz, 2 H, C(25)H_2), 3.47 (t, *J*=8.5 Hz, 2 H, C(26)H_2), 3.62 - 3.69 (m, 4 H, C(20)H_2+C(22)H_2), 4.21 (t, *J*=6.5 Hz, 2 H, C(16)H_2), 7.15 (dd, *J*=8.0, 1.0 Hz, 1 H, C(2)*H*), 7.38 (d, *J*=8.0 Hz, 1 H, C(3)*H*), 7.49 (t, *J*=8.0 Hz, 1 H, C(29)*H*), 7.59 - 7.67 (m, 2 H, C(4)*H*+C(28)*H*)), 8.11 (d, *J*=8.0 Hz, 1 H, C(30)*H*), 8.17 (s, 1 H, C(32)*H*); ^{13}C NMR (101 MHz, $CDCl_3$) δ ppm 10.9 (s, 1 C, *C*(14)), 11.6 (s, 1 C, *C*(15)), 28.8 (s, 1 C, *C*(25)), 32.7 (s, 1 C, *C*(26)), 41.6 (s, 1 C, *C*(10)), 54.1 (s, 2 C, *C*(19)+*C*(23)), 57.7 (s, 1 C, *C*(17)), 66.8 (s, 2 C, *C*(20)+*C*(22)), 109.4 (s, 1 C, *C*(3)), 117.0 (s, 1 C, *C*(7)), 120.0 (s, 1 C, *C*(6)), 121.6 (s, 1 C, *C*(30)), 123.1 (s, 1 C, *C*(32)), 123.7 (s, 1 C, *C*(2)), 124.4 (s, 1 C, *C*(1)), 129.6 (s, 1 C, *C*(29)), 134.3 (s, 1 C, *C*(4)), 134.9 (s, 1 C, *C*(28)), 142.8 (s, 1 C, *C*(5/27)), 142.9 (s, 1 C, *C*(5/27)), 148.4 (s, 1 C, *C*(31)), 154.2 (s, 1 C, *C*(24)), 158.9 (s, 1 C, *C*(10)), 165.0 (s, 1 C, *C*(13)); LRMS *m/z* (ESI$^+$) 498 [(M+Na)$^+$], 476 [MH$^+$]; HRMS (ESI$^+$) found 476.2277, calculated for $C_{26}H_{30}N_5O_4^+$ 476.2292; HPLC (System E) t_r 3.8 min (95%).

5-(3,5-Dimethyl-1,2-oxazol-4-yl)-1-[2-(morpholin-4-yl)ethyl]-2-[2-(4-nitrophenyl)ethyl]-1*H*-benzimidazole (329)

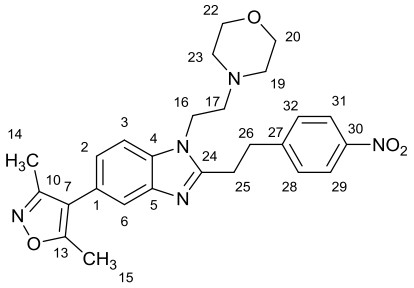

3-(4-Nitrophenyl)propanoic acid (27 mg, 0.14 mmol) was reacted with compound **316** (0.13 mmol) according to general procedure H. The product was obtained as a brown/orange gum (18 mg, 29%); R_f 0.15 (EtOAc:MeOH:NEt_3, 95:5:0.5); ν_{max} (neat) 2934 (C-H), 2854 (C-H), 1516 (N-O), 1344 (N-O); ^{1}H NMR (400 MHz, $CDCl_3$) δ ppm 2.30 (s, 3 H, C(14)H_3), 2.43 (s, 3 H, C(15)H_3), 2.45 - 2.53 (m, 4 H, C(19)H_2+C(23)H_2), 2.66 (t, *J*=6.5 Hz, 2 H, C(17)H_2), 3.26 (t, *J*=8.5 Hz, 2 H, C(25)H_2), 3.47 (t, *J*=8.5 Hz, 2 H, C(26)H_2), 3.62 - 3.72 (m, 4 H, C(20)H_2+C(22)H_2), 4.18 (t, *J*=6.5 Hz, 2 H, C(16)H_2), 7.15 (dd, *J*=8.0, 1.0 Hz, 1 H, C(3)*H*), 7.37 (d, *J*=8.0 Hz, 1 H, C(2)*H*), 7.45 (d, *J*=8.5 Hz, 2 H, C(28)*H*+C(32)*H*), 7.63 (s, 1 H, C(6)*H*), 8.18 (d, *J*=8.5 Hz, 2 H, C(29)*H*+C(31)*H*); ^{13}C NMR (101 MHz, $CDCl_3$) δ ppm 10.9 (s, 1 C, *C*(14)), 11.6 (s, 1 C, *C*(15)), 28.7 (s, 1 C, *C*(25)), 33.1 (s, 1 C, *C*(26)), 41.6 (s, 1 C, *C*(16)), 54.0 (s, 2 C, *C*(19)+*C*(23)), 57.6 (s, 1 C, *C*(17)), 66.8 (s, 2 C, *C*(20)+*C*(22)), 109.5 (s, 1 C, *C*(3)), 117.0 (s, 1 C, *C*(7)), 119.9 (s, 1 C, *C*(2)), 123.7 (s, 1 C, *C*(6)), 123.9 (s, 2 C, *C*(29)+*C*(31)), 124.5 (s, 1 C, *C*(1)), 129.3 (s, 2 C, *C*(28)+*C*(32)), 134.2 (s, 1 C, *C*(4)), 142.8 (s, 1 C, *C*(5)), 146.7 (s, 1 C, *C*(30)), 148.5 (s, 1 C, *C*(27)), 154.2 (s, 1 C, *C*(24)), 158.9 (s, 1 C, *C*(10)), 165.0 (s, 1 C, *C*(13)); LRMS *m/z* (ESI$^+$) 476 [MH^+], (ESI$^-$) 474 [$(M-H)^-$]; HRMS (ESI$^+$) found 476.2282, calculated for $C_{26}H_{30}N_5O_4^+$ 476.2292; HPLC (System E) t_r 3.8 min (97%).

5-(3,5-Dimethyl-1,2-oxazol-4-yl)-2-{2-[4-(methylsulfonyl)phenyl]ethyl}-1-[2-(morpholin-4-yl)ethyl]-1*H*-benzimidazole (330)

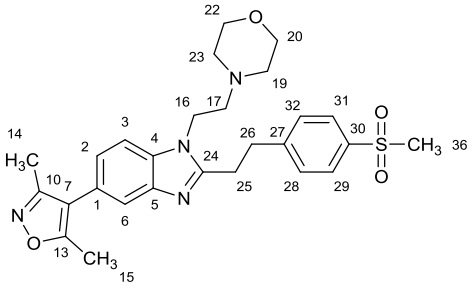

3-[4-(Methylsulfonyl)phenyl]propanoic acid (32 mg, 0.14 mmol) was reacted with compound **316** (0.13 mmol) according to general procedure H. The product was obtained as a pale-orange gum (19 mg, 29%); R_f 0.05 (EtOAc:MeOH:NEt_3, 95:5:0.5); ν_{max} (neat) 2918 (C-H), 2850 (C-H), 1301 (S=O), 1147 (S=O); ^{1}H NMR (400 MHz, $CDCl_3$) δ ppm 2.30 (s, 3 H, C(14)H_3), 2.43 (s, 3 H, C(15)H_3), 2.45 - 2.50 (m, 4 H, C(19)H_2+C(23)H_2), 2.65 (t, J=6.5 Hz, 2 H, C(17)H_2), 3.05 (s, 3 H, C(36)H_3), 3.25 (t, J=8.5 Hz, 2 H, C(25)H_2), 3.45 (t, J=8.5 Hz, 2 H, C(26)H_2), 3.63 - 3.70 (m, 4 H, C(20)H_2+C(22)H_2), 4.17 (t, J=6.5 Hz, 2 H, C(16)H_2), 7.15 (dd, J=8.5, 1.0 Hz, 1 H, C(2)H), 7.37 (d, J=8.5 Hz, 1 H, C(3)H), 7.48 (d, J=8.0 Hz, 2 H, C(28)H+C(32)H), 7.64 (s, 1 H, C(6)H), 7.89 (d, J=8.0 Hz, 2 H, C(29)H+C(31)H); ^{13}C NMR (101 MHz, $CDCl_3$) δ ppm 10.9 (s, 1 C, C(14)), 11.6 (s, 1 C, C(15)), 28.8 (s, 1 C, C(25)), 33.2 (s, 1 C, C(26)), 41.5 (s, 1 C, C(16)), 44.5 (s, 1 C, C(36)), 54.0 (s, 2 C, C(19)+C(23)), 57.6 (s, 1 C, C(17)), 66.7 (s, 2 C, C(20)+C(22)), 109.5 (s, 1 C, C(3)), 117.0 (s, 1 C, C(7)), 119.9 (s, 1 C, C(6)), 123.7 (s, 1 C, C(2)), 124.4 (s, 1 C, C(1)), 127.8 (s, 2 C, C(29)+C(31)), 129.4 (s, 2 C, C(28)+C(32)), 134.2 (s, 1 C, C(4)), 138.8 (s, 1 C, C(30)), 142.8 (s, 1 C, C(5)), 147.4 (s, 1 C, C(27)), 154.3 (s, 1 C, C(24)), 158.9 (s, 1 C, C(10)), 165.0 (s, 1 C, C(13)); LRMS m/z (ESI^+) 531 [$(M+Na)^+$], 509 [MH^+]; HRMS (ESI^+) found 509.2205, calculated for $C_{27}H_{33}N_4O_4S^+$ 509.2217; HPLC (System E) t_r 3.4 min (92%).

4-(2-{5-(3,5-Dimethyl-1,2-oxazol-4-yl)-1-[2-(morpholin-4-yl)ethyl]-1*H*-benzimidazol-2-yl}ethyl)-*N,N*-dimethylaniline (331)

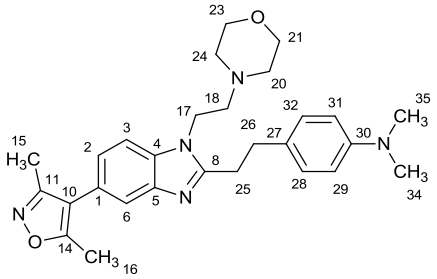

3-[4-(Dimethylamino)phenyl]propanoic acid (27 mg, 0.14 mmol) was reacted with compound **316** (0.13 mmol) according to general procedure H. The product was obtained as a colourless gum (29 mg, 47%); R_f 0.40 (EtOAc:MeOH:NEt_3, 90:10:1); ν_{max} (neat) 2962 (C-H), 2851 (C-H); ^{1}H NMR (400 MHz, $CDCl_3$) δ ppm 2.30 (s, 3 H, C(15)H_3), 2.43 (s, 3 H, C(16)H_3), 2.45 - 2.52 (m, 4 H, C(20)H_2+C(24)H_2), 2.58 (t, J=7.0 Hz, 2 H, C(18)H_2), 2.93 (s, 6 H, C(34)H_3+C(35)H_3), 3.05 - 3.27 (m, 4 H, C(25)H_2+C(26)H_2), 3.63 - 3.80 (m, 4 H, C(21)H_2+C(23)H_2), 4.14 (t, J=7.0 Hz, 2 H, C(17)H_2), 6.62 - 6.77 (m, 2 H, C(29)H+C(31)H), 7.02 - 7.17 (m, 3 H, C(2)H+C(28)H+C(32)H), 7.38 (d, J=8.5 Hz, 1 H, C(3)H), 7.64 (d, J=1.0 Hz, 1 H, C(6)H); ^{13}C NMR (101 MHz, $CDCl_3$) δ ppm 10.9 (s, 1 C, C(15)), 11.5 (s, 1 C, C(16)), 30.0 (s, 1 C, C(25)), 33.1 (s, 1 C, C(26)), 40.7 (s, 2 C, C(34)+C(35)), 41.2 (s, 1 C, C(17)), 53.9 (s, 2 C, C(20)+C(24)), 57.3 (s, 1 C, C(18)), 66.6 (s, 2 C, C(21)+C(23)), 109.4 (s, 1 C, C(3)), 113.0 (s, 2 C, C(29)+C(31)), 117.0 (s, 1 C, C(10)), 119.7 (s, 1 C, C(6)), 123.4 (s, 1 C, C(2)), 124.3 (s, 1 C, C(1)), 128.7 (s, 1 C, C(27)), 129.0 (s, 2 C, C(28)+C(32)), 134.1 (s, 1 C, C(4)), 142.7 (s, 1 C, C(5)), 149.4 (s, 1 C, C(30)), 155.6 (s, 1 C, C(8)), 159.0 (s, 1 C, C(11)), 165.0 (s, 1 C, C(14)); LRMS *m/z* (ESI$^+$), 474 [MH$^+$]; HRMS (ESI$^+$) found 474.2851, calculated for $C_{28}H_{36}N_5O_2^+$ 474.2864; HPLC (System D) t_r 8.3 min (99%).

2-[2-(3,4-Dimethoxyphenyl)ethyl]-5-(3,5-dimethyl-1,2-oxazol-4-yl)-1-[2-(morpholin-4-yl)ethyl]-1*H*-benzimidazole (332)

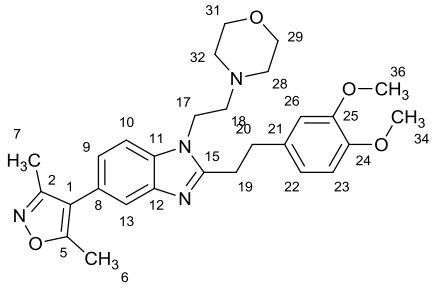

3-(3,4-Dimethoxyphenyl)propionic acid (38 mg, 0.18 mmol) was reacted with compound **316** (50 mg, 0.16 mmol) according to general procedure G. Chromatography was carried out with a gradient of CH_2Cl_2:MeOH:NH_4OH, which was increased linearly from 99:1:0.1 to 92:8:0.8 over 30 CVs. The product was obtained as a pale yellow gum (45 mg, 57%); R_f 0.35 (CH_2Cl_2:MeOH:NH_4OH, 90:10:1); ν_{max} (neat) 2958 (C-H), 2934 (C-H), 2855 (C-H), 2834 (C-H); ^{1}H NMR (400 MHz, $CDCl_3$) δ ppm 2.29 (s, 3 H, C(7)H_3), 2.42 (s, 3 H, C(6)H_3), 2.43 - 2.48 (m, 4 H, C(28)H_2+C(32)H_2), 2.57 (t, *J*=7.0 Hz, 2 H, C(18)H_2), 3.14 - 3.28 (m, 4 H, C(19)H_2+C(20)H_2), 3.64 - 3.69 (m, 4 H, C(29)H_2+C(31)H_2), 3.72 (s, 3 H, C(34/36)H_3), 3.86 (s, 3 H, C(34/36)H_3), 4.08 (t, *J*=7.0 Hz, 2 H, C(17)H_2), 6.67 (d, *J*=2.0 Hz, 1 H, C(26)*H*) .78 (dd, *J*=8.0, 2.0 Hz, 1 H, C(22)*H*), 6.81 (d, *J*=8.0 Hz, 1 H, C(23)*H*), 7.12 (dd, *J*=8.0, 1.5 Hz, 1 H, C(9)*H*), 7.34 (d, *J*=8.0 Hz, 1 H, C(10)*H*), 7.63 (d, *J*=1.5 Hz, 1 H, C(13)*H*); ^{13}C NMR (101 MHz, $CDCl_3$) δ ppm 10.8 (s, 1 C, *C*(7)), 11.5 (s, 1 C, *C*(6)), 29.9 (s, 1 C, *C*(19)), 33.6 (s, 1 C, *C*(20)), 41.4 (s, 1 C, *C*(17)), 54.0 (s, 2 C, *C*(28)+*C*(32)), 55.6 (s, 1 C, *C*(34/36)), 55.9 (s, 1 C, *C*(34/36)), 57.5 (s, 1 C, *C*(18)), 66.8 (s, 2 C, *C*(29)+*C*(31)), 109.4 (s, 1 C, *C*(10)), 111.3 (s, 1 C, *C*(23)), 111.7 (s, 1 C, *C*(26)), 117.1 (s, 1 C, *C*(8)), 119.8 (s, 1 C, *C*(13)), 120.1 (s, 1 C, *C*(22)), 123.4 (s, 1 C, *C*(9)), 124.2 (s, 1 C, *C*(8)), 133.4 (s, 1 C, *C*(21)), 134.2 (s, 1 C, *C*(11)), 143.0 (s, 1 C, *C*(12)), 147.6 (s, 1 C, *C*(24/25)), 148.9 (s, 1 C, *C*(24/25)), 155.3 (s, 1 C, *C*(15)), 158.9 (s, 1 C, *C*(2)), 165.0 (s, 1 C, *C*(5)); LRMS *m/z* (ESI$^+$) 981 [(2M+Na)$^+$], 513 [(M+Na)$^+$], 491 [MH$^+$]; HRMS (ESI$^+$) found 491.2648, calculated for $C_{28}H_{35}N_4O_4^+$ 491.2653; HPLC (System E) t_r 3.3 min (88%).

2-[2-(3,4-Difluorophenyl)ethyl]-5-(3,5-dimethyl-1,2-oxazol-4-yl)-1-[2-(morpholin-4-yl)ethyl]-1*H*-benzimidazole (333)

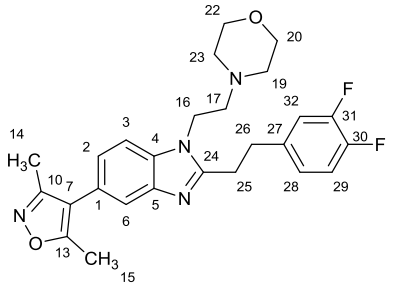

3-(3,4-Difluorophenyl)propanoic acid (26 mg, 0.14 mmol) was reacted with compound **316** (0.13 mmol) according to general procedure H. The product was obtained as a pale pink solid (24 mg, 41%); R_f 0.20 (EtOAc:MeOH:NEt_3, 95:5:0.5); mp 77-80 °C; ν_{max} (neat) 2941 (C-H), 2829 (C-H); ^{1}H NMR (400 MHz, $CDCl_3$) δ ppm 2.30 (s, 3 H, C(14)H_3), 2.43 (s, 3 H, C(15)H_3), 2.44 - 2.50 (m, 4 H, C(19)H_2+C(23)H_2), 2.64 (t, J=7.0 Hz, 2 H, C(17)H_2), 3.14 - 3.22 (m, 2 H, C(25)), 3.24 - 3.33 (m, 2 H, C(26)H_2), 3.63 - 3.71 (m, 4 H, C(20)H_2+C(22)H_2), 4.17 (t, J=7.0 Hz, 2 H, C(16)H_2), 6.93 - 6.99 (m, 1 H, C(28)H), 7.03 - 7.11 (m, 2 H, C(29)H+C(32)H), 7.14 (dd, J=8.0, 1.5 Hz, 1 H, C(2)H), 7.37 (d, J=8.0 Hz, 1 H, C(3)H), 7.62 (s, 1 H, C(6)H); ^{13}C NMR (101 MHz, $CDCl_3$) δ ppm 10.8 (s, 1 C, C(14)), 11.5 (s, 1 C, C(13)), 29.2 (s, 1 C, C(25)), 32.6 (s, 1 C, C(26)), 41.5 (s, 1 C, C(16)), 54.0 (s, 2 C, C(19)+C(23)), 57.6 (s, 1 C, C(17)), 66.8 (s, 2 C, C(20)+C(22)), 109.4 (s, 1 C, C(3)), 117.0 (s, 1 C, C(7)), 117.2 (t, J=17.0 Hz, 2 C, C(29)+C(32)), 119.9 (s, 1 C, C(6)), 123.6 (s, 1 C, C(2)), 124.2 - 124.3 (m, 1 C, C(28)), 124.3 (s, 1 C, C(1)), 134.2 (s, 1 C, C(4)), 137.7 - 137.8 (m, 1 C, C(27)), 142.9 (s, 1 C, C(5)), 147.6 - 149.2 (m, 2 C, C(30)+C(31)), 154.6 (s, 1 C, C(24)), 158.9 (s, 1 C, C(10)), 165.0 (s, 1 C, C(13)); ^{19}F NMR (377 MHz, $CDCl_3$) δ ppm -141.1 (d, J=21.5 Hz, 1 F) -137.62 (d, J=21.5 Hz, 1 F); LRMS *m/z* (ESI^+) 467 [MH^+], 465 [$(M-H)^-$]; HRMS (ESI^+) found 467.2235, calculated for $C_{26}H_{29}F_2N_4O_2^+$ 467.2253; HPLC (System D) t_r 9.9 min (91%).

2-[2-(2-Chloro-3-methoxyphenyl)ethyl]-5-(3,5-dimethyl-1,2-oxazol-4-yl)-1-[2-(morpholin-4-yl)ethyl]-1*H*-benzimidazole (334)

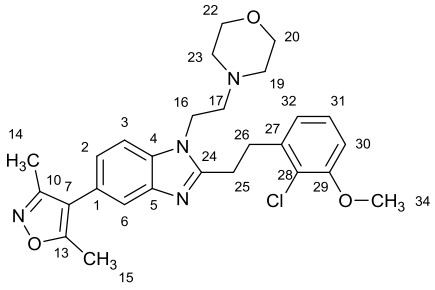

3-(2-Chloro-3-methoxyphenyl)propanoic acid (30 mg, 0.14 mmol) was reacted with compound **316** (0.13 mmol) according to general procedure H. The product was obtained as a pale yellow gum (22 mg, 35%); R_f 0.25 (EtOAc:MeOH:NEt_3, 95:5:0.5); ν_{max} (neat) 2936 (C-H), 2854 (C-H), 2815 (C-H); ^{1}H NMR (400 MHz, $CDCl_3$) δ ppm 2.30 (s, 3 H, C(14)H_3), 2.43 (s, 3 H, C(15)H_3), 2.45 - 2.53 (m, 4 H, C(19)H_2+C(23)H_2), 2.64 (t, *J*=7.0 Hz, 2 H, C(17)H_2), 3.20 - 3.28 (m, 2 H, C(25)H_2), 3.35 - 3.42 (m, 2 H, C(26)H_2), 3.64 - 3.69 (m, 4 H, C(20)H_2+C(22)H_2), 3.92 (s, 3 H, C(34)H_3), 4.19 (t, *J*=7.0 Hz, 2 H, C(16)H_2), 6.86 (d, *J*=8.0 Hz, 1 H, C(30)*H*), 6.91 (d, *J*=8.0 Hz, 1 H, C(32)*H*), 7.13 (dd, *J*=8.5, 1.5 Hz, 1 H, C(2)*H*), 7.17 (t, *J*=8.0 Hz, 1 H, C(31)*H*), 7.37 (d, *J*=8.5 Hz, 1 H, C(3)*H*), 7.63 (s, 1 H, C(6)*H*); ^{13}C NMR (101 MHz, $CDCl_3$) δ ppm 10.8 (s, 1 C, *C*(14)), 11.5 (s, 1 C, *C*(15)), 27.6 (s, 1 C, *C*(25)), 32.5 (s, 1 C, *C*(26)), 41.5 (s, 1 C, *C*(16)), 54.0 (s, 2 C, *C*(19)+*C*(23)), 56.2 (s, 1 C, *C*(34)), 57.5 (s, 1 C, *C*(17)), 66.8 (s, 2 C, *C*(20)+*C*(22)), 109.4 (s, 1 C, *C*(3)), 110.3 (s, 1 C, *C*(30)), 117.1 (s, 1 C, *C*(7)), 119.9 (s, 1 C, *C*(6)), 122.0 (s, 1 C, *C*(28)), 122.5 (s, 1 C, *C*(32)), 123.4 (s, 1 C, *C*(2)), 124.2 (s, 1 C, *C*(1)), 127.4 (s, 1 C, *C*(31)), 134.2 (s, 1 C, *C*(4)), 139.9 (s, 1 C, *C*(27)), 143.0 (s, 1 C, *C*(5)), 155.1 (s, 1 C, *C*(24/29)), 155.3 (s, 1 C, *C*(24/29)), 159.0 (s, 1 C, *C*(10)), 165.0 (s, 1 C, *C*(13)); LRMS *m/z* (ESI$^+$) 497 [M(^{37}Cl)H$^+$] 495 [M(^{35}Cl)H$^+$]; HRMS (ESI$^+$) found 495.2147, calculated for $C_{27}H_{32}{}^{35}ClN_4O_3^+$ 495.2157; HPLC (System D) t_r 9.7 min (95%).

2-[2-(3-Chloro-4-methoxyphenyl)ethyl]-5-(3,5-dimethyl-1,2-oxazol-4-yl)-1-[2-(morpholin-4-yl)ethyl]-1*H*-benzimidazole (335)

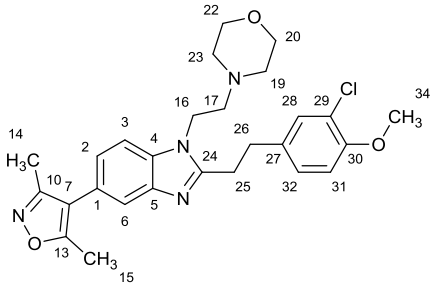

3-(3-Chloro-4-methoxyphenyl)propanoic acid (30 mg, 0.14 mmol) was reacted with compound **316** (0.13 mmol) according to general procedure H. The product was obtained as a pale orange gum (27 mg, 43%); R_f 0.25 (EtOAc:MeOH:NEt_3, 95:5:0.5); ν_{max} (neat) 2955 (C-H), 2934 (C-H), 2851 (C-H); ^{1}H NMR (400 MHz, $CDCl_3$) δ ppm 2.29 (s, 3 H, C(14)H_3), 2.42 (s, 3 H, C(15)H_3), 2.44 - 2.50 (m, 4 H, C(19)H_2+C(23)H_2), 2.62 (t, J=7.0 Hz, 2 H, C(17)H_3), 3.13 - 3.20 (m, 2 H, C(25)H_2), 3.20 - 3.27 (m, 2 H, C(26)H_2), 3.65 - 3.70 (m, 4 H, C(20)H_2+C(22)H_2), 3.88 (s, 3 H, C(34)H_3), 4.15 (t, J=7.0 Hz, 2 H, C(16)H_2), 6.86 (d, J=8.5 Hz, 1 H, C(31)H), 7.09 (dd, J=8.5, 2.0 Hz, 1 H, C(32)H), 7.13 (dd, J=8.0, 1.0 Hz, 1 H, C(2)H), 7.27 (d, J=2.0 Hz, 1 H, C(28)H), 7.36 (d, J=8.0 Hz, 1 H, C(3)H), 7.62 (d, J=1.0 Hz, 1 H, C(6)H); ^{13}C NMR (101 MHz, $CDCl_3$) δ ppm 10.8 (s, 1 C, C(14)), 11.5 (s, 1 C, C(15)), 29.5 (s, 1 C, C(25)), 32.5 (s, 1 C, C(26)), 41.5 (s, 1 C, C(16)), 54.0 (s, 2 C, C(19)+C(23)), 56.2 (s, 1 C, C(34)), 57.6 (s, 1 C, C(17)), 66.8 (s, 2 C, C(20)+C(22)), 109.4 (s, 1 C, C(3)), 112.2 (s, 1 C, C(31)), 117.0 (s, 1 C, C(7)), 119.9 (s, 1 C, C(6)), 122.3 (s, 1 C, C(29)), 123.5 (s, 1 C, C(2)), 124.2 (s, 1 C, C(1)), 127.6 (s, 1 C, C(32)), 130.0 (s, 1 C, C(28)), 133.9 (s, 1 C, C(4/27)), 134.2 (s, 1 C, C(4/27)), 142.9 (s, 1 C, C(5)), 153.6 (s, 1 C, C(30)), 154.9 (s, 1 C, C(24)), 159.0 (s, 1 C, C(10)), 165.0 (s, 1 C, C(13)); LRMS (ESI^+) *m/z* 497 [M(^{37}Cl)H^+], 495 [M(^{35}Cl)H^+]; HRMS (ESI^+) found 495.2138, calculated for $C_{27}H_{32}{}^{35}ClN_4O_3^+$ 495.2157; HPLC (System D) t_r 9.9 min (92%).

5-(3,5-Dimethyl-1,2-oxazol-4-yl)-2-[2-(2-fluoro-4-methoxyphenyl)ethyl]-1-[2-(morpholin-4-yl)ethyl]-1*H*-benzimidazole (336)

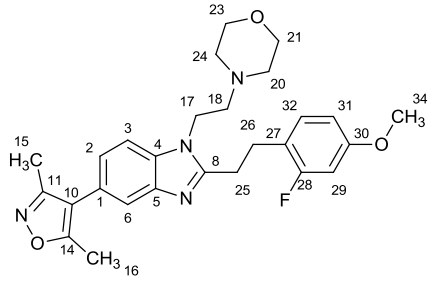

3-(2-Fluoro-4-methoxyphenyl)propanoic acid (28 mg, 0.14 mmol) was reacted with compound **316** (0.13 mmol) according to general procedure H. The product was obtained as a colourless gum (39 mg, 63%); R_f 0.50 (EtOAc:MeOH:NEt_3, 90:10:1); ν_{max} (neat) 2943 (C-H), 1739; ^{1}H NMR (400 MHz, $CDCl_3$) δ ppm 2.29 (s, 3 H, C(15)H_3), 2.43 (s, 3 H, C(16)H_3), 2.48 - 2.59 (m, 4 H, C(20)H_2+C(24)H_2), 2.68 (t, *J*=7.0 Hz, 2 H, C(18)H_2), 3.14 - 3.34 (m, 4 H, C(25)H_2+C(26)H_2), 3.57 - 3.75 (m, 4 H, C(21)H_2+C(23)H_2), 3.79 (s, 3 H, C(34)H_3), 4.22 (t, *J*=7.0 Hz, 2 H, C(17)H_2), 6.59 - 6.70 (m, 2 H, C(29)*H*+C(31)*H*), 7.11 - 7.20 (m, 2 H, C(2)*H*+C(32)*H*), 7.40 (d, *J*=8.5 Hz, 1 H, C(3)*H*), 7.64 (d, *J*=1.0 Hz, 1 H, C(6)*H*); ^{13}C NMR (101 MHz, $CDCl_3$) δ ppm 10.8 (s, 1 C, *C*(14)), 11.5 (s, 1 C, *C*(16)), 27.3 (s, 1 C, *C*(26)), 28.3 (s, 1 C, *C*(25)), 41.3 (s, 1 C, *C*(17)), 53.9 (s, 2 C, *C*(20)+*C*(24)), 55.5 (s, 1 C, *C*(34)), 57.4 (s, 1 C, *C*(18)), 66.6 (s, 2 C, *C*(21)+*C*(23)), 101.8 (d, *J*=25.5 Hz, 1 C, *C*(29)), 109.5 (s, 1 C, *C*(3)), 109.8 (d, *J*=3.0 Hz, 1 C, *C*(31)), 116.9 (s, 1 C, *C*(10)), 119.1 (d, *J*=16.0 Hz, 1 C, *C*(27)), 119.7 (s, 1 C, *C*(6)), 123.7 (s, 1 C, *C*(2)), 124.5 (s, 1 C, *C*(1)), 131.1 (d, *J*=7.0 Hz, 1 C, *C*(32)), 134.0 (s, 1 C, *C*(4)), 142.3 (s, 1 C, *C*(5)), 155.1 (s, 1 C, *C*(8)), 158.9 (s, 1 C, *C*(11)), 159.7 (d, *J*=11.0 Hz, 1 C, *C*(30)), 161.5 (d, *J*=244.0 Hz, 1 C, *C*(28)), 165.0 (s, 1 C, *C*(14)); ^{19}F NMR (377 MHz, $CDCl_3$) δ ppm -116.8 (s, 1 F); LRMS *m/z* (ESI$^+$) 501 [(M+Na)$^+$], 479 [MH$^+$]; HRMS (ESI$^+$) found 479.2442, calculated for $C_{27}H_{32}FN_4O_3^+$ 479.2453; HPLC (System D) t_r 9.8 min (>99%).

5-(3,5-Dimethyl-1,2-oxazol-4-yl)-2-[2-(3-fluoro-4-methoxyphenyl)ethyl]-1-[2-(morpholin-4-yl)ethyl]-1*H*-benzimidazole (337)

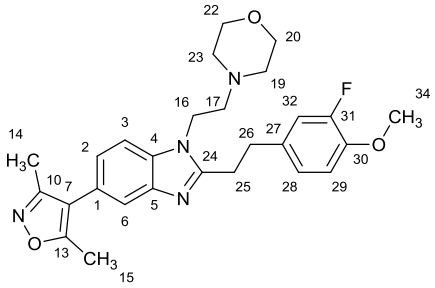

3-(3-Fluoro-4-methoxyphenyl)propanoic acid (28 mg, 0.14 mmol) was reacted with compound **316** (0.13 mmol) according to general procedure H. The product was obtained as an off-white solid (19 mg, 31%); R_f 0.25 (EtOAc:MeOH:NEt_3, 90:10:1); mp 119-122 °C; ν_{max} (neat) 2956 (C-H), 2928 (C-H), 2856 (C-H); ^{1}H NMR (400 MHz, $CDCl_3$) δ ppm 2.30 (s, 3 H, C(14)H_3), 2.43 (s, 3 H, C(15)H_3), 2.45 - 2.51 (m, 4 H, C(19)H_2+C(23)H_2), 2.63 (t, *J*=7.0 Hz, 2 H, C(17)H_2), 3.11 - 3.21 (m, 2 H, C(25)H_2), 3.21 - 3.29 (m, 2 H, C(26)H_2), 3.63 - 3.71 (m, 4 H, C(20)H_2+C(22)H_2), 3.87 (s, 3 H, C(34)H_3), 4.15 (t, *J*=7.0 Hz, 2 H, C(16)H_2), 6.85 - 7.02 (m, 3 H, 3×Ar*H*), 7.13 (d, *J*=8.5 Hz, 1 H, C(2)*H*), 7.36 (d, *J*=8.5 Hz, 1 H, C(3)*H*), 7.63 (s, 1 H, C(6)*H*); ^{13}C NMR (101 MHz, $CDCl_3$) δ ppm 10.9 (s, 1 C, *C*(14)), 11.6 (s, 1 C, *C*(15)), 29.5 (s, 1 C, *C*(25)), 32.7 (s, 1 C, *C*(26)), 41.5 (s, 1 C, *C*(16)), 54.0 (s, 2 C, *C*(19)+*C*(23)), 56.3 (s, 1 C, *C*(34)), 57.6 (s, 1 C, *C*(17)), 66.8 (s, 2 C, *C*(20)+*C*(22)), 109.4 (s, 1 C, *C*(3)), 113.6 (d, *J*=2.5 Hz, 1 C, *C*(29)), 116.0 (d, *J*=17.5 Hz, 1 C, *C*(32)), 117.0 (s, 1 C, *C*(7)), 119.9 (s, 1 C, *C*(6)), 123.5 (s, 1 C, *C*(2)), 123.9 (d, *J*=3.0 Hz, 1 C, *C*(28)), 124.2 (s, 1 C, *C*(1)), 133.8 (d, *J*=5.5 Hz, 1 C, *C*(27)), 134.2 (s, 1 C, *C*(4)), 142.9 (s, 1 C, *C*(5)), 146.1 (d, *J*=10.5 Hz, 1 C, *C*(30)), 152.3 (d, *J*=246.0 Hz, 1 C, *C*(21)), 155.0 (s, 1 C, *C*(24)), 159.0 (s, 1 C, *C*(10)), 165.0 (s, 1 C, *C*(13)); ^{19}F NMR (377 MHz, $CDCl_3$) δ ppm -135.0 (s, 1 F); LRMS *m/z* (ESI^+) 479 [MH^+]; HRMS (ESI^+) found 479.2445, calculated for $C_{27}H_{32}FN_4O_3^+$ 479.2453; HPLC (System D) t_r 9.5 min (96%).

2-[2-(1,3-Benzodioxol-5-yl)ethyl]-5-(3,5-dimethyl-1,2-oxazol-4-yl)-1-[2-(morpholin-4-yl)ethyl]-1*H*-benzimidazole (338)

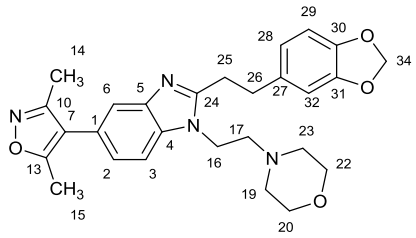

3-(1,3-Benzodioxol-5-yl)propanoic acid (27 mg, 0.14 mmol) was reacted with compound **316** (0.13 mmol) according to general procedure H. The product was obtained as a pale-yellow gum (9 mg, 15%); R_f 0.25 (EtOAc:MeOH:NEt_3, 95:5:0.5); ν_{max} (neat) 2922 (C-H), 2852 (C-H); ^{1}H NMR (500 MHz, $CDCl_3$) δ ppm 2.31 (s, 3 H, C(14)H_3), 2.44 (s, 3 H, C(15)H_3), 2.46 - 2.54 (m, 4 H, C(19)H_2+C(23)H_2), 2.63 (t, J=7.0 Hz, 2 H, C(17)H_2), 3.14 - 3.20 (m, 2 H, C(25)H_2), 3.20 - 3.28 (m, 2 H, C(26)H_2), 3.65 - 3.75 (m, 4 H, C(20)H_2+C(22)H_2), 4.16 (t, J=7.0 Hz, 2 H, C(16)H_2), 5.94 (s, 2 H, C(34)H_2), 6.70 (dd, J=8.0, 1.5 Hz, 1 H, C(28)H), 6.73 - 6.78 (m, 2 H, C(29)H+C(32)H), 7.14 (dd, J=8.0, 1.5 Hz, 1 H, C(2)H), 7.37 (d, J=8.0 Hz, 1 H, C(3)H), 7.64 (d, J=1.5 Hz, 1 H, C(6)H); ^{13}C NMR (126 MHz, $CDCl_3$) δ ppm 10.9 (s, 1 C, C(14)), 11.6 (s, 1 C, C(15)), 29.9 (s, 1 C, C(25)), 33.6 (s, 1 C, C(26)), 41.5 (s, 1 C, C(16)), 54.0 (s, 2 C, C(19)+C(23)), 57.6 (s, 1 C, C(17)), 66.8 (s, 2 C, C(20)+C(22)), 100.9 (s, 1 C, C(34)), 108.4 (s, 1 C, C(32)), 108.8 (s, 1 C, C(29)), 109.4 (s, 1 C, C(3)), 117.0 (s, 1 C, C(7)), 119.9 (s, 1 C, C(6)), 121.2 (s, 1 C, C(28)), 123.5 (s, 1 C, C(2)), 124.3 (s, 1 C, C(1)), 134.2 (s, 1 C, C(4)), 134.6 (s, 1 C, C(27)), 142.9 (s, 1 C, C(5)), 146.1 (s, 1 C, C(30)), 147.8 (s, 1 C, C(31)), 155.2 (s, 1 C, C(24)), 159.0 (s, 1 C, C(10)), 165.0 (s, 1 C, C(13)); R_f 0.25 (EtOAc:MeOH:NEt_3, 95:5:0.5); LRMS m/z (ESI^+) 475 [MH^+]; HRMS (ESI^+) found 475.2325, calculated for $C_{27}H_{31}N_4O_4^+$ 475.2340; HPLC (System E) t_r 3.6 min (88%).

2-[2-(2,3-Dihydro-1-benzofuran-5-yl)ethyl]-5-(3,5-dimethyl-1,2-oxazol-4-yl)-1-[2-(morpholin-4-yl)ethyl]-1*H*-benzimidazole (339)

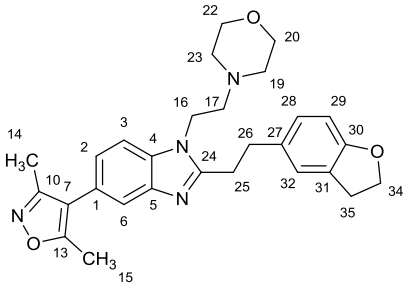

3-(2,3-Dihydro-1-benzofuran-5-yl)propanoic acid (27 mg, 0.14 mmol) was reacted with compound **316** (0.13 mmol) according to general procedure H. The product was obtained as an orange/brown gum (17 mg, 28%); R_f 0.25 (EtOAc:MeOH:NEt_3, 95:5:0.5); ν_{max} (neat) 2926 (C-H), 2855 (C-H), 2817 (C-H); ^{1}H NMR (400 MHz, $CDCl_3$) δ ppm 2.30 (s, 3 H, C(14)H_3), 2.43 (s, 3 H, C(15)H_3), 2.49 (m, *J*=4.0 Hz, 4 H, C(19)H_2+C(23)H_2), 2.63 (t, *J*=7.0 Hz, 2 H, C(17)H_2), 3.13 - 3.27 (m, 6 H, C(25)H_2+C(26)H_2+C(33)H_2), 3.65 - 3.73 (m, 4 H, C(20)H_2+C(22)H_2), 4.15 (t, *J*=7.0 Hz, 2 H, C(16)H_2), 4.56 (t, *J*=8.5 Hz, 2 H, C(34)H_2), 6.73 (d, *J*=8.0 Hz, 1 H, C(29)*H*), 6.97 (d, *J*=8.0 Hz, 1 H, C(28)*H*), 7.09 (s, 1 H, C(32)*H*), 7.13 (d, *J*=8.5 Hz, 1 H, C(2)*H*), 7.37 (d, *J*=8.5 Hz, 1 H, C(3)*H*), 7.64 (s, 1 H, C(6)*H*); ^{13}C NMR (101 MHz, $CDCl_3$) δ ppm 10.9 (s, 1 C, *C*(14)), 11.6 (s, 1 C, *C*(15)), 29.7 (s, 1 C, *C*(35)), 30.2 (s, 1 C, *C*(25)), 33.3 (s, 1 C, *C*(26)), 41.4 (s, 1 C, *C*(16)), 54.0 (s, 2 C, *C*(19)+*C*(23)), 57.5 (s, 1 C, *C*(17)), 66.8 (s, 2 C, *C*(20)+*C*(22)), 71.2 (s, 1 C, *C*(34)), 109.3 (s, 1 C, *C*(3/29)), 109.4 (s, 1 C, *C*(3/29)), 117.0 (s, 1 C, *C*(7)), 119.8 (s, 1 C, *C*(6)), 123.4 (s, 1 C, *C*(2)), 124.3 (s, 1 C, *C*(1)), 125.0 (s, 1 C, *C*(32)), 127.4 (s, 1 C, *C*(31)), 127.7 (s, 1 C, *C*(28)), 132.8 (s, 1 C, *C*(27)), 134.2 (s, 1 C, *C*(4)), 142.9 (s, 1 C, *C*(5)), 155.4 (s, 1 C, *C*(24)), 158.7 (s, 1 C, *C*(30)), 159.0 (s, 1 C, *C*(10)), 165.0 (s, 1 C, *C*(13)); LRMS *m/z* (ESI^+) 473 [MH^+]; HRMS (ESI^+) found 473.2535, calculated for $C_{28}H_{33}N_4O_3^+$ 473.2547; HPLC (System E) t_r 3.6 min (87%).

5-(3,5-Dimethyl-1,2-oxazol-4-yl)-1-[2-(morpholin-4-yl)ethyl]-2-[2-(thiophen-2-yl)ethyl]-1*H*-benzimidazole (340)

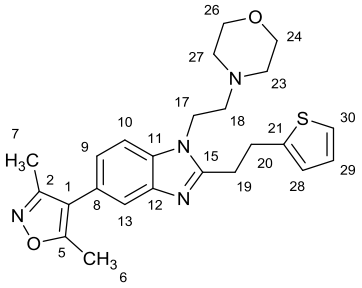

2-Thiophenepropionic acid (28 mg, 0.18 mmol) was reacted with compound **316** (50 mg, 0.16 mmol) according to general procedure G. Chromatography was carried out with a gradient of CH_2Cl_2:MeOH:NH_4OH, which was increased linearly from 99:1:0.1 to 92:8:0.8 over 30 CVs. The product was obtained as a colourless gum (31 mg, 44%); R_f 0.45 (CH_2Cl_2:MeOH:NH_4OH, 90:10:1); ν_{max} (neat) 2964 (C-H), 2924 (C-H), 2847, (C-H), 2817 (C-H); ^{1}H NMR (400 MHz, $CDCl_3$) δ ppm 2.30 (s, 3 H, C(7)H_3), 2.43 (s, 3 H, C(6)H_3), 2.45 - 2.51 (m, 4 H, C(23)H_2+C(37)H_2), 2.63 (t, J=6.5 Hz, 2 H, C(18)H_2), 3.24 - 3.33 (m, 2 H, C(19)H_2), 3.51 - 3.58 (m, 2 H, C(20)H_2), 3.64 - 3.71 (m, 4 H, C(24)H_2+C(26)H_2), 4.17 (t, J=6.5 Hz, 2 H, C(17)H_2), 6.86 (d, J=3.5 Hz, 1 H, C(28)H), 6.93 (dd, J=5.0, 3.5 Hz, 1 H, C(29)H), 7.10 - 7.19 (m, 2 H, C(9)H+C(30)H), 7.36 (d, J=8.0 Hz, 1 H, C(10)H), 7.63 (d, J=1.0 Hz, 1 H, C(13)H); ^{13}C NMR (101 MHz, $CDCl_3$) δ ppm 10.9 (s, 1 C, C(7)), 11.5 (s, 1 C, C(6)), 27.8 (s, 1 C, C(20)), 29.9 (s, 1 C, C(19)), 41.4 (s, 1 C, C(17)), 54.0 (s, 2 C, C(23)+C(27)), 57.6 (s, 1 C) 66.8 (s, 2 C, C(24)+C(26)), 109.4 (s, 1 C, C(10)), 117.0 (s, 1 C, C(1)), 119.9 (s, 1 C, C(13)), 123.5 (s, 1 C, C(9)), 123.6 (s, 1 C, C(28)), 124.2 (s, 1 C, C(8)), 124.9 (s, 1 C, C(30)), 127.0 (s, 1 C, C(29)), 134.2 (s, 1 C, C(11)), 143.0 (s, 1 C, C(12/21)), 143.2 (s, 1 C, C(12/21)), 154.7 (s, 1 C, C(15)), 159.0 (s, 1 C, C(2)), 165.0 (s, 1 C, C(5)); LRMS *m/z* (ESI$^+$) 895 [(2M+Na)$^+$], 873 [(2M+H)$^+$], 459 [(M+Na)$^+$], 437 [MH$^+$]; HRMS (ESI$^+$) found 437.2011, calculated for $C_{24}H_{29}N_4O_2S^+$ 437.2006; HPLC (System E) t_r 3.4 min (94%).

5-(3,5-Dimethyl-1,2-oxazol-4-yl)-2-[2-(1*H*-indol-1-yl)ethyl]-1-[2-(morpholin-4-yl)ethyl]-1*H*-benzimidazole (341)

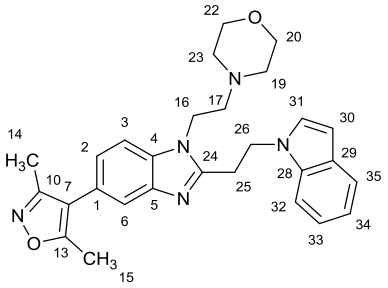

3-(1*H*-Indol-1-yl)propanoic acid (26 mg, 0.14 mmol) was reacted with compound **316** (0.13 mmol) according to general procedure H. The product was obtained as a pale brown gum (25 mg, 41%); R_f 0.20 (EtOAc:MeOH:NEt_3, 90:10:1); ν_{max} (neat) 2965 (C-H), 2846 (C-H), 2813 (C-H); ^{1}H NMR (400 MHz, $CDCl_3$) δ ppm 2.14 - 2.18 (m, 4 H, C(19)H_2+C(23)H_2), 2.26 - 2.34 (m, 5 H, C(17)H_2+C(14)H_3), 2.44 (s, 3 H, C(15)H_3), 3.40 (t, *J*=6.5 Hz, 2 H, C(25)H_2), 3.53 - 3.58 (m, 4 H, C(20)H_2+C(22)H_2), 3.61 (t, *J*=7.0 Hz, 2 H, C(16)H_2), 4.80 (t, *J*=6.5 Hz, 2 H, C(26)H_2), 6.43 (d, *J*=3.0 Hz, 1 H, C(30)*H*), 6.91 (d, *J*=3.0 Hz, 1 H, C(31)*H*), 7.08 - 7.15 (m, 2 H, C(2)*H*+C(34)*H*), 7.19 (t, *J*=7.5 Hz, 1 H, C(33)*H*), 7.26 - 7.31 (m, 1 H, C(2)*H*), 7.36 (d, *J*=8.5 Hz, 1 H, C(3)*H*), 7.56 - 7.66 (m, 2 H, C(6)*H*+C(35)*H*); ^{13}C NMR (101 MHz, $CDCl_3$) δ ppm 10.9 (s, 1 C, *C*(14)), 11.6 (s, 1 C, *C*(15)), 28.4 (s, 1 C, *C*(25)), 40.9 (s, 1 C, *C*(16)), 45.0 (s, 1 C, *C*(26)), 53.6 (s, 2 C, *C*(19)+*C*(23)), 57.2 (s, 1 C, *C*(17)), 66.7 (s, 2 C, *C*(20)+*C*(22)), 101.8 (s, 1 C, *C*(30)), 108.9 (s, 1 C, *C*(32)), 109.6 (s, 1 C, *C*(3)), 117.0 (s, 1 C, *C*(7)), 119.7 (s, 1 C, *C*(6/34)), 119.8 (s, 1 C, *C*(6/34)), 121.3 (s, 1 C, *C*(35)), 121.8 (s, 1 C, *C*(33)), 123.7 (s, 1 C, *C*(2)), 124.5 (s, 1 C, *C*(1)), 127.9 (s, 1 C, *C*(31)), 128.8 (s, 1 C, *C*(29)), 134.1 (s, 1 C, *C*(4)), 135.4 (s, 1 C, *C*(28)), 142.9 (s, 1 C, *C*(5)), 153.2 (s, 1 C, *C*(24)), 158.9 (s, 1 C, *C*(10)), 165.0 (s, 1 C, *C*(13)); LRMS *m/z* (ESI$^+$) 492 [(M+Na)$^+$], 470 [MH$^+$]; HRMS (ESI$^+$) found 470.2540, calculated for $C_{28}H_{32}N_5O_2^+$ 470.2551; HPLC (System D) t_r 10.1 min (93%).

2-(2-{5-(3,5-Dimethyl-1,2-oxazol-4-yl)-1-[2-(morpholin-4-yl)ethyl]-1*H*-benzimidazol-2-yl}ethyl)-1,3-benzothiazole (342)

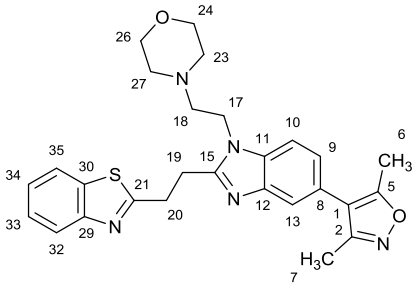

3-(1,3-Benzothiazol-2-yl)propanoic acid (37 mg, 0.14 mmol) was reacted with compound **316** (50 mg, 0.16 mmol) according to general procedure G. Chromatography was carried out with a gradient of CH_2Cl_2:MeOH:NH_4OH, which was increased linearly from 99:1:0.1 to 92:8:0.8 over 30 CVs. The product was obtained as a light brown gum (30 mg, 38%); R_f 0.40 (CH_2Cl_2:MeOH:NH_4OH, 90:10:1); ν_{max} (neat) 2926 (C-H), 2854 (C-H), 2816 (C-H); ^{1}H NMR (400 MHz, $CDCl_3$) δ ppm 2.30 (s, 3 H, C(7)H_3), 2.43 (s, 3 H, C(6)H_3), 2.46 - 2.54 (m, 4 H, C(23)H_2+C(27)H_2), 2.71 (t, J=6.5 Hz, 2 H, C(18)H_2), 3.52 - 3.62 (m, 2 H, C(19)H_2), 3.63 - 3.73 (m, 4 H, C(24)H_2+C(26)H_2), 3.82 - 3.93 (m, 2 H, C(20)H_2), 4.30 (t, J=6.5 Hz, 2 H, C(17)H_2), 7.13 (d, J=8.5 Hz, 1 H, C(9)H), 7.33 - 7.40 (m, 2 H, C(10)H+C(33/34)H), 7.47 (t, J=8.0 Hz, 1 H, C(33/34)H), 7.63 (s, 1 H, C(13)H), 7.84 (d, J=8.0 Hz, 1 H, C(32/35)H), 7.97 (d, J=8.0 Hz, 1 H, C(32/35)H); ^{13}C NMR (101 MHz, $CDCl_3$) δ ppm 10.8 (s, 1 C, C(7)), 11.5 (s, 1 C, C(6)), 26.3 (s, 1 C, C(19)), 31.5 (s, 1 C, C(20)), 41.5 (s, 1 C, C(17)), 54.0 (s, 2 C, C(23)+C(27)), 57.8 (s, 1 C, C(18)), 66.8 (s, 2 C, C(24)+C(26)), 109.4 (s, 1 C, C(10)), 117.0 (s, 1 C, C(1)), 119.9 (s, 1 C, C(10)), 121.6 (s, 1 C, C(32/35)), 122.5 (s, 1 C, C(32/35)), 123.5 (s, 1 C, C(9)), 124.3 (s, 1 C, C(8)), 124.9 (s, 1 C, C(33/34)), 126.0 (s, 1 C, C(33/34)), 134.4 (s, 1 C, C(11)), 135.2 (s, 1 C, C(30)), 142.9 (s, 1 C, C(12)), 153.1 (s, 1 C, C(29)), 154.3 (s, 1 C, C(15)), 159.0 (s, 1 C, C(7)), 165.0 (s, 1 C, C(6)), 169.7 (s, 1 C, C(21)); LRMS *m/z* (ESI$^+$) 997 [(2M+Na)$^+$], 975 [(2M+H)$^+$], 510 [(M+Na)$^+$], 488 [MH$^+$]; HRMS (ESI$^+$) found 488.2103, calculated for $C_{27}H_{30}N_5O_2S^+$ 488.2115; HPLC (System E) t_r 3.7 min (93%).

5-(3,5-Dimethyl-1,2-oxazol-4-yl)-2-[2-(1-methyl-1*H*-indol-5-yl)ethyl]-1-[2-(morpholin-4-yl)ethyl]-1*H*-benzimidazole (343)

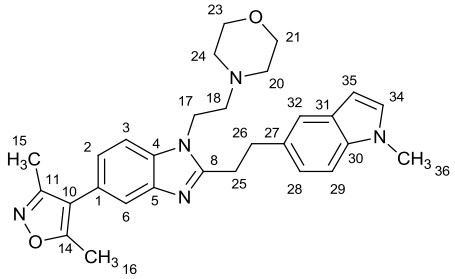

3-(1-Methyl-1*H*-indol-5-yl)propanoic acid (28 mg, 0.14 mmol) was reacted with compound **316** (0.13 mmol) according to general procedure H. The product was obtained as a colourless gum (35 mg, 56%); R_f 0.45 (EtOAc:MeOH:NEt_3, 90:10:1); ν_{max} (neat) 2930 (C-H), 2856 (C-H), 2818 (C-H); ^{1}H NMR (400 MHz, $CDCl_3$) δ ppm 2.31 (s, 3 H, C(15)H_3), 2.38 - 2.42 (m, 4 H, C(20)H_2+C(24)H_2), 2.44 (s, 3 H, C(16)H_3), 2.51 (t, *J*=7.0 Hz, 2 H, C(18)H_2), 3.20 - 3.33 (m, 2 H, C(25)H_2), 3.33 - 3.49 (m, 2 H, C(26)H_2), 3.61 - 3.74 (m, 4 H, C(21)H_2+C(23)H_2), 3.79 (s, 3 H, C(36)H_3), 4.11 (t, *J*=7.0 Hz, 2 H, C(17)H_2), 6.43 (dd, *J*=3.0, 0.8 Hz, 1 H, C(35)*H*), 7.06 (d, *J*=3.0 Hz, 1 H, C(34)*H*), 7.09 (dd, *J*=8.5, 1.5 Hz, 1 H, C(28)*H*), 7.13 (dd, *J*=8.5, 1.5 Hz, 1 H, C(2)*H*), 7.26 (d, *J*=8.5 Hz, 1 H, C(29)*H*), 7.38 (d, *J*=8.5 Hz, 1 H, C(3)*H*), 7.50 (d, *J*=1.5 Hz, 1 H, C(32)*H*), 7.66 (d, *J*=1.5 Hz, 1 H, C(6)*H*); ^{13}C NMR (101 MHz, $CDCl_3$) δ ppm 10.9 (s, 1 C, *C*(15)), 11.6 (s, 1 C, *C*(16)), 30.6 (s, 1 C, *C*(25)), 32.9 (s, 1 C, *C*(36)), 34.2 (s, 1 C, *C*(26)), 41.2 (s, 1 C, *C*(17)), 53.7 (s, 2 C, *C*(20)+*C*(24)), 57.2 (s, 1 C, *C*(18)), 66.6 (s, 2 C, *C*(21)+*C*(23)), 100.5 (s, 1 C, *C*(35)), 109.4 (s, 1 C, *C*(3/29)), 109.5 (s, 1 C, *C*(3/29)), 117.0 (s, 1 C, *C*(10)), 119.7 (s, 1 C, *C*(6)), 120.1 (s, 1 C, *C*(32)), 122.2 (s, 1 C, *C*(28)), 123.4 (s, 1 C, *C*(2)), 124.3 (s, 1 C, *C*(1)), 128.8 (s, 1 C, *C*(31)), 129.3 (s, 1 C, *C*(34)), 131.6 (s, 1 C, *C*(27)), 134.1 (s, 1 C, *C*(4)), 135.6 (s, 1 C, *C*(30)), 142.7 (s, 1 C, *C*(5)), 155.7 (s, 1 C, *C*(8)), 159.0 (s, 1 C, *C*(11)), 165.0 (s, 1 C, *C*(14)); LRMS *m/z* (ESI$^+$) 506 [(M+Na)$^+$], 484 [MH$^+$]; HRMS (ESI$^+$) found 484.2699, calculated for $C_{29}H_{34}N_5O_2^+$ 484.2707; HPLC (System D) t_r 9.5 min (>99%).

5-(3,5-Dimethyl-1,2-oxazol-4-yl)-2-[2-(2-methyl-1*H*-benzimidazol-5-yl)ethyl]-1-[2-(morpholin-4-yl)ethyl]-1*H*-benzimidazole (344)

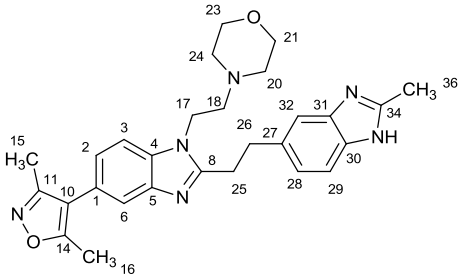

3-(2-methyl-1*H*-benzimidazol-5-yl)propanoic acid (53 mg, 0.26 mmol) was reacted with compound **316** (40mg, 0.13 mmol) according to general procedure I. Chromatography was carried out with a gradient of CH_2Cl_2:MeOH:NH_4OH which was increased linearly from 99:1:0.1 to 90:10:1 over 20 CVs. The product was obtained as a brown gum (39 mg, 62%); R_f 0.35 (EtOAc:MeOH:NEt_3, 90:10:1); ν_{max} (neat) 2927 (C-H), 2855 (C-H), 2814 (C-H); ^{1}H NMR (400 MHz, $CDCl_3$) δ ppm 2.27 (s, 3 H, C(15)H_3), 2.41 (s, 3 H, C(16)H_3), 2.43 - 2.48 (m, 4 H, C(20)H_2+C(24)H_2), 2.58 - 2.66 (m, 5 H, C(18)H_2+C(36)H_3), 3.24 - 3.32 (m, 2 H, C(25)H_2), 3.33 - 3.41 (m, 2 H, C(26)H_2), 3.63 - 3.70 (m, 4 H, C(21)H_2+C(23)H_2), 4.16 (t, *J*=6.5 Hz, 2 H, C(17)H_2), 5.43 (br. s, 1 H, N*H*), 7.06 (dd, *J*=8.5, 1.5 Hz, 1 H, C(28)*H*), 7.14 (dd, *J*=8.0, 1.5 Hz, 1 H, C(2)*H*), 7.35 - 7.41 (m, 3 H, C(3)*H*+C(29)*H*+C(32)*H*), 7.57 (d, *J*=1.5 Hz, 1 H, C(6)*H*); ^{13}C NMR (126 MHz, $CDCl_3$) δ ppm 10.8 (s, 1 C, *C*(15)), 11.5 (s, 1 C, *C*(16)), 14.9 (s, 1 C, *C*(36)), 30.2 (s, 1 C, *C*(25)), 34.1 (s, 1 C, *C*(26)), 41.5 (s, 1 C, *C*(17)), 54.0 (s, 2 C, *C*(20)+*C*(24)), 57.6 (s, 1 C, *C*(18)), 66.8 (s, 2 C, *C*(21)+*C*(23)), 109.5 (s, 1 C, *C*(3)), 114.0 (s, 1 C, *C*(29/32)), 114.4 (s, 1 C, *C*(29/32)), 117.0 (s, 1 C, *C*(10)), 119.7 (s, 1 C, *C*(6)), 122.8 (s, 1 C, *C*(28)), 123.5 (s, 1 C, *C*(2)), 124.3 (s, 1 C, *C*(1)), 134.2 (s, 1 C, *C*(4)), 134.9 (s, 1 C, *C*(27)), 137.0 (s, 1 C, *C*(30/31)), 138.7 (s, 1 C, *C*(30/31)), 142.8 (s, 1 C, *C*(5)), 151.1 (s, 1 C, *C*(34)), 155.4 (s, 1 C, *C*(8)), 158.9 (s, 1 C, *C*(11)), 165.0 (s, 1 C, *C*(14)); LRMS *m/z* (ESI$^+$) 485 [MH$^+$], 483 [(M-H)$^-$]; HRMS (ESI$^+$) found 485.2653, calculated for $C_{28}H_{33}N_6O_2^+$ 485.2660; HPLC (System E) t_r 2.9 min (93%).

4-(2-{5-(3,5-Dimethyl-1,2-oxazol-4-yl)-1-[2-(morpholin-4-yl)ethyl]-1*H*-benzimidazol-2-yl}ethyl)-3,4-dihydro-2*H*-1,4-benzoxazine (345)

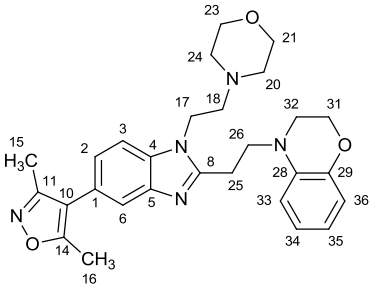

3-(2,3-Dihydro-4*H*-1,4-benzoxazin-4-yl)propanoic acid (29 mg, 0.14 mmol) was reacted with compound **316** (0.13 mmol) according to general procedure H. The product was obtained as a pale-yellow gum (17 mg, 43%); R_f 0.45 (EtOAc:MeOH:NEt_3, 90:10:1); ν_{max} (neat) 2950 (C-H), 2853 (C-H), 1502; ^{1}H NMR (400 MHz, $CDCl_3$) δ ppm 2.30 (s, 3 H, C(15)H_3), 2.43 (s, 7 H, C(16)H_3+C(20)H_2+C(24)H_2), 2.67 (t, *J*=6.5 Hz, 2 H, C(18)H_2), 3.24 (t, *J*=7.0 Hz, 2 H, C(25)H_2), 3.27 - 3.33 (m, 2 H, C(32)H_2), 3.58 - 3.78 (m, 4 H, C(21)H_2+C(23)H_2), 3.99 (t, *J*=7.0 Hz, 2 H, C(26)H_2), 4.11 - 4.18 (m, 2 H, C(31)H_2), 4.18 - 4.30 (m, 2 H, C(17)H_2), 6.61 - 6.69 (m, 1 H, C(34/35)*H*), 6.76 (dd, *J*=8.0, 1.5 Hz, 1 H, C(33/36)*H*), 6.82 (dd, *J*=8.0, 1.5 Hz, 1 H, C(33/36)*H*), 6.84 - 6.89 (m, 1 H, C(34/35)*H*), 7.16 (dd, *J*=8.5, 1.5 Hz, 1 H, C(2)*H*), 7.38 - 7.48 (m, 1 H, C(3)*H*), 7.63 (d, *J*=1.5 Hz, 1 H, C(6)*H*); ^{13}C NMR (101 MHz, $CDCl_3$) δ ppm 10.9 (s, 1 C, *C*(15)), 11.6 (s, 1 C, *C*(16)), 23.7 (s, 1 C, *C*(25)), 41.2 (s, 1 C, *C*(17)), 47.8 (s, 1 C, *C*(20)), 49.4 (s, 1 C, *C*(18)), 53.7 (s, 2 C, *C*(20)+*C*(24)), 57.3 (s, 1 C, *C*(18)), 64.4 (s, 1 C, *C*(31)), 66.4 (s, 2 C, *C*(21)+*C*(23)), 109.6 (s, 1 C, *C*(3)), 111.6 (s, 1 C, *C*(36)), 116.8 (s, 1 C, *C*(33)), 116.9 (s, 1 C, *C*(10)), 117.9 (s, 1 C, *C*(34/35)), 119.7 (s, 1 C, *C*(6)), 121.8 (s, 1 C, *C*(34/37)), 123.8 (s, 1 C, *C*(2)), 124.7 (s, 1 C, *C*(1)), 133.9 (s, 1 C, *C*(4/5)), 134.1 (s, 1 C, *C*(4/5)), 144.2 (s, 1 C, *C*(4/5)), 153.9 (s, 1 C, *C*(8)), 158.9 (s, 1 C, *C*(11)), 165.1 (s, 1 C, *C*(14)); LRMS *m/z* (ESI^+) 510 [$(M+Na)^+$], 488 [MH^+]; HRMS (ESI^+) found 488.2637, calculated for $C_{28}H_{34}N_5O_3^+$ 488.2656; HPLC (System D) t_r 9.9 min (92%).

4-(3-{5-(3,5-Dimethyl-1,2-oxazol-4-yl)-1-[2-(morpholin-4-yl)ethyl]-1*H*-benzimidazol-2-yl}propyl)-3,4-dihydro-2*H*-1,4-benzoxazine (346)

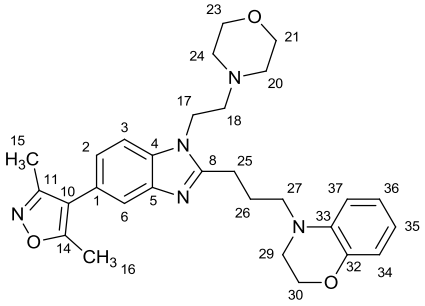

4-(2,3-Dihydro-4*H*-1,4-benzoxazin-4-yl)butanoic acid (31 mg, 0.14 mmol) was reacted with compound **316** (0.13 mmol) according to general procedure H. The product was obtained as a pale-brown gum (18 mg, 28%); R_f 0.40 (EtOAc:MeOH:NEt_3, 90:10:1); ν_{max} (neat) 2932 (C-H), 2855 (C-H); ^{1}H NMR (500 MHz, $CDCl_3$) δ ppm 2.25 - 2.36 (m, 5 H, C(15)H_3+C(26)H_2), 2.41 - 2.44 (m, 3 H, C(16)H_3), 2.46 - 2.54 (m, 4 H, C(20)H_2+C(24)H_2), 2.71 (t, J=6.5 Hz, 2 H, C(18)H_2), 3.01 (t, J=7.5 Hz, 2 H, C(25)H_2), 3.36 - 3.41 (m, 2 H, C(29)H_2), 3.48 (t, J=7.0 Hz, 2 H, C(27)H_2), 3.66 - 3.75 (m, 4 H, C(21)H_2+C(23)H_2), 4.19 - 4.23 (m, 2 H, C(30)H_2), 4.26 (t, J=6.5 Hz, 2 H, C(17)H_2), 6.60 (td, J=7.5, 1.5 Hz, 1 H, C(35)H), 6.63 (dd, J=8.0, 1.5 Hz, 1 H, C(37)H), 6.73 - 6.79 (m, 2 H, C(34)H+C(36)H), 7.15 (dd, J=8.5, 1.5 Hz, 1 H, C(2)H), 7.40 (d, J=8.5 Hz, 1 H, C(3)H), 7.63 (d, J=1.5 Hz, 1 H, C(6)H); ^{13}C NMR (126 MHz, $CDCl_3$) δ ppm 10.8 (s, 1 C, C(15)), 11.5 (s, 1 C, C(16)), 24.3 (s, 1 C, C(26)), 24.5 (s, 1 C, C(25)), 41.2 (s, 1 C, C(17)), 47.1 (s, 1 C, C(29)), 50.0 (s, 1 C, C(27)), 53.8 (s, 2 C, C(20)+C(24)), 57.3 (s, 1 C, C(18)), 64.4 (s, 1 C, C(30)), 66.5 (s, 2 C, C(21)+C(23)), 109.5 (s, 1 C, C(3)), 112.0 (s, 1 C, C(34/37)), 116.5 (s, 1 C, C(35/36)), 116.9 (s, 1 C, C(10)), 117.6 (s, 1 C, C(35/36)), 119.7 (s, 1 C, C(6)), 121.5 (s, 1 C, C(34/37)), 123.8 (s, 1 C, C(2)), 124.6 (s, 1 C, C(1)), 134.0 (s, 1 C, C(4)), 135.2 (s, 1 C, C(33)), 144.0 (s, 1 C, C(32)), 155.1 (s, 1 C, C(8)), 158.9 (s, 1 C, C(11)), 165.1 (s, 1 C, C(14)); LRMS *m/z* (ESI$^+$) 524 [(M+Na)$^+$], 502 [MH$^+$]; HRMS (ESI$^+$) found 502.2806, calculated for $C_{29}H_{36}N_5O_3^+$ 502.2813; HPLC (System D) t_r 10.0 min (99%).

4-Bromo-2-(bromomethyl)-1-nitrobenzene (348)

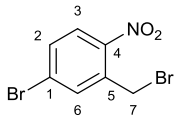

3-Bromobenzyl bromide (5.00 g, 20.0 mmol) was added portion-wise to cooled (-10 °C) *c*.H_2SO_4 (20 mL). *c*.HNO_3 (4 mL) was added drop-wise at a rate which maintained the temperature below 0 °C. The mixture was allowed to warm to room temperature over 2 h then poured onto crushed ice (50 mL). Once all the ice had melted, the resultant mixture was extracted with EtOAc (20 mL). The phases were separated then the organic phase was washed with water (3×20 mL) and brine (20 mL) then dried over $MgSO_4$ and evaporated directly onto silica. The crude material was purified by flash column chromatography on a silica column (330 g). The column was eluted with a gradient of EtOAc:*c*-hexane which was increased linearly from 2:98 to 20:80 over 10 CVs. The desired fractions were combined and evaporated to yield the product as a pale-yellow solid (2.27 g, 39%); mp 75-78 °C {lit.[278] mp 77-78 °C}; R_f 0.35 (EtOAc:*c*-hexane, 10:90); ^{1}H NMR (500 MHz, $CDCl_3$) δ ppm 4.79 (s, 2 H, C(7)H_2), 7.63 (dd, *J*=8.5, 2.0 Hz, 1 H, C(2)*H*), 7.75 (d, *J*=2.0 Hz, 1 H, C(6)*H*), 7.95 (d, *J*=8.5 Hz, 1 H, C(3)*H*); ^{13}C NMR (126 MHz, $CDCl_3$) δ ppm 27.9 (s, 1 C, *C*(10)), 127.0 (s, 1 C, *C*(3)), 128.4 (s, 1 C, *C*(1)), 132.7 (s, 1 C, *C*(2)), 134.7 (s, 1 C, *C*(5)), 135.4 (s, 1 C, *C*(6)), 146.6 (s, 1 C, *C*(4)); HRMS (FI$^+$) found 294.8723, calculated for $C_7H_5Br_2NO_2^+$ 294.8667; HPLC (System E) t_r 5.8 min (>99%).

(5-Bromo-2-nitrobenzyl)(triphenyl)phosphonium bromide (349)

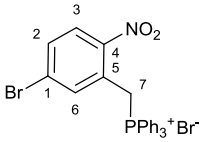

Triphenyl phosphine (1.95 g, 7.46 mmol) was added to a stirred solution of compound **348** (2.20 g, 7.45 mmol) in $CHCl_3$ (15 mL). The mixture was stirred for 64 h at room temperature

then concentrate *in vacuo*. $CHCl_3$ (15 mL) and Et_2O (15 mL) were added then the solid was collected by filtration. The solid was dried under vacuum to yield the product as a pale yellow solid (4.15 g, quant.); mp 269-271 °C {lit.[278] mp 256-258 °C}; ^{1}H NMR (400 MHz, $CDCl_3$) δ ppm 6.23 (d, *J*=15.0 Hz, 2 H, C(7)H_2), 7.61 (dt, *J*=9.0, 2.5 Hz, 1 H, C(2)*H*), 7.63 - 7.70 (m, 6 H, 6×Ph*H*), 7.70 - 7.78 (m, 6 H, 6×Ph*H*), 7.78 - 7.85 (m, 4 H, 3×Ph*H*+C(3)*H*), 8.16 (t, *J*=2.5 Hz, 1 H, C(6)*H*); ^{13}C NMR (101 MHz, $CDCl_3$) δ ppm 28.2 (d, *J*=48.5 Hz, 1 C, *C*(7)), 116.9 (d, *J*=86.0 Hz, 3 C, 3×Ar*C*) 126.6 (d, *J*=8.5 Hz, 1 C, *C*(5) 126.9 (d, *J*=2.5 Hz, 1 C, *C*(3)), 129.8 (d, *J*=3.0 Hz, 1 C, *C*(1)), 130.4 (d, *J*=12.5 Hz, 6 C, 6×Ar*C*) 133.1 (d, *J*=3.0 Hz, 1 C, *C*(2)), 134.2 (d, *J*=10.5 Hz, 6 C, 6×Ar*C*) 135.4 (d, *J*=3.0 Hz, 3 C, 3×Ar*C*) 137.6 (d, *J*=5.5 Hz, 1 C, *C*(6)), 147.1 (d, *J*=5.5 Hz, 1 C, *C*(4)); ^{31}P NMR (162 MHz, $CDCl_3$) δ ppm 24.8 (s, 1 P); LRMS *m/z* (ESI$^+$) 478 [M(^{81}Br)$^+$], 476 [M(^{79}Br)$^+$]; HPLC (System E) t_r 4.7 min (93%).

(2-Amino-5-bromobenzyl)(triphenyl)phosphonium chloride hydrochloride (350)

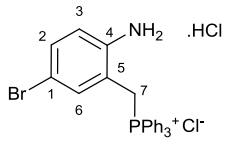

Zinc dust (2.96 g, 45.3 mmol) was added portion-wise to a solution of compound **349** (5.05 g, 9.06 mmol) in AcOH (90 mL). The resultant suspension was stirred at room temperature for 1 h then filtered through Celite. The filter cake was washed with MeCN then the filtrate was concentrated *in vacuo*. The residue was azeotroped with toluene (2×50 mL) then dried under high vacuum to yield the desired product as a beige foam (4.67 g, 99%); ^{1}H NMR (400 MHz, DMSO-d_6) δ ppm 4.94 (d, *J*=15.0 Hz, 2 H, C(7)H_2), 6.54 (d, *J*=8.5 Hz, 1 H, C(2)*H*), 6.60 (t, *J*=2.5 Hz, 1 H, C(3)*H*), 7.13 (dt, *J*=9.0, 2.0 Hz, 1 H, C(6)*H*), 7.62 - 7.80 (m, 12 H, 12×Ph*H*), 7.85 - 8.01 (m, 3 H, 3×Ph*H*); ^{13}C NMR (101 MHz, DMSO-d_6) δ ppm 24.3 (d, *J*=47.5 Hz, 1 C, *C*(7)), 106.6 (d, *J*=4.0 Hz, 1 C, *C*(1)), 112.4 (d, *J*=8.0 Hz, 1 C, *C*(5)), 117.9 (d, *J*=85.0 Hz, 3 C, 3×Ph*C*) 118.0 (d, *J*=3.0 Hz, 1 C, *C*(2)), 130.1 (d, *J*=12.0 Hz, 6 C, 6×Ph*C*) 131.8 (d, *J*=3.0 Hz, 1 C, *C*(6)), 133.6 (d, *J*=5.0 Hz, 1 C, *C*(3)), 134.1 (d, *J*=9.5 Hz, 6 C, 6×Ph*C*) 135.2 (d, *J*=2.5 Hz, 3 C, 3×Ph*C*)

146.9 (d, *J*=5.5 Hz, 1 C, *C*(4)); ^{31}P NMR (162 MHz, DMSO-d_6) δ ppm 21.5 (s, 1 P); LRMS *m/z* (ESI$^+$) 448 [M(^{81}Br)$^+$], 446[M(^{79}Br)$^+$]; HPLC (System E) t_r 4.7 min (99%).

(5-Bromo-2-{[3-(3-chloro-4-methoxyphenyl)propanoyl]amino}benzyl)(triphenyl)phosphonium chloride (351)

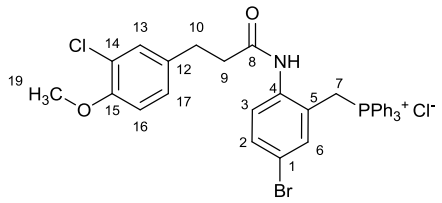

Oxalyl chloride (239 µL, 2.83 mmol) was added to a solution of 3-(3-chloro-4-methoxyphenyl)propanoic acid (488 mg, 0.94 mmol) in CH_2Cl_2 (5 mL). DMF (1 drop) was added then the resultant solution was stirred at room temperature for 1 h. The solvent was evaporated by nitrogen blow-down. The residue was re-dissolved in CH_2Cl_2 (5 mL) then evaporated by blow-down. The residue was dissolved in CH_2Cl_2 (1 mL) then added drop-wise to a cooled (0 °C) solution of compound **350** (202 mg, 0.94 mmol) in DMF (1.5 mL) and pyridine (0.5 mL). The mixture was allowed to warm to room temperature then stirred for 16 h. The solvent was evaporated by nitrogen blow-down then the residue was partitioned between EtOAc (5 mL) and 1 M aq. HCl solution (5 mL). The phases were separated then the organic phase was washed with brine (5 mL) then dried over $MgSO_4$ and evaporated. The crude material was suspended in Et_2O (5 mL) then the supernatant was decanted off with a pipette. The solid material was dried under vacuum to yield the product as a yellow solid (243 mg, 56%); mp 169-171 °C; ν_{max} (neat) 3064 (C-H), 2909 (C-H), 1687 (C=O) ; ^{1}H NMR (400 MHz, $CDCl_3$) δ ppm 2.41 - 2.49 (m, 2 H, C(10)H_2), 2.56 - 2.64 (m, 2 H, C(9)H_2), 3.76 (s, 3 H, C(19)H_3), 5.61 (d, *J*=14.5 Hz, 2 H, C(7)H_2), 6.69 - 6.79 (m, 2 H, C(6)*H*+C(16)*H*), 7.06 - 7.19 (m, 3 H, C(2)*H*+C(13)*H*+C(17)*H*), 7.44 - 7.56 (m, 7 H, C(3)*H*+6×Ph*H*), 7.56 - 7.71 (m, 9 H, 9×Ph*H*), 10.28 (br. s., 1 H, N*H*); ^{13}C NMR (101 MHz, $CDCl_3$) δ ppm 27.5 (d, *J*=46.0 Hz, 1 C, *C*(7)), 30.1 (s, 1 C, *C*(10)), 37.6 (s, 1 C, *C*(9)), 56.1 (s, 1 C, *C*(19)), 112.1 (s, 1 C, *C*(16)), 116.9

(d, *J*=4.0 Hz, 1 C, *C*(1)), 117.6 (d, *J*=86.0 Hz, 3 C, 3×Ph*C*) 121.6 (s, 1 C, *C*(14)), 121.9 (d, *J*=8.5 Hz, 1 C, *C*(5)), 127.5 (s, 1 C, *C*(12)), 127.7 (d, *J*=4.0 Hz, 1 C, *C*(3)), 128.0 (s, 1 C, *C*(17)), 130.1 (d, *J*=12.0 Hz, 6 C, 6×Ph*C*) 130.3 (s, 1 C, *C*(13)), 131.7 (d, *J*=4.0 Hz, 1 C, *C*(2)), 134.3 (d, *J*=9.5 Hz, 6 C, 6×Ph*C*) 134.5 (d, *J*=18.5 Hz, 1 C, *C*(6)), 134.9 (d, *J*=3.0 Hz, 3 C, 3×Ph*C*) 137.4 (d, *J*=5.5 Hz, 1 C, *C*(4)), 153.0 (s, 1 C, *C*(15)), 171.9 (s, 1 C, *C*(8)); LRMS *m/z* (ESI$^+$) 645 [M(^{81}Br)$^+$], 643 [M(^{79}Br)$^+$]; HRMS found 644.0943, calculated for $C_{35}H_{31}(^{81}Br)ClNO_2P^+$ 644.0939, found 642.0959, calculated for $C_{35}H_{31}(^{79}Br)ClNO_2P^+$ 642.0959; HPLC (System E) t_r 6.2 min (85%).

2-[2-(3-Chloro-4-methoxyphenyl)ethyl]-5-(3,5-dimethyl-1,2-oxazol-4-yl)-1*H*-indole (353)

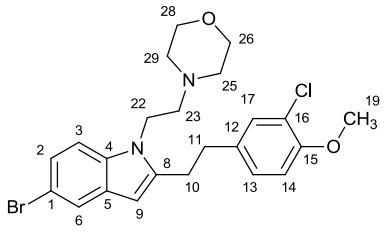

A suspension of compound **351** (318 mg, 0.46 mmol) and KO*t*-Bu (63 mg, 0.57 mmol) in anhydrous toluene (4 mL) was crimp-sealed in a microwave vial then heated under microwave irradiation for 15 minutes at 130 °C. The resultant mixture was partitioned between EtOAc (5 mL) and 1 M aq. HCl (5 mL). The phases were separated then the organic phase was washed with water (5 mL) and brine (5 mL) then dried over $MgSO_4$ and evaporated directly onto silica. The crude material was purified by flash column chromatography on a silica column (4 g). The column was eluted with a gradient of EtOAc:*c*-hexane which was increased linearly from 10:90 to 30:70 over 12 CVs. The desired fractions were combined and evaporated to yield the intermediate bromoindole **352** as an off-white solid (94 mg, 56%). The bromoindole **352** was dissolved in DMF (1 mL) then 4-(2-chloroethyl)morpholine hydrochloride (53 mg, 0.28 mmol), and K_2CO_3 (108 mg, 0.78 mmol) were added. The mixture was heated at 80 °C for 2 h then potassium iodide (46 mg, 0.28 mmol) was added. The mixture was heated at 80°C for 16 h then allowed to cool. The solids

were removed by filtration then NaH (60% dispersion in mineral oil, 11 mg, 0.28 mmol) was added. The mixture was heated at 80 °C for 3 h then more 4-(2-chloroethyl)morpholine hydrochloride (53 mg, 0.28 mmol) and NaH (60% dispersion in mineral oil, 11 mg, 0.28 mmol) were added. The mixture was heated at 80 °C for a further 24 h then allowed to cool. The mixture was partitioned between EtOAc (5 mL) and water (5 mL). The phases were separated then the organic phase was washed with water (5 mL) and brine (5 mL) then dried over $MgSO_4$ and evaporated. The crude material was purified by flash column chromatography on a silica column (4 g) which was eluted with EtOAc. The desired fractions were combined and evaporated to yield the product as a yellow/brown gum (30 mg, 24% from bromoindole); R_f 0.30 (EtOAc); mp 157-160 °C; ^{1}H NMR (400 MHz, $CDCl_3$) δ ppm 2.31 - 2.42 (m, 4 H, C(25)H_2+C(29)H_2), 2.50 (t, *J*=7.0 Hz, 2 H, C(23)H_2), 2.93 (s, 4 H, C(10)H_2+C(11)H_2), 3.56 - 3.68 (m, 4 H, C(26)H_2+C(28)H_2), 3.81 (s, 3 H, C(19)H_3), 4.05 (t, *J*=7.0 Hz, 2 H, C(22)H_2), 6.15 (s, 1 H, C(9)*H*), 6.78 (d, *J*=8.5 Hz, 1 H, C(14)*H*), 6.97 (dd, *J*=8.5, 2.0 Hz, 1 H, C(13)*H*), 7.07 (d, *J*=8.5 Hz, 1 H, C(3)*H*), 7.15 (dd, *J*=8.5, 2.0 Hz, 1 H, C(2)*H*), 7.18 (d, *J*=2.0 Hz, 1 H, C(17)*H*), 7.57 (d, *J*=2.0 Hz, 1 H, C(6)*H*); ^{13}C NMR (101 MHz, $CDCl_3$) δ ppm 28.6 (s, 1 C, *C*(10)), 33.4 (s, 1 C, *C*(11)), 41.0 (s, 1 C, *C*(22)), 54.0 (s, 2 C, *C*(25)+*C*(29)), 56.2 (s, 1 C, *C*(19)), 57.7 (s, 1 C, *C*(23)), 66.7 (s, 2 C, *C*(26)+*C*(28)), 98.9 (s, 1 C, *C*(9)), 110.3 (s, 1 C, *C*(3)), 112.1 (s, 1 C, *C*(14)), 112.7 (s, 1 C, *C*(1)), 122.3 (s, 1 C, *C*(16)), 122.5 (s, 1 C, *C*(6)), 123.5 (s, 1 C, *C*(2)), 127.5 (s, 1 C, *C*(13)), 129.7 (s, 1 C, *C*(5)), 130.0 (s, 1 C, *C*(17)), 134.1 (s, 1 C, *C*(12)), 135.1 (s, 1 C, *C*(4)), 141.1 (s, 1 C, *C*(8)), 153.5 (s, 1 C, *C*(15)); LRMS *m/z* (ESI$^+$) 479 [M(^{81}Br)H$^+$], 477 [M(^{79}Br)H$^+$]; HRMS (ESI$^+$) found 479.0902, calculated for $C_{23}H_{27}(^{81}Br)ClN_2O_2^+$ 479.0918, found 477.0926, calculated for $C_{23}H_{27}(^{79}Br)ClN_2O_2^+$ 477.0939; HPLC (System E) t_r 6.5 min (72%).

2-[2-(3-Chloro-4-methoxyphenyl)ethyl]-5-(3,5-dimethyl-1,2-oxazol-4-yl)-1-[2-(morpholin-4-yl)ethyl]-1*H*-indole (354)

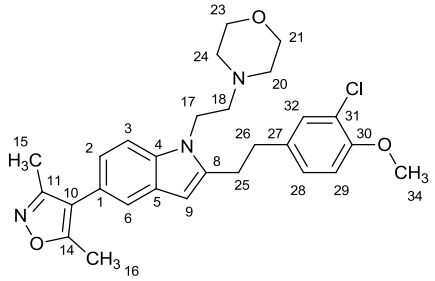

$Pd(dppf)Cl_2$ (5 mg, 0.0063 mmol) was added to a solution of compound **353** (30 mg, 0.063 mmol) and 3,5-dimethylisoxazole-4-boronic acid pinacol ester (17 mg, 0.075 mmol) in DME (0.5 mL). The mixture was stirred then saturated aq. $NaHCO_3$ solution (0.2 mL) was added. The mixture was degassed by evacuating and refilling with nitrogen (×3) then heated at 80 °C for 2 h. The reaction was allowed to cool then partitioned between EtOAc (1 mL) and water (1 mL). The phases were separated then organic phase was passed through a hydrophobic frit then evaporated. The crude material was purified by flash column chromatography on a silica column (4 g). The column was eluted with a gradient of EtOAc:*c*-hexane, which was increased linearly from 80:20 to 100:0 over 30 column volumes (CVs). The desired fractions were combined and evaporated then then the material was dissolved in MeOH and loaded onto a pre-wetted SCX-cartridge (1 g). Non-basic components were eluted with MeOH then the captured product was released by elution with methanolic ammonia solution (7 M). The basic eluent was evaporate to yield the product as a yellow gum (13 mg, 42%); R_f 0.45 (EtOAc); ν_{max} (neat) 2958 (C-H), 2854 (C-H); ^{1}H NMR (400 MHz, $CDCl_3$) δ ppm 2.29 (s, 3 H, C(15)H_3), 2.42 (s, 3 H, C(16)H_3), 2.46 - 2.57 (m, 4 H, C(20)H_2+C(24)H_2), 2.66 (t, *J*=6.5 Hz, 2 H, C(18)H_2), 2.97 - 3.15 (m, 4 H, C(25)H_2+C(26)H_2), 3.64 - 3.78 (m, 4 H, C(21)H_2+C(23)H_2), 3.91 (s, 3 H, C(34)H_3), 4.16 - 4.28 (m, 2 H, C(17)H_2), 6.33 (s, 1 H, C(9)*H*), 6.88 (d, *J*=8.5 Hz, 1 H, C(29)*H*), 7.04 (dd, *J*=8.5, 1.5 Hz, 1 H, C(2)*H*), 7.10 (dd, *J*=8.5, 2.0 Hz, 1 H, C(28)*H*), 7.30 (d, *J*=2.0 Hz, 1 H, C(32)*H*), 7.35 (d, *J*=8.5 Hz, 1 H, C(3)*H*), 7.41 (d, *J*=1.5 Hz, 1 H, C(6)*H*); ^{13}C NMR (126 MHz, $CDCl_3$) δ ppm 10.9 (s, 1 C, *C*(15)), 11.5 (s, 1

C, *C*(16)), 28.6 (s, 1 C, *C*(25)), 33.6 (s, 1 C, *C*(26)), 40.8 (s, 1 C, *C*(17)), 53.9 (s, 2 C, *C*(20)+*C*(24)), 56.2 (s, 1 C, *C*(34)), 57.7 (s, 1 C, *C*(18)), 66.7 (s, 2 C, *C*(21)+*C*(23)), 99.5 (s, 1 C, *C*(9)), 109.2 (s, 1 C, *C*(3)), 112.2 (s, 1 C, *C*(29)), 117.5 (s, 1 C, *C*(10)), 120.7 (s, 1 C, *C*(6)), 121.6 (s, 1 C, *C*(1)), 122.3 (s, 2 C, *C*(2)+*C*(31)), 127.6 (s, 1 C, *C*(28)), 128.3 (s, 1 C, *C*(5)), 130.0 (s, 1 C, *C*(32)), 134.2 (s, 1 C, *C*(27)), 135.7 (s, 1 C, *C*(4)), 140.7 (s, 1 C, *C*(8)), 153.5 (s, 1 C, *C*(30)), 159.2 (s, 1 C, *C*(11)), 164.7 (s, 1 C, *C*(14)); LRMS *m/z* (ESI$^+$) 496 [M(^{37}Cl)H$^+$], 494[M(^{35}Cl)H$^+$]; HRMS (ESI$^+$) found 494.2191, calculated for $C_{28}H_{33}(^{35}Cl)N_3O_3^+$ 494.2205, found 496.2182, calculated for $C_{28}H_{33}(^{37}Cl)N_3O_3^+$ 496.2178; HPLC (System E) t_r 5.0 min (94%).

{5-(3,5-Dimethyl-1,2-oxazol-4-yl)-1-[2-(morpholin-4-yl)ethyl]-1*H*-benzimidazol-2-yl}methanol (355)

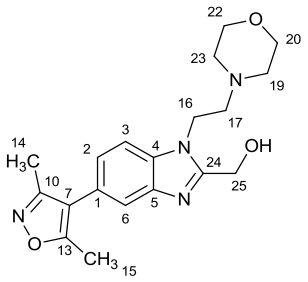

A mixture of compound **316** (316 mg, 1.00 mmol) and glycolic acid (114 mg, 1.50 mmol) in 6 M aq. HCl (5 mL) was heated under microwave irradiation for 20 minutes at 180 °C. The pH of the resultant solution was made basic by drop-wise addition of 20% aq. NaOH solution. The mixture was extracted with EtOAc (10 mL). The phases were separated then the organic phase was washed with water (10 mL) and brine (10 mL) then dried over $MgSO_4$ and evaporated. The crude material was purified by flash column chromatography on a silica column (24 g). The column was eluted with a gradient of CH_2Cl_2:MeOH:NH_4OH which was increased linearly from 99:1:0.1 to 90:10:1 over 12 CVs. The desired fractions were combined and evaporated to yield the product as a pale-orange solid (221 mg, 62%); R_f 0.35 (CH_2Cl_2:MeOH:NH_4OH, 90:10:1); mp 154-158 °C; ν_{max} (neat) 3122 (O-H), 2842 (C-H), 2813

(C-H); ^{1}H NMR (400 MHz, $CDCl_3$) δ ppm 2.28 (s, 3 H, C(14)H_3), 2.41 (s, 3 H, C(15)H_3), 2.49 - 2.70 (m, 4 H, C(19)H_2+C(23)H_2), 2.88 (t, *J*=5.5 Hz, 2 H, C(17)H_2), 3.66 - 3.83 (m, 4 H, C(20)H_2+C(22)H_2), 4.43 (t, *J*=5.5 Hz, 2 H, C(16)H_2), 4.91 (s, 2 H, C(25)H_2), 7.18 (dd, *J*=8.5, 1.5 Hz, 1 H, C(2)*H*), 7.41 (d, *J*=8.5 Hz, 1 H, C(3)*H*), 7.64 (d, *J*=1.5 Hz, 1 H, C(6)*H*); ^{13}C NMR (101 MHz, $CDCl_3$) δ ppm 10.8 (s, 1 C, *C*(14)), 11.5 (s, 1 C, *C*(15)), 42.0 (s, 1 C, *C*(16)), 54.3 (s, 2 C, *C*(19)+*C*(23)), 56.8 (s, 1 C, *C*(25)), 57.8 (s, 1 C, *C*(17)), 66.1 (s, 2 C, *C*(20)+*C*(22)), 109.6 (s, 1 C, *C*(6)), 116.8 (s, 1 C, *C*(7)), 120.6 (s, 1 C, *C*(3)), 124.4 (s, 1 C, *C*(2)), 125.0 (s, 1 C, *C*(1)), 134.1 (s, 1 C, *C*(5)), 142.3 (s, 1 C, *C*(4)), 154.7 (s, 1 C, *C*(24)), 158.8 (s, 1 C, *C*(10)), 165.1 (s, 1 C, *C*(13)); LRMS *m/z* (ESI$^+$) 379 [(M+Na)$^+$], 357 [MH$^+$], (ESI$^-$) 355 [(M-H)$^-$]; HRMS (ESI$^+$) found 357.1914, calculated for $C_{19}H_{25}N_4O_3^+$ 357.1921; HPLC (System E) t_r 2.7 min (>99%).

2-(Chloromethyl)-5-(3,5-dimethyl-1,2-oxazol-4-yl)-1-[2-(morpholin-4-yl)ethyl]-1*H*-benzimidazole (356)

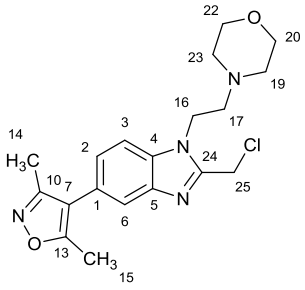

A mixture of compound **316** (300 mg, 0.95 mmol) and chloroacetic acid (83 mg, 0.88 mmol) in 6 M aq. HCl (5 mL) was heated at 100 °C for 16 h. The resultant brown solution was allowed to cool to room temperature then cooled further in an ice bath. The pH was made basic by drop-wise addition of 20% aq. NaOH solution. The mixture was extracted with EtOAc (5 mL). The organic phase was separated then washed with water (5 mL) and brine (5 mL) then dried over $MgSO_4$ and evaporated. The crude material was purified by flash column chromatography on a silica column (24 g). The column was eluted with a gradient of EtOAc:MeOH, which was increased linearly from 100:0 to 90:10 over 12 CVs. The desired fractions were combined and evaporated to yield the product as a pale brown residue (49

mg, 14%); R_f 0.30 (EtOAc:MeOH, 90:10); ^{1}H NMR (400 MHz, $CDCl_3$) δ ppm 2.27 (s, 3 H, C(14)H_3), 2.41 (s, 3 H, C(15)H_3), 2.48 - 2.59 (m, 4 H, C(19)H_2+C(23)H_2), 2.81 (t, J=6.5 Hz, 2 H, C(17)H_2), 3.66 - 3.73 (m, 4 H, C(20)H_2+C(22)H_2), 4.41 (t, J=6.5 Hz, 2 H, C(16)H_2), 4.98 (s, 2 H, C(25)H_2), 7.20 (dd, J=8.5, 1.0 Hz, 1 H, C(2)H), 7.44 (d, J=8.5 Hz, 1 H, C(3)H), 7.63 (s, 1 H, C(6)H); ^{13}C NMR (101 MHz, $CDCl_3$) δ ppm 10.8 (s, 1 C, C(14)), 11.5 (s, 1 C, C(15)), 37.0 (s, 1 C, C(25)), 42.2 (s, 1 C, C(16)), 54.1 (s, 2 C, C(19)+C(23)), 57.8 (s, 1 C, C(17)), 66.8 (s, 2C, C(20)+C(22)), 110.0 (s, 1 C, C(3)), 116.8 (s, 1 C, C(7)), 120.9 (s, 1 C, C(6)), 124.9 (s, 1 C, C(2)), 125.0 (s, 1 C, C(1)), 134.7 (s, 1 C, C(4)), 142.5 (s, 1 C, C(5)), 150.2 (s, 1 C, C(24)), 158.8 (s, 1 C, C(10)), 165.1 (s, 1 C, C(13)); LRMS *m/z* (ESI$^+$) 375 [MH$^+$]; HRMS (ESI$^+$) found 375.1573, calculated for $C_{19}H_{24}ClN_4O_2^+$ 375.1582; HPLC (System D) t_r 9.0 min (91%).

5-(3,5-Dimethyl-1,2-oxazol-4-yl)-1-ethenyl-2-(morpholin-4-ylmethyl)-1*H*-benzimidazole (357)

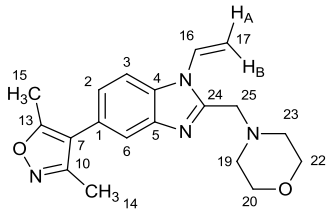

A mixture of compound **356** (50 mg, 0.13 mmol), 3-chloro-4-methoxyaniline (42 mg, 0.27 mmol) and K_2CO_3 (37 mg, 0.27 mmol) in DMF (1 mL) was heated at 70 °C for 16 h. The mixture was allowed to cool then partitioned between EtOAc and water (5 mL). The phases were separated then the organic phase was washed with water (5 mL) and brine (5 mL) then dried over $MgSO_4$ and concentrated *in vacuo*. The crude material was purified by flash column chromatography on a silica column (4 g). The column was eluted with a gradient of EtOAc:MeOH:NEt_3 which was increased linearly from 99:1:0.1 to 96:4:0.4 over 30 CVs. The desired fractions were combined and evaporated to yield the product as a pale brown gum (18 mg, 41%); R_f 0.45 (EtOAc:MeOH:NEt_3, 90:10:1); ^{1}H NMR (400 MHz, $CDCl_3$) δ ppm 2.29 (s, 3 H, C(14)H_3), 2.42 (s, 3 H, C(15)H_3), 2.51 - 2.67 (m, 4 H, C(19)H_2+C(23)H_2), 3.68 - 3.78 (m, 4

H, C(20)H_2+C(22)H_2), 3.84 (s, 2 H, C(25)H_2), 5.29 (d, J=9.0 Hz, 1 H, C(17)H_AH_B), 5.68 (d, J=16.0 Hz, 1 H, C(17)H_AH_B), 7.20 (dd, J=8.5, 1.5 Hz, 1 H, C(2)H), 7.48 (dd, J=16.0, 9.0 Hz, 1 H, C(16)H), 7.63 (d, J=1.5 Hz, 1 H, C(6)H), 7.69 (d, J=8.5 Hz, 1 H, C(3)H); ^{13}C NMR (101 MHz, $CDCl_3$) δ ppm 10.8 (s, 1 C, C(14)), 11.5 (s, 1 C, C(15)), 53.4 (s, 2 C, C(19)+C(23)), 55.9 (s, 1 C, C(25)), 66.8 (s, 2 C, C(20)+C(22)), 106.6 (s, 1 C, C(17)), 111.7 (s, 1 C, C(3)), 116.7 (s, 1 C, C(7)), 120.5 (s, 1 C, C(6)), 124.8 (s, 1 C, C(2)), 125.1 (s, 1 C, C(1)), 129.3 (s, 1 C, C(16)), 133.5 (s, 1 C, C(4)), 143.0 (s, 1 C, C(5)), 150.8 (s, 1 C, C(24)), 158.9 (s, 1 C, C(10)), 165.1 (s, 1 C, C(13)); LRMS m/z (ESI$^+$) 361 [(M+Na)$^+$], 339 [MH$^+$], HRMS (ESI$^+$) found 339.1813, calculated for $C_{19}H_{23}N_4O_2^+$ 339.1816; HPLC (System E) t_r 3.5 min (97%).

5-(3,5-Dimethyl-1,2-oxazol-4-yl)-1-[2-(morpholin-4-yl)ethyl]-1,3-dihydro-2*H*-benzimidazol-2-one (358)

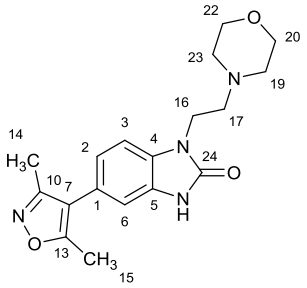

A solution of compound **316** (1.00 g, 3.16 mmol) and CDI (1.02 g, 6.32 mmol) in THF (10 mL) was heated under reflux for 16 h. The reaction mixture was allowed to cool then partitioned between EtOAc (20 mL) and water (20 mL). The phases were separated then the organic phase was washed with water (20 mL) and brine (20 mL) then dried over $MgSO_4$ and evaporated. The crude material was purified by flash column chromatography on silica (80 g). The column was eluted with a gradient of EtOAc:MeOH, which was increased linearly from 100:0 to 80:20 over 11 CVs. The desired fractions were combined and evaporated then the resultant material re-dissolved in EtOAc (20 mL). The solution was washed with water (2×20 mL) and brine (20 mL) then dried over $MgSO_4$ to yield the product as an off-white solid (0.78 g, 78%); R_f 0.25 (EtOAc:MeOH:NEt_3, 90:10:1); mp 180-183 °C; ν_{max} (neat) 2930

(C-H), 2857 (C-H), 2828 (C-H), 1703 (C=O); ^{1}H NMR (400 MHz, $CDCl_3$) δ ppm 2.26 (s, 3 H, C(14)H_3), 2.40 (s, 3 H, C(15)H_3), 2.52 - 2.64 (m, 4 H, C(19)H_2+C(23)H_2), 2.75 (t, J=7.0 Hz, 2 H, C(17)H_2), 3.61 - 3.75 (m, 4 H, C(20)H_2+C(22)H_2), 4.06 (t, J=7.0 Hz, 2 H, C(16)H_2), 6.96 (dd, J=8.0, 1.5 Hz, 1 H, C(2)H), 7.00 (s, 1 H, C(6)H), 7.10 (d, J=8.0 Hz, 1 H, C(3)H), 10.29 (s, 1 H, NH); ^{13}C NMR (101 MHz, $CDCl_3$) δ ppm 10.8 (s, 1 C, C(14)), 11.5 (s, 1 C, C(15)), 38.4 (s, 1 C, C(16)), 53.7 (s, 2 C, C(19)+C(23)), 56.2 (s, 1 C, C(17)), 66.9 (s, 2 C, C(20)+C(22)), 108.1 (s, 1 C, C(3)), 110.3 (s, 1 C, C(6)), 116.7 (s, 1 C, C(7)), 122.5 (s, 1 C, C(2)), 123.8 (s, 1 C, C(1)), 128.4 (s, 1 C, C(5)), 129.8 (s, 1 C, C(4)), 155.7 (s, 1 C, C(24)), 158.8 (s, 1 C, C(10)), 165.0 (s, 1 C, C(13)); LRMS *m/z* (ESI$^+$) 365 [(M+Na)$^+$], 343 [MH$^+$], (ESI$^-$) 341 [(M-H)$^-$]; HRMS (ESI$^+$) found 343.1752, calculated for $C_{18}H_{23}N_4O_3^+$ 343.1765; HPLC (System E) t_r 3.0 min (99%).

2-Chloro-5-(3,5-dimethyl-1,2-oxazol-4-yl)-1-[2-(morpholin-4-yl)ethyl]-1*H*-benzimidazole (359)

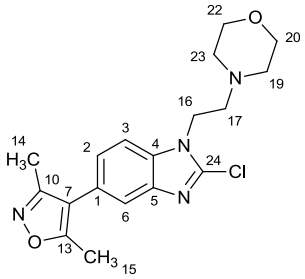

A suspension of compound **358** (319 mg, 0.93 mmol) in MeCN (10 mL) and $POCl_3$ (10 mL) was heated under reflux for 6 h. The resultant solution was allowed to cool then added drop-wise to warm water (*ca.* 40 °C). The resultant solution was cooled in an ice-bath then the pH was adjusted to 8 by careful addition of 10% aq. NaOH solution. The resultant suspension was extracted with EtOAc (20 mL). The organic phase was separated then dried over $MgSO_4$ and evaporated. The crude material was purified by flash column chromatography on a silica column (12 g). Eluted with EtOAc:MeOH:NEt_3, which was increased linearly from 100:0:0 to 90:10:1 over 12 CVs. The desired fractions were combined and evaporated to yield the product as a white solid (184 mg, 55%); R_f 0.30

(EtOAc); mp 164-166 °C; ν_{max} (neat) 2961 (C-H), 2922 (C-H), 2868 (C-H), 2849 (C-H); ^{1}H NMR (400 MHz, $CDCl_3$) δ ppm 2.28 (s, 3 H, C(14)H_3), 2.41 (s, 3 H, C(15)H_3), 3.24 - 3.37 (m, 4 H, C(19)H_2+C(23)H_2), 3.86 (t, *J*=7.0 Hz, 2 H, C(16)H_2), 3.90 - 3.94 (m, 4 H, C(20)H_2+C(22)H_2), 4.40 (t, *J*=7.0 Hz, 2 H, C(16)H_2), 7.09 (dd, *J*=8.5, 1.5 Hz, 1 H, C(2)*H*), 7.32 (d, *J*=8.5 Hz, 1 H, C(3)*H*), 7.52 (d, *J*=1.5 Hz, 1 H, C(6)*H*); ^{13}C NMR (101 MHz, $CDCl_3$) δ ppm 10.8 (s, 1 C, *C*(14)), 11.5 (s, 1 C, *C*(15)), 40.4 (s, 1 C, *C*(17)), 45.4 (s, 1 C, *C*(16)), 51.3 (s, 2 C, *C*(19)+*C*(23)), 66.5 (s, 2 C, *C*(20)+*C*(22)), 109.2 (s, 1 C, *C*(3)), 117.0 (s, 1 C, *C*(7)), 119.3 (s, 1 C, *C*(6)), 123.1 (s, 1 C, *C*(2)), 124.5 (s, 1 C, *C*(1)), 133.7 (s, 1 C, *C*(4)), 141.8 (s, 1 C, *C*(5)), 158.1 (s, 1 C, *C*(10/24)), 158.9 (s, 1 C, *C*(10/24)), 165.0 (s, 1 C, *C*(13)); LRMS *m/z* (ESI^+) 361 [MH^+]; HRMS (ESI^+) found 361.1417, calculated for $C_{18}H_{22}ClN_4O_2^+$ 361.1426, HPLC (System D) t_r 10.1 min (>99%).

5-(3,5-Dimethyl-1,2-oxazol-4-yl)-1-ethenyl-2-(morpholin-4-yl)-1*H*-benzimidazole (360)

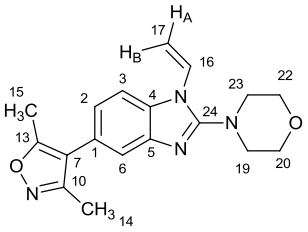

A mixture of 2-chloro-5-(3,5-dimethyl-1,2-oxazol-4-yl)-1-[2-(morpholin-4-yl)ethyl]-1*H*-benzimidazole (23 mg, 0.065 mmol) 4-methoxybenzyl alcohol (40 µL, 0.33 mmol) and KOH (11 mg, 0.20 mmol) in DMSO (0.1 mL) was heated at 70 °C for 3 h then allowed to cool. The mixture was partitioned between EtOAc (0.5 mL) and water (0.5 mL). The aqueous phase was decanted off with a pipette then the organic phase was washed with water (0.5 mL) and brine (0.5 mL) then passed through a hydrophobic frit. The crude material was purified by flash column chromatography on a silica column (4 g). The column was eluted with a gradient of EtOAc:MeOH:NEt_3 which was increased linearly from 99:1:0.1 to 97:3:0.3 over 30 CVs. The desired fractions were combined and evaporated then the resultant material

was re-purified on silica (4 g). The column was eluted with a gradient of EtOAc:*c*-hexane, which was increased from 50:50 to 100:0 over 30 CVs. The desired fractions were combined and evaporated to yield the product as a white solid (8 mg, 38%); R_f 0.50 (EtOAc:MeOH:NEt_3, 90:10:1); mp 119-123 °C; ν_{max} (neat) 2966 (C-H), 2920 (C-H), 2850 (C-H); ^{1}H NMR (500 MHz, $CDCl_3$) δ ppm 2.29 (s, 3 H, C(14)H_3), 2.42 (s, 3 H, C(15)H_3), 3.33 - 3.49 (m, 4 H, C(19)H_2+C(23)H_2), 3.81 - 3.94 (m, 4 H, C(20)H_2+C(22)H_2), 5.28 (d, *J*=8.5 Hz, 1 H, C(17)H_AH$_B$), 5.61 (dd, *J*=16.0, 1.0 Hz, 1 H, C(17)H$_A$$H_B$), 6.92 (dd, *J*=16.0, 8.5 Hz, 1 H, C(16)*H*), 7.08 (dd, *J*=8.0, 1.5 Hz, 1 H, C(2)*H*), 7.50 (d, *J*=1.5 Hz, 1 H, C(6)*H*), 7.53 (d, *J*=8.0 Hz, 1 H, C(2)*H*); ^{13}C NMR (126 MHz, $CDCl_3$) δ ppm 10.8 (s, 1 C, *C*(14)), 11.5 (s, 1 C, *C*(15)), 50.4 (s, 2 C, *C*(19)+*C*(23)), 66.4 (s, 2 C, *C*(20)+*C*(22)), 105.9 (s, 1 C, *C*(17)), 110.3 (s, 1 C, *C*(3)), 116.9 (s, 1 C, *C*(7)), 118.7 (s, 1 C, *C*(6)), 123.1 (s, 1 C, *C*(2)), 125.0 (s, 1 C, *C*(1)), 129.4 (s, 1 C, *C*(16)), 132.9 (s, 1 C, *C*(4)), 141.8 (s, 1 C, *C*(5)), 156.9 (s, 1 C, *C*(24)), 158.9 (s, 1 C, *C*(10)), 165.0 (s, 1 C, *C*(13)); LRMS *m/z* (ESI$^+$) 347 [(M+Na)$^+$], 325 [MH$^+$], HRMS (ESI$^+$) found 325.1650, calculated for $C_{18}H_{21}N_4O_2^+$ 325.1659; HPLC (System E) t_r 2.9 min (93%).

5-(3,5-Dimethyl-1,2-oxazol-4-yl)-2-[(3-fluoro-4-methoxyphenoxy)methyl]-1-[2-(morpholin-4-yl)ethyl]-1*H*-benzimidazole (361)

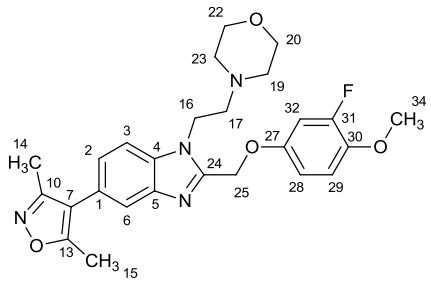

Tri-*n*-butylphosphine (165 µL, 0.66 mmol) was added to a solution of {5-(3,5-dimethyl-1,2-oxazol-4-yl)-1-[2-(morpholin-4-yl)ethyl]-1*H*-benzimidazol-2-yl}methanol (120 mg, 0.33 mmol), 3-fluoro-4-methoxyphenol (72 mg, 0.51 mmol) and ADDP (168 mg, 0.66 mmol) in CH_2Cl_2 (2 mL). The solution was stirred at room temperature for 16 h then diluted with methanol (3 mL) and loaded onto a pre-wetted SCX cartridge (2 g). Eluted with MeOH then

the captured basic components were eluted with CH_2Cl_2:MeOH:NH_4OH (90:10:1). The basic eluent was evaporated then the crude material was purified by flash column chromatography on a silica column (12 g). The column was eluted with a gradient of EtOAc:MeOH:NEt_3 which was increased linearly from 100:0:0 to 98:2:0.2 over 20 CVs. The desired fractions were combined and evaporated to yield the product as a yellow gum (107 mg, 67%); R_f 0.15 (EtOAc); ν_{max} (neat) 2953 (C-H), 2836 (C-H), 2800 (C-H), 1512; ^{1}H NMR (400 MHz, $CDCl_3$) δ ppm 2.29 (s, 3 H, C(14)H_3), 2.42 (s, 3 H, C(15)H_3), 2.48 - 2.71 (m, 4 H, C(19)H_2+C(23)H_2), 2.75 - 2.96 (m, 2 H, C(17)H_2), 3.67 - 3.81 (m, 4 H, C(20)H_2+C(22)H_2), 3.84 (s, 3 H, C(34)H_3), 4.42 - 4.61 (m, 2 H, C(16)H_2), 5.41 (s, 2 H, C(25)H_2), 6.80 - 6.93 (m, 3 H, C(28)H+C(29)H+C(32)H), 7.21 (dd, J=8.5, 1.5 Hz, 1 H, C(2)H), 7.46 - 7.59 (m, 1 H, C(2)H), 7.66 (d, J=1.5 Hz, 1 H, C(6)H); ^{13}C NMR (101 MHz, $CDCl_3$) δ ppm 10.8 (s, 1 C, C(14)), 11.5 (s, 1 C, C(15)), 41.5 (s, 1 C, C(16)), 53.8 (s, 2 C, C(19)+C(23)), 56.9 (s, 1 C, C(34)), 57.6 (s, 1 C, C(17)), 64.3 (s, 1 C, C(25)), 66.4 (s, 2 C, C(20)+C(22)), 104.6 (d, J=22.5 Hz, 1 C, C(32)), 109.3 (d, J=3.0 Hz, 1 C, C(29)), 110.0 (s, 1 C, C(3)), 114.4 (d, J=2.5 Hz, 1 C, C(28)), 116.8 (s, 1 C, C(7)), 120.8 (s, 1 C, C(6)), 124.8 (s, 1 C, C(2)), 124.9 (s, 1 C, C(1)), 134.7 (s, 1 C, C(4)), 142.5 (s, 1 C, C(5)), 142.7 (d, J=11.0 Hz, 1 C, C(24)), 150.0 (s, 1 C, C(24)), 152.7 (d, J=247.0 Hz, 1 C, C(31)), 151.8 (d, J=9.5 Hz, 1 C, C(27)), 158.9 (s, 1 C, C(10)), 165.1 (s, 1 C, C(13)); ^{19}F NMR (377 MHz, $CDCl_3$) δ ppm -131.4 (s, 1 F); LRMS *m/z* (ESI^+) 503 [$(M+Na)^+$], 481 [MH^+]; HRMS (ESI^+) found 481.2240, calculated for $C_{26}H_{30}FN_4O_4^+$ 481.2246; HPLC (System D) t_r 10.5 min (98%).

2-(Benzyloxy)-5-(3,5-dimethyl-1,2-oxazol-4-yl)-1-[2-(morpholin-4-yl)ethyl]-1*H*-benzimidazole (362)

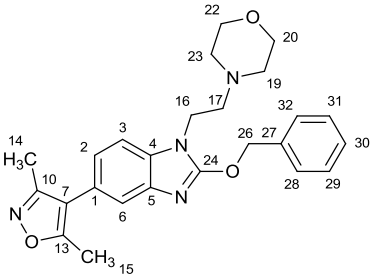

Benzyl bromide (59 µL, 0.50 mmol) was added to a suspension of 5-(3,5-dimethyl-1,2-oxazol-4-yl)-1-[2-(morpholin-4-yl)ethyl]-1,3-dihydro-2*H*-benzimidazol-2-one (100 mg, 0.33 mmol) and Ag_2CO_3 (182 mg, 0.66 mmol) in toluene (2 mL). The resultant suspension was heated at 80 °C for 16 h then allowed to cool. The mixture was evaporated directly onto silica then purified by flash column chromatography on a silica column (4 g). The column was eluted with a gradient of EtOAc:MeOH:NEt_3 which was increased linearly from 99:1:0.1 to 90:10:1 over 30 CVs. The desired fractions were combined and evaporated then the material was re-purified on silica (4 g). Eluted with a gradient of CH_2Cl_2:MeOH:NH_4OH which was increased linearly from 99:1:0.1 to 94:6:0.6 over 30 CVs. The desired fractions were combined and evaporated to yield the product as a colourless gum (33 mg, 23%); R_f 0.50 (EtOAc:MeOH:NEt_3, 90:10:1); ν_{max} (neat) 2970 (C-H), 1739; ^{1}H NMR (400 MHz, $CDCl_3$) δ ppm 2.30 (s, 3 H, C(14)H_3), 2.42 (s, 3 H, C(15)H_3), 2.44 - 2.53 (m, 4 H, C(19)H_2+C(23)H_2), 2.71 (t, *J*=6.5 Hz, 2 H, C(17)H_2), 3.55 - 3.64 (m, 4 H, C(20)H_2+C(22)H_2), 4.15 (t, *J*=6.5 Hz, 2 H, C(16)H_2), 5.61 (s, 2 H, C(26)H_2), 7.04 (dd, *J*=8.0, 1.5 Hz, 1 H, C(2)*H*), 7.25 (d, *J*=8.0 Hz, 1 H, C(3)*H*), 7.37 - 7.52 (m, 6 H, C(6)*H*+5×Ph*H*); ^{13}C NMR (101 MHz, $CDCl_3$) δ ppm 10.9 (s, 1 C, *C*(14)), 11.5 (s, 1 C, *C*(15)), 39.5 (s, 1 C, *C*(16)), 53.7 (s, 2 C, *C*(19)+*C*(23)), 56.9 (s, 1 C, *C*(17)), 66.7 (s, 2 C, *C*(20)+*C*(22)), 72.0 (s, 1 C, *C*(26)), 108.4 (s, 1 C, *C*(3)), 117.2 (s, 1 C, *C*(7)), 118.4 (s, 1 C, *C*(6)), 122.1 (s, 1 C, *C*(2)), 123.7 (s, 1 C, *C*(1)), 128.2 (s, 2 C, 2×Ar*C*) 128.7 (s, 3 C, 3×Ar*C*) 133.0 (s, 1 C, *C*(4)), 135.4 (s, 1 C, *C*(27)), 140.4 (s, 1 C, *C*(5)), 157.8 (s, 1 C, *C*(24)), 159.0 (s, 1 C, *C*(10)), 164.9 (s, 1 C, *C*(13)); LRMS *m/z* (ESI$^+$) 455 [(M+Na)$^+$], 433 [MH$^+$]; HRMS

(ESI$^+$) found 433.2218, calculated for $C_{25}H_{29}N_4O_3^+$ 433.2234; HPLC (System E) t_r 4.0 min (91%).

4-Bromo-5-fluoro-*N*-[2-(morpholin-4-yl)ethyl]-2-nitroaniline (364)

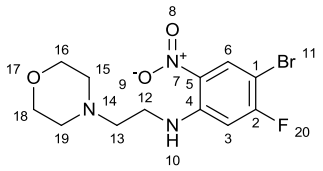

A solution of 4-(2-aminoethyl)morpholine (133 µL, 1.01 mmol) and EtN(*i*-Pr)$_2$ (261 µL, 1.50 mmol) in THF (2 mL) was added to a solution of 5-bromo-2,4-difluoronitrobenzene (238 mg, 1.00 mmol) in THF (3 mL). The mixture was left to stir at 0 °C for 1 h, allowed to warm to room temperature then stirred for 16 h at room temperature. The solution was concentrated *in vacuo* then partitioned between EtOAc (10 mL) and water (10 mL). The phases were separated then the organic phase was washed with water (10 mL) and brine (10 mL) then dried over $MgSO_4$ and evaporated. The organic phase was separated then dried over $MgSO_4$ and evaporated. The crude material was purified by flash column chromatography on a silica column (24 g). The column was eluted with EtOAc:*c*-hexane, which was increased linearly from 30:70 to 50:50 over 12 CVs. The desired fractions were combined and evaporated to yield the product as a yellow solid (230 mg, 66%); R_f 0.25 (EtOAc:*c*-hexane, 60:40); mp 139-144 °C; ν_{max} (neat) 3344 (N-H), 2922 (C-H), 2859 (C-H), 2813 (C-H), 1556 (N-O), 1397 (N-O); ^{1}H NMR (400 MHz, $CDCl_3$) δ ppm 2.47 - 2.60 (m, 4 H, C(15)H_2+C(19)H_2), 2.73 (t, *J*=5.5 Hz, 2 H, C(13)H_2), 3.30 (q, *J*=5.5 Hz, 2 H, C(12)H_2), 3.75 - 3.84 (m, 4 H, C(16)H_2+C(18)H_2), 6.57 (d, *J*=11.0 Hz, 1 H, C(3)*H*), 8.43 (d, *J*=7.0 Hz, 1 H, C(6)*H*), 8.64 (br. s., 1 H, N*H*); ^{13}C NMR (101 MHz, $CDCl_3$) δ ppm 39.6 (s, 1 C, *C*(12)), 53.1 (s, 2 C, *C*(15)+*C*(19)), 55.6 (s, 1 C, *C*(13)), 66.9 (s, 2 C, *C*(16)+*C*(18)), 94.3 (d, *J*=24.0 Hz, 1 C, *C*(1)), 100.6 (d, *J*=28.0 Hz, 1 C, *C*(3)), 129.2 (s, 1 C, *C*(5)), 132.1 (d, *J*=4.0 Hz, 1 C, *C*(6)), 146.1 (d, *J*=13.0 Hz, 1 C, *C*(4)), 163.5 (d, *J*=255.5 Hz, 1 C, *C*(2)); ^{19}F NMR (377 MHz, $CDCl_3$) δ ppm -94.9 (s, 1 F); LRMS *m/z* (ESI$^+$) 350 [(M(^{81}Br)+H)$^+$], 348 [(M(^{79}Br)+H)$^+$]; HRMS (ESI$^+$) found

348.0349, calculated for $C_{12}H_{16}(^{79}Br)FN_3O_3^+$ 348.0354; found 350.0329, calculated for $C_{12}H_{16}(^{81}Br)FN_3O_3^+$ 350.0334; HPLC (System E) t_r 3.5 min (>99%).

4-(3,5-Dimethyl-1,2-oxazol-4-yl)-5-fluoro-*N*-[2-(morpholin-4-yl)ethyl]-2-nitroaniline (365)

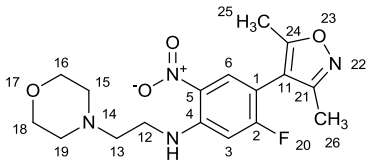

Pd(dppf)Cl_2 (24 mg, 0.033 mmol) was added to a solution of compound **364** (230 mg, 0.66 mmol) and 3,5-dimethylisoxazole-4-boronic acid pinacol ester (176 mg, 0.79 mmol) in DME (3 mL). The mixture was stirred then saturated aq. $NaHCO_3$ solution (2 mL) was added. The mixture was degassed by evacuating and refilling with nitrogen (×3) then heated at 80 °C for 6 h. The reaction was allowed to cool then partitioned between EtOAc (10 mL) and water (10 mL). The phases were separated then the organic phase was dried over $MgSO_4$ then evaporated. The crude material was purified by flash column chromatography on a silica column (25 g). The column was eluted with a gradient of EtOAc:*c*-hexane, which was increased linearly from 10:90 to 30:70 over 20 CVs. The desired fractions were combined and evaporated to yield the product as a yellow gum (112 mg, 16%); R_f 0.15 (EtOAc:*c*-hexane, 30:70); ν_{max} (neat) 2956 (C-H), 2920 (C-H), 2851 (C-H), 2816 (C-H), 1530 (N-O), 1356 (N-O); ^{1}H NMR (400 MHz, $CDCl_3$) δ ppm 2.21 (s, 3 H, C(26)H_3), 2.36 (s, 3 H, C(25)H_3), 2.50 - 2..62 (m, 4 H, C(15)H_2+C(19)H_2), 2.76 (t, *J*=6.0 Hz, 2 H, C(13)H_2), 3.36 (q, *J*=6.0 Hz, 2 H, C(12)H_2), 3.77 (t, *J*=4.5 Hz, 4 H, C(16)H_2+C(18)H_2), 6.59 (d, *J*=12.0 Hz, 1 H, C(3)*H*), 8.12 (d, *J*=8.0 Hz, 1 H, C(6)*H*), 8.70 (br. s., 1 H, N*H*); ^{13}C NMR (101 MHz, $CDCl_3$) δ ppm 10.5 (s, 1 C, *C*(26)), 11.6 (s, 1 C, *C*(25)), 39.6 (s, 1 C, *C*(12)), 53.1 (s, 2 C, *C*(15)+*C*(19)), 55.7 (s, 1 C, *C*(13)), 67.0 (s, 2 C, *C*(16)+*C*(18)), 100.2 (d, *J*=28.0 Hz, 1 C, *C*(3)), 109.4 (s, 1 C, *C*(1)), 118.8 (s, 1 C, *C*(11)), 128.9 (s, 1 C, *C*(5)), 130.8 (d, *J*=7.0 Hz, 1 C, *C*(6)), 146.7 (d, *J*=13.5 Hz, 1 C, *C*(4)), 159.2 (s, 1 C, *C*(21)), 164.7 (d, *J*=223.5 Hz, 1 C, *C*(2)), 166.7 (s, 1 C, *C*(24)); ^{19}F NMR (377 MHz,

$CDCl_3$) δ ppm -100.5 (s, 1 F); LRMS *m/z* (ESI^+) 365 [MH^+], (ESI^-) 363 [$(M-H)^-$]; HRMS (ESI^+) found 365.1608, calculated for $C_{11}H_9FN_2NaO_3^+$ 365.1620; HPLC (System E) t_r 2.8 min (95%).

5-(3,5-Dimethyl-1,2-oxazol-4-yl)-6-fluoro-1-[2-(morpholin-4-yl)ethyl]-2-(2-phenylethyl)-1*H*-benzimidazole (366)

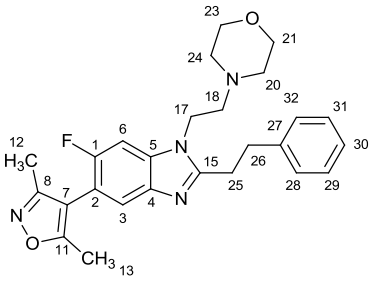

A freshly prepared aq. solution of $Na_2S_2O_4$ (1.0 M, 80 µL, 0.080 mmol) was added to a solution of compound **365** (10 mg, 0.027 mmol) and 2-phenylpropanal (3.6 µL mg, 0.027 mmol) in EtOH (0.1 mL) and DMSO (0.1 mL). The mixture was heated at 80 °C for 4 h then partitioned between water (1 mL) and EtOAc (1 mL). The aqueous phase was decanted off with a pipette then more water (1 mL) was added and the process repeated. The organic phase was dried by passing it through a hydrophobic frit. The solvent was evaporated then the crude material was purified by flash column chromatography on a silica column (4 g). The column was eluted with a gradient of EtOAc:*c*-hexane, which was increased linearly from 80:20 to 100:0 over 20 CVs. The desired fractions were combined and evaporated to yield the product as a colourless gum (12 mg, quant.); R_f 0.30 (EtOAc); ; ν_{max} (neat) 2923 (C-H), 2953 (C-H); ^{1}H NMR (500 MHz, $CDCl_3$) δ ppm 2.25 (s, 3 H, C(12)H_3), 2.38 (s, 3 H, C(13)H_3), 2.43 - 2.48 (m, 4 H, C(20)H_2+C(24)H_2), 2.59 (t, *J*=7.0 Hz, 2 H, C(18)H_2), 3.17 - 3.23 (m, 2 H, C(25)H_2), 3.26 - 3.33 (m, 2 H, C(26)H_2), 3.62 - 3.70 (m, 4 H, C(21)H_2+C(23)H_2), 4.06 (t, *J*=7.0 Hz, 2 H, C(17)H_2), 7.11 (d, *J*=9.5 Hz, 1 H, C(6)*H*), 7.25 (d, *J*=8.0 Hz, 3 H, C(28)*H*+C(30)*H*+C(32)*H*), 7.30 - 7.35 (m, 2 H, C(29)*H*+C(31)*H*), 7.56 (d, *J*=6.5 Hz, 1 H, C(3)*H*); ^{13}C NMR (126 MHz, $CDCl_3$) δ ppm 10.6 (s, *J*=3.0 Hz, 1 C, *C*(12)), 11.6 (s, 1 C, *C*(13)), 29.7 (s, 1 C, *C*(25)), 33.8 (s, 1 C, *C*(26)), 41.7 (s, 1 C, *C*(17)), 54.0 (s, 2 C, *C*(20)+*C*(24)), 57.5 (s,

1 C, *C*(18)), 66.8 (s, 2 C, *C*(21)+*C*(23)), 96.7 (d, *J*=28.5 Hz, 1 C, *C*(6)), 111.6 (s, 1 C, *C*(7)), 112.5 (d, *J*=19.0 Hz, 1 C, *C*(2)), 121.3 (d, *J*=5.0 Hz, 1 C, *C*(3)), 126.6 (s, 1 C, *C*(30)), 128.4 (s, 2 C, *C*(28)+*C*(32)), 128.7 (s, 2 C, *C*(29)+*C*(31)), 134.9 (d, *J*=12.5 Hz, 1 C, *C*(5)), 139.0 (s, 1 C, *C*(4)), 140.8 (s, 1 C, *C*(27)), 156.8 (d, *J*=240.5 Hz, 1 C, *C*(1)), 155.9 (s, 1 C, *C*(15)), 159.6 (s, 1 C, *C*(8)), 166.4 (s, 1 C, *C*(11)); ^{19}F NMR (377 MHz, $CDCl_3$) δ ppm -119.4 (s, 1 F); LRMS *m/z* (ESI^+) 471 [$(M+Na)^+$], 449 [MH^+]; HRMS (ESI^+) found 449.2339, calculated for $C_{26}H_{30}FN_4O_2^+$ 449.2347; HPLC (System E) t_r 2.9 min (94%).

5-(3,5-Dimethyl-1,2-oxazol-4-yl)-1-[2-(morpholin-4-yl)ethyl]-2-(2-phenylethyl)-1*H*-benzimidazol-6-ol (367)

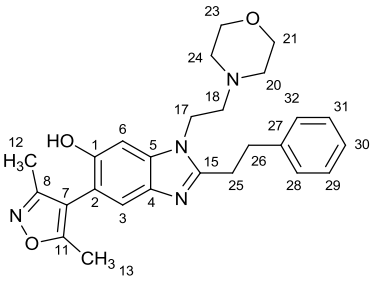

10% aq. KOH solution (50 µL) was added to a solution of **366** (10 mg, 0.027 mmol) in DMSO (0.1 mL). The solution was heated at 80 °C for 1 h then allowed to cool. The reaction mixture was partitioned between saturated aq. NH_4Cl (1 mL) and EtOAc (1 mL). The phases were separated then the organic phase was washed with water (1 mL) then passed through a hydrophobic frit and evaporated by N_2 blow-down. The residue was re-dissolved in EtOH (0.1 mL) and DMSO (0.1 mL) then 2-phenylpropanal (3.6 µL mg, 0.027 mmol) was added followed by a freshly prepared aq. solution of $Na_2S_2O_4$ (1.0 M, 80 µL, 0.080 mmol). The mixture was stirred at 80 °C for 4 h then allowed to cool. The solution was partitioned between water (1 mL) and EtOAc (1 mL). The aqueous phase was decanted off with a pipette then more water (1 mL) was added and the process repeated. The organic phase was dried by passing it through a hydrophobic frit. The solvent was evaporated then the crude material was purified by flash column chromatography on a silica column (4 g). The

column was eluted with a gradient of CH_2Cl_2:MeOH:NH_4OH, which was increased linearly from 99:1:0.1 to 90:10:1 over 30 CVs. The desired fractions were combined and evaporated to yield the product as a colourless gum (8.5mg, 71%); R_f 0.10 (CH_2Cl_2:MeOH:NH_4OH, 90:10:1); ν_{max} (neat) 2923 (C-H), 2852 (C-H); ^{1}H NMR (500 MHz, $CDCl_3$) δ ppm 2.18 (s, 3 H, C(12)H_3), 2.33 (s, 3 H, C(13)H_3), 2.38 - 2.52 (m, 4 H, C(20)H_2+C(24)H_2), 2.59 (t, *J*=7.0 Hz, 2 H, C(16)H_2), 3.12 - 3.19 (m, 2 H, C(25)H_2), 3.24 - 3.30 (m, 2 H, C(26)H_2), 3.64 - 3.71 (m, 4 H, C(21)H_2+C(23)H_2), 4.04 (t, *J*=7.0 Hz, 2 H, C(17)H_2), 5.50 (br. s., 1 H, O*H*), 6.92 (s, 1 H, C(6)*H*), 7.22 - 7.26 (m, 3 H, C(28)*H*+C(30)*H*+C(32)*H*), 7.29 - 7.34 (m, 2 H, C(29)*H*+C(31)*H*), 7.42 (s, 1 H, C(3)*H*); ^{13}C NMR (126 MHz, $CDCl_3$) δ ppm 10.5 (s, 1 C, *C*(12)), 11.5 (s, 1 C, *C*(13)), 29.6 (s, 1 C, *C*(25)), 33.8 (s, 1 C, *C*(26)), 41.4 (s, 1 C, *C*(17)), 54.0 (s, 2 C, *C*(20)+*C*(24)), 57.3 (s, 1 C, *C*(18)), 66.8 (s, 2 C, *C*(21)+*C*(23)), 95.7 (s, 1 C, *C*(6)), 111.7 (s, 1 C, *C*(2/7)), 112.0 (s, 1 C, *C*(2/7)), 121.1 (s, 1 C, *C*(3)), 126.5 (s, 1 C, *C*(30)), 128.4 (s, 2 C, *C*(28)+*C*(32)), 128.7 (s, 2 C, *C*(29)+*C*(31)), 136.0 (s, 1 C, *C*(5)), 137.0 (s, 1 C, *C*(4)), 140.9 (s, 1 C, *C*(27)), 150.2 (s, 1 C, *C*(15)), 154.5 (s, 1 C, *C*(1)), 160.3 (s, 1 C, *C*(8)), 167.3 (s, 1 C, *C*(11)); LRMS *m/z* (ESI$^+$) 469 [(M+Na)$^+$], 447 [MH$^+$], 445 [(M-H)$^-$]; HRMS (ESI$^+$) found 447.2386, calculated for $C_{26}H_{31}N_4O_3^+$ 447.2391; HPLC (System E) t_r 2.7 min (77%).

5-(3,5-Dimethyl-1,2-oxazol-4-yl)-1-[2-(morpholin-4-yl)ethyl]-2-[(2*R*)-2-phenylpropyl]-1*H*-benzimidazole (368)

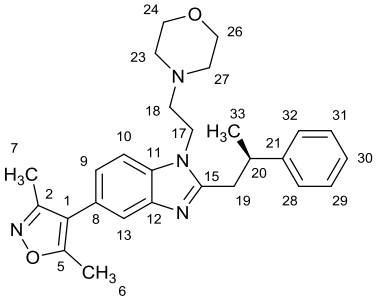

(*R*)-3-Phenylbutyric acid (28 µL, 0.18 mmol) was reacted with compound **316** (50 mg, 0.16 mmol) according to general procedure G. Chromatography was carried out with a gradient of CH_2Cl_2:MeOH:NH_4OH, which was increased linearly from 99:1:0.1 to 92:8:0.8 over 30 CVs.

The product was obtained as a pale yellow gum (34 mg, 48%); R_f 0.45 (CH_2Cl_2:MeOH:NH_4OH, 90:10:1); $[\alpha]_D^{22}$ -91.4 (*c* 2.8 in $CHCl_3$); ν_{max} (neat) 2961 (C-H), 2931 (C-H), 2855 (C-H), 2815 (C-H); ^{1}H NMR (400 MHz, $CDCl_3$) δ ppm 1.46 (d, *J*=7.0 Hz, 3 H, C(33)H_3), 2.31 (s, 3 H, C(7)H_3), 2.37 - 2.62 (m, 9 H, C(6)H_3+C(18)H_2+C(23)H_2+C(27)H_2), 3.16 (d, *J*=7.0 Hz, 2 H, C(19)H_2), 3.53 - 3.64 (m, 1 H, C(20)*H*), 3.64-3.71 (m, 4 H, C(24)H_2+C(26)H_2), 3.92 - 4.07 (m, 2 H, C(17)H_2), 7.11 (dd, *J*=8.0, 1.5 Hz, 1 H, C(9)*H*), 7.19 - 7.26 (m, 3 H, 3×Ph*H*), 7.28 - 7.35 (m, 3 H, C(10)*H*+2×Ph*H*), 7.63 (d, *J*=1.5 Hz, 1 H, C(13)*H*); ^{13}C NMR (101 MHz, $CDCl_3$) δ ppm 10.9 (s, 1 C, *C*(7)), 11.6 (s, 1 C, *C*(6)), 21.2 (s, 1 C, *C*(33)), 36.6 (s, 1 C, *C*(19)), 39.0 (s, 1 C, *C*(20)), 41.2 (s, 1 C, *C*(17)), 53.9 (s, 2 C, *C*(23)+*C*(27)), 57.5 (s, 1 C, *C*(18)), 66.7 (s, 2 C, *C*(24)+*C*(26)), 109.4 (s, 1 C, *C*(10)), 117.0 (s, 1 C, *C*(1)), 119.8 (s, 1 C, *C*(13)), 123.2 (s, 1 C, *C*(9)), 124.1 (s, 1 C, *C*(8)), 126.6 (s, 1 C, *C*(30)), 126.7 (s, 2 C, *C*(28/29)+*C*(32/31)), 128.6 (s, 2 C, *C*(28/29)+*C*(32/31)), 134.1 (s, 1 C, *C*(11)), 143.1 (s, 1 C, *C*(12)), 145.9 (s, 1 C, *C*(21)), 154.7 (s, 1 C, *C*(15)), 159.0 (s, 1 C, *C*(2)), 165.0 (s, 1 C, *C*(5)); LRMS *m/z* (ESI$^+$) 911 [(2M+Na)$^+$], 889 [(2M+H)$^+$], 467 [(M+Na)$^+$], 445 [MH$^+$]; HRMS (ESI$^+$) found 445.2596, calculated for $C_{27}H_{33}N_4O_2^+$ 445.2598; HPLC (System E) t_r 3.5 min (90%).

5-(3,5-Dimethyl-1,2-oxazol-4-yl)-1-[2-(morpholin-4-yl)ethyl]-2-[(2*S*)-2-phenylpropyl]-1*H*-benzimidazole (369)

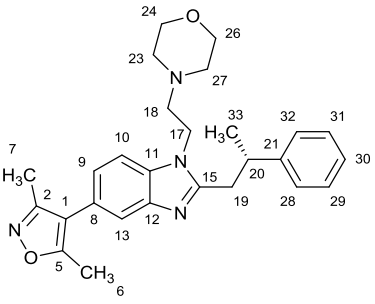

(*S*)-3-Phenylbutyric acid (28 µL, 0.18 mmol) was reacted with compound **316** (50 mg, 0.16 mmol) according to general procedure G. Chromatography was carried out with a gradient of EtOAc:MeOH:NEt_3, which was increased linearly from 99:1:0.1 to 95:5:0.5 over 20 CVs. The product was obtained as a colourless gum (26 mg, 36%); R_f 0.25 (EtOAc:MeOH:NEt_3,

90:10:1); $[\alpha]_D^{20}$ +99.6 (*c* 2.8 in $CHCl_3$); ν_{max} (neat) 2960 (C-H), 2929 (C-H), 2854 (C-H), 2815 (C-H); ^{1}H NMR (400 MHz, $CDCl_3$) δ ppm 1.46 (d, *J*=7.0 Hz, 3 H, C(33)H_3), 2.30 (s, 3 H, C(14)H_3), 2.41 - 2.52 (m, 8 H, C(15)H_3+C(17)H_AH$_B$+C(19)H_2+C(23)H_2), 2.53 - 2.62 (m, 1 H, C(17)H$_A$$H_B$), 3.09 - 3.22 (m, 2 H, C(25)H_2), 3.52 - 3.64 (m, 1 H, C(26)*H*), 3.65 - 3.71 (m, 4 H, C(20)H_2+C(22)H_2), 3.92 - 4.11 (m, 2 H, C(16)H_2), 7.11 (dd, *J*=8.5, 1.5 Hz, 1 H, C(3)*H*), 7.18 - 7.26 (m, 3 H, 3×Ph*H*), 7.28 - 7.36 (m, 3 H, C(3)*H*+2×Ph*H*), 7.63 (s, 1 H, C(6)*H*); ^{13}C NMR (101 MHz, $CDCl_3$) δ ppm 10.9 (s, 1 C, *C*(14)), 11.6 (s, 1 C, *C*(15)), 21.2 (s, 1 C, *C*(33)), 36.6 (s, 1 C, *C*(25)), 39.1 (s, 1 C, *C*(26)), 41.2 (s, 1 C, *C*(16)), 53.9 (s, 2 C, *C*(19)+*C*(23)), 57.4 (s, 1 C, *C*(17)), 66.7 (s, 2 C, *C*(20)+*C*(22)), 109.5 (s, 1 C, *C*(3)), 117.0 (s, 1 C, *C*(7)), 119.8 (s, 1 C, *C*(6)), 123.3 (s, 1 C, *C*(2)), 124.2 (s, 1 C, *C*(1)), 126.6 (s, 1 C, *C*(30)), 126.7 (s, 2 C, *C*(28/29)+*C*(32/31)), 128.7 (s, 2 C, *C*(28/29)+*C*(32/31)), 134.0 (s, 1 C, *C*(4)), 142.9 (s, 1 C, *C*(27)), 145.9 (s, 1 C, *C*(5)), 154.7 (s, 1 C, *C*(24)), 159.0 (s, 1 C, *C*(10)), 165.0 (s, 1 C, *C*(13)); LRMS *m/z* (ESI$^+$) 911 [(2M+Na)$^+$], 889 [(2M+H)$^+$], 467 [(M+Na)$^+$], 445 [MH$^+$], (ESI$^-$) 443 [(M-H)$^-$]; HRMS (ESI$^+$) found 445.2580, calculated for $C_{29}H_{31}N_4O_2^+$ 445.2598; HPLC (System E) t_r 3.6 min (93%).

5-(3,5-Dimethyl-1,2-oxazol-4-yl)-1-[2-(morpholin-4-yl)ethyl]-2-(1-phenylpropan-2-yl)-1*H*-benzimidazole (370)

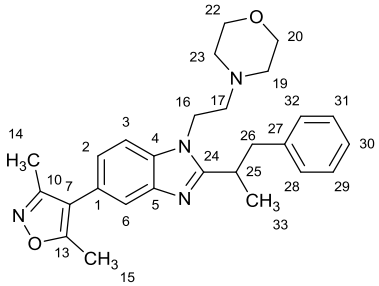

2-Methyl-3-phenylpropanoic acid (30 mg, 0.18 mmol) was reacted with compound **316** (50 mg, 0.16 mmol) according to general procedure G. Chromatography was carried out with a gradient of EtOAc:MeOH:NEt_3, which was increased linearly from 99:1:0.1 to 95:5:0.5 over 20 CVs. The product was obtained as a colourless gum (26 mg, 36%); R_f 0.30 (EtOAc:MeOH:NEt_3, 90:10:1); ν_{max} (neat) 2966 (C-H), 2923 (C-H), 2857 (C-H); ^{1}H NMR (400

MHz, $CDCl_3$) δ ppm 1.53 (d, *J*=6.5 Hz, 3 H, C(33)H_3), 2.22 - 2.35 (m, 4 H, C(14)H_3+C(17)H_AH_B), 2.35 - 2.55 (m, 8 H, C(15)H_3+C(17)H_AH_B+C(19)H_2+C(23)H_2), 2.95 - 3.12 (m, 1 H, C(26)H_AH_B), 3.21 - 3.37 (m, 2 H, C(25)*H*+C(26)H_AH_B), 3.63 - 3.72 (t, *J*=4.5 Hz, 4 H, C(20)H_2+C(22)H_2), 3.83 - 4.03 (m, 2 H, C(16)H_2), 7.03 - 7.13 (m, 3 H, C(2)*H*+2×Ph*H*), 7.14 - 7.25 (m, 3 H, 3×Ph*H*), 7.31 (d, *J*=8.5 Hz, 1 H, C(3)*H*), 7.67 (s, 1 H, C(6)*H*); ^{13}C NMR (101 MHz, $CDCl_3$) δ ppm 10.9 (s, 1 C, *C*(14)), 11.6 (s, 1 C, *C*(15)), 20.5 (s, 1 C, *C*(33)), 34.7 (s, 1 C, *C*(25)), 40.9 (s, 1 C, *C*(16)), 43.1 (s, 1 C, *C*(26)), 53.9 (s, 2 C, *C*(19)+*C*(23)), 57.5 (s, 1 C, *C*(17)), 66.7 (s, 2 C, *C*(20)+*C*(22)), 109.4 (s, 1 C, *C*(3)), 117.1 (s, 1 C, *C*(7)), 119.9 (s, 1 C, *C*(6)), 123.2 (s, 1 C, *C*(2)), 124.1 (s, 1 C, *C*(1)), 126.4 (s, 1 C, *C*(30)), 128.5 (s, 2 C, *C*(28/29)+*C*(32/31)), 128.9 (s, 2 C, *C*(28/29)+*C*(32/31)), 133.8 (s, 1 C, *C*(4)), 140.0 (s, 1 C, *C*(27)), 143.0 (s, 1 C, *C*(5)), 159.0 (s, 1 C, *C*(24)), 159.5 (s, 1 C, *C*(10)), 165.0 (s, 1 C, *C*(13)); LRMS *m/z* (ESI^+) 911 [$(2M+Na)^+$], 889 [$(2M+H)^+$], 467 [$(M+Na)^+$], 445 [MH^+]; HRMS (ESI^+) found 445.2580, calculated for $C_{29}H_{31}N_4O_2^+$ 445.2598; HPLC (System E) t_r 3.6 min (90%).

(1*S*)-1-{5-(3,5-Dimethyl-1,2-oxazol-4-yl)-1-[2-(morpholin-4-yl)ethyl]-1*H*-benzimidazol-2-yl}-2-phenylethanol (371)

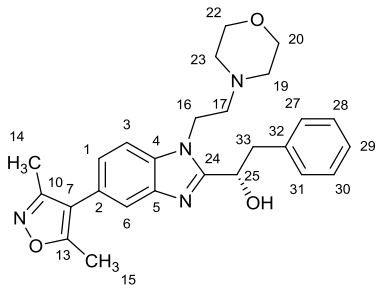

L-(-)-phenyllactic acid (43 mg, 0.26 mmol) was reacted with compound **316** (40 mg, 0.13 mmol) according to general procedure I. Chromatography was carried out with a gradient of EtOAc:MeOH:NEt_3, which was increased linearly from 99:1:0.1 to 90:10:1 over 20 CVs. The desired fractions were combined and evaporated to yield the product as a brown gum (9 mg, 16%); R_f 0.40 (EtOAc:MeOH:NEt_3, 90:10:1); $[\alpha]_D^{20}$ +24.9 (*c* 0.5 in $CHCl_3$); ν_{max} (neat) 3252 (O-H), 2923 (C-H), 2853 (C-H); ^{1}H NMR (500 MHz, $CDCl_3$) δ ppm 2.31 (s, 3 H, C(14)H_3), 2.40 -

2.46 (m, 5 H, C(15)H_3+C(19)H_AH$_B$+C(23)H_AH$_B$), 2.51 - 2.60 (m, 2 H, C(19)H$_A$$H_B$+C(23)H$_A$$H_B$), 2.70 - 2.87 (m, 2 H, C(17)H_2), 3.43 (dd, *J*=14.0, 7.5 Hz, 1 H, C(33)H_AH$_B$), 3.58 (dd, *J*=14.0, 5.5 Hz, 1 H, C(33)H$_A$$H_B$), 3.67 - 3.73 (m, 4 H, C(20)H_2+C(22)H_2), 4.23 - 4.35 (m, 2 H, C(16)H_2), 5.20 (dd, *J*=7.5, 5.5 Hz, 1 H, C(25)*H*), 7.18 (dd, *J*=8.0, 1.5 Hz, 1 H, C(1)*H*), 7.21 - 7.33 (m, 5 H, 5×Ph*H*), 7.39 (d, *J*=8.0 Hz, 1 H, C(3)*H*), 7.70 (d, *J*=1.5 Hz, 1 H, C(6)*H*); ^{13}C NMR (126 MHz, $CDCl_3$) δ ppm 10.9 (s, 1 C, *C*(14)), 11.6 (s, 1 C, *C*(15)), 41.5 (s, 2 C, *C*(16)+*C*(33)), 54.3 (s, 2 C, *C*(19)+*C*(23)), 57.4 (s, 1 C, *C*(17)), 66.0 (s, 2 C, *C*(20)+*C*(22)), 67.5 (s, 1 C, *C*(25)), 109.6 (s, 1 C, *C*(3)), 116.9 (s, 1 C, *C*(7)), 120.7 (s, 1 C, *C*(6)), 124.3 (s, 1 C, *C*(1)), 125.0 (s, 1 C, *C*(2)), 126.7 (s, 1 C, *C*(29)), 128.4 (s, 2 C, *C*(27/28)+*C*(31/30)), 129.7 (s, 2 C, *C*(27/28)+*C*(31/30)), 134.0 (s, 1 C, *C*(4)), 137.8 (s, 1 C, *C*(32)), 142.4 (s, 1 C, *C*(5)), 156.3 (s, 1 C, *C*(24)), 158.9 (s, 1 C, *C*(10)), 165.1 (s, 1 C, *C*(13)); LRMS *m/z* (ESI$^+$) 447 [MH$^+$]; HRMS (ESI$^+$) found 447.2395, calculated for $C_{26}H_{31}N_4O_3^+$ 447.2391; HPLC (System E) t_r 3.6 min (79%).

(2,3-Dihydro-1-benzofuran-2-yl)-5-(3,5-dimethyl-1,2-oxazol-4-yl)-1-[2-(morpholin-4-yl)ethyl]-1*H*-benzimidazole (372)

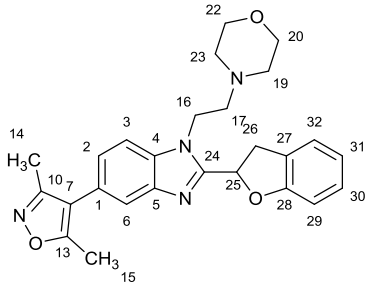

3-(2,3-Dihydro-1-benzofuran-5-yl)propanoic acid (27 mg, 0.14 mmol) was reacted with compound **316** (0.13 mmol) according to general procedure H. The product was obtained as a pale yellow gum (27 mg, 48%); R_f 0.35 (EtOAc:MeOH:NEt$_3$, 95:5:0.5); ν_{max} (neat) 2927 (C-H), 2854 (C-H), 2814 (C-H); ^{1}H NMR (400 MHz, $CDCl_3$) δ ppm 2.27 (s, 3 H, C(14)H_3), 2.40 (s, 3 H, C(15)H_3), 2.45 - 2.54 (m, 2 H, C(19)H_AH$_B$+C(23)H_AH$_B$), 2.58 - 2.67 (m, 2 H, C(19)H$_A$$H_B$+C(23)H$_A$$H_B$), 2.86 (t, *J*=7.0 Hz, 2 H, C(17)H_2), 3.64 - 3.75 (m, 5 H, C(20)H_2+C(22)H_2+C(26)H_AH$_B$), 4.30 (dd, *J*=15.5, 7.5 Hz, 1 H, C(26)H$_A$$H_B$), 4.39 - 4.48 (m, 1 H,

C(16)H_AH_B), 4.54 - 4.65 (m, 1 H, C(16)H_AH_B), 6.15 (dd, *J*=9.5, 7.5 Hz, 1 H, C(25)*H*), 6.80 (d, *J*=8.0 Hz, 1 H, C(3)*H*), 6.93 (t, *J*=7.5 Hz, 1 H, C(31)*H*), 7.15 (t, *J*=7.5 Hz, 1 H, C(30)*H*), 7.19 (dd, *J*=8.0, 1.5 Hz, 1 H, C(2)*H*), 7.31 (d, *J*=7.5 Hz, 1 H, C(32)*H*), 7.48 (d, *J*=7.5 Hz, 1 H, C(29)*H*), 7.65 (s, 1 H, C(6)*H*); ^{13}C NMR (101 MHz, $CDCl_3$) δ ppm 10.8 (s, 1 C, *C*(14)), 11.5 (s, 1 C, *C*(15)), 33.5 (s, 1 C, *C*(26)), 42.1 (s, 1 C, *C*(16)), 54.0 (s, 2 C, *C*(19)+*C*(23)), 57.8 (s, 1 C, *C*(17)), 66.9 (s, 2 C, *C*(20)+*C*(22)), 76.8 (s, 1 C, *C*(25)), 109.4 (s, 1 C, *C*(3)), 110.0 (s, 1 C, *C*(29)), 116.9 (s, 1 C, *C*(7)), 120.9 (s, 1 C, *C*(6)), 121.4 (s, 1 C, *C*(31)), 124.5 (s, 1 C, *C*(2)), 124.6 (s, 1 C, *C*(1)), 125.1 (s, 1 C, *C*(32)), 126.0 (s, 1 C, *C*(27)), 128.2 (s, 1 C, *C*(30)), 135.4 (s, 1 C, *C*(4)), 142.3 (s, 1 C, *C*(5)), 152.6 (s, 1 C, *C*(24)), 158.2 (s, 1 C, *C*(28)), 158.9 (s, 1 C, *C*(10)), 165.0 (s, 1 C, *C*(13)); LRMS (ESI$^+$) *m/z* 445 [MH$^+$]; HRMS (ESI$^+$) found 445.2215, calculated for $C_{26}H_{29}N_4O_3^+$ 445.2234; HPLC (System D) t_r 10.5 min (94%).

2-(2,3-Dihydro-1*H*-inden-2-yl)-5-(3,5-dimethyl-1,2-oxazol-4-yl)-1-[2-(morpholin-4-yl)ethyl]-1*H*-benzimidazole (373)

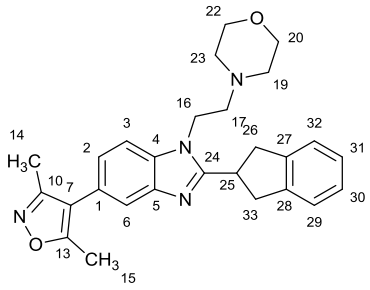

3-(2,3-Dihydro-1*H*-inden-5-yl)propanoic acid (26 mg, 0.14 mmol) was reacted with compound **316** (0.13 mmol) according to general procedure H. The product was obtained as a pale yellow gum (13 mg, 23%); R_f 0.30 (EtOAc:MeOH:NEt_3, 95:5:0.5); ν_{max} (neat) 2926 (C-H), 2853 (C-H), 2815 (C-H); ^{1}H NMR (500 MHz, $CDCl_3$) δ ppm 2.29 (s, 3 H, C(14)H_3), 2.42 (s, 3 H, C(15)H_3), 2.52 - 2.58 (m, 4 H, C(19)H_2+C(23)H_2), 2.80 (t, *J*=7.0 Hz, 2 H, C(17)H_2), 3.43 (dd, *J*=15.5, 9.0 Hz, 2 H, C(26)H_AH_B+C(33)H_AH_B), 3.62 (dd, *J*=15.5, 9.0 Hz, 2 H, C(26)H_AH_B+C(33)H_AH_B), 3.69 - 3.75 (m, 4 H, C(20)H_2+C(22)H_2), 4.01 (quin, *J*=9.0 Hz, 1 H, C(25)*H*), 4.37 (t, *J*=7.0 Hz, 2 H, C(16)H_2), 7.15 (dd, *J*=8.0, 1.5 Hz, 1 H, C(2)*H*), 7.20 - 7.23 (m, 2

H, C(30)*H*+C(31)*H*), 7.27 - 7.30 (m, 2 H, C(29)*H*+C(32)*H*), 7.43 (d, *J*=8.0 Hz, 1 H, C(3)*H*), 7.63 (d, *J*=1.5 Hz, 1 H, C(6)*H*); ^{13}C NMR (126 MHz, $CDCl_3$) δ ppm 10.8 (s, 1 C, *C*(14)), 11.5 (s, 1 C, *C*(15)), 37.5 (s, 1 C, *C*(25)), 38.9 (s, 2 C, *C*(26)+*C*(33)), 41.7 (s, 1 C, *C*(16)), 54.1 (s, 2 C, *C*(19)+*C*(23)), 57.8 (s, 1 C, *C*(17)), 66.8 (s, 2 C, *C*(20)+*C*(22)), 109.5 (s, 1 C, *C*(3)), 117.1 (s, 1 C, *C*(7)), 120.1 (s, 1 C, *C*(6)), 123.6 (s, 1 C, *C*(2)), 124.3 (s, 3 C, *C*(1)+*C*(29)+*C*(32)), 126.8 (s, 2 C, *C*(30)+*C*(31)), 134.6 (s, 1 C, *C*(4)), 141.5 (s, 2 C, *C*(28)+*C*(27)), 142.8 (s, 1 C, *C*(5)), 158.2 (s, 1 C, *C*(24)), 159.0 (s, 1 C, *C*(10)), 165.0 (s, 1 C, *C*(13)) ; LRMS *m/z* (ESI$^+$) 443 [MH$^+$]; HRMS (ESI$^+$) found 443.2435, calculated for $C_{27}H_{31}N_4O_2^+$ 443.2442; HPLC (System D) t_r 9.6min (94%).

5-(3,5-Dimethyl-1,2-oxazol-4-yl)-1-[2-(morpholin-4-yl)ethyl]-2-(1,2,3,4-tetrahydronaphthalen-2-yl)-1*H*-benzimidazole (374)

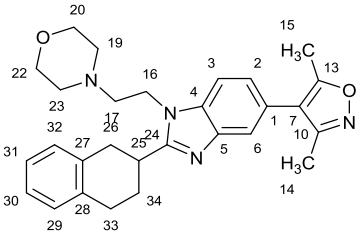

1,2,3,4-Tetrahydronaphthalene-2-carboxylic acid (26 mg, 0.14 mmol) was reacted with compound **316** (0.13 mmol) according to general procedure H. The product was obtained as a pale orange solid (11 mg, 19%); R_f 0.30 (EtOAc:MeOH:NEt_3, 95:5:0.5); mp 87-90 °C; ν_{max} (neat) 2921 (C-H), 2851 (C-H), ^{1}H NMR (500 MHz, $CDCl_3$) δ ppm 2.26 - 2.34 (m, 5 H, C(14)H_3+C(34)H_2), 2.42 - 2.44 (m, 3 H, C(15)H_3), 2.48 - 2.61 (m, 4 H, C(19)H_2+C(23)H_2), 2.74 - 2.86 (m, 2 H, C(17)H_2), 2.98 - 3.18 (m, 3 H, C(26)H_AH_B+C(33)H_2), 3.29 - 3.38 (m, 1 H, C(25)*H*), 3.42 - 3.51 (m, 1 H, C(26)H$_A$*H*$_B$), 3.65 - 3.75 (m, 4 H, C(20)H_2+C(22)H_2), 4.30 - 4.41 (m, 2 H, C(16)H_2), 7.12 - 7.22 (m, 5 H, C(2)*H*+4×Ar*H*), 7.44 (d, *J*=8.0 Hz, 1 H, C(3)*H*), 7.68 (s, 1 H, C(6)*H*); ^{13}C NMR (126 MHz, $CDCl_3$) δ ppm 10.9 (s, 1 C, *C*(14)), 11.6 (s, 1 C, *C*(15)), 29.0 (s, 1 C, *C*(34)), 29.4 (s, 1 C, *C*(33)), 33.3 (s, 1 C, *C*(25)), 35.1 (s, 1 C, *C*(26)), 41.5 (s, 1 C, *C*(16)), 54.1 (s, 2 C, *C*(19)+*C*(23)), 57.8 (s, 1 C, *C*(17)), 66.7 (s, 2 C, *C*(20)+*C*(22)), 109.6 (s, 1 C, *C*(3)),

117.0 (s, 1 C, *C*(7)), 120.1 (s, 1 C, *C*(6)), 123.7 (s, 1 C, *C*(2)), 124.5 (s, 1 C, *C*(1)), 126.0 (s, 1 C, *C*(30/32)), 126.2 (s, 1 C, *C*(30/32)), 129.0 (s, 2 C, *C*(29)+*C*(31)), 134.1 (s, 1 C, *C*(4)), 135.2 (s, 1 C, *C*(27/28)), 135.4 (s, 1 C, *C*(27/28)), 143.3 (s, 1 C, *C*(5)), 159.0 (s, 2 C, *C*(10)+*C*(24)), 165.1 (s, 1 C, *C*(13)); LRMS *m/z* (ESI$^+$) 457 [MH$^+$]; HRMS (ESI$^+$) found 457.2581, calculated for $C_{28}H_{33}N_4O_2^+$ 457.2598; HPLC (System D) t_r 10.0 min (91%).

5-(3,5-Dimethyl-1,2-oxazol-4-yl)-1-[2-(morpholin-4-yl)ethyl]-2-[*trans*-2-phenylcyclopropyl]-1*H*-benzimidazole (375)

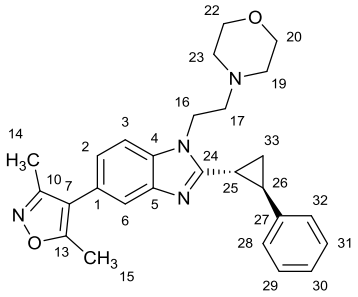

(*trans*)-2-Phenylcyclopropanecarboxylic acid (26 mg, 0.14 mmol) was reacted with compound **316** (0.13 mmol) according to general procedure H. The product was obtained as a pale orange gum (14 mg, 25%); R_f 0.35 (EtOAc:MeOH:NEt_3, 95:5:0.5); ν_{max} (neat) 2958 (C-H), 2924 (C-H), 2854 (C-H), 2814 (C-H); ^{1}H NMR (500 MHz, $CDCl_3$) δ ppm 1.70 (dt, *J*=8.5, 5.5 Hz, 1 H, C(33)H_AH_B), 2.10 (dt, *J*=8.5, 5.5 Hz, 1 H, C(33)H_AH_B), 2.27 - 2.34 (m, 4 H, C(14)H_3+C(25)*H*), 2.34 - 2.44 (m, 7 H, C(14)H_3+C(19)H_2+C(23)H_2), 2.61 - 2.68 (m, 1 H, C(26)*H*), 2.69 - 2.80 (m, 2 H, C(17)H_2), 3.53 - 3.68 (m, 4 H, C(20)H_2+C(22)H_2), 4.27 - 4.41 (m, 2 H, C(16)H_2), 7.12 (dd, *J*=8.0, 1.5 Hz, 1 H, C(2)*H*), 7.18 - 7.21 (m, 2 H, C(28)*H*+C(32)*H*), 7.22 - 7.27 (m, 1 H, C(30)*H*), 7.31 - 7.42 (m, 3 H, C(29)*H*+C(31)*H*), 7.59 (d, *J*=1.5 Hz, 1 H, C(6)*H*); ^{13}C NMR (126 MHz, $CDCl_3$) δ ppm 10.8 (s, 1 C, *C*(14)), 11.5 (s, 1 C, *C*(15)), 17.1 (s, 1 C, *C*(33)), 20.0 (s, 1 C, *C*(25)), 27.4 (s, 1 C, *C*(26)), 41.4 (s, 1 C, *C*(16)), 53.8 (s, 2 C, *C*(19)+*C*(23)), 57.6 (s, 1 C, *C*(17)), 66.6 (s, 2 C, *C*(20)+*C*(22)), 109.1 (s, 1 C, *C*(3)), 117.1 (s, 1 C, *C*(7)), 119.7 (s, 1 C, *C*(3)), 123.4 (s, 1 C, *C*(2)), 124.4 (s, 1 C, *C*(1)), 125.7 (s, 2 C, *C*(28)+*C*(32)), 126.5 (s, 1 C, *C*(30)), 128.7 (s, 2 C, *C*(29)+*C*(31)), 134.6 (s, 1 C, *C*(4)), 140.6 (s, 1 C, *C*(27)), 142.5 (s, 1 C,

C(5)), 156.1 (s, 1 C, *C*(24)), 159.0 (s, 1 C, *C*(10)), 165.0 (s, 1 C, *C*(13)); LRMS *m/z* (ESI$^+$) 443 [MH$^+$]; HRMS (ESI$^+$) found 443.2432, calculated for $C_{27}H_{31}N_4O_2^+$ 443.2442; HPLC (System D) t_r 9.7 min (96%).

5-(3,5-Dimethyl-1,2-oxazol-4-yl)-1-[2-(morpholin-4-yl)ethyl]-2-(naphthalen-1-ylmethyl)-1*H*-benzimidazole (376)

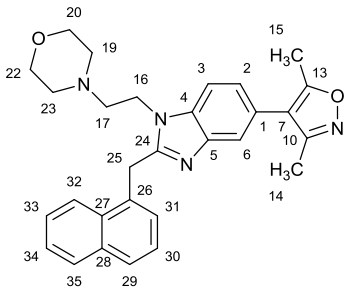

Naphthalen-1-ylacetic acid (34 mg, 0.18 mmol) was reacted with compound **316** (50 mg, 0.16 mmol) according to general procedure G. Chromatography was carried out with a gradient of EtOAc:MeOH:NEt_3, which was increased linearly from 99:1:0.1 to 95:5:0.5 over 20 CVs. The product was obtained as a colourless gum (34 mg, 45%); R_f 0.30 (EtOAc:MeOH:NEt_3, 90:10:1); ν_{max} (neat) 2959 (C-H), 2855 (C-H), 2816 (C-H); ^{1}H NMR (400 MHz, $CDCl_3$) δ ppm 2.22 - 2.28 (m, 4 H, C(19)H_2+C(23)H_2), 2.31 (s, 3 H, C(14)H_3), 2.37 (t, *J*=7.0 Hz, 2 H, C(17)H_2), 2.44 (s, 3 H, C(15)H_3), 3.58-3.68 (m, 4 H, C(20)H_2+C(22)H_2), 4.14 (t, *J*=7.0 Hz, 2 H, C(16)H_2), 4.86 (s, 2 H, C(25)H_2), 7.15 (dd, *J*=8.0, 1.5 Hz, 1 H, C(2)*H*), 7.23 (d, *J*=7.0 Hz, 1 H, C(31)*H*), 7.35 - 7.42 (m, 2 H, C(3)*H*+C(30)*H*), 7.50 - 7.61 (m, 2 H, C(33)*H*+C(34)*H*), 7.67 (s, 1 H, C(6)*H*), 7.81 (d, *J*=8.5 Hz, 1 H, C(29)*H*), 7.91 (d, *J*=7.5 Hz, 1 H C(29)*H*), 8.25 (d, *J*=8.0 Hz, 1 H, C(32)*H*); ^{13}C NMR (101 MHz, $CDCl_3$) δ ppm 10.9 (s, 1 C, *C*(14)), 11.5 (s, 1 C, *C*(15)), 32.0 (s, 1 C, *C*(25)), 41.9 (s, 1 C, *C*(16)), 53.7 (s, 2 C, *C*(19)+*C*(23)), 57.1 (s, 1 C, *C*(17)), 66.6 (s, 2 C, *C*(20)+*C*(22)), 109.5 (s, 1 C, *C*(3)), 117.0 (s, 1 C, *C*(7)), 120.2 (s, 1 C, *C*(6)), 123.4 (s, 1 C, *C*(32)), 123.7 (s, 1 C, *C*(2)), 124.3 (s, 1 C, *C*(1)), 125.5 (s, 1 C, *C*(30)), 126.0 (s, 1 C, *C*(31)), 126.5 (s, 1 C, *C*(33/34)), 126.6 (s, 1 C, *C*(33/34)), 128.0 (s, 1 C, *C*(29)), 128.9 (s, 1 C, *C*(35)), 131.7 (s, 1 C, *C*(28)), 132.1 (s, 1 C, *C*(27)), 133.9 (s, 1 C, *C*(26)),

134.7 (s, 1 C, *C*(4)), 143.0 (s, 1 C, *C*(5)), 154.1 (s, 1 C, *C*(24)), 159.0 (s, 1 C, *C*(10)), 165.0 (s, 1 C, *C*(13)); LRMS *m/z* (ESI$^+$) 955 [(2M+Na)$^+$], 933 [(2M+H)$^+$], 489 [(M+Na)$^+$], 467 [MH$^+$], (ESI$^-$) 465 [(M-H)$^-$]; HRMS (ESI$^+$) found 467.2428, calculated for $C_{29}H_{31}N_4O_2^+$ 467.2442; HPLC (System E) t_r 3.8 min (87%).

5-(3,5-Dimethyl-1,2-oxazol-4-yl)-1-[2-(morpholin-4-yl)ethyl]-2-(naphthalen-2-ylmethyl)-1*H*-benzimidazole (377)

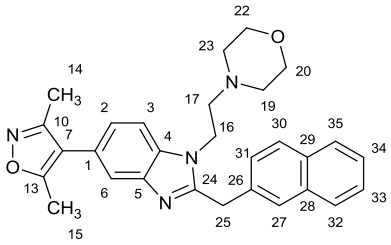

2-Naphthaleneacetic acid (34 mg, 0.18 mmol) was reacted with compound **316** (50 mg, 0.16 mmol) according to general procedure G to yield the product as a yellow gum (55 mg, 74%); R_f 0.20 (EtOAc:MeOH:NEt_3, 90:10:1); ν_{max} (neat) 2960 (C-H), 2855 (C-H), 2816 (C-H); ^{1}H NMR (400 MHz, $CDCl_3$) δ ppm 2.26 - 2.30 (m, 4 H, C(19)H_2+C(23)H_2), 2.31 (s, 3 H, C(14)H_3), 2.40 (t, *J*=7.0 Hz, 2 H, C(17)H_2), 2.44 (s, 3 H, C(15)H_3), 3.59 - 3.67 (m, 4 H, C(20)H_2+C(22)H_2), 4.17 (t, *J*=7.0 Hz, 2 H, C(25)H_2), 4.57 (s, 2 H, C(17)H_2), 7.15 (dd, *J*=8.5, 1.0 Hz, 1 H, C(2)*H*), 7.37 (d, *J*=8.5 Hz, 1 H, C(3)*H*), 7.41 (dd, *J*=8.5, 1.5 Hz, 1 H, C(31)*H*), 7.43 - 7.50 (m, 2 H, C(33)*H*+C(34)*H*), 7.68 (d, *J*=1.0 Hz, 1 H, C(6)*H*), 7.71 (s, 1 H, C(27)*H*), 7.74 - 7.78 (m, 1 H, C(35)*H*), 7.78 - 7.83 (m, 2 H, C(30)*H*+C(32)*H*); ^{13}C NMR (101 MHz, $CDCl_3$) δ ppm 10.8 (s, 1 C, *C*(14)), 11.5 (s, 1 C, *C*(15)), 34.8 (s, 1 C, *C*(25)), 41.9 (s, 1 C, *C*(16)), 53.8 (s, 2 C, *C*(19)+*C*(23)), 57.1 (s, 1 C, *C*(17)), 66.7 (s, 2 C, *C*(20)+*C*(22)), 109.5 (s, 1 C, *C*(3)), 117.0 (s, 1 C, *C*(7)), 120.2 (s, 1 C, *C*(6)), 123.6 (s, 1 C, *C*(2)), 124.3 (s, 1 C, *C*(1)), 126.0 (s, 1 C, *C*(31)), 126.4 (s, 1 C, *C*(33/34)), 126.5 (s, 1 C, *C*(33/34)), 127.0 (s, 1 C, *C*(27)), 127.4 (s, 1 C, *C*(35)), 127.6 (s, 1 C, *C*(30)), 128.7 (s, 1 C, *C*(32)), 132.4 (s, 1 C, *C*(26/28/29)), 133.4 (s, 1 C, *C*(26/28/29)), 133.5 (s, 1 C, *C*(26/28/29)), 134.7 (s, 1 C, *C*(4)), 143.0 (s, 1 C, *C*(5)), 154.0 (s, 1 C, *C*(24)), 158.9 (s, 1 C, *C*(10)), 165.0 (s, 1 C, *C*(13)); LRMS *m/z* (ESI$^+$) 955 [(2M+Na)$^+$], 933 [(2M+H)$^+$], 489

[(M+Na)$^+$], 467 [MH$^+$], (ESI$^-$) 465 [(M-H)$^-$]; HRMS (ESI$^+$) found 467.2430, calculated for $C_{29}H_{31}N_4O_2^+$ 467.2442; HPLC (System E) t_r 4.0 min (91%).

4-(3,5-Dimethyl-1,2-oxazol-4-yl)-*N*-[2-(morpholin-4-yl)-1-phenylethyl]-2-nitroaniline (378)

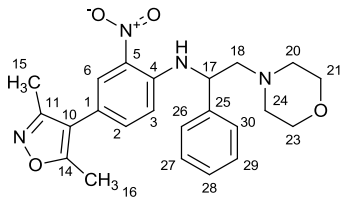

2-(Morpholin-4-yl)-2-phenylethanamine (52 mg, 0.25 mmol) was added to a solution of compound **251** (60 mg, 0.25 mmol) and EtN(*i*-Pr)$_2$ (35 µL, 0.30 mmol) in THF (2 mL) in a sealable vial. The vial was sealed then the solution was heated at 80 °C for 16 h. The resultant mixture was partitioned between CH_2Cl_2 (3 mL) and water (3 mL). The organic phase was collected by passing it through a hydrophobic frit then evaporated by nitrogen blow-down. The crude material was purified by flash column chromatography on a silica column (4 g). The column was eluted with a gradient of EtOAc:*c*-hexane which was increased linearly from 10:90 to 100:0 over 30 CVs. The desired fractions were combined and evaporated to yield the product as a bright-orange solid (62 mg, 59%); R_f 0.60 (EtOAc:*c*-hexane, 80:20); mp 155-160 °C; ν_{max} (neat) 3309 (N-H), 2915 (C-H), 2858 (C-H), 2818 (C-H); ^{1}H NMR (400 MHz, $CDCl_3$) δ ppm 2.22 (s, 3 H, C(15)H_3), 2.36 (s, 3 H, C(16)H_3), 2.42 - 2.53 (m, 2 H, C(20)H_AH_B+C(24)H_AH_B), 2.56 - 2.67 (m, 2 H, C(20)H_AH_B+C(24)H_AH_B), 2.69 - 2.81 (m, 2 H, C(18)H_2), 3.67 - 3.89 (m, 4 H, C(21)H_2+C(23)H_2), 4.53 - 4.66 (m, 1 H, C(17)*H*), 6.59 (d, *J*=8.5 Hz, 1 H, C(3)*H*), 7.11 (d, *J*=8.5 Hz, 1 H, C(2)*H*), 7.29 - 7.35 (m, 1 H, C(28)*H*), 7.35 - 7.43 (m, 4 H, 4×Ph*H*), 8.09 (d, *J*=2.0 Hz, 1 H, C(6)*H*), 9.17 (br. s., 1 H, N*H*); ^{13}C NMR (101 MHz, $CDCl_3$) δ ppm 10.7 (s, 1 C, *C*(15)), 11.5 (s, 1 C, *C*(16)), 53.3 (s, 2 C, *C*(20)+*C*(24)), 55.1 (s, 1 C, *C*(17)), 64.9 (s, 1 C, *C*(18)), 66.9 (s, 2 C, *C*(21)+*C*(23)), 114.8 (s, 1 C, *C*(10)), 116.3 (s, 1 C, *C*(3)), 117.8 (s, 1 C, *C*(1)), 126.1 (s, 2 C, *C*(26/27)+*C*(30/29)), 126.8 (s, 1 C, *C*(6)), 127.9 (s, 1 C, *C*(28)),

129.1 (s, 2 C, *C*(26/27)+*C*(30/29)), 132.7 (s, 1 C, *C*(5)), 136.2 (s, 1 C, *C*(2)), 140.7 (s, 1 C, *C*(25)), 143.8 (s, 1 C, *C*(4)), 158.5 (s, 1 C, *C*(11)), 165.3 (s, 1 C, *C*(14)); LRMS *m/z* (ESI^+) 445 [$(M+Na)^+$], 423 [MH^+]; HRMS (ESI^+) found 423.2025, calculated for $C_{23}H_{27}N_4O_4^+$ 423.2027; HPLC (System E) t_r 4.3 min (96%).

4-(3,5-Dimethyl-1,2-oxazol-4-yl)-*N*-[2-(morpholin-4-yl)-2-phenylethyl]-2-nitroaniline (379)

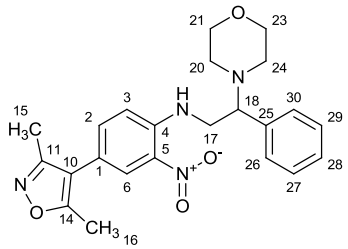

2-(Morpholin-4-yl)-2-phenylethanamine (52 mg, 0.25 mmol) was added to a solution of compound **251** (60 mg, 0.25 mmol) and EtN(*i*-Pr)$_2$ (35 µL, 0.30 mmol) in THF (2 mL) in a sealable vial. The vial was sealed then the solution was heated at 80 °C for 16 h. The resultant mixture was partitioned between CH_2Cl_2 (3 mL) and water (3 mL). The organic phase was collected by passing it through a hydrophobic frit then evaporated by nitrogen blow-down. The crude material was purified by flash column chromatography on a silica column (4 g). The column was eluted with a gradient of EtOAc:*c*-hexane which was increased linearly from 10:90 to 100:0 over 30 CVs. The desired fractions were combined and evaporated to yield the product as a bright-orange solid (72 mg, 68%); R_f 0.50 (EtOAc:*c*-hexane, 80:20); mp 176-180 °C; ν_{max} (neat) 3383 (N-H), 2947 (C-H), 2838 (C-H), 1559 (N-O), 1354 (N-O), ; ^{1}H NMR (400 MHz, $CDCl_3$) δ ppm 2.26 (s, 3 H, C(15)H_3), 2.39 (s, 3 H, C(16)H_3), 2.45 - 2.65 (m, 4 H, C(20)H_2+C(24)H_2), 3.52 - 3.73 (m, 2 H, C(17)H_2), 3.73 - 3.91 (m, 5 H, C(16)*H*+C(21)H_2+C(23)H_2), 6.87 (d, *J*=9.0 Hz, 1 H, C(3)*H*), 7.28 - 7.48 (m, 6 H, C(2)*H*+5×Ph*H*), 8.09 (d, *J*=2.0 Hz, 1 H, C(6)*H*), 8.83 (br. s., 1 H, N*H*); 13C NMR (101 MHz, $CDCl_3$) δ ppm 10.7 (s, 1 C, C(15)), 11.5 (s, 1 C, C(16)), 44.0 (s, 1 C, C(17)), 50.1 (s, 2 C, C(20)+C(24)), 67.1 (s, 2 C, C(21)+C(23)), 67.6 (s, 1 C, C(18)), 114.7 (s, 1 C, C(3)), 114.9 (s, 1

C, C(10)), 117.3 (s, 1 C, C(1)), 127.0 (s, 1 C, C(6)), 128.2 (s, 1 C, C(28)), 128.4 (s, 2 C, C(26/27)+C(30/29)), 128.6 (s, 2 C, C(26/27)+C(30/29)), 131.9 (s, 1 C, C(5)), 136.7 (s, 1 C, C(2)), 136.8 (s, 1 C, C(25)), 144.2 (s, 1 C, C(4)), 158.5 (s, 1 C, C(11)), 165.3 (s, 1 C, C(14)); LRMS *m/z* (ESI^+) 445 [$(M+Na)^+$], 423 [MH^+]; HRMS (ESI^+) found 423.2011, calculated for $C_{23}H_{27}N_4O_4^+$ 423.2027; HPLC (System E) t_r 4.0 min (99%).

5-(3,5-Dimethyl-1,2-oxazol-4-yl)-1-[2-(morpholin-4-yl)-1-phenylethyl]-1*H*-benzimidazole (380)

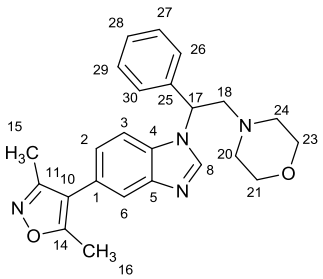

Freshly prepared 1 M aq. $Na_2S_2O_4$ (0.35 mL, 0.35 mmol) was added to a suspension compound **378** (29 mg, 0.069 mmol) in EtOH (0.5 mL) in a sealable vial. The vial was sealed then heated at 80°C for 2 h then more 1 M aq. $Na_2S_2O_4$ (0.35 mL, 0.35 mmol) was added. The mixture was heated for a further 2 h then allowed to cool. The resultant mixture was partitioned between 10% aq. NH_3 (1.5 mL) and EtOAc (1.5 mL). The organic phase was passed through $MgSO_4$ on a hydrophobic frit then evaporated by nitrogen blow-down. The residue was dissolved in EtOH (0.5 mL) then triethyl orthoformate (0.5 mL) was added. The solution was heated under reflux for 18 h then allowed to cool. The resultant solution was evaporated by nitrogen blow-down. The crude material was purified by flash column chromatography on a silica column (4 g). The column was eluted with a gradient of EtOAc:MeOH:NEt_3 which was increased linearly from 99:1:0.1 to 95:5:0.5 over 30 CVs. The desired fractions were combined and evaporated to yield the product as a yellow gum (7 mg, 25%); R_f 0.45 (EtOAc:MeOH:NEt_3, 90:10:1); ν_{max} (neat) 2959 (C-H), 2918 (C-H), 2850 (C-H); ^{1}H NMR (500 MHz, $CDCl_3$) δ ppm 2.26 (s, 3 H, C(15)H_3), 2.40 (s, 3 H, C(16)H_3), 2.80 - 3.24

(m, 4 H, C(20)H_2+C(24)H_2), 3.63 - 4.02 (m, 6 H, C(18)H+C(21)H_2+C(23)H_2), 4.52 - 4.83 (m, 1 H, C(17)H), 7.31 - 7.53 (m, 5 H, 5×ArH), 7.56 - 7.70 (m, 2 H, 2×ArH), 7.81 - 7.94 (m, 2 H, 2×ArH); ^{13}C NMR (126 MHz, $CDCl_3$) δ ppm 10.8 (s, 1 C, C(15)), 11.6 (s, 1 C, C(16)), 45.8 (s, 1 C, C(17)), 53.0 (s, 2 C, C(20)+C(24)), 57.6 (s, 1 C) 60.2 (s, 1 C) 64.8 (s, 2 C, C(21)+C(23)), 113.1 (s, 1 C) 115.5 (s, 1 C) 117.0 (s, 1 C, C(10)), 127.0 (s, 1 C) 127.8 (s, 1 C) 129.5 (s, 1 C) 130.0 (s, 1 C) 130.0 (s, 1 C) 130.4 (s, 1 C) 135.3 (s, 1 C) 141.2 (s, 1 C) 158.4 (s, 1 C, C(11)), 165.9 (s, 1 C, C(14)); LRMS *m/z* (ESI$^+$) 403 [MH$^+$]; HRMS (ESI$^+$) found 403.2119, calculated for $C_{24}H_{27}N_4O_2^+$ 403.2129; HPLC (System E) t_r 3.8 min (>99%).

5-(3,5-Dimethyl-1,2-oxazol-4-yl)-2-methyl-1-[2-(morpholin-4-yl)-1-phenylethyl]-1*H*-benzimidazole (381)

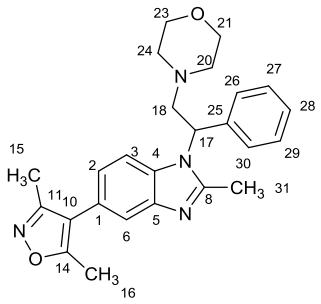

Freshly prepared 1 M aq. $Na_2S_2O_4$ (0.35 mL, 0.35 mmol) was added to a suspension compound **378** (29 mg, 0.069 mmol) in EtOH (0.5 mL) in a sealable vial. The vial was sealed then heated at 80°C for 2 h then more 1 M aq. $Na_2S_2O_4$ (0.35 mL, 0.35 mmol) was added. The mixture was heated for a further 2 h then allowed to cool. The resultant mixture was partitioned between 10% aq. NH_3 (1.5 mL) and EtOAc (1.5 mL). The organic phase was passed through $MgSO_4$ on a hydrophobic frit then evaporated by nitrogen blow-down. The residue was dissolved in EtOH (0.5 mL) then triethyl orthoacetate (0.5 mL) was added. The solution was heated under reflux for 18 h then allowed to cool. The resultant solution was evaporated by nitrogen blow-down. The crude material was purified by flash column chromatography on a silica column (4 g). The column was eluted with a gradient of EtOAc:-MeOH:NEt_3 which was increased linearly from 99:1:0.1 to 95:5:0.5 over 30 CVs. The desired

fractions were combined and evaporated to yield the product as a colourless gum (5 mg, 17%); R_f 0.40 (EtOAc:MeOH:NEt_3, 90:10:1); ν_{max} (neat) 2957 (C-H), 2918 (C-H), 2850 (C-H); ^{1}H NMR (500 MHz, $CDCl_3$) δ ppm 1.42 - 2.04 (m, 3 H, CH_3), 2.25 (s, 3 H, C(15)H_3), 2.41 (s, 3 H, C(16)H_3), 2.57 - 4.52 (m, 11 H), 7.27 - 7.55 (m, 7 H, 7×Ar*H*), 7.82 (s, 1 H, Ar*H*); ^{13}C NMR (126 MHz, $CDCl_3$) δ ppm 10.8 (s, 1 C, *C*(15)), 10.9 (s, 1 C, *C*(16)), 11.6 (s, 1 C) 11.7 (s, 1 C) 21.2 (s, 1 C) 29.7 (s, 1 C) 41.8 (s, 1 C) 46.7 (s, 1 C) 53.7 (s, 1 C) 66.6 (s, 1 C) 66.8 (s, 1 C) 113.4 (s, 1 C) 114.3 (s, 1 C) 115.2 (s, 1 C) 115.9 (s, 1 C) 127.2 (s, 1 C) 127.4 (s, 1 C) 129.4 (s, 1 C) 129.9 (s, 1 C) 130.1 (s, 1 C) 133.5 (s, 1 C) 151.9 (s, 1 C) 158.3 (s, 1 C, *C*(11)), 166.0 (s, 1 C, *C*(14)); LRMS *m/z* (ESI$^+$) 417 [MH$^+$]; HRMS (ESI$^+$) found 417.2276, calculated for $C_{25}H_{29}N_4O_2^+$ 417.2285; HPLC (System E) t_r 3.8 min (80%).

5-(3,5-Dimethyl-1,2-oxazol-4-yl)-1-[2-(morpholin-4-yl)-2-phenylethyl]-1*H*-benzimidazole (382)

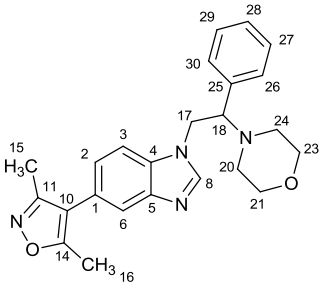

Freshly prepared 1 M aq. $Na_2S_2O_4$ (0.4 mL, 0.4 mmol) was added to a suspension of compound **379** (34 mg, 0.080 mmol) in EtOH (0.5 mL) in a sealable vial. The vial was sealed then heated at 80°C for 2 h then more 1 M aq. $Na_2S_2O_4$ (0.4 mL, 0.4 mmol) was added. The mixture was heated for a further 2 h then allowed to cool. The resultant mixture was partitioned between 10% aq. NH_3 (1.5 mL) and EtOAc (1.5 mL). The organic phase was passed through $MgSO_4$ on a hydrophobic frit then evaporated by nitrogen blow-down. The residue was dissolved in EtOH (0.5 mL) then triethyl orthoformate (0.5 mL) was added. The solution was heated under reflux for 18 h then allowed to cool. The resultant solution was evaporated by nitrogen blow-down. The crude material was purified by flash column

chromatography on a silica column (4 g). The column was eluted with a gradient of EtOAc:-MeOH:NEt_3 which was increased linearly from 99:1:0.1 to 95:5:0.5 over 30 CVs. The desired fractions were combined and evaporated to yield the product as a yellow gum (26 mg, 81%); R_f 0.35 (EtOAc:MeOH:NEt_3, 90:10:1); ν_{max} (neat) 2958 (C-H), 2916 (C-H), 2889 (C-H), 2856 (C-H), 2815 (C-H); ^{1}H NMR (400 MHz, $CDCl_3$) δ ppm 2.30 (s, 3 H, C(15)H_3), 2.43 (s, 3 H, C(16)H_3), 2.48 - 2.72 (m, 4 H, C(20)H_2+C(24)H_2), 3.70 - 3.87 (m, 5 H, C(18)H+C(21)H_2+C(23)H_2), 4.43 (dd, J=14.0, 7.5 Hz, 1 H, C(17)H_AH_B), 4.82 (dd, J=14.0, 6.0 Hz, 1 H, C(17)H_AH_B), 7.09 - 7.19 (m, 3 H, C(2)H+2×PhH), 7.29 - 7.35 (m, 3 H, 3×PhH), 7.38 (d, J=8.5 Hz, 1 H, C(3)H), 7.57 - 7.67 (m, 2 H, C(6)H+C(8)H); ^{13}C NMR (126 MHz, $CDCl_3$) δ ppm 10.8 (s, 1 C, C(15)), 11.5 (s, 1 C, C(16)), 47.0 (s, 1 C, C(17)), 51.1 (s, 2 C, C(20)+C(24)), 66.8 (s, 2 C, C(21)+C(23)), 69.5 (s, 1 C, C(18)), 109.6 (s, 1 C, C(3)), 116.9 (s, 1 C, C(10)), 120.8 (s, 1 C, C(6)), 124.2 (s, 1 C, C(2)), 124.3 (s, 1 C, C(1)), 128.3 (s, 2 C, 2×PhC) 128.5 (s, 1 C, C(28)), 128.8 (s, 2 C, 2×PhC) 133.1 (s, 1 C, C(4)), 136.2 (s, 1 C, C(25) 143.4 (s, 1 C, C(5)), 144.2 (s, 1 C, C(8)), 158.9 (s, 1 C, C(11)), 165.0 (s, 1 C, C(14)); LRMS m/z (ESI^+) 403 [MH^+]; HRMS (ESI^+) found 425.1946, calculated for $C_{24}H_{26}N_4NaO_2^+$ 425.1948; HPLC (System E) t_r 3.5 min (96%).

5-(3,5-Dimethyl-1,2-oxazol-4-yl)-2-methyl-1-[2-(morpholin-4-yl)-2-phenylethyl]-1*H*-benzimidazole (383)

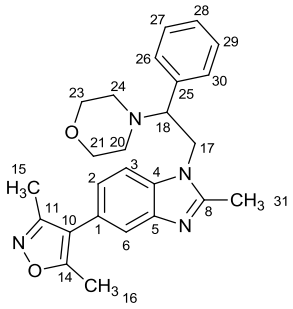

Freshly prepared 1 M aq. $Na_2S_2O_4$ (0.4 mL, 0.4 mmol) was added to a suspension of compound **379** (34 mg, 0.080 mmol) in EtOH (0.5 mL) in a sealable vial. The vial was sealed then heated at 80°C for 2 h then more 1 M aq. $Na_2S_2O_4$ (0.4 mL, 0.4 mmol) was added. The mixture was heated for a further 2 h then allowed to cool. The resultant mixture was

partitioned between 10% aq. NH_3 (1.5 mL) and EtOAc (1.5 mL). The organic phase was passed through $MgSO_4$ on a hydrophobic frit then evaporated by nitrogen blow-down. The residue was dissolved in EtOH (0.5 mL) then triethyl orthoacetate (0.5 mL) was added. The solution was heated under reflux for 18 h then allowed to cool. The resultant solution was evaporated by nitrogen blow-down. The crude material was purified by flash column chromatography on a silica column (4 g). The column was eluted with a gradient of EtOAc:-MeOH:NEt_3 which was increased linearly from 99:1:0.1 to 95:5:0.5 over 30 CVs. The desired fractions were combined and evaporated to yield the product as a colourless gum (15 mg, 45%); R_f 0.35 (EtOAc:MeOH:NEt_3, 90:10:1); ν_{max} (neat) 2959 (C-H), 2917 (C-H), 2861 (C-H), 2922 (C-H); ^{1}H NMR (400 MHz, $CDCl_3$) δ ppm 2.12 (s, 3 H, C(31)H_3), 2.21 (s, 3 H, C(15)H_3), 2.35 (s, 3 H, C(16)H_3), 2.42 - 2.63 (m, 4 H, C(20)H_2+C(24)H_2), 3.58 - 3.76 (m, 5 H, C(18)H+C(21)H_2+C(23)H_2), 4.17 (dd, J=14.0, 8.5 Hz, 1 H, C(17)H_AH_B), 4.71 (dd, J=14.0, 5.0 Hz, 1 H, C(17)H_AH_B), 6.97 - 7.09 (m, 3 H, C(2)H+2×PhH), 7.16 - 7.27 (m, 4 H, C(3)H+3×PhH), 7.50 (s, 1 H, C(6)H); ^{13}C NMR (126 MHz, $CDCl_3$) δ ppm 10.8 (s, 1 C, C(15)), 11.6 (s, 1 C, C(16)), 13.0 (s, 1 C, C(31)), 47.2 (s, 1 C, C(17)), 51.7 (s, 2 C, C(20)+C(24)), 66.8 (s, 2 C, C(21)+C(23)), 69.5 (s, 1 C, C(18)), 109.8 (s, 1 C, C(3)), 116.7 (s, 1 C, C(10)), 118.9 (s, 1 C, C(6)), 124.0 (s, 1 C, C(2)), 125.1 (s, 1 C, C(1)), 128.4 (s, 2 C, 2×PhC) 128.6 (s, 1 C, C(28)), 128.9 (s, 2 C, 2×PhC) 133.6 (s, 1 C, C(4)), 136.9 (s, 1 C, C(25)), 140.4 (s, 1 C, C(5)), 152.7 (s, 1 C, C(8)), 158.8 (s, 1 C, C(11)), 165.1 (s, 1 C, C(14)); LRMS *m/z* (ESI$^+$) 417 [MH$^+$]; HRMS (ESI$^+$) found 417.2282, calculated for $C_{25}H_{29}N_4O_2^+$ 417.2285; HPLC (System E) t_r 3.5 min (98%).

4-(3,5-Dimethyl-1,2-oxazol-4-yl)-*N*-[1-(morpholin-4-yl)propan-2-yl]-2-nitroaniline (384)

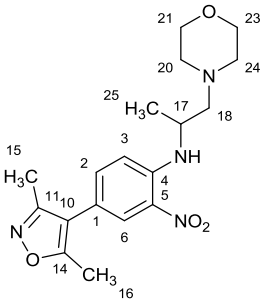

1-(Morpholin-4-yl)propan-2-amine (37 mg, 0.26 mmol) was added to a solution of compound **251** (60 mg, 0.25 mmol) and EtN(*i*-Pr)$_2$ (35 µL, 0.30 mmol) in THF (2 mL) in a sealable vial. The vial was sealed then the solution was heated at 80 °C for 16 h. The resultant mixture was partitioned between CH_2Cl_2 (3 mL) and water (3 mL). The organic phase was collected by passing it through a hydrophobic frit then evaporated by nitrogen blow-down. The crude material was purified by flash column chromatography on a silica column (4 g). The column was eluted with a gradient of EtOAc:*c*-hexane which was increased linearly from 10:90 to 100:0 over 30 CVs. The desired fractions were combined and evaporated to yield the product as a bright-orange solid (61 mg, 68%); R_f (0.30); mp 214-217°C; ν_{max} (neat) 3362 (N-H), 2934 (C-H), 2929 (C-H), 2850 (C-H), 2809 (C-H), 1561 (N-O), 1355 (N-O); ^{1}H NMR (400 MHz, $CDCl_3$) δ ppm 1.35 (d, *J*=6.5 Hz, 3 H, C(25)H_3), 2.27 (s, 3 H, C(15)H_3), 2.41 (s, 3 H, C(16)H_3), 2.46 - 2.67 (m, 6 H, C(18)H_2+C(20)H_2+C(24)H_2), 3.64 - 3.76 (m, 4 H, C(21)H_2+C(23)H_2), 3.79 - 3.89 (m, 1 H, C(17)*H*), 6.97 (d, *J*=9.0 Hz, 1 H, C(3)*H*), 7.33 (dd, *J*=9.0, 2.0 Hz, 1 H, C(2)*H*), 8.08 (d, *J*=2.0 Hz, 1 H, C(6)*H*), 8.28 - 8.50 (m, 1 H, N*H*); ^{13}C NMR (101 MHz, $CDCl_3$) δ ppm 10.8 (s, 1 C, *C*(15)), 11.6 (s, 1 C, *C*(16)), 19.3 (s, 1 C, *C*(25)), 45.8 (s, 1 C, *C*(17)), 53.9 (s, 2 C, *C*(20)+*C*(24)), 63.7 (s, 1 C, *C*(18)), 66.9 (s, 2 C, *C*(21)+*C*(23)), 114.7 - 114.9 (m, 2 C, *C*(3)+*C*(10)), 117.1 (s, 1 C, *C*(1)), 127.2 (s, 1 C, *C*(6)), 132.0 (s, 1 C, *C*(5)), 136.6 (s, 1 C, *C*(2)), 144.0 (s, 1 C, *C*(4)), 158.6 (s, 1 C, *C*(11)), 165.3 (s, 1 C, *C*(14));

LRMS *m/z* (ESI$^+$) 383 [(M+Na)$^+$], 361 [MH$^+$], 359 [(M-H)$^-$]; HRMS (ESI$^+$) found 361.1858, calculated for $C_{18}H_{25}N_4O_4^+$ 361.1870; HPLC (System E) t_r 3.6 min (99%).

4-(3,5-Dimethyl-1,2-oxazol-4-yl)-*N*-[2-(morpholin-4-yl)propyl]-2-nitroaniline (385)

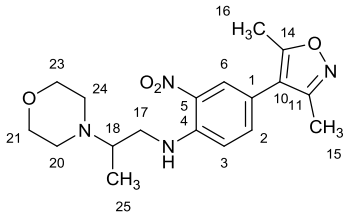

2-(Morpholin-4-yl)propan-1-amine (37 mg, 0.26 mmol) was added to a solution of compound **251** (60 mg, 0.25 mmol) and EtN(*i*-Pr)$_2$ (35 µL, 0.30 mmol) in THF (2 mL) in a sealable vial. The vial was sealed then the solution was heated at 80 °C for 16 h. The resultant mixture was partitioned between CH_2Cl_2 (3 mL) and water (3 mL). The organic phase was collected by passing it through a hydrophobic frit then evaporated by nitrogen blow-down. The crude material was purified by flash column chromatography on a silica column (4 g). The column was eluted with a gradient of EtOAc:*c*-hexane which was increased linearly from 10:90 to 100:0 over 30 CVs. The desired fractions were combined and evaporated to yield the product as a bright-orange solid (73 mg, 81%); R_f 0.35 (EtOAc:*c*-hexane, 80:20); mp 184-187 °C; ν_{max} (neat) 3321 (N-H), 2970 (C-H), 2857 (C-H), 2815 (C-H), 1352 (N-O), 1556 (N-O); ^{1}H NMR (400 MHz, $CDCl_3$) δ ppm 1.13 (d, *J*=6.5 Hz, 3 H, C(25)H_3), 2.26 (s, 3 H, C(15)H_3), 2.40 (s, 3 H, C(16)H_3), 2.45 - 2.57 (m, 2 H, C(20)H_AH_B+C(24)H_AH_B), 2.59 - 2.74 (m, 2 H, C(20)H$_A$$H_B$+C(24)H$_A$$H_B$), 2.97 - 3.07 (m, 1 H, C(18)*H*), 3.07 - 3.18 (m, 1 H, C(17)H_AH_B), 3.27 - 3.37 (m, 1 H, C(17)H$_A$$H_B$), 3.71 - 3.87 (m, 4 H, C(21)H_2+C(23)H_2), 6.89 (d, *J*=8.5 Hz, 1 H, C(3)*H*), 7.33 (dd, *J*=8.5, 2.0 Hz, 1 H, C(2)*H*), 8.09 (d, *J*=2.0 Hz, 1 H, C(6)*H*), 8.80 - 8.93 (m, 1 H, N*H*); ^{13}C NMR (101 MHz, $CDCl_3$) δ ppm 10.7 (s, 1 C, *C*(15)), 11.3 (s, 1 C, *C*(16/25)), 11.5 (s, 1 C, *C*(16/25)), 45.3 (s, 1 C, *C*(17)), 48.0 (s, 2 C, *C*(20)+*C*(24)), 57.4 (s, 1 C, *C*(18)), 67.2 (s, 2 C, *C*(21)+*C*(23)), 114.9 (s, 1 C, *C*(3)), 114.9 (s, 1 C, *C*(10)), 116.9 (s, 1 C, *C*(1)), 127.0 (s, 1 C, *C*(6)), 131.7 (s, 1 C, *C*(5)), 136.6 (s, 1 C, *C*(2)), 144.2 (s, 1 C, *C*(4)), 158.6

(s, 1 C, *C*(2)), 165.2 (s, 1 C, *C*(6)); LRMS *m/z* (ESI+) 383 [(M+Na)+], 361 [MH+]; HRMS (ESI+) found 361.1859, calculated for $C_{18}H_{25}N_4O_4^+$ 361.1870; HPLC (System E) t_r 3.6 min (>99%).

2-[2-(3-Chloro-4-methoxyphenyl)ethyl]-5-(3,5-dimethyl-1,2-oxazol-4-yl)-1-[1-(morpholin-4-yl)propan-2-yl]-1*H*-benzimidazole (386)

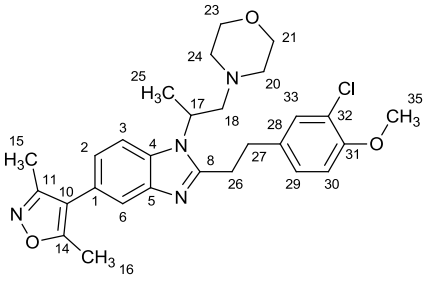

Freshly prepared 1 M aq. $Na_2S_2O_4$ (0.4 mL, 0.4 mmol) was added to a suspension of compound **384** (28 mg, 0.078 mmol) in EtOH (0.5 mL) in a sealable vial. The vial was sealed then heated at 80°C for 2 h then more 1 M aq. $Na_2S_2O_4$ (0.4 mL, 0.4 mmol) was added. The mixture was heated for a further 2 h then allowed to cool. The resultant mixture was partitioned between 10% aq. NH_3 (1.5 mL) and EtOAc (1.5 mL). The organic phase was passed through $MgSO_4$ on a hydrophobic frit then evaporated by nitrogen blow-down. The residue was dissolved in EtOAc (2 mL) then 3-(3-chloro-4-methoxyphenyl)propanoic acid (14 mg, 0.065 mmol), DIPEA (15 µL, 0.086 mmol) and T3P (50 wt.% in EtOAc, 0.2 mL, 0.31 mmol) were added. The solution was heated under reflux for 18 h then allowed to cool. The resultant solution was partitioned between EtOAc (3 mL) and 1 M aq. NaOH (3 mL). The organic phase was passed through a little $MgSO_4$ on a hydrophobic frit then evaporated by nitrogen blow-down. The crude material was purified by flash column chromatography on a silica column (4 g). The column was eluted with a gradient of EtOAc:MeOH:NEt_3 which was increased linearly from 99:1:0.1 to 95:5:0.5 over 30 CVs. The desired fractions were combined and evaporated to yield the product as a colourless gum (9 mg, 23%); R_f 0.50 (EtOAc:MeOH:NEt_3, 90:10:1); ν_{max} (neat) 2957 (C-H), 2923 (C-H), 2857 (C-H); ^{1}H NMR (400 MHz, $CDCl_3$) δ ppm 1.60 (d, *J*=7.0 Hz, 3 H, C(25)H_3), 2.24 - 2.35 (m, 5 H,

C(15)H_3+C(20)H_AH$_B$+C(24)H_AH$_B$), 2.41 - 2.52 (m, 5 H, C(16)H_3+C(20)H$_A$$H_B$+C(24)H$_A$$H_B$), 2.78 (dd, J=13.5, 5.5 Hz, 1 H, C(18)H_AH$_B$), 2.96 (dd, J=13.5, 8.5 Hz, 1 H, C(18)H$_A$$H_B$), 3.08 - 3.30 (m, 4 H, C(26)H_2+C(27)H_2), 3.55 - 3.64 (m, 4 H, C(21)H_2+C(23)H_2), 3.90 (s, 3 H, C(35)H_3), 4.53 - 4.67 (m, 1 H, C(17)H), 6.88 (d, J=8.5 Hz, 1 H, C(30)H), 7.09 (dd, J=8.5, 1.5 Hz, 1 H, C(2)H), 7.13 (dd, J=8.5, 2.0 Hz, 1 H, C(29)H), 7.29 (d, J=2.0 Hz, 1 H, C(33)H), 7.49 (d, J=8.5 Hz, 1 H, C(3)H), 7.64 (d, J=1.5 Hz, 1 H, C(6)H); ^{13}C NMR (126 MHz, $CDCl_3$) δ ppm 10.9 (s, 1 C, C(15)), 11.6 (s, 1 C, C(16)), 18.0 (s, 1 C, C(25)), 30.2 (s, 1 C, C(26)), 32.7 (s, 1 C, C(26)), 50.8 (s, 1 C, C(27)), 54.1 (s, 2 C, C(20)+C(24)), 56.2 (s, 1 C, C(35)), 62.2 (s, 1 C, C(18)), 66.9 (s, 2 C, C(21)+C(23)), 111.5 (s, 1 C, C(3)), 112.3 (s, 1 C, C(30)), 116.9 (s, 1 C, C(10)), 120.1 (s, 1 C, C(6)), 122.4 (s, 1 C, C(32)), 123.2 (s, 1 C, C(2)), 124.1 (s, 1 C, C(1)), 127.6 (s, 1 C, C(29)), 130.0 (s, 1 C, C(33)), 132.6 (s, 1 C, C(28)), 133.9 (s, 1 C, C(4)), 143.2 (s, 1 C, C(5)), 153.6 (s, 1 C, C(31)), 155.0 (s, 1 C, C(8)), 159.0 (s, 1 C, C(11)), 165.1 (s, 1 C, C(14)); LRMS *m/z* (ESI$^+$) 509 [MH$^+$]; HRMS (ESI$^+$) found 509.2305, calculated for $C_{28}H_{34}ClN_4O_3^+$ 509.2314; HPLC (System E) t_r 5.8 min (86%).

5-(3,5-Dimethyl-1,2-oxazol-4-yl)-2-[2-(1*H*-indol-1-yl)ethyl]-1-[1-(morpholin-4-yl)propan-2-yl]-1*H*-benzimidazole (387)

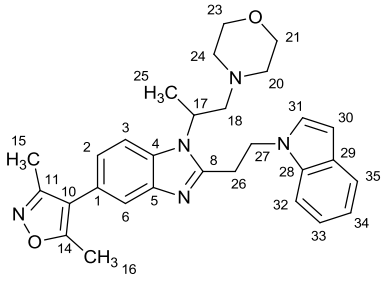

Freshly prepared 1 M aq. $Na_2S_2O_4$ (0.4 mL, 0.4 mmol) was added to a suspension of compound **384** (28 mg, 0.078 mmol) in EtOH (0.5 mL) in a sealable vial. The vial was sealed then heated at 80°C for 2 h then more 1 M aq. $Na_2S_2O_4$ (0.4 mL, 0.4 mmol) was added. The mixture was heated for a further 2 h then allowed to cool. The resultant mixture was partitioned between 10% aq. NH_3 (1.5 mL) and EtOAc (1.5 mL). The organic phase was

passed through $MgSO_4$ on a hydrophobic frit then evaporated by nitrogen blow-down. The residue was dissolved in EtOAc (2 mL) then 3-(1*H*-indol-1-yl)propanoic acid (12 mg, 0.063 mmol), DIPEA (15 µL, 0.086 mmol) and T3P (50 wt.% in EtOAc, 0.2 mL, 0.31 mmol) were added. The solution was heated under reflux for 18 h then allowed to cool. The resultant solution was partitioned between EtOAc (3 mL) and 1 M aq. NaOH (3 mL). The organic phase was passed through a little $MgSO_4$ on a hydrophobic frit then evaporated by nitrogen blow-down. The crude material was purified by flash column chromatography on a silica column (4 g). The column was eluted with a gradient of EtOAc:MeOH:NEt_3 which was increased linearly from 99:1:0.1 to 95:5:0.5 over 30 CVs. The desired fractions were combined and evaporated to yield the product as a colourless gum (11 mg, 29%); R_f 0.45 (EtOAc:MeOH:NEt_3, 90:10:1); ν_{max} (neat) 2927 (C-H), 2853 (C-H); ^{1}H NMR (400 MHz, $CDCl_3$) δ ppm 1.37 (d, *J*=7.0 Hz, 3 H, C(25)H_3), 2.06 - 2.16 (m, 2 H, C(20)H_AH_B+C(24)H_AH_B)), 2.22 - 2.36 (m, 5 H, C(15)H_3+C(20)H_AH_B+C(24)H_AH_B), 2.46 (s, 3 H, C(16)H_3), 2.60 (dd, *J*=13.0, 6.0 Hz, 1 H, C(18)H_AH_B), 2.72 (dd, *J*=13.0, 8.0 Hz, 1 H, C(18)H_AH_B), 3.35 - 3.45 (m, 2 H, C(26)H_2), 3.46 - 3.55 (m, 4 H, C(21)H_2+C(23)H_2), 4.15 - 4.28 (m, 1 H, C(17)*H*), 4.76 - 4.95 (m, 2 H, C(27)H_2), 6.47 (dd, *J*=3.0, 0.5 Hz, 1 H, C(30)*H*), 7.04 - 7.16 (m, 3 H, C(2)*H*+C(31)*H*+C(34)*H*), 7.21 (td, *J*=7.5, 1.0 Hz, 1 H, C(33)*H*), 7.39 (d, *J*=8.0 Hz, 1 H, C(3)*H*), 7.45 (d, *J*=8.5 Hz, 1 H, C(32)*H*), 7.62 - 7.69 (m, 2 H, C(6)*H*+C(35)*H*); ^{13}C NMR (126 MHz, $CDCl_3$) δ ppm 10.9 (s, 1 C, *C*(15)), 11.6 (s, 1 C, *C*(16)), 17.6 (s, 1 C, *C*(25)), 28.9 (s, 1 C, *C*(26)), 44.7 (s, 1 C, *C*(27)), 50.8 (s, 1 C, *C*(17)), 54.0 (s, 2 C, *C*(20)+*C*(24)), 62.2 (s, 1 C, *C*(18)), 66.8 (s, 2 C, *C*(21)+*C*(23)), 101.8 (s, 1 C, *C*(30)), 108.9 (s, 1 C, *C*(3)), 111.6 (s, 1 C, *C*(32)), 116.9 (s, 1 C, *C*(10)), 119.7 (s, 1 C, *C*(34)), 120.1 (s, 1 C, *C*(6)), 121.3 (s, 1 C, *C*(35)), 121.8 (s, 1 C, *C*(33)), 123.3 (s, 1 C, *C*(2)), 124.1 (s, 1 C, *C*(1)), 127.9 (s, 1 C, *C*(31)), 128.9 (s, 1 C, *C*(29)), 132.7 (s, 1 C, *C*(4)), 135.5 (s, 1 C, *C*(28)), 143.5 (s, 1 C, *C*(5)), 153.1 (s, 1 C, *C*(8)), 159.0 (s, 1 C, *C*(11)), 165.1 (s, 1 C, *C*(14)); LRMS *m/z* (ESI$^+$) 484 [MH$^+$]; HRMS (ESI$^+$) found 484.2698, calculated for $C_{29}H_{34}N_5O_2^+$ 484.2707; HPLC (System E) t_r 6.0 min (90%).

2-[2-(3-Chloro-4-methoxyphenyl)ethyl]-5-(3,5-dimethyl-1,2-oxazol-4-yl)-1-[2-(morpholin-4-yl)propyl]-1*H*-benzimidazole (388)

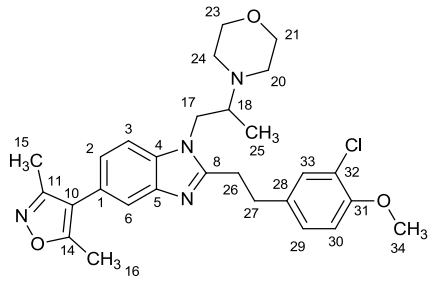

Freshly prepared 1 M aq. $Na_2S_2O_4$ (0.5 mL, 0.5 mmol) was added to a suspension of compound **385** (35 mg, 0.096 mmol) in EtOH (0.5 mL) in a sealable vial. The vial was sealed then heated at 80°C for 2 h then more 1 M aq. $Na_2S_2O_4$ (0.5 mL, 0.5 mmol) was added. The mixture was heated for a further 2 h then allowed to cool. The resultant mixture was partitioned between 10% aq. NH_3 (1.5 mL) and EtOAc (1.5 mL). The organic phase was passed through $MgSO_4$ on a hydrophobic frit then evaporated by nitrogen blow-down. The residue was dissolved in EtOAc (2 mL) then 3-(3-chloro-4-methoxyphenyl)propanoic acid (16 mg, 0.075 mmol), DIPEA (15 µL, 0.086 mmol) and T3P (50 wt.% in EtOAc, 0.2 mL, 0.31 mmol) were added. The solution was heated under reflux for 18 h then allowed to cool. The resultant solution was partitioned between EtOAc (3 mL) and 1 M aq. NaOH (3 mL). The organic phase was passed through a little $MgSO_4$ on a hydrophobic frit then evaporated by nitrogen blow-down. The crude material was purified by flash column chromatography on a silica column (4 g). The column was eluted with a gradient of EtOAc:MeOH:NEt_3 which was increased linearly from 99:1:0.1 to 95:5:0.5 over 30 CVs. The desired fractions were combined and evaporated to yield the product as a colourless gum (19 mg, 39%); R_f 0.45 (EtOAc:MeOH:NEt_3, 90:10:1); ν_{max} (neat) 2968 (C-H), 2855 (C-H) 1503 (C-H); ^{1}H NMR (400 MHz, $CDCl_3$) δ ppm 1.04 (d, *J*=6.5 Hz, 3 H, C(25)H_3), 2.32 (s, 3 H, C(15)H_3), 2.45 (s, 3 H, C(16)H_3), 2.50 - 2.66 (m, 2 H, C(20)H_AH_B+C(24)H_AH_B), 2.64 - 2.79 (m, 2 H, C(20)H_AH_B+C(24)H_AH_B), 2.95 - 3.06 (m, 1 H, C(18)H), 3.13 - 3.33 (m, 4 H, C(26)H_2+C(27)H_2)), 3.63 - 3.82 (m, 4 H, C(17)H_AH_B+C(34)H_3), 3.83 - 3.99 (m, 4 H, C(21)H_2+C(23)H_2), 4.18 - 4.37

(m, 1 H, C(17)H_AH_B), 6.88 (d, *J*=8.5 Hz, 1 H, C(30)*H*), 7.07 - 7.20 (m, 2 H, C(2)*H*+C(29)*H*), 7.29 (d, *J*=2.0 Hz, 1 H, C(33)*H*), 7.40 (d, *J*=7.0 Hz, 1 H, C(3)*H*), 7.67 (d, *J*=1.0 Hz, 1 H, C(6)*H*); ^{13}C NMR (126 MHz, $CDCl_3$) δ ppm 10.9 (s, 1 C, *C*(15)), 11.6 (s, 1 C, *C*(16)), 12.0 (s, 1 C, *C*(25)), 29.6 (s, 1 C, *C*(26)), 32.5 (s, 1 C, *C*(27)), 46.5 (s, 1 C, *C*(17)), 49.3 (s, 2 C, *C*(20)+*C*(24)), 56.2 (s, 1 C, *C*(34)), 59.5 (s, 1 C, *C*(18)), 66.6 (s, 1 C, *C*(21)+*C*(23)), 109.9 (s, 1 C, *C*(3)), 112.3 (s, 1 C, *C*(30)), 116.9 (s, 1 C, *C*(10)), 119.7 (s, 1 C, *C*(6)), 122.4 (s, 1 C, *C*(32)), 123.7 (s, 1 C, *C*(2)), 124.6 (s, 1 C, *C*(1)), 127.7 (s, 1 C, *C*(29)), 130.0 (s, 1 C, *C*(33)), 133.8 (s, 1 C, *C*(28)), 134.3 (s, 1 C, *C*(4)), 142.2 (s, 1 C, *C*(5)), 153.6 (s, 1 C, *C*(31)), 155.0 (s, 1 C, *C*(8)), 158.9 (s, 1 C, *C*(11)), 165.1 (s, 1 C, *C*(14)); LRMS *m/z* (ESI^+) 509 [MH^+]; HRMS (ESI^+) found 509.2314, calculated for $C_{28}H_{34}ClN_4O_3^+$ 509.2314; HPLC (System E) t_r 5.6 min (96%).

5-(3,5-Dimethyl-1,2-oxazol-4-yl)-2-[2-(1*H*-indol-1-yl)ethyl]-1-[2-(morpholin-4-yl)propyl]-1*H*-benzimidazole (389)

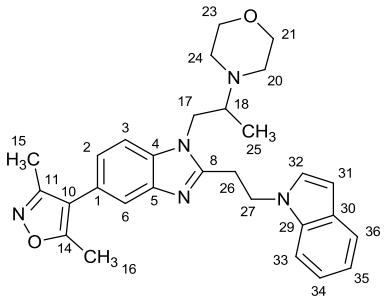

Freshly prepared 1 M aq. $Na_2S_2O_4$ (0.5 mL, 0.5 mmol) was added to a suspension of compound **385** (35 mg, 0.096 mmol) in EtOH (0.5 mL) in a sealable vial. The vial was sealed then heated at 80°C for 2 h then more 1 M aq. $Na_2S_2O_4$ (0.5 mL, 0.5 mmol) was added. The mixture was heated for a further 2 h then allowed to cool. The resultant mixture was partitioned between 10% aq. NH_3 (1.5 mL) and EtOAc (1.5 mL). The organic phase was passed through $MgSO_4$ on a hydrophobic frit then evaporated by nitrogen blow-down. The residue was dissolved in EtOAc (2 mL) then 3-(1*H*-indol-1-yl)propanoic acid (14 mg, 0.085 mmol), DIPEA (15 µL, 0.086 mmol) and T3P (50 wt.% in EtOAc, 0.2 mL, 0.31 mmol) were added. The solution was heated under reflux for 18 h then allowed to cool. The resultant

solution was partitioned between EtOAc (3 mL) and 1 M aq. NaOH (3 mL). The organic phase was passed through a little $MgSO_4$ on a hydrophobic frit then evaporated by nitrogen blow-down. The crude material was purified by flash column chromatography on a silica column (4 g). The column was eluted with a gradient of EtOAc:MeOH:NEt_3 which was increased linearly from 99:1:0.1 to 95:5:0.5 over 30 CVs. The desired fractions were combined and evaporated to yield the product as a colourless gum (12 mg, 26%); R_f 0.35 (EtOAc:MeOH:NEt_3, 90:10:1); ν_{max} (neat) 2963 (C-H), 2855 (C-H); ^{1}H NMR (400 MHz, $CDCl_3$) δ ppm 0.74 (d, *J*=6.5 Hz, 3 H, C(25)H_3)), 1.60 - 2.81 (m, 12 H, C(15)H_3+C(16)H_3+C(18)*H*+C(20)H_2+C(24)H_2), 3.10 - 3.91 (m, 7 H, C(17)H_2+C(21)H_2+C(23)H_2+ C(27)H_2), 4.81 (t, *J*=6.0 Hz, 2 H, C(26)H_2), 6.41 (d, *J*=2.5 Hz, 1 H, 1 H, C(31)*H*), 6.87 (d, *J*=2.5 Hz, 1 H, 1 H, C(32)*H*), 7.05 - 7.16 (m, 2 H, C(2)*H*+C(34)*H*), 7.20 (t, *J*=7.5 Hz, 1 H, 1 H, C(35)*H*), 7.27 - 7.33 (m, 1 H, C(3)*H*), 7.38 (d, *J*=7.5 Hz, 1 H, C(33)*H*), 7.61 - 7.70 (m, 2 H, C(6)*H*+C(36)*H*); ^{13}C NMR (126 MHz, $CDCl_3$) δ ppm 10.9 (s, 1 C, *C*(15)), 11.6 (s, 2 C, *C*(16)+*C*(25)), 28.6 (s, 1 C, *C*(26)), 45.4 (s, 2 C, *C*(17)+*C*(27)), 48.9 (s, 2 C, *C*(20)+*C*(24)), 59.4 (s, 1 C, *C*(18)), 66.5 (s, 2 C, *C*(21)+*C*(23)), 101.8 (s, 1 C, *C*(31)), 109.2 (s, 1 C, *C*(33)), 110.0 (s, 1 C, *C*(3)), 116.9 (s, 1 C, *C*(10)), 119.8 (s, 1 C, *C*(34)), 119.8 (s, 1 C, *C*(6)), 121.3 (s, 1 C, *C*(36)), 121.9 (s, 1 C, *C*(35)), 123.9 (s, 1 C, *C*(2)), 124.8 (s, 1 C, *C*(1)), 128.1 (s, 1 C, *C*(32)), 128.8 (s, 1 C, *C*(30)), 134.4 (s, 1 C, *C*(4)), 135.3 (s, 1 C, *C*(29)), 142.7 (s, 1 C, *C*(5)), 153.5 (s, 1 C, *C*(8)), 158.9 (s, 1 C, *C*(11)), 165.1 (s, 1 C, *C*(14)); LRMS *m/z* (ESI$^+$) 484 [MH$^+$]; HRMS (ESI$^+$) found 484.2698, calculated for $C_{29}H_{34}N_5O_2^+$ 484.2707; HPLC (System E) t_r 3.9 min (98%).

(2*R*)-*N*^{1}-[4-(3,5-Dimethyl-1,2-oxazol-4-yl)-2-nitrophenyl]propane-1,2-diamine (390)

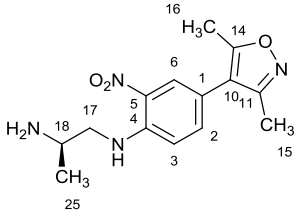

EtN(*i*-Pr)$_2$ (1.29 mL, 7.40 mmol) was added to a suspension of (*R*)-propane-1,2-diamine dihydrochloride (374 mg, 2.54 mmol) and compound **251** (500 mg, 2.12 mmol) and in THF (20 mL). The mixture was stirred at room temperature for 16 h then at reflux for 2 h then allowed to cool. K_2CO_3 (1.02 g, 7.40 mmol) and DMF (5 mL) were added then the mixture was heated under reflux for 4 h then allowed to cool. The resultant mixture was partitioned between EtOAc (10 mL) and water (10 mL). The phases were separated then the organic phase was washed with water (10 mL) and brine (10 mL) then dried over $MgSO_4$ and evaporated. The crude material was purified by flash column chromatography on a silica column (40 g). The column was eluted with a gradient of CH_2Cl_2:MeOH:NH_4OH which was increased linearly from 99:1:0.1 to 90:10:1 over 12 CVs. The desired fractions were combined and evaporated to yield the product (4:1 ratio of regioisomers in favour of desired) as a bright-orange solid (233 mg, 38%); R_f 0.15 (CH_2Cl_2:MeOH:NH_4OH, 90:10:1); mp 124-127 °C; $[\alpha]_D^{20}$ -20.4 (*c* 0.44 in $CHCl_3$); ν_{max} (neat) 3372 (N-H), 2964 (C-H), 2928 (C-H), 2869 (C-H), 1528 (N-O), 1353 (N-O); ^{1}H NMR (400 MHz, $CDCl_3$) δ ppm 1.24 (d, *J*=6.0 Hz, 3 H, C(15)H_3), 2.26 (s, 3 H), 2.40 (s, 3 H, C(16)H_3), 3.11 - 3.24 (m, 1 H, C(17)H_AH_B), 3.25 - 3.41 (m, 2 H, C(17)H_AH_B+C(18)*H*), 6.96 (d, *J*=9.0 Hz, 1 H, C(3)*H*), 7.33 (dd, *J*=9.0, 2.0 Hz, 1 H, C(2)*H*), 8.08 (d, *J*=2.0 Hz, 1 H, C(6)*H*), 8.41 (br. s., 1 H, *N*H); ^{13}C NMR (101 MHz, $CDCl_3$) δ ppm 10.7 (s, 1 C, *C*(15)), 11.5 (s, 1 C, *C*(16)), 22.1 (s, 1 C, *C*(20)), 46.0 (s, 1 C, *C*(18)), 50.9 (s, 1 C, *C*(17)), 114.6 (s, 1 C, *C*(3)), 114.8 (s, 1 C, *C*(10)), 117.4 (s, 1 C, *C*(1)), 127.0 (s, 1 C, *C*(6)), 131.9 (s, 1 C, *C*(5)), 136.7 (s, 1 C, *C*(2)), 144.7 (s, 1 C, *C*(4)), 158.5 (s, 1 C, *C*(11)), 165.3 (s, 1 C, *C*(14)); LRMS *m/z* (ESI$^+$) 313 [(M+Na)$^+$], 291 [MH$^+$]; HRMS (ESI$^+$) found 291.1444, calculated for $C_{14}H_{19}N_4O_3^+$ 291.1452; HPLC (System E) t_r 3.6 min (81%).

(2*S*)-*N*^{1}-[4-(3,5-Dimethyl-1,2-oxazol-4-yl)-2-nitrophenyl]propane-1,2-diamine (391)

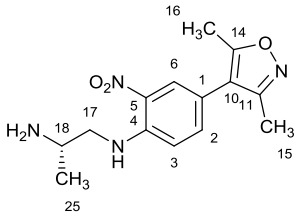

EtN(*i*-Pr)$_2$ (1.29 mL, 7.40 mmol) was added to a suspension of (*R*)-propane-1,2-diamine dihydrochloride (374 mg, 2.54 mmol) and compound **251** (500 mg, 2.12 mmol) and in THF (20 mL). The mixture was stirred at room temperature for 16 h then at reflux for 2 h then allowed to cool. K_2CO_3 (1.02 g, 7.40 mmol) and DMF (5 mL) were added then the mixture was heated under reflux for 4 h then allowed to cool. The resultant mixture was partitioned between EtOAc (10 mL) and water (10 mL). The phases were separated then the organic phase was washed with water (10 mL) and brine (10 mL) then dried over $MgSO_4$ and evaporated. The crude material was purified by flash column chromatography on a silica column (40 g). The column was eluted with a gradient of CH_2Cl_2:MeOH:NH_4OH which was increased linearly from 99:1:0.1 to 90:10:1 over 12 CVs. The desired fractions were combined and evaporated to yield the product (4:1 ratio of regioisomers in favour of desired) as a bright-orange solid (254 mg, 41%); R_f 0.15 (CH_2Cl_2:MeOH:NH_4OH, 90:10:1); mp 126-129 °C; $[\alpha]_D^{20}$ +17.7 (*c* 1.4 in $CHCl_3$); ν_{max} (neat) 3369 (N-H), 2964 (C-H), 2928 (C-H), 2871 (C-H), 1526 (N-O), 1352 (N-O); ^{1}H NMR (400 MHz, $CDCl_3$) δ ppm 1.24 (d, *J*=6.0 Hz, 3 H, C(15)*H*$_3$), 2.26 (s, 3 H), 2.40 (s, 3 H, C(16)*H*$_3$), 3.11 - 3.24 (m, 1 H, C(17)H_AH_B), 3.25 - 3.41 (m, 2 H, C(17)H_AH_B+C(18)*H*), 6.96 (d, *J*=9.0 Hz, 1 H, C(3)*H*), 7.33 (dd, *J*=9.0, 2.0 Hz, 1 H, C(2)*H*), 8.08 (d, *J*=2.0 Hz, 1 H, C(6)*H*), 8.41 (br. s., 1 H, *N*H); ^{13}C NMR (101 MHz, $CDCl_3$) δ ppm 10.7 (s, 1 C, *C*(15)), 11.5 (s, 1 C, *C*(16)), 22.1 (s, 1 C, *C*(20)), 46.0 (s, 1 C, *C*(18)), 50.9 (s, 1 C, *C*(17)), 114.6 (s, 1 C, *C*(3)), 114.8 (s, 1 C, *C*(10)), 117.4 (s, 1 C, *C*(1)), 127.0 (s, 1 C, *C*(6)), 131.9 (s, 1 C, *C*(5)), 136.7 (s, 1 C, *C*(2)), 144.7 (s, 1 C, *C*(4)), 158.5 (s, 1 C, *C*(11)), 165.3 (s, 1 C, *C*(14));

LRMS *m/z* (ESI$^+$) 313 [(M+Na)$^+$], 291 [MH$^+$]; HRMS (ESI$^+$) found 291.1446, calculated for $C_{14}H_{19}N_4O_3^+$ 291.1452; HPLC (System E) t_r 3.6 min (87%).

4-(3,5-Dimethyl-1,2-oxazol-4-yl)-*N*^{1}-[(2*R*)-2-(morpholin-4-yl)propyl]-2-nitroaniline (392)

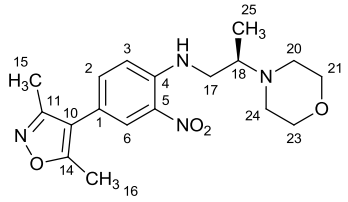

2-Bromoethyl ether (100 µL, 0.79 mmol) was added to a suspension of compound **390** (210 mg, 0.72 mmol) and K_2CO_3 (299 mg, 2.16 mmol) in DMF (5 mL) . The mixture was heated in a sealed vial at 70 °C for 16 h then allowed to cool. The resultant mixture was partitioned between water (5 mL) and EtOAc (5 mL). The phases were separated then the aqueous phase was extracted with more EtOAc (5 mL). The combined organic phases were washed with water (5 mL) and brine (5 mL) then dried over $MgSO_4$ and evaporated directly onto silica. The crude material was purified by flash column chromatography on a silica column (24 g). The column was eluted with a gradient of acetone:CH_2Cl_2 which was increased linearly from 0:100 to 6:94 over 6 CVs then isocratic at 6:94 for 10 CVs. The desired fractions were combined and evaporated then the resultant material was purified again by flash column chromatography on a silica column (12 g). The column was eluted with acetone:*c*-hexane (1:9). The desired fractions were combined and evaporated to yield the product as a pale orange solid (71 mg, 27%); R_f 0.20 (acetone:*c*-hexane, 20:80); ^{1}H NMR (400 MHz, $CDCl_3$) δ ppm 1.13 (d, *J*=6.5 Hz, 3 H, C(25)H_3), 2.26 (s, 3 H, C(15)H_3), 2.40 (s, 3 H, C(16)H_3), 2.45 - 2.57 (m, 2 H, C(20)H_AH_B+C(24)H_AH_B), 2.59 - 2.74 (m, 2 H, C(20)H_AH_B+C(24)H_AH_B), 2.97 - 3.07 (m, 1 H, C(18)*H*), 3.07 - 3.18 (m, 1 H, C(17)H_AH_B), 3.27 - 3.37 (m, 1 H, C(17)H_AH_B), 3.71 - 3.87 (m, 4 H, C(21)H_2+C(23)H_2), 6.89 (d, *J*=8.5 Hz, 1 H, C(3)*H*), 7.33 (dd, *J*=8.5, 2.0 Hz, 1 H, C(2)*H*), 8.09 (d, *J*=2.0 Hz, 1 H, C(6)*H*), 8.80 - 8.93 (m, 1 H,

N*H*); ^{13}C NMR (101 MHz, $CDCl_3$) δ ppm 10.7 (s, 1 C, *C*(15)), 11.3 (s, 1 C, *C*(16/25)), 11.5 (s, 1 C, *C*(16/25)), 45.3 (s, 1 C, *C*(17)), 48.0 (s, 2 C, *C*(20)+*C*(24)), 57.4 (s, 1 C, *C*(18)), 67.2 (s, 2 C, *C*(21)+*C*(23)), 114.9 (s, 1 C, *C*(3)), 114.9 (s, 1 C, *C*(10)), 116.9 (s, 1 C, *C*(1)), 127.0 (s, 1 C, *C*(6)), 131.7 (s, 1 C, *C*(5)), 136.6 (s, 1 C, *C*(2)), 144.2 (s, 1 C, *C*(4)), 158.6 (s, 1 C, *C*(2)), 165.2 (s, 1 C, *C*(6)); LRMS *m/z* (ESI$^+$) 361 [MH$^+$]; HRMS (ESI$^+$) found 361.1858, calculated for $C_{18}H_{25}N_4O_4^+$ 361.1870; HPLC (System E), 3.6 min (>99%).

4-(3,5-Dimethyl-1,2-oxazol-4-yl)-*N*^{1}-[(2*S*)-2-(morpholin-4-yl)propyl]-2-nitroaniline (393)

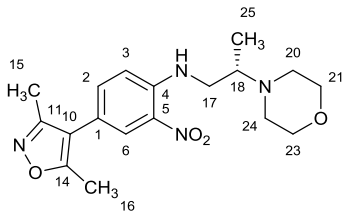

2-Bromoethyl ether (0.68 mL, 5.4 mmol) was added to a suspension of compound **391** (1.43 g, 4.92 mmol) and K_2CO_3 (2.04 g, 14.8 mmol) in DMF (50 mL). The mixture was heated at 70 °C for 16 h then allowed to cool and partitioned between EtOAc (50 mL) and water (50 mL). The phases were separated then the organic phase was extracted with more EtOAc (50 mL). The combined organic phases were washed with 1:1 brine:water (3×50 mL) then brine (50 mL) then dried over $MgSO_4$ and evaporated. The crude material was purified by flash column chromatography on a silica column (80 g). The column was eluted with a gradient of acetone:CH_2Cl_2, which was increased linearly from 0:100 to 10:90 over 10 CVs. The desired fractions were combined and evaporated. The resultant material was purified further by flash column chromatography on a silica column (80 g). The column was eluted with a gradient of acetone:*c*-hexane, which was increased linearly from 10:90 to 20:80 over 20 CVs. The desired fractions were combined and evaporated to yield the product as an orange solid (620 mg, 35%); R_f 0.20 (acetone:*c*-hexane, 20:80); mp 182-185 °C; ν_{max} (neat) 3321 (N-H), 2964 (C-H), 2858 (C-H), 2815 (C-H), 1525 (N-O), 1353 (N-O); ^{1}H NMR (400 MHz, $CDCl_3$) δ

ppm 1.13 (d, *J*=6.5 Hz, 3 H, C(25)H_3), 2.26 (s, 3 H, C(15)H_3), 2.40 (s, 3 H, C(16)H_3), 2.45 - 2.57 (m, 2 H, C(20)H_AH_B+C(24)H_AH_B), 2.59 - 2.74 (m, 2 H, C(20)H_AH_B+C(24)H_AH_B), 2.97 - 3.07 (m, 1 H, C(18)*H*), 3.07 - 3.18 (m, 1 H, C(17)H_AH_B), 3.27 - 3.37 (m, 1 H, C(17)H_AH_B), 3.71 - 3.87 (m, 4 H, C(21)H_2+C(23)H_2), 6.89 (d, *J*=8.5 Hz, 1 H, C(3)*H*), 7.33 (dd, *J*=8.5, 2.0 Hz, 1 H, C(2)*H*), 8.09 (d, *J*=2.0 Hz, 1 H, C(6)*H*), 8.80 - 8.93 (m, 1 H, N*H*); ^{13}C NMR (101 MHz, $CDCl_3$) δ ppm 10.7 (s, 1 C, *C*(15)), 11.3 (s, 1 C, *C*(16/25)), 11.5 (s, 1 C, *C*(16/25)), 45.3 (s, 1 C, *C*(17)), 48.0 (s, 2 C, *C*(20)+*C*(24)), 57.4 (s, 1 C, *C*(18)), 67.2 (s, 2 C, *C*(21)+*C*(23)), 114.9 (s, 1 C, *C*(3)), 114.9 (s, 1 C, *C*(10)), 116.9 (s, 1 C, *C*(1)), 127.0 (s, 1 C, *C*(6)), 131.7 (s, 1 C, *C*(5)), 136.6 (s, 1 C, *C*(2)), 144.2 (s, 1 C, *C*(4)), 158.6 (s, 1 C, *C*(2)), 165.2 (s, 1 C, *C*(6)); LRMS *m/z* (ESI$^+$) 383 [(M+Na)$^+$], 361 [MH$^+$]; HRMS (ESI$^+$) found 361.1856, calculated for $C_{18}H_{25}N_4O_4^+$ 361.1870; HPLC (System E) t_r 3.7 min (>99%).

2-[2-(3-Chloro-4-methoxyphenyl)ethyl]-5-(3,5-dimethyl-1,2-oxazol-4-yl)-1-[(2*R*)-2-(morpholin-4-yl)propyl]-1*H*-benzimidazole (394)

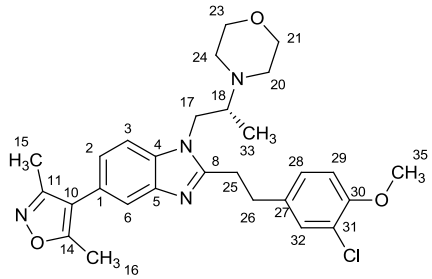

Freshly prepared 1 M aq. $Na_2S_2O_4$ (0.32 mL, 0.32 mmol) was added to a suspension of compound **392** (23 mg, 0.065 mmol) in EtOH (0.5 mL) in a sealable vial. The vial was sealed then heated at 80°C for 1 h then allowed to cool. The resultant mixture was partitioned between 10% aq. NH_3 (1 mL) and EtOAc (1 mL). The organic phase was passed through a hydrophobic frit then evaporated by nitrogen blow-down. The residue was dissolved in EtOAc (2 mL) then added to a vial containing 3-(3-chloro-4-methoxyphenyl)propanoic acid (13 mg, 0.061 mmol). DIPEA (23 µL, 0.13 mmol) and T3P (50 wt.% in EtOAc, 0.2 mL, 0.31 mmol) were added then the solution was heated at 80 °C for 16 h then allowed to cool. 1 M

aq. NaOH solution (1 mL) was added and the phases were mixed then allowed to separate. The organic phase was passed through a hydrophobic frit then evaporated by nitrogen blow-down. The crude material was purified by flash column chromatography on a silica column (4 g). The column was eluted with a gradient of EtOAc:MeOH:NEt_3 which was increased linearly from 99:1:0.1 to 95:5:0.5 over 30 CVs. The desired fractions were combined and evaporated to yield the product as a colourless gum (15 mg, 46%); R_f 0.50 (EtOAc:MeOH:NEt_3, 90:10:1); $[\alpha]_D^{20}$ -3.8 (*c* 0.6 in $CHCl_3$); ν_{max} (neat) 2964 (C-H), 2933 (C-H), 2854 (C-H); ^{1}H NMR (400 MHz, $CDCl_3$) δ ppm 0.93 (d, *J*=7.0 Hz, 3 H, C(33)H_3), 2.23 (s, 3 H, C(15)H_3), 2.36 (s, 3 H, C(16)H_3), 2.38 - 2.48 (m, 2 H, C(20)$H_A$$H_B$+C(24)$H_A$$H_B$), 2.53 - 2.61 (m, 2 H, C(20)$H_A$$H_B$+C(24)$H_A$$H_B$), 2.81 - 2.94 (m, 1 H, C(18)*H*), 3.00 - 3.12 (m, 2 H, C(25)H_2), 3.12 - 3.22 (m, 2 H, C(26)H_2), 3.51 - 3.65 (m, 4 H, C(21)H_2+C(23)H_2), 3.76 - 3.84 (m, 4 H, C(17)$H_A$$H_B$+C(35)$H_3$), 4.08 (dd, *J*=14.5, 6.5 Hz, 1 H, C(17)$H_A$$H_B$), 6.79 (d, *J*=8.5 Hz, 1 H, C(3)*H*), 6.99 - 7.07 (m, 2 H, C(2)*H*+C(28)*H*), 7.20 (d, *J*=1.5 Hz, 1 H, C(32)*H*), 7.26 (d, *J*=8.5 Hz, 1 H, C(3)*H*), 7.56 (d, *J*=1.0 Hz, 1 H, C(6)*H*); ^{13}C NMR (101 MHz, $CDCl_3$) δ ppm 10.9 (s, 1 C, *C*(15)), 11.6 (s, 1 C, *C*(16)), 12.2 (s, 1 C, *C*(33)), 29.7 (s, 1 C, *C*(25)), 32.5 (s, 1 C, *C*(26)), 46.6 (s, 1 C, *C*(17)), 49.3 (s, 2 C, *C*(20)+*C*(24)), 56.2 (s, 1 C, *C*(35)), 59.5 (s, 1 C, *C*(18)), 66.9 (s, 2 C, *C*(21)+*C*(23)), 109.8 (s, 1 C, *C*(3)), 112.2 (s, 1 C, *C*(29)), 117.0 (s, 1 C, *C*(10)), 119.8 (s, 1 C, *C*(6)), 122.4 (s, 1 C, *C*(31)), 123.5 (s, 1 C, *C*(2)), 124.3 (s, 1 C, *C*(1)), 127.7 (s, 1 C, *C*(28)), 130.0 (s, 1 C, *C*(32)), 133.9 (s, 1 C, *C*(27)), 134.5 (s, 1 C, *C*(4)), 142.7 (s, 1 C, *C*(5)), 153.6 (s, 1 C, *C*(30)), 155.1 (s, 1 C, *C*(8)), 159.0 (s, 1 C, *C*(11)), 165.0 (s, 1 C, *C*(14)); LRMS *m/z* (ESI$^+$) 511 [M(^{37}Cl)H$^+$] 509 [M(^{35}Cl)H$^+$]; HRMS (ESI$^+$) found 511.2297, calculated for $C_{28}H_{34}(^{37}Cl)N_4O_3^+$ 511.2287; HRMS (ESI$^+$) found 509.2312, calculated for $C_{28}H_{34}(^{35}Cl)N_4O_3^+$ 509.2314; HPLC (System E) t_r 3.8 min (97%); *er* >99:1 (HPLC Chiralpak AD column, λ 220 nm, *n*-hexane/*i*-PrOH (70:30), flow rate 0.9 mL/min, t_r 19.5 min (minor), 26.2 min (major)).

5-(3,5-Dimethyl-1,2-oxazol-4-yl)-2-[2-(1*H*-indol-1-yl)ethyl]-1-[(2*R*)-2-(morpholin-4-yl)propyl]-1*H*-benzimidazole (395)

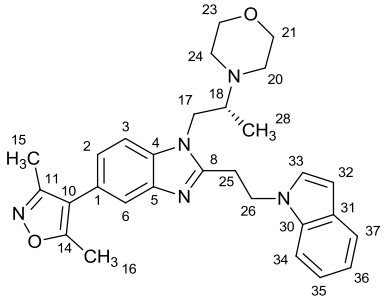

Freshly prepared 1 M aq. $Na_2S_2O_4$ (0.32 mL, 0.32 mmol) was added to a suspension of compound **392** (23 mg, 0.065 mmol) in EtOH (0.5 mL) in a sealable vial. The vial was sealed then heated at 80°C for 1 h then allowed to cool. The resultant mixture was partitioned between 10% aq. NH_3 (1 mL) and EtOAc (1 mL). The organic phase was passed through a hydrophobic frit then evaporated by nitrogen blow-down. The residue was dissolved in EtOAc (2 mL) then added to a vial containing 3-(1*H*-indol-1-yl)propanoic acid (11 mg, 0.058 mmol). DIPEA (23 μL, 0.13 mmol) and T3P (50 wt.% in EtOAc, 0.2 mL, 0.31 mmol) were added then the solution was heated at 80 °C for 16 h then allowed to cool. 1 M aq. NaOH solution (1 mL) was added and the phases were mixed then allowed to separate. The organic phase was passed through a hydrophobic frit then evaporated by nitrogen blow-down. The crude material was purified by flash column chromatography on a silica column (4 g). The column was eluted with a gradient of EtOAc:MeOH:NEt_3 which was increased linearly from 99:1:0.1 to 95:5:0.5 over 30 CVs. The desired fractions were combined and evaporated to yield the product as a colourless gum (12 mg, 38%); R_f 0.35 (EtOAc:MeOH:NEt_3, 90:10:1); $[\alpha]_D^{20}$ +6.4 (*c* 0.5 in $CHCl_3$); ν_{max} (neat) 2964 (C-H), 2855 (C-H), 2819 (C-H); ^{1}H NMR (400 MHz, $CDCl_3$) δ ppm 0.76 (d, *J*=6.5 Hz, 3 H, C(28)H_3), 2.12 - 2.24 (m, 2 H, C(20)H_AH_B+C(24)H_AH_B), 2.27 - 2.38 (m, 5 H, C(15)H_3+C(20)H_AH_B+C(24)H_AH_B), 2.46 (s, 3 H, C(16)H_3), 2.53 - 2.69 (m, 1 H, C(18)*H*), 3.21 - 3.44 (m, 3 H, C(17)H_AH_B+C(25)H_2), 3.47 - 3.66 (m, 5 H, C(17)H_AH_B+C(21)H_2+C(23)H_2), 4.80 (t, *J*=6.5 Hz, 2 H, C(26)H_2), 6.43 (d, *J*=3.0

Hz, 1 H, C(32)*H*), 6.89 (d, *J*=3.0 Hz, 1 H, C(33)*H*), 7.09 - 7.14 (m, 2 H, C(2)*H*+C(35)*H*), 7.16 - 7.22 (m, 1 H, C(36)*H*), 7.25 (d, *J*=8.5 Hz, 1 H, C(3)*H*), 7.36 (d, *J*=8.0 Hz, 1 H, C(34)*H*), 7.57 - 7.70 (m, 2 H, C(6)*H*+C(37)*H*); ^{13}C NMR (101 MHz, $CDCl_3$) δ ppm 10.9 (s, 1 C, *C*(15)), 11.6 (s, 1 C, *C*(16)), 11.8 (s, 1 C, *C*(33)), 28.6 (s, 1 C, *C*(25)), 45.2 (s, 1 C, *C*(26)), 46.2 (s, 1 C, *C*(17)), 49.0 (s, 2 C, *C*(20)+*C*(24)), 59.2 (s, 1 C, *C*(18)), 66.9 (s, 2 C, *C*(21)+*C*(23)), 101.8 (s, 1 C, *C*(32)), 109.0 (s, 1 C, *C*(34)), 109.9 (s, 1 C, *C*(3)), 117.0 (s, 1 C, *C*(10)), 119.7 (s, 1 C, *C*(35)), 119.8 (s, 1 C, *C*(6)), 121.3 (s, 1 C, *C*(37)), 121.8 (s, 1 C, *C*(36)), 123.7 (s, 1 C, *C*(2)), 124.5 (s, 1 C, *C*(1)), 128.0 (s, 1 C, *C*(33)), 128.9 (s, 1 C, *C*(31)), 134.5 (s, 1 C, *C*(4)), 135.4 (s, 1 C, *C*(30)), 142.8 (s, 1 C, *C*(5)), 153.5 (s, 1 C, *C*(8)), 159.0 (s, 1 C, *C*(11)), 165.1 (s, 1 C, *C*(14)); LRMS *m/z* (ESI$^+$) 484 [MH$^+$]; HRMS (ESI$^+$) found 484.2701, calculated for $C_{29}H_{34}N_5O_2^+$ 484.2707; HPLC (System E) t_r 3.9 min (98%); *er* 99:1 (HPLC Chiralpak AD column, λ 220 nm, *n*-hexane/*i*-PrOH (80:20), flow rate 1.0 mL/min, t_r 25.1 min (minor), 27.7 min (major)).

5-(3,5-Dimethyl-1,2-oxazol-4-yl)-2-[2-(3-fluoro-4-methoxyphenyl)ethyl]-1-[(2*R*)-2-(morpholin-4-yl)propyl]-1*H*-benzimidazole (396)

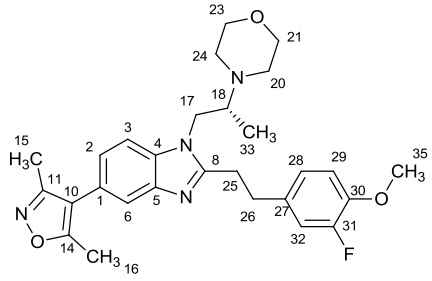

Freshly prepared 1 M aq. $Na_2S_2O_4$ (0.32 mL, 0.32 mmol) was added to a suspension of compound **392** (23 mg, 0.065 mmol) in EtOH (0.5 mL) in a sealable vial. The vial was sealed then heated at 80°C for 1 h then allowed to cool. The resultant mixture was partitioned between 10% aq. NH_3 (1 mL) and EtOAc (1 mL). The organic phase was passed through a hydrophobic frit then evaporated by nitrogen blow-down. The residue was dissolved in EtOAc (2 mL) then added to a vial containing 3-(3-fluoro-4-methoxyphenyl)propanoic acid (12 mg, 0.061 mmol). DIPEA (23 μL, 0.13 mmol) and T3P (50 wt.% in EtOAc, 0.2 mL, 0.31

mmol) were added then the solution was heated at 80 °C for 16 h then allowed to cool. 1 M aq. NaOH solution (1 mL) was added and the phases were mixed then allowed to separate. The organic phase was passed through a hydrophobic frit then evaporated by nitrogen blow-down. The crude material was purified by flash column chromatography on a silica column (4 g). The column was eluted with a gradient of EtOAc:MeOH:NEt_3 which was increased linearly from 99:1:0.1 to 95:5:0.5 over 30 CVs. The desired fractions were combined and evaporated to yield the product as a colourless gum (12 mg, 38%); R_f 0.50 (EtOAc:MeOH:NEt_3, 90:10:1); $[\alpha]_D^{20}$ -11.5 (*c* 0.6 in $CHCl_3$); ν_{max} (neat) 2963 (C-H), 2934 (C-H), 2855 (C-H); ^{1}H NMR (400 MHz, $CDCl_3$) δ ppm 1.01 (d, *J*=7.0 Hz, 3 H, C(33)*H*$_3$), 2.31 (s, 3 H, C(15)*H*$_3$), 2.44 (s, 3 H, C(16)*H*$_3$), 2.45 - 2.54 (m, 2 H, C(20)*H*$_A$H$_B$+C(24)*H*$_A$H$_B$), 2.61 - 2.69 (m, 2 H, C(20)H$_A$*H*$_B$+C(24)H$_A$*H*$_B$), 2.90 - 3.02 (m, 1 H, C(18)*H*), 3.08 - 3.20 (m, 2 H, C(25/26)*H*$_2$), 3.20 - 3.30 (m, 2 H, C(25/26)*H*$_2$), 3.60 - 3.73 (m, 4 H, C(21)*H*$_2$+C(23)*H*$_2$), 3.81 - 3.92 (m, 4 H, C(17)*H*$_A$H$_B$+C(35)*H*$_3$), 4.16 (dd, *J*=14.5, 6.5 Hz, 1 H, C(17)H$_A$*H*$_B$), 6.85 - 6.93 (m, 1 H, C(29)*H*), 6.93 - 7.02 (m, 2 H, C(28)*H*+C(32)*H*), 7.13 (dd, *J*=8.5, 1.5 Hz, 1 H, C(2)*H*), 7.33 (d, *J*=8.5 Hz, 1 H, C(3)*H*), 7.64 (d, *J*=1.5 Hz, 1 H, C(6)*H*); ^{13}C NMR (126 MHz, $CDCl_3$) δ ppm 10.9 (s, 1 C, *C*(15)), 11.6 (s, 1 C, *C*(16)), 12.2 (s, 1 C, *C*(33)), 29.7 (s, 1 C, *C*(25)), 32.7 (s, 1 C, *C*(26)), 46.6 (s, 1 C, *C*(17)), 49.3 (s, 2 C, *C*(20)+*C*(24)), 56.3 (s, 1 C, *C*(35)), 59.5 (s, 1 C, *C*(18)), 66.9 (s, 2 C, *C*(21)+*C*(23)), 109.8 (s, 1 C, *C*(3)), 113.6 (d, *J*=2.0 Hz, 1 C, *C*(29)), 116.0 (d, *J*=17.0 Hz, 1 C, *C*(32)), 117.0 (s, 1 C, *C*(10)), 119.8 (s, 1 C, *C*(6)), 123.5 (s, 1 C, *C*(2)), 124.0 (d, *J*=3.0 Hz, 1 C, *C*(28)), 124.3 (s, 1 C, *C*(1)), 133.8 (d, *J*=6.0 Hz, 1 C, *C*(27)), 134.5 (s, 1 C, *C*(4)), 142.6 (s, 1 C, *C*(5)), 146.2 (d, *J*=10.5 Hz, 1 C, *C*(30)), 152.3 (d, *J*=245.0 Hz, 1 C, *C*(31)), 155.1 (s, 1 C, *C*(8)), 159.0 (s, 1 C, *C*(11)), 165.0 (s, 1 C, *C*(14)); ^{19}F NMR (377 MHz, $CDCl_3$) δ ppm -135.0 (s, 1 F); LRMS *m/z* (ESI$^+$) 493 [MH$^+$]; HRMS (ESI$^+$) found 493.2591, calculated for $C_{28}H_{34}FN_4O_3^+$ 493.2609; HPLC (System E) t_r 3.7 min (96%); *er* >99:1 (HPLC Chiralpak AD column, λ 220 nm, *n*-hexane/*i*-PrOH (80:20), flow rate 1.0 mL/min, t_r 36.9 min (minor), 51.8 min (major)).

2-[2-(3-Chloro-4-methoxyphenyl)ethyl]-5-(3,5-dimethyl-1,2-oxazol-4-yl)-1-[(2*S*)-2-(morpholin-4-yl)propyl]-1*H*-benzimidazole (397)

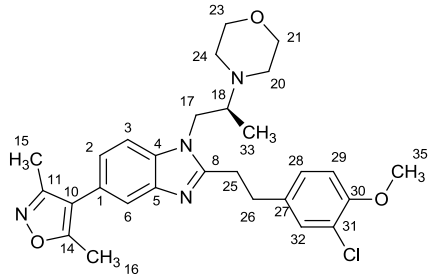

Freshly prepared 1 M aq. $Na_2S_2O_4$ (0.50 mL, 0.50 mmol) was added to a suspension of compound **393** (35 mg, 0.097 mmol) in EtOH (0.5 mL) in a sealable vial. The vial was sealed then heated at 80°C for 1 h then allowed to cool. The resultant mixture was partitioned between 10% aq. NH_3 (1 mL) and EtOAc (1 mL). The organic phase was passed through a hydrophobic frit then evaporated by nitrogen blow-down. The residue was dissolved in EtOAc (3 mL) then added to a vial containing 3-(3-chloro-4-methoxyphenyl)propanoic acid (19 mg, 0.089 mmol). DIPEA (34 µL, 0.19 mmol) and T3P (50 wt.% in EtOAc, 0.3 mL, 0.47 mmol) were added then the solution was heated at 80 °C for 16 h then allowed to cool. 1 M aq. NaOH solution (1 mL) was added and the phases were mixed then allowed to separate. The organic phase was passed through a hydrophobic frit then evaporated by nitrogen blow-down. The crude material was purified by flash column chromatography on a silica column (4 g). The column was eluted with a gradient of EtOAc:MeOH:NEt_3 which was increased linearly from 99:1:0.1 to 95:5:0.5 over 30 CVs. The desired fractions were combined and evaporated to yield the product as a colourless gum (26 mg, 52%); R_f 0.50 (EtOAc:MeOH:NEt_3, 90:10:1); $[\alpha]_D^{20}$ +4.0 (*c* 1.1 in $CHCl_3$); ν_{max} (neat) 2963 (C-H), 2933 (C-H), 2854 (C-H); ^{1}H NMR (400 MHz, $CDCl_3$) δ ppm 0.93 (d, *J*=7.0 Hz, 3 H, C(33)H_3), 2.23 (s, 3 H, C(15)H_3), 2.36 (s, 3 H, C(16)H_3), 2.38 - 2.48 (m, 2 H, C(20)$H_A$$H_B$+C(24)$H_A$$H_B$), 2.53 - 2.61 (m, 2 H, C(20)$H_A$$H_B$+C(24)$H_A$$H_B$), 2.81 - 2.94 (m, 1 H, C(18)H), 3.00 - 3.12 (m, 2 H, C(25)H_2), 3.12 - 3.22 (m, 2 H, C(26)H_2), 3.51 - 3.65 (m, 4 H, C(21)H_2+C(23)H_2), 3.76 - 3.84 (m, 4 H,

C(17)H_AH_B+C(35)H_3), 4.08 (dd, *J*=14.5, 6.5 Hz, 1 H, C(17)H_AH_B), 6.79 (d, *J*=8.5 Hz, 1 H, C(3)*H*), 6.99 - 7.07 (m, 2 H, C(2)*H*+C(28)*H*), 7.20 (d, *J*=1.5 Hz, 1 H, C(32)*H*), 7.26 (d, *J*=8.5 Hz, 1 H, C(3)*H*), 7.56 (d, *J*=1.0 Hz, 1 H, C(6)*H*); ^{13}C NMR (101 MHz, $CDCl_3$) δ ppm 10.9 (s, 1 C, *C*(15)), 11.6 (s, 1 C, *C*(16)), 12.2 (s, 1 C, *C*(33)), 29.7 (s, 1 C, *C*(25)), 32.5 (s, 1 C, *C*(26)), 46.8 (s, 1 C, *C*(17)), 49.3 (s, 2 C, *C*(20)+*C*(24)), 56.2 (s, 1 C, *C*(35)), 59.4 (s, 1 C, *C*(18)), 67.1 (s, 2 C, *C*(21)+*C*(23)), 109.7 (s, 1 C, *C*(3)), 112.2 (s, 1 C, *C*(29)), 117.0 (s, 1 C, *C*(10)), 119.8 (s, 1 C, *C*(6)), 122.3 (s, 1 C, *C*(31)), 123.4 (s, 1 C, *C*(2)), 124.1 (s, 1 C, *C*(1)), 127.6 (s, 1 C, *C*(28)), 130.0 (s, 1 C, *C*(32)), 134.0 (s, 1 C, *C*(27)), 134.6 (s, 1 C, *C*(4)), 142.9 (s, 1 C, *C*(5)), 153.6 (s, 1 C, *C*(30)), 155.1 (s, 1 C, *C*(8)), 159.0 (s, 1 C, *C*(11)), 165.0 (s, 1 C, *C*(14)); LRMS *m/z* (ESI$^+$) 511 [M(^{37}Cl)H$^+$] 509 [M(^{35}Cl)H$^+$]; HRMS (ESI$^+$) found 511.2290, calculated for $C_{28}H_{34}(^{37}Cl)N_4O_3^+$ 511.2287; HRMS (ESI$^+$) found 509.2308, calculated for $C_{28}H_{34}(^{35}Cl)N_4O_3^+$ 509.2314; HPLC (System E) t_r 3.9 min (97%); *er* >99:1 (HPLC Chiralpak AD column, λ 220 nm, *n*-hexane/*i*-PrOH (70:30), flow rate 0.9 mL/min, t_r 19.7 min (major), 26.7 min (minor)).

5-(3,5-Dimethyl-1,2-oxazol-4-yl)-2-[2-(1*H*-indol-1-yl)ethyl]-1-[(2*S*)-2-(morpholin-4-yl)propyl]-1*H*-benzimidazole (398)

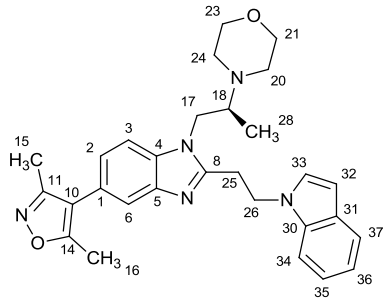

Freshly prepared 1 M aq. $Na_2S_2O_4$ (0.50 mL, 0.50 mmol) was added to a suspension of compound **393** (35 mg, 0.097 mmol) in EtOH (0.5 mL) in a sealable vial. The vial was sealed then heated at 80°C for 1 h then allowed to cool. The resultant mixture was partitioned between 10% aq. NH_3 (1 mL) and EtOAc (1 mL). The organic phase was passed through a hydrophobic frit then evaporated by nitrogen blow-down. The residue was dissolved in EtOAc (3 mL) then added to a vial containing 3-(1*H*-indol-1-yl)propanoic acid (17 mg, 0.090

mmol). DIPEA (34 μL, 0.19 mmol) and T3P (50 wt.% in EtOAc, 0.3 mL, 0.47 mmol) were added then the solution was heated at 80 °C for 16 h then allowed to cool. 1 M aq. NaOH solution (1 mL) was added and the phases were mixed then allowed to separate. The organic phase was passed through a hydrophobic frit then evaporated by nitrogen blow-down. The crude material was purified by flash column chromatography on a silica column (4 g). The column was eluted with a gradient of EtOAc:MeOH:NEt_3 which was increased linearly from 99:1:0.1 to 95:5:0.5 over 30 CVs. The desired fractions were combined and evaporated to yield the product as a colourless gum (26 mg, 52%); R_f 0.35 (EtOAc:MeOH:NEt_3, 90:10:1); $[\alpha]_D^{20}$ -5.2 (*c* 1.2 in $CHCl_3$); ν_{max} (neat) 2963 (C-H), 2955 (C-H), 2819 (C-H); ^{1}H NMR (400 MHz, $CDCl_3$) δ ppm 0.76 (d, *J*=6.5 Hz, 3 H, C(28)H_3), 2.12 - 2.24 (m, 2 H, C(20)H_AH$_B$+C(24)H_AH$_B$), 2.27 - 2.38 (m, 5 H, C(15)H_3+C(20)H$_A$$H_B$+C(24)H$_A$$H_B$), 2.46 (s, 3 H, C(16)$H_3$), 2.53 - 2.69 (m, 1 H, C(18)*H*), 3.21 - 3.44 (m, 3 H, C(17)H_AH$_B$+C(25)H_2), 3.47 - 3.66 (m, 5 H, C(17)H$_A$$H_B$+C(21)$H_2$+C(23)$H_2$), 4.80 (t, *J*=6.5 Hz, 2 H, C(26)H_2), 6.43 (d, *J*=3.0 Hz, 1 H, C(32)*H*), 6.89 (d, *J*=3.0 Hz, 1 H, C(33)*H*), 7.09 - 7.14 (m, 2 H, C(2)*H*+C(35)*H*), 7.16 - 7.22 (m, 1 H, C(36)*H*), 7.25 (d, *J*=8.5 Hz, 1 H, C(3)*H*), 7.36 (d, *J*=8.0 Hz, 1 H, C(34)*H*), 7.57 - 7.70 (m, 2 H, C(6)*H*+C(37)*H*); ^{13}C NMR (101 MHz, $CDCl_3$) δ ppm 10.9 (s, 1 C, *C*(15)), 11.6 (s, 1 C, *C*(16)), 11.9 (s, 1 C, *C*(33)), 28.6 (s, 1 C, *C*(25)), 45.1 (s, 1 C, *C*(26)), 46.2 (s, 1 C, *C*(17)), 49.0 (s, 2 C, *C*(20)+*C*(24)), 59.1 (s, 1 C, *C*(18)), 67.0 (s, 2 C, *C*(21)+*C*(23)), 101.7 (s, 1 C, *C*(32)), 108.9 (s, 1 C, *C*(34)), 109.9 (s, 1 C, *C*(3)), 117.0 (s, 1 C, *C*(10)), 119.7 (s, 1 C, *C*(35)), 119.8 (s, 1 C, *C*(6)), 121.3 (s, 1 C, *C*(37)), 121.8 (s, 1 C, *C*(36)), 123.6 (s, 1 C, *C*(2)), 124.4 (s, 1 C, *C*(1)), 127.9 (s, 1 C, *C*(33)), 128.8 (s, 1 C, *C*(31)), 134.5 (s, 1 C, *C*(4)), 135.4 (s, 1 C, *C*(30)), 142.9 (s, 1 C, *C*(5)), 153.5 (s, 1 C, *C*(8)), 159.0 (s, 1 C, *C*(11)), 165.0 (s, 1 C, *C*(14)); LRMS *m/z* (ESI$^+$) 484 [MH$^+$]; HRMS (ESI$^+$) found 484.2695, calculated for $C_{29}H_{34}N_5O_2^+$ 484.2707; HPLC (System E) t_r 3.9 min (98%); *er* >99:1 (HPLC Chiralpak AD column, λ 220 nm, *n*-hexane/*i*-PrOH (80:20), flow rate 1.0 mL/min, t_r 24.7 min (major), 27.6 min (minor)).

5-(3,5-Dimethyl-1,2-oxazol-4-yl)-2-[2-(3-fluoro-4-methoxyphenyl)ethyl]-1-[(2*S*)-2-(morpholin-4-yl)propyl]-1*H*-benzimidazole (399)

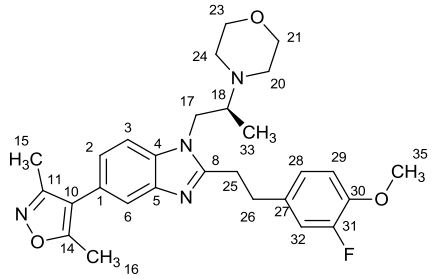

Freshly prepared 1 M aq. $Na_2S_2O_4$ (0.50 mL, 0.50 mmol) was added to a suspension of compound **393** (35 mg, 0.097 mmol) in EtOH (0.5 mL) in a sealable vial. The vial was sealed then heated at 80°C for 1 h then allowed to cool. The resultant mixture was partitioned between 10% aq. NH_3 (1 mL) and EtOAc (1 mL). The organic phase was passed through a hydrophobic frit then evaporated by nitrogen blow-down. The residue was dissolved in EtOAc (3 mL) then added to a vial containing 3-(3-fluoro-4-methoxyphenyl)propanoic acid (17 mg, 0.086 mmol). DIPEA (34 µL, 0.19 mmol) and T3P (50 wt.% in EtOAc, 0.3 mL, 0.47 mmol) were added then the solution was heated at 80 °C for 16 h then allowed to cool. 1 M aq. NaOH solution (1 mL) was added and the phases were mixed then allowed to separate. The organic phase was passed through a hydrophobic frit then evaporated by nitrogen blow-down. The crude material was purified by flash column chromatography on a silica column (4 g). The column was eluted with a gradient of EtOAc:MeOH:NEt_3 which was increased linearly from 99:1:0.1 to 95:5:0.5 over 30 CVs. The desired fractions were combined and evaporated to yield the product as a colourless gum (21 mg, 43%); R_f 0.50 (EtOAc:MeOH:NEt_3, 90:10:1); $[\alpha]_D^{20}$ +12.3 (*c* 1.1 in $CHCl_3$); ν_{max} (neat) 2963 (C-H), 2934 (C-H), 2854 (C-H); ^{1}H NMR (400 MHz, $CDCl_3$) δ ppm 1.01 (d, *J*=7.0 Hz, 3 H, C(33)H_3), 2.31 (s, 3 H, C(15)H_3), 2.44 (s, 3 H, C(16)H_3), 2.45 - 2.54 (m, 2 H, C(20)H_AH_B+C(24)H_AH_B), 2.61 - 2.69 (m, 2 H, C(20)H_AH_B+C(24)H_AH_B), 2.90 - 3.02 (m, 1 H, C(18)*H*), 3.08 - 3.20 (m, 2 H, C(25/26)H_2), 3.20 - 3.30 (m, 2 H, C(25/26)H_2), 3.60 - 3.73 (m, 4 H, C(21)H_2+C(23)H_2), 3.81 -

3.92 (m, 4 H, C(17)$H_A$$H_B$+C(35)$H_3$), 4.16 (dd, *J*=14.5, 6.5 Hz, 1 H, C(17)H$_A$$H_B$), 6.85 - 6.93 (m, 1 H, C(29)*H*), 6.93 - 7.02 (m, 2 H, C(28)*H*+C(32)*H*), 7.13 (dd, *J*=8.5, 1.5 Hz, 1 H, C(2)*H*), 7.33 (d, *J*=8.5 Hz, 1 H, C(3)*H*), 7.64 (d, *J*=1.5 Hz, 1 H, C(6)*H*); ^{13}C NMR (101 MHz, $CDCl_3$) δ ppm 10.9 (s, 1 C, *C*(15)), 11.6 (s, 1 C, *C*(16)), 12.2 (s, 1 C, *C*(33)), 29.7 (s, 1 C, *C*(25)), 32.6 (s, 1 C, *C*(26)), 46.8 (s, 1 C, *C*(17)), 49.3 (s, 2 C, *C*(20)+*C*(24)), 56.3 (s, 1 C, *C*(35)), 59.4 (s, 1 C, *C*(18)), 67.1 (s, 2 C, *C*(21)+*C*(23)), 109.7 (s, 1 C, *C*(3)), 113.6 (d, *J*=1.5 Hz, 1 C, *C*(29)), 116.0 (d, *J*=17.5 Hz, 1 C, *C*(32)), 117.0 (s, 1 C, *C*(10)), 119.9 (s, 1 C, *C*(6)), 123.4 (s, 1 C, *C*(2)), 123.9 (d, *J*=4.0 Hz, 1 C, *C*(28)), 124.2 (s, 1 C, *C*(1)), 133.9 (d, *J*=5.5 Hz, 1 C, *C*(27)), 134.6 (s, 1 C, *C*(4)), 142.9 (s, 1 C, *C*(5)), 146.1 (d, *J*=10.5 Hz, 1 C, *C*(30)), 152.3 (d, *J*=245.5 Hz, 1 C, *C*(31)), 155.2 (s, 1 C, *C*(8)), 159.0 (s, 1 C, *C*(11)), 165.0 (s, 1 C, *C*(14)); ^{19}F NMR (377 MHz, $CDCl_3$) δ ppm -135.0 (s, 1 F); LRMS *m/z* (ESI$^+$) 493 [MH$^+$]; HRMS (ESI$^+$) found 493.2603, calculated for $C_{28}H_{34}FN_4O_3^+$ 493.2609; HPLC (System E) t_r 3.7 min (97%); *er* >99:1 (HPLC Chiralpak AD column, λ 220 nm, *n*-hexane/*i*-PrOH (80:20), flow rate 1.0 mL/min, t_r 36.9 min (major), 52.3 min (minor)).

2-[(Tripropan-2-ylsilyl)ethynyl]pyrimidine (405)

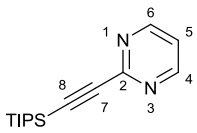

A mixture of 2-bromo-pyrimidine (690 mg, 5.00 mmol), (triisopropylsilyl)acetylene (1.94 mL, 10.0 mmol), $Pd(PPh_3)_2Cl_2$ (152 mg, 0.05 mmol) CuI (10 mg, 0.10 mmol) and Et_3N (1.80 mL, 15.0 mmol) in DMF (20 mL) was degassed by evacuating the apparatus then refilling with nitrogen (×3). The reaction mixture was stirred for 16 h at room temperature then concentrated *in vacuo*. The residue was suspended in EtOAc then pre-adsorbed onto silica. The crude material was purified by flash column chromatography on a silica column (40 g). The column was eluted with a gradient of EtOAc:*c*-hexane which was increased linearly from 0:100 to 40:60 over 12 CVs. The desired fractions were combined and evaporated to yield the product as a brown oil (584 mg, 45%); R_f 0.20 (EtOAc); ν_{max} (neat) 2944 (C-H),

2892 (C-H), 2866 (C-H), ; ^{1}H NMR (400 MHz, $CDCl_3$) δ ppm 1.04 - 1.27 (m, 21 H, (21×TIPS-*H*)), 7.23 (t, *J*=5.0 Hz, 1 H, C(5)*H*), 8.72 (d, *J*=5.0 Hz, 2 H, C(4)*H*+C(6)*H*); ^{13}C NMR (101 MHz, $CDCl_3$) δ ppm 11.2 (s, 3 C, (3×TIPS *C*H)), 18.6 (s, 6C (6×TIPS *C*H_3) 91.2 (s, 1 C, *C*(8)), 104.7 (s, 1 C, *C*(7)), 119.9 (s, 1 C, *C*(5)), 152.7 (s, 1 C, *C*(2)), 157.2 (s, 2 C, *C*(4)+*C*(6)); LRMS *m/z* (ESI^+) 283 [$(M+Na)^+$], 261 [MH^+]; HRMS (ESI^+) found 261.1785, calculated for $C_{15}H_{25}N_2Si^+$ 261.1782; HPLC (System D) t_r 17.8 min (92%).

2-Ethynylpyrimidine (406)[322]

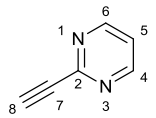

A mixture of compound **405** (260 mg, 1.0 mmol) and TBAF on silica (1.5 mmol/g, 733 mg, 1.1 mmol) in THF (10 mL) was stirred at room temperature for 2 h then evaporated. The crude material was purified by flash column chromatography on a silica column (24 g). The column was eluted with a gradient of EtOAc:*c*-hexane which was increased linearly from 20:80 to 60:40 over 12 CVs. The desired fractions were combined and evaporated to yield the product as a pale-brown oil (47 mg, 45%); R_f 0.25 (EtOAc:*c*-hexane, 40:60); ^{1}H NMR (400 MHz, $CDCl_3$) δ ppm 3.10 (s, 1 H, C(8)*H*), 7.24 (t, *J*=5.0 Hz, 1 H, C(5)*H*), 8.67 (d, *J*=5.0 Hz, 2 H, C(4)*H*+C(6)*H*); ^{13}C NMR (101 MHz, $CDCl_3$) δ ppm 75.8 (s, 1 C, *C*(8)), 81.7 (s, 1 C, *C*(7)), 120.4 (s, 1 C, *C*(5)), 152.1 (s, 1 C, *C*(2)), 157.2 (s, 2 C, *C*(4)+*C*(6)).

2-Ethynyl-1-methyl-1*H*-imidazole (408)[323]

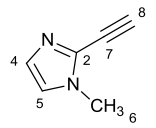

A solution of the Bestmann-Ohira (dimethyl (-diazo-2-oxo-propyl)phosphonate, 409 μL, 2.72 mmol) in MeOH (5 mL) was added drop-wise to a suspension of 1-methyl-1*H*-imidazole-2-carbaldehyde (250 mg, 2.27 mmol) and K_2CO_3 (627 mg, 2.27 mmol) in MeOH (5

mL). The mixture was stirred at room temperature for 3 h then concentrated *in vacuo*. The residue was partitioned between Et_2O (10 mL) and saturated aq. $NaHCO_3$ (10 mL). The phases were separated then the aqueous phase was extracted with Et_2O (4×10 ml). The combined organic phases were dried over $MgSO_4$ and evaporated. The crude material was purified by flash column chromatography on a silica column (12 g). The column was eluted with a gradient of EtOAc:*c*-hexane which was increased linearly from 80:20 to 100:0 over 12 CVs. The desired fractions were combined and evaporated to yield the product as a pale brown oil (208 mg, 86%); R_f 0.30 (EtOAc); ν_{max} (neat) 3280 (alkenyl C-H) 2951 (C-H), 2116 (C≡C); ^{1}H NMR (400 MHz, $CDCl_3$) δ ppm 3.31 (s, 1 H, C(8)*H*), 3.72 (s, 3 H, C(6)H_3), 6.89 (d, *J*=1.0 Hz, 1 H, C(5)*H*), 7.02 (d, *J*=1.0 Hz, 1 H, C(4)*H*); ^{13}C NMR (101 MHz, $CDCl_3$) δ ppm 33.4 (s, 1 C, *C*(6)), 73.1 (s, 1 C, *C*(7)), 81.1 (s, 1 C, *C*(8)), 121.5 (s, 1 C, *C*(5)), 129.4 (s, 1 C, *C*(4)), 131.4 (s, 1 C, *C*(2)); LRMS *m/z* (ESI$^+$) 107 [MH$^+$]; HRMS (ESI$^+$) found 107.0607, calculated for $C_6H_7N_2^+$ 107.0604; HPLC (System E) t_r 0.4 min (99%).

4-Propoxypyridine (410)

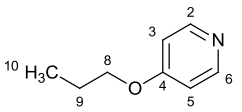

Sodium metal (345 mg, 15.00 mmol) was added in portions to anhydrous *n*-PrOH (8 mL) at room temperature using a water bath to dissipate evolved heat. Once all sodium had dissolved, the resulting colourless solution was added drop-wise to a suspension of 4-chloropyridine hydrochloride (750 mg, 5.00 mmol) in *n*-PrOH (2 mL). The resultant suspension was heated at reflux for 16 h. The mixture was allowed to cool, neutralised by addition of 1 M aq. HCl, and then concentrated *in vacuo*. The material thus obtained was partitioned between EtOAc (10 mL) and water (10 mL). The phases were separated then the organic phase was washed with brine (10 mL) then dried over $MgSO_4$ and concentrated *in vacuo*. The crude material was purified by flash column chromatography on a silica column (24 g). The column was eluted with a gradient of EtOAc:*c*-hexane which was increased

linearly from 40:60 to 80:20 over 12 CVs. The desired fractions were combined and evaporated to yield the product as a colourless oil (637 mg, 93%); R_f 0.10 (EtOAc:*c*-hexane, 40:60); ν_{max} (neat) 3031 (C-H), 2967 (C-H), 2939 (C-H), 2880 (C-H); ^{1}H NMR (400 MHz, $CDCl_3$) δ ppm 1.03 (t, *J*=7.5 Hz, 3 H, C(10)H_3), 1.81 (sxt, *J*=7.5 Hz, C(9)H_2), 3.95 (t, *J*=6.5 Hz, 2 H, C(8)H_2), 6.74 - 6.84 (m, 2 H, C(3)*H*+C(5)*H*), 8.31 - 8.50 (m, 2 H, C(2)*H*+C(6)*H*); ^{13}C NMR (101 MHz, $CDCl_3$) δ ppm 10.3 (s, 1 C, *C*(10)), 22.2 (s, 1 C, *C*(9)), 69.3 (s, 1 C, *C*(8)), 110.2 (s, 2 C, *C*(3)+*C*(5)), 150.9 (s, 2 C, *C*(2)+*C*(6)), 165.0 (s, 1 C, *C*(4)); LRMS *m/z* (ESI$^+$) 138 [MH$^+$]; HRMS (ESI$^+$) found 138.0907, calculated for $C_8H_{12}O^+$ 138.0913; HPLC (System E) t_r 1.1 min (>99%).

1-(2-Oxopropyl)-4-propoxypyridinium chloride (411)

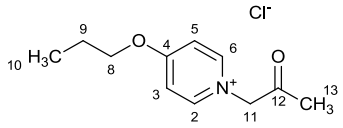

Chloroacetone (293 µL, 3.56 mmol) was added to a stirred solution of compound **410** (630 mg, 3.24 mmol) in THF (15 mL). The resultant mixture was left to stir for 16 h at room temperature then more chloroacetone (293 µL, 3.56 mmol) was added. The mixture was refluxed for 6 h then allowed to cool. Et_2O (10 mL) was added then the suspension was stirred gently for 16 h. The solid was collected by filtration, washed with Et_2O then dried under vacuum to yield the product as a white solid (558 mg, 75%); mp 170-174°C; ν_{max} (neat) 3002 (C-H), 2981 (C-H), 2990 (C-H), 1728 (C=O); ^{1}H NMR (400 MHz, DMSO-d_6) δ ppm 0.98 (t, *J*=7.5 Hz, 3 H, C(15)H_3), 1.71 - 1.87 (m, 2 H, C(9)H_2), 2.27 (s, 3 H, C(13)H_2), 4.32 (t, *J*=6.5 Hz, 2 H, C(8)H_2), 5.70 (s, 2 H, C(11)H_2), 7.68 (d, *J*=7.5 Hz, 2 H, C(3)*H*+C(5)*H*), 8.73 (d, *J*=7.5 Hz, 2 H, C(2)*H*+C(6)*H*); ^{13}C NMR (101 MHz, DMSO-d_6) δ ppm 10.0 (s, 1 C, *C*(10)), 21.4 (s, 1 C, *C*(9)), 27.0 (s, 1 C, *C*(13)), 66.3 (s, 1 C, *C*(11)), 72.2 (s, 1 C, *C*(8)), 113.2 (s, 2 C, *C*(3)+*C*(5)), 147.2 (s, 2 C, *C*(2)+*C*(6)), 170.2 (s, 1 C, *C*(4)), 200.2 (s, 1 C, *C*(12)); LRMS *m/z*

(ESI$^+$) 194 [M$^+$]; HRMS (ESI$^+$) found 194.1183, calculated for $C_{11}H_{16}NO_2^+$ 194.1176; HPLC (System E) t_r 3.8 min (>99%).

1-[7-Propoxy-1-(pyridine-2-yl)indolizin-3-yl]ethanone (402)

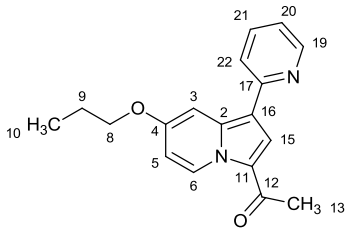

A mixture of compound **411** (84 mg, 0.30 mmol) and K_2CO_3 (83 mg, 0.60 mmol) in DMF (2 mL) was stirred for 15 minutes. 2-Ethynylpyridine (36 µL, 0.36 mmol) was added then the resultant mixture was heated at 90 °C for 2 h then allowed to cool. The mixture was partitioned between EtOAc (10 mL) and water (10 mL). The organic phase was washed with water (10 mL) and brine (10 mL) then dried over $MgSO_4$ and evaporated. The crude material was purified by flash column chromatography on a silica column (12 g). The column was eluted with a gradient of EtOAc:*c*-hexane which was increased linearly from 20:80 to 50:50 over 12 CVs. The desired fractions were combined and evaporated to yield the product as a pale brown solid (17 mg, 19%); R_f 0.30 (EtOAc:*c*-hexane, 40:60); mp 125-129 °C; ν_{max} (neat) 3051 (C-H), 2964 (C-H), 2922 (C-H), 1638 (C=O); ^{1}H NMR (400 MHz, $CDCl_3$) δ ppm 1.09 (t, *J*=7.5 Hz, 3 H, C(10)H_3), 1.77 - 1.96 (m, 2 H, C(9)H_2), 2.57 (s, 3 H, C(13)H_3), 4.08 (t, *J*=6.5 Hz, 2 H, C(8)H_2), 6.66 (dd, *J*=7.5, 3.0 Hz, 1 H, C(5)*H*), 7.09 (ddd, *J*=7.5, 5.0, 1.0 Hz, 1 H, C(20)*H*), 7.57 - 7.64 (m, 1 H, C(22)*H*), 7.64 - 7.73 (m, 1 H, C(21)*H*), 7.83 (s, 1 H, C(15)*H*), 8.11 (d, *J*=3.0 Hz, 1 H, C(3)*H*), 8.65 (d, *J*=5.0 Hz, 1 H, C(19)*H*), 9.79 (dd, *J*=7.5, 1.0 Hz, 1 H, C(6)*H*); ^{13}C NMR (101 MHz, $CDCl_3$) δ ppm 10.5 (s, 1 C, *C*(10)), 22.3 (s, 1 C, *C*(9)), 26.8 (s, 1 C, *C*(13)), 69.7 (s, 1 C, *C*(8)), 98.5 (s, 1 C, *C*(3)), 108.6 (s, 1 C, *C*(5)), 112.9 (s, 1 C, *C*(16)), 119.8 (s, 1 C, *C*(20/22)), 119.8 (s, 1 C, *C*(20/22)), 121.6 (s, 1 C, *C*(11)), 123.2 (s, 1 C, *C*(15)), 130.1 (s, 1 C, *C*(6)), 136.3 (s, 1 C, *C*(21)), 139.2 (s, 1 C, *C*(2)), 149.2 (s, 1 C, *C*(19)), 154.7 (s, 1

C, *C*(17)), 157.7 (s, 1 C, *C*(4)), 185.6 (s, 1 C, *C*(12)); LRMS *m/z* (ESI$^+$) 295 [MH$^+$]; HRMS (ESI$^+$) found 295.1431, calculated for $C_{18}H_{19}N_2O_2^+$ 295.1441; HPLC (System E) t_r 4.3 min (98%).

1-[1-(6-Chloropyridin-2-yl)-7-propoxyindolizin-3-yl]ethanone (412)

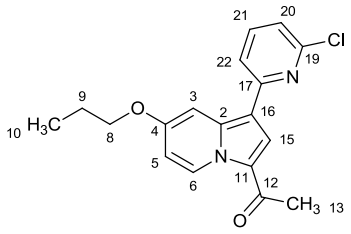

A mixture of compound **411** (84 mg, 0.30 mmol) and K_2CO_3 (83 mg, 0.60 mmol) in DMF (2 mL) was stirred for 15 minutes. 2-Chloro-6-ethynylpyridine (50 mg, 0.36 mmol) was added then the resultant mixture was heated at 90 °C for 2 h then allowed to cool. The mixture was partitioned between EtOAc (10 mL) and water (10 mL). The organic phase was washed with water (10 mL) and brine (10 mL) then dried over $MgSO_4$ and evaporated. The crude material was purified by flash column chromatography on a silica column (12 g). The column was eluted with a gradient of EtOAc:*c*-hexane which was increased linearly from 20:80 to 50:50 over 12 CVs. The desired fractions were combined and evaporated to yield the product as a beige solid (38 mg, 39%); R_f 0.35 (EtOAc:*c*-hexane, 40:60); mp 184-188 °C; ν_{max} (neat) 3106 (C-H), 2963 (C-H), 2939 (C-H), 2881 (C-H), 1642 (C=O); ^{1}H NMR (400 MHz, $CDCl_3$) δ ppm 1.10 (t, *J*=7.5 Hz, 3 H, C(10)*H*$_3$), 1.84 - 1.97 (m, 2 H, C(9)*H*$_2$), 2.55 (s, 3 H, C(13)*H*$_3$), 4.10 (t, *J*=6.5 Hz, 2 H, C(8)*H*$_2$), 6.66 (dd, *J*=7.5, 2.5 Hz, 1 H, C(5)*H*), 7.07 (dd, *J*=8.0, 1.0 Hz, 1 H, C(20)*H*), 7.49 (dd, *J*=8.0, 1.0 Hz, 1 H, C(22)*H*), 7.60 (t, *J*=8.0 Hz, 1 H, C(21)*H*), 7.77 (s, 1 H, C(15)*H*), 8.19 (d, *J*=2.5 Hz, 1 H, C(3)*H*), 9.74 (dd, *J*=7.5, 0.5 Hz, 1 H, C(6)*H*); ^{13}C NMR (101 MHz, $CDCl_3$) δ ppm 10.4 (s, 1 C, *C*(10)), 22.1 (s, 1 C, *C*(9)), 26.8 (s, 1 C, *C*(13)), 69.7 (s, 1 C, *C*(8)), 98.8 (s, 1 C, *C*(3)), 108.9 (s, 1 C, *C*(5)), 111.0 (s, 1 C, *C*(16)), 117.4 (s, 1 C, *C*(22)), 119.4 (s, 1 C, *C*(20)), 121.8 (s, 1 C, *C*(11)), 122.9 (s, 1 C, *C*(15)), 130.1 (s, 1 C, *C*(6)), 138.6 (s, 1 C, *C*(21)), 139.5 (s, 1 C, *C*(2)), 150.4 (s, 1 C, *C*(19)), 155.1 (s, 1 C, *C*(17)), 158.0 (s, 1 C, *C*(4)),

185.8 (s, 1 C, *C*(12)); LRMS *m/z* (ESI$^+$) 329 [MH$^+$]; HRMS (ESI$^+$) found 351.0874, calculated for $C_{18}H_{17}ClN_2NaO_2^+$ 351.0871; HPLC (System E) t_r 7.3 min (97%).

Methyl 2-(3-acetyl-7-propoxyindolizin-1-yl)pyridine-4-carboxylate (413)

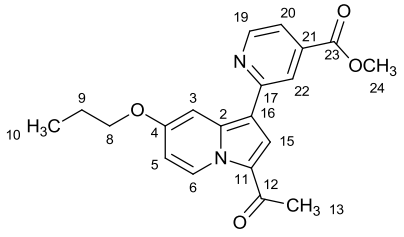

A mixture of compound **411** (84 mg, 0.30 mmol) and K_2CO_3 (83 mg, 0.60 mmol) in DMF (2 mL) was stirred for 15 minutes. Methyl 2-ethynylisonicotinate (58 mg, 0.36 mmol) was added then the resultant mixture was heated at 90 °C for 2 h then allowed to cool. The mixture was partitioned between EtOAc (10 mL) and water (10 mL). The organic phase was washed with water (10 mL) and brine (10 mL) then dried over $MgSO_4$ and evaporated. The crude material was purified by flash column chromatography on a silica column (12 g). The column was eluted with a gradient of EtOAc:*c*-hexane which was increased linearly from 20:80 to 50:50 over 12 CVs. The desired fractions were combined and evaporated then the resultant material was purified further by flash column chromatography on a C-18 column (13 g). The column was eluted with a gradient of H_2O:MeCN (+0.1% CF_3CO_2H) which was increased linearly from 95:5 to 95:5 over 30 CVs. The desired fractions were combined and concentrated *in vacuo* to remove most of the solvent. The residual material was partitioned between CH_2Cl_2 (5 mL) and saturated aq. $NaHCO_3$ (5 mL). The organic phase was separated then dried over $MgSO_4$ and evaporated to yield the product as a yellow solid (25 mg, 24%); R_f 0.30 (EtOAc:*c*-hexane, 40:60); mp 154-159°C; ν_{max} (neat) 3088 (C-H), 2976 (C-H), 2942 (C-H), 1727 (ester C=O), 1643 (ketone C=O); ^{1}H NMR (400 MHz, $CDCl_3$) δ ppm 1.01 (t, *J*=7.5 Hz, 3 H, C(10)H_3), 1.68 - 1.93 (m, 2 H, C(9)H_2), 2.51 (s, 3 H, C(13)H_3), 3.78 - 3.95 (m, 3 H, C(24)H_3), 4.00 (t, *J*=6.5 Hz, 2 H, C(8)H_2), 6.60 (dd, *J*=7.5, 3.0 Hz, 1 H, C(5)*H*), 7.50 (dd, *J*=5.0, 1.5 Hz, 1 H, C(20)*H*), 7.82 (s, 1 H, C(15)*H*), 8.06 - 8.08 (m, 1 H, C(22)*H*), 8.09 (d, *J*=3.0 Hz, 1 H,

C(3)*H*), 8.67 (dd, *J*=5.0, 1.5 Hz, 1 H, C(19)*H*), 9.70 (d, *J*=7.5 Hz, 1 H, C(6)*H*); ^{13}C NMR (101 MHz, $CDCl_3$) δ ppm 10.5 (s, 1 C, *C*(10)), 22.3 (s, 1 C, *C*(9)), 26.9 (s, 1 C, *C*(13)), 52.7 (s, 1 C, *C*(24)), 69.8 (s, 1 C, *C*(8)), 98.8 (s, 1 C, *C*(3)), 108.7 (s, 1 C, *C*(5)), 112.0 (s, 1 C, *C*(16)), 118.2 (s, 1 C, *C*(20)), 118.9 (s, 1 C, *C*(22)), 121.9 (s, 1 C, *C*(11)), 123.3 (s, 1 C, *C*(15)), 130.1 (s, 1 C, *C*(6)), 137.5 (s, 1 C, *C*(21)), 139.4 (s, 1 C, *C*(2)), 149.9 (s, 1 C, *C*(19)), 155.7 (s, 1 C, *C*(17)), 158.0 (s, 1 C, *C*(4)), 166.1 (s, 1 C, *C*(23)), 185.9 (s, 1 C, *C*(12)); LRMS *m/z* (ESI$^+$) 353 [MH$^+$]; HRMS (ESI$^+$) found 375.1309, calculated for $C_{20}H_{20}N_2NaO_4^+$ 375.1315; HPLC (System E) t_r 6.5 min (97%).

4-(Morpholin-4-yl)-1-(2-oxopropyl)pyridinium chloride (415)

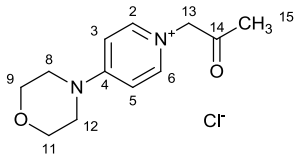

Chloroacetone (0.820 mL, 10.0 mmol) was added to a stirred solution of 4-morpholinopyridine (1.64 g, 10.0 mmol) in THF (5 mL). The resultant mixture was left to stir for 16 h at room temperature then diluted with EtOAc (5 mL). The solid was filtered then dried under vacuum to yield the product as a white solid (2.15 g, 84%); mp 304-307 °C; ν_{max} (neat) 3039 (C-H), 3000 (C-H), 2941 (C-H), 2857 (C-H), 1724 (C=O); ^{1}H NMR (400 MHz, DMSO-d_6) δ ppm 2.22 (s, 3 H, C(15)H_3), 3.64 - 3.79 (m, 8 H, C(8)H_2+C(9)H_2+C(11)H_2+C(12)H_2), 5.36 (s, 2 H, C(13)H_2), 7.30 (d, *J*=8.0 Hz, 2 H, C(3)*H*+C(5)*H*), 8.17 (d, *J*=8.0 Hz, 2 H, C(2)*H*+C(6)*H*); ^{13}C NMR (101 MHz, DMSO-d_6) δ ppm 26.9 (s, 1 C, *C*(15)), 46.1 (s, 2 C, *C*(8)+*C*(12)), 64.6 (s, 1 C, *C*(13)), 65.5 (s, 2 C, *C*(9)+*C*(11)), 107.6 (s, 2 C, *C*(3)+*C*(5)), 143.6 (s, 2 C, *C*(2)+*C*(6)), 155.7 (s, 1 C, *C*(4)), 201.0 (s, 1 C, *C*(14)); LRMS *m/z* (ESI$^+$) 221 [M$^+$]; HRMS (ESI$^+$) found 221.1282, calculated for $C_{12}H_{17}N_2O_2$ 221.1285$^+$; HPLC (System E) t_r 0.4 min (80%).

1-[7-(Morpholin-4-yl)-1-(pyridin-2-yl)indolizin-3-yl]ethanone (403)

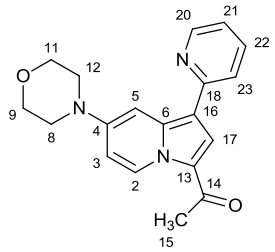

A mixture of compound **415** (80 mg, 0.31 mmol), 2-ethynylpyridine (38 µL, 0.37 mmol) and K_2CO_3 (86 mg, 0.62 mmol) in DMF (2 mL) was heated in a sealed vial for 2 h at 90 °C then allowed to cool. The mixture was then partitioned between water (3 mL) and EtOAc (3 mL). The phases were separated then the organic phase was washed with water (3 mL) and brine (3 mL) then dried over $MgSO_4$ and evaporated. The crude material was purified by flash column chromatography on a silica column (4 g). The column was eluted with a gradient of EtOAc:*c*-hexane which was increased linearly from 40:60 to 100:0 over 30 CVs. The desired fractions were combined and evaporated to yield the product as a yellow solid (17 mg, 17%); R_f 0.35 (EtOAc) ; mp 180-185 °C; ν_{max} (neat) 3111 (C-H), 2964 (C-H), 2849 (C-H), 1642 (C=O); ^{1}H NMR (400 MHz, $CDCl_3$) δ ppm 2.54 - 2.71 (m, 3 H, C(15)*H*$_3$), 3.32 - 3.48 (m, 4 H, C(8)*H*$_2$+C(12)*H*$_2$), 3.78 - 3.96 (m, 4 H, C(9)*H*$_2$+C(11)*H*$_2$), 6.69 (dd, *J*=8.0, 2.5 Hz, 1 H, C(3)*H*), 7.07 (ddd, *J*=7.5, 5.0, 1.0 Hz, 1 H, C(21)*H*), 7.59 - 7.64 (m, 1 H, C(23)*H*), 7.64 - 7.73 (m, 1 H, C(22)*H*), 7.82 (s, 1 H, C(17)*H*), 8.05 (d, *J*=2.5 Hz, 1 H, C(5)*H*), 8.58 - 8.68 (m, 1 H, C(20)*H*), 9.77 (d, *J*=7.8 Hz, 1 H, C(2)*H*); ^{13}C NMR (101 MHz, $CDCl_3$) δ ppm 26.7 (s, 1 C, *C*(15)), 47.6 (s, 2 C, *C*(8)+*C*(12)), 66.5 (s, 2 C, *C*(9)+*C*(11)), 99.5 (s, 1 C, *C*(5)), 106.0 (s, 1 C, *C*(3)), 112.3 (s, 1 C, *C*(16)), 119.6 (s, 1 C, *C*(21/23)), 119.8 (s, 1 C, *C*(21/23)), 121.3 (s, 1 C, *C*(13)), 123.5 (s, 1 C, *C*(17)), 129.7 (s, 1 C, *C*(2)), 136.3 (s, 1 C, *C*(22)), 139.3 (s, 1 C, *C*(6)), 148.7 (s, 1 C, *C*(4)), 149.1 (s, 1 C, *C*(20)), 154.8 (s, 1 C, *C*(18)), 185.1 (s, 1 C, *C*(14)); LRMS *m/z* (ESI$^+$) 322 [MH$^+$]; HRMS (ESI$^+$) found 322.1538, calculated for $C_{19}H_{20}N_3O_2^+$ 322.1550; HPLC (System E) t_r 3.4 min (97%).

1-[1-(6-Chloropyridin-2-yl)-7-(morpholin-4-yl)indolizin-3-yl]ethanone (416)

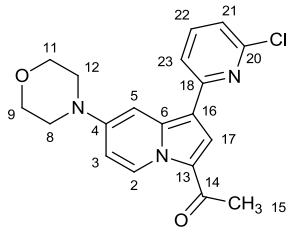

K_2CO_3 (323 mg, 2.34 mmol) was added to a solution of compound **415** (300 mg, 1.17 mmol) in DMF (10 mL). The resultant suspension was stirred at room temperature for 15 minutes then 2-ethynylpyridine (189 µL, 1.40 mmol) was added. The mixture was then heated at 90 °C for 2 h then allowed to cool. The solvent was evaporated by N_2 blow-down then the mixture was then partitioned between water (5 mL) and CH_2Cl_2 (5 mL). The organic phase was collected by passing it through a hydrophobic frit then concentrated by nitrogen blow-down. The crude material was purified by flash column chromatography on a silica column (20 g). The column was eluted with a gradient of EtOAc:*c*-hexane which was increased linearly from 40:60 to 80:20 over 12 CVs. The desired fractions were combined and evaporated to a yellow solid (180 mg). This material was suspended in MeOH (3 mL) then the supernatant was decanted off with a pipette. This process was repeated (×2) then the residual solid was dried under vacuum to yield the product as a yellow solid (166 mg, 40%) R_f 0.45 (EtOAc); mp 215-220 °C; ν_{max} (neat) 3104 (C-H), 2964 (C-H), 2864 (C-H), 1641 (C=O); ^{1}H NMR (400 MHz, $CDCl_3$) δ ppm 2.54 (s, 3 H, C(15)H_3), 3.34 - 3.43 (m, 4 H, C(8)H_2+C(12)H_2), 3.81 - 4.02 (m, 4 H, C(9)H_2+C(11)H_2), 6.69 (dd, *J*=8.0, 3.0 Hz, 1 H, C(3)*H*), 7.05 (d, *J*=7.5 Hz, 1 H, C(21)*H*), 7.50 (d, *J*=7.5 Hz, 1 H, C(23)*H*), 7.60 (t, *J*=7.5 Hz, 1 H, C(22)*H*), 7.77 (s, 1 H, C(17)*H*), 8.15 (d, *J*=3.0 Hz, 1 H, C(5)*H*), 9.73 (d, *J*=8.0 Hz, 1 H, C(2)*H*); ^{13}C NMR (101 MHz, $CDCl_3$) δ ppm 26.7 (s, 1 C, *C*(15)), 47.4 (s, 2 C, *C*(8)+*C*(12)), 66.5 (s, 2 C, *C*(9)+*C*(11)), 99.7 (s, 1 C, *C*(5)), 106.0 (s, 1 C, *C*(3)), 110.4 (s, 1 C, *C*(16)), 117.3 (s, 1 C, *C*(23)), 119.1 (s, 1 C, *C*(21)), 121.4 (s, 1 C, *C*(13)), 123.2 (s, 1 C, *C*(17)), 129.7 (s, 1 C, *C*(2)), 138.6 (s, 1 C, *C*(22)), 139.6 (s, 1 C, *C*(6)), 148.9 (s, 1 C, *C*(4)), 150.4 (s, 1 C, *C*(20)), 155.3 (s, 1 C, *C*(18)),

185.2 (s, 1 C, *C*(14)); LRMS *m/z* (ESI+) 356 [MH+]; HRMS (ESI+) found 378.0979, calculated for $C_{19}H_{18}ClN_3NaO_2^+$ 378.0980; HPLC (System D) t_r 17.8 min (91%).

1-[1-(6-Methylpyridin-2-yl)-7-(morpholin-4-yl)indolizin-3-yl]ethanone (417)

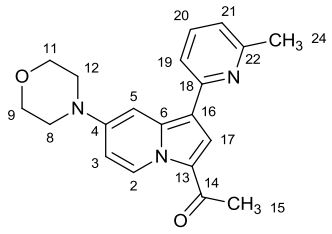

K_2CO_3 (47 mg, 0.34 mmol) was added to a solution of compound **415** (80 mg, 0.31 mmol) in DMF (2 mL). The resultant suspension was stirred at room temperature for 10 minutes then 2-ethynyl-6-methylpyridine (40 mg, 0.34 mmol) was added. The mixture was then heated at 90 °C for 2 h then allowed to cool. The mixture was then partitioned between water (3 mL) and CH_2Cl_2 (3 mL). The organic phase was collected by passing it through a hydrophobic frit then concentrated by nitrogen blow-down. The crude material was purified by flash column chromatography on a silica column (4 g). The column was eluted with a gradient of EtOAc:*c*-hexane + 0.1% NEt_3 which was increased linearly from 40:60 to 80:20 over 20 CVs. The desired fractions were combined and evaporated. The resultant solid was suspended in MeOH then filtered to yield the product as a yellow solid (29 mg, 28%); R_f 0.25 (EtOAc:*c*-hexane, 60:40 + 1% NEt_3); mp 168-173 °C; ν_{max} (neat) 3113 (C-H), 2950 (C-H), 2849 (C-H), 1640 (C=O); ^{1}H NMR (400 MHz, $CDCl_3$) δ ppm 2.55 (s, 3 H, C(15)H_3), 2.62 (s, 3 H, C(24)H_3), 3.31 - 3.50 (m, 4 H, C(8)H_2+C(12)H_2), 3.79 - 3.96 (m, 4 H, C(9)H_2, C(11)H_2), 6.69 (dd, *J*=8.0, 2.5 Hz, 1 H, C(3)*H*), 6.95 (d, *J*=7.5 Hz, 1 H, C(21)*H*), 7.43 (d, *J*=7.5 Hz, 1 H, C(19)*H*), 7.59 (t, *J*=7.5 Hz, 1 H, C(20)*H*), 7.83 (s, 1 H, C(17)*H*), 8.14 (s, 1 H, C(5)*H*), 9.76 (d, *J*=8.0 Hz, 1 H, C(2)*H*); ^{13}C NMR (101 MHz, $CDCl_3$) δ ppm 24.7 (s, 1 C, *C*(24)), 26.7 (s, 1 C, *C*(15)), 47.6 (s, 2 C, *C*(8)+*C*(12)), 66.5 (s, 2 C, *C*(9)+*C*(11)), 99.9 (s, 1 C, *C*(5)), 106.1 (s, 2 C, *C*(3)+*C*(16)), 116.8 (s, 1 C, *C*(19)), 119.0 (s, 1 C, *C*(21)), 121.2 (s, 1 C, *C*(13)), 123.5 (s, 1 C, *C*(17)), 129.7 (s, 1 C, *C*(2)), 136.7 (s, 1 C, *C*(20)), 139.3 (s, 1 C, *C*(6)), 148.6 (s, 1 C, *C*(4)), 154.0 (s, 1 C, *C*(18/22)),

157.3 (s, 1 C, *C*(18/22)), 185.1 (s, 1 C, *C*(14)); LRMS *m/z* (ESI$^+$) 336 [MH$^+$]; HRMS (ESI$^+$) found 336.1692, calculated for $C_{20}H_{22}N_3O_2^+$ 336.1707; HPLC (System D) t_r 9.5 min (97%).

1-[1-(6-Methoxypyridin-2-yl)-7-(morpholin-4-yl)indolizin-3-yl]ethanone (418)

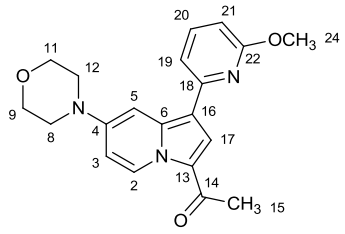

K_2CO_3 (47 mg, 0.34 mmol) was added to a solution of 4 compound **415** (80 mg, 0.31 mmol) in DMF (2 mL). The resultant suspension was stirred at room temperature for 10 minutes then 2-ethynyl-6-methoxypyridine (46 mg, 0.34 mmol) was added. The mixture was then heated at 90 °C for 2 h then allowed to cool. The mixture was then partitioned between water (3 mL) and CH_2Cl_2 (3 mL). The organic phase was collected by passing it through a hydrophobic frit then concentrated by nitrogen blow-down. The crude material was purified by flash column chromatography on a silica column (4 g). The column was eluted with a gradient of EtOAc:*c*-hexane + 0.1% NEt_3 which was increased linearly from 40:60 to 80:20 over 20 CVs. The desired fractions were combined and evaporated. The resultant solid was suspended in MeOH then filtered to yield the product as a yellow solid (29 mg, 28%); R_f 0.25 (EtOAc:*c*-hexane, 60:40 + 1% NEt_3); mp 177-181 °C; ν_{max} (neat) 3124 (C-H), 2957 (C-H), 2821 (C-H), 1643 (C=O); ^{1}H NMR (400 MHz, $CDCl_3$) δ ppm 2.55 (s, 3 H, C(15)H_3), 3.21 - 3.36 (m, 4 H, C(8)H_2+C(12)H_2), 3.84 - 3.97 (m, 4 H, C(9)H_2+C(12)H_2), 4.07 (s, 3 H, C(24)H_3), 6.55 (d, *J*=8.0 Hz, 1 H, C(21)*H*), 6.68 (dd, *J*=8.0, 3.0 Hz, 1 H, C(3)*H*), 7.23 (d, *J*=8.0 Hz, 1 H, C(19)*H*), 7.58 (t, *J*=8.0 Hz, 1 H, C(20)*H*), 7.79 (s, 1 H, C(17)*H*), 8.15 (d, *J*=3.0 Hz, 1 H, C(5)*H*), 9.75 (d, *J*=8.0 Hz, 1 H, C(2)*H*); ^{13}C NMR (101 MHz, $CDCl_3$) δ ppm 26.7 (s, 1 C, *C*(15)), 47.9 (s, 2 C, *C*(8)+*C*(12)), 53.2 (s, 1 C, *C*(24)), 66.4 (s, 2 C, *C*(9)+*C*(11)), 100.2 (s, 1 C, *C*(5)), 106.3 (s, 2 C, *C*(3)+*C*(21)), 112.1 (s, 1 C, *C*(19)), 112.3 (s, 1 C, *C*(16)), 121.2 (s, 1 C, *C*(13)), 123.4 (s, 1 C, *C*(17)), 129.7 (s, 1 C, *C*(2)), 138.8 (s, 1 C, *C*(20)), 139.1 (s, 1 C, *C*(6)), 148.4 (s, 1 C, *C*(4)),

152.4 (s, 1 C, *C*(18)), 163.4 (s, 1 C, *C*(22)), 185.2 (s, 1 C, *C*(14)); LRMS *m/z* (ESI^+) 352 [MH^+]; HRMS (ESI^+) found 352.1665, calculated for $C_{20}H_{22}N_3O_2^+$ 352.1656; HPLC (System D) t_r 17.0 min (94%).

1-[1-(5-Chloropyridin-2-yl)-7-(morpholin-4-yl)indolizin-3-yl]ethanone (419)

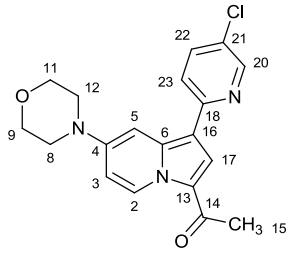

K_2CO_3 (108 mg, 0.78 mmol) was added to a solution of compound **415** (100 mg, 0.39 mmol) in DMF (2 mL). The resultant suspension was stirred at room temperature for 15 minutes then 5-chloro-2-ethynylpyridine (59 mg, 0.43 mmol) was added. The mixture was then heated at 90 °C for 2 h then allowed to cool. The solvent was evaporated by N_2 blow-down then the mixture was then partitioned between water (5 mL) and CH_2Cl_2 (5 mL). The organic phase was collected by passing it through a hydrophobic frit then concentrated by nitrogen blow-down. The crude material was purified by flash column chromatography on a silica column (12 g). The column was eluted with a gradient of EtOAc:*c*-hexane + 0.1% NEt_3 which was increased linearly from 40:60 to 80:20 over 12 CVs. The desired fractions were combined and evaporated to an orange solid (39 mg). This material was suspended in MeOH, refluxed, allowed to cool, then filtered to yield the product as a yellow solid (34 mg, 25%); R_f 0.30 (EtOAc:*c*-hexane, 60:40 + 1% NEt_3); mp 282-286 °C; ν_{max} (neat) 3114 (C-H), 2958 (C-H), 2923 (C-H), 2870 (C-H), 1642 (C=O); ^{1}H NMR (400 MHz, $CDCl_3$) δ ppm 2.54 (s, 3 H, C(15)H_3), 3.29 - 3.39 (m, 4 H, C(8)H_2+C(12)H_2), 3.83 - 3.95 (m, 4 H, C(9)H_2+C(11)H_2), 6.70 (dd, *J*=7.8, 2.7 Hz, 1 H, C(3)*H*), 7.55 (d, *J*=8.5 Hz, 1 H, C(23)*H*), 7.64 (dd, *J*=8.5, 2.5 Hz, 1 H, C(22)*H*), 7.76 (s, 1 H, C(17)*H*), 7.93 - 8.01 (m, 1 H, C(5)*H*), 8.56 (d, *J*=2.0 Hz, 1 H, C(20)*H*), 9.69 - 9.78 (m, 1 H, C(2)*H*); ^{13}C NMR (101 MHz, $CDCl_3$) δ ppm 26.5 (s, 1 C, *C*(15)), 47.4 (s, 2 C, *C*(8)+*C*(12)), 66.4 (s, 2 C, *C*(9)+*C*(11)), 99.3 (s, 1 C, *C*(5)), 106.0 (s, 1 C, *C*(3)), 111.3 (s, 1 C,

C(16)), 120.4 (s, 1 C, *C*(23)), 121.2 (s, 1 C, *C*(13)), 123.6 (s, 1 C, *C*(17)), 127.3 (s, 1 C, *C*(21)), 129.7 (s, 1 C, *C*(2)), 136.0 (s, 1 C, *C*(22)), 139.4 (s, 1 C, *C*(6)), 147.7 (s, 1 C, *C*(20)), 148.9 (s, 1 C, *C*(4)), 152.9 (s, 1 C, *C*(18)), 185.2 (s, 1 C, *C*(14)); LRMS *m/z* (ESI$^+$) 356 [MH$^+$]; HRMS (ESI$^+$) found 378.0971, calculated for $C_{19}H_{18}ClN_3NaO_2^+$ 378.0980; HPLC (System E) t_r 5.9 min (96%).

1-{7-(Morpholin-4-yl)-1-[5-(trifluoromethyl)pyridin-2-yl]indolizin-3-yl}ethanone (420)

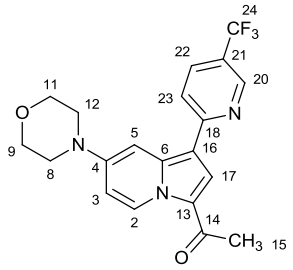

K_2CO_3 (108 mg, 0.78 mmol) was added to a solution of compound **415** (100 mg, 0.39 mmol) in DMF (2 mL). The resultant suspension was stirred at room temperature for 15 minutes then 5-2-ethynyl-5-(trifluoromethyl)pyridine (74 mg, 0.43 mmol) was added. The mixture was then heated at 90 °C for 2 h then allowed to cool. The solvent was evaporated by N_2 blow-down then the mixture was then partitioned between water (5 mL) and CH_2Cl_2 (5 mL). The organic phase was collected by passing it through a hydrophobic frit then concentrated by nitrogen blow-down. The crude material was purified by flash column chromatography on a silica column (12 g). The column was eluted with a gradient of EtOAc:*c*-hexane + 0.1% NEt_3 which was increased linearly from 40:60 to 80:20 over 12 CVs. The desired fractions were combined and evaporated to a yellow solid (40 mg). The material thus obtained was purified further by flash column chromatography on a C-18 column (13 g). The column was eluted with a gradient of H_2O:MeCN (+0.1% CF_3CO_2H) which was increased linearly from 95:5 to 5:95 over 20 CVs. The desired fractions were combined and evaporated then partitioned between CH_3Cl (5 mL) and saturated aq. $NaHCO_3$ (5 mL). The organic phase was

collected by passing through a hydrophobic frit then evaporated to yield the product as a yellow solid (26 mg, 17%); R_f 0.30 (EtOAc:*c*-hexane, 60:40 + 1% NEt_3); mp 271-278 °C; ν_{max} (neat) 3102 (C-H), 2966 (C-H), 2854 (C-H), 1644 (C=O); ^{1}H NMR (200 MHz, $CDCl_3$) δ ppm 2.58 (s, 3 H, C(15)H_3), 3.35 - 3.48 (m, 4 H, C(8)H_2+C(12)H_2), 3.87 - 3.98 (m, 4 H, C(9)H_2+C(11)H_2), 6.74 (dd, *J*=8.0, 3.0 Hz, 1 H, C(3)*H*), 7.71 (m, 1 H, C(23)*H*), 7.83 - 7.92 (m, 2 H, C(17)*H*+C(22)*H*), 8.17 (d, *J*=3.0 Hz, 1 H, C(5)*H*), 8.87 - 8.95 (m, 1 H, C(20)*H*), 9.79 (d, *J*=8.0 Hz, 1 H, C(2)*H*); ^{13}C NMR (126 MHz, CHLOROFORM-*d*) δ ppm 26.8 (s, 1 C, *C*(15)), 47.4 (s, 2 C, *C*(8)+*C*(12)), 66.4 (s, 2 C, *C*(9)+*C*(11)), 99.6 (s, 1 C, *C*(5)), 106.0 (s, 1 C, *C*(3)), 110.3 - 110.5 (m, 1 C, *C*(16)), 118.8 (s, 1 C, *C*(23)), 124.0 (q, *J*=271.5 Hz, 1 C, *C*(24)), 121.5 (q, *J*=33.0 Hz, 1 C, *C*(21)), 121.8 (s, 1 C, *C*(13)), 123.9 (s, 1 C, *C*(17)), 129.9 (s, 1 C, *C*(2)), 132.9 - 133.3 (m, 1 C, *C*(22)), 139.9 (s, 1 C, *C*(6)), 145.9 - 146.1 (m, 1 C, *C*(20)), 149.3 (s, 1 C, *C*(4)), 157.7 - 158.1 (m, 1 C, *C*(18)), 185.6 (s, 1 C, *C*(14)); LRMS *m/z* (ESI$^+$) 390 [MH$^+$]; HRMS (ESI$^+$) found 412.1259, calculated for $C_{20}H_{18}F_3N_3NaO_3^+$ 412.1243; HPLC (System D) t_r 18.1 min (91%).

3-Acetyl-1-[5-(trifluoromethyl)pyridin-2-yl]-5,6-dihydroindolizin-7(8*H*)-one (429)

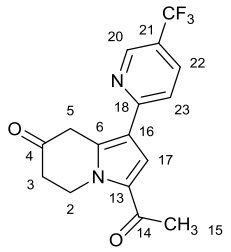

Compound **429** was isolated as a by-product from the formation of compound **420**. Compound **429** was obtained as a yellow solid (5 mg, 3.9%); R_f 0.45 (EtOAc:*c*-hexane, 60:40 + 1% NEt_3); ν_{max} (neat) 3030 (C-H), 2970 (C-H), 2925 (C-H), 1720 (cyclic ketone C=O), 1650 (acetyl ketone C=O); ^{1}H NMR (400 MHz, $CDCl_3$) δ ppm 2.53 (s, 3 H, C(15)H_3), 2.79 (t, *J*=6.5 Hz, 2 H, C(3)H_2), 4.29 (s, 2 H, C(5)H_2), 4.98 (t, *J*=6.5 Hz, 2 H, C(2)H_2), 7.41 (s, 1 H, C(17)*H*), 7.59 (d, *J*=8.5 Hz, 1 H, C(23)*H*), 7.90 (dd, *J*=8.5, 2.5 Hz, 1 H, C(22)*H*), 8.78 - 8.84 (m, 1 H, C(20)*H*); ^{13}C NMR (126 MHz, $CDCl_3$) δ ppm 27.3 (s, 1 C, *C*(15)), 38.8 (s, 1 C, *C*(3)), 40.1 (s, 1 C, *C*(5)), 42.2 (s, 1 C, *C*(2)), 118.4 (s, 1 C, *C*(17)), 119.3 (s, 1 C, *C*(23)), 119.6 (s, 1 C, *C*(16)),

123.7 (q, *J*=272.0 Hz, 1 C, *C*F_3) 123.2 (q, *J*=33.0 Hz, 1 C, *C*(21)), 130.0 (s, 1 C, *C*(13)), 133.5 (q, *J*=3.5 Hz, 1 C, *C*(22)), 135.5 (s, 1 C, *C*(6)), 146.2 (q, *J*=4.5 Hz, 1 C, *C*(20)), 157.1 (d, *J*=2.0 Hz, 1 C, *C*(18)), 188.6 (s, 1 C, *C*(14)), 204.4 (s, 1 C, *C*(4)); ^{19}F NMR (377 MHz, $CDCl_3$) δ ppm -62.15 (s, 3 F); LRMS *m/z* (ESI^+) 323 (MH^+), (ESI^-) 321 [$M-H^-$]; HRMS (ESI^+) found 345.0820, calculated for $C_{16}H_{13}F_3N_2NaO_2^+$ 345.0821; HPLC (System E) t_r 5.9 min (>99%).

1-[1-(3-Fluoropyridin-2-yl)-7-(morpholin-4-yl)indolizin-3-yl]ethanone (421)

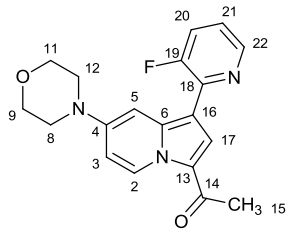

K_2CO_3 (47 mg, 0.34 mmol) was added to a solution of compound **415** (80 mg, 0.31 mmol) in DMF (2 mL). The resultant suspension was stirred at room temperature for 10 minutes then 2-ethynyl-3-fluoropyridine (42 mg, 0.34 mmol) was added. The mixture was then heated at 90 °C for 2 h then allowed to cool. The mixture was then partitioned between water (3 mL) and CH_2Cl_2 (3 mL). The organic phase was collected by passing it through a hydrophobic frit then concentrated by nitrogen blow-down. The crude material was purified by flash column chromatography on a silica column (4 g). The column was eluted with a gradient of EtOAc:*c*-hexane + 0.1% NEt_3 which was increased linearly from 40:60 to 80:20 over 20 CVs. The desired fractions were combined and evaporated. The resultant solid was suspended in MeOH then filtered to yield the product as a yellow solid (16 mg, 28%); R_f 0.25 (EtOAc:*c*-hexane, 60:40 + 1% NEt_3); mp 191-195 °C; ν_{max} (neat) 3104 (C-H), 2961 (C-H), 2925 (C-H), 2864 (C-H), 1645 (C=O); ^{1}H NMR (400 MHz, $CDCl_3$) δ ppm 2.56 (s, 3 H, C(15)H_3), 3.22 - 3.39 (m, 4 H, C(8)H_2+C(12)H_2), 3.82 - 4.03 (m, 4 H, C(9)H_2+C(11)H_2), 6.72 (dd, *J*=8.0, 3.0 Hz, 1 H, C(3)*H*), 7.07 - 7.24 (m, 1 H, C(21)*H*), 7.44 (ddd, *J*=12.0, 8.0, 1.5 Hz, 1 H, C(20)*H*), 8.03 (d, *J*=3.0 Hz, 1 H, C(17)*H*), 8.12 (d, *J*=3.0 Hz, 1 H, C(5)*H*), 8.46 (dt, *J*=4.5, 1.5 Hz, 1 H, C(22)*H*), 9.80 (d, *J*=8.0 Hz, 1 H, C(2)*H*); ^{13}C NMR (101 MHz, $CDCl_3$) δ ppm 26.7 (s, 1 C, *C*(15)), 47.6 (s, 2

C, *C*(8)+*C*(12)), 66.5 (s, 2 C, *C*(9)+*C*(11)), 99.7 (s, 1 C, *C*(5)), 106.1 (s, 1 C, *C*(3)), 106.9 (d, *J*=5.5 Hz, 1 C, *C*(3)), 120.1 (d, *J*=4.0 Hz, 1 C, *C*(21)), 121.4 (d, *J*=3.0 Hz, 1 C, *C*(13)), 122.9 (d, *J*=20.0 Hz, 1 C, *C*(20)), 126.0 (d, *J*=15.0 Hz, 1 C, *C*(17)), 129.7 (s, 1 C, *C*(2)), 140.1 (s, 1 C, *C*(6)), 143.7 (d, *J*=10.5 Hz, 1 C, *C*(18)), 144.5 (d, *J*=5.0 Hz, 1 C, *C*(22)), 148.8 (s, 1 C, *C*(4)), 156.3 (d, *J*=259.0 Hz, 1 C, *C*(19)), 185.5 (s, 1 C, *C*(14)); ^{19}F NMR (377 MHz, $CDCl_3$) δ ppm -121.8 (s, 1 F); LRMS *m/z* (ESI^+) 340 [MH^+]; HRMS (ESI^+) found 340.1440, calculated for $C_{19}H_{19}FN_3O_2^+$ 340.1456; HPLC (System D) t_r 15.3 min (97%).

1-[1-(3-Fluoro-5-methylpyridin-2-yl)-7-(morpholin-4-yl)indolizin-3-yl]ethanone (422)

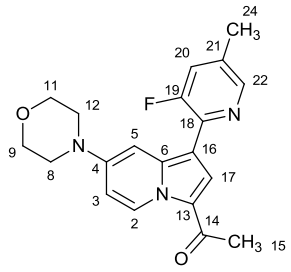

K_2CO_3 (47 mg, 0.34 mmol) was added to a solution of compound **415** (80 mg, 0.31 mmol) in DMF (2 mL). The resultant suspension was stirred at room temperature for 10 minutes then 2-ethynyl-3-fluoro-5-methylpyridine (46 mg, 0.34 mmol) was added. The mixture was then heated at 90 °C for 2 h then allowed to cool. The mixture was then partitioned between water (3 mL) and CH_2Cl_2 (3 mL). The organic phase was collected by passing it through a hydrophobic frit then concentrated by nitrogen blow-down. The crude material was purified by flash column chromatography on a silica column (4 g). The column was eluted with a gradient of EtOAc:*c*-hexane + 0.1% NEt_3 which was increased linearly from 40:60 to 80:20 over 20 CVs. The desired fractions were combined and evaporated. The resultant solid was suspended in MeOH then filtered to yield the product as a yellow solid (16 mg, 28%); R_f 0.25 (EtOAc:*c*-hexane, 60:40 + 1% NEt_3); mp 235-239 °C; ν_{max} (neat) 3119 (C-H), 2965 (C-H), 2917 (C-H), 2861 (C-H), 1643 (C=O); ^{1}H NMR (400 MHz, $CDCl_3$) δ ppm 2.31 (s, 3 H, C(24)H_3),

2.42 - 2.53 (m, 3 H, C(15)H_3), 3.14 - 3.30 (m, 4 H, C(8)H_2+C(12)H_2), 3.70 - 3.94 (m, 4 H, C(9)H_2+C(11)H_2), 6.63 (dd, *J*=8.0, 2.5 Hz, 1 H, C(3)*H*), 7.15 - 7.38 (m, 1 H, C(20)*H*), 7.90 (d, *J*=3.0 Hz, 1 H, C(17)*H*), 7.96 (d, *J*=2.5 Hz, 1 H, C(5)*H*), 8.12 - 8.34 (m, 1 H, C(22)*H*), 9.72 (d, *J*=8.0 Hz, 1 H, C(2)*H*); ^{13}C NMR (101 MHz, $CDCl_3$) δ ppm 17.8 (s, 1 C, *C*(24)), 26.7 (s, 1 C, *C*(15)), 47.6 (s, 2 C, *C*(8)+*C*(12)), 66.5 (s, 2 C, *C*(9)+*C*(11)), 99.6 (s, 1 C, *C*(5)), 106.1 (s, 1 C, *C*(3)), 107.1 (d, *J*=6.5 Hz, 1 C, *C*(16)), 121.3 (d, *J*=3.0 Hz, 1 C, *C*(13)), 123.6 (d, *J*=20.0 Hz, 1 C, *C*(20)), 125.7 (d, *J*=13.5 Hz, 1 C, *C*(17)), 129.6 (s, 1 C, *C*(2)), 130.7 (d, *J*=4.0 Hz, 1 C, *C*(2)), 139.8 (s, 1 C, *C*(6)), 140.7 (d, *J*=11.0 Hz, 1 C, *C*(18)), 144.8 (d, *J*=4.0 Hz, 1 C, *C*(22)), 148.6 (s, 1 C, *C*(4)), 156.1 (d, *J*=259.0 Hz, 1 C, *C*(19)), 185.4 (s, 1 C, *C*(14)); ^{19}F NMR (377 MHz, $CDCl_3$) δ ppm -123.6 (s, 1 F); LRMS *m/z* (ESI$^+$) 354 [MH$^+$]; HRMS (ESI$^+$) found 354.1596, calculated for $C_{20}H_{21}FN_3O_2^+$ 354.1612; HPLC (System D) t_r 15.8 min (92%).

1-[7-(Morpholin-4-yl)-1-(pyrimidin-2-yl)indolizin-3-yl]ethanone (423)

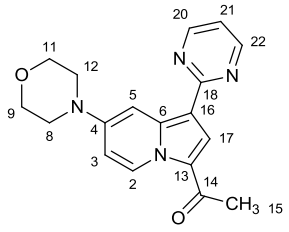

A mixture of compound **415** (100 mg, 0.39 mmol) and K_2CO_3 (108 mg, 0.78 mmol) in DMF (2 mL) was stirred at room temperature for 15 minutes then 2-ethynylpyrimidine (45 mg, 0.43 mmol) was added. The resultant mixture was stirred for 2 h at 90 °C then allowed to cool. The mixture was then partitioned between water (5 mL) and CH_2Cl_2 (5 mL). The phases were separated using a hydrophobic frit then the organic phase was evaporated. The crude material was purified by flash column chromatography on a silica column (12 g). The column was eluted with a gradient of EtOAc:*c*-hexane which was increased linearly from 60:40 to 100:0 over 10 CVs. The desired fractions were combined and evaporated to a yellow solid (28 mg). This material thus obtained was suspended in MeOH (5 mL), refluxed, allowed to cool, sonicated, then filtered and dried under vacuum to yield the product as a

pale-yellow solid (19 mg, 15%); R_f 0.30 (EtOAc + 1% NEt_3); mp 213-217 °C; ν_{max} (neat) 3114 (C-H), 3023 (C-H), 2858 (C-H), 2831 (C-H), 1643 (C=O); ^{1}H NMR (400 MHz, $CDCl_3$) δ ppm 2.50 (s, 3 H, C(15)H_3), 3.27 - 3.38 (m, 4 H, C(8)H_2+C(12)H_2), 3.72 - 3.88 (m, 4 H, C(9)H_2+C(11)H_2), 6.63 (dd, *J*=8.0, 3.0 Hz, 1 H, C(3)*H*), 6.91 (t, *J*=5.0 Hz, 1 H, C(21)*H*), 8.09 (d, *J*=3.0 Hz, 1 H, C(5)*H*), 8.20 (s, 1 H, C(17)*H*), 8.63 (d, *J*=5.0 Hz, 2 H, C(20)*H*+C(22)*H*), 9.69 (d, *J*=8.0 Hz, 1 H, C(2)*H*); ^{13}C NMR (101 MHz, $CDCl_3$) δ ppm 26.8 (s, 1 C, *C*(15)), 47.5 (s, 2 C, *C*(8)+*C*(12)), 66.5 (s, 2 C, *C*(9)+*C*(11)), 99.9 (s, 1 C, *C*(5)), 105.7 (s, 1 C, *C*(3)), 111.2 (s, 1 C, *C*(16)), 116.1 (s, 1 C, *C*(21)), 121.7 (s, 1 C, *C*(13)), 126.2 (s, 1 C, *C*(17)), 130.0 (s, 1 C, *C*(2)), 140.6 (s, 1 C, *C*(6)), 149.1 (s, 1 C, *C*(4)), 156.8 (s, 2 C, *C*(20)+*C*(22)), 163.1 (s, 1 C, *C*(18)), 186.1 (s, 1 C, *C*(14)); LRMS *m/z* (ESI$^+$) 323 [MH$^+$]; HRMS (ESI$^+$) found 345.1327, calculated for $C_{18}H_{18}N_4NaO_2^+$ 345.1322; HPLC (System E) t_r 4.5 min (96%).

1-[1-(1,3-Benzothiazol-2-yl)-7-(morpholin-4-yl)indolizin-3-yl]ethanone (424)

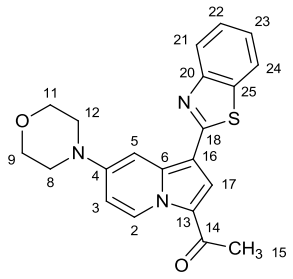

K_2CO_3 (47 mg, 0.34 mmol) was added to a solution of compound **415** (80 mg, 0.31 mmol) in DMF (2 mL). The resultant suspension was stirred at room temperature for 10 minutes then 2-ethynyl-1,3-benzothiazole (55 mg, 0.34 mmol) was added. The mixture was then heated at 90 °C for 2 h then allowed to cool. The mixture was then partitioned between water (3 mL) and CH_2Cl_2 (3 mL). The organic phase was collected by passing it through a hydrophobic frit then concentrated by nitrogen blow-down. The crude material was purified by flash column chromatography on a silica column (4 g). The column was eluted with a gradient of EtOAc:*c*-hexane + 0.1% NEt_3 which was increased linearly from 40:60 to 80:20 over 20 CVs. The desired fractions were combined and evaporated. The resultant solid was suspended in

MeOH then filtered to yield the product as an orange solid (14 mg, 12%); R_f 0.25 (EtOAc:*c*-hexane, 60:40 + 1% NEt_3); mp 212-217 °C; ν_{max} (neat) 3061 (C-H), 2963 (C-H), 2856 (C-H), 1645 (C=O); ^{1}H NMR (500 MHz, $CDCl_3$) δ ppm 2.57 (s, 3 H, C(15)H_3), 3.39 - 3.49 (m, 4 H, C(8)H_2+C(12)H_2), 3.84 - 4.01 (m, 4 H, C(9)H_2+C(11)H_2), 6.72 (dd, *J*=7.5, 2.5 Hz, 1 H, C(3)*H*), 7.32 (t, *J*=7.5 Hz, 1 H, C(22/23)*H*), 7.45 (t, *J*=7.5 Hz, 1 H, C(23/24)*H*), 7.80 - 7.91 (m, 2 H, C(17)*H*+C(21/24)*H*), 7.92 - 8.06 (m, 2 H, C(5)*H*+C(21/24)*H*), 9.73 (d, *J*=8.0 Hz, 1 H, C(2)*H*); ^{13}C NMR (126 MHz, $CDCl_3$) δ ppm 26.8 (s, 1 C, *C*(15)), 47.2 (s, 2 C, *C*(8)+*C*(12)), 66.4 (s, 2 C, *C*(9)+*C*(11)), 98.8 (s, 1 C, *C*(5)), 106.0 (s, 1 C, *C*(3)), 107.0 (s, 1 C, *C*(16)), 121.2 (s, 1 C, *C*(21/24)), 121.8 (s, 1 C, *C*(13/21/24)), 121.9 (s, 1 C, *C*(13/21/24)), 124.0 (s, 1 C, *C*(22/23)), 124.9 (s, 1 C, *C*(17)), 126.0 (s, 1 C, *C*(22/23)), 130.1 (s, 1 C, *C*(2)), 133.3 (s, 1 C, *C*(25)), 139.2 (s, 1 C, *C*(6)), 149.5 (s, 1 C, *C*(4)), 154.2 (s, 1 C, *C*(20)), 162.7 (s, 1 C, *C*(18)), 185.8 (s, 1 C, *C*(14)); LRMS *m/z* (ESI$^+$) 378 [MH$^+$]; HRMS (ESI$^+$) found 378.1274, calculated for $C_{21}H_{20}N_3O_2S^+$ 378.1271; HPLC (System D) t_r 18.4 min (92%).

1-[1-(Imidazo[1,2-*a*]pyridin-5-yl)-7-(morpholin-4-yl)indolizin-3-yl]ethanone (425)

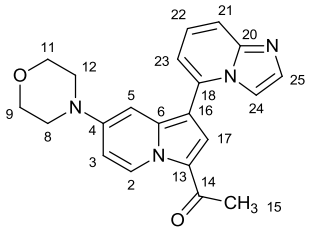

K_2CO_3 (108 mg, 0.78 mmol) was added to a solution of compound **415** (100 mg, 0.39 mmol) in DMF (2 mL). The resultant suspension was stirred at room temperature for 15 minutes then 5-ethynylimidazo[1,2*a*]pyridine (61 mg, 0.43 mmol) was added. The mixture was then heated at 90 °C for 2 h then allowed to cool. The solvent was evaporated by N_2 blow-down then the mixture was then partitioned between water (5 mL) and CH_2Cl_2 (5 mL). The organic phase was collected by passing it through a hydrophobic frit then concentrated by nitrogen blow-down. The crude material was purified by flash column chromatography on a silica column (12 g). The column was eluted with a gradient of EtOAc:MeOH:NEt_3 which was

increased linearly from 99:1:0.1 to 90:10:1 over 12 CVs. The desired fractions were combined and evaporated to a cream solid (32 mg). The material thus obtained was purified further by flash column chromatography on a C-18 column (4.3 g). The column was eluted with a gradient of H_2O:MeCN (+0.1% CF_3CO_2H) which was increased linearly from 95:5 to 5:95 over 12 CVs. The desired fractions were combined and evaporated then partitioned between CH_2Cl_2 (2 mL) and saturated aq. $NaHCO_3$ (2 mL). The organic phase was collected by passing through a hydrophobic frit then evaporated to yield the product as a yellow solid (5 mg, 4%); R_f 0.25 (EtOAc:MeOH:NEt_3, 90:10:1); mp 212-217 °C; ν_{max} (neat) 3079 (C-H), 2952 (C-H), 2867 (C-H), 1644 (C=O); ^{1}H NMR (200 MHz, $CDCl_3$) δ ppm 2.56 (s, 3 H, C(15)H_3), 3.11 - 3.32 (m, 4 H, C(8)H_2+C(12)H_2), 3.75 - 3.91 (m, 4 H, C(9)H_2+C(11)H_2), 6.46 (d, *J*=2.4 Hz, 1 H, C(24/25)*H*), 6.75 (dd, *J*=7.9, 2.7 Hz, 1 H, C(3)*H*), 6.88 (dd, *J*=7.0, 1.1 Hz, 1 H, C(23)*H*), 7.23 - 7.35 (m, 1 H, C(22)*H*), 7.54 - 7.74 (m, 4 H, C(5)*H*+C(17)*H*+C(21)*H*+C(24/25)*H*), 9.81 (d, *J*=7.9 Hz, 1 H, C(2)*H*); ^{13}C NMR (101 MHz, $CDCl_3$) δ ppm 26.7 (s, 1 C, *C*(15)), 47.4 (s, 2 C, *C*(8)+*C*(12)), 66.2 (s, 2 C, *C*(9)+*C*(11)), 96.4 (s, 1 C, *C*(5)), 105.8 (s, 1 C, *C*(16)), 106.2 (s, 1 C, *C*(3)), 111.5 (s, 1 C, *C*(24)), 113.0 (s, 1 C, *C*(23)), 115.6 (s, 1 C, *C*(21)), 121.5 (s, 1 C, *C*(13)), 124.4 (s, 1 C, *C*(17)), 124.7 (s, 1 C, *C*(22)), 130.1 (s, 1 C, *C*(2)), 132.8 (s, 1 C, *C*(18)), 132.9 (s, 1 C, *C*(25)), 138.3 (s, 1 C, *C*(6)), 146.1 (s, 1 C, *C*(20)), 148.2 (s, 1 C, *C*(4)), 185.5 (s, 1 C, *C*(14)); LRMS *m/z* (ESI$^+$) 361 [MH$^+$]; HRMS (ESI$^+$) found 361.1643, calculated for $C_{21}H_{21}N_4O_2^+$ 361.1659; HPLC (System E) t_r 3.8 min (99%).

1-{3-[3-Acetyl-7-(morpholin-4-yl)indolizin-1-yl]phenyl}-3,3-dimethylazetidin-2-one (426)

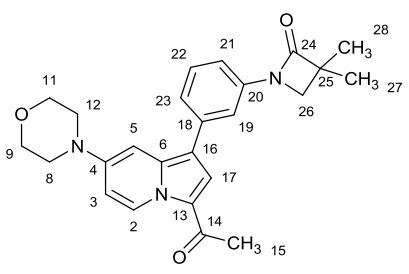

K_2CO_3 (69 mg, 0.25 mmol) was added to a solution of compound **415** (64 mg, 0.25 mmol) in DMF (2 mL). The resultant suspension was stirred at room temperature for 10 minutes then 1-(3-ethynylphenyl)-3,3-dimethyl-2-azetidinone (50 mg, 0.25 mmol) was added. The mixture was then heated at 90 °C for 3 h then allowed to cool. The mixture was partitioned between water (5 mL) and EtOAc (5 mL). The organic phase was washed with water (5 mL) and brine (5 mL) then dried ($MgSO_4$) and evaporated. The crude material was purified by flash column chromatography on a silica column (12 g). The column was eluted with a gradient of EtOAc:*c*-hexane which was increased linearly from 60:40 to 100:0 over 10 CVs. The desired fractions were combined and evaporated to a yellow gum (17 mg). This material was re-dissolved in CH_2Cl_2/MeOH then pre-adsorbed onto silica. The material was then re-purified by flash column chromatography on a C-18 column (4.3 g). The column was eluted with a gradient of MeCN:H_2O+0.1% CF_3CO_2H, which was increased linearly from 5:95 to 95:5 over 20 CVs. The desired fractions were combined and evaporated to yield the product as a yellow gum (8 mg, 8%); R_f 0.30 (EtOAc:*c*-hexane, 80:20); ν_{max} (neat) 2962 (C-H), 2925 (C-H), 2855 (C-H), 1735 (lactam C=O), 1642 (ketone C=O); ^{1}H NMR (700 MHz, $CDCl_3$) δ ppm 1.36 (s, 6 H, C(27)H_3+C(28)H_3), 2.48 (s, 3 H, C(15)H_3), 3.17 - 3.28 (m, 4 H, C(8)H_2+C(12)H_2), 3.42 (s, 2 H, C(26)H_2), 3.76 - 3.85 (m, 4 H, C(9)H_2+C(11)H_2), 6.61 (dd, *J*=8.0, 2.5 Hz, 1 H, C(3)*H*), 6.99 - 7.06 (m, 2 H, C(5)*H*+C(21)*H*), 7.22 (d, *J*=7.5 Hz, 1 H, C(23)*H*), 7.31 - 7.36 (m, 1 H, C(22)*H*), 7.47 (s, 1 H, C(17)*H*), 7.68 (s, 1 H, C(19)*H*), 9.70 (d, *J*=8.0 Hz, 1 H, C(2)*H*); ^{13}C NMR (176 MHz, $CDCl_3$) δ ppm 21.5 (s, 2 C, *C*(27)+*C*(28)), 26.5 (s, 1 C, *C*(15)), 47.9 (s, 2 C, *C*(8)+*C*(12)), 50.0 (s, 1 C, *C*(25)), 53.4 (s, 1 C, *C*(26)), 66.4 (s, 2 C, *C*(9)+*C*(11)), 97.1 (s, 1 C, *C*(5)), 106.1 (s, 1 C, *C*(3)), 113.4 (s, 1 C, *C*(21)), 114.3 (s, 1 C, *C*(16)), 115.8 (s, 1 C, *C*(19)), 121.1 (s, 1 C, *C*(13)), 122.6 (s, 1 C, *C*(23)), 124.0 (s, 1 C, *C*(17)), 129.6 (s, 1 C, *C*(22)), 130.1 (s, 1 C, *C*(2)), 136.3 (s, 1 C, *C*(18/20)), 138.3 (s, 1 C, *C*(6)), 139.2 (s, 1 C, *C*(18/20)), 148.2 (s, 1 C, *C*(4)) 171.2 (s, 1 C, *C*(24)), 184.3 (s, 1 C, *C*(14)); LRMS *m/z* (ESI$^+$) 418 [MH$^+$]; HRMS (ESI$^+$) found 440.1947, calculated for $C_{25}H_{27}N_3NaO_3^+$ 440.1945; HPLC (System E) t_r 3.6 min (95%).

Methyl 2-[3-acetyl-7-(morpholin-4-yl)indolizin-1-yl]pyridine-4-carboxylate (427)

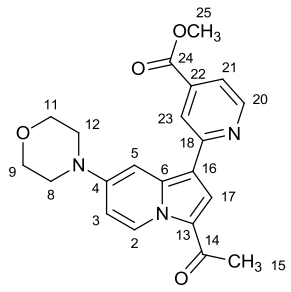

K_2CO_3 (216 mg, 1.56 mmol) was added to a solution of compound **415** (200 mg, 0.78 mmol) in DMF (4 mL). The resultant suspension was stirred at room temperature for 15 minutes then methyl 2-ethynylisonicotinate (151 mg, 0.93 mmol) was added. The mixture was then heated at 90 °C for 2 h then allowed to cool. The solvent was evaporated by N_2 blow-down then the mixture was then partitioned between water (5 mL) and CH_2Cl_2 (5 mL). The organic phase was collected by passing it through a hydrophobic frit then concentrated by nitrogen blow-down. The crude material was purified by flash column chromatography on a silica column (12 g). The column was eluted with a gradient of EtOAc:*c*-hexane which was increased linearly from 60:40 to 100:0 over 12 CVs. The desired fractions were combined and evaporated to an orange solid (127 mg). This material was suspended in MeOH (3 mL) then the supernatant was decanted off with a pipette. This process was repeated (×2) then the residual solid was dried under vacuum to yield the product as a yellow solid (96 mg, 32%) R_f 0.45 (EtOAc); mp 212-216 °C; ν_{max} (neat) 3112 (C-H), 2994 (C-H), 2954 (C-H), 2867 (C-H), 2838 (C-H), 1723 (ester C=O), 1643 (ketone C=O); ^{1}H NMR (400 MHz, $CDCl_3$) δ ppm 2.57 (s, 3 H, C(15)H_3), 3.33 - 3.48 (m, 4 H, C(8)H_2+C(12)H_2), 3.79 - 3.94 (m, 4 H, C(9)H_2+C(11)H_2), 4.00 (s, 3 H, C(25)*H*), 6.70 (dd, *J*=8.0, 3.0 Hz, 1 H, C(3)*H*), 7.55 (dd, *J*=5.0, 1.5 Hz, 1 H, C(21)*H*), 7.88 (s, 1 H, C(17)*H*), 8.12 (d, *J*=3.0 Hz, 1 H, C(5)*H*), 8.15 (s, 1 H, C(23)*H*), 8.74 (d, *J*=5.0 Hz, 1 H, C(20)*H*), 9.76 (d, *J*=8.0 Hz, 1 H, C(2)*H*); ^{13}C NMR (101 MHz, $CDCl_3$) δ ppm 26.8 (s, 1 C, *C*(15)), 47.5 (s, 2 C, *C*(8)+*C*(12)), 52.6 (s, 1 C, *C*(25)), 66.5 (s, 2 C, *C*(9)+*C*(11)), 99.6 (s, 1 C, *C*(5)), 106.0 (s, 1 C, *C*(3)), 111.4 (s, 1 C, *C*(16)), 118.0 (s, 1 C, *C*(21)),

118.9 (s, 1 C, *C*(23)), 121.4 (s, 1 C, *C*(13)), 123.6 (s, 1 C, *C*(17)), 129.7 (s, 1 C, *C*(2)), 137.4 (s, 1 C, *C*(22)), 139.5 (s, 1 C, *C*(6)), 148.9 (s, 1 C, *C*(4)), 149.8 (s, 1 C, *C*(20)), 155.9 (s, 1 C, *C*(18)), 166.1 (s, 1 C, *C*(24)), 185.3 (s, 1 C, *C*(14)); LRMS *m/z* (ESI^+) 380 [MH^+]; HRMS (ESI^+) found 402.1417, calculated for $C_{21}H_{21}N_3NaO_4^+$ 402.1424; HPLC (System D) t_r 15.0 min (95%).

2-[3-Acetyl-7-(morpholin-4-yl)indolizin-1-yl]pyridine-4-carboxylic acid (428)

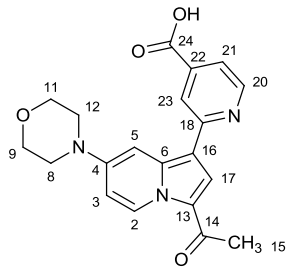

1.0 M aq. LiOH solution (0.26 mL, 0.26 mmol) was added to a stirred suspension of methyl compound **427** (50 mg, 0.13 mmol) in THF (1.0 mL) and MeOH (1 mL). The mixture was heated at 50 °C for 2 h then allowed to cool. The reaction mixture was neutralised by addition of 1 M aq. HCl. The resultant precipitate was collected by filtration, washed with a small volume of MeOH, then dried under vacuum to yield the product as a brick-red solid (37 mg, 78%); R_f 0.10 (CH_2Cl_2:MeOH, 80:20); mp 212-217 °C; ν_{max} (neat) 3118 (C-H), 2947 (C-H), 2875 (C-H), 1713 (acid C=O) 1646 (ketone C=O); ^{1}H NMR (500 MHz, DMSO-d_6) δ ppm 2.53 (s, 3 H, C(15)H_3) 3.25 - 3.47 (m, 4 H+H_2O, C(8)H_2+C(12)H_2) 3.71 - 3.87 (m, 4 H, C(9)H_2+C(11)H_2) 7.09 (dd, *J*=8.0, 3.0 Hz, 1 H, C(3)*H*) 7.51 (dd, *J*=5.0, 1.5 Hz, 1 H, C(21)*H*) 8.18 (d, *J*=3.0 Hz, 1 H, C(5)*H*) 8.29 (s, 1 H, C(23)*H*) 8.40 (s, 1 H, C(17)*H*) 8.73 (d, *J*=5.0 Hz, 1 H, C(20)*H*) 9.64 (d, *J*=8.0 Hz, 1 H, C(2)*H*); ^{13}C NMR (126 MHz, DMSO-d_6) δ ppm 26.6 (s, 1 C, *C*(15)), 46.8 (s, 2 C, *C*(8)+*C*(12)), 65.8 (s, 2 C, *C*(9)+*C*(11)), 98.8 (s, 1 C, *C*(5)), 106.4 (s, 1 C, *C*(3)), 110.6 (s, 1 C, *C*(16)), 118.1 (s, 1 C, *C*(21)), 118.7 (s, 1 C, *C*(23)), 120.8 (s, 1 C, *C*(13)), 124.4 (s, 1 C, *C*(17)), 128.7 (s, 1 C, *C*(2)), 138.9 (s, 1 C, *C*(22)), 139.7 (s, 1 C, *C*(6)), 148.6 (s, 1 C, *C*(4)), 149.7 (s, 1 C, *C*(20)), 155.5 (s, 1 C, *C*(18)), 166.8 (s, 1 C, *C*(24)), 185.0 (s, 1 C, *C*(14));

LRMS *m/z* (ESI$^+$) 366 [MH$^+$], 364 [(M-H)$^-$]; HRMS found 366.1443, calculated for $C_{20}H_{20}N_3O_4^+$ 366.1448; HPLC (System D) t_r 11.4 min (98%).

1-Methyl-4-(pyridin-4-yl)piperazine (437)

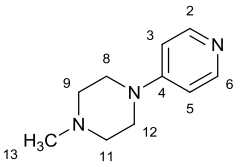

Iodomethane (6.15 g, 43.3 mmol) was added drop-wise to a stirred suspension of 1-(piperidine-4-yl)piperazine (7.00 g, 42.9 mmol) and K_2CO_3 (11.9 g, 85.8 mmol) in DMF (200 mL). The resultant mixture was stirred at room temperature for 4 h then quenched by addition of *conc*. NH_4OH (0.5 mL). The mixture was concentrated *in vacuo* then partitioned between EtOAc (200 mL) and water (200 mL). The phases were separated then the aqueous phase was extracted with EtOAc (5 × 200 mL). The combined organic phases were washed with brine (200 mL) then dried over $MgSO_4$ and evaporated. The material thus obtained was re-dissolved in MeOH then loaded onto a pre-wetted SCX cartridge (70 g, Biotage). The cartridge was eluted with MeOH then the basic components were recovered through elution with 7 M NH_3 in MeOH. The ammonia eluent was evaporated to yield the product as a pale-yellow oil (4.24 g, 56%); R_f 0.25 (CH_2Cl_2:MeOH:NH_4OH, 90:10:1); ν_{max} (neat) 3030 (C-H), 2939 (C-H), 2843 (C-H), 2797 (C-H); ^{1}H NMR (400 MHz, $CDCl_3$) δ ppm 2.27 (s, 3 H, C(13)H_3), 2.40 - 2.50 (m, 4 H, C(9)H_2+C(11)H_2), 3.25 - 3.31 (m, 4 H, C(8)H_2+C(12)H_2), 6.54 - 6.64 (m, 2 H, C(3)*H*+C(5)*H*), 8.16 - 8.25 (m, 2 H, C(2)*H*+C(6)*H*); ^{13}C NMR (101 MHz, $CDCl_3$) δ ppm 45.8 (s, 2 C, *C*(9)+*C*(11)), 46.1 (s, 1 C, *C*(13)), 54.4 (s, 2 C, *C*(8)+*C*(12)), 108.3 (s, 2 C, *C*(3)+*C*(5)), 150.1 (s, 2 C, *C*(2)+*C*(6)), 154.8 (s, 1 C, *C*(4)); LRMS *m/z* (ESI$^+$) 200 [(M+Na)$^+$], 178 [MH$^+$]; HRMS (ESI$^+$) found 178.1339, calculated for $C_{10}H_{16}N_3^+$ 178.1339; HPLC (System E) t_r 0.4 min (>99%).

4-(4-Methylpiperazin-1-yl)-1-(2-oxopropyl)pyridinium chloride (438)

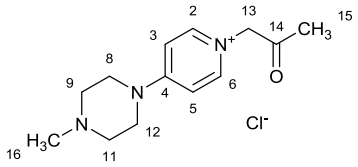

Chloroacetone (90 μL, 1.1 mmol) was added drop-wise to a stirred solution of compound **437** (200 mg, 1.1 mmol) in THF (6 mL). The resultant mixture was left to stir at room temperature for 18 h. The resultant suspension was filtered then the solid was washed with THF and dried under vacuum to yield the product as a pale-yellow solid (104 mg, 34%); mp 238-242 °C; ν_{max} (neat) 3036 (C-H), 2988 (C-H), 2939 (C-H), 2839 (C-H), 2787 (C-H), 2750 (C-H), 2707 (C-H), 1730 (C=O); ^{1}H NMR (400 MHz, DMSO-d_6) δ ppm 2.06 - 2.26 (m, 6 H, C(15)H_3+C(16)H_3), 2.36 - 2.47 (m, 4 H, C(9)H_2+C(11)H_2), 3.51 - 3.77 (m, 4 H, C(8)H_2+C(12)H_2), 5.36 (s, 2 H, C(13)H_2), 7.30 (d, J=8.0 Hz, 2 H, C(3)H+C(5)H), 8.14 (d, J=8.0 Hz, 2 H, C(2)H+C(6)H); ^{13}C NMR (101 MHz, DMSO-d_6) δ ppm 26.9 (s, 1 C, C(15)), 45.3 (s, 1 C, C(16)), 45.9 (s, 2 C, C(8)+C(12)), 53.9 (s, 2 C, C(9)+C(11)), 64.5 (s, 1 C, C(13)), 107.6 (s, 2 C, C(3)+C(5)), 143.6 (s, 2 C, C(2)+C(6)), 155.4 (s, 1 C, C(4)), 201.0 (s, 1 C, C(14)); LRMS m/z (ESI$^+$) 234 [M$^+$]; HRMS (ESI$^+$) found 234.1610, calculated for $C_{13}H_{20}N_3O^+$ 234.1601; HPLC (System E) t_r 0.6 min (>99%).

1-[1-(Imidazo[1,2-*a*]pyridin-5-yl)-7-(4-methylpiperazin-1-yl)indolizin-3-yl]ethanone (434)

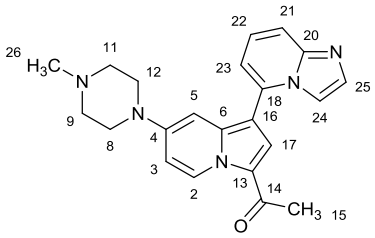

K_2CO_3 (138 mg, 1.00 mmol) was added to a solution of compound **438** (135 mg, 0.50 mmol) in DMF (5 mL). The resultant suspension was stirred at room temperature for 1 minutes

then 5-ethynylimidazo[1,2*a*]pyridine (78 mg, 0.55 mmol) was added. The mixture was then heated at 90 °C for 4 h, allowed to cool, then partitioned between water (10 mL) and $CHCl_3$ (10 mL). The organic phase was collected by passing it through a hydrophobic frit then concentrated by nitrogen blow-down. The crude material was purified by flash column chromatography on a silica column (24 g). The column was eluted with a gradient of CH_2Cl_2:MeOH:NH_4OH which was increased linearly from 99:1:0.1 to 95:5:0.5 over 10 CVs. The desired fractions were combined and evaporated to a red gum (39 mg). The material thus obtained was purified further by flash column chromatography on a C-18 column (13 g). The column was eluted with a gradient of H_2O:MeCN (+0.1% CF_3CO_2H) which was increased linearly from 95:5 to 5:95 over 20 CVs. The desired fractions were combined and evaporated then partitioned between $CHCl_3$ (5 mL) and saturated aq. $NaHCO_3$ (5 mL). The organic phase was collected by passing through a hydrophobic frit then evaporated to a red gum (19 mg). The material thus obtained was re-dissolved in the minimum of $CHCl_3$ then loaded onto a preparative TLC plate (Analtech, 20×20 cm, 2000 μm). Eluted with CH_2Cl_2:MeOH:NH_4OH (95:5:0.5). The desired band was scratched from the TLC plate with a spatula then suspended in CH_2Cl_2:MeOH:NH_4OH (90:10:1). The mixture was filtered then the filtrate was evaporated to yield the product as a tan-brown residue (5 mg, 2.7%); R_f 0.45 (CH_2Cl_2:MeOH:NH_4OH, 90:10:1); ν_{max} (neat) 3096 (C-H), 2925 (C-H), 2875 (C-H), 2841 (C-H), 2803 (C-H), 2771 (C-H), 1645 (C=O); ^{1}H NMR (500 MHz, $CDCl_3$) δ ppm 2.37 (s, 3 H, C(26)*H*$_3$), 2.55 (s, 3 H, C(15)*H*$_3$), 2.56 - 2.60 (m, 4 H, C(9)*H*$_2$+C(11)*H*$_2$), 3.27 - 3.32 (m, 4 H, C(8)*H*$_2$+C(12)*H*$_2$), 6.45 (d, *J*=2.5 Hz, 1 H, C(5)*H*), 6.75 (dd, *J*=8.0, 2.5 Hz, 1 H, C(3)*H*), 6.89 (d, *J*=7.0 Hz, 1 H, C(23)*H*), 7.28 - 7.34 (m, 1 H, C(22)*H*), 7.61 - 7.73 (m, 4 H, C(17)*H*+C(21)*H*+C(24)*H*+C(25)*H*), 9.79 (d, *J*=8.0 Hz, 1 H, C(2)*H*); ^{13}C NMR (126 MHz, $CDCl_3$) δ ppm 26.7 (s, 1 C, *C*(15)), 45.9 (s, 1 C, *C*(26)), 47.1 (s, 2 C, *C*(8)+*C*(12)), 54.3 (s, 2 C, *C*(9)+*C*(11)), 96.6 (s, 1 C, *C*(5)), 105.8 (s, 1 C, *C*(16)), 106.5 (s, 1 C, *C*(3)), 111.6 (s, 1 C, *C*(24)), 113.0 (s, 1 C, *C*(23)), 115.6 (s, 1 C, *C*(21)), 121.5 (s, 1 C, *C*(13)), 124.5 (s, 1 C, *C*(17)), 124.7 (s, 1 C, *C*(22)), 130.1 (s, 1 C, *C*(2)), 132.9 (s, 1 C, *C*(18)), 133.0 (s, 1 C, *C*(25)), 138.5 (s, 1 C, *C*(6)),

146.2 (s, 1 C, *C*(20)), 148.0 (s, 1 C, *C*(4)), 185.4 (s, 1 C, *C*(14)); LRMS *m/z* (ESI$^+$) 374 [MH$^+$]; HRMS (ESI$^+$) found 374.1980, calculated for $C_{22}H_{24}N_5O^+$ 374.1975; HPLC (System D) t_r 7.7 min (91%).

tert-Butyl 4-(pyridin-4-yl)piperazine-1-carboxylate (439)

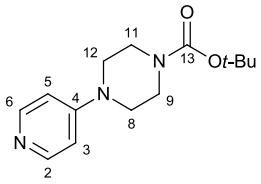

Di-*tert*-butyl dicarbonate (2.18 g, 10.0 mmol) was added to a solution of 1-(pyridine-4-yl)piperazine (1.63 g, 10.0 mmol) in THF (50 mL). The resultant solution was left to stir at room temperature for 2 h then concentrated *in vacuo*. The residue was partitioned between EtOAc (50 mL) and water (50 mL). The phases were separated then the organic phase was washed with brine (50 mL) then dried over $MgSO_4$ and evaporated to yield the product as a white solid (2.34 g, 89%); R_f 0.30 (CH_2Cl_2:MeOH:NH_4OH, 90:10:1); mp 99-104 °C; ν_{max} (neat) 2978 (C-H), 2862 (C-H), 1686 (C=O); ^{1}H NMR (400 MHz, $CDCl_3$) δ ppm 1.48 (s, 9 H, 9×Boc-*H*), 3.27 - 3.42 (m, 4 H, C(8)*H*$_2$+C(12)*H*$_2$), 3.47 - 3.59 (m, 4 H, C(9)*H*$_2$+C(11)*H*$_2$), 6.61 - 6.71 (m, 2 H, C(3)*H*+C(5)*H*), 8.28 (d, *J*=6.5 Hz, 2 H, C(2)*H*+C(6)*H*)); ^{13}C NMR (101 MHz, $CDCl_3$) δ ppm 28.3 (s, 3 C, 3×Boc-*C*) 42.9 (s, 2 C, *C*(9)+*C*(11)), 45.8 (s, 2 C, *C*(8)+*C*(12)), 80.2 (s, 1 C, Boc-*C*) 108.5 (s, 2 C, *C*(3)+*C*(5)), 150.3 (s, 2 C, *C*(2)+*C*(6)), 154.5 (s, 1 C, *C*(4/13)), 154.7 (s, 1 C, *C*(4/13)); LRMS *m/z* (ESI$^+$) 264 [MH$^+$]; HRMS (ESI$^+$) found 264.1695, calculated for $C_{22}H_{24}N_5O^+$ 264.1707; HPLC (System D) t_r 9.1 min (98%).

4-[4-(_tert_-Butoxycarbonyl)piperazin-1-yl]-1-(2-oxopropyl)pyridinium chloride (440)

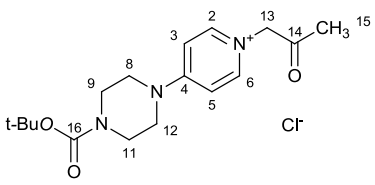

Chloroacetone (0.233 mL, 2.85 mmol) was added to a stirred solution of compound **439** (750 mg, 2.85 mmol) in THF (20 mL). The resultant mixture was left to stir for 18 h at room temperature then diluted with Et_2O (20 mL). The solid was filtered then dried under vacuum to yield the product as a pale-yellow solid (662 mg, 65%); mp 229-231 °C; ν_{max} (neat) 3034 (C-H), 2982 (C-H), 2921 (C-H), 2866 (C-H), 1735 (ketone C=O), 1692 (carbamate C=O); ^{1}H NMR (400 MHz, $CDCl_3$) δ ppm 1.44 (s, 9 H, 9×Boc-*H*), 2.34 (s, 3 H, C(15)*H*$_3$), 3.56 - 3.66 (m, 4 H, C(8/9)*H*$_2$+C(11/12)*H*$_2$), 3.66 - 3.80 (m, 4 H, C(8/9)*H*$_2$+C(11/12)*H*$_2$), 5.87 - 6.01 (m, 2 H, C(13)*H*$_2$), 7.07 - 7.19 (m, 2 H, C(3)*H*+C(5)*H*), 8.42 - 8.57 (m, 2 H, C(2)*H*+C(6)*H*); ^{13}C NMR (101 MHz, $CDCl_3$) δ ppm 27.6 (s, 1 C, *C*(15)), 28.2 (s, 3 C, 3×Boc-*C*) 46.1 (s, 4 C, *C*(8)+*C*(9)+*C*(11)+*C*(12)), 65.3 (s, 1 C, *C*(13)), 80.7 (s, 1 C, Boc-*C*) 107.9 (s, 2 C, *C*(3)+*C*(5)), 144.3 (s, 2 C, *C*(2)+*C*(6)), 154.2 (s, 1 C, *C*(4/16)), 155.9 (s, 1 C, *C*(4/16)), 200.7 (s, 1 C, *C*(21)); LRMS *m/z* (ESI$^+$) 320 [M$^+$]; HRMS (ESI$^+$) found 320.1954, calculated for $C_{17}H_{26}N_3O_3^+$ 320.1969; HPLC (System D) t_r 9.2 min (91%).

tert-Butyl 4-[3-acetyl-1-(imidazo[1,2-*a*]pyridin-5-yl)indolizin-7-yl]piperazine-1-carboxylate (441)

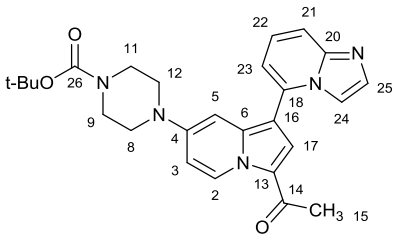

A suspension of K_2CO_3 (66 mg, 0.48 mmol) was added to a solution of compound **440** (155 mg, 0.44 mmol) in DMF (5 mL). The resultant suspension was stirred at room temperature for 5 minutes then 5-ethynylimidazo[1,2*a*]pyridine (68 mg, 0.48 mmol) was added. The mixture was then heated at 90 °C for 2 h, allowed to cool, then concentrated *in vacuo*. The residue was then partitioned between water (5 mL) and EtOAc (5 mL). The aqueous phase was extracted with more EtOAc (5 mL) then the combined organic phases were washed water (5 mL) and brine (5 mL) then dried over $MgSO_4$ and evaporated. The crude material

was purified by flash column chromatography on a silica column (12 g). The column was eluted with a gradient of CH_2Cl_2:MeOH:NH_4OH which was increased linearly from 99:1:0.1 to 90:10:1 over 12 CVs. The desired fractions were combined and evaporated to yield a yellow gum (132 mg). The material thus obtained was purified further by flash column chromatography on a C-18 column (13 g). The column was eluted with a gradient of H_2O:MeCN (+0.1% CF_3CO_2H) which was increased linearly from 95:5 to 5:95 over 20 CVs. The desired fractions were combined and evaporated then partitioned between CH_2Cl_2 (5 mL) and saturated aq. $NaHCO_3$ (5 mL). The organic phase was collected by passing through a hydrophobic frit then evaporated to yield the product as a yellow gum (74 mg, 20%); R_f 0.50 (CH_2Cl_2:MeOH:NH_4OH, 90:10:1); ν_{max} (neat) 3105 (C-H), 2975 (C-H), 2922 (C-H), 2853 (C-H), 1689 (carbamate C=O), 1644 (ketone C=O); ^{1}H NMR (400 MHz, $CDCl_3$) δ ppm 1.46 (s, 9 H, 9×Boc-*H*), 2.55 (s, 3 H, C(15)H_3), 3.09 - 3.33 (m, 4 H, C(8)H_2+C(12)H_2), 3.47 - 3.68 (m, 4 H, C(9)H_2+C(11)H_2), 6.44 (d, *J*=2.5 Hz, 1 H, C(5)*H*), 6.75 (dd, *J*=8.0, 2.5 Hz, 1 H, C(3)*H*), 6.93 (d, *J*=7.0 Hz, 1 H, C(23)*H*), 7.36 (dd, *J*=9.0, 7.0 Hz, 1 H, C(22)*H*), 7.50 - 7.81 (m, 4 H, C(17)*H*+C(21)*H*+C(24)*H*+C(25)*H*), 9.79 (d, *J*=8.0 Hz, 1 H, C(2)*H*); ^{13}C NMR (101 MHz, $CDCl_3$) δ ppm 26.7 (s, 1 C, *C*(15)), 28.3 (s, 3 C, 3×Boc-*C*) 43.0 (s, 2 C, *C*(9)+*C*(11)), 47.3 (s, 2 C, *C*(8)+*C*(12)), 80.3 (s, 1 C, Boc-*C*) 96.7 (s, 1 C, *C*(5)), 105.4 (s, 1 C, *C*(16)), 106.8 (s, 1 C, *C*(3)), 111.8 (s, 1 C, *C*(24)), 113.5 (s, 1 C, *C*(23)), 115.2 (s, 1 C, *C*(21)), 121.6 (s, 1 C, *C*(13)), 124.4 (s, 1 C, *C*(17)), 125.6 (s, 1 C, *C*(22)), 130.1 (s, 1 C, *C*(2)), 131.8 (s, 1 C, *C*(18)), 133.0 (s, 1 C, *C*(25)), 138.4 (s, 1 C, *C*(6)), 146.2 (s, 1 C, *C*(20)), 148.1 (s, 1 C, *C*(4)), 154.4 (s, 1 C, *C*(26)), 185.6 (s, 1 C, *C*(14)); LRMS *m/z* (ESI$^+$) 460 [MH$^+$]; HRMS (ESI$^+$) found 460.2358, calculated for $C_{26}H_{30}N_5O_3^+$ 460.2343; HPLC (System E) t_r 4.4 min (92%).

tert-Butyl 4-[3-acetyl-1-(pyridin-2-yl)indolizin-7-yl]piperazine-1-carboxylate (442)

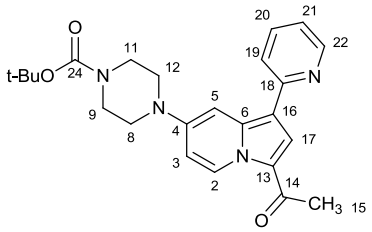

A suspension of K_2CO_3 (40 mg, 0.29 mmol) was added to a solution of compound **440** (93 mg, 0.26 mmol) in DMF (2 mL). The resultant suspension was stirred at room temperature for 10 minutes then 2-ethynylpyridine (29 µL, 0.29 mmol) was added. The mixture was then heated at 90 °C for 2 h then allowed to cool. The mixture was then partitioned between water (5 mL) and CH_2Cl_2 (5 mL). The organic phase was collected by passing it through a hydrophobic frit then evaporated. The crude material was purified by flash column chromatography on a silica column (4 g). The column was eluted with a gradient of EtOAc:*c*-hexane + 0.1% NEt_3 which was increased linearly from 10:90 to 50:50 over 20 CVs. The desired fractions were combined and evaporated to yield the product as a yellow resin (23 mg, 21%); R_f 0.25 (EtOAc:*c*-hexane, 60:40 + 1% NEt_3); ν_{max} (neat) 3107 (C-H), 3049 (C-H), 2979 (C-H), 2923 (C-H), 2822 (C-H), 1696 (carbamate C=O), 1639 (ketone C=O); ^{1}H NMR (400 MHz, $CDCl_3$) δ ppm 1.49 (s, 9 H, 9×Boc-*H*), 2.55 (s, 3 H, C(15)H_3), 3.30 - 3.47 (m, 4 H, C(8)H_2+C(12)H_2), 3.50 - 3.68 (m, 4 H, C(9)H_2+C(11)H_2), 6.69 (dd, *J*=8.0, 2.5 Hz, 1 H, C(3)*H*), 7.07 (ddd, *J*=7.5, 5.0, 1.0 Hz, 1 H, C(21)*H*), 7.57 - 7.65 (m, 1 H, C(19)*H*), 7.65 - 7.73 (m, 1 H, C(20)*H*), 7.81 (s, 1 H, C(17)*H*), 8.04 (d, *J*=2.5 Hz, 1 H, C(5)*H*), 8.57 - 8.67 (m, 1 H, C(22)*H*), 9.76 (d, *J*=8.0 Hz, 1 H, C(2)*H*); ^{13}C NMR (101 MHz, $CDCl_3$) δ ppm 26.7 (s, 1 C, *C*(15)), 28.4 (s, 3 C, 3×Boc-*C*) 42.7 (s, 2 C, *C*(9)+*C*(11)), 47.5 (s, 2 C, *C*(8)+*C*(12)), 80.1 (s, 1 C, Boc-*C*) 100.0 (s, 1 C, *C*(5)), 106.6 (s, 1 C, *C*(3)), 112.2 (s, 1 C, *C*(16)), 119.6 (s, 1 C, *C*(19/21)), 119.9 (s, 1 C, *C*(19/21)), 121.3 (s, 1 C, *C*(13)), 123.5 (s, 1 C, *C*(17)), 129.7 (s, 1 C, *C*(2)), 136.3 (s, 1 C, *C*(20)), 139.2 (s, 1 C, *C*(6)), 148.5 (s, 1 C, *C*(4)), 149.0 (s, 1 C, *C*(22)), 154.6 (s, 1 C, *C*(22/24)), 154.7 (s, 1 C, *C*(22/24)), 185.1 (s, 1 C, *C*(14)); LRMS *m/z* (ESI$^+$) 443 ([M+Na]$^+$), 421 [MH$^+$];

HRMS (ESI$^+$) found 421.2238, calculated for $C_{24}H_{29}N_4O_3^+$ 421.2234; HPLC (System D) t_r 11.7 min (89%).

1-[1-(Imidazo[1,2-*a*]pyridin-5-yl)-7-(piperazin-1-yl)indolizin-3-yl]ethanone dihydrochloride (435)

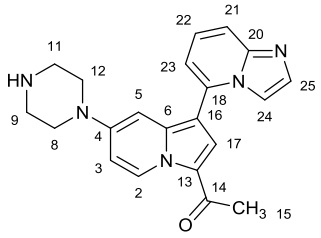

4 M HCl in dioxane (2 mL, 8 mmol) was added to a stirred suspension of compound **441** (70 mg, 0.15 mmol) in dioxane (2 mL) and MeOH (0.5 mL). The suspension was stirred at room temperature for 1 h then evaporated to yield the product as a dark green solid (66 mg, quant.); mp 320 °C (dec); ν_{max} (neat) 3473 (N-H), 3383 (N-H), 2914 (C-H), 2833 (C-H), 2757 (C-H), 2635 (C-H), 1648 (C=O); ^{1}H NMR (500 MHz, CD_3OD) δ ppm 2.49 (s, 3 H, C(15)H_3), 3.24 - 3.31 (m, 4 H, C(9)H_2+C(11)H_2), 3.50 - 3.58 (m, 4 H, C(8)H_2+C(12)H_2), 6.77 (d, *J*=2.5 Hz, 1 H, C(5)*H*), 7.01 (dd, *J*=8.0, 2.5 Hz, 1 H, C(3)*H*), 7.53 (dd, *J*=7.5, 0.5 Hz, 1 H, C(23)*H*), 7.81 (d, *J*=9.0 Hz, 1 H, C(21)*H*), 7.95 - 7.99 (m, 2 H, C(22)*H*+C(25)*H*), 7.99 (s, 1 H, C(17)*H*), 8.03 (d, *J*=1.5 Hz, 1 H, C(24)*H*), 9.68 (d, *J*=8.0 Hz, 1 H, C(2)*H*); ^{13}C NMR (126 MHz, CD_3OD) δ ppm 26.9 (s, 1 C, *C*(15)), 44.3 (s, 2 C, *C*(9)+*C*(11)), 45.7 (s, 2 C, *C*(8)+*C*(12)), 98.3 (s, 1 C, *C*(5)), 104.6 (s, 1 C, *C*(16)), 108.6 (s, 1 C, *C*(3)), 110.7 (s, 1 C, *C*(21)), 115.5 (s, 1 C, *C*(24)), 119.2 (s, 1 C, *C*(23)), 123.7 (s, 1 C, *C*(25)), 123.7 (s, 1 C, *C*(13)), 127.2 (s, 1 C, *C*(17)), 131.5 (s, 1 C, *C*(2)), 135.3 (s, 1 C, *C*(22)), 137.2 (s, 1 C, *C*(18/20)), 140.7 (s, 1 C, *C*(6)), 142.7 (s, 1 C, *C*(18/20)), 149.8 (s, 1 C, *C*(4)), 188.4 (s, 1 C, *C*(14)); LRMS *m/z* (ESI$^+$) 360 [MH$^+$]; HRMS (ESI$^+$) found 360.1814, calculated for $C_{21}H_{22}N_5O^+$ 360.1819; HPLC (System E) t_r 2.7 min (95%).

1-[7-(Piperazin-1-yl)-1-(pyridin-2-yl)indolizin-3-yl]ethanone dihydrochloride (443)

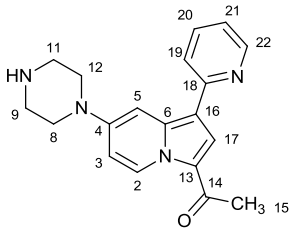

4 M HCl in dioxane (1 mL, 4 mmol) was added to a stirred suspension of compound **442** (35 mg, 0.083 mmol) in dioxane (1 mL). The suspension was stirred at room temperature for 16 h then evaporated to yield the product as a yellow solid (33 mg, quant.); mp 210 °C (dec) ν_{max} (neat) 3356 (N-H), 2805 (C-H), 1644 (C=O); ^{1}H NMR (500 MHz, CD_3OD) δ ppm 2.62 (s, 3 H, C(15)H_3), 3.35 - 3.55 (m, 4 H, C(9)H_2+C(11)H_2), 3.77 - 3.90 (m, 4 H, C(8)H_2+C(12)H_2), 7.17 (d, *J*=8.0 Hz, 1 H, C(3)*H*), 7.39 (s, 1 H, C(5)*H*), 7.72 – 7.87 (m, 1 H, C(21)*H*), 8.28 (s, 1 H, C(17)*H*), 8.39 (d, *J*=8.0 Hz, 1 H, C(19)*H*), 8.48 - 8.60 (m, 1 H, C(20)*H*), 8.66 (d, *J*=5.5 Hz, 1 H, C(22)*H*), 9.78 (d, *J*=8.0 Hz, 1 H, C(2)*H*); ^{13}C NMR (126 MHz, CD_3OD) δ ppm 26.9 (s, 1 C, *C*(15)), 44.4 (s, 2 C, *C*(9)+*C*(11)), 45.4 (s, 2 C, *C*(8)+*C*(12)), 97.8 (s, 1 C, *C*(5)), 104.6 (s, 1 C, *C*(16)), 108.4 (s, 1 C, *C*(3)), 123.0 (s, 1 C, *C*(21)), 124.8 (s, 1 C, *C*(13)), 126.4 (s, 1 C, *C*(19)), 126.9 (s, 1 C, *C*(17)), 131.9 (s, 1 C, *C*(2)), 140.8 (s, 1 C, *C*(6)), 141.9 (s, 1 C, *C*(22)), 147.3 (s, 1 C, *C*(20)), 149.5 (s, 1 C, *C*(4)), 150.9 (s, 1 C, *C*(18)), 188.7 (s, 1 C, *C*(14)); LRMS *m/z* (ESI$^+$) 321 [MH$^+$]; HRMS (ESI$^+$) found 321.1700, calculated for $C_{19}H_{21}N_4O^+$ 321.1710; HPLC (System D) t_r 7.5 min (99%).

4-(Morpholin-4-yl)-1-(2-oxobutyl)pyridinium bromide (444)

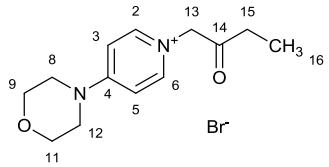

1-Bromo-2-butanone (311 µL, 3.05 mmol) was added to a stirred solution of 4-morpholinopyridine (500 mg, 3.05 mmol) in THF (15 mL). The resultant mixture was left to

stir for 1 h at room temperature then the solid precipitate was filtered and dried under vacuum to yield the product as a white solid (858 mg, 89%); mp 320-325°C; ν_{max} (neat) 3036 (C-H), 2996 (C-H), 2902 (C-H), 2857 (C-H), 1721 (C=O); ^{1}H NMR (400 MHz, DMSO-d_6) δ ppm 1.00 (t, *J*=7.0 Hz, 3 H, C(16)H_3), 2.59 (q, *J*=7.0 Hz, 2 H, C(15)H_2), 3.59 - 3.80 (m, 8 H+solvent, C(8)H_2+C(9)H_2+C(11)H_2+ C(12)H_2), 5.29 (s, 2 H, C(13)H_2), 7.24 (d, *J*=8.0 Hz, 2 H, C(3)*H*+C(5)*H*), 8.08 (d, *J*=8.0 Hz, 2 H, C(2)*H*+C(6)*H*); ^{13}C NMR (101 MHz, DMSO-d_6) δ ppm 7.3 (s, 1 C, *C*(16)), 32.6 (s, 1 C, *C*(15)), 46.3 (s, 2 C, *C*(8)+*C*(12)), 64.2 (s, 1 C, *C*(13)), 65.8 (s, 2 C, *C*(9)+*C*(11)), 107.8 (s, 2 C, *C*(3)+*C*(5)), 143.9 (s, 2 C, *C*(2)+*C*(6)), 156.0 (s, 1 C, *C*(4)), 204.0 (s, 1 C, *C*(14)); LRMS *m/z* (ESI$^+$) 235 [M$^+$]; HRMS (ESI$^+$) found 235.1443, calculated for $C_{13}H_{19}N_2O_2^+$ 235.1441; HPLC (System E) t_r 2.7 min (90%).

4-(Morpholin-4-yl)-1-(3,3,3-trifluoro-2,2-dihydroxypropyl)pyridinium bromide (445)

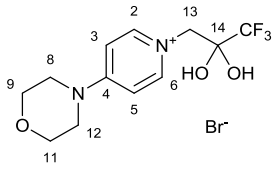

3-Bromo-1,1,1-trifluoroacetone (632 µL, 6.09 mmol) was added to a stirred solution of 4-morpholinopyridine (1.00 g, 6.09 mmol) in THF (15 mL). The resultant mixture was left to stir for 1 h at room temperature then filtered to remove the precipitate. The filtrate was left to stand for 64 h, resulting in further precipitation. The supernatant was decanted off then the solid was suspended in acetone, filtered, and dried under vacuum to yield the product as a cream solid (337 mg, 15%); mp 235-239 °C; ν_{max} (neat) 3213 (O-H), 3055 (C-H); ^{1}H NMR (400 MHz, DMSO-d_6) δ ppm 3.63 - 3.86 (m, 8 H, C(8)H_2+C(9)H_2+C(11)H_2+C(12)H_2), 4.46 (s, 2 H, C(13)H_2), 7.29 (d, *J*=8.0 Hz, 2 H, C(3)*H*+C(5)*H*), 7.72 (s, 2 H, 2×O*H*), 8.21 (d, *J*=8.0 Hz, 2 H, C(2)*H*+C(6)*H*); ^{13}C NMR (101 MHz, DMSO-d_6) δ ppm 46.1 (s, 2 C, *C*(8)+*C*(12)), 58.8 (s, 1 C, *C*(13)), 65.5 (s, 2 C, *C*(9)+*C*(11)), 91.2 (q, *J*=31.0 Hz, 1 C, *C*(14)), 107.2 (s, 2 C, *C*(3)+*C*(5)), 123.2 (q, *J*=285.0 Hz, 1 C, *C*F$_3$) 144.4 (s, 2 C, *C*(2)+*C*(6)), 155.9 (s, 1 C, *C*(4)); ^{19}F NMR (377

MHz, DMSO-d_6) δ ppm -82.40 (s, 3 F); LRMS *m/z* (ESI$^+$) 307 [(M-H_2O+MeOH)$^+$], 293 [M^+]; HRMS (ketone) (ESI$^+$) found 275.1001, calculated for $C_{12}H_{14}F_3N_2O_2^+$ 275.1002; HRMS (MeOH adduct) (ESI$^+$) found 307.1263, calculated for $C_{15}H_{18}F_3N_2O_3^+$ 307.1264; HPLC (System E) t_r 2.5 min (98%).

4-(4-Methylpiperazin-1-yl)-1-(2-oxobutyl)pyridinium bromide (446)

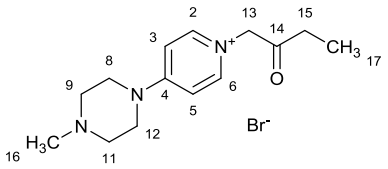

1-Bromo-2-butanone (115 µL, 1.13 mmol) was added drop-wise to a stirred solution of compound **437** (200 mg, 1.13 mmol) in THF (6 mL). The resultant mixture was left to stir at room temperature for 18 h. The resultant suspension was filtered then the solid was washed with THF and dried under vacuum to yield the product as a pale-yellow solid (268 mg, 72%); mp 255-259 °C; ν_{max} (neat) 3038 (C-H), 2977 (C-H), 2940 (C-H), 2909 (C-H), 2954 (C-H), 2790 (C-H), 2745 (C-H), 1725 (C=O); ^{1}H NMR (400 MHz, DMSO-d_6) δ ppm 1.02 (t, *J*=7.5 Hz, 3 H, C(17)H_3), 2.24 (s, 3 H, C(16)H_3), 2.41 - 2.50 (m, 4 H, C(9)H_2+C(11)H_2), 2.59 (q, *J*=7.5 Hz, 2 H, C(15)H_2), 3.61 - 3.78 (m, 4 H, C(8)H_2+C(12)H_2), 5.32 (s, 2 H, C(13)H_2), 7.31 (d, *J*=8.0 Hz, 2 H, C(3)*H*+C(5)*H*), 8.12 (d, *J*=8.0 Hz, 2 H, C(2)*H*+C(6)*H*); ^{13}C NMR (101 MHz, DMSO-d_6) δ ppm 7.0 (s, 1 C, *C*(17)), 32.3 (s, 1 C, *C*(15)), 45.3 (s, 1 C, *C*(16)), 45.9 (s, 2 C, *C*(8)+*C*(12)), 53.9 (s, 2 C, *C*(9)+*C*(11)), 63.8 (s, 1 C, *C*(13)), 107.6 (s, 2 C, *C*(3)+*C*(5)), 143.6 (s, 2 C, *C*(2)+*C*(6)), 155.4 (s, 1 C, *C*(4)), 203.6 (s, 1 C, *C*(14)); LRMS *m/z* (ESI$^+$) 248 [M^+]; HRMS (ESI$^+$) found 248.1756, calculated for $C_{14}H_{22}N_3O^+$ 248.1757; HPLC (System E) t_r 0.8 min (>99%).

1-(3-Methyl-2-oxobutyl)-4-(4-methylpiperazin-1-yl)pyridinium bromide (447)

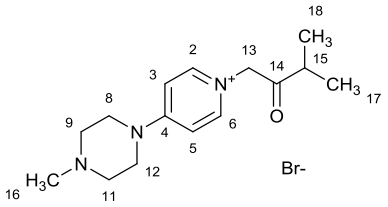

1-Bromo-3-methyl-2-butanone (489 mg, 2.96 mmol) was added drop-wise to a stirred solution of compound **437** (500 mg, 2.82 mmol) in THF (15 mL). The resultant mixture was left to stir at room temperature for 4 h. The resultant suspension was filtered then the solid was washed with acetone and dried under vacuum to yield the product as a pale-yellow solid (672 mg, 70%); mp 198-201°C; ν_{max} (neat) 3034 (C-H), 2936 (C-H), 2797 (C-H), 1721 (C=O); ^{1}H NMR (400 MHz, DMSO-d_6) δ ppm 1.13 (d, *J*=7.0 Hz, 6 H, C(17)H_3+C(18)H_3), 2.26 (s, 3 H, C(16)H_3), 2.43 - 2.52 (m, 4 H, C(9)H_2+C(11)H_2), 2.80 (spt, *J*=7.0 Hz, 1 H, C(15)*H*), 3.69 - 3.79 (m, 4 H, C(8)H_2+C(12)H_2), 5.48 (s, 2 H, C(13)H_2), 7.32 (d, *J*=8.0 Hz, 2 H, C(3)*H*+C(5)*H*), 8.17 (d, *J*=8.0 Hz, 2 H, C(2)*H*+C(6)*H*); ^{13}C NMR (101 MHz, DMSO-d_6) δ ppm 17.6 (s, 2 C, *C*(17)+*C*(18)), 37.7 (s, 1 C, *C*(15)), 45.1 (s, 1 C, *C*(16)), 45.8 (s, 2 C, *C*(8)+*C*(12)), 53.8 (s, 2 C, *C*(9)+*C*(11)), 62.7 (s, 1 C, *C*(13)), 107.7 (s, 2 C, *C*(3)+*C*(5)), 143.6 (s, 2 C, *C*(2)+*C*(6)), 155.4 (s, 1 C, *C*(4)), 206.6 (s, 1 C, *C*(14)); LRMS *m/z* (ESI$^+$) 262 [M$^+$]; HRMS (ESI$^+$) found 262.1918, calculated for $C_{15}H_{24}N_3O^+$ 262.1914; HPLC (System D) t_r 2.2 min (83%).

1-(2-Cyclopropyl-2-oxoethyl)-4-(4-methylpiperazin-1-yl)pyridinium bromide (448)

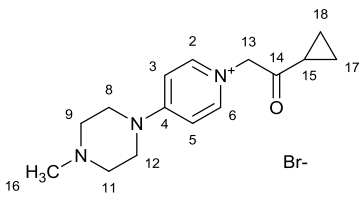

2-Bromo-1-cyclopropylethanone (483 mg, 2.96 mmol) was added drop-wise to a stirred solution of compound **437** (500 mg, 2.82 mmol) in THF (15 mL). The resultant mixture was left to stir at room temperature for 4 h. The resultant suspension was filtered then the solid

was washed with acetone and dried under vacuum to yield the product as an off-white solid (427 mg, 44%); mp 233-237 °C; ν_{max} (neat) 3034 (C-H), 2936 (C-H), 2903 (C-H), 2793 (C-H), 1707 (C=O); ^{1}H NMR (400 MHz, DMSO-d_6) δ ppm 0.95 - 1.12 (m, 4 H, C(17)H_2+C(18)H_2), 2.14 - 2.23 (m, 1 H, C(15)*H*), 2.26 (s, 3 H, C(16)H_3), 2.44 - 2.50 (m, 4 H, C(9)H_2+C(11)H_2), 3.69 - 3.76 (m, 4 H, C(8)H_2+C(12)H_2), 5.51 (s, 2 H, C(13)H_2), 7.30 (d, *J*=8.0 Hz, 2 H, C(3)*H*+C(5)*H*), 8.16 (d, *J*=8.0 Hz, 2 H, C(2)*H*+C(6)*H*); ^{13}C NMR (101 MHz, DMSO-d_6) δ ppm 11.2 (s, 2 C, *C*(17)+*C*(18)), 18.3 (s, 1 C, *C*(15)), 45.1 (s, 1 C, *C*(16)), 45.8 (s, 2 C, *C*(8)+*C*(12)), 53.8 (s, 2 C, *C*(9)+*C*(11)), 64.2 (s, 1 C, *C*(13)), 107.6 (s, 2 C, *C*(3)+*C*(5)), 143.6 (s, 2 C, *C*(2)+*C*(6)), 155.4 (s, 1 C, *C*(4)), 202.9 (s, 1 C, *C*(14)); LRMS *m/z* (ESI$^+$) 260 [M$^+$]; HRMS (ESI$^+$) found 260.1761, calculated for $C_{15}H_{22}N_3O^+$ 260.1757; HPLC (System D) t_r 2.3 min (73%).

Ethyl 2-chloro-3-oxoheptanoate (459)[324, 325]

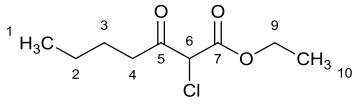

SO_2Cl_2 (426 µL, 5.25 mmol) was added drop-wise to a stirred solution of ethyl 3-oxoheptanoate (800 µL, 5.00 mmol) in CH_2Cl_2 (4 mL). The resultant solution was left to stir at room temperature for 1 h then added to water (5 mL). The phases were separated then the organic phase was washed with water (5 mL) and brine (5 mL) then dried by passing it through a hydrophobic frit. The dried solution was evaporated to yield the product as a colourless oil (1.01 g, 98%); R_f 0.50 (EtOAc:*c*-hexane, 20:80); ν_{max} (neat) 2962 (C-H), 2937 (C-H), 2875 (C-H), 1729 (C=O); ^{1}H NMR (400 MHz, $CDCl_3$) δ ppm 0.92 (t, *J*=7.5 Hz, 3 H, C(1)H_3), 1.26 - 1.45 (m, 5 H, C(2)H_2+C(10)H_3), 1.62 (quin, *J*=7.5 Hz, 2 H, C(3)H_2), 2.71 (q, *J*=7.5 Hz, 2 H, C(4)H_2), 4.29 (q, *J*=7.0 Hz, 2 H, C(9)H_2), 4.78 (s, 1 H, C(6)*H*); ^{13}C NMR (101 MHz, $CDCl_3$) δ ppm 13.7 (s, 1 C, *C*(1)), 13.9 (s, 1 C, *C*(10)), 22.0 (s, 1 C, *C*(2)), 25.5 (s, 1 C, *C*(3)), 38.6 (s, 1 C, *C*(4)), 60.9 (s, 1 C, *C*(6)), 63.1 (s, 1 C, *C*(9)), 165.1 (s, 1 C, *C*(7)), 199.1 (s, 1 C, *C*(5)); LRMS *m/z* (ESI$^+$) 229 [(M+Na)$^+$] 224 [(M+H_2O)$^+$]; HRMS (ESI$^+$) found 229.0610, calculated for $C_9H_{15}ClNaO_3^+$ 229.0602.

1-Chlorohexan-2-one (460)[326]

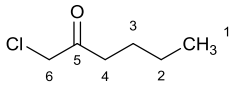

A mixture of compound **459** in H_2O (2.4 g) and H_2SO_4(2.4 g) was heated under reflux for 24 h. The reaction mixture was added onto H_2O (15 mL) then extracted with CH_2Cl_2 (2×15 mL). The combined organic phases were dried over $MgSO_4$ and evaporated to a brown oil (415 mg, 64%); ν_{max} (neat) 2961 (C-H), 2934 (C-H), 2874 (C-H), 1739 (C=O); ^{1}H NMR (400 MHz, $CDCl_3$) δ ppm 0.85 (t, *J*=7.5 Hz, 3 H, C(1)H_3), 1.27 (sxt, *J*=7.5 Hz, 2 H, C(2)H_2), 1.54 (quin, *J*=7.5 Hz, 1 H, C(3)H_2), 2.52 (t, *J*=7.5 Hz, 2 H, C(4)H_2), 4.01 (s, 2 H, C(6)H_2); ^{13}C NMR (101 MHz, $CDCl_3$) δ ppm 14.2 (s, 1 C, *C*(1)), 22.6 (s, 1 C, *C*(2)), 26.1 (s, 1 C, *C*(3)), 39.9 (s, 1 C, *C*(4)), 48.7 (s, 1 C, *C*(6)), 203.2 (s, 1 C, *C*(5)).

4-(4-Methylpiperazin-1-yl)-1-(2-oxohexyl)pyridinium chloride (449)

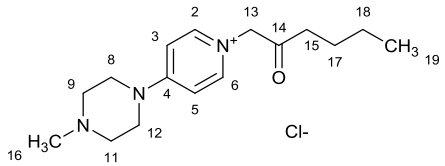

Compound **460** (228 mg, 1.69 mmol) was added drop-wise to a stirred solution of compound **437** (300 mg, 1.69 mmol) in THF (10 mL). The resultant mixture was left to stir at room temperature for 18 h. The resultant suspension was filtered then the filtrate was left to stand for 24 h, resulting in further precipitation. The precipitate was filtered, to yield the product as a beige solid (427 mg, 44%); mp 210-214 °C; ν_{max} (neat) 3036 (C-H), 2948 (C-H), 2869 (C-H), 2810 (C-H), 2778 (C-H), 1727 (C=O); ^{1}H NMR (500 MHz, DMSO-d_6) δ ppm 0.89 (t, *J*=7.5 Hz, 3 H, C(19)H_3), 1.31 (sxt, *J*=7.5 Hz, 2 H, C(18)H_2), 1.52 (quin, *J*=7.5 Hz, 2 H, C(17)H_2), 2.24 (s, 3 H, C(16)H_3), 2.41 - 2.50 (m, 4 H, C(9)H_2+C(11)H_2), 2.57 (t, *J*=7.5 Hz, 2 H, C(15)H_2), 3.66 - 3.76 (m, 4 H, C(8)H_2+C(12)H_2), 5.30 (s, 2 H, C(13)H_2), 7.29 (d, *J*=8.0 Hz, 2 H, C(3)*H*+C(5)*H*), 8.11 (d, *J*=8.0 Hz, 2 H, C(2)*H*+C(6)*H*); ^{13}C NMR (126 MHz, DMSO-d_6) δ ppm

13.8 (s, 1 C, *C*(19)), 21.7 (s, 1 C, *C*(18)), 24.7 (s, 1 C, *C*(17)), 38.6 (s, 1 C, *C*(15)), 45.3 (s, 1 C, *C*(16)), 45.9 (s, 2 C, *C*(8)+*C*(12)), 53.9 (s, 2 C, *C*(9)+*C*(11)), 64.0 (s, 1 C, *C*(13)), 107.6 (s, 2 C, *C*(3)+*C*(5)), 143.6 (s, 2 C, *C*(2)+*C*(6)), 155.4 (s, 1 C, *C*(4)), 203.2 (s, 1 C, *C*(14)); LRMS *m/z* (ESI+) 276 [M+]; HRMS (ESI+) found 276.2063, calculated for $C_{16}H_{26}N_3O^+$ 276.2070; HPLC (System D) t_r 2.4 min (76%).

4-(4-Methylpiperazin-1-yl)-1-(3,3,3-trifluoro-2,2-dihydroxypropyl)pyridinium bromide (450)

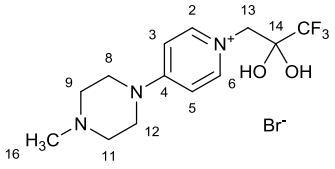

3-Bromo-1,1,1-trifluoroacetone (293 µL, 2.82 mmol) was added to a stirred solution of compound **437** (500 mg, 2.82 mmol) in acetone (15 mL). The resultant mixture was left to stir for 16 h at room temperature then filtered. The solid was washed with acetone then dried under vacuum to yield the product as a beige solid (261 mg, 25%); mp 188-192 °C; ν_{max} (neat) 2986 (C-H), 2963 (C-H), 2868 (C-H); ^{1}H NMR (400 MHz, DMSO-d_6) δ ppm 2.31 (s, 3 H, C(16)H_3), 2.53 - 2.59 (m, 4 H, C(9)H_2+C(11)H_2), 3.72 - 3.79 (m, 4 H, C(8)H_2+C(12)H_2), 4.45 (s, 2 H, C(13)H_2), 7.30 (d, *J*=8.0 Hz, 2 H, C(3)*H*+C(5)*H*), 7.72 (br. s., 2 H, 2×O*H*), 8.19 (d, *J*=8.0 Hz, 2 H, C(2)*H*+C(6)*H*); ^{13}C NMR (101 MHz, DMSO-d_6) δ ppm 44.9 (s, 1 C, *C*(16)), 45.6 (s, 2 C, *C*(8)+*C*(12)), 53.6 (s, 2 C, *C*(9)+*C*(11)), 58.7 (s, 1 C, *C*(13)), 91.2 (q, *J*=31.5 Hz, 1 C, *C*(14)), 107.3 (s, 2 C, *C*(3)+*C*(5)), 123.1 (q, *J*=285.0 Hz, 1 C, *C*F_3) 144.4 (s, 2 C, *C*(2)+*C*(6)), 155.7 (s, 1 C, *C*(14)); ^{19}F NMR (377 MHz, DMSO-d_6) δ ppm -82.42 (s, 3 F); LRMS *m/z* (ESI+) 320 [(M-H_2O+MeOH)+], 306 [M+]; HRMS (ESI+) found 306.1423, calculated for $C_{13}H_{19}F_3N_3O_2^+$ 306.1424; HPLC (System D) t_r 1.5 min (>99%).

1-[1-(Imidazo[1,2-*a*]pyridin-5-yl)-7-(morpholin-4-yl)indolizin-3-yl]propan-1-one (451)

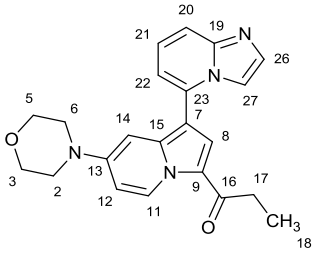

K_2CO_3 (111 mg, 0.80 mmol) was added to a solution of compound **444** (126 mg, 0.40 mmol) in DMF (5 mL). The resultant suspension was stirred at room temperature for 15 minutes then 5-ethynylimidazo[1,2*a*]pyridine (63 mg, 0.44 mmol) was added. The mixture was then heated at 90 °C for 3 h then allowed to cool. The resultant mixture was partitioned between water (5 mL) and EtOAc (5 mL). The phases were separated then the aqueous phase was extracted with more EtOAc (2×5 mL). The combined organic phases were washed with water (2×5mL) and brine (5 mL) then dried over $MgSO_4$ and evaporated. The crude material was pre-adsorbed onto silica then purified by flash column chromatography on a silica column (12 g). The column was eluted with a gradient of CH_2Cl_2:MeOH:NH_4OH which was increased linearly from 99:1:0.1 to 95:5:0.5 over 12 CVs. The desired fractions were combined and evaporated to a beige solid (56 mg). The material thus obtained was purified further by flash column chromatography on a C-18 column (13 g). The column was eluted with a gradient of H_2O:MeCN (+0.1% CF_3CO_2H) which was increased linearly from 95:5 to 5:95 over 20 CVs. The desired fractions were combined and evaporated then partitioned between $CHCl_3$ (5 mL) and saturated aq. $NaHCO_3$ (5 mL). The organic phase was collected by passing through a hydrophobic frit then evaporated to yield the product as a yellow gum (5 mg, 3.3%); R_f 0.55 (CH_2Cl_2:MeOH:NH_4OH, 90:10:1); ν_{max} (neat) 3071 (C-H), 2973 (C-H), 2943 (C-H), 2868 (C-H), 1644 (C=O); ^{1}H NMR (700 MHz, $CDCl_3$) δ ppm 1.30 (t, *J*=7.5 Hz, 3 H, C(18)H_3), 2.91 (q, *J*=7.5 Hz, 2 H, C(17)H_2), 3.12 - 3.23 (m, 4 H, C(2)H_2+C(6)H_2), 3.76 - 3.86 (m, 4 H, C(3)H_2+C(5)H_2), 6.46 (d, *J*=2.5 Hz, 1 H, C(14)*H*), 6.75 (dd, *J*=8.0, 2.5 Hz, 1 H, C(12)*H*),

6.90 (d, *J*=7.0 Hz, 1 H, C(22)*H*), 7.31 (dd, *J*=9.0, 7.0 Hz, 1 H, C(21)*H*), 7.59 (s, 1 H, C(27)*H*), 7.65 - 7.69 (m, 2 H, C(20)*H*+C(26)*H*), 7.72 (s, 1 H, C(8)*H*), 9.84 (d, *J*=8.0 Hz, 1 H, C(11)*H*); ^{13}C NMR (176 MHz, $CDCl_3$) δ ppm 9.7 (s, 1 C, *C*(18)), 32.0 (s, 1 C, *C*(17)), 47.5 (s, 2 C, *C*(2)+*C*(6)), 66.3 (s, 2 C, *C*(3)+*C*(5)), 96.5 (s, 1 C, *C*(14)), 105.7 (s, 1 C, *C*(7)), 106.2 (s, 1 C, *C*(12)), 111.6 (s, 1 C, *C*(27)), 113.1 (s, 1 C, *C*(22)), 115.6 (s, 1 C, *C*(20) 121.1 (s, 1 C, *C*(9)), 123.6 (s, 1 C, *C*(8)), 124.8 (s, 1 C, *C*(21)), 130.1 (s, 1 C, *C*(11)), 132.8 (s, 1 C, *C*(26)), 132.9 (s, 1 C, *C*(23)), 138.3 (s, 1 C, *C*(15)), 146.1 (s, 1 C, *C*(19)), 148.2 (s, 1 C, *C*(13)), 189.4 (s, 1 C, *C*(16)); LRMS *m/z* (ESI^+) 375 [MH^+]; HRMS (ESI^+) found 375.1806, calculated for $C_{22}H_{23}N_4O_2^+$ 375.1816; HPLC (System E) t_r 4.3 min (97%).

2,2,2-Trifluoro-1-[1-(imidazo[1,2-*a*]pyridin-5-yl)-7-(morpholin-4-yl)indolizin-3-yl]ethanone (452)

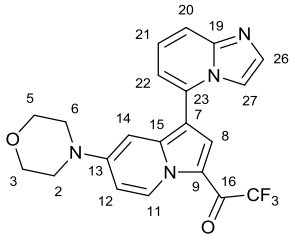

K_2CO_3 (111 mg, 0.80 mmol) was added to a solution of compound **445** (149 mg, 0.40 mmol) in DMF (5 mL). The resultant suspension was stirred at room temperature for 15 minutes then 5-ethynylimidazo[1,2*a*]pyridine (63 mg, 0.44 mmol) was added. The mixture was then heated at 90 °C for 3 h then allowed to cool. The resultant mixture was partitioned between water (5 mL) and EtOAc (5 mL). The phases were separated then the aqueous phase was extracted with more EtOAc (2×5 mL). The combined organic phases were washed with water (2×5mL) and brine (5 mL) then dried over $MgSO_4$ and evaporated. The crude material was purified by flash column chromatography on a silica column (12 g). The column was eluted with a gradient of CH_2Cl_2:MeOH:NH_4OH which was increased linearly from 99:1:0.1 to 95:5:0.5 over 12 CVs. The desired fractions were combined and evaporated to yield the product as a yellow residue (24 mg, 14%); R_f 0.50 (CH_2Cl_2:MeOH:NH_4OH, 90:10:1); ν_{max}

(neat) 2960 (C-H), 2854 (C-H), 1649 (C=O); ^{1}H NMR (400 MHz, $CDCl_3$) δ ppm 3.23 - 3.36 (m, 4 H, C(2)H_2+C(6)H_2), 3.79 - 3.87 (m, 4 H, C(3)H_2+C(5)H_2), 6.51 (d, *J*=2.5 Hz, 1 H, C(14)*H*), 6.87 (dd, *J*=8.0, 2.5 Hz, 1 H, C(12)*H*), 6.91 (dd, *J*=7.0, 1.0 Hz, 1 H, C(22)*H*), 7.30 (dd, *J*=9.0, 7.0 Hz, 1 H, C(21)*H*), 7.49 - 7.55 (m, 1 H, C(27)*H*), 7.66 - 7.72 (m, 2 H, C(20)*H*+C(26)*H*), 7.86 (q, *J*=2.0 Hz, 1 H, C(8)*H*), 9.79 (d, *J*=8.0 Hz, 1 H, C(11)*H*); ^{13}C NMR (176 MHz, $CDCl_3$) δ ppm 46.8 (s, 2 C, *C*(2)+*C*(6)), 66.1 (s, 2 C, *C*(3)+*C*(5)), 96.6 (s, 1 C, *C*(14)), 106.4 (s, 1 C, *C*(12)), 109.7 (s, 1 C, *C*(7)), 111.4 (s, 1 C, *C*(27)), 113.6 (s, 1 C, *C*(22)), 117.8 (q, *J*=289.5 Hz, 1 C, *C*F_3) 116.5 (s, 1 C, *C*(9)), 116.6 (s, 1 C, *C*(20)), 124.4 (s, 1 C, *C*(21)), 126.9 (q, *J*=4.0 Hz, 1 C, *C*(8)), 131.0 (s, 1 C, *C*(11)), 131.4 (s, 1 C, *C*(23)), 133.4 (s, 1 C, *C*(26)), 141.3 (s, 1 C, *C*(15)), 146.1 (s, 1 C, *C*(19)), 150.1 (s, 1 C, *C*(13)), 166.0 (q, *J*=35.0 Hz, 1 C, *C*(16)); ^{19}F NMR (377 MHz, $CDCl_3$) δ ppm -70.22 (s, 3 F); LRMS *m/z* (ESI$^+$) 415 [MH$^+$]; HRMS (ESI$^+$) found 415.1379, calculated for $C_{21}H_{18}F_3N_4O_2$ 415.1376; HPLC (System D) t_r 10.7 min (99%).

1-[1-(Imidazo[1,2-*a*]pyridin-5-yl)-7-(4-methylpiperazin-1-yl)indolizin-3-yl]propan-1-one (453)

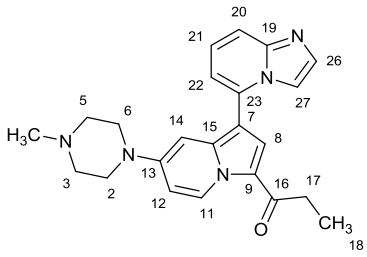

K_2CO_3 (111 mg, 0.80 mmol) was added to a solution of compound **446** (131 mg, 0.40 mmol) in DMF (5 mL). The resultant suspension was stirred at room temperature for 15 minutes then 5-ethynylimidazo[1,2*a*]pyridine (63 mg, 0.44 mmol) was added. The mixture was then heated at 90 °C for 3 h then allowed to cool and stirred at room temperature for 16 h. The resultant mixture was partitioned between water (5 mL) and EtOAc (5 mL). The phases were separated then the aqueous phase was extracted with more EtOAc (2×5 mL). The combined organic phases were washed with water (2×5mL) and brine (5 mL) then dried over $MgSO_4$ and evaporated. The crude material was purified by flash column

chromatography on a silica column (12 g). The column was eluted with a gradient of CH_2Cl_2:MeOH:NH_4OH which was increased linearly from 99:1:0.1 to 90:10:1 over 20 CVs. The desired fractions were combined and evaporated to a brown/orange gum (28 mg). The material thus obtained was purified further by flash column chromatography on a silica column (12 g). The column was eluted with a gradient of CH_2Cl_2:MeOH:NH_4OH which was increased linearly from 96:4:0.4 to 93:7:0.7 over 12 CVs. The desired fractions were combined and evaporated then the material thus obtained was purified once more by column chromatography silica column (4 g). The column was eluted isocratically with EtOAc:MeOH:NEt_3 (90:10:1). The desired fractions were combined and evaporated to yield the product as a pale-orange solid (15 mg, 10%); R_f 0.25 (CH_2Cl_2:MeOH:NH_4OH, 90:10:1); ν_{max} (neat) 2977 (C-H), 2941 (C-H), 2807 (C-H), 1645 (C=O);^{1}H NMR (700 MHz, $CDCl_3$) δ ppm 1.29 (t, *J*=7.5 Hz, 3 H, C(18)H_3), 2.34 (s, 3 H, NCH_3), 2.50 - 2.58 (m, 4 H, C(3)H_2+C(5)H_2), 2.89 (q, *J*=7.5 Hz, 2 H, C(17)H_2), 3.22 - 3.30 (m, 4 H, C(2)H_2+C(6)H_2), 6.44 (d, *J*=2.5 Hz, 1 H, C(14)*H*), 6.75 (dd, *J*=8.0, 2.5 Hz, 1 H, C(12)*H*), 6.87 (d, *J*=7.0 Hz, 1 H, C(22)*H*), 7.28 (dd, *J*=9.0, 7.0 Hz, 1 H+solvent, C(21)*H*), 7.58 (s, 1 H, C(27)*H*), 7.63 (d, *J*=9.0 Hz, 1 H, C(20)*H*), 7.65 (s, 1 H, C(26)*H*), 7.70 (s, 1 H, C(8)*H*), 9.81 (d, *J*=8.0 Hz, 1 H, C(11)*H*); ^{13}C NMR (176 MHz, $CDCl_3$) δ ppm 9.7 (s, 1 C, *C*(18)), 31.9 (s, 1 C, *C*(17)), 46.0 (s, 1 C, N*C*H_3) 47.2 (s, 2 C, *C*(2)+*C*(6)), 54.4 (s, 2 C, *C*(3)+*C*(5)), 96.6 (s, 1 C, *C*(14)), 105.7 (s, 1 C, *C*(7)), 106.4 (s, 1 C, *C*(12)), 111.6 (s, 1 C, *C*(27)), 112.8 (s, 1 C, *C*(22)), 115.6 (s, 1 C, *C*(20)), 121.0 (s, 1 C, *C*(9)), 123.6 (s, 1 C, *C*(8)), 124.5 (s, 1 C, *C*(21)), 130.0 (s, 1 C, *C*(11)), 132.9 (s, 1 C, *C*(23)), 133.1 (s, 1 C, *C*(26)), 138.4 (s, 1 C, *C*(15)), 146.3 (s, 1 C, *C*(19)), 148.0 (s, 1 C, *C*(13)), 189.2 (s, 1 C, *C*(16)); LRMS *m/z* (ESI^+) 388 [MH^+]; HRMS (ESI^+) found 388.2135, calculated for $C_{23}H_{26}N_5O$ 388.2132; HPLC (System D) t_r 8.2 min (99%).

1-[1-(Imidazo[1,2-*a*]pyridin-5-yl)-7-(4-methylpiperazin-1-yl)indolizin-3-yl]-2-methylpropan-1-one (454)

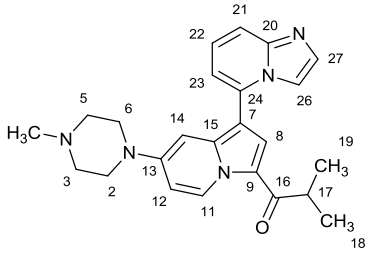

K_2CO_3 (138 mg, 1.00 mmol) was added to a solution of compound **447** (171 mg, 0.50 mmol) in DMF (5 mL). The resultant suspension was stirred at room temperature for 10 minutes then 5-ethynylimidazo[1,2*a*]pyridine (78 mg, 0.55 mmol) was added. The mixture was then heated at 90 °C for 4 h then allowed to cool. The resultant mixture was partitioned between water (10 mL) and $CHCl_3$ (10 mL). The phases were separated then the organic phase was evaporated under a stream of nitrogen. The crude material was purified by flash column chromatography on a silica column (24 g). The column was eluted with a gradient of CH_2Cl_2:MeOH:NH_4OH which was increased linearly from 99:1:0.1 to 95:5:0.5 over 10 CVs. The desired fractions were combined and evaporated to an red gum (54 mg). The material thus obtained was purified further by flash column chromatography on a C-18 column (13 g). The column was eluted with a gradient of H_2O:MeCN (+0.1% CF_3CO_2H) which was increased linearly from 95:5 to 5:95 over 20 CVs. The desired fractions were combined and evaporated then partitioned between $CHCl_3$ (5 mL) and saturated aq. $NaHCO_3$ (5 mL). The organic phase was collected by passing through a hydrophobic frit then evaporated to yield the product as a yellow gum (41 mg, 20%); R_f 0.45 (CH_2Cl_2:MeOH:NH_4OH, 90:10:1); ν_{max} (neat) 2967 (C-H), 2936 (C-H), 2844 (C-H), 2799 (C-H), 1644 (C=O); ^{1}H NMR (400 MHz, $CDCl_3$) δ ppm 1.27 (d, *J*=7.0 Hz, 6 H, C(18)H_3+C(19)H_3), 2.34 (s, 3 H, NCH_3), 2.50 - 2.59 (m, 4 H, C(3)H_2+C(5)H_2), 3.22 - 3.30 (m, 4 H, C(2)H_2+C(6)H_2), 3.40 (spt, *J*=7.0 Hz, 1 H, C(17)*H*), 6.45 (d, *J*=2.5 Hz, 1 H, C(14)*H*), 6.75 (dd, *J*=8.0, 2.5 Hz, 1 H, C(12)*H*), 6.88 (dd, *J*=7.0, 1.0 Hz, 1 H, C(23)*H*), 7.28 (dd, *J*=9.0, 7.0 Hz, 1 H+solvent, C(22)*H*), 7.58 - 7.60 (m, 1 H, C(26)*H*), 7.61 -

7.67 (m, 2 H, C(25)*H*+C(27)*H*), 7.73 (s, 1 H, C(8)*H*), 9.84 (d, *J*=8.0 Hz, 1 H, C(11)*H*); ^{13}C NMR (101 MHz, $CDCl_3$) δ ppm 20.1 (s, 2 C, *C*(18)+*C*(19)), 36.2 (s, 1 C, *C*(17)), 46.0 (s, 1 C, N*C*H_3) 47.2 (s, 2 C, *C*(2)+*C*(6)), 54.4 (s, 2 C, *C*(3)+*C*(5)), 96.6 (s, 1 C, *C*(14)), 105.7 (s, 1 C, *C*(7)), 106.4 (s, 1 C, *C*(12)), 111.6 (s, 1 C, *C*(26)), 112.8 (s, 1 C, *C*(23)), 115.6 (s, 1 C, *C*(21)), 120.3 (s, 1 C, *C*(9)), 123.5 (s, 1 C, *C*(8)), 124.5 (s, 1 C, *C*(22)), 130.2 (s, 1 C, *C*(11)), 132.9 (s, 1 C, *C*(24)), 133.2 (s, 1 C, *C*(27)), 138.7 (s, 1 C, *C*(15)), 146.3 (s, 1 C, *C*(20)), 148.1 (s, 1 C, *C*(13)), 192.9 (s, 1 C, *C*(16)); LRMS *m/z* (ESI^+) 402 [MH^+]; HRMS (ESI^+) found 402.2297, calculated for $C_{24}H_{28}N_5O$ 402.2288; HPLC (System D) t_r 8.5 min (95%).

Cyclopropyl[1-(imidazo[1,2-*a*]pyridin-5-yl)-7-(4-methylpiperazin-1-yl)indolizin-3-yl]methanone (455)

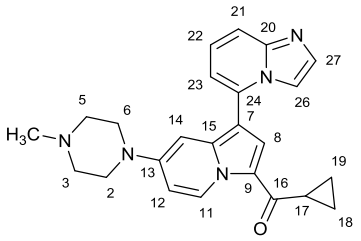

K_2CO_3 (138 mg, 1.00 mmol) was added to a solution of compound **448** (170 mg, 0.50 mmol) in DMF (5 mL). The resultant suspension was stirred at room temperature for 10 minutes then 5-ethynylimidazo[1,2*a*]pyridine (78 mg, 0.55 mmol) was added. The mixture was then heated at 90 °C for 4 h then allowed to cool. The resultant mixture was partitioned between water (10 mL) and $CHCl_3$ (10 mL). The phases were separated then the organic phase was evaporated under a stream of nitrogen. The crude material was purified by flash column chromatography on a silica column (24 g). The column was eluted with a gradient of CH_2Cl_2:MeOH:NH_4OH which was increased linearly from 99:1:0.1 to 95:5:0.5 over 10 CVs. The desired fractions were combined and evaporated to a red gum (52 mg). The material thus obtained was purified further by flash column chromatography on a C-18 column (13 g). The column was eluted with a gradient of H_2O:MeCN (+0.1% CF_3CO_2H) which was increased linearly from 95:5 to 5:95 over 20 CVs. The desired fractions were combined and

evaporated then partitioned between $CHCl_3$ (5 mL) and saturated aq. $NaHCO_3$ (5 mL). The organic phase was collected by passing through a hydrophobic frit then evaporated to yield the product as a red/brown gum (28 mg, 14%); R_f 0.45 (CH_2Cl_2:MeOH:NH_4OH, 90:10:1); ν_{max} (neat) 3088 (C-H), 3004 (C-H), 2941 (C-H), 2844 (C-H), 1642 (C=O); ^{1}H NMR (400 MHz, $CDCl_3$) δ ppm 0.89 - 0.99 (m, 2 H, C(18)H_AH_B+C(19)H_AH_B), 1.18 - 1.26 (m, 2 H, C(18)H_AH_B+C(19)H_AH_B), 2.35 (s, 3 H, NCH_3), 2.45 - 2.58 (m, 5 H, C(3)H_2+C(5)H_2+C(17)*H*), 3.24 - 3.32 (m, 4 H, C(2)H_2+C(6)H_2), 6.46 (d, *J*=2.5 Hz, 1 H, C(14)*H*), 6.73 (dd, *J*=8.0, 2.5 Hz, 1 H, C(12)*H*), 6.90 (dd, *J*=7.0, 1.0 Hz, 1 H, C(23)*H*), 7.30 (dd, *J*=9.0, 7.0 Hz, 1 H+solvent, C(22)*H*), 7.60 - 7.68 (m, 3 H, C(21)*H*+C(26)*H*+C(27)*H*), 7.85 (s, 1 H, C(8)*H*), 9.80 (d, *J*=8.0 Hz, 1 H, C(11)*H*); ^{13}C NMR (101 MHz, $CDCl_3$) δ ppm 9.7 (s, 2 C, *C*(18)+*C*(19)), 17.5 (s, 1 C, *C*(17)), 46.0 (s, 1 C, N*C*H_3) 47.2 (s, 2 C, *C*(2)+*C*(6)), 54.4 (s, 2 C, *C*(3)+*C*(5)), 96.5 (s, 1 C, *C*(14)), 105.9 (s, 1 C, *C*(7)), 106.4 (s, 1 C, *C*(12)), 111.6 (s, 1 C, *C*(21)), 112.9 (s, 1 C, *C*(23)), 115.6 (s, 1 C, *C*(21)), 122.0 (s, 1 C, *C*(9)), 123.7 (s, 1 C, *C*(8)), 124.6 (s, 1 C, *C*(22)), 130.0 (s, 1 C, *C*(11)), 133.0 (s, 1 C, *C*(24)), 133.1 (s, 1 C, *C*(27)), 138.4 (s, 1 C, *C*(15)), 146.3 (s, 1 C, *C*(20)), 147.9 (s, 1 C, *C*(13)), 187.4 (s, 1 C, *C*(16)); LRMS *m/z* (ESI$^+$) 400 [MH$^+$]; HRMS (ESI$^+$) found 400.2129, calculated for $C_{24}H_{26}N_5O$ 400.2132; HPLC (System D) t_r 8.4 min (95%).

1-[1-(Imidazo[1,2-*a*]pyridin-5-yl)-7-(4-methylpiperazin-1-yl)indolizin-3-yl]propan-1-one (456)

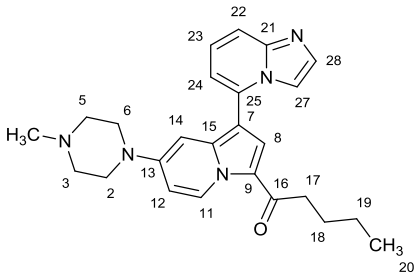

K_2CO_3 (53 mg, 0.38 mmol) was added to a solution of compound **449** (60 mg, 0.19 mmol) in DMF (2 mL). The resultant suspension was stirred at room temperature for 10 minutes then 5-ethynylimidazo[1,2*a*]pyridine (30 mg, 0.21 mmol) was added. The mixture was then

heated at 90 °C for 4 h then allowed to cool. The resultant mixture was partitioned between water (5 mL) and $CHCl_3$ (5 mL). The organic phase was collected by passing it through a hydrophobic frit, then evaporated using a stream of nitrogen. The crude material was purified by flash column chromatography on a silica column (12 g). The column was eluted with a gradient of CH_2Cl_2:MeOH:NH_4OH which was increased linearly from 99:1:0.1 to 95:5:0.5 over 10 CVs, then isocratic at 95:5:0.5 for 5 CVs. The desired fractions were combined and evaporated to an orange gum (15 mg). The material thus obtained was purified further by flash column chromatography on a C-18 column (13 g). The column was eluted with a gradient of H_2O:MeCN (+0.1% CF_3CO_2H) which was increased linearly from 95:5 to 5:95 over 20 CVs. The desired fractions were combined and evaporated then partitioned between $CHCl_3$ (5 mL) and saturated aq. $NaHCO_3$ (5 mL). The organic phase was collected by passing through a hydrophobic frit then evaporated to yield the product as a brown gum (6 mg, 7.6%); R_f 0.45 (CH_2Cl_2:MeOH:NH_4OH, 90:10:1); ν_{max} (neat) 2955 (C-H), 2932 (C-H), 2844 (C-H), 2802 (C-H), 1644 (C=O); ^{1}H NMR (500 MHz, $CDCl_3$) δ ppm 0.97 (t, *J*=7.5 Hz, 3 H, C(20)*H*$_3$), 1.44 (sxt, *J*=7.5 Hz, 2 H, C(19)*H*$_2$), 1.79 (quin, *J*=7.5 Hz, 2 H, C(18)*H*$_2$), 2.37 (s, 3 H, NC*H*$_3$), 2.54 - 2.64 (m, 4 H, C(3)*H*$_2$+C(5)*H*$_2$), 2.86 (t, *J*=7.5 Hz, 2 H, C(17)*H*$_2$), 3.23 - 3.33 (m, 4 H, C(2)*H*$_2$+C(6)*H*$_2$), 6.46 (d, *J*=2.5 Hz, 1 H, C(14)*H*), 6.75 (dd, *J*=8.0, 2.5 Hz, 1 H, C(12)*H*), 6.89 (dd, *J*=7.0, 1.0 Hz, 1 H, C(24)*H*), 7.30 (dd, *J*=9.0, 7.0 Hz, 1 H, C(23)*H*), 7.59 (s, 1 H, C(27)*H*), 7.63 - 7.68 (m, 2 H, C(22)*H*+C(28)*H*), 7.70 (s, 1 H, C(8)*H*), 9.83 (d, *J*=8.0 Hz, 1 H, C(11)*H*); ^{13}C NMR (126 MHz, $CDCl_3$) δ ppm 14.0 (s, 1 C, *C*(20)), 22.7 (s, 1 C, *C*(19)), 28.2 (s, 1 C, *C*(18)), 38.8 (s, 1 C, *C*(17)), 45.9 (s, 1 C, N*C*H$_3$) 47.2 (s, 2 C, *C*(2)+*C*(6)), 54.3 (s, 2 C, *C*(3)+*C*(5)), 96.6 (s, 1 C, *C*(14)), 105.7 (s, 1 C, *C*(7)), 106.5 (s, 1 C, *C*(12)), 111.6 (s, 1 C, *C*(27)), 113.0 (s, 1 C, *C*(24)), 115.6 (s, 1 C, *C*(22)), 121.4 (s, 1 C, *C*(9)), 123.9 (s, 1 C, *C*(8)), 124.7 (s, 1 C, *C*(23)), 130.1 (s, 1 C, *C*(11)), 133.0 (s, 1 C, *C*(25)), 133.0 (s, 1 C, *C*(28)), 138.5 (s, 1 C, *C*(15)), 146.3 (s, 1 C, *C*(21)), 148.0 (s, 1 C, *C*(13)), 188.9 (s, 1 C, *C*(16)); LRMS *m/z* (ESI$^+$) 416 [MH$^+$]; HRMS (ESI$^+$) found 416.2448, calculated for $C_{25}H_{30}N_5O$ 416.2445; HPLC (System D) t_r 9.0 min (92%).

2,2,2-Trifluoro-1-[1-(imidazo[1,2-*a*]pyridin-5-yl)-7-(4-methylpiperazin-1-yl)indolizin-3-yl]ethanone (457)

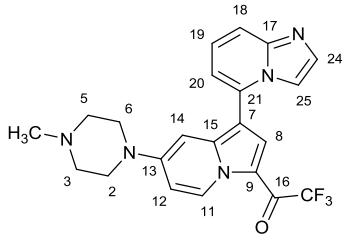

K_2CO_3 (138 mg, 1.00 mmol) was added to a solution of compound **450** (193 mg, 0.50 mmol) in DMF (5 mL). The resultant suspension was stirred at room temperature for 10 minutes then 5-ethynylimidazo[1,2*a*]pyridine (78 mg, 0.55 mmol) was added. The mixture was then heated at 90 °C for 4 h then allowed to cool. The resultant mixture was partitioned between water (10 mL) and $CHCl_3$ (10 mL). The phases were separated then the organic phase was evaporated under a stream of nitrogen. The crude material was purified by flash column chromatography on a silica column (24 g). The column was eluted with a gradient of CH_2Cl_2:MeOH:NH_4OH which was increased linearly from 99:1:0.1 to 95:5:0.5 over 10 CVs. The desired fractions were combined and evaporated to an orange gum (15 mg). The material thus obtained was purified further by flash column chromatography on a C-18 column (13 g). The column was eluted with a gradient of H_2O:MeCN (+0.1% CF_3CO_2H) which was increased linearly from 95:5 to 5:95 over 20 CVs. The desired fractions were combined and evaporated then partitioned between $CHCl_3$ (5 mL) and saturated aq. $NaHCO_3$ (5 mL). The organic phase was collected by passing through a hydrophobic frit then evaporated to yield the product as a red/brown gum (5 mg, 2.3%); R_f 0.45 (CH_2Cl_2:MeOH:NH_4OH, 90:10:1); ν_{max} (neat) 2957 (C-H), 2929 (C-H), 2845 (C-H), 2808 (C-H), 2760 (C-H), 1650 (C=O); ^{1}H NMR (500 MHz, $CDCl_3$) δ ppm 2.35 (s, 3 H, NH_3), 2.51 - 2.57 (m, 4 H, C(3)H_2+C(5)H_2), 3.33 - 3.40 (m, 4 H, C(2)H_2+C(6)H_2), 6.50 (d, *J*=2.5 Hz, 1 H, C(14)*H*), 6.87 (dd, *J*=8.0, 2.5 Hz, 1 H, C(12)*H*), 6.91 (dd, *J*=7.0, 0.5 Hz, 1 H, C(20)*H*), 7.30 (dd, *J*=9.0, 7.0 Hz, 1 H, C(19)*H*), 7.52 (s, 1 H, C(25)*H*), 7.66 - 7.71 (m, 2 H, C(18)*H*+C(24)*H*), 7.83 - 7.87 (m, 1 H, C(8)*H*), 9.78 (d, *J*=8.0

Hz, 1 H, C(11)*H*); ^{13}C NMR (126 MHz, $CDCl_3$) δ ppm 46.0 (s, 1 C, N*C*H_3), 46.7 (s, 2 C, *C*(2)+*C*(6)), 54.2 (s, 2 C, *C*(3)+*C*(5)), 96.6 (s, 1 C, *C*(14)), 106.6 (s, 1 C, *C*(12)), 109.7 (s, 1 C, *C*(7)), 111.5 (s, 1 C, *C*(25)), 113.5 (s, 1 C, *C*(20)), 117.9 (q, *J*=289.5 Hz, 1 C, *C*F_3) 116.5 (s, 1 C, *C*(9)), 116.6 (s, 1 C, *C*(18)), 124.4 (s, 1 C, *C*(19)), 127.0 (q, *J*=3.5 Hz, 1 C, *C*(8)), 131.0 (s, 1 C, *C*(11)), 131.5 (s, 1 C, *C*(21)), 133.5 (s, 1 C, *C*(24)), 141.5 (s, 1 C, *C*(15)), 146.2 (s, 1 C, *C*(17)), 150.0 (s, 1 C, *C*(13)), 165.8 (q, *J*=35 Hz, 1 C, *C*(16)); LRMS *m/z* (ESI^+) 428 [MH^+]; HRMS (ESI^+) found 428.1697, calculated for $C_{22}H_{21}F_3N_5O$ 428.1693; HPLC (System D) t_r 8.7 min (96%).

EXPERIMENTAL – PROTEIN EXPRESSION AND PURIFICATION

cDNAs encoding human BRD4 (NCBI accession numbers NP 055114.1) and human CBP (NCBI accession number 004371.1) were obtained from FivePrime and were used as template to amplify the BRD regions of the proteins. Proteins were cloned, expressed and purified as previously described.[327] Media, trypsin, and antibiotics for tissue culture were purchased from Mediatech. Colonies from freshly transformed plasmid DNA in competent *E. coli* BL21(DE3)-R3-pRARE2 cells (phage-resistant derivative of BL21(DE3) strain), with a pRARE plasmid encoding rare codon tRNAs were grown overnight at 37 °C in 5 ml of Terrific Broth medium (TB-broth, Merck) with 50 μg/ml kanamycin and 34 μg/ml chloramphenicol (start-up culture). The start-up culture was diluted 1:1000 in fresh medium (6×1 L) and cell growth was allowed at 37 °C to an optical density of about 3.0 (OD600) before the temperature was decreased to 18 °C. When the system equilibrated at 18 °C the protein expression was induced over night at 18 °C with 0.1 mM isopropyl-β-D-thiogalactopyranoside (IPTG). The bacteria were harvested by centrifugation (6000 rpm, 20 min, 4 °C, JLA 81,000 rotor, on a Beckman Coulter Avanti J-20 XP centrifuge) and were frozen at -20 °C as pellets for storage. Cells expressing His6-tagged proteins were re-suspended in lysis buffer (50 mM HEPES, pH 7.5 at 25 °C, 500 mM NaCl, 5 mM imidazole, 5% glycerol and 0.5 mM TCEP (Tris(2-carboxyethyl)phosphine hydrochloride)) in the presence of protease inhibitor cocktail (1 μl/ml) and lysed using an EmulsiFlex-C5 high pressure homogenizer (Avestin - Mannheim, Germany) at 4 °C. The lysate was cleared by centrifugation (20,000 rpm for 1 h at 4 °C, JA 25.50 rotor, on a Beckman Coulter Avanti J-20 XP centrifuge) and was applied to 10 g of pre-activated DE52 (diethylaminoethyl cellulose) ion-exchange resin in a gravity column. The resin was eluted with lysis buffer (10 mL) then the eluent was applied to a nickel-nitrilotriacetic acid agarose column (Ni-NTA, Qiagen Ltd., 5 ml, equilibrated with 20 ml lysis buffer). The column was washed once with 10 ml of lysis buffer then twice with 10 ml of lysis buffer containing 30 mM Imidazole. The protein was

eluted using a step elution of Imidazole in lysis buffer (50, 100, 150, 2 x 250 mM imidazole in 50 mM HEPES, pH 7.5 at 25 °C, 500 mM NaCl). All fractions were collected and monitored by SDS-polyacrylamide gel electrophoresis (Bio-Rad Criterion™ Precast Gels, 4-12% Bis-Tris, 1.0 mm, from Bio-Rad, CA.). After the addition of 10 mM dithiothreitol (DTT), the eluted protein was treated overnight at 4 °C with Tobacco Etch Virus (TEV) protease to remove the hexa-histidine tag. The protein was further purified with size exclusion chromatography on a Superdex 75 16/60 HiLoad gel filtration column (GE/Amersham Biosciences) on an ÄktaPrime™ plus system (GE/Amersham Biosciences). Samples were monitored by SDS-polyacrylamide gel electrophoresis. The desired fractions were combined then passed through 1 mL of Ni-NTA 50% resin in a small gravity column. Flow through (FT) was collected then the beads were rinsed with 3 mL of gel filtration buffer. Bound proteins were eluted with 3 mL of elution buffer (50 mM Hepes, 500 mM NaCl, 250 mM imidazole). The flow through was concentrated to 10 mg/ml in the gel filtration buffer, 10 mM Hepes pH 7.5, 150 mM NaCl, 0.5 mM TCEP and were used for crystallisation. Samples for isothermal calorimetry were dialysed over night at 4 °C in a D-Tube™ Dialyser Midi, MWCO 3.5 kDa to a final buffer of 50 mM HEPES, pH 7.4 (at 25 °C), 150 mM NaCl. Protein handling was carried out on ice or in a cold room in all the above steps. Electro-spray Mass Spectrometry (ESI-TOF). Concentrated protein samples were diluted at 1 mg/ml in 0.1% formic acid and 30 µl were injected on an Agilent 1100 Series LC/MSD TOF (Agilent Technologies Inc. - Palo Alto, CA) mass spectrometer with a Zorbax 5 µm 300SB-C3 column (Agilent Technologies Inc. - Palo Alto, CA) in order to ascertain the correct mass of the protein constructs (14.897 kDa for BRD2(1), 15.084 kDa for BRD4(1) and 14.207 kDa for CBP). Raw ion count data were deconvoluted using the software package Proteins (version A.01.00, Agilent Technologies Inc. - Palo Alto, CA), or MAGTRAN49 (version 1.02). The corrected mass and purity was confirmed for all recombinant proteins.

CBP mass purified: 42 mg.

Mass spectrum:

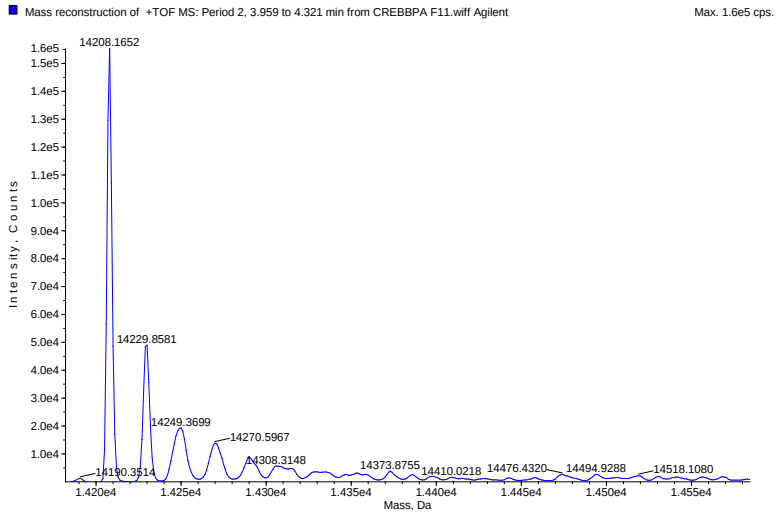

BRD4(1) mass purified = 52 mg.

Mass spectrum:

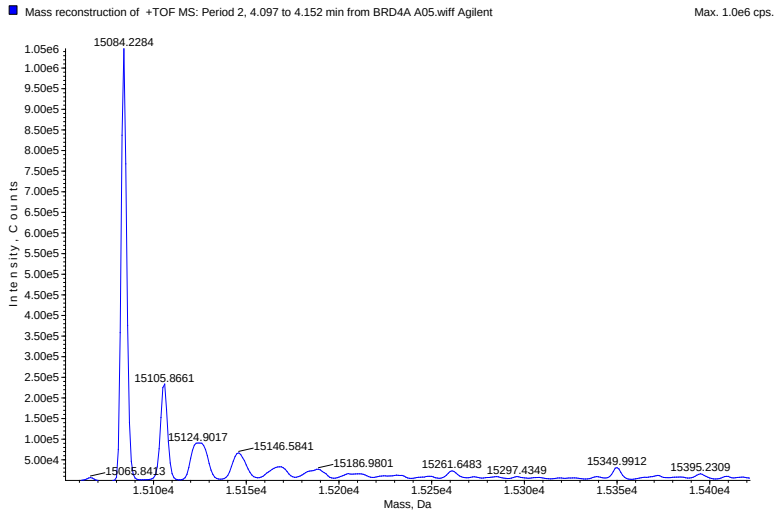

EXPERIMENTAL – ISOTHERMAL TITRATION CALORIMETRY

Experiments were carried out on a VP-ITC titration microcalorimeter from MicroCal™, LLC (Northampton, MA) with a cell volume of 1.4189 ml and a 250 µL microsyringe and equipped with a ThermoVac module. Experiments were carried out at 15 °C while stirring at 295 rpm, in ITC buffer (50 mM HEPES pH 7.4 (at 25 °C), 150 mM NaCl). The microsyringe was loaded with a solution of the protein sample (200-350 µM protein in ITC buffer) and was carefully inserted into the calorimetric cell which was filled with an amount of the ligand (200 µL, 20-30 µM in ITC buffer). The system was first allowed to equilibrate until the cell temperature reached 15 °C and an additional delay of 120 s was applied. All titrations were conducted using an initial control injection of 2 µL followed by 34 identical injections of 8 µl with a duration of 4 sec per injection and a spacing of 250 sec between injections. The titration experiments were designed in such a fashion, as to ensure complete saturation of the enzymes before the final injection. The heat of dilution for the proteins were independent of their concentration and corresponded to the heat observed from the last injection, following saturation of ligand binding, thus facilitating the estimation of the baseline of each titration from the last injection. The collected data were corrected for protein heats of dilution (measured on separate experiments by titrating the proteins into ITC buffer) and deconvoluted using the MicroCal™ Origin software supplied with the instrument to yield enthalpies of binding (ΔH) and binding constants (K_B) in the same fashion to that previously described.[328] Thermodynamic parameters were calculated using the basic equation of thermodynamics ($\Delta G = \Delta H - T\Delta S = -RT\ln K_B$, where ΔG, ΔH and ΔS are the changes in free energy, enthalpy and entropy of binding respectively). In all cases a single binding site model was employed, supplied with the MicroCal™ Origin software package.

EXPERIMENTAL – CRYSTALLISATION TRIALS

Aliquots of the purified proteins were set up for crystallisation using a mosquito® crystallisation robot (TTP Labtech, Royston UK). Coarse screens were typically setup onto Greiner 3-well plates using three different drop ratios of precipitant to protein per condition (100+50 nL, 75+75 nL and 50+100 nL). Initial hits were optimized further scaling up the drop sizes. Crystallisation was carried out using the sitting drop vapor diffusion method at 4 °C. BRD4(1) crystals with compound **308** were grown by mixing 100 nL of the protein (9.0 mg/ml and 5 mM final ligand concentration) with 100 nL of reservoir solution containing 0.20 M NaI, 0.1 M BT-Propane pH 8.5, 20% PEG3350 and 10% ethylene glycol. Diffraction quality crystals grew within a few days.

REFERENCES

1. B. Alberts, A. Johnson, J. Lewis, M. Raff, K. Roberts and P. Walter, *Molecular Biology of the Cell, Fifth Edition*, Taylor & Francis Group, 2007.
2. B. M. Turner, *Chromatin and Gene Regulation: Molecular Mechanisms in Epigenetics*, Wiley, 2008.
3. R. A. Meyers, *Epigenetic Regulation and Epigenomics*, Wiley, 2012.
4. P. B. Talbert and S. Henikoff, *Nat. Rev. Mol. Cell Biol.*, 2010, **11**, 264-275.
5. S. C. R. Elgin and S. I. S. Grewal, *Curr. Biol.*, 2003, **13**, R895-R898.
6. C. P. Ponting, P. L. Oliver and W. Reik, *Cell*, 2009, **136**, 629-641.
7. J. L. Rinn, M. Kertesz, J. K. Wang, S. L. Squazzo, X. Xu, S. A. Brugmann, L. H. Goodnough, J. A. Helms, P. J. Farnham, E. Segal and H. Y. Chang, *Cell*, 2007, **129**, 1311-1323.
8. R. F. Luco, M. Allo, I. E. Schor, A. R. Kornblihtt and T. Misteli, *Cell*, 2011, **144**, 16-26.
9. C. H. Waddington, *Endeavour*, 1942, 18-20.
10. V. E. A. Russo, R. A. Martienssen and A. D. Riggs, *Epigenetic mechanisms of gene regulation*, Cold Spring Harbor Laboratory Press, 1996.
11. A. Bird, *Nature*, 2007, **447**, 396-398.
12. T. C. Roloff and U. A. Nuber, *Eur. J. Cell Biol.*, 2005, **84**, 123-135.
13. S. L. Berger, T. Kouzarides, R. Shiekhattar and A. Shilatifard, *Genes Dev.*, 2009, **23**, 781-783.
14. M. M. Suzuki and A. Bird, *Nat. Rev. Genet.*, 2008, **9**, 465-476.
15. M. Okano, D. W. Bell, D. A. Haber and E. Li, *Cell*, 1999, **99**, 247-257.
16. T. H. Bestor, *Hum. Mol. Genet.*, 2000, **9**, 2395-2402.
17. J. Sharif, M. Muto, S.-i. Takebayashi, I. Suetake, A. Iwamatsu, T. A. Endo, J. Shinga, Y. Mizutani-Koseki, T. Toyoda, K. Okamura, S. Tajima, K. Mitsuya, M. Okano and H. Koseki, *Nature*, 2007, **450**, 908-912.
18. G. V. Avvakumov, J. R. Walker, S. Xue, Y. Li, S. Duan, C. Bronner, C. H. Arrowsmith and S. Dhe-Paganon, *Nature*, 2008, **455**, 822-825.
19. G. Vilkaitis, E. Merkiene˙, S. Serva, E. Weinhold and S. Klimašauskas, *J. Biol. Chem.*, 2001, **276**, 20924-20934.
20. S. Klimasauskas, S. Kumar, R. J. Roberts and X. Cheng, *Cell*, 1994, **76**, 357-369.
21. S. Kagiwada, K. Kurimoto, T. Hirota, M. Yamaji and M. Saitou, *EMBO J.*, 2013, **32**, 340-353.
22. Z. D. Smith and A. Meissner, *EMBO J.*, 2013, **32**, 318-321.
23. Z. Z. Gong and J. K. Zhu, *Cell Res*, 2011, **21**, 1649-1651.
24. Y.-F. He, B.-Z. Li, Z. Li, P. Liu, Y. Wang, Q. Tang, J. Ding, Y. Jia, Z. Chen, L. Li, Y. Sun, X. Li, Q. Dai, C.-X. Song, K. Zhang, C. He and G.-L. Xu, *Science*, 2011, **333**, 1303-1307.
25. W. A. Pastor, L. Aravind and A. Rao, *Nat. Rev. Mol. Cell Biol.*, 2013, **14**, 341-356.
26. M. R. Branco, G. Ficz and W. Reik, *Nat. Rev. Genet.*, 2012, **13**, 7-13.
27. V. K. C. Ponnaluri, J. P. Maciejewski and M. Mukherji, *Biochem. Biophys. Res. Commun.*, 2013, **436**, 115-120.
28. L. Hu, Z. Li, J. Cheng, Q. Rao, W. Gong, M. Liu, Y. G. Shi, J. Zhu, P. Wang and Y. Xu, *Cell*, 2013, **155**, 1545-1555.
29. S. J. Clark and J. Melki, *Oncogene*, 2002, **21**, 5380-5387.
30. S. H. Cross, R. R. Meehan, X. Nan and A. Bird, *Nat. Genet.*, 1997, **16**, 256-259.
31. B. Hendrich and A. Bird, *Mol. Cell. Biol.*, 1998, **18**, 6538-6547.
32. X. Nan, H.-H. Ng, C. A. Johnson, C. D. Laherty, B. M. Turner, R. N. Eisenman and A. Bird, *Nature*, 1998, **393**, 386-389.
33. R. Jaenisch and A. Bird, *Nat. Genet.*, 2003, **33**, 245-254.

34. K. L. Ho, I. W. McNae, L. Schmiedeberg, R. J. Klose, A. P. Bird and M. D. Walkinshaw, *Mol. Cell*, 2008, **29**, 525-531.
35. S. H. Cross and A. P. Bird, *Curr. Opin. Genet. Dev.*, 1995, **5**, 309-314.
36. M. Weber, I. Hellmann, M. B. Stadler, L. Ramos, S. Paabo, M. Rebhan and D. Schubeler, *Nat. Genet.*, 2007, **39**, 457-466.
37. A. K. Maunakea, R. P. Nagarajan, M. Bilenky, T. J. Ballinger, C. D'Souza, S. D. Fouse, B. E. Johnson, C. B. Hong, C. Nielsen, Y. J. Zhao, G. Turecki, A. Delaney, R. Varhol, N. Thiessen, K. Shchors, V. M. Heine, D. H. Rowitch, X. Y. Xing, C. Fiore, M. Schillebeeckx, S. J. M. Jones, D. Haussler, M. A. Marra, M. Hirst, T. Wang and J. F. Costello, *Nature*, 2010, **466**, 253-U131.
38. M. T. McCabe, J. C. Brandes and P. M. Vertino, *Clin Cancer Res*, 2009, **15**, 3927-3937.
39. E. Li, T. H. Bestor and R. Jaenisch, *Cell*, 1992, **69**, 915-926.
40. T. Mohandas, R. S. Sparkes and L. J. Shapiro, *Science*, 1981, **211**, 393-396.
41. M. Esteller, *Nat. Rev. Genet.*, 2007, **8**, 286-298.
42. J. G. Herman and S. B. Baylin, *N. Engl. J. Med.*, 2003, **349**, 2042-2054.
43. J. G. Herman and S. B. Baylin, *N. Engl. J. Med.*, 2003, **349**, 2042-2054.
44. F. Gaudet, J. G. Hodgson, A. Eden, L. Jackson-Grusby, J. Dausman, J. W. Gray, H. Leonhardt and R. Jaenisch, *Science*, 2003, **300**, 489-492.
45. G. S. Mack, *Nat. Biotechnol.*, 2010, **28**, 1259-1266.
46. E. Kaminskas, A. T. Farrell, Y.-C. Wang, R. Sridhara and R. Pazdur, *The Oncologist*, 2005, **10**, 176-182.
47. H. M. Kantarjian, S. O'Brien, X. Huang, G. Garcia-Manero, F. Ravandi, J. Cortes, J. Shan, J. Davisson, C. E. Bueso-Ramos and J.-P. Issa, *Cancer (Hoboken, NJ, U. S.)*, 2007, **109**, 1133-1137.
48. K. Ghoshal, J. Datta, S. Majumder, S. Bai, H. Kutay, T. Motiwala and S. T. Jacob, *Mol. Cell. Biol.*, 2005, **25**, 4727-4741.
49. C. Flotho, R. Claus, C. Batz, M. Schneider, I. Sandrock, S. Ihde, C. Plass, C. M. Niemeyer and M. Luebbert, *Leukemia*, 2009, **23**, 1019-1028.
50. S. L. Berger, *Nature (London, U. K.)*, 2007, **447**, 407-412.
51. J. A. Latham and S. Y. R. Dent, *Nat. Struct. Mol. Biol.*, 2007, **14**, 1017-1024.
52. J.-S. Lee, E. Smith and A. Shilatifard, *Cell (Cambridge, MA, U. S.)*, 2010, **142**, 682-685.
53. A. J. Ruthenburg, H. Li, D. J. Patel and C. D. Allis, *Nat. Rev. Mol. Cell Biol.*, 2007, **8**, 983-994.
54. S. Messner and M. O. Hottiger, *Trends in Cell Biology*, 2011, **21**, 534-542.
55. T. D. Heightman, *Curr. Chem. Genomics*, 2011, **5**, 62-71.
56. B. M. Turner, *Cell*, 2002, **111**, 285-291.
57. S. L. Berger, *Curr. Opin. Genet. Dev.*, 2002, **12**, 142-148.
58. T. Jenuwein and C. D. Allis, *Science*, 2001, **293**, 1074-1080.
59. K. Helin and D. Dhanak, *Nature*, 2013, **502**, 480-488.
60. A. D. Goldberg, C. D. Allis and E. Bernstein, *Cell*, 2007, **128**, 635-638.
61. C. Martin and Y. Zhang, *Nat. Rev. Mol. Cell Biol.*, 2005, **6**, 838-849.
62. J. C. Black, C. Van Rechem and J. R. Whetstine, *Mol. Cell*, 2012, **48**, 491-507.
63. M. Lachner and T. Jenuwein, *Curr. Opin. Cell Biol.*, 2002, **14**, 286-298.
64. H. Santos-Rosa, R. Schneider, A. J. Bannister, J. Sherriff, B. E. Bernstein, N. C. T. Emre, S. L. Schreiber, J. Mellor and T. Kouzarides, *Nature*, 2002, **419**, 407-411.
65. M. Lachner, N. O'Carroll, S. Rea, K. Mechtler and T. Jenuwein, *Nature*, 2001, **410**, 116-120.
66. A. J. Bannister, P. Zegerman, J. F. Partridge, E. A. Miska, J. O. Thomas, R. C. Allshire and T. Kouzarides, *Nature*, 2001, **410**, 120-124.
67. B. Czermin, R. Melfi, D. McCabe, V. Seitz, A. Imhof and V. Pirrotta, *Cell*, 2002, **111**, 185-196.
68. J. Müller, C. M. Hart, N. J. Francis, M. L. Vargas, A. Sengupta, B. Wild, E. L. Miller, M. B. O'Connor, R. E. Kingston and J. A. Simon, *Cell*, 2002, **111**, 197-208.

69. Y.-i. Tsukada, J. Fang, H. Erdjument-Bromage, M. E. Warren, C. H. Borchers, P. Tempst and Y. Zhang, *Nature*, 2006, **439**, 811-816.
70. Y. Shi, F. Lan, C. Matson, P. Mulligan, J. R. Whetstine, P. A. Cole, R. A. Casero and Y. Shi, *Cell*, 2004, **119**, 941-953.
71. H. Hou and H. Yu, *Curr. Opin. Struct. Biol.*, 2010, **20**, 739-748.
72. J. Wysocka, T. Swigut, H. Xiao, T. A. Milne, S. Y. Kwon, J. Landry, M. Kauer, A. J. Tackett, B. T. Chait, P. Badenhorst, C. Wu and C. D. Allis, *Nature*, 2006, **442**, 86-90.
73. X. Shi, I. Kachirskaia, K. L. Walter, J.-H. A. Kuo, A. Lake, F. Davrazou, S. M. Chan, D. G. E. Martin, I. M. Fingerman, S. D. Briggs, L. Howe, P. J. Utz, T. G. Kutateladze, A. A. Lugovskoy, M. T. Bedford and O. Gozani, *J. Biol. Chem.*, 2007, **282**, 2450-2455.
74. D. G. E. Martin, K. Baetz, X. Shi, K. L. Walter, V. E. MacDonald, M. J. Wlodarski, O. Gozani, P. Hieter and L. Howe, *Mol. Cell. Biol.*, 2006, **26**, 7871-7879.
75. S. A. Jacobs and S. Khorasanizadeh, *Science*, 2002, **295**, 2080-2083.
76. P. R. Nielsen, D. Nietlispach, H. R. Mott, J. Callaghan, A. Bannister, T. Kouzarides, A. G. Murzin, N. V. Murzina and E. D. Laue, *Nature*, 2002, **416**, 103-107.
77. J. Lee, J. R. Thompson, M. V. Botuyan and G. Mer, *Nat. Struct. Mol. Biol.*, 2008, **15**, 109-111.
78. Y. Huang, J. Fang, M. T. Bedford, Y. Zhang and R. M. Xu, *Science*, 2006, **312**, 748-751.
79. J. Kim, J. Daniel, A. Espejo, A. Lake, M. Krishna, L. Xia, Y. Zhang and M. T. Bedford, *EMBO Rep.*, 2006, **7**, 397-403.
80. C. Grimm, R. Matos, N. Ly-Hartig, U. Steuerwald, D. Lindner, V. Rybin, J. Muller and C. W. Muller, *EMBO J.*, 2009, **28**, 1965-1977.
81. C. Grimm, A. G. de Ayala Alonso, V. Rybin, U. Steuerwald, N. Ly-Hartig, W. Fischle, J. Mueller and C. W. Mueller, *EMBO Rep.*, 2007, **8**, 1031-1037.
82. A. K. Upadhyay and X. D. Cheng, *Prog Drug Res*, 2011, **67**, 107-124.
83. B. Xiao, C. Jing, J. R. Wilson, P. A. Walker, N. Vasisht, G. Kelly, S. Howell, I. A. Taylor, G. M. Blackburn and S. J. Gamblin, *Nature*, 2003, **421**, 652-656.
84. J. Min, Q. Feng, Z. Li, Y. Zhang and R.-M. Xu, *Cell*, 2003, **112**, 711-723.
85. T. Schalch, G. Job, V. J. Noffsinger, S. Shanker, C. Kuscu, L. Joshua-Tor and J. F. Partridge, *Mol. Cell*, 2009, **34**, 36-46.
86. H. Li, W. Fischle, W. Wang, E. M. Duncan, L. Liang, S. Murakami-Ishibe, C. D. Allis and D. J. Patel, *Mol. Cell*, 2007, **28**, 677-691.
87. B. Karasulu, M. Patil and W. Thiel, *J. Am. Chem. Soc.*, 2013, **135**, 13400-13413.
88. F. Chen, H. Yang, Z. Dong, J. Fang, P. Wang, T. Zhu, W. Gong, R. Fang, Y. G. Shi, Z. Li and Y. Xu, *Cell Res*, 2013, **23**, 306-309.
89. L. Kruidenier, C.-w. Chung, Z. Cheng, J. Liddle, K. Che, G. Joberty, M. Bantscheff, C. Bountra, A. Bridges, H. Diallo, D. Eberhard, S. Hutchinson, E. Jones, R. Katso, M. Leveridge, P. K. Mander, J. Mosley, C. Ramirez-Molina, P. Rowland, C. J. Schofield, R. J. Sheppard, J. E. Smith, C. Swales, R. Tanner, P. Thomas, A. Tumber, G. Drewes, U. Oppermann, D. J. Patel, K. Lee and D. M. Wilson, *Nature*, 2012, **488**, 404-408.
90. L. Ringrose and R. Paro, *Annu. Rev. Genet.*, 2004, **38**, 413-443.
91. S. R. Bhaumik, E. Smith and A. Shilatifard, *Nat. Struct. Mol. Biol.*, 2007, **14**, 1008-1016.
92. S. Varambally, S. M. Dhanasekaran, M. Zhou, T. R. Barrette, C. Kumar-Sinha, M. G. Sanda, D. Ghosh, K. J. Pienta, R. G. A. B. Sewalt, A. P. Otte, M. A. Rubin and A. M. Chinnaiyan, *Nature*, 2002, **419**, 624-629.
93. S. K. Knutson, N. M. Warholic, T. J. Wigle, C. R. Klaus, C. J. Allain, A. Raimondi, M. Porter Scott, R. Chesworth, M. P. Moyer, R. A. Copeland, V. M. Richon, R. M. Pollock, K. W. Kuntz and H. Keilhack, *Proceedings of the National Academy of Sciences*, 2013, **110**, 7922-7927.
94. Epizyme Inc, *EZH2 Inhibitor — EPZ-6438 for Genetically Defined Non-Hodgkin Lymphoma and INI1-Deficient Tumors*, http://www.epizyme.com/programs/ezh2-inhibitor, Accessed February 25, 2014.
95. S. R. Daigle, E. J. Olhava, C. A. Therkelsen, A. Basavapathruni, L. Jin, P. A. Boriack-Sjodin, C. J. Allain, C. R. Klaus, A. Raimondi, M. P. Scott, N. J. Waters, R. Chesworth, M.

P. Moyer, R. A. Copeland, V. M. Richon and R. M. Pollock, *Blood*, 2013, **122**, 1017-1025.
96. Epizyme Inc, *DOT1L Inhibitor – EPZ-5676 for Acute Leukemias with Genetic Alterations of MLL*, http://www.epizyme.com/programs/dot1l-inhibitor/, Accessed February 26, 2014.
97. C. Choudhary, C. Kumar, F. Gnad, M. L. Nielsen, M. Rehman, T. C. Walther, J. V. Olsen and M. Mann, *Science*, 2009, **325**, 834-840.
98. S. C. Kim, R. Sprung, Y. Chen, Y. Xu, H. Ball, J. Pei, T. Cheng, Y. Kho, H. Xiao, L. Xiao, N. V. Grishin, M. White, X.-J. Yang and Y. Zhao, *Mol. Cell*, 2006, **23**, 607-618.
99. S. Zhao, W. Xu, W. Jiang, W. Yu, Y. Lin, T. Zhang, J. Yao, L. Zhou, Y. Zeng, H. Li, Y. Li, J. Shi, W. An, S. M. Hancock, F. He, L. Qin, J. Chin, P. Yang, X. Chen, Q. Lei, Y. Xiong and K.-L. Guan, *Science*, 2010, **327**, 1000-1004.
100. B. M. Turner, *BioEssays*, 2000, **22**, 836-845.
101. M. D. Shahbazian and M. Grunstein, *Annu. Rev. Biochem.*, 2007, **76**, 75-100.
102. P. Close, C. Creppe, M. Gillard, A. Ladang, J.-P. Chapelle, L. Nguyen and A. Chariot, *Cell. Mol. Life Sci.*, 2010, **67**, 1255-1264.
103. L. Hong, G. P. Schroth, H. R. Matthews, P. Yau and E. M. Bradbury, *J. Biol. Chem.*, 1993, **268**, 305-314.
104. P. Filippakopoulos and S. Knapp, *FEBS Lett.*, 2012, **586**, 2692-2704.
105. R. Sanchez and M.-M. Zhou, *Curr. Opin. Drug Discovery Dev.*, 2009, **12**, 659-665.
106. S. Mujtaba, L. Zeng and M. M. Zhou, *Oncogene*, 2007, **26**, 5521-5527.
107. R. Marmorstein and S. L. Berger, *Gene*, 2001, **272**, 1-9.
108. D. E. Sterner and S. L. Berger, *Microbiol. Mol. Biol. Rev.*, 2000, **64**, 435-459.
109. T. Kouzarides, *EMBO J.*, 2000, **19**, 1176-1179.
110. K. Struhl, *Genes Dev.*, 1998, **12**, 599-606.
111. M. Grunstein, *Nature*, 1997, **389**, 349-352.
112. V. Di Cerbo and R. Schneider, *Briefings in Functional Genomics*, 2013, **12**, 231-243.
113. J. R. Rojas, R. C. Trievel, J. Zhou, Y. Mo, X. Li, S. L. Berger, C. D. Allis and R. Marmorstein, *Nature*, 1999, **401**, 93-98.
114. A. J. M. de Ruijter, A. H. van Gennip, H. N. Caron, S. Kemp and A. B. P. van Kuilenburg, *Biochem. J.*, 2003, **370**, 737-749.
115. S. G. Gray and T. J. Ekstrom, *Exp. Cell Res.*, 2001, **262**, 75-83.
116. G. Blander and L. Guarente, *Annu. Rev. Biochem.*, 2004, **73**, 417-435.
117. P. M. Lombardi, K. E. Cole, D. P. Dowling and D. W. Christianson, *Curr. Opin. Struct. Biol.*, 2011, **21**, 735-743.
118. T. K. Nielsen, C. Hildmann, A. Dickmanns, A. Schwienhorst and R. Ficner, *J. Mol. Biol.*, 2005, **354**, 107-120.
119. B. J. North, B. L. Marshall, M. T. Borra, J. M. Denu and E. Verdin, *Mol. Cell*, 2003, **11**, 437-444.
120. Z. Liang, T. Shi, S. Ouyang, H. Li, K. Yu, W. Zhu, C. Luo and H. Jiang, *J. Phys. Chem. B*, 2010, **114**, 11927-11933.
121. K. H. Zhao, X. M. Chai and R. Marmorstein, *Structure*, 2003, **11**, 1403-1411.
122. P. Filippakopoulos, S. Picaud, M. Mangos, T. Keates, J.-P. Lambert, D. Barsyte-Lovejoy, I. Felletar, R. Volkmer, S. Müller, T. Pawson, A.-C. Gingras, Cheryl H. Arrowsmith and S. Knapp, *Cell*, 2012, **149**, 214-231.
123. SGC, http://www.thesgc.org/, Accessed February 27, 2014.
124. S. Muller, P. Filippakopoulos and S. Knapp, *Expert Rev. Mol. Med.*, 2011, **13**, e29/21-21).
125. H. S. Mellert and S. B. McMahon, *Trends Biochem. Sci.*, 2009, **34**, 571-578.
126. J. H. Roelfsema and D. J. M. Peters, *Expert Reviews in Molecular Medicine*, 2007, **9**, 1-16.
127. F. Petrif, R. H. Giles, H. G. Dauwerse, J. J. Saris, R. C. M. Hennekam, M. Masuno, N. Tommerup, G.-J. B. van Ommen, R. H. Goodman, D. J. M. Peters and M. H. Breuning, *Nature*, 1995, **376**, 348-351.

128. J. H. Roelfsema, S. J. White, Y. Ariyürek, D. Bartholdi, D. Niedrist, F. Papadia, C. A. Bacino, J. T. den Dunnen, G.-J. B. van Ommen, M. H. Breuning, R. C. Hennekam and D. J. M. Peters, *The American Journal of Human Genetics*, 2005, **76**, 572-580.
129. N. G. Iyer, H. Oezdag and C. Caldas, *Oncogene*, 2004, **23**, 4225-4231.
130. J. M. Alarcon, G. Malleret, K. Touzani, S. Vronskaya, S. Ishii, E. R. Kandel and A. Barco, *Neuron*, 2004, **42**, 947-959.
131. G. A. Blobel, *Blood*, 2000, **95**, 745-755.
132. Y. Oike, N. Takakura, A. Hata, T. Kaname, M. Akizuki, Y. Yamaguchi, H. Yasue, K. Araki, K. Yamamura and T. Suda, *Blood*, 1999, **93**, 2771-2779.
133. Y. Tanaka, I. Naruse, T. Maekawa, H. Masuya, T. Shiroishi and S. Ishii, *Proceedings of the National Academy of Sciences*, 1997, **94**, 10215-10220.
134. Merck Sharp & Dohme Corp, *Zolinza*, http://www.zolinza.com/vorinostat/zolinza/, Accessed February 26, 2014.
135. Celgene, *Istodax*, http://www.istodax.com/dtc/Default.aspx, Accessed February 26, 2014.
136. W. S. Xu, R. B. Parmigiani and P. A. Marks, *Oncogene*, 2007, **26**, 5541-5552.
137. Cancer Research UK, *A trial of azacitidine with or without vorinostat for acute myeloid leukaemia or high risk myelodysplastic syndrome (RAvVA)*, http://www.cancerresearchuk.org/cancer-help/trials/a-trial-azacitidine-with-or-without-vorinostat-for-aml-that-has-come-back-ravva, Accessed February 26, 2014.
138. B. E. L. Lauffer, R. Mintzer, R. Fong, S. Mukund, C. Tam, I. Zilberleyb, B. Flicke, A. Ritscher, G. Fedorowicz, R. Vallero, D. F. Ortwine, J. Gunzner, Z. Modrusan, L. Neumann, C. M. Koth, P. J. Lupardus, J. S. Kaminker, C. E. Heise and P. Steiner, *J. Biol. Chem.*, 2013, **288**, 26926-26943.
139. R. Furumai, A. Matsuyama, N. Kobashi, K. H. Lee, N. Nishiyama, I. Nakajima, A. Tanaka, Y. Komatsu, N. Nishino, M. Yoshida and S. Horinouchi, *Cancer Res.*, 2002, **62**, 4916-4921.
140. K. E. Cole, D. P. Dowling, M. A. Boone, A. J. Phillips and D. W. Christianson, *J. Am. Chem. Soc.*, 2011, **133**, 12474-12477.
141. C. A. French, *Cancer Genetics and Cytogenetics*, 2010, **203**, 16-20.
142. Y. J. Zhao, C. Y. Yang and S. M. Wang, *J. Med. Chem.*, 2013, **56**, 7498-7500.
143. GlaxoSmithKline plc., *Studies filtered by compound GSK525762*, http://www.gsk-clinicalstudyregister.com/compounds/gsk525762+#ps, Accessed February 26, 2014.
144. S. Picaud, C. Wells, I. Felletar, D. Brotherton, S. Martin, P. Savitsky, B. Diez-Dacal, M. Philpott, C. Bountra, H. Lingard, O. Fedorov, S. Muller, P. E. Brennan, S. Knapp and P. Filippakopoulos, *Proc. Natl. Acad. Sci. U. S. A.*, 2013, **110**, 19754-19759,S19754/19751-S19754/19710.
145. D. Bailey, R. Jahagirdar, A. Gordon, A. Hafiane, S. Campbell, S. Chatur, G. S. Wagner, H. C. Hansen, F. S. Chiacchia, J. Johansson, L. Krimbou, N. C. W. Wong and J. Genest, *J. Am. Coll. Cardiol.*, 2010, **55**, 2580-2589.
146. C. W. Chung, H. Coste, J. H. White, O. Mirguet, J. Wilde, R. L. Gosmini, C. Delves, S. M. Magny, R. Woodward, S. A. Hughes, E. V. Boursier, H. Flynn, A. M. Bouillot, P. Bamborough, J. M. G. Brusq, F. J. Gellibert, E. J. Jones, A. M. Riou, P. Homes, S. L. Martin, I. J. Uings, J. Toum, C. A. Clement, A. B. Boullay, R. L. Grimley, F. M. Blande, R. K. Prinjha, K. Lee, J. Kirilovsky and E. Nicodeme, *J. Med. Chem.*, 2011, **54**, 3827-3838.
147. J. Lovén, Heather A. Hoke, Charles Y. Lin, A. Lau, David A. Orlando, Christopher R. Vakoc, James E. Bradner, Tong I. Lee and Richard A. Young, *Cell*, 2013, **153**, 320-334.
148. J. A. Mertz, A. R. Conery, B. M. Bryant, P. Sandy, S. Balasubramanian, D. A. Mele, L. Bergeron and R. J. Sims, III, *Proc. Natl. Acad. Sci. U. S. A.*, 2011, **108**, 16669-16674.
149. Constellation Pharmaceuticals, http://www.constellationpharma.com/2013/09/constellation-pharmaceuticals-initiates-clinical-development-of-cpi-0610-a-novel-bet-protein-bromodomain-inhibitor-in-patients-with-lymphoma/, Accessed 26 February, 2014.

150. Tensha Therapeutics, *Therapeutic Program*, http://www.tenshatherapeutics.com/program-ten-010.php, Accessed February 26, 2014.
151. Oncoethix, *OTC015*, http://www.oncoethix.com/product/otx015, Accessed February 26, 2014.
152. W. A. Weiss, S. S. Taylor and K. M. Shokat, *Nat. Chem. Biol.*, 2007, **3**, 739-744.
153. M. E. Bunnage, E. L. P. Chekler and L. H. Jones, *Nat. Chem. Biol.*, 2013, **9**, 195-199.
154. R. Garcia-Serna and J. Mestres, *Drug Discovery Today*, 2011, **16**, 99-106.
155. S. V. Frye, *Nat. Chem. Biol.*, 2010, **6**, 159-161.
156. A. M. Edwards, C. Bountra, D. J. Kerr and T. M. Willson, *Nat. Chem. Biol.*, 2009, **5**, 436-440.
157. S. Muller and S. Knapp, *MedChemComm*, 2014, **5**, 288-296.
158. R. H. Goodman and S. Smolik, *Genes Dev.*, 2000, **14**, 1553-1577.
159. N. Vo and R. H. Goodman, *J. Biol. Chem.*, 2001, **276**, 13505-13508.
160. E. Kalkhoven, *Biochem. Pharmacol.*, 2004, **68**, 1145-1155.
161. K. J. McManus and M. J. Hendzel, *Biochem. Cell Biol.*, 2001, **79**, 253-266.
162. D. C. Bedford, L. H. Kasper, T. Fukuyama and P. K. Brindle, *Epigenetics*, 2010, **5**, 9-15.
163. J. C. Chrivia, R. P. S. Kwok, N. Lamb, M. Hagiwara, M. R. Montminy and R. H. Goodman, *Nature*, 1993, **365**, 855-859.
164. R. W. Stein, M. Corrigan, P. Yaciuk, J. Whelan and E. Moran, *J. Virol.*, 1990, **64**, 4421-4427.
165. R. Eckner, M. E. Ewen, D. Newsome, M. Gerdes, J. A. DeCaprio, J. B. Lawrence and D. M. Livingston, *Genes Dev.*, 1994, **8**, 869-884.
166. M. Delvecchio, J. Gaucher, C. Aguilar-Gurrieri, E. Ortega and D. Panne, *Nat. Struct. Mol. Biol.*, 2013, **20**, 1040-1046.
167. S. J. Freedman, Z. Y. J. Sun, A. L. Kung, D. S. France, G. Wagner and M. J. Eck, *Nat Struct Biol*, 2003, **10**, 504-512.
168. S. J. Freedman, Z. Y. J. Sun, F. Poy, A. L. Kung, D. M. Livingston, G. Wagner and M. J. Eck, *Proc. Natl. Acad. Sci. U. S. A.*, 2002, **99**, 5367-5372.
169. I. Radhakrishnan, G. C. Pérez-Alvarado, D. Parker, H. J. Dyson, M. R. Montminy and P. E. Wright, *Cell*, 1997, **91**, 741-752.
170. G. B. Legge, M. A. Martinez-Yamout, D. M. Hambly, T. Trinh, B. M. Lee, H. J. Dyson and P. E. Wright, *J. Mol. Biol.*, 2004, **343**, 1081-1093.
171. L. J. Jensen, M. Kuhn, M. Stark, S. Chaffron, C. Creevey, J. Muller, T. Doerks, P. Julien, A. Roth, M. Simonovic, P. Bork and C. von Mering, *Nucleic Acids Res.*, 2009, **37**, D412-D416.
172. Z. Deng, C.-J. Chen, M. Chamberlin, F. Lu, G. A. Blobel, D. Speicher, L. A. Cirillo, K. S. Zaret and P. M. Lieberman, *Mol. Cell. Biol.*, 2003, **23**, 2633-2644.
173. A. Tomita, M. Towatari, S. Tsuzuki, F. Hayakawa, H. Kosugi, K. Tamai, T. Miyazaki, T. Kinoshita and H. Saito, *Oncogene*, 2000, **19**, 444-451.
174. E. T. Manning, T. Ikehara, T. Ito, J. T. Kadonaga and L. Kraus, *Mol. Cell. Biol.*, 2001, **21**, 3876-3887.
175. P. R. Thompson, D. X. Wang, L. Wang, M. Fulco, N. Pediconi, D. Z. Zhang, W. J. An, Q. Y. Ge, R. G. Roeder, J. M. Wong, M. Levrero, V. Sartorelli, R. J. Cotter and P. A. Cole, *Nat. Struct. Mol. Biol.*, 2004, **11**, 308-315.
176. J. C. Black, A. Mosley, T. Kitada, M. Washburn and M. Carey, *Mol. Cell*, 2008, **32**, 449-455.
177. H. M. Chan and T. N. B. La, *J. Cell Sci.*, 2001, **114**, 2363-2373.
178. Z.-Q. Huang, J. Li, L. M. Sachs, P. A. Cole and J. Wong, *EMBO J.*, 2003, **22**, 2146-2155.
179. W. Zhang, S. Kadam, B. M. Emerson and J. J. Bieker, *Mol. Cell. Biol.*, 2001, **21**, 2413-2422.
180. V. V. Ogryzko, R. L. Schiltz, V. Russanova, B. H. Howard and Y. Nakatani, *Cell*, 1996, **87**, 953-959.
181. A. J. Bannister and T. Kouzarides, *Nature*, 1996, **384**, 641-643.

182. S. Spange, T. Wagner, T. Heinzel and O. H. Kraemer, *Int. J. Biochem. Cell Biol.*, 2009, **41**, 185-198.
183. M. A. Glozak, N. Sengupta, X. Zhang and E. Seto, *Gene*, 2005, **363**, 15-23.
184. F. Petrij, R. Giles, H. Dauwerse, J. Saris, R. Hennekam, M. Masuno, N. Tommerup, G. van Ommen, R. Goodman and D. Peters, *Nature*, 1995, **376**, 348 - 351.
185. L. M. Valor, J. Viosca, J. P. Lopez-Atalaya and A. Barco, *Curr. Pharm. Des.*, 2013, **19**, 5051-5064.
186. Y. Oike, N. Takakura, K. I. Yamamura and T. Suda, *Circulation*, 1999, **100**, 404-404.
187. T.-P. Yao, S. P. Oh, M. Fuchs, N.-D. Zhou, L.-E. Ch'ng, D. Newsome, R. T. Bronson, E. Li, D. M. Livingston and R. Eckner, *Cell*, 1998, **93**, 361-372.
188. A. L. Kung, V. I. Rebel, R. T. Bronson, L. E. Ch'ng, C. A. Sieff, D. M. Livingston and T. P. Yao, *Genes Dev.*, 2000, **14**, 272-277.
189. E. Park, Y. Kim, H. Ryu, N. W. Kowall, J. Lee and H. Ryu, *NeuroMol. Med.*, 2014, **16**, 16-24.
190. D. Tsui, A. Voronova, D. Gallagher, D. R. Kaplan, F. D. Miller and J. Wang, *Dev. Biol. (Amsterdam, Neth.)*, 2014, **385**, 230-241.
191. W. X. Guo, E. L. Crossey, L. Zhang, S. Zucca, O. L. George, C. F. Valenzuela and X. Y. Zhao, *PLoS One*, 2011, **6**.
192. E. Korzus, M. G. Rosenfeld and M. Mayford, *Neuron*, 2004, **42**, 961-972.
193. G. Q. Chen, X. Y. Zou, H. Watanabe, J. M. van Deursen and J. Shen, *J. Neurosci.*, 2010, **30**, 13066-13077.
194. L. M. Valor, M. M. Pulopulos, M. Jimenez-Minchan, R. Olivares, B. Lutz and A. Barco, *J. Neurosci.*, 2011, **31**, 1652-1663.
195. R. M. Barrett, M. Malvaez, E. Kramar, D. P. Matheos, A. Arrizon, S. M. Cabrera, G. Lynch, R. W. Greene and M. A. Wood, *Neuropsychopharmacol*, 2011, **36**, 1545-1556.
196. C. A. Saura, S. Y. Choi, V. Beglopoulos, S. Malkani, D. W. Zhang, B. S. S. Rao, S. Chattarji, R. J. Kelleher III, E. R. Kandel, K. Duff, A. Kirkwood and J. Shen, *Neuron*, 2004, **42**, 23-36.
197. Y. I. Francis, A. Stephanou and D. S. Latchman, *Neuroreport*, 2006, **17**, 917-921.
198. Y. I. Francis, J. K. J. Diss, M. Kariti, A. Stephanou and D. S. Latchman, *Neurosci. Lett.*, 2007, **413**, 137-140.
199. E. C. Stack, S. J. Del Signore, R. Luthi-Carter, B. Y. Soh, D. R. Goldstein, S. Matson, S. Goodrich, A. L. Markey, K. Cormier, S. W. Hagerty, K. Smith, H. Ryu and R. J. Ferrante, *Hum. Mol. Genet.*, 2007, **16**, 1164-1175.
200. G. Sadri-Vakili and J. H. J. Cha, *Nat Clin Pract Neuro*, 2006, **2**, 330-338.
201. G. Sadri-Vakili, P. Chawla, K. E. Glajch, R. P. Overland and J. H. J. Cha, *Annals of Neurology*, 2005, **58**, S1-S2.
202. P. O. Bauer and N. Nukina, *J. Neurochem.*, 2009, **110**, 1737-1765.
203. G. Schaffar, P. Breuer, R. Boteva, C. Behrends, N. Tzvetkov, N. Strippel, H. Sakahira, K. Siegers, M. Hayer-Hartl and F. U. Hartl, *Mol. Cell*, 2004, **15**, 95-105.
204. H. J. Jin, A. Kanthasamy, A. Ghosh, Y. J. Yang, V. Anantharam and A. G. Kanthasamy, *J. Neurosci.*, 2011, **31**, 2035-2051.
205. F. J. Dekker and H. J. Haisma, *Drug Discovery Today*, 2009, **14**, 942-948.
206. O. M. Sobulo, J. Borrow, R. Tomek, S. Reshmi, A. Harden, B. Schlegelberger, D. Housman, N. A. Doggett, J. D. Rowley and N. J. Zeleznik-Le, *Proceedings of the National Academy of Sciences*, 1997, **94**, 8732-8737.
207. I. Panagopoulos, T. Fioretos, M. Isaksson, U. Samuelsson, R. Billström, B. Strömbeck, F. Mitelman and B. Johansson, *Hum. Mol. Genet.*, 2001, **10**, 395-404.
208. K. Ida, I. Kitabayashi, T. Taki, M. Taniwaki, K. Noro, M. Yamamoto, M. Ohki and Y. Hayashi, *Blood*, 1997, **90**, 4699-4704.
209. L. H. Kasper, P. K. Brindle, C. A. Schnabel, C. E. Pritchard, M. L. Cleary and J. M. van Deursen, *Mol. Cell. Biol.*, 1999, **19**, 764-776.
210. K. Deguchi, P. M. Ayton, M. Carapeti, J. L. Kutok, C. S. Snyder, I. R. Williams, N. C. P. Cross, C. K. Glass, M. L. Cleary and D. G. Gilliland, *Cancer Cell*, 2003, **3**, 259-271.

211. L. Pasqualucci, D. Dominguez-Sola, A. Chiarenza, G. Fabbri, A. Grunn, V. Trifonov, L. H. Kasper, S. Lerach, H. Y. Tang, J. Ma, D. Rossi, A. Chadburn, V. V. Murty, C. G. Mullighan, G. Gaidano, R. Rabadan, P. K. Brindle and R. Dalla-Favera, *Nature*, 2011, **471**, 189-U175.
212. J. Bouchal, F. R. Santer, P. P. S. Hoschele, E. Tomastikova, H. Neuwirt and Z. Culig, *Prostate*, 2011, **71**, 431-437.
213. R. Ward, M. Johnson, V. Shridhar, J. van Deursen and F. J. Couch, *Journal of Medical Genetics*, 2005, **42**, 514-518.
214. Y. T. Gui, G. W. Guo, Y. Huang, X. D. Hu, A. F. Tang, S. J. Gao, R. H. Wu, C. Chen, X. X. Li, L. Zhou, M. H. He, Z. S. Li, X. J. Sun, W. L. Jia, J. N. Chen, S. M. Yang, F. J. Zhou, X. K. Zhao, S. Q. Wan, R. Ye, C. Z. Liang, Z. S. Liu, P. D. Huang, C. X. Liu, H. Jiang, Y. Wang, H. C. Zheng, L. Sun, X. W. Liu, Z. M. Jiang, D. F. Feng, J. Chen, S. Wu, J. Zou, Z. F. Zhang, R. L. Yang, J. Zhao, C. J. Xu, W. H. Yin, Z. C. Guan, J. X. Ye, H. Zhang, J. X. Li, K. Kristiansen, M. L. Nickerson, D. Theodorescu, Y. R. Li, X. Q. Zhang, S. G. Li, J. Wang, H. M. Yang, J. Wang and Z. M. Cai, *Nat. Genet.*, 2011, **43**, 875-U884.
215. T. Ohshima, T. Suganuma and M.-a. Ikeda, *Biochem. Biophys. Res. Commun.*, 2001, **281**, 569-575.
216. K. Shigeno, H. Yoshida, L. Pan, J. Min Luo, S. Fujisawa, K. Naito, S. Nakamura, K. Shinjo, A. Takeshita, R. Ohno and K. Ohnishi, *Cancer Letters*, 2004, **213**, 11-20.
217. D. A. Santillan, C. M. Theisler, A. S. Ryan, R. Popovic, T. Stuart, M.-M. Zhou, S. Alkan and N. J. Zeleznik-Le, *Cancer Res.*, 2006, **66**, 10032-10039.
218. K. C. Choi, Y. H. Lee, M. G. Jung, S. H. Kwon, M. J. Kim, W. J. Jun, J. Lee, J. M. Lee and H. G. Yoon, *Mol. Cancer Res.*, 2009, **7**, 2011-2021.
219. S. Rajendrasozhan, H. W. Yao and I. Rahman, *Copd*, 2009, **6**, 291-297.
220. W. G. Deng, Y. Zhu and K. K. Wu, *Blood*, 2004, **103**, 2135-2142.
221. X.-Y. Zhu, C.-S. Huang, Q. Li, R.-m. Chang, Z.-b. Song, W.-y. Zou and Q.-L. Guo, *Molecular Pain*, 2012, **8**, 84.
222. D. Boehm, R. J. Conrad and M. Ott, *Viruses*, 2013, **5**, 1571-1586.
223. G. Marzio, M. Tyagi, M. I. Gutierrez and M. Giacca, *Proc. Natl. Acad. Sci. U. S. A.*, 1998, **95**, 13519-13524.
224. A. Cereseto, L. Manganaro, M. I. Gutierrez, M. Terreni, A. Fittipaldi, M. Lusic, A. Marcello and M. Giacca, *EMBO J.*, 2005, **24**, 3070-3081.
225. T. Kino, A. Gragerov, O. Slobodskaya, M. Tsopanomichalou, G. P. Chrousos and G. N. Pavlakis, *J. Virol.*, 2002, **76**, 9724-9734.
226. B. Vogelstein, D. Lane and A. J. Levine, *Nature*, 2000, **408**, 307-310.
227. A. J. Levine, *Cell*, 1997, **88**, 323-331.
228. C. Prives and P. A. Hall, *J Pathol*, 1999, **187**, 112-126.
229. A. S. Coutts and N. B. La Thangue, *Biochem. Biophys. Res. Commun.*, 2005, **331**, 778-785.
230. D. Alarcon-Vargas and Z. Ronai, *Carcinogenesis*, 2002, **23**, 541-547.
231. S. Mujtaba, Y. He, L. Zeng, S. Yan, O. Plotnikova, Sachchidanand, R. Sanchez, N. J. Zeleznik-Le, Z. Ronai and M. M. Zhou, *Mol. Cell*, 2004, **13**, 251-263.
232. A. V. Gudkov and E. A. Komarova, *Biochem. Biophys. Res. Commun.*, 2005, **331**, 726-736.
233. S. K. Nayak, P. S. Panesar and H. Kumar, *Curr. Med. Chem.*, 2009, **16**, 2627-2640.
234. J. D. Li, C. A. Ghiani, J. Y. Kim, A. X. Liu, J. Sandoval, J. DeVellis and P. Casaccia-Bonnefil, *J. Neurosci.*, 2008, **28**, 6118-6127.
235. W. Duan, X. Zhu, B. Ladenheim, Q.-S. Yu, Z. Guo, J. Oyler, R. G. Cutler, J. L. Cadet, N. H. Greig and M. P. Mattson, *Annals of Neurology*, 2002, **52**, 597-606.
236. L.-Z. Hong, X.-Y. Zhao and H.-L. Zhang, *Neurosci. Bull.*, 2010, **26**, 232-240.
237. J. Tashiro, S. Kikuchi, K. Shinpo, R. Kishimoto, S. Tsuji and H. Sasaki, *J. Neurosci. Res.*, 2007, **85**, 395-401.
238. N. Pietrancosta, C. Garino, Y. Laras, G. Quéléver, P. Pierre, G. Clavarino and J.-L. Kraus, *Drug Dev. Res.*, 2005, **65**, 43-49.

239. C. J. Schofield and P. J. Ratcliffe, *Nat. Rev. Mol. Cell Biol.*, 2004, **5**, 343-354.
240. M. Ivan, K. Kondo, H. F. Yang, W. Kim, J. Valiando, M. Ohh, A. Salic, J. M. Asara, W. S. Lane and W. G. Kaelin, *Science*, 2001, **292**, 464-468.
241. P. Jaakkola, D. R. Mole, Y. M. Tian, M. I. Wilson, J. Gielbert, S. J. Gaskell, A. von Kriegsheim, H. F. Hebestreit, M. Mukherji, C. J. Schofield, P. H. Maxwell, C. W. Pugh and P. J. Ratcliffe, *Science*, 2001, **292**, 468-472.
242. S. A. Dames, M. Martinez-Yamout, R. N. De Guzman, H. J. Dyson and P. E. Wright, *Proceedings of the National Academy of Sciences*, 2002, **99**, 5271-5276.
243. K. Balasubramanyam, V. Swaminathan, A. Ranganathan and T. K. Kundu, *J. Biol. Chem.*, 2003, **278**, 19134-19140.
244. K. Balasubramanyam, M. Altaf, R. A. Varier, V. Swaminathan, A. Ravindran, P. P. Sadhale and T. K. Kundu, *J. Biol. Chem.*, 2004, **279**, 33716-33726.
245. K. Mantelingu, B. A. A. Reddy, V. Swaminathan, A. H. Kishore, N. B. Siddappa, G. V. P. Kumar, G. Nagashankar, N. Natesh, S. Roy, P. P. Sadhale, U. Ranga, C. Narayana and T. K. Kundu, *Chem. Biol.*, 2007, **14**, 645-657.
246. V. Sarli and A. Giannis, *Chem. Biol.*, 2007, **14**, 605-606.
247. K. Balasubramanyam, R. A. Varier, M. Altaf, V. Swaminathan, N. B. Siddappa, U. Ranga and T. K. Kundu, *J. Biol. Chem.*, 2004, **279**, 51163-51171.
248. M. G. Marcu, Y.-J. Jung, S. Lee, E.-J. Chung, M.-J. Lee, J. Trepel and L. Neckers, *Med. Chem.*, 2006, **2**, 169-174.
249. Y. Chen, W. Shu, W. Chen, Q. Wu, H. Liu and G. Cui, *Basic Clin. Pharmacol. Toxicol.*, 2007, **101**, 427-433.
250. S. B. Kutluay, J. Doroghazi, M. E. Roemer and S. J. Triezenberg, *Virology*, 2008, **373**, 239-247.
251. K. C. Ravindra, B. R. Selvi, M. Arif, B. A. A. Reddy, G. R. Thanuja, S. Agrawal, S. K. Pradhan, N. Nagashayana, D. Dasgupta and T. K. Kundu, *J. Biol. Chem.*, 2009, **284**, 24453-24464.
252. E. M. Bowers, G. Yan, C. Mukherjee, A. Orry, L. Wang, M. A. Holbert, N. T. Crump, C. A. Hazzalin, G. Liszczak, H. Yuan, C. Larocca, S. A. Saldanha, R. Abagyan, Y. Sun, D. J. Meyers, R. Marmorstein, L. C. Mahadevan, R. M. Alani and P. A. Cole, *Chem. Biol.*, 2010, **17**, 471-482.
253. B. M. Dancy, N. T. Crump, D. J. Peterson, C. Mukherjee, E. M. Bowers, Y. H. Ahn, M. Yoshida, J. Zhang, L. C. Mahadevan, D. J. Meyers, J. D. Boeke and P. A. Cole, *ChemBioChem*, 2012, **13**, 2113-2121.
254. S. D. Furdas, S. Shekfeh, S. Kannan, W. Sippl and M. Jung, *MedChemComm*, 2012, **3**, 305-311.
255. X. N. Gao, J. Lin, Q. Y. Ning, L. Gao, Y. S. Yao, J. H. Zhou, Y. H. Li, L. L. Wang and L. Yu, *PLoS One*, 2013, **8**.
256. B. B. X. Li and X. S. Xiao, *ChemBioChem*, 2009, **10**, 2721-2724.
257. C. Y. Majmudar, J. W. Hojfeldt, C. J. Arevang, W. C. Pomerantz, J. K. Gagnon, P. J. Schultz, L. C. Cesa, C. H. Doss, S. P. Rowe, V. Vasquez, G. Tamayo-Castillo, T. Cierpicki, C. L. Brooks, D. H. Sherman and A. K. Mapp, *Angew Chem Int Edit*, 2012, **51**, 11258-11262.
258. Sachchidanand, L. Resnick-Silverman, S. Yan, S. Mutjaba, W.-j. Liu, L. Zeng, J. J. Manfredi and M.-M. Zhou, *Chem. Biol.*, 2006, **13**, 81-90.
259. Jagat C. Borah, S. Mujtaba, I. Karakikes, L. Zeng, M. Muller, J. Patel, N. Moshkina, K. Morohashi, W. Zhang, G. Gerona-Navarro, Roger J. Hajjar and M.-M. Zhou, *Chem. Biol.*, 2011, **18**, 531-541.
260. G. Gerona-Navarro, Yoel-Rodriguez, S. Mujtaba, A. Frasca, J. Patel, L. Zeng, A. N. Plotnikov, R. Osman and M. M. Zhou, *J. Am. Chem. Soc.*, 2011, **133**, 2040-2043.
261. D. Hay, O. Fedorov, P. Filippakopoulos, S. Martin, M. Philpott, S. Picaud, D. S. Hewings, S. Uttakar, T. D. Heightman, S. J. Conway, S. Knapp and P. E. Brennan, *MedChemComm*, 2013, **4**, 140-144.

262. T. Ryckmans, M. P. Edwards, V. A. Horne, A. M. Correia, D. R. Owen, L. R. Thompson, I. Tran, M. F. Tutt and T. Young, *Bioorg. Med. Chem. Lett.*, 2009, **19**, 4406-4409.
263. M. D. Shultz, *Bioorg. Med. Chem. Lett.*, 2013, **23**, 5980-5991.
264. A. L. Hopkins, C. R. Groom and A. Alex, *Drug Discovery Today*, 2004, **9**, 430-431.
265. D. S. Hewings, M. H. Wang, M. Philpott, O. Fedorov, S. Uttarkar, P. Filippakopoulos, S. Picaud, C. Vuppusetty, B. Marsden, S. Knapp, S. J. Conway and T. D. Heightman, *J. Med. Chem.*, 2011, **54**, 6761-6770.
266. D. S. Hewings, O. Fedorov, P. Filippakopoulos, S. Martin, S. Picaud, A. Tumber, C. Wells, M. M. Olcina, K. Freeman, A. Gill, A. J. Ritchie, D. W. Sheppard, A. J. Russell, E. M. Hammond, S. Knapp, P. E. Brennan and S. J. Conway, *J. Med. Chem.*, 2013, **56**, 3217-3227.
267. M. A. Dawson, R. K. Prinjha, A. Dittmann, G. Giotopoulos, M. Bantscheff, W. I. Chan, S. C. Robson, C. W. Chung, C. Hopf, M. M. Savitski, C. Huthmacher, E. Gudgin, D. Lugo, S. Beinke, T. D. Chapman, E. J. Roberts, P. E. Soden, K. R. Auger, O. Mirguet, K. Doehner, R. Delwel, A. K. Burnett, P. Jeffrey, G. Drewes, K. Lee, B. J. P. Huntly and T. Kouzarides, *Nature*, 2011, **478**, 529-533.
268. M. Philpott, J. Yang, T. Tumber, O. Fedorov, S. Uttarkar, P. Filippakopoulos, S. Picaud, T. Keates, I. Felletar, A. Ciulli, S. Knapp and T. D. Heightman, *Mol. BioSyst.*, 2011, **7**, 2899-2908.
269. P. Filippakopoulos, J. Qi, S. Picaud, Y. Shen, W. B. Smith, O. Fedorov, E. M. Morse, T. Keates, T. T. Hickman, I. Felletar, M. Philpott, S. Munro, M. R. McKeown, Y. C. Wang, A. L. Christie, N. West, M. J. Cameron, B. Schwartz, T. D. Heightman, N. La Thangue, C. A. French, O. Wiest, A. L. Kung, S. Knapp and J. E. Bradner, *Nature*, 2010, **468**, 1067-1073.
270. M. P. Jacobson, R. A. Friesner, Z. X. Xiang and B. Honig, *J. Mol. Biol.*, 2002, **320**, 597-608.
271. C. R. Sondergaard, A. E. Garrett, T. Carstensen, G. Pollastri and J. E. Nielsen, *J. Med. Chem.*, 2009, **52**, 5673-5684.
272. S. V. Ryabukhin, A. S. Plaskon, D. M. Volochnyuk, S. E. Pipko, A. N. Shivanyuk and A. A. Tolmachev, *J. Comb. Chem.*, 2007, **9**, 1073-1078.
273. R. D. Clark and A. Jahangir, in *Organic Reactions*, John Wiley & Sons, Inc., 2004.
274. A. D. Scott, C. Phillips, A. Alex, M. Flocco, A. Bent, A. Randall, R. O'Brien, L. Damian and L. H. Jones, *ChemMedChem*, 2009, **4**, 1985-1989.
275. P. V. Fish, P. Filippakopoulos, G. Bish, P. E. Brennan, M. E. Bunnage, A. S. Cook, O. Federov, B. S. Gerstenberger, H. Jones, S. Knapp, B. Marsden, K. Nocka, D. R. Owen, M. Philpott, S. Picaud, M. J. Primiano, M. J. Ralph, N. Sciammetta and J. D. Trzupek, *J. Med. Chem.*, 2012, **55**, 9831-9837.
276. O. Mirguet, R. Gosmini, J. Toum, C. A. Clement, M. Barnathan, J.-M. Brusq, J. E. Mordaunt, R. M. Grimes, M. Crowe, O. Pineau, M. Ajakane, A. Daugan, P. Jeffrey, L. Cutler, A. C. Haynes, N. N. Smithers, C.-w. Chung, P. Bamborough, I. J. Uings, A. Lewis, J. Witherington, N. Parr, R. K. Prinjha and E. Nicodeme, *J. Med. Chem.*, 2013, **56**, 7501-7515.
277. S. i. Taira, H. Danjo and T. Imamoto, *Tetrahedron Lett.*, 2002, **43**, 2885-2888.
278. N. Prasitpan, J. N. Patel, P. Z. Decroos, B. L. Stockwell, P. Manavalan, L. Kar, M. E. Johnson and B. L. Currie, *J. Heterocycl. Chem.*, 1992, **29**, 335-341.
279. T. Tsunoda, C. Nagino, M. Oguri and S. Itô, *Tetrahedron Lett.*, 1996, **37**, 2459-2462.
280. G. Collina, L. Forlani, E. Mezzina, M. Sintoni and P. E. Todesco, *Gazz. Chim. Ital.*, 1987, **117**, 281-285.
281. B. K. Singh, C. Cavalluzzo, M. De Maeyer, Z. Debyser, V. S. Parmar and E. Van der Eycken, *Synthesis*, 2009, 2725-2728.
282. A. F. Morel, E. L. Larghi and M. M. Selvero, *Synlett*, 2005, 2755-2758.
283. Y. Miyake, E. Nomura, A. Hosoda, H. Mori, M. Takagaki and H. Taniguchi, *Kenkyu Hokoku - Wakayama-ken Kogyo Gijutsu Senta*, 2006, 22.

284. C. A. French, C. L. Ramirez, J. Kolmakova, T. T. Hickman, M. J. Cameron, M. E. Thyne, J. L. Kutok, J. A. Toretsky, A. K. Tadavarthy, U. R. Kees, J. A. Fletcher and J. C. Aster, *Oncogene*, 2008, **27**, 2237-2242.
285. A. Rehemtulla, N. Taneja and B. D. Ross, *Molecular imaging*, 2004, **3**, 63-68.
286. H. J. S. Stewart, G. A. Horne, S. Bastow and T. J. T. Chevassut, *Cancer Med.*, 2013, **2**, 826-835.
287. Jake E. Delmore, Ghayas C. Issa, Madeleine E. Lemieux, Peter B. Rahl, J. Shi, Hannah M. Jacobs, E. Kastritis, T. Gilpatrick, Ronald M. Paranal, J. Qi, M. Chesi, Anna C. Schinzel, Michael R. McKeown, Timothy P. Heffernan, Christopher R. Vakoc, P. L. Bergsagel, Irene M. Ghobrial, Paul G. Richardson, Richard A. Young, William C. Hahn, Kenneth C. Anderson, Andrew L. Kung, James E. Bradner and Constantine S. Mitsiades, *Cell*, 2011, **146**, 904-917.
288. A. Miyawaki, *Dev. Cell*, 2003, **4**, 295-305.
289. T. Mosmann, *J. Immunol. Methods*, 1983, **65**, 55-63.
290. F. Lamoureux, M. Baud'huin, L. Rodriguez Calleja, C. Jacques, M. Berreur, F. Rédini, F. Lecanda, J. E. Bradner, D. Heymann and B. Ory, *Nat Commun*, 2014, **5**.
291. C. A. Lipinski, *J. Pharmacol. Toxicol. Methods*, 2000, **44**, 235-249.
292. C. L. Cummins, W. Jacobsen and L. Z. Benet, *J. Pharmacol. Exp. Ther.*, 2002, **300**, 1036-1045.
293. R. S. Obach, J. G. Baxter, T. E. Liston, B. M. Silber, B. C. Jones, F. MacIntyre, D. J. Rance and P. Wastall, *J. Pharmacol. Exp. Ther.*, 1997, **283**, 46-58.
294. E. Middeljans, X. Wan, P. W. Jansen, V. Sharma, H. G. Stunnenberg and C. Logie, *PLoS One*, 2012, **7**.
295. C. Kadoch, D. C. Hargreaves, C. Hodges, L. Elias, L. Ho, J. Ranish and G. R. Crabtree, *Nat. Genet.*, 2013, **45**, 592-601.
296. M. D. Kaeser, A. Aslanian, M.-Q. Dong, J. R. Yates, III and B. M. Emerson, *J. Biol. Chem.*, 2008, **283**, 32254-32263.
297. S. Tae, V. Karkhanis, K. Velasco, M. Yaneva, H. Erdjument-Bromage, P. Tempst and S. Sif, *Nucleic Acids Res.*, 2011, **39**, 5424-5438.
298. C. Peng, J. Zhou, H. Y. Liu, M. Zhou, L. L. Wang, Q. H. Zhang, Y. X. Yang, W. Xiong, S. R. Shen, X. L. Li and G. Y. Li, *J. Cell. Biochem.*, 2006, **97**, 882-892.
299. J. U. Kang, S. H. Koo, K. C. Kwon, J. W. Park and J. M. Kim, *Cancer Genet. Cytogenet.*, 2008, **182**, 1-11.
300. L. Scotto, G. Narayan, S. V. Nandula, S. Subramaniyam, A. M. Kaufmann, J. D. Wright, B. Pothuri, M. Mansukhani, A. Schneider, H. Arias-Pulido and V. V. Murty, *Mol Cancer*, 2008, **7**.
301. J. Zhou, J. Ma, B.-C. Zhang, X.-L. Li, S.-R. Shen, S.-G. Zhu, W. Xiong, H.-Y. Liu, H. Huang, M. Zhou and G.-Y. Li, *J. Cell. Physiol.*, 2004, **200**, 89-98.
302. C. Peng, H. Y. Liu, M. Zhou, L. M. Zhang, X. L. Li, S. R. Shen and G. Y. Li, *Mol. Cell. Biochem.*, 2007, **303**, 141-149.
303. A. E. Burrows, A. Smogorzewska and S. J. Elledge, *Proc. Natl. Acad. Sci. U. S. A.*, 2010, **107**, 14280-14285, S14280/14281-S14280/14284.
304. J. Drost, F. Mantovani, F. Tocco, R. Elkon, A. Comel, H. Holstege, R. Kerkhoven, J. Jonkers, P. M. Voorhoeve, R. Agami and G. Del Sal, *Nat. Cell Biol.*, 2010, **12**, 380-389.
305. F. Mantovani, J. Drost, P. M. Voorhoeve, G. Del Sal and R. Agami, *Cell Cycle*, 2010, **9**, 2777-2781.
306. M. T. Harte, G. J. O'Brien, N. M. Ryan, J. J. Gorski, K. I. Savage, N. T. Crawford, P. B. Mullan and D. P. Harkin, *Cancer Res.*, 2010, **70**, 2538-2547.
307. W.-J. Wu, K.-S. Hu, D.-L. Chen, Z.-L. Zeng, H.-Y. Luo, F. Wang, D.-S. Wang, Z.-Q. Wang, F. He and R.-H. Xu, *Eur. J. Clin. Invest.*, 2013, **43**, 131-140.
308. Y.-A. Park, J.-W. Lee, H.-S. Kim, Y.-Y. Lee, T.-J. Kim, C. H. Choi, J.-J. Choi, H.-K. Jeon, Y. J. Cho, J. Y. Ryu, B.-G. Kim and D.-S. Bae, *Clin Cancer Res*, 2014, **20**, 565-575.
309. J. Penkert, B. Schlegelberger, D. Steinemann and D. Gadzicki, *Fam. Cancer*, 2012, **11**, 601-606.

310. Y.-A. Park, J.-W. Lee, J.-J. Choi, H.-K. Jeon, Y. Cho, C. Choi, T.-J. Kim, N. W. Lee, B.-G. Kim and D.-S. Bae, *Gynecol. Oncol.*, 2012, **124**, 125-133.
311. SGC, *GSK2801: A Selective Chemical Probe for BAZ2B/A bromodomains*, http://www.thesgc.org/chemical-probes/GSK2801, Accessed March 21, 2014, 2014.
312. M. K. Dahlgren, P. Schyman, J. Tirado-Rives and W. L. Jorgensen, *J. Chem. Inf. Model.*, 2013, **53**, 1191-1199.
313. R. S. Kulkarni, B. Padmashali and Sandeep, *Tetrahedron Lett.*, 2013, **54**, 6411 - 6414.
314. X. He, K. Ju, Y. Shang, C. Wang, S. Yu and M. Zhang, *Tetrahedron Lett.*, 2009, **50**, 6981 - 6984.
315. L. Guo, J. Li, L. Li, T. Li, Z. Li, J. Lin, L. Lin, J. Wang, P. G. Wang, Y. Zhang, Z. Zhang and W. Zhao, *Carbohydr. Res.*, 2011, **346**, 1083 - 1092.
316. O.-U.-R. Abid, V. Iaroshenko, M. F. Ibad, R. A. Khera, P. Langer and M. Nawaz, *Organic and Biomolecular Chemistry*, 2011, **9**, 2185 - 2191.
317. R. P. Alexander, S. Bailey, S. Brand, D. C. Brookings, J. A. Brown, A. F. Haughan, N. Kinsella, C. Lowe, S. R. Mack, W. R. Pitt, M. D. Richard, A. Sharpe and L. J. Tait, *Fused thiophene derivatives as kinase inhibitors*, WO2007/141504, 2007.
318. E. Koenigs and L. Neumann, *Berichte der deutschen chemischen Gesellschaft*, 1915, **48**, 956-963.
319. SGC, *Bromosporine*, http://www.thesgc.org/chemical-probes/bromosporine, Accessed March 21, 2014, 2014.
320. A. J. Williams and V. Kulkov, *Web-based access to structure-based prediction and databases for spectroscopy and physical properties*, Book of Abstracts, 218th ACS National Meeting, New Orleans, Aug. 22-26, 1999.
321. A. Demeijere, *Angewandte Chemie-International Edition in English*, 1979, **18**, 809-826.
322. U. Lottermoser, P. Rademacher, M. Mazik and K. Kowski, *Eur. J. Org. Chem.*, 2005, **2005**, 522-531.
323. Y. Nakamura, N. Aratani, H. Shinokubo, A. Takagi, T. Kawai, T. Matsumoto, Z. S. Yoon, D. Y. Kim, T. K. Ahn, D. Kim, A. Muranaka, N. Kobayashi and A. Osuka, *J. Am. Chem. Soc.*, 2006, **128**, 4119-4127.
324. A. Takeda and et al., *Bull. Chem. Soc. Jpn.*, 1977, **50**, 2191 - 2192.
325. T. Kitamura, S. Kobayashi, M. H. Morshed and Y. Tazawa, *Synthesis*, 2012, **44**, 1159 - 1162.
326. F. Segat-Dioury, O. Lingibé, B. Graffe, M.-C. Sacquet and G. Lhommet, *Tetrahedron*, 2000, **56**, 233-248.
327. P. Filippakopoulos, J. Qi, S. Picaud, Y. Shen, W. B. Smith, O. Fedorov, E. M. Morse, T. Keates, T. T. Hickman, I. Felletar, M. Philpott, S. Munro, M. R. McKeown, Y. Wang, A. L. Christie, N. West, M. J. Cameron, B. Schwartz, T. D. Heightman, N. La Thangue, C. A. French, O. Wiest, A. L. Kung, S. Knapp and J. E. Bradner, *Nature*, 2010, **468**, 1067-1073.
328. T. Wiseman, S. Williston, J. F. Brandts and L. N. Lin, *Anal. Biochem.*, 1989, **179**, 131-137.

APPENDIX 1. CARBOXYLIC ACID HETEROARYL BROMIDES FOR PARALLEL SUZUKI COUPLINGS

Compounds used, along with yields in parenthesis. Little/no detectable product was observed in reactions with 'failed reaction'. Product was not isolated in sufficient quantity or purity with those reactions labelled with 'failed purification'.

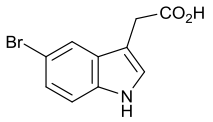

32 (10%)

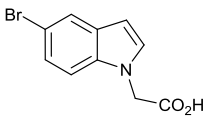

33 (46%)

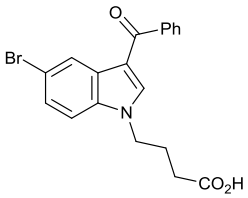

34 (55%)

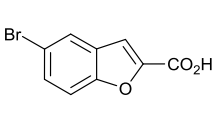

35 (54%)

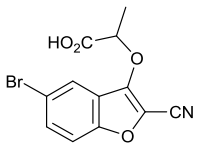

36 (17%)

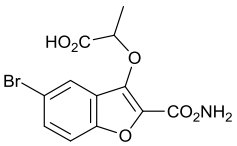

37 (19%)

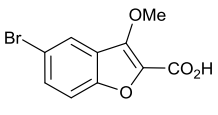

38 (21%)

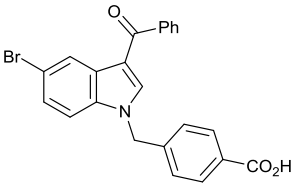

39 (55%)

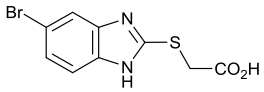

40 (35%)

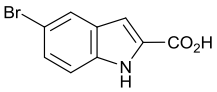

41 (24%)

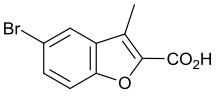

42 (16%)

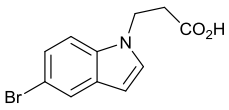

43 (28%)

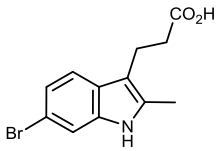

44 (10%)

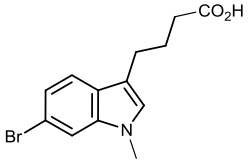

45 (13%)

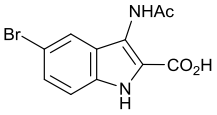

46 (15%)

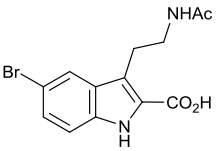

47 (45%)

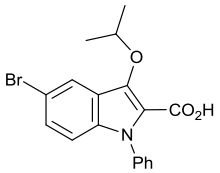

48 (31%)

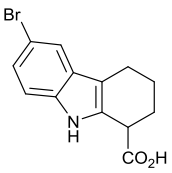

49 (41%)

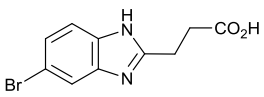

50 (failed purification)

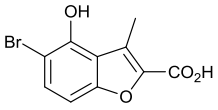

51 (failed reaction)

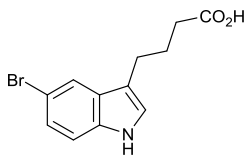

52 (failed purification)

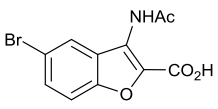

53 (failed purification)

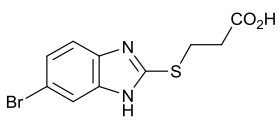

54 (failed purification)

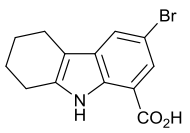

55 (failed purification)

APPENDIX 2. ADDITIONAL SAR FOR CARBOXYLIC ACIDS FROM PARALLEL SUZUKI COUPLINGS

		Alpha Screen IC_{50} (µM)[*]		*DSF ΔT_m (°C)*[*]	
Cmpd	*Structural formula*	*CBP*	*BRD4(1)*	*CBP*	*BRD4(1)*
56	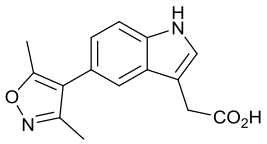	8.9 (1)	28 (1)		
57	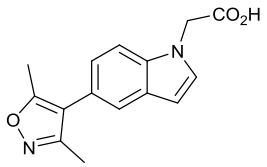	14 (1)	450 (1)		
58	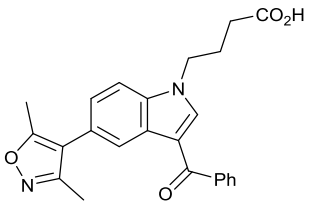	1.8 (1)	2.1 (1)		
59	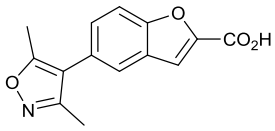	14 (1)	2.1 (1)		
60	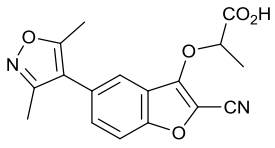	22 (1)	4.4 (1)		
61	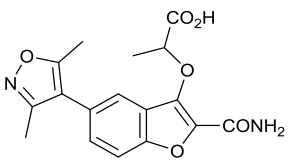	11 (1)	9.0 (1)		

		Alpha Screen IC_{50} (µM)[*]		*DSF ΔT_m (°C)*[*]	
Cmpd	*Structural formula*	*CBP*	*BRD4(1)*	*CBP*	*BRD4(1)*
62	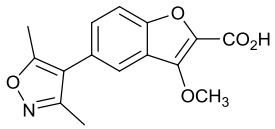	64 (1)	24 (1)		
63	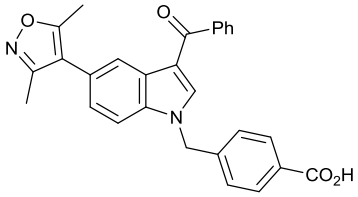	4.3 (1)	5.0 (1)		
64	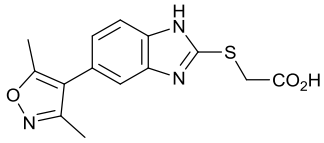	30 (1)	22 (1)	1.4 (1)	
65	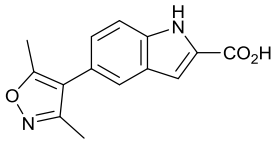	8.4 (1)	3.2 (1)		
66	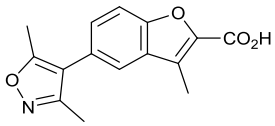	14 (1)	25 ± 19 (2)		
67	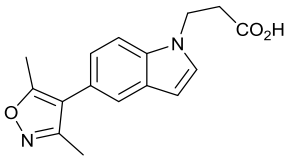	12 (1)	84 ± 66 (2)		
68	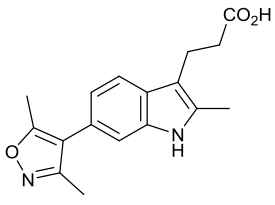			1.6 ± 0.24 (2)	0.98 (1)

		Alpha Screen IC_{50} (μM)[*]		*DSF ΔT_m (°C)*[*]	
Cmpd	*Structural formula*	*CBP*	*BRD4(1)*	*CBP*	*BRD4(1)*
69	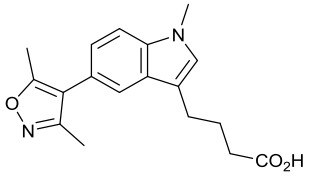			0.55 ± 0.035 (2)	0.77 (1)
70	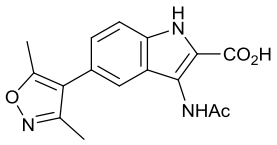	8.7 (1)	17 ± 13 (2)		
71	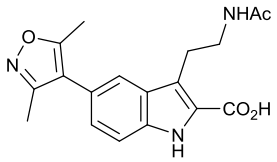	3.7 (1)	10 ± 8.0 (2)		
72	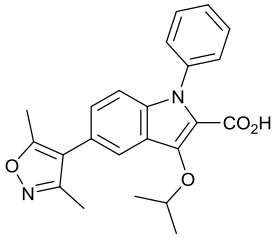	3.0 ± 2.1 (2)	15 ± 11 (2)		
73	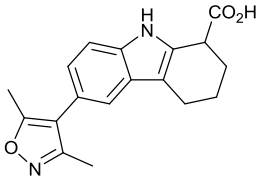	24 (1)	46 ± 38 (2)		

[*]Mean value ± SEM (number of measurements).

APPENDIX 3. NEUTRAL AND BASIC HETEROARYL BROMIDES FOR PARALLEL SUZUKI COUPLINGS

Compounds used, along with yields in parenthesis. Little/no detectable product was observed in reactions with 'failed reaction'. Product was not isolated in sufficient quantity or purity with those reactions labelled with 'failed purification'.

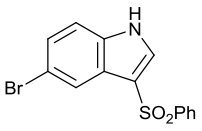

74 (38%)

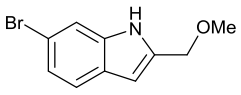

75 (17%)

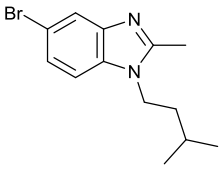

76 (52%)

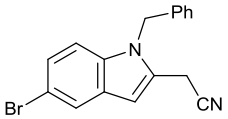

77 (13%)

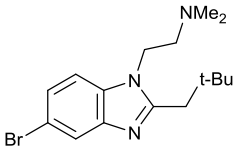

78 (52%)

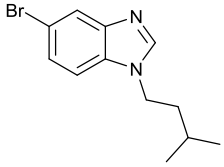

79 (23%)

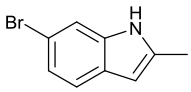

80 (58%)

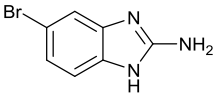

81 (48%)

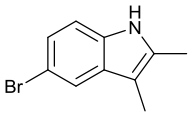

82 (50%)

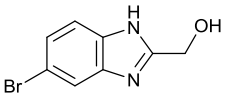

83 (63%)

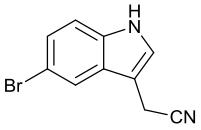

84 (61%)

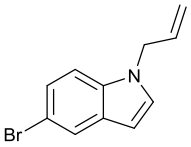

85 (48%)

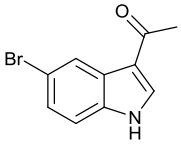

86 (45%)

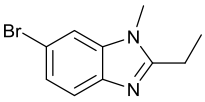

87 (74%)

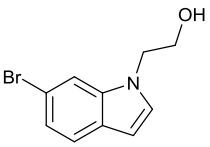

88 (23%)

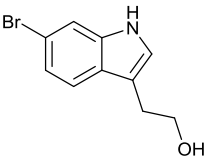

89 (66%)

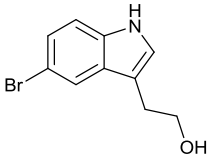

90 (36%)

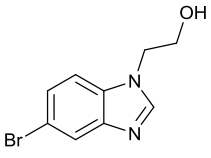

91 (70%)

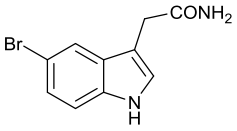

92 (44%)

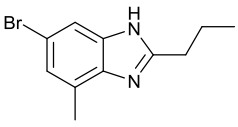

93 (59%)

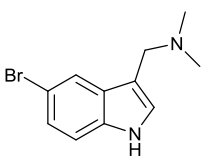

94 (9%)

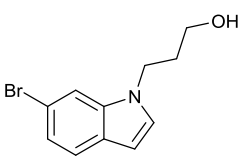

95 (39%)

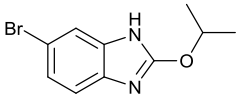

96 (33%)

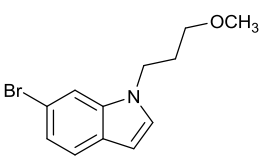

97 (70%)

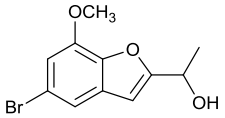

98 (93%)

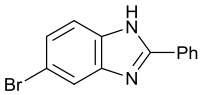

99 (23%)

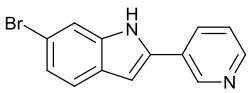

100 (44%)

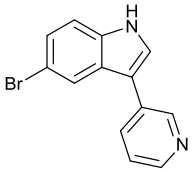

101 (62%)

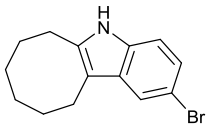

102 (62%)

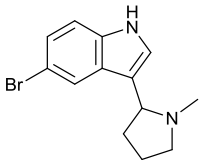

103 (81%)

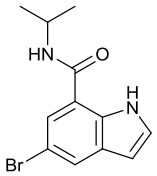

104 (70%)

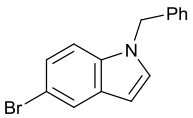

105 (58%)

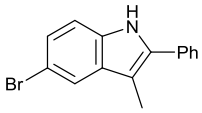

106 (40%)

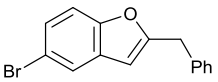

107 (46%)

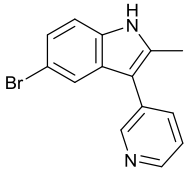

108 (26%)

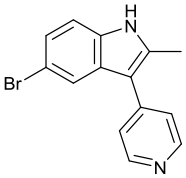

109 (11%)

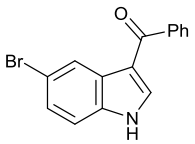

110 (5%)

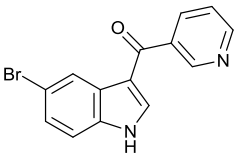

111 (35%)

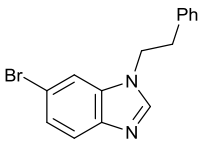

112 (23%)

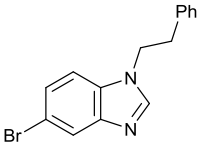

113 (21%)

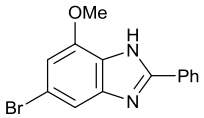

114 (27%)

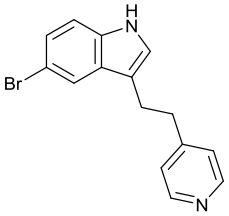

115 (56%)

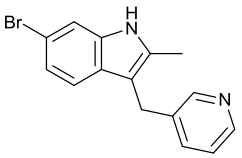

116 (34%)

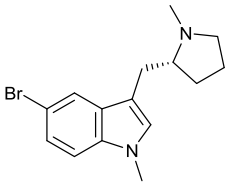

117 (31%)

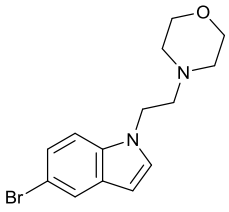

118 (79%)

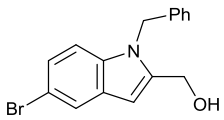

119 (39%)

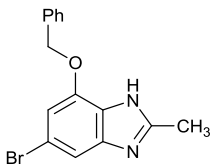

120 (39%)

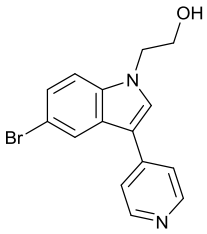

121 (25%)

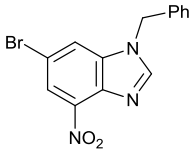

122 (19%)

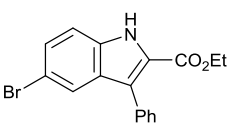

123 (11%)

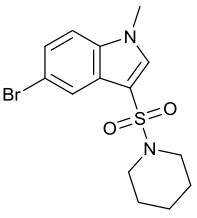

124 (18%)

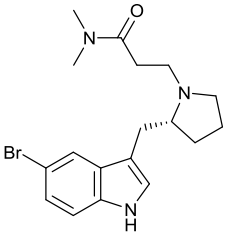

125 (27%)

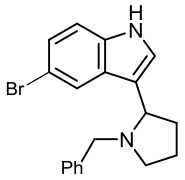

126 (37%)

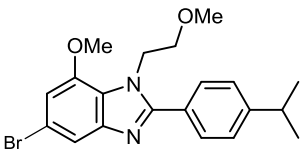

127 (32%)

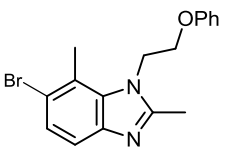

128 (21%)

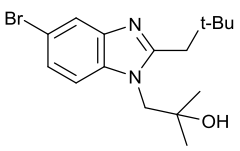

129 (15%)

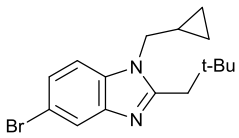

130 (57%)

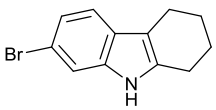

131 (54%)

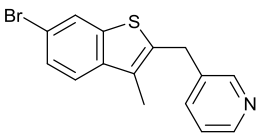

132 (50%)

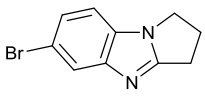

133 (30%)

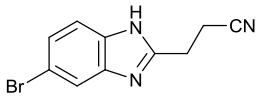

134 (10%)

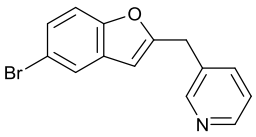

135 (42%)

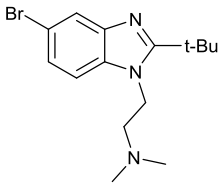

136 (13%)

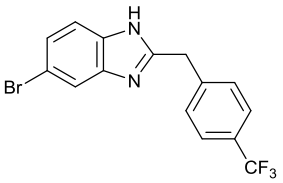

137 (82%)

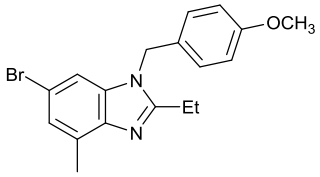

138 (68%)

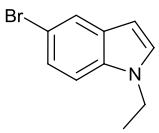

139 (failed purification)

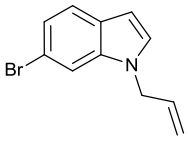

140 (failed purification)

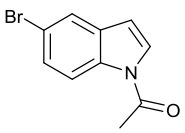

141 (failed purification)

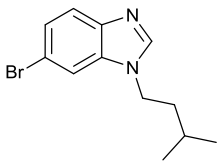

142 (failed purification)

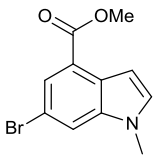

143 (failed purification)

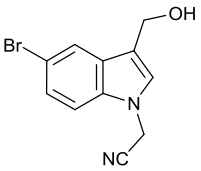

144 (failed purification)

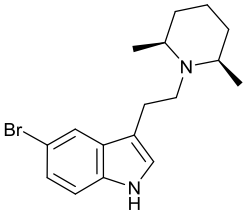

145 (failed purification)

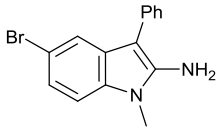

146 (failed purification)

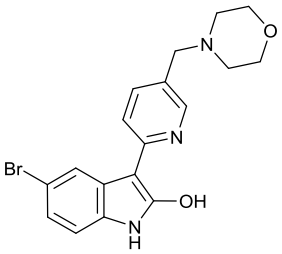

147 (failed purification)

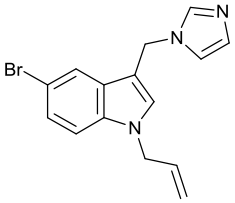

148 (failed purification)

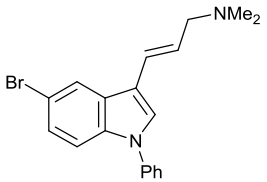

149 (failed purification)

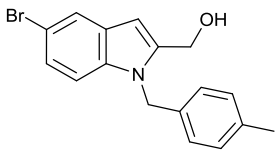

150 (failed purification)

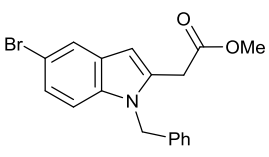

151 (failed reaction)

APPENDIX 4. ADDITIONAL SAR FROM NEUTRAL AND BASIC PARALLEL SUZUKI ANALOGUES

		*Alpha Screen IC_{50} (µM)***		*DSF ΔT_m (°C)**	
Cmpd	*Structural formula*	*CBP*	*BRD4(1)*	*CBP*	*BRD4(1)*
152	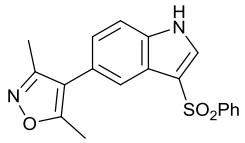	1.2 (1)	1.1 (1)		
153	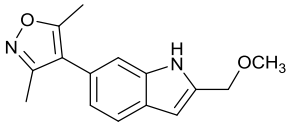	4.1 (1)	15 (1)		
154	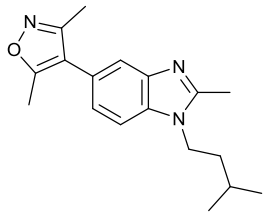	2.0 (1)	8.2 (1)	4.3 (1)	
155	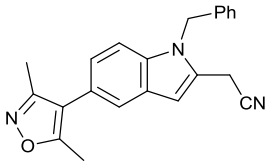	2.2 (1)	11 (1)		
156	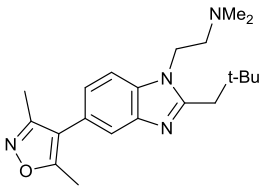	1.6 (1)	15 (1)		
157	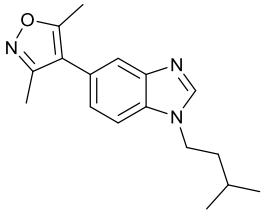	4.8 (1)	0.44 (1)	3.2 (1)	

		Alpha Screen IC_{50} (μM)[*]		*DSF ΔT_m (°C)*[*]	
Cmpd	*Structural formula*	*CBP*	*BRD4(1)*	*CBP*	*BRD4(1)*
158	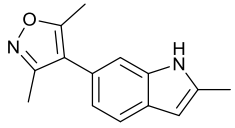	10 (1)	15 (1)		
160	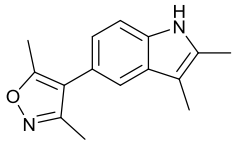	13 (1)	22 (1)		
162	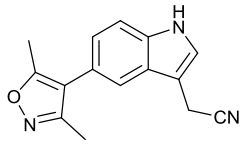	3.1 (1)	5.4 (1)		
163	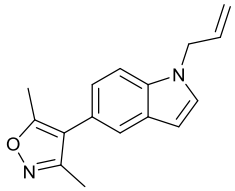	14 (1)	21 (1)		
164	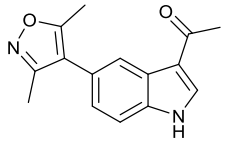	24 (1)	10 (1)		
165	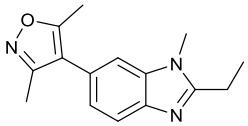	3.4 (1)	5.4 (1)		
166	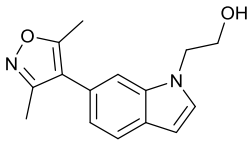	10 (1)	15 (1)		

		Alpha Screen IC_{50} (µM)[*]		*DSF ΔT_m (°C)*[*]	
Cmpd	*Structural formula*	*CBP*	*BRD4(1)*	*CBP*	*BRD4(1)*
167	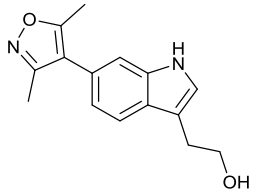	6.5 (1)	22 (1)		
168	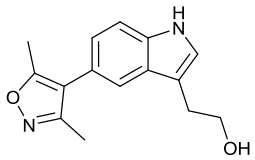	10 (1)	16 (1)		
169	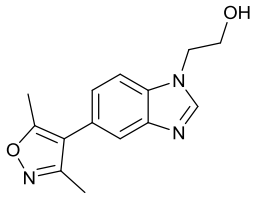	5.9 (1)	22 (1)	0.8 (1)	
170	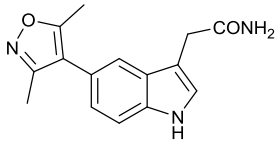	15 (1)	4.6 (1)		
171	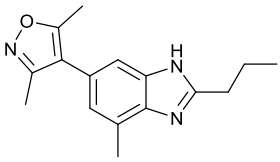	1.8 (1)	3.3 (1)		
172	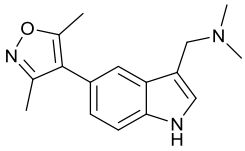	22 (1)	16 (1)		
173	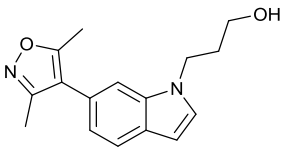	13 (1)	10 (1)		

		Alpha Screen IC_{50} (μM)[*]		*DSF ΔT_m (°C)*[*]	
Cmpd	*Structural formula*	*CBP*	*BRD4(1)*	*CBP*	*BRD4(1)*
174	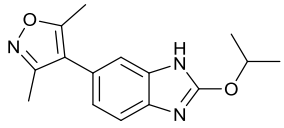	100 (1)	100 (1)		
175	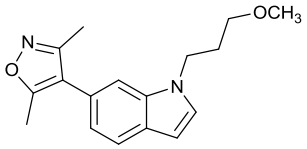	35 (1)	9.2 (1)		
176	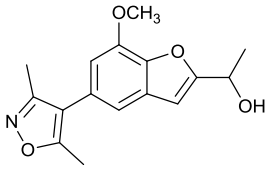	7.3 (1)	17 (1)		
177	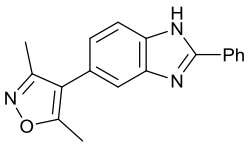	3.4 (1)	2.6 (1)	2.4 (1)	
178	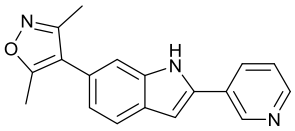	4.8 (1)	6.3 (1)		
179	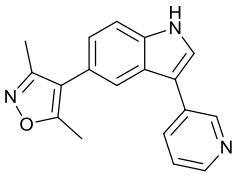	130 (1)	84 (1)		
180	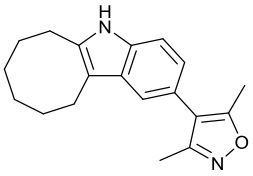	10 (1)	15 (1)	4.3 (1)	

		Alpha Screen IC_{50} (μM)[*]		*DSF ΔT_m (°C)*[*]	
Cmpd	*Structural formula*	*CBP*	*BRD4(1)*	*CBP*	*BRD4(1)*
181	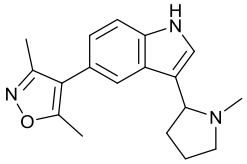	31 (1)	5.5 (1)		
182	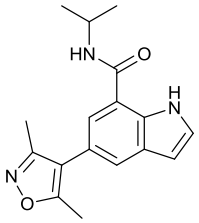	13 (1)	16 (1)		
183	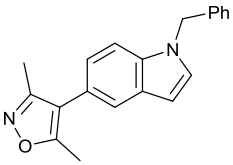	9.0 (1)	16 (1)		
184	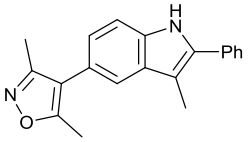	13 (1)	28 (1)		
185	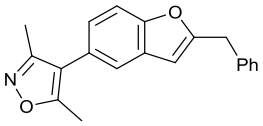	4.3 ± 2.5 (2)	3.3 (1)		
186	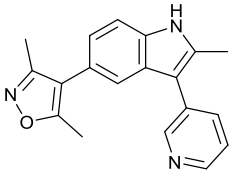	11 (1)	5.2 (1)		
187	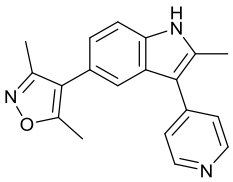	>100 μM	>100 μM		

		Alpha Screen IC_{50} (μM)[*]		*DSF ΔT_m (°C)*[*]	
Cmpd	*Structural formula*	*CBP*	*BRD4(1)*	*CBP*	*BRD4(1)*
188	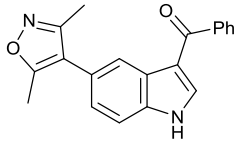	6.6 (1)	9.1 (1)		
189	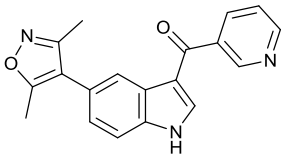	35 (1)	2.9 (1)		
190	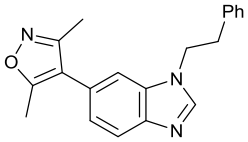	5.3 (1)	2.4 (1)	1.9 (1)	
191	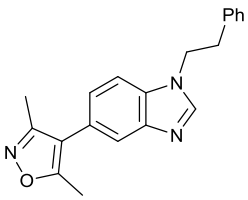	2.8 (1)	4.1 (1)	3.2 (1)	
192	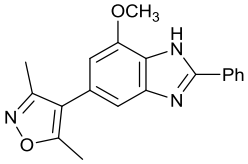	5.3 ± 2.7 (2)	2.1 (1)	4.3 (1)	
193	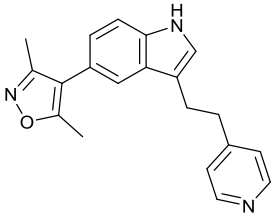	35 (1)	5.2 (1)		
194	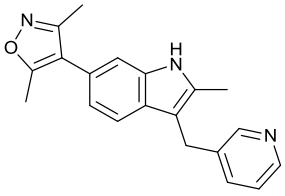	2.7 ± 1.3 (2)	5.4 (1)		

		Alpha Screen IC_{50} (μM)[*]		*DSF ΔT_m (°C)*[*]	
Cmpd	*Structural formula*	*CBP*	*BRD4(1)*	*CBP*	*BRD4(1)*
195	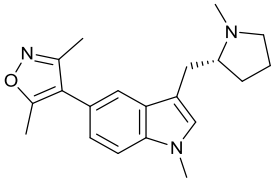	35 (1)	2.1 (1)		
196	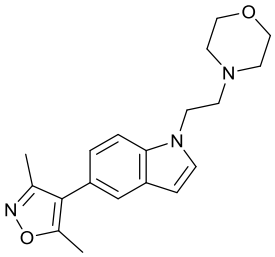	7.0 (1)	14 (1)		
197	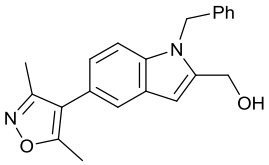	4.7 (1)	15 (1)		
198	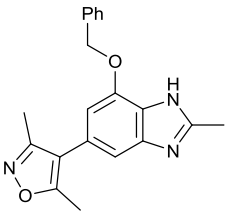	1.4 ± 0.74 (3)	0.86 (1)	6.9 (1)	
199	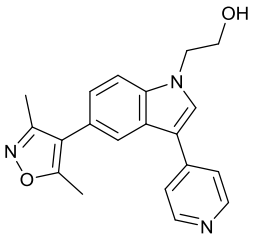	3.4 (1)	3.4 (1)		
200	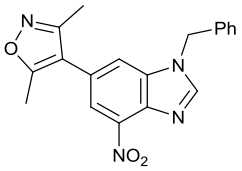	4.7 ± 2.6 (2)	0.30 (1)		

		Alpha Screen IC_{50} (μM)[*]		*DSF ΔT_m (°C)*[*]	
Cmpd	*Structural formula*	*CBP*	*BRD4(1)*	*CBP*	*BRD4(1)*
201	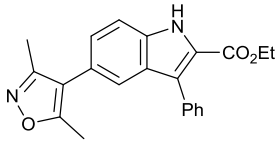	11 (1)	6.9 (1)		
202	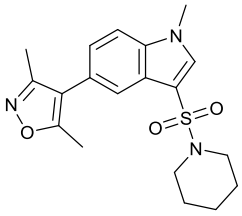	>100 μM	10 (1)		
203	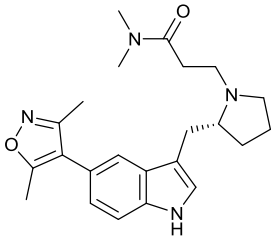	>100 μM (1)	5.4 (1)		
204	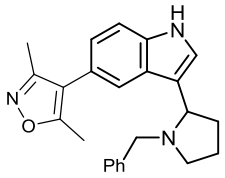	29 (1)	1.7 (1)		
205	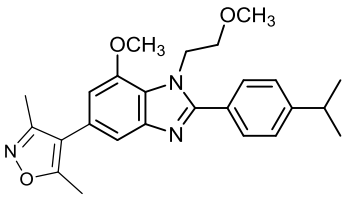	>100 μM (1)	20 (1)	3.1 (1)	
206	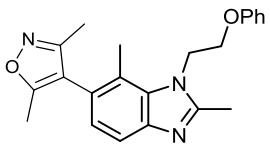	16 (1)	6.8 (1)	0.15 (1)	

		Alpha Screen IC_{50} (μM)[*]		*DSF ΔT_m (°C)*[*]	
Cmpd	*Structural formula*	*CBP*	*BRD4(1)*	*CBP*	*BRD4(1)*
207	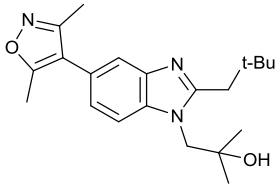			2.6 ± 0.050 (2)	0.23 (1)
208	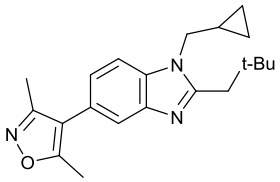	0.55 (1)		4.7 ± 0.23 (2)	1.2 (1)
209	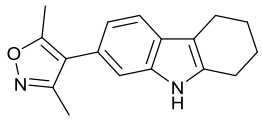			1.8 (1)	0.12 (1)
210	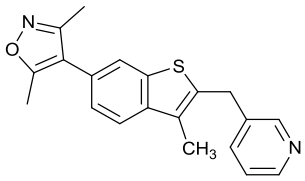			0.68 ± 0.33 (2)	0.80 (1)
211	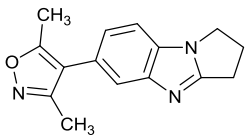			0.94 ± 0.050 (2)	0.040 (1)
212	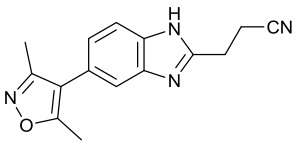			2.5 ± 0.67 (2)	0.65 (1)
213	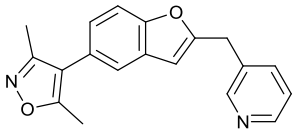			0.62 ± 0.035 (2)	0.56 (1)

		Alpha Screen IC_{50} (μM)[*]		*DSF ΔT_m (°C)*[*]	
Cmpd	*Structural formula*	*CBP*	*BRD4(1)*	*CBP*	*BRD4(1)*
214	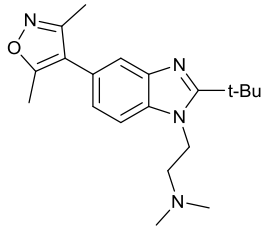			3.3 (1)	0.4 (1)
215	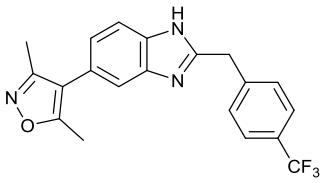			3.1 ± 0.24 (2)	1.1 (1)
216	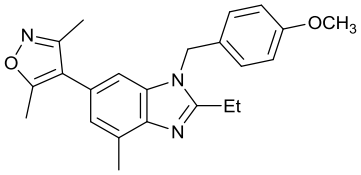			2.2 ± 0.15 (2)	2.4 (1)

APPENDIX 5. ALDEHYDES FOR PARALLEL BENZIMIDAZOLE-FORMING REACTIONS

Compounds used, along with yields in parenthesis. Little/no detectable product was observed in reactions with 'failed reaction'. Product was not isolated in sufficient quantity or purity with those reactions labelled with 'failed purification'.

218 (31%)

219 (30%)

220 (17%)

221 (49%)

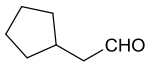

222 (50%)

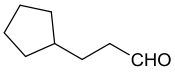

223 (9%)

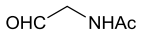

224 (54%)

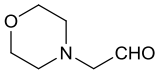

225 (13%)

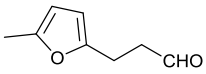

226 (24%)

227 (12%)

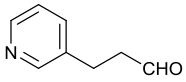

228 (34%)

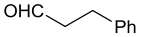

229 (34%)

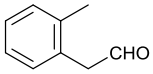

230 (8%)

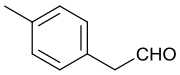

231 (34%)

232 (54%)

233 (36%)

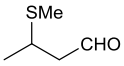

234 (10%)

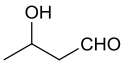

235 (16%)

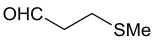

236 (12%)

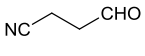

237 (failed reaction)

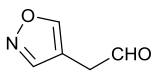

238 (failed purification)

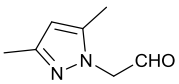

239 (failed purification)

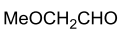

240 (failed purification)

241 (failed reaction)

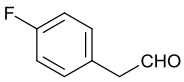

242 (failed purification)

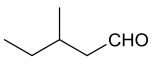

243 (failed reaction)

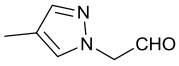

244 (failed purification)

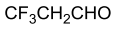

245 (failed reaction)

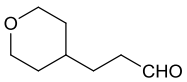

246 (failed reaction)

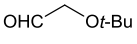

247 (failed reaction)

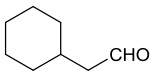

248 (failed reaction)

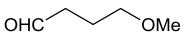

249 (failed purification)

APPENDIX 6. ADDITIONAL SAR FROM PARALLEL BENZIMIDAZOLE FORMING REACTIONS

		Alpha Screen IC_{50} (µM)[*]		*DSF ΔT_m (°C)*[*]	
Cmpd	*Structural formula*	*CBP*	*BRD4(1)*	*CBP*	*BRD4(1)*
251	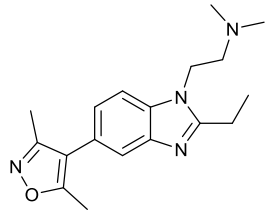			1.4 ± 0.12 (2)	0.35 (1)
253	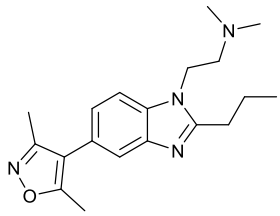			3.0 (1)	0.20 (1)
254	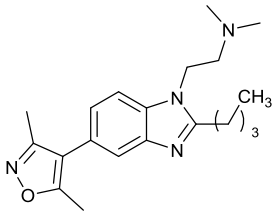			2.0 ± 0.075 (2)	0.71 (1)
255	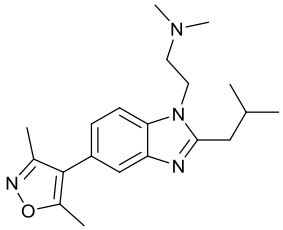			1.9 ± 0.32 (2)	0.42 (1)
256	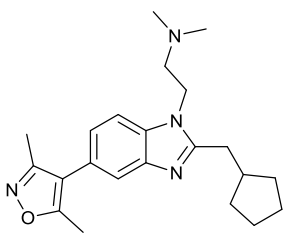			3.2 ± 0.060 (2)	0.55 (1)

		Alpha Screen IC_{50} (µM)[*]		*DSF ΔT_m (°C)*[*]	
Cmpd	*Structural formula*	*CBP*	*BRD4(1)*	*CBP*	*BRD4(1)*
257	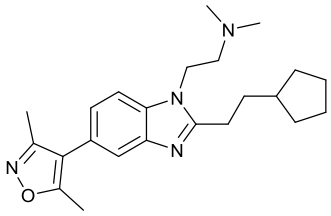			3.8 ± 0.41 (2)	0.78 (1)
258	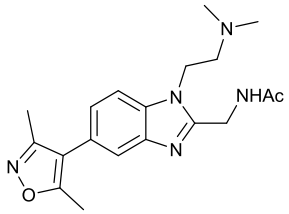			0.84 ± 0.080 (2)	0.17 (1)
259	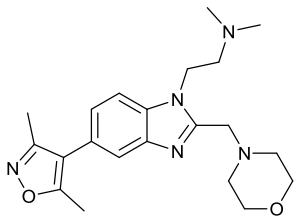			0.78 ± 0.16 (2)	0.14 (1)
260	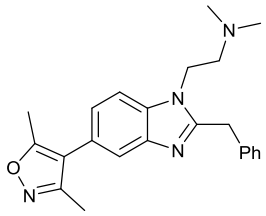			3.1 ± 0.43 (2)	0.25 (1)
261	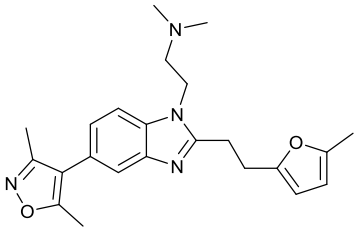			3.0 ± 0.24 (2)	0.75 (1)
262	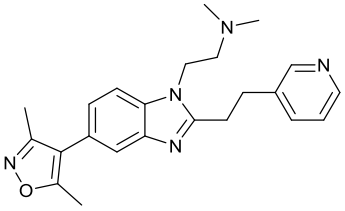			2.2 ± 0.040 (2)	0.53 (1)

		Alpha Screen IC_{50} (µM)[*]		*DSF ΔT_m (°C)*[*]	
Cmpd	*Structural formula*	*CBP*	*BRD4(1)*	*CBP*	*BRD4(1)*
263	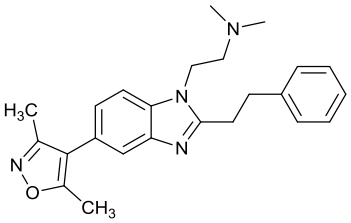	0.49		6.3 ± 0.27 (3)	2.9 ± 0.20 (3)
264	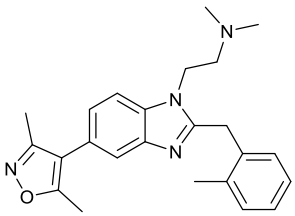			2.7 ± 0.44 (2)	0.27 (1)
265	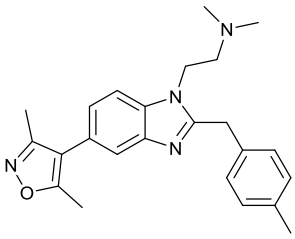			4.0 ± 0.075 (2)	0.38 (1)
267	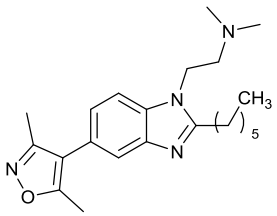			3.0 ± 0.040 (2)	0.62 (1)
268	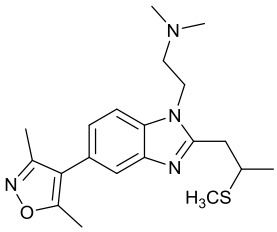			2.0 ± 0.11 (2)	0.22 (1)

		Alpha Screen IC_{50} (µM)[*]		*DSF ΔT_m (°C)*[*]	
Cmpd	*Structural formula*	*CBP*	*BRD4(1)*	*CBP*	*BRD4(1)*
269	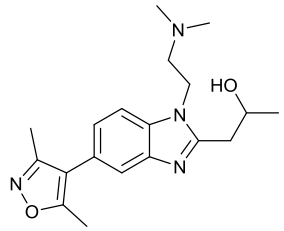			0.7 ± 0.035 (2)	0.30 (1)
270	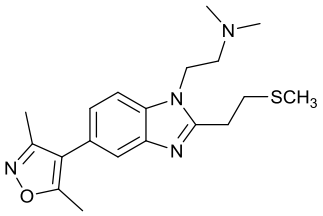			1.9 ± 0.090 (2)	0.43 (1)

[*]Mean value ± SEM (number of measurements).

APPENDIX 7. CEREP WIDE-LIGAND PROFILING FOR COMPOUND **397**

Target	*$IC_{50}(\mu M)$*
alpha 2C (h) (antagonist radioligand)	0.11
PDE5 (h) (non-selective)	0.15
PAF (h) (agonist radioligand)	0.54
alpha 2A (h) (antagonist radioligand)	0.57
5-HT1A (h) (agonist radioligand)	1.2
CB2 (h) (agonist radioligand)	1.9
Ca2+ channel (L, diltiazem site) (benzothiazepines) (antagonist radioligand)	2.9
NK2 (h) (agonist radioligand)	3.9
alpha 2B (h) (antagonist radioligand)	4.2
MT1 (ML1A) (h) (agonist radioligand)	4.3
Cl- channel (GABA-gated) (antagonist radioligand)	4.6
CB1 (h) (agonist radioligand)	5.5
sigma (non-selective) (h) (agonist radioligand)	5.7
Na+ channel (site 2) (antagonist radioligand)	6.6
5-HT transporter (h) (antagonist radioligand)	>10
5-HT1B (antagonist radioligand)	>10
5-HT1D (agonist radioligand)	>10
5-HT2A (h) (agonist radioligand)	>10
5-HT2B (h) (agonist radioligand)	>10
5-HT2C (h) (agonist radioligand)	>10
5-HT3 (h) (antagonist radioligand)	>10
5-HT4e (h) (antagonist radioligand)	>10
5-HT6 (h) (agonist radioligand)	>10
5-HT7 (h) (agonist radioligand)	>10
A1 (h) (agonist radioligand)	>10
A2A (h) (agonist radioligand)	>10
A2B (h) (antagonist radioligand)	>10
A3 (h) (agonist radioligand)	>10
Abl kinase (h)	>10
ACE (h)	>10
ACE-2 (h)	>10
acetylcholinesterase (h)	>10
alpha 1A (h) (antagonist radioligand)	>10
alpha 1B (h) (antagonist radioligand)	>10
AMPA (agonist radioligand)	>10
APJ (apelin) (h) (agonist radioligand)	>10
AR (h) (agonist radioligand)	>10
AT1 (h) (antagonist radioligand)	>10

Target	*$IC_{50}(\mu M)$*
AT2 (h) (agonist radioligand)	>10
ATPase (Na+/K+)	>10
B2 (h) (agonist radioligand)	>10
BACE-1 (h) (beta -secretase)	>10
BB3 (h) (agonist radioligand)	>10
beta 1 (h) (agonist radioligand)	>10
beta 2 (h) (agonist radioligand)	>10
beta 3 (h) (antagonist radioligand)	>10
BLT1 (LTB4) (h) (agonist radioligand)	>10
BZD (central) (agonist radioligand)	>10
Ca2+ channel (L, dihydropyridine site) (antagonist radioligand)	>10
Ca2+ channel (L, verapamil site) (phenylalkylamine) (antagonist radioligand)	>10
Ca2+ channel (N) (antagonist radioligand)	>10
CaMK2alpha (h)	>10
caspase-3 (h)	>10
CCK1 (CCKA) (h) (agonist radioligand)	>10
CCK2 (CCKB) (h) (agonist radioligand)	>10
CCR2 (h) (agonist radioligand)	>10
CDK2 (h) (cycA)	>10
choline transporter (CHT1) (h) (antagonist radioligand)	>10
COMT (catechol- O-methyl transferase)	>10
COX1 (h)	>10
COX2 (h)	>10
CRF1 (h) (agonist radioligand)	>10
CysLT1 (LTD4) (h) (agonist radioligand)	>10
D1 (h) (antagonist radioligand)	>10
D2S (h) (agonist radioligand)	>10
D3 (h) (antagonist radioligand)	>10
delta 2 (DOP) (h) (agonist radioligand)	>10
dopamine transporter (h) (antagonist radioligand)	>10
EP2 (h) (agonist radioligand)	>10
ERalpha (h) (agonist fluoligand)	>10
ERK2 (h) (P42mapk)	>10
ETA (h) (agonist radioligand)	>10
ETB (h) (agonist radioligand)	>10
FLT-1 kinase (h) (VEGFR1)	>10
FP (h) (agonist radioligand)	>10
Fyn kinase (h)	>10
GABA transporter (antagonist radioligand)	>10
GABAA1 (h) (alpha 1,beta 2,gamma 2) (agonist radioligand)	>10
GABAB(1b) (h) (antagonist radioligand)	>10
glucagon (h) (agonist radioligand)	>10
glycine (strychnine-insensitive) (antagonist radioligand)	>10
GR (h) (agonist radioligand)	>10

Target	*$IC_{50}(\mu M)$*
guanylyl cyclase (h) (activator effect)	>10
H1 (h) (antagonist radioligand)	>10
H2 (h) (antagonist radioligand)	>10
H3 (h) (agonist radioligand)	>10
H4 (h) (agonist radioligand)	>10
HIV-1 protease (h)	>10
inducible NOS	>10
IP (PGI2) (h) (agonist radioligand)	>10
IRK (h) (InsR)	>10
kainate (agonist radioligand)	>10
kappa (KOP) (agonist radioligand)	>10
LXRbeta (h) (agonist radioligand)	>10
Lyn A kinase (h)	>10
M1 (h) (antagonist radioligand)	>10
M2 (h) (antagonist radioligand)	>10
M3 (h) (antagonist radioligand)	>10
M4 (h) (antagonist radioligand)	>10
MAO-A (antagonist radioligand)	>10
MC1 (agonist radioligand)	>10
MC3 (h) (agonist radioligand)	>10
MC4 (h) (agonist radioligand)	>10
MCH1 (h) (agonist radioligand)	>10
MMP-1 (h)	>10
MMP-2 (h)	>10
MMP-9 (h)	>10
motilin (h) (agonist radioligand)	>10
MT3 (ML2) (agonist radioligand)	>10
mu (MOP) (h) (agonist radioligand)	>10
N muscle-type (h) (antagonist radioligand)	>10
N neuronal alpha 4beta 2 (h) (agonist radioligand)	>10
neutral endopeptidase (h)	>10
NK1 (h) (agonist radioligand)	>10
NMDA (antagonist radioligand)	>10
NOP (ORL1) (h) (agonist radioligand)	>10
norepinephrine transporter (h) (antagonist radioligand)	>10
p38alpha kinase (h)	>10
PCP (antagonist radioligand)	>10
PDE2A1 (h)	>10
PDE3B (h)	>10
PDE4D2 (h)	>10
PDE6 (non-selective)	>10
PPARgamma (h) (agonist radioligand)	>10
SKCa channel (antagonist radioligand)	>10
sst1 (h) (agonist radioligand)	>10

Target	*$IC_{50}(\mu M)$*
sst4 (h) (agonist radioligand)	>10
TNF-alpha (h) (agonist radioligand)	>10
TR (TH) (agonist radioligand)	>10
UT (h) (agonist radioligand)	>10
V1a (h) (agonist radioligand)	>10
V2 (h) (agonist radioligand)	>10
VPAC1 (VIP1) (h) (agonist radioligand)	>10
xanthine oxidase/ superoxide O2- scavenging	>10
Y1 (h) (agonist radioligand)	>10
ZAP70 kinase (h)	>10